1834

Isotope and Radiation Techniques in Soil Physics and Irrigation Studies 1983

INTERNATIONAL ATOMIC ENERGY AGENCY, VIENNA, 1983

ISOTOPE AND RADIATION TECHNIQUES
IN SOIL PHYSICS
AND IRRIGATION STUDIES 1983

ISOTOPE AND RADIATION TECHNIQUES IN SOIL PHYSICS AND IRRIGATION STUDIES 1983

PROCEEDINGS OF AN INTERNATIONAL SYMPOSIUM
ON ISOTOPE AND RADIATION TECHNIQUES
IN SOIL PHYSICS AND IRRIGATION STUDIES
JOINTLY ORGANIZED BY THE
INTERNATIONAL ATOMIC ENERGY AGENCY
AND THE
FOOD AND AGRICULTURE ORGANIZATION
OF THE UNITED NATIONS
AND HELD IN
AIX-EN-PROVENCE, FRANCE, 18–22 APRIL 1983

ISOTOPE AND RADIATION TECHNIQUES
IN SOIL PHYSICS AND IRRIGATION STUDIES 1983
IAEA, VIENNA, 1983
STI/PUB/647
ISBN 92—0—010083—X

FOREWORD

The understanding of the process by which water moves within the soil profile and by which water and nutrients are made available to plants started with theories developed from laboratory experiments carried out in columns filled with glass beads to simulate a homogeneous soil. More than half a century has passed since Richards, on the basis of these experiments, suggested that Darcy's equation could be combined with that of mass conservation to describe the movement and retention of water within unsaturated soils. At a later stage the soil physicist moved out into the fields and tried to use the laboratory models to describe water behaviour in the soil and to suggest management practices to optimize crop production. A fair amount of field data is available today, obtained on small experimental plots and disregarding the spatial co-ordinate at which observations were made. Tremendous difficulties are being encountered in using this information to describe important practical problems dealing with the transport of water through large fields given over to crop production.

This Symposium has shown that a major effort is being made to make soil physics applicable to the analysis of the behaviour of field soils in relation to crop production and to the development of effective management practices that improve and conserve the quality and the quantity of agricultural lands. However, the development of a valuable field technology has been slow. Soil hydraulic conductivity is highly sensitive to small changes in soil water content and texture, being extremely variable spatially and temporally. It has been a great challenge to earth and geophysical scientists to cope with this problem. One promising direction, indicated at the meeting, is to take advantage of stochastic concepts and equations rather than treat the process of soil water movement in a strictly deterministic manner. The application of scaling and geostatistical methods coupled with available soil survey information seems to be one way of making better use of available data and describing the behaviour of water over large fields. Observations should be made so as to take advantage of the spatial variability of soil properties and less emphasis should be given to the identification of average values, their potential dispersion within a given parcel of land and the regression of one attribute versus another.

This Symposium, like that on the same topic held in 1973, concentrated on the use of isotope and radiation techniques in soil physics and irrigation studies. Attention was focused on the possibilities of using isotopes and various types of radiation equipment in irrigation and crop water requirements.

Attention was also paid to crop production in saline soils and the problem of how the improved insight gained with the aid of isotopes can be of advantage in making more efficient use of applied fertilizer or in developing more adequate management practices aimed at conserving the soil and increasing productivity.

More than 100 participants from 33 countries and 2 international organiza- tions attended the Symposium and 43 papers were presented. The IAEA and the FAO wish to thank the authors, session chairmen and participants for their contribution to the success of the meeting. Gratitude is expressed to the French Atomic Energy Commission and the Centre d'études nucléaires de Cadarache for their excellent arrangements and for the assistance rendered by the staff in the organization of the Symposium. Finally, special thanks are extended to the authorities of Aix-en-Provence for the hospitality extended to the participants.

EDITORIAL NOTE

CONTENTS

SOIL WATER (Session 5)

CHARACTERIZATION OF FIELD SOILS

(Sessions 1 and 2)

Chairman (Session 1)

D.R. NIELSEN
United States of America

Chairman (Session 2)

E.G. YOUNGS
United Kingdom

Invited Paper

SOIL PHYSICS AND THE WATER MANAGEMENT OF SPATIALLY VARIABLE SOILS

E.G. YOUNGS
Rothamsted Experimental Station,
Harpenden, Herts,
United Kingdom

Abstract

SOIL PHYSICS AND THE WATER MANAGEMENT OF SPATIALLY VARIABLE SOILS.
The physics of macroscopic soil-water behaviour in inert porous materials has been
developed by considering water flow to take place in a continuum. This requires the flow
region to consist of an assembly of representative elementary volumes, repeated throughout
space and small compared with the scale of observations. Soil-water behaviour in swelling soils
may also be considered as a continuum phenomenon so long as the soil is saturated and swells
and shrinks in the normal range. Macroscale heterogeneity superimposed on the inherent micro-
scale heterogeneity can take many forms and may pose difficulties in the definition and
measurement of soil physical properties and also in the development and use of predictive
theories of soil-water behaviour. Thus, measurement techniques appropriate for uniform soils
are often inappropriate, and criteria for soil-water management, obtained from theoretical con-
siderations of behaviour in equivalent uniform soils, are not applicable without modification
when there is soil heterogeneity. The spatial variability of soil-water properties is shown in
results from field experiments concerned with water flow measurements; these illustrate both
stochastic and deterministic heterogeneity in soil-water properties. Problems of water manage-
ment of spatially variable soils when there is stochastic heterogeneity appear to present an
insuperable problem in the application of theory. However, for soils showing deterministic
heterogeneity, soil-water theory has been used in the solution of soil-water management problems.
Thus, scaling using similar media theory has been applied to the infiltration of water into soils
that vary over a catchment area. Also, the drain spacing to control the water-table height in soils
in which the hydraulic conductivity varies with depth has been calculated using groundwater
seepage theory.

1. INTRODUCTION

The aim of good soil-water management is the efficient
production of the soil-water environment required for a given
purpose. The latter is usually the maximum yield of
agricultural crops. Irrigation and drainage systems are
installed to give the required soil-water conditions. The
resulting soil-water behaviour is dependent on the properties

3

of the soil medium and on the physical boundary conditions
imposed on the flow region, both by these installations and at
the natural boundaries of the region as well as by growing
plants. A quantitative approach to soil-water management
problems is therefore through soil-water physics.

The extensive theoretical work on the movement of water
from irrigation channels and on the control of water tables by
land drains in uniform soils has led to rational approaches to
soil-water management being discussed mainly for such very
ideal soil conditions [1,2,3]. However, soils are very often
far from uniform (see, for example, [4]). The application of
the rational approaches that assume a uniform soil may not
therefore give a correct design and operation of soil-water
management systems when there is soil variability. In this
paper we consider the physics of soil water in spatially
variable soils, and then go on to apply these considerations
to infiltration and drainage problems.

2.   THE CONTINUUM CONCEPT IN SOIL PHYSICS

Quantitative soil-water physics has been developed
largely from studies on inert porous materials (see, for
example, [5]). To a lesser extent, the swelling and shrinking
behaviour of ideal clay soils has been considered
quantitatively [6]. Soils, however, may not conform to either
of these simple patterns. They are, nevertheless, porous
materials, and an understanding of their physical behaviour
comes from building on to the extensive knowledge we have
concerning the physics of simple porous materials.

2.1. Inert porous materials

Every soil physicist knows of the experiments that Darcy
performed last century on saturated columns of sand, from
which he deduced the law, now known as Darcy's law,

$$Q/t = - K_s A \Delta h/L \qquad (1)$$

that describes the volume of water Q flowing in time t down a
column of length L and cross-section A when a head difference
Δh is applied between the base and surface. The constant of
proportionality K_s is now known as the hydraulic conductivity
of the porous material, and the law is the basis for the
quantitative description of flow through soils. Indeed, most
of quantitative soil physics describes the water in inert
uniform porous materials, and hence it should perhaps be
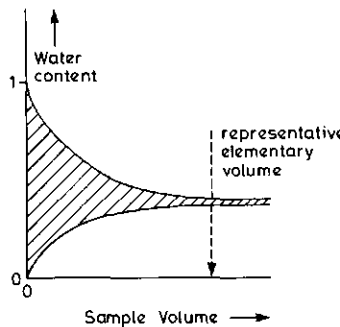
FIG.1.   *Measurement of soil-water content of a simple saturated porous material.*

better referred to as "sand physics". Thus, Richards [7]
assumed that soils were inert uniform porous materials in his
development of the unsaturated flow equation

$$\frac{\partial \theta}{\partial t} = \text{div}(K \text{ grad } \phi) , \qquad\qquad (2)$$

where θ is the water content at a point at time t, ϕ the
hydraulic potential and K the hydraulic conductivity that
varies with the water content θ. Similarly, Haines [8]
explained the hysteresis observed in the relationship between
soil-water content and pressure by referring to the physical
behaviour of water in materials such as sands. The tradition
of developing and testing soil physical principles with
experiments on sand-like materials is thus well established.
      One implication of Darcy's law, and also of Richards'
equation, is that water flow though a porous material may be
considered as if the water moved not through discrete non-
uniform channels between particles of various sizes but
through a continuum. This continuum approach, and therefore
Darcy's law, must obviously fail if the distances over which
the flow is being considered become too small. The continuum
approach is thus linked with the concept of the representative
elementary volume of a porous material which may be regarded
as that volume that contains a sufficient number of pores to
be representative of the pore space and so may be considered
to be repeated throughout the flow region.
      The measurement of water content in a saturated uniformly
packed sand simply illustrates the concept of the
representative elementary volume of a porous material.
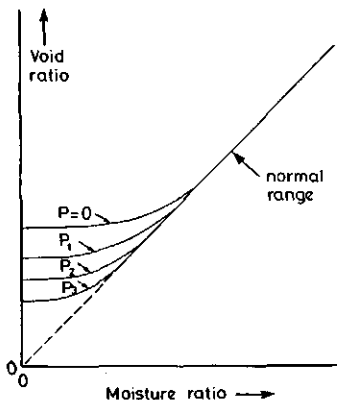
FIG.2. Shrinkage curves for a swelling soil under different loads P = O, P₁, P₂, P₃...
(O < P₁ < P₂ < P₃).

Sampling a very small volume gives a variation in the
volumetric water content between zero (when the volume sampled
lies wholly within a solid particle) and unity (when the
volume sampled lies wholly within the water-filled pore
space). Sampling a larger volume reduces the range of
results, as shown in Fig. 1, until, if large enough samples
are taken, the values of water content become practically the
same. The smallest volume where this occurs is the
representative elementary volume. The water in the sand may
be supposed to be uniformly distributed throughout the volume
and the inherent heterogeneity at the microscale ignored.

2.2. Swelling soils in normal range

The behaviour of clays during swelling and shrinking is
described by shrinkage diagrams in which the void ratio is
plotted against the moisture ratio for a given loading, as
illustrated in Fig. 2. Diagrams usually shown in the
literature (for example, [9] and as shown in Fig. 2) give
different intercepts for different loadings on the void ratio
axis in spite of the fact that this would imply some
irreversible structural change on loading. Hence the
application of reversible thermodynamics, although used in the
development of theory relating to swelling soils [10], is
inappropriate. More experimental evidence is required on this
point.
Again the theory concerning the physical behaviour of
swelling soils is that of continuum physics. Because of the

smaller size of clay particles, the representative elementary
volume of clay materials may be supposed to be much smaller
than those for sands.

     Using the continuum concept, Smiles and Rosenthal [11]
considered the mechanism of flow through saturated clay
slurries by postulating that Darcy's law would be expected to
hold if flow were considered relative to material coordinates
rather than spatial coordinates. This led to the equation to
describe one-dimensional flow phenomena, validated by
experiment,

$$\frac{\partial e}{\partial t} = \frac{\partial}{\partial m} \left(D_m \frac{\partial e}{\partial m} \right) \tag{3}$$

where e is the void ratio, m is the material coordinate and
D_m a soil-water diffusivity. The diffusion approach can be
applied only to one-dimensional flow with the clay swelling
and shrinking in the normal range, that is, with all swelling
or shrinking being accounted for wholly by the addition or
subtraction of water. This approach may be referred to
appropriately as "slurry physics".

2.3. Porous materials not behaving as continua

     The continued shrinkage of clays below the normal range
leads to the formation of cracks. The physical mechanism of
crack formation is not well understood, but must involve the
tensile strength of the clay at the moment of cracking. Once
cracks are formed, the shrinkage is no longer one-dimensional
so that Eq. (3) no longer describes the water movement in the
soil of the micropore space between the cracks, even though it
is still shrinking in the normal range. The cracks themselves
form a macropore region of pore space that forms a boundary to
the micropore space. Similar structural formations occur
during the mechanical disturbance of soils during cultivation
and on account of plant roots and soil animals. In these
situations the soil-water behaviour is no longer described by
simple sand or slurry physics.

3. APPLICATION OF SOIL-WATER THEORY

     In inert uniform soils the development of soil-water
profiles is predicted from Richards' equation (Eq. (2)) with
the given boundary conditions of the physical situation.
However, in swelling soils this is not the case, not only
because the soil particles move to accommodate the changing
water content, but also because the overburden pressure, due
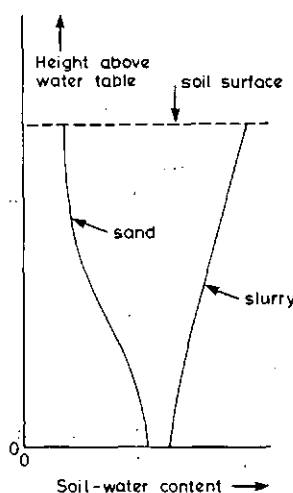
FIG. 3. Equilibrium moisture profiles above a water table in a uniform inert soil and in a swelling slurry.

to the load at a point in the soil, compresses the soil and so alters the water content at a given soil-water pressure. The soil-water profile development for swelling soils is thus different from that for inert soils.

The difference that the nature of the soil can make on soil-water profiles is illustrated in Fig. 3 in which soil-water profiles for a sand and for a slurry are in static equilibrium with a water table. For the sand, the water content decreases with height above the saturated capillary fringe that exists for a small height above the water table. However, for the slurry, the overburden decreases with height, and this has the effect of increasing the water content as the height above the water table increases.

Except perhaps in unstructured saturated clays, it would seem to be unusual for field soils to behave as slurries. Thus sand physics would appear to be the most promising theoretical basis for soil-water predictions in the field. Nevertheless, there is a need to establish how far the swelling of many natural soils needs to be considered in the analysis of soil-water behaviour.

4.   SOIL HETEROGENEITY

Soil heterogeneity of many types occurs at many scales in the field. It results, for example, from natural cracks and

fissures, from inclusions of different materials, from
variations imparted during soil formation, and from root,
animal and man-made disturbances. The heterogeneity may be
stochastic with the soil variation too complex to be known and
hence physical measurements may be difficult to interpret for
predictive use; or it may be deterministic in that the spatial
variability is known and physical measurements can be made
that can be used in soil physical analyses. The scale may be
as small, for example, as the aggregates produced during
cultivation, or as large, for example, as that occurring over
a large catchment area. In all cases it is a complicating
factor in the definition and measurement of soil physical
properties and the use of these in physical analyses.

4.1. Stochastic heterogeneity

Philip [12] suggested that flow regions with random soil
variability could well present the physicist with an
insuperable task of physically characterising the soil for the
purpose of predicting soil physical behaviour under known
imposed conditions. Perhaps it is only possible to consider
the behaviour of the soil region as a whole in these cases. A
system approach such as this would allow only integral
behaviour of the region to be assessed, not the soil-water
properties from point to point throughout the region.
However, just as even the simplest soil material is
inherently heterogeneous at the microscale and yet its
soil-water behaviour is subject to analytical treatment at the
macroscale using continuum physics, so water movement in a
soil showing stochastic heterogeneity at the macroscale should
be subject to analytical treatment at a smaller scale than
that of the bulk system, if the scale of macroscopic
heterogeneity is relatively small. This is the case, for
instance, for aggregated soils in which a heterogeneous array
of macropores encloses the micropore regions of the
individual aggregates. In these soil systems, if the variation
of water content with sample volume size is measured, then the
result would be as shown in Fig. 4 with a wide range of
results found at the representative elementary volume of the
micropore space, and only when a much larger sample is
measured, will the results from different samples become
approximately the same. When this occurs, we have a
macroscale representative elementary volume that can be
assumed to be repeated throughout space. For volumes larger
than this size, continuum physics can be applied to the flow
region. Thus we can measure a hydraulic conductivity K_e of
the whole system to be applied to these larger flow regions.
It can be demonstrated [13] that the value of K_e is dependent
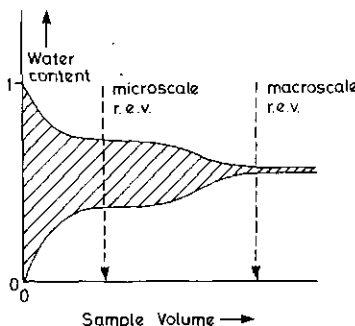
FIG.4.   Measurement of soil-water content of a saturated soil showing macroscale heterogeneity, illustrating the representative elementary volume (r.e.v.) at the microscale and at the macroscale.

on the configuration of the flow lines. If the macroscopic flow lines are parallel and straight, then

$$K_a > K_e > K_h \qquad\qquad (4)$$

where K_a and K_h are the arithmetic and harmonic means of the hydraulic conductivity values of the constituent elemental volumes making up the representative elementary volume. $(K_a^2/K_h)^{1/3}$ can be shown to be the value of K_e for a special isotropic porous material and can be taken as a convenient estimate.

        We have argued that the continuum concept can be applied to stochastic heterogeneous soil systems if a representative elementary volume at the macroscale can be defined and, of course, if physical measurements are made at this scale. However, it cannot be assumed without further consideration that the continuum physics of soil water applied to uniform porous materials will apply in such soils. While Darcy's law for saturated heterogeneous soils is still valid, it does not appear, for instance, that Richards' equation would apply at this larger scale. Additionally with aggregated soils, it has been shown [14] that the displaced air phase during the wetting of soils can no longer be ignored as is usually the case with simple soil systems.

4.2. Deterministic Heterogeneity

        When the variation of soil physical properties is known throughout a region, there is, in principle, no obstacle to

using theory to determine the soil-water behaviour. The flow
velocity V(x,y,z) at the position (x,y,z) is given by

$$V(x,y,z) = - K(x,y,z) \text{ grad } \phi \qquad (5)$$

where K(x,y,z) is the hydraulic conductivity at (x,y,z) where
the hydraulic potential is ϕ. Everywhere in the flow region
there is continuity of soil-water pressure and potential, as
well as continuity of flux. It follows that the streamlines
across a boundary between two soils of conductivity K_1 and
K_2 are refracted according to the cotangent law (see, for
example [5])

$$K_1 \cot \alpha_1 = K_2 \cot \alpha_2 \qquad (6)$$

where α_1 and α_2 are the angles to the normal at the boundary
that the streamlines make in the two soils. Because of the
different relationships between soil-water content and
pressure, there can be abrupt changes in water content at
boundaries. Thus textural changes in the soil result often in
zones of different water content persisting side by side for
long periods of time.

5. DEFINITION AND MEASUREMENT OF SOIL PHYSICAL PROPERTIES

     Soil physical properties are defined as if the soil were
a continuum. From our previous discussion, this implies the
existence of a representative elementary volume for the soil
material, and that measurements of the physical properties are
made on volumes of soil greater than this volume.
     For an additive soil physical property, such as water
content, the value for the bulk material is the weighted
arithmetic mean of the values of the constituent elemental
volumes making up the representative elementary volume [13].
In contrast, no similar simple relationship exists for
transport coefficients, such as hydraulic conductivity,
because of the complex series-parallel flow that occurs in any
porous system. Thus it is not possible to calculate
accurately the hydraulic conductivity from measurements made
on a number of samples smaller than the representative
elementary volume; measurements must be made on volume samples
larger than this.
     If there is a gradual change of soil properties over a
given region, it is not possible to reason as previously and
argue the existence of a representative elementary volume from

FIG.5.   Measurements of infiltration rates through infiltrometer rings of different sizes into a sandy soil. The relationship for an equivalent uniform soil is shown by the full line.
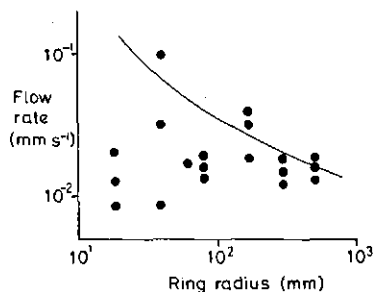
which soil physical properties can be defined. Instead, with increasing sample size, the "noise" in the measurements on account of the inherent microheterogeneity at the scale of particle dimensions becomes less, and the trend of the observed measurements allows the variation of the soil physical property with position to be inferred.

It is impossible to make soil physical measurements without affecting the results by disturbances of the soil in the installation of instruments and by perturbations of the physical field during the measurement. Because of the necessity to include a volume of soil larger than the representative elementary volume, disturbances often have to be large. For example, the use of small wells in the measurement of hydraulic conductivity below the water table gives unrepresentative results for the soil as a whole; the well has to be large enough to give a representative value, and hence a large volume of soil is disturbed. Soil-water pressure measurements, on the other hand, attempt to give the actual pressure of the soil water at a given point by measuring the pressure of bulk water in equilibrium with it through a porous membrane. The latter short circuits many pores because in practice its size cannot be too small, and thus the streamlines and potential patterns are different than would have been the case if the sensor were not present.

The soil physicist is concerned with the use of soil physical measurements in theories for soil-water management. It is necessary to make physical measurements on the soil that are appropriate for the purpose for which they are to be used. Thus, if there is soil heterogeneity, .methods must be used that allow the effect of the soil variability on the results obtained to be assessed when the object of the measurements is to gain information for the design of water management installations. To assume that results, given by an
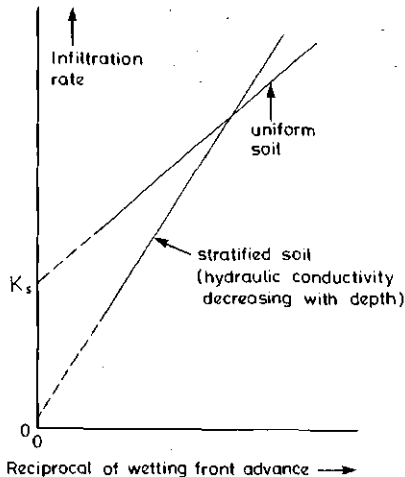
FIG.6.   Infiltration into a uniform soil and into a stratified soil that behaves as a uniform soil.

experimental method that assumes the soil to be homogeneous, can give average results for the design of such installations, may lead to very wrong conclusions concerning the soil-water management. Soil heterogeneity complicates the pattern of streamlines and potentials when there is water flow. Analyses applied both to experimental methods to obtain transport coefficients, and to given field problems, must take cognizance of this.

6.   FIELD MEASUREMENTS OF WATER TRANSPORT PROPERTIES IN HETEROGENEOUS SOILS

6.1. Flow rates from infiltrometer rings

Water flow into the soil from infiltrometer rings is used to obtain the infiltration capacity of the given soil. The proportion of lateral flow from the rings is greater the smaller the diameter. Measured flow rates in field experiments, undertaken to extend the laboratory sand tank work that tested the theoretical relationship between flow rate and ring diameter [15], showed the effect of structural channels in a sandy soil. These channels, originating mainly from worm activity, made the representative elementary volume larger than that expected for a sandy soil. The measurements, shown in Fig. 5, were very variable for small rings; only when

Hydraulic conductivity
values in mm d⁻¹
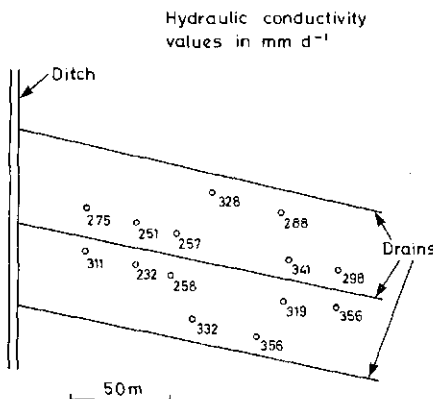
FIG.7. *Hydraulic conductivity values obtained with wells sunk below the water table in a sandy-silt field.*

the ring diameter exceeded 150 mm did the measurements from site to site become repeatable. Thus measurements of infiltration into this soil need to be done on areas at least 0.18 m² to overcome the stochastic heterogeneity.

6.2. Infiltration into stratified soil

The physically-based infiltration equation of Green and Ampt [16] into a unform soil is

$$\frac{di}{dt} = K_s(1 - H_f/Z) \tag{7}$$

where i is the cumulative infiltration at time t, K_s the hydraulic conductivity of the saturated soil, and H_f is the soil-water pressure at the wetting front at depth Z below the surface. Thus a plot of the infiltration rate against the reciprocal of the wetting front advance Z gives an intercept K_s on the infiltration rate axis, as indicated in Fig. 6. However, Swartzendruber and Huberty [17] found this intercept to be zero or even negative in some field experiments. This was shown by Childs [18] to be consistent with theory if the soil were stratified with the conductivity decreasing with depth, and laboratory experiments with layers of graded sands [19] demonstrated that straight line relationships with zero or negative intercepts were possible in practice. As shown in Fig. 6, for these particular stratified soils showing deterministic heterogeneity, the soil system behaves analogously to a uniform soil with a smaller hydraulic

Hydraulic conductivity (m d^{-1})
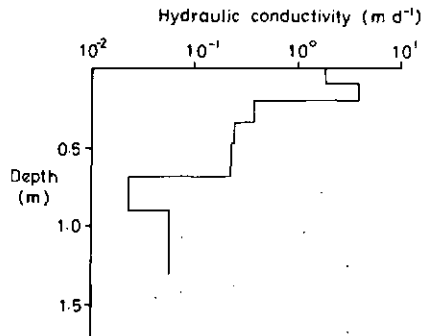
FIG.8. The variation of hydraulic conductivity down the profile of a saturated clay-soil monolith.

conductivity (possibly even negative) and with a larger value of $-H_f$.

6.3. Well measurements of hydraulic conductivity

A survey done in connection with a drainage experiment at the Unit of Soil Physics at Cambridge by G.D. Towner and myself in 1960 gave the results shown in Fig. 7 for the hydraulic conductivity of a very uniform sandy silt soil using Childs' two-well method [20]. The range of results over the 2 ha experimental area is seen to be small. The results themselves show that there is slight stochastic heterogeneity in the hydraulic conductivity measurements. A geometric mean value would give a hydraulic conductivity value suitable for drain design purposes.

6.4. Measurement of hydraulic conductivity profiles in soil monoliths

The most common occurrence of deterministic heterogeneity is the variation of soils down the profile. It is perhaps surprising that soil physicists have not paid more attention to depth-dependence of soil properties in studying soil-water profile development and especially in considering water-table control by drainage. While Childs' two-well method allows the determination of the hydraulic conductivity profile by using Youngs' seepage analysis [21] as does the analysis of drain hydrographs [22], these methods require high water tables. Instead, soil monoliths, obtained without disturbing the soil, can be used for the purpose. With the soil in the monolith saturated, the conductance between the ponded soil surface and different depths can be measured [23], allowing the hydraulic

conductivity at any depth to be obtained. Results for a clay
soil obtained in a lysimeter at Letcombe Laboratory are shown
in Fig. 8. It is seen that the hydraulic conductivity near
the soil surface is, as expected, much greater than at depth,
with an indication that there may be surface capping to a
slight extent.

7. APPLICATION OF THEORY TO THE WATER MANAGEMENT OF SPATIALLY
VARIABLE SOILS

7.1. Use of similar media theory in considering the
infiltration into soils of a catchment area

The collection of sufficient data to use in physically-
based infiltration equations is very time consuming when
carried out over large areas whose soils vary spatially. In
an attempt to provide a simpler means to obtain the physical
data required for calculating the infiltration and runoff from
catchment areas, several studies (for example, [24,25,26]),
have used similar media theory [27]. Laboratory studies using
columns of many porous materials, dissimilar in both size and
shape of particle, have shown that microscopic characteristic
lengths in this theory, calculated from soil physical
properties such as hydraulic conductivity, can be used in
scaling infiltration and runoff relationships [28, 29]. Thus,
using a microscopic characteristic length λ_k given by

$$\lambda_k = (\eta K_s / \rho g) \qquad (8)$$

where η is the viscosity of water, ρ the density of water,
K_s the hydraulic conductivity of the saturated soil, and g
the acceleration due to gravity, the scaled cumulative
infiltration i^* and scaled time t^*, given in terms of the
actual cumulative infiltration i and time t by

$$i^* = \{\rho g \lambda_k / [\sigma(\theta_o - \theta_i)]\} i \qquad (9)$$

and

$$t^* = \{(\rho g)^2 \lambda_k^3 / [\eta(\theta_o - \theta_i)]\} t \quad , \qquad (10)$$

are related by

$$i^* = 0.233 \, t^{*1/2} + t^* \quad . \qquad (11)$$
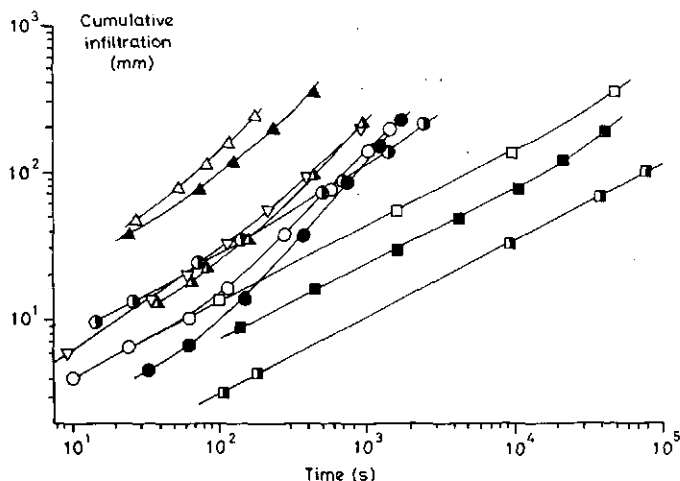
FIG.9.   Infiltration into simple soil materials (after Youngs and Price [28]).   The materials were glass beads (circles), sands (triangles) and a slate dust and sieved soils (squares).

In Eqs. (9) and (10), σ is the surface tension of water and θ_0 and θ_i are the saturated and initial water contents of the soil.

The infiltration results obtained by Youngs and Price [28] for various porous materials are shown in Fig. 9. When these results are scaled, they all fit Eq. (11) well, as shown in Fig. 10. Thus scaling allows the infiltration process to be characterised by microscopic characteristic lengths that can be easily measured, instead of making time-consuming measurements of the infiltration itself.

In addition to hydraulic conductivity, Youngs and Price [28] used the soil-water pressure at half saturation and also the integral of the hydraulic conductivity with soil-water pressure to define the microscopic characteristic length to use in scaling the infiltration behaviour. Alternatively, a mean soil particle size might be used. The object is to be able to infer the infiltration from some easily measured soil property so that such data, collected over the study area, can provide the distribution of infiltration and runoff.

7.2. Land drainage in soils with hydraulic conductivity varying with depth

Drainage equations relate the water-table height above drain lines to drain discharge, drain spacing and the hydraulic conductivity of the soil. Reference to standard
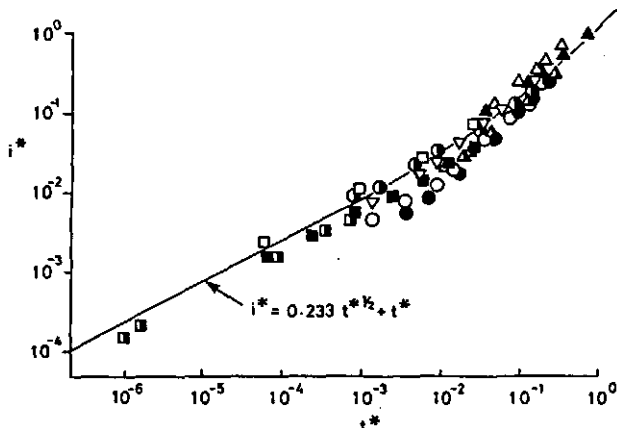
FIG.10. The results of Fig. 9 scaled using similar media theory.

works on land drainage [2,3] shows that most drainage analyses
assume uniform hydraulic conductivity in the groundwater zone.
The assumption that the hydraulic conductivity of soils is
uniform makes these drainage equations of little use in
drainage design work when there is soil variability, since the
form of the hydrograph is very different when the hydraulic
conductivity varies with depth compared with when it is
uniform [22]. However, some analyses do take into account
soil variability. For example, the seepage analysis [21] can
be used for cases of ditch drainage in heterogeneous soils,
especially those with hydraulic conductivity varying with
depth, and is an alternative to the application of numerical
methods of solution (see, for example, [30]).

The seepage analysis gives the maximum height of the
water table H_m above an impermeable floor between two
bounds given by the inequality

$$\int_0^{H_m} K(z)(H_m-z)dz > qD^2/2$$

$$> \int_0^{H_m} K(z)(H_m-z)dz - \int_0^{H_m} K(z) \left[\int_z^{H_m} q/K(z)dz \right]dz \qquad (12)$$

where $K(z)$ is the hydraulic conductivity value at height z and
q the steady rainfall rate applied at the surface. Thus, if
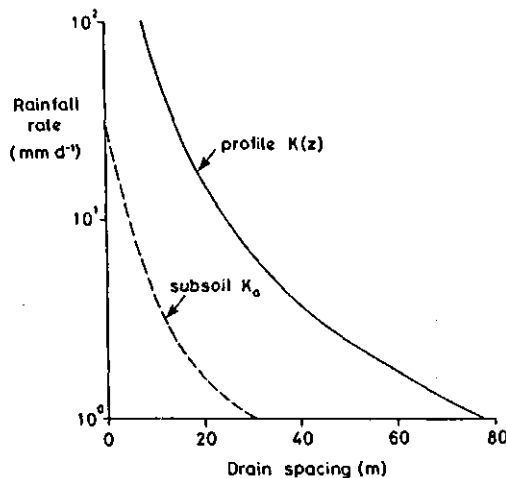
FIG.11. The relationship between drain spacing and steady rainfall rate for the water table just at the soil surface with drains at 1 m depth, calculated for the hydraulic conductivity profile given in Fig. 8. The relationship calculated for a uniform soil with hydraulic conductivity that of the subsoil is also shown.

$K(z)$ is known, the half-drain spacing D can be calculated for a given steady rainfall rate q, which is the drain discharge per unit surface area, that would maintain the water-table height at the level required.

In Fig. 11, the drain spacing, as calculated from Ineq.[1] (12) when the drain is at 1 m depth and the water table just comes to the soil surface, is shown as a function of applied steady rainfall rate for the clay soil whose hydraulic conductivity profile is given in Fig. 8. For this profile the bounds given by Ineq. (12) are close. For comparison, the spacing calculated for a uniform soil with a hydraulic conductivity value K_0 of the subsoil is also shown. From this comparison it is clear that the greater hydraulic conductivity values near the soil surface have the effect of allowing saving in the drain installation cost.

8. CONCLUSION

In this paper an attempt has been made to show how the concepts on which soil physical theory has been developed over

---

[1] Ineq. = inequality

the years can be used in studies concerning water movement in
variable soils. These studies are particularly important to
soil-water management problems. The difficulties that the
soil physicist faces in dealing with soil heterogeneity are
indeed great, but they need to be overcome if rational
approaches, based on soil physical principles, are to be used
in soil-water management.

<div align="center">REFERENCES</div>

[1] HAGAN, R.M., HAISE, H.R., EDMINSTER, T.W., (Eds.),
     "Irrigation of Agricultural Lands", Agronomy Monograph
     No. 11, Amer. Soc. Agron., Madison, Wisconsin (1967).
[2] LUTHIN, J.N., (Ed.), "Drainage of Agricultural Lands",
     Agoronomy Monograph No. 7, Amer. Soc. Agron., Madison,
     Wisconsin (1957).
[3] VAN SCHILFGAARDE, J., (Ed.), "Drainage for Agriculture",
     Agronomy Monograph No. 17, Amer. Soc. Agron., Madison,
     Wisconsin (1974).
[4] NIELSEN, D.R., BIGGAR, J.W., ERH, K.T., Spatial
     variability of field-measured soil-water properties,
     Hilgardia 42, 7 (1973) 215.
[5] CHILDS, E.C., "An Introduction to the Physical Basis of
     Soil Water Phenomena", John Wiley and Sons, Ltd.,
     London (1969).
[6] PHILIP, J.R., SMILES, D.E., Kinematics of sorption and
     volume change in three component systems, Aust. J. Soil
     Res. 7 (1969) 1.
[7] RICHARDS, L.A., Capillary conduction of liquids through
     porous mediums, Physics 1 (1931) 318.
[8] HAINES, W.B., Studies in the physical properties of
     soils. V. The hysteresis effect in capillary properties
     and the modes of moisture distribution associated
     therewith, J. Agr. Sci. 20 (1930) 97.
[9] GROENEVELT, P.H., BOLT, G.H., Water retention in soils,
     Soil Sci. 133 (1972) 238.
[10] COLEMAN, J.D., CRONEY, D., The estimation of the
     vertical moisture distribution with depth in unsaturated
     cohesive soils, Road Res. Road Note No. RN/1709/JDC.DC
     (1952).
[11] SMILES, D.E., ROSENTHAL, M.J., The movement of water in
     swelling soils, Aust. J. Soil Res. 6 (1968) 237.
[12] PHILIP, J.R., Field heterogeneity: some basic issues,
     Water Resour. Res. 16 (1980) 443.
[13] YOUNGS. E.G., Soil physical theory and heterogeneity,
     Agric. Water Manage. 6 (1983).

[14] YOUNGS, E.G., PECK, A.J., Moisture profile development
and air compression during water uptake by bounded
porous bodies: 1. Theoretical introduction, Soil Sci.
98 (1964), 290.

[15] YOUNGS, E.G., Two- and three-dimensional infiltration:
seepage from irrigation channels and infiltration rings,
J. Hydrol. 15 (1972) 301.

[16] GREEN, W.H., AMPT, G.A., Studies on soil physics: 1.
The flow of air and water through soils, J. Agric. Sci.
4 (1911) 1.

[17] SWARTZENDRUBER, D., HUBERTY, M.R., Use of infiltration
equation parameters to evaluate infiltration differences
in the field, Trans. Amer. Geophys. Un. 39 (1958) 84.

[18] CHILDS, E.C., Soil moisture theory, Advances in
Hydroscience 4 (1967) 73.

[19] CHILDS, E.C., BYBORDI, M., The vertical movement of
water in stratified porous material. 1. Infiltration,
Water Resour. Res. 5 (1969) 446.

[20] CHILDS, E.C., COLLIS-GEORGE, N., HOLMES, J.W.,
Permeability measurements in the field as an assessment
of anisotropy and structure development, J. Soil Sci.
8 (1957) 27.

[21] YOUNGS, E.G., The analysis of groundwater seepage in
heterogeneous aquifers, Hydrol. Sci. Bul. 25 (1980) 155.

[22] YOUNGS, E.G., Determination of the variation of
hydraulic conductivity with depth in drained lands and
the design of drainage installations, Agric. Water
Manage. 1 (1976) 57.

[23] YOUNGS, E.G., The measurement of the variation with
depth of the hydraulic conductivity of saturated soil
monoliths, J. Soil Sci. 33 (1982) 3.

[24] PECK, A.J., LUXMOORE, R.J., STOLZY, J.L., Effects of
spatial variability of soil hydraulic properties in
water budget modeling, Water Resour. Res. 13 (1977) 348.

[25] WARRICK, A.W., MULLEN, G.J., NIELSEN, D.R., Scaling
field-measured soil hydraulic properties using a similar
media concept, Water Resour. Res. 13 (1977) 355.

[26] SHARMA, M.L., GANDER, G.A., HUNT, C.G., Spatial
variability of infiltration in a watershed, J. Hydrol.
45 (1980) 101.

[27] MILLER, E.E., MILLER, R.D., Physical theory for
capillary flow phenomena, J. Appl. Phys. 27 (1956)
324.

[28] YOUNGS, E.G., PRICE, R.I., Scaling of infiltration
behaviour in dissimilar porous materials, Water
Resour. Res. 17 (1981) 1065.

[29] YOUNGS, E.G., "Modeling Components of Hydrologic Cycle"
(Ed. V.P. Singh), Use of similar media theory in

infiltration and runoff relationships, (Proc. Int. Symp. Rainfall/Runoff Modeling, Mississippi State University, 1981) Water Resources Publication, Littleton, Colorado (1982) 149.

[30] GUREGHIAN, A.B., YOUNGS, E.G., The calculation of steady-state water-table heights in drained soils by means of the finite-element method, J. Hydrol. $\underline{27}$ (1975) 15.

SUR UN MODE DE CALCUL SIMPLIFIE DES CARACTERISTIQUES HYDRODYNAMIQUES D'UN SOL NON SATURE A NAPPE PEU PROFONDE [†]

J. VIEILLEFON
Office de la recherche scientifique
    et technique outrè-mer (France),
Mission ORSTOM en Tunisie,
Tunis, Tunisie

Abstract–Résumé

A SIMPLIFIED METHOD OF CALCULATING THE HYDRODYNAMIC CHARACTERISTICS
OF A NON-SATURATED SOIL WITH A SHALLOW WATER TABLE.
    Recalling the problems which arise during measurements of the hydrodynamic character-
istics of saline and gypsum soils with a shallow water table, especially for neutron calibration
and for monitoring of variations in the water content and hydraulic pressure head, the author
suggests some methods of calculating the instantaneous flux and driving gradient, giving a
reliable estimate of the $h(\theta)$ and $K(\theta)$ relationships.

SUR UN MODE DE CALCUL SIMPLIFIE DES CARACTERISTIQUES HYDRODYNAMIQUES
D'UN SOL NON SATURE A NAPPE PEU PROFONDE.
    Après avoir évoqué les problèmes qui se posent lors de la réalisation de mesures des
caractéristiques hydrodynamiques de sols à nappe peu profonde, salés et gypseux, notamment
pour l'étalonnage neutronique et le suivi des variations de la teneur en eau et de la charge
hydraulique, on propose quelques méthodes de calcul du flux instantané et de la pente motrice
aboutissant à une estimation fiable des relations $h(\theta)$ et $K(\theta)$.

INTRODUCTION

Dans les études sur la dynamique de l'eau, l'emploi de plus en plus fréquent
de la sonde à neutrons et du tensiomètre a permis de faire passer du laboratoire
au terrain la mesure des caractéristiques hydrodynamiques, comme les relations
succion/teneur en eau, ou h (θ), et conductibilité hydraulique/teneur en eau,
ou $K(\theta)$.

Cette approche en vraie grandeur a permis de pallier aux insuffisances des
mesures effectuées sur des échantillons de petit volume, perturbés ou non.

[†] Ce mémoire s'inscrit dans un programme de recherches effectué en Tunisie dans le
cadre d'un accord de coopération scientifique avec la Direction des ressources en eau et en sol
du Ministère de l'agriculture de la République tunisienne.

Diverses procédures, basées sur l'application de la loi de Darcy généralisée, ont été mises au point, comme la méthode du «drainage interne» ou la méthode du «bilan» [1, 2].

Ces méthodes ayant, semble-t-il, fait leurs preuves dans le cas de sols bien drainés ne comportant pas de nappe à proximité de la base des profils étudiés, il était intéressant de tester leur applicabilité dans le cas de sols à nappe peu profonde, de niveau fixe ou variable, comme on en trouve dans la plupart des périmètres irrigués de Tunisie, et où se posent des problèmes d'économie de l'eau et de lutte contre la salure.

1. LES CONDITIONS MATERIELLES DE REALISATION DES MESURES

L'utilisation de la loi de Darcy généralisée, exprimée par:

$$q = - K(\theta) \frac{dH}{dz}$$

nécessite la mesure simultanée de la teneur en eau à des cotes aussi rapprochées que possible, et de la charge hydraulique ($H = h - z$) aux mêmes cotes.

1.1. Etalonnage

Comme nous l'avons vu, la première série de mesures concernant la teneur en eau se fait à l'aide d'une sonde neutronique. Elle nécessite qu'aient été auparavant déterminées les relations entre les comptages neutroniques et l'humidité volumique θ.

Ces relations, qui peuvent être établies, soit par la mesure des coefficients d'absorption et de diffusion des neutrons par l'échantillon de sol dans un bloc de graphite [3], soit in situ par prélèvement simultané aux comptages, posent quelques problèmes. En effet, l'analyse en pile, qui fonctionne bien pour la caractérisation de sols courants, donne des résultats très différents de l'étude in situ pour les sols gypseux ou salés.

D'un autre côté, l'étalonnage in situ n'est réalisable que si l'on peut, naturelle-ment ou artificiellement, faire des mesures sur une large gamme d'humidité, autorisant l'obtention de corrélations fiables. Ceci n'est malheureusement pas réalisable sur une grande partie du profil des sols à nappe peu profonde.

C'est pourquoi nous avons dû opter pour une méthode mixte. Si le sol ne comporte pas de trop grandes différences de composition, on s'assure dans un premier temps, sur les horizons superficiels, de la concordance des étalonnages in situ et en pile. Le parallélisme des droites d'étalonnage obtenues est générale-ment bon, mais les ordonnées sont souvent différentes, sans doute en raison de

la teneur en sels d'une part et de la teneur en gypse, par son eau de constitution, d'autre part. L'étalonnage in situ est donc en général retenu.

Pour les couches profondes, où les mesures in situ ne donnent qu'un nuage de points sans axe préférentiel, on prend la valeur moyenne des comptages et des teneurs en eau pour fixer l'ordonnée à l'origine de la droite d'étalonnage, en utilisant d'autre part la pente calculée en pile.

Dans le cas des sols gypseux, il semble que l'on puisse obtenir d'assez bonnes relations entre les coefficients A et B de l'équation de la droite d'étalonnage $\theta = A \cdot N + B$, respectivement avec la densité apparente et la teneur en gypse, mais les recherches doivent être pousuivies en ce sens.

On sait enfin qu'il est nécessaire de connaître avec assez de précision la densité apparente de chaque couche. La nécessité de ne pas perturber le sol à proximité du site de mesure oblige à répéter ces mesures en des points pas trop éloignés. On notera, en effet, qu'un approximation de $\pm 0,1$ sur la densité apparente produit une erreur de $\pm 1,25\%$ sur la pente et jusqu'à $\pm 3\%$ sur l'ordonnée à l'origine, dans le cas du sol gypseux étudié ci-après.

Pour ce sol, le coefficient A s'écarte peu de 0,1 (0,086 à 0,108) sauf pour la couche 0–10 cm (0,158), tandis que le coefficient B varie de 9,3 à 27,5%!

Ces étalonnages peuvent être contrôlés lors d'un essai d'infiltration en comparant la lame d'eau infiltrée à différents instants de l'expérience avec les variations de stock d'eau calculées.

Lors d'une expérience d'infiltration, on a obtenu successivement:

Temps d'arrosage (min)	Lame infiltrée (mm)	Variation de stock (mm)
20	93,1	71
30	98,4	83
50	109,1	106
60	126,3	118
70	136,5	129
120	136,5	135

L'écart est assez important au début mais s'amenuise fortement en fin d'infiltration. Au cours de la redistribution, l'évasion latérale perturbe le bilan.

1.2 Critique des mesures

L'examen des résultats des comptages neutroniques montre d'assez nombreuses irrégularités. On peut alors:
— soit rechercher de bonnes relations entre h et θ en travaillant sur un grand nombre de mesures et utiliser ensuite les variations relativement plus régulières de h pour calculer θ, sous réserves de se placer dans des conditions analogues à celles qui ont servi à définir les relations h(θ);
— soit ajuster les variations de θ en fonction du temps [4, 5].
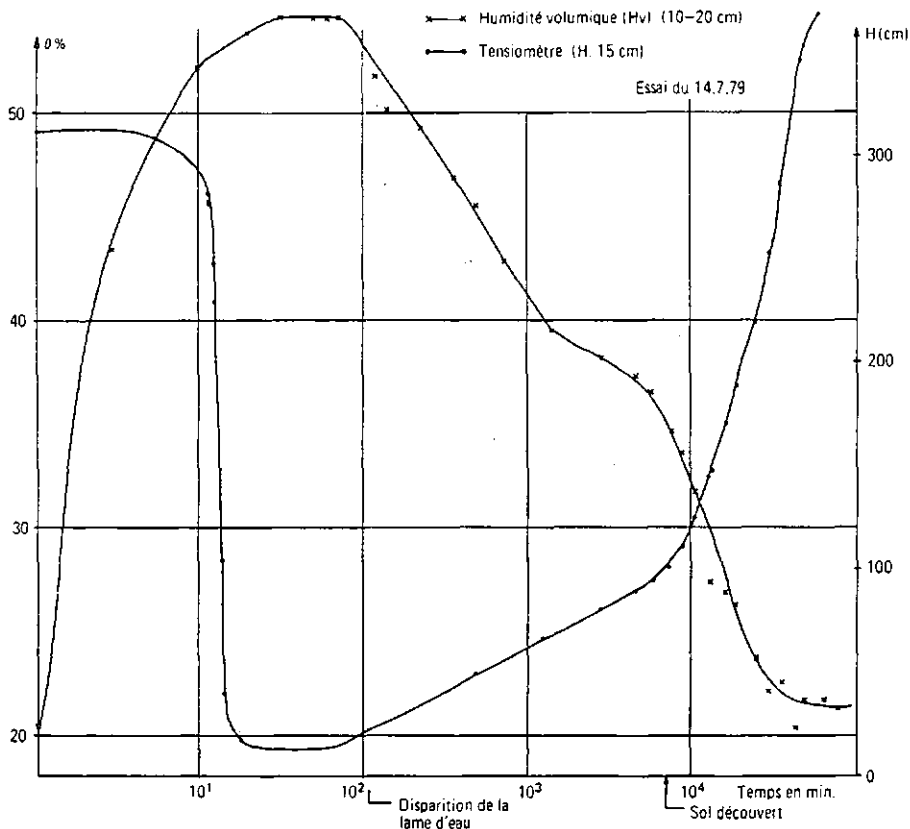
FIG. 1.   Evolution de l'humidité volumique (θ) et de la charge hydraulique (H).

La première méthode a été employée avec quelque succès sur un sol très argileux de drainance moyenne étudié en monolithe [6].

Nous avons utilisé la seconde, notamment au cours de la phase d'évaporation, et la même procédure a été par ailleurs appliquée aux variations de H ou h (figure 1) [7].

Lorsque l'on suit les variations de la teneur en eau, on peut mettre en évidence des phases de saturation qui correspondent à des périodes où la teneur en eau ne varie pas, pendant l'infiltration, mais également quand le ressuyage a commencé. Dans ce cas, les mesures de la charge hydraulique peuvent mettre en évidence des valeurs négatives de la succion h, qui indiqueraient apparemment l'existence de micronappes perchées temporaires, retardant le ressuyage des horizons situés au-dessus d'elles.

En effet, bien que la nappe soit restée à son niveau minimum (180 cm) au cours de l'essai, les profils de charge indiquent des saturations qui durent jusqu'à 8 jours à la cote 120. Ces états sont dus au freinage des flux dans une zone de moindre perméabilité marquée par la présence d'un encroûtement gypseux de nappe.

La mise en évidence de ces phases permet d'éliminer une partie des mesures qui ne pourrait être utilisées pour l'estimation de la conductibilité hydraulique (figure 2).

Un autre intérêt de l'examen des profils de charge est de mettre en évidence la fin de la période favorable aux mesures par la méthode du drainage interne. En effet, en l'absence d'un flux ascendant évaporatoire, la valeur minimum de la charge hydraulique est commandée par la profondeur de la nappe, où $H = -z$ ($h = 0$). Ce point est l'intersection de la cote de la nappe avec la droite $H/z = -1$ [8]. Tout se passe comme si, au cours de la redistribution en sol couvert, le profil de charge effectuait une rotation autour de ce point jusqu'à une verticale qui marque l'arrêt de tous les flux. On a ainsi en tout point du profil

$$H = h - z = Cte = z_{nappe}$$

ce qui se produit au bout de 5 jours dans l'expérience rapportée ici. Ceci ne semble cependant valable que pour des sols légers ou à texture franche. Dans les sols argileux et à structure peu nette ou grossière, des phénomènes de retard, avec manifestation de plusieurs plans de flux nul, sont à craindre [8, 9].

2.   CALCUL DES CARACTERISTIQUES HYDRODYNAMIQUES

2.1. Relation $h(\theta)$

On a vu précédemment que, pour des périodes de temps données, les variations de la succion h (ou de la charge hydraulique H) et de la teneur en eau (ou des comptages) pouvaient être reliées linéairement au logarithme du temps. La combinaison de ces relations pour les mêmes périodes doit permettre de calculer la relation $h(\theta)$.

Si l'on compare en effet des valeurs isolées de ces deux paramètres mesurés sur d'assez longues périodes, en ressuyage mais également au cours de l'évaporation, on peut voir que la relation générale, toutes périodes confondues, est encore acceptable. Les données portées dans le tableau I montrent en effet que les corrélations sont significatives et ne diffèrent pas énormément d'un horizon à l'autre (figure 3).

Ces relations sont naturellement meilleures quand on procède par périodes uniformes, à partir des variations de h et de θ par rapport au temps.
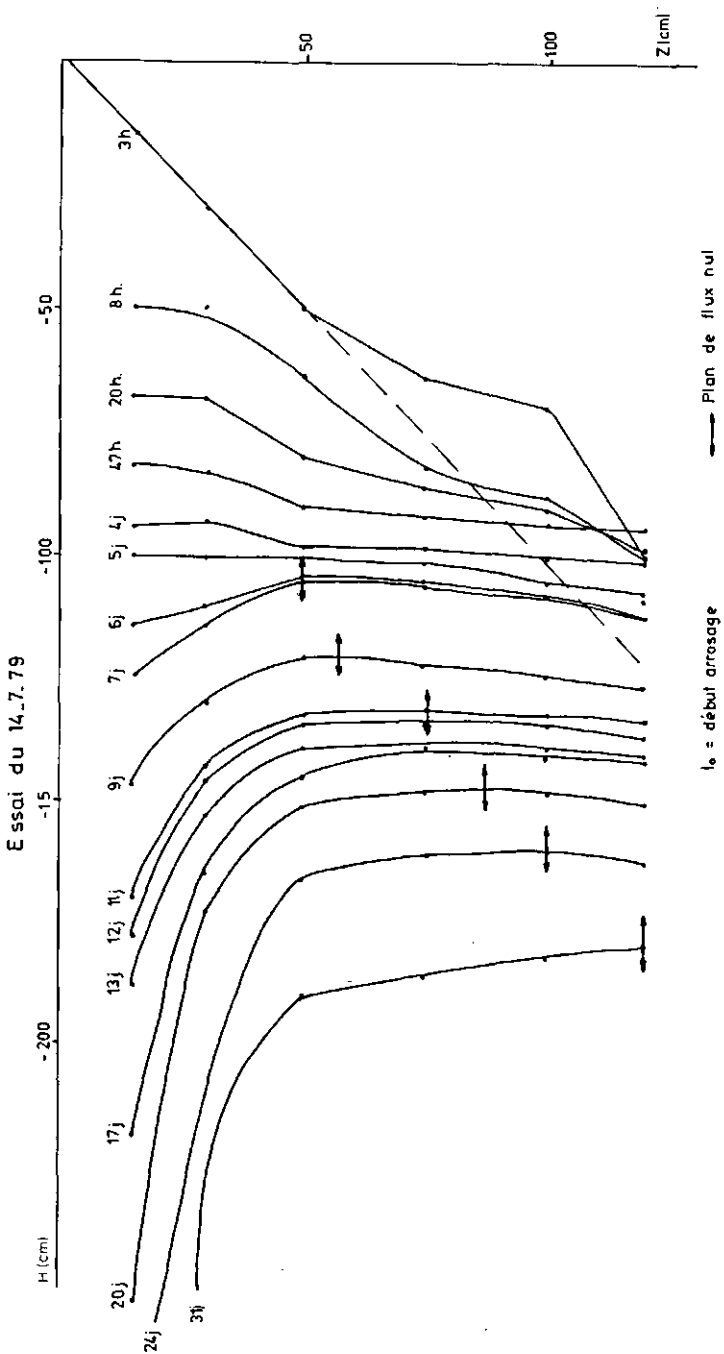
FIG.2. Evolution des profils de charge.

TABLEAU I. RELATIONS GENERALES $h(\theta)$

Profondeur (cm)	Equations	Corrélations
15	$h = 592,7 - 14,541 \, \theta$	$r = -0,923$
30	$h = 635,1 - 15,550 \, \theta$	$r = -0,940$
50	$h = 767,9 - 20,000 \, \theta$	$r = -0,948$
75	$h = 836,1 - 19,697 \, \theta$	$r = -0,950$
100	$h = 617,1 - 15,004 \, \theta$	$r = -0,974$
120	$h = 575,8 - 14,986 \, \theta$	$r = -0,928$

2.2. Evolution de h et θ en fonction du temps

Des diagrammes des figures 1 et 4, on peut retenir les fractions de droites où l'évolution de ces deux paramètres est assez rigoureusement linéaire. A l'aide du graphique semi-logarithmique, il est aisé de déduire sans calcul les équations de ces droites. Leurs pentes étant régulièrement croissantes pour chaque niveau séparant la phase de ressuyage de différentes phases d'évaporation, il peut être plus judicieux d'ajuster ces courbes (figure 2) sur des équations adéquates, par exemple sur des régressions exponentielles.

Les résultats obtenus montrent que les corrélations sont très hautement significatives, du moins pour les variations de h en fonction du temps (tableau II).

2.3. Calcul de $K(\theta)$

Par la méthode du drainage interne comme par celle du bilan, le calcul de la conductibilité hydraulique s'obtient à partir des estimations du flux instantané dS/dt et de la pente motrice dH/dz [2].

2.3.1. Calcul de dS/dt

Le flux instantané peut être obtenu par estimation graphique de la pente de la tangente à la courbe de variation du flux à une cote Z [1], ou par ajustement de cette courbe sur une loi en log t [5]. De même, Libardi et al. [4] ont utilisé des régressions liant la teneur en eau θ, ou la différence $(\theta_0 - \theta)$, θ_0 étant la teneur en eau à la fin du processus d'infiltration, au logarithme du temps.

Si nous observons une loi du type $S = a \cdot \log t + b$ pour toutes les cotes de mesure surmontant un niveau de cote Z, il est évident que la teneur en eau dans chaque couche de sol le surmontant suit une variation du même type.
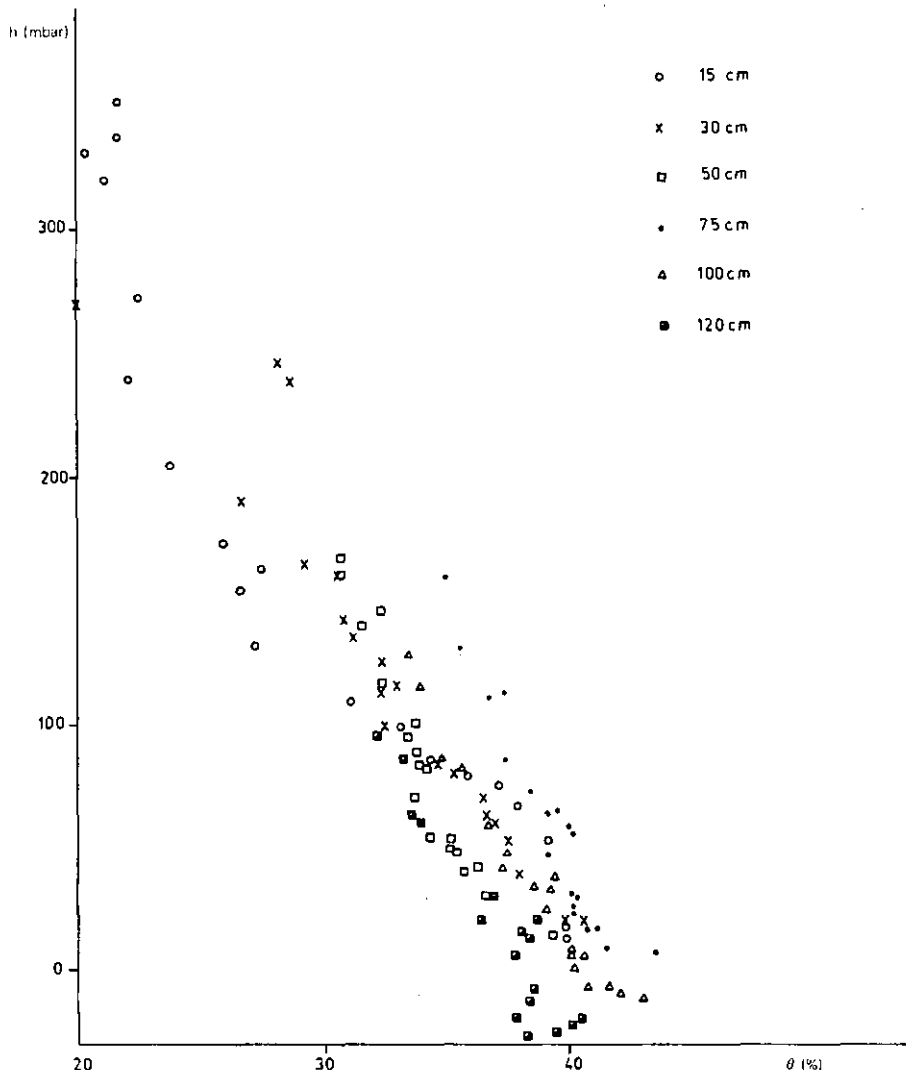
FIG.3.   Relations h (θ).

En effet, si nous nous intéressons à la première couche de sol entre la surface et Z_1, la variation de stock est égale au produit de la teneur en eau moyenne de la couche par son épaisseur. Si donc S est lié au temps par la relation citée plus haut, il en est de même pour θ et pour le taux de comptage N de la sonde à neutrons qui lui est proportionnel (équation d'étalonnage).

Pour une couche de sol deux fois plus épaisse, de 0 à Z_2, une relation de même type ($S_{Z_2} = a_2 \cdot \log t + b_2$) entraîne, par différence, une relation identique pour

ESSAI DU 14_7_1979
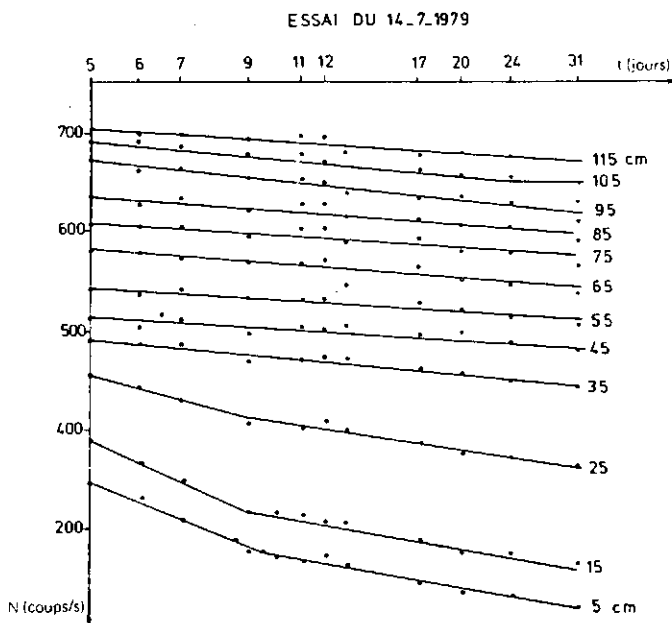
FIG.4.   Evolution de N (coups par seconde) en fonction du temps.

la couche de sol située entre Z_1 et Z_2, donc pareillement pour le taux de comptage qui y est mesuré, et ainsi de suite.

Il devient ainsi plus avantageux de relier, chaque fois que cela est possible, les taux de comptage de chaque niveau au logarithme du temps, pour en tirer, avec l'estimation graphique de la dérivée, une méthode de calcul rapide qui peut être appliquée aussi bien en «drainage interne» qu'en «bilan».

2.3.1.1. Sol couvert — Drainage interne

Cette phase a duré cinq jours dans notre expérience, pendant laquelle le flux évaporatif est resté nul ($q_0 = 0$).

Pour chaque tranche de sol d'épaisseur unitaire U (ici 10 cm) on peut écrire:

$$\theta = A_i \cdot N + B_i = A_i(a_i \cdot \log t + b_i) + B_i$$

et pour l'ensemble des tranches surmontant une cote Z, le stock d'eau au temps t s'écrit:

$$S_{z,t} = \Sigma_0^z \theta \cdot u = \Sigma_0^z (A_i (a_i \cdot \log t + b_i) + B_i) \cdot u$$

$$= \Sigma_0^z (A_i \cdot a_i \cdot \log t + A_i \cdot b_i + B_i) \cdot u$$

TABLEAU II. RELATIONS GENERALES h(log t) $h = A \cdot B^{\log t}$

Profondeur (cm)	A	B	Corrélations
15	33,77	4,69	$r = 0,9995$
30	49,74	2,71	$r = 0,9972$
50	55,07	2,25	$r = 0,9903$
75	55,93	2,22	$r = 0,9851$
100	59,91	2,09	$r = 0,9877$
120	64,32	1,98	$r = 0,9898$

Le flux instantané de drainage à travers la cote Z est la dérivée de cette expression par rapport au temps, soit:

$$q = \frac{dS}{dt_{z,t}} = \frac{\Sigma_0^z A_i \cdot a_i}{2,3\, t}$$

a_i (et b_i) étant définis sur un graphique semi-log décimal.

Ainsi, entre la disparition de la lame d'eau et 33 heures, on a obtenu les valeurs suivantes pour q en drainage interne (tableau III).

Ces valeurs sont sensiblement proches de celles qui sont citées [5] pour un sol sableux surmontant une couche gypseuse.

2.3.1.2. Sol soumis à l'évaporation (bilan)

L'intervention de l'évaporation simultanément au drainage introduit la création d'un plan de flux nul séparant ces deux régimes de circulation opposés [2].

Pour les cotes situées entre ce plan de flux nul et la surface, on doit donc tenir compte de l'évaporation pour calculer le flux les traversant.

$1°)\ 0 < z < z_{fn}$

Le flux ascendant, déterminé par les profils de charge, et traversant une cote Z est donnée par:

$$q_{z,t} = q_{0(t)} - dS/dt \qquad [5]$$

TABLEAU III. VARIATION DU FLUX EN FONCTION DU TEMPS POUR
LES COTES 10 A 60 cm (EN mm/h)

Profondeur (cm)	Temps (h)						
	3	5	8	12	15	20	33
10	2,02	1,21	0,49	0,32	0,26	0,19	0,07
20	2,96	1,78	1,11	0,74	0,59	0,44	0,12
30	3,62	2,17	1,35	0,90	0,72	0,54	0,15
40	4,05	2,43	1,52	1,01	0,81	0,61	0,18
50	4,34	2,61	1,63	1,09	0,87	0,65	0,23
60	4,85	2,91	1,82	1,22	0,95	0,74	0,26

Or q_0 (flux évaporatif à la surface) n'est autre que la variation instantanée
de stock au-dessus du plan de flux nul:

$$q_0 = \frac{\Sigma_0^z \, fn \, A_i \cdot a_i}{2,3 \, t}$$

où z_{fn} = cote du plan de flux nul.

Et comme

$$\frac{dS}{dt} = \frac{\Sigma_0^z \, A_i \cdot a_i}{2,3 \, t}$$

il vient:

$$q = \frac{\Sigma_0^z \, fn \, A_i \cdot a_i - \Sigma_0^z \, A_i \cdot a_i}{2,3 \, t} = \frac{\Sigma_z^z \, fn \, A_i \cdot a_i}{2,3 \, t}$$

Il suffit donc de calculer le produit $A_i \cdot a_i$ pour toutes les cotes au-dessus du
plan de flux nul pour connaître immédiatement q par cumul ascendant (tableau IV).

TABLEAU IV. ELEMENTS DE CALCUL DE q POUR LES COTES 10 A 50 cm
DE 5 A 11 JOURS

Cotes (cm)	Etalonnage		Lissage N		Dérivée × 2,3	Cumul
	$\theta = A \cdot N + B$		$N = a \cdot \log t + b$		$|A \cdot a|$	$\Sigma_z^{z_{fn}} A \cdot a$
	A	B	a	b		
10	0,158	−13,4	−259	529	17,79	39,91
20	0,108	−10,3	−238	552	11,17	22,12
30	0,095	−9,3	−170	573	7,02	10,95
40	0,095	−16,6	−59	532	2,44	3,93
50	0,102	−22,1	−34	536	1,49	1,49

2°) $z > z_{fn}$

On se trouve ici ramené au calcul en drainage interne, le plan de flux nul
remplaçant alors la cote 0 (surface). Il vient alors:

$$q = \left(\frac{dS}{dt}\right)^{z_{fn}} = \frac{\Sigma_{z_{fn}}^z A_i \cdot a_i}{2,3\, t}$$

L'analogie de ces formules montre qu'en résumé, l'intégration des variations
de flux se fait toujours entre la cote de mesure et celle du plan de flux nul, que
celui-ci se trouve au sein du profil ou qu'il soit ramené en surface (évaporation nulle)
ou au niveau de la nappe (drainage nul).

2.3.2. Calcul de dH/dz

Dans un sol relativement homogène, les profils de charge présentent en général
une certaine uniformité, en dehors du maximum de la courbe H(z) indiquant le
plan de flux nul.

Ainsi, en dehors des zones de forte courbure, il est possible d'utiliser les
variations de H mesurées sur deux tensiomètres bornant les cotes intermédiaires
dont on veut connaître la pente motrice.

Au centre de la courbe qui joint ces deux points connus du profil de charge,
on assimile la pente de la tangente à celle de la droite joignant ces deux points.

Pour les autres cotes intermédiaires, une méthode possible est de calculer
les paramètres d'un arc de cercle passant par trois points, donc trois valeurs tensio-
métriques, et de calculer les tangentes à ce cercle aux cotes voulues.
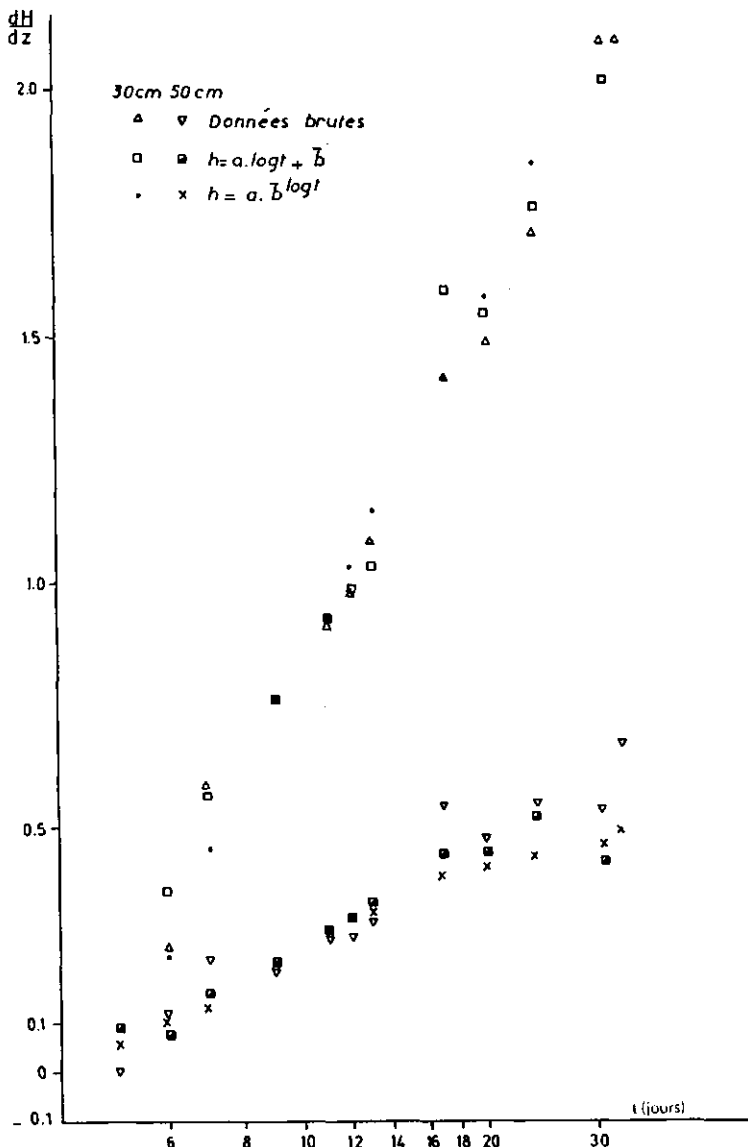
FIG.5.   Comparaison des valeurs calculées dH/dz.

TABLEAU V. EVOLUTION DE dH/dz (LISSAGE DE $h = a \cdot b^{\log t}$)

Profondeur (cm) \ Temps (d)	6	7	9	11	12	13	17	20	24	31
10	0,31 ?	1,14 ?	3,71 ?							
20	0,27	0,74	1,51	2,68	3,14	3,80	7,14	11,36	17,79	41,35
30	0,23	0,45	0,76	0,92	1,03	1,14	1,41	1,57	1,84	21,23
40	0,19	0,25	0,35	0,55	0,65	0,75	1,00	1,15	1,40	1,75
50	0,10	0,13	0,22	0,29	0,32	0,33	0,40	0,42	0,44	0,47
60	0,01	0,01	0,02	0,06	0,07	0,07	0,11	0,11	0,11	0,15
70	−0,04	−0,04	−0,02	0,00	0,01	0,03	0,04	0,05	0,06	0,09
80	−0,05	−0,05	−0,02	−0,01	−0,01	0,01	0,04	0,07	0,07	0,11
90	−0,08	−0,08	−0,04	−0,04	−0,04	−0,01	0,03	0,05	0,07	0,11
100	−0,11	−0,11	−0,07	−0,07	−0,04	−0,05	−0,01	0,03	0,06	0,10
110	−0,14	−0,14	−0,09	−0,09	−0,05	−0,03	−0,01	0,00	0,05	0,10
120	−0,18	−0,18	−0,12	−0,12	−0,05	−0,04	−0,04	−0,03	0,03	0,09

Par exemple, entre 15 et 50 cm, nous pouvons calculer les pentes dH/dz aux cotes 20, 30 et 40 cm, puis entre 30 et 75, aux cotes 40, 50, 60 cm, et ainsi de suite jusqu'à 120.

Il ne s'agit bien sûr que d'une approximation qui doit être critiquée, notamment par la comparaison des doubles valeurs obtenues à l'aide des différents cercles, par exemple aux cotes 40, 60, 70, 80, 90 cm.

Il faut, en effet, vérifier que la courbure est bien maximale près du plan de flux nul et que les centres des cercles successifs ne s'éloignent pas trop de cette cote. Ceci est généralement vérifié pour les arcs de cercle qui encadrent le plan de flux nul, mais ne l'est pas pour les cercles extérieurs. Par contre, les arcs de cercle doivent être approximativement tangents.

Par ailleurs, comme c'est au voisinage du plan de flux nul que l'approximation circulaire semble la plus valable, on peut en tirer par le calcul une estimation relativement précise de sa cote Z_{fn}, par la comparaison du signe des tangentes ainsi calculées, en interpolant entre deux valeurs de signe opposé. Cette valeur sert ensuite dans le calcul du flux instantané au-dessus et en-dessous du plan de flux nul.

Néanmoins, cette procédure n'est possible que dans le cas de sols relativement homogènes ne présentant pas de discontinuités majeures.

En résumé nous disposons de plusieurs options possibles:

1) Lissage des profils de charge puis mesure graphique de dH/dz. C'est la méthode classique sujette à des incertitudes notamment au voisinage du plan de flux nul.

2) Calcul de dH/dz à partir des données brutes par la méthode des cercles.

3) Lissage des variations de H en fonction du temps et calcul des valeurs ajustées de H pour le calcul de dH/dz par la méthode précédente.

La phase d'évaporation de l'essai rapporté ci-dessus a servi à comparer les deux dernières méthodes, en appliquant pour la troisième les deux types de relations h(t) précédemment évoquées, soit $h = a \cdot \log t + b$ et $h = a \cdot b^{\log t}$.

On trouvera sur la figure 5, pour les cotes 30 et 50 cm, le résultat des calculs. On peut voir que l'utilisation des relations du type $h = a \cdot b^{\log t}$ conduit à une représentation plus régulière.

Les données obtenues pour les différentes cotes (tableau V) ont servi au calcul de la conductibilité hydraulique.

On a porté sur la figure 6 les résultats obtenus par la méthode classique (.) et par le lissage des valeurs de N et H combiné au calcul automatique de dS/dt et dH/dz (x). Le groupement des valeurs, toutes sections confondues, est meilleur dans le second cas.

CONCLUSION

Les quelques recettes simples présentées ci-dessus permettent d'affiner l'approche des caractéristiques hydrodynamiques des sols et d'automatiser presque
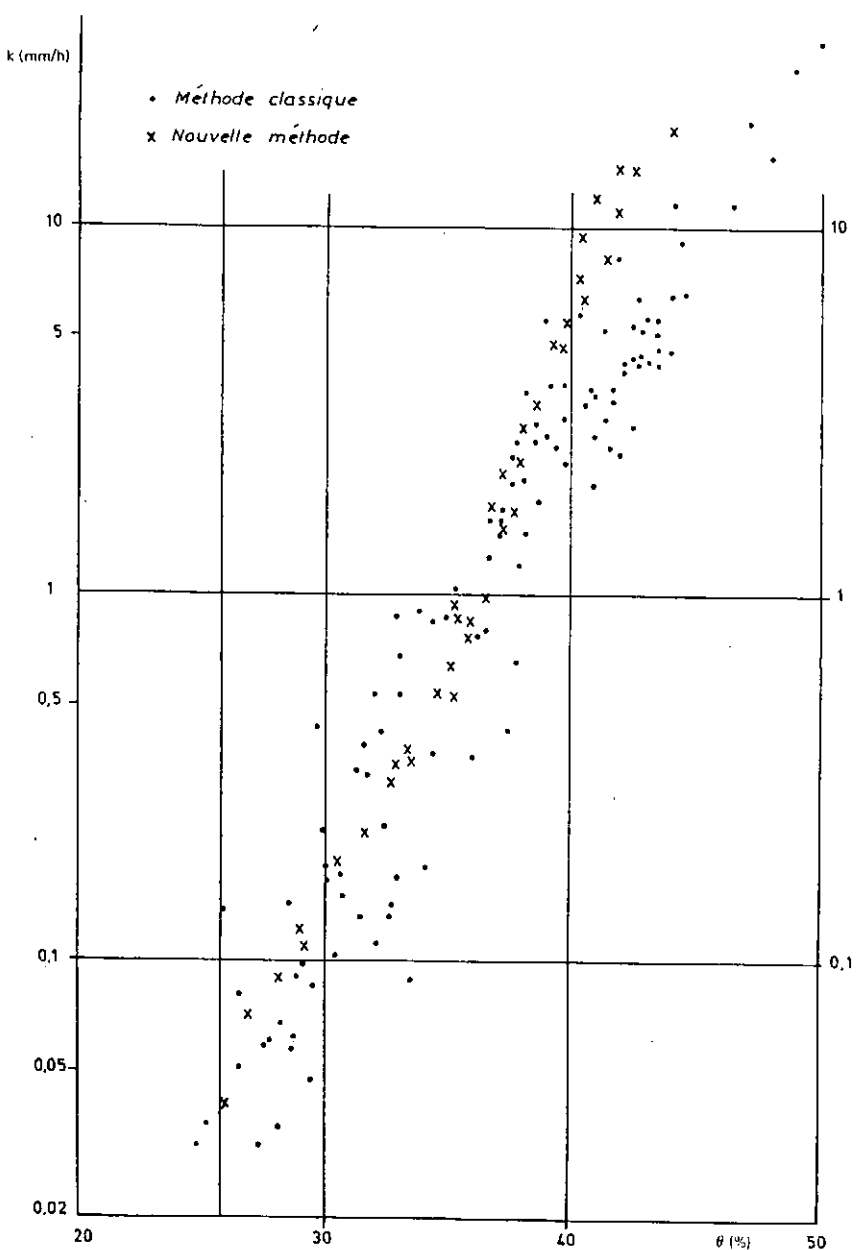
FIG. 6.   Caractéristiques k (θ).

complètement les calculs, dans le cas de sols homogènes sans stratification notable. Cette automatisation doit cependant être précédée d'une étude critique des résultats bruts en autorisant l'utilisation. Il est probable que ces méthodes ne sont qu'une étape vers un meilleur ajustement des paramètres réels.

REFERENCES

[1] HILLEL, D., L'eau et le sol (1974).
[2] VACHAUD, G., DANCETTE, C., SONKO, S., THONY, J.L., Ann. Agron. **29** 1 (1978).
[3] COUCHAT, P., Mesure neutronique de l'humidité des sols, Thèse d'état, UPST (1974).
[4] LIBARDI, P.L., REICHARDT, K., NIELSEN, D.R., BIGGAR, J.W., Soil Sci. Soc. Am. J. **44** 1 (1980) 3.
[5] VACHAUD, G., VAUCLIN, M., COLOMBANI, J., J. Hydrol. **49** (1981) 31.
[6] VALLES, V., VALLES, A.M., Etude méthodologique des transferts d'eau et de sels dans un monolithe de sol argileux. IIème partie: caractérisation hydrodynamique et modélisation des transferts d'eau, ES-199 multigr. ORSTOM/DRES, Tunis (1982).
[7] VIEILLEFON, J., ZANTE, P., Etude du régime hydrique et de la salure en périmètre irrigué sur sol gypseux salé, ES-190, multigr. ORSTOM/DRES, Tunis (1981).
[8] MECHERGUI, M., VIEILLEFON, J., Bull. GFHN **10** (1981) 29.
[9] MECHERGUI, M., Etude dynamique de l'eau dans le sol dans les conditions naturelles par les méthodes tensiométrique et neutronique, Mém. INAT, TUNIS (1980).

VARIABILITE SPATIALE DES CARACTERISTIQUES NEUTRONIQUES D'UN SOL

Incidence sur la détermination des courbes d'étalonnage des humidimètres à neutrons

P. MOUTONNET, P. PERROCHET, Ph. COUCHAT
Service de radio-agronomie,
CEA, Centre d'études nucléaires de Cadarache,
Saint-Paul-lez-Durance, France

Abstract–Résumé

SPATIAL VARIABILITY OF THE NEUTRON CHARACTERISTICS OF A SOIL: IMPACT ON THE PLOTTING OF NEUTRON MOISTURE GAUGE CALIBRATION CURVES.
 In homogeneous sandy loam 66 soil samples were taken for the purpose of measuring the neutron absorption and neutron diffusion constants. Statistical analysis in terms of spatial variability shows that the samples are not interdependent even when they are separated by a distance of no more than 2 m, and that there is no anisotropy in the surface layer, while the deep horizon is anisotropic. By plotting neutron moisture gauge calibration curves using the neutron constants Σ_a and Σ_d it is possible to test the sensitivity of the measurement to the heterogeneity of the medium: at a standard deviation of ± 1 the heterogeneity affects the water balance calculation by $\pm 4\%$ and the determination of an absolute water content in the neighbourhood of 25% by $\pm 10\%$. Lastly, the number of samples necessary if the medium is to be satisfactorily representative was calculated in accordance with the accuracy anticipated for the physical measurement itself: 12 to 22 soil cores are required, depending whether Σ_a or Σ_d is used.

VARIABILITE SPATIALE DES CARACTERISTIQUES NEUTRONIQUES D'UN SOL: INCIDENCE SUR LA DETERMINATION DES COURBES D'ETALONNAGE DES HUMIDIMETRES A NEUTRONS.
 Sur un sol limono-sableux homogène, nous avons procédé au prélèvement de 66 échantillons de sol destinés à la mesure des constantes neutroniques d'absorption et de diffusion des neutrons. L'analyse statistique en terme de variabilité spatiale montre que les échantillons ne sont pas interdépendants, même lorsque la distance qui les sépare n'est que de 2 m et que, s'il n'y a pas d'anisotropie dans la couche de surface, l'horizon profond est par contre anisotrope. Le calcul des courbes d'étalonnage d'un humidimètre à neutrons, à partir des constantes neutroniques Σ_a et Σ_d, permet de tester la sensibilité de la mesure à l'hétérogénéité du milieu: à ± 1 écart-type, elle affecte de $\pm 4\%$ le calcul du bilan d'eau et de $\pm 10\%$ la détermination des valeurs absolues de teneur en eau proche de 25%. Enfin, en terme d'échantillonnage, on a calculé le nombre de prélèvements nécessaires à une bonne représentativité du milieu, en accord avec la précision attendue sur la mesure physique elle-même: il faut 12 à 22 carottages selon que l'on s'attache à Σ_a ou Σ_d.

INTRODUCTION

La mise en œuvre des humidimètres à neutrons sur le terrain implique la
détermination de la relation permettant de passer des vitesses de comptage (N)
mesurées in situ à l'humidité volumique du sol (Θ_v). On sait que la mesure
neutronique repose sur le principe du ralentissement puis de la diffusion d'un flux
de neutrons. L'hydrogène, essentiellement présent dans l'eau du sol, a le plus fort
pouvoir ralentisseur, si bien que le flux de neutrons lents mesuré près de la source
de neutrons rapides est très dépendant de Θ_v. Mais ce flux dépend aussi des
caractéristiques neutroniques de la matrice sol puisque chaque élément intervient
dans le processus par ses sections efficaces d'absorption Σ_a et de diffusion Σ_d.
Les sols étant chimiquement très variables, il en résulte pour chaque utilisateur
la sujétion d'étalonner son appareil sur son point d'essais. Pour ce faire, il dispose
de deux méthodes:

1) La méthode gravimétrique [1, 2] consiste à faire correspondre aux
vitesses de comptage, N, mesurées in situ, les humidités volumiques du sol, Θ_v,
déterminées à partir d'échantillons séchés en étuve, Hts, et des mesures de densités
apparentes, ds; on obtient une relation du type:

$$N = a\,(Hts \times ds) + b$$

$$avec\ \Theta_v = Hts \times ds$$

Il convient de travailler sur une gamme très large de teneur en eau du sol
(ce qui n'est pas toujours facile dans les conditions naturelles), et de procéder au
calcul de la droite de régression, $N(\Theta_v)$, pour chacun des horizons pédologiques
reconnus. Cette méthode est la méthode de référence; elle est laborieuse et de
ce fait onéreuse; d'autre part, la représentativité du résultat obtenu est très
dépendante de l'hétérogénéité spatiale des sols.

2) Pour l'étalonnage à partir des constantes neutroniques d'échantillons
de sol, les travaux réalisés antérieurement [3, 4] ont mis en évidence la relation
existant entre la composition chimique du sol et l'étalonnage des appareils.
A l'usage, il est apparu que le calcul des constantes neutroniques du sol, à partir
de sa composition chimique totale, pouvait être avantageusement remplacé par
une mesure directe de ces paramètres [5–7].

Il s'agit essentiellement de deux comptages neutroniques effectués dans un
bloc de graphite de 1 m^3 contenant une source de 3 Ci de ^{241}Am–Be, en présence
d'un échantillon d'environ 250 g de sol. Des paramètres Σ_a et Σ_d, on déduit,
par calcul du ralentissement et de la diffusion des neutrons, les paramètres de la
courbe d'étalonnage de l'appareil [7]:

$$N = (\alpha ds + \beta)\,\Theta_v + \nu ds + \delta$$

Cette méthode, pratiquée depuis plusieurs années au Centre d'études
nucléaires de Cadarache, s'est révélée sûre et pratique. Elle n'a de sens, cependant,
que si l'échantillon analysé est représentatif de la parcelle ou d'un horizon
pédologique particulier. Il se pose donc un problème d'échantillonnage que l'on
devra résoudre à la lumière des résultats d'une analyse de la variabilité spatiale des
paramètres Σ_a et Σ_d [8].

MATERIEL ET METHODES

a)   Approche mathématique

Les propriétés neutroniques du sol, en un point, sont définissables par une
fonction des coordonnées spatiales de ce point:

$$\Sigma = f(x, y, z)$$

Cette fonction variant a priori d'une manière irrégulière, la prédiction d'une
valeur en un point du site $f(x, y, z)$ à partir de mesures en quelques autre points
$f(x_i, y_i, z_i)$ du même site est évidemment sujette à une incertitude. Afin de décrire
cette incertitude d'une manière rationnelle, nous devons supposer que la fonction
spatiale f est aléatoire.

Cependant, une interdépendance entre des mesures faites à différents points
ne peut être écartée. Considérons une couche de sol plane: si, de plusieurs mesures
de la variable aléatoire f aux points (x_i, y_i), on déduit une valeur moyenne f, et
qu'en un point particulier (x, y) la variable a une valeur différente de cette
moyenne, on peut s'attendre à ce que les valeurs de f aux points immédiatement
voisins $(x + \Delta x, y + \Delta y)$ soient également différentes de la moyenne. Autrement
dit, $f(x, y)$ et $f(x + \Delta x, y + \Delta y)$ ont entre elles un certain degré de corrélation.
Or, l'existence de cette corrélation, dont le degré est lié à la grandeur du vecteur
$(\Delta x, \Delta y)$, est contraire à la définition même de la fonction aléatoire. Si l'on
souhaite ajuster les valeurs mesurées à une loi de distribution statistique, la
connaissance d'une valeur en un point ne doit théoriquement donner aucune
information sur l'obervation adjacente. La distance entre prélèvements déterminant
leur degré d'interdépendance, le problème se ramènera à trouver le pas moyen
d'échantillonnage $\sqrt{\Delta x^2 + \Delta y^2}$ pour lequel il n'y a plus de corrélation entre les
mesures. Le vecteur $(\Delta x, \Delta y)$ possède une direction et une longueur. Pour
simplifier l'analyse, nous lui attribuerons une direction fixe et ne considérerons
que ses variations de longueur. L'analyse devient donc unidirectionnelle. Afin
de mettre en évidence la variabilité spatiale, nous utiliserons deux méthodes de
représentation relatives aux effets d'autocorrélation [9, 10].

1)   Le *corrélogramme:* c'est la représentation graphique de la fonction d'auto-corrélation définissant le degré de dépendance, r, entre observations séparées d'une distance, h:

$$r(h) = \frac{\text{Cov}[f(x), f(x+h)]}{\sqrt{\text{Var}[f(x)] \times \text{Var}[f(x+h)]}}$$

avec r, Cov, Var: corrélation, covariance et variance de l'échantillonnage.

2)   Le *variogramme:* c'est également un mode de représentation de l'auto-corrélation déterminant les écarts quadratiques moyens existants entre des mesures distantes de h. Il est défini par:

$$\nu(h) = \frac{1}{n(h)} \sum_{i=1}^{n(h)} [f(x_i + h) - f(x_i)]^2$$

Le corrélogramme met en évidence l'évolution de l'autocorrélation selon la distance choisie et par suite l'évolution spatiale de l'infrastructure pédologique, régissant le degré de dépendance des couples de mesures. C'est le mode d'exploitation que nous retiendrons.

b)   Echantillonnage

Il a été conduit sur le point d'essais du CEN de Cadarache. Le sol est un limon de type brun calcaire, non différencié, formé à partir d'alluvions pontiennes fines et reposant sur un socle calcaire à une profondeur de 2 à 3 m. Les prélèvements de sol sont effectués à la tarière (diam: 45 mm) selon deux profils longitudinaux π_1 et π_2, de 100 m de longueur, disposés en une croix, couvrant ainsi une surface de 1 ha. Une distance régulière 10 m sépare chaque point, excepté sur le profil π_1 où l'on a prélevé du sol par intervalles de 2 m sur une séquence de 30 m. Le sol est interrogé selon ce modèle aux horizons 0–30 cm et 30–60 cm (fig. 1). On dispose donc au total de 66 échantillons de sol à analyser.

c)   Mesures des paramètres neutroniques

Le sol a été séché à 105°C pendant 24 heures, puis broyé si nécessaire, à moins de 2 mm. Il est ensuite compacté de manière uniforme dans un conteneur en aluminium de 150 ml.

On procède, en position A puis B, à des comptages neutroniques successifs dont on déduit les valeurs Σ_a et Σ_d (mm^2·g^{-1}). Le dispositif actuel permet
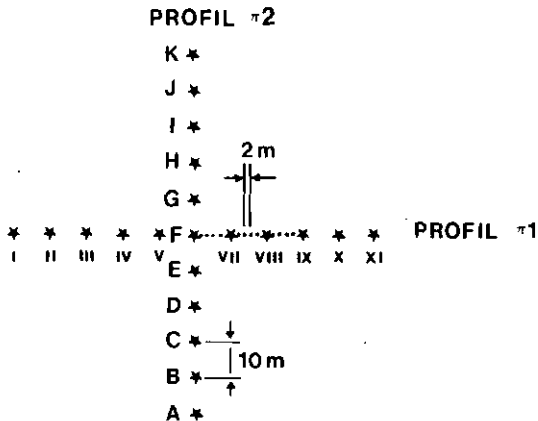
FIG.1.   Disposition des profils π_1, π_2, sur le point d'essais de Cadarache, pour l'échantillonnage du sol.

d'analyser 3 à 4 échantillons par jour. Compte tenu des incertitudes sur les comptages, les fluctuations de l'électronique, la préparation des échantillons, on considère que Σ_a est mesuré à ±0,070 mm$^2 \cdot$g^{-1} et que Σ_d est mesuré à ±1,58 mm$^2 \cdot$g^{-1} [8].

RESULTATS ET DISCUSSION

L'ensemble des résultats est porté dans le tableau I: on a successivement, pour les profils π_1 et π_2, les valeurs de Σ_a et Σ_d pour les horizons 0–30 cm et 30–60 cm. Ces informations, pour le profil π_1, sont reprises en figure 2 où on donne, en fonction de l'ordre de prélèvement des échantillons, les valeurs respectives de Σ_a puis de Σ_d. On observe une grande variabilité spatiale, particulièrement pour Σ_d; cette hétérogénéité est plus forte que l'imprécision sur les mesures indiquées sur chaque figure par un segment ± 1σ.

Avant de procéder aux calculs statistiques classiques, nous allons analyser l'autocorrélation pouvant exister entre les mesures selon le pas d'échantillonnage. La figure 3 donne la relation r(h) pour chacun des 8 cas possibles: 2 horizons X 2 profils X 2 sigma.

Nous avons figuré 2 seuils à ± 1/e que l'on considère comme seuil d'indépendance; cette valeur empirique de 36% correspond à la corrélation admise sur différentes mesures d'une variable aléatoire. Sur deux des graphes de la figure 3,

TABLEAU I. RESULTATS DES ANALYSES NEUTRONIQUES FAITES SUR LES 66 ECHANTILLONS DU POINT D'ESSAIS DE CADARACHE (VALEURS EN $mm^2 \cdot g^{-1}$)

	Echantillons	Prof.: 0-30 cm		Prof.: 30-60 cm	
		Σ_a	Σ_d	Σ_a	Σ_d
PROFIL π_1	I	1.022	21.89	1.119	29.80
	II	1.168	26.99	1.011	19.77
	III	1.130	27.60	0.972	25.48
	IV	1.079	20.71	0.971	18.59
	V	0.934	22.51	0.908	24.00
	VI	0.976	20.20	0.733	17.55
	VI_2	0.967	19.73	0.937	26.12
	VI_4	1.021	21.11	0.856	24.82
	VI_6	0.935	24.01	0.883	20.24
	VI_8	0.945	23.32	0.917	19.18
	VII	0.904	23.26	0.779	21.12
	VII_2	1.060	25.66	0.851	16.65
	VII_4	0.830	20.01	0.719	16.53
	VII_6	0.921	16.85	0.957	19.33
	VII_8	0.803	17.86	0.974	21.75
	VIII	0.823	16.94	0.806	16.42
	$VIII_2$	0.987	23.22	0.944	21.32
	$VIII_4$	1.006	22.71	0.912	21.81
	$VIII_6$	0.952	22.47	0.943	23.03
	$VIII_8$	1.039	27.02	0.988	26.71
	IX	1.038	20.22	0.761	19.73
	X	0.943	16.06	0.790	16.22
	XI	1.006	23.35	0.951	23.07
PROFIL π_2	A	0.911	20.04	0.741	19.36
	B	0.951	25.36	0.753	18.72
	C	0.927	20.56	0.852	19.35
	D	0.906	23.37	0.785	18.54
	E	0.963	21.88	0.904	17.13
	F	0.976	20.20	0.733	17.55
	G	1.033	19.17	0.868	16.62
	H	0.857	16.80	0.786	16.25
	I	0.955	22.16	0.977	18.56
	J	0.967	17.30	0.856	18.63
	K	0.837	17.78	0.625	16.34
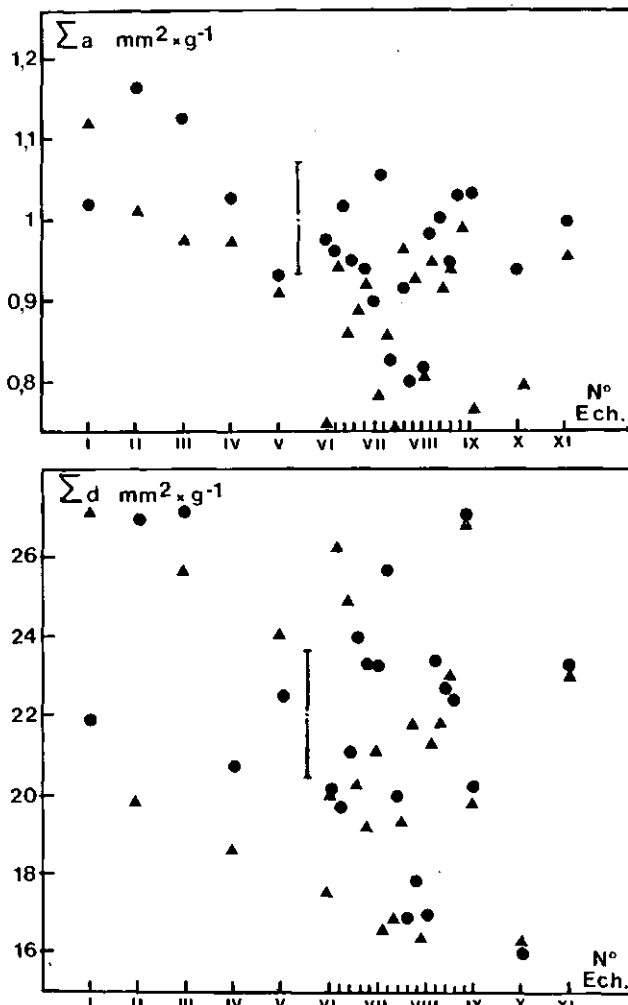
FIG.2. Distribution des sections efficaces d'absorption Σ_a, et de diffusion Σ_d, en fonction de leur position sur le profil π_1 (●: Horizon 0–30 cm; ▲: Horizon 30–60 cm).

nous avons indiqué pour chacun des points expérimentaux le nombre de couples utilisés pour le calcul r(h): il varie entre 9 et 18 selon les distances. Selon M. Vauclin (communication orale), on considère que le nombre de couples pour le calcul de l'autocorrélation devrait être supérieur à 20; on n'accordera donc pas d'attention particulière aux points extérieurs à la fourchette ± 1/e et on considérera qu'à partir de 2 m d'écartement il n'y a pas d'interdépendance entre échantillons lorsqu'on considère leurs valeurs de Σ_a et Σ_d. La figure 4 montre que, pour le profil π_1 sur lequel l'échantillonnage était plus important et pour

FIG.3. Corrélogrammes établis en fonction de h, distance séparant les prélèvements, pour $\Sigma_a - \Sigma_d$, les horizons 0−30 et 30−60 cm, et les profils π_1 et π_2.
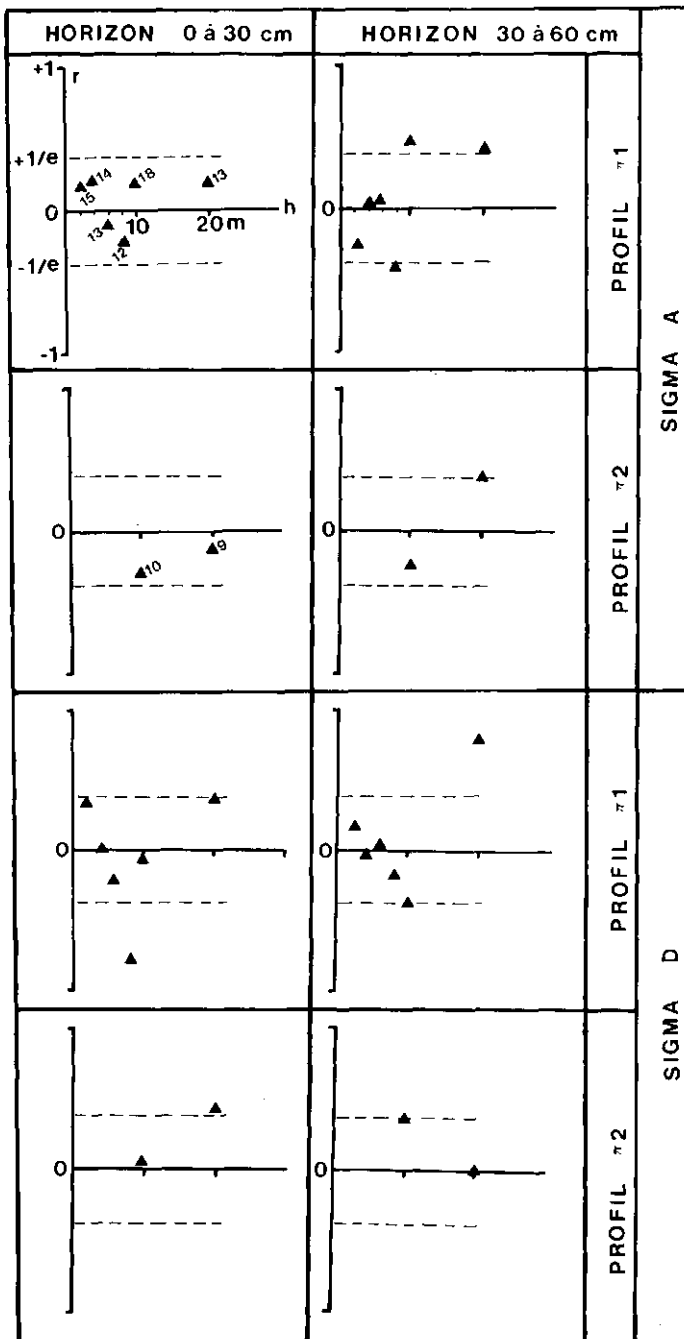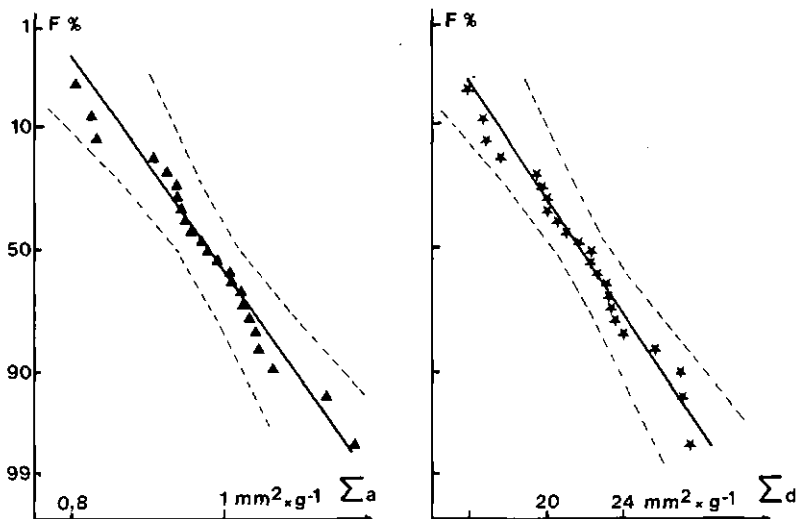
FIG.4. Histogramme des répartitions, en fréquences cumulées, des mesures de Σ_a et Σ_d sur le profil π_1 pour l'horizon 0–30 cm.

l'horizon 0–30 cm, les distributions des fréquences cumulées suivent des lois normales; il en est de même pour l'autre profil et les autres profondeurs. Nous avons donc calculé les valeurs moyennes et les écarts-types pour Σ_a et Σ_d dans les différents cas (tableau II). La comparaison des écarts-types entre profils confirme ce que nous avons déjà constaté sur les graphiques des variations spatiales: les σ_{Σ_a} et σ_{Σ_d} sont systématiquement plus grands sur π_1 que sur π_2. La comparaison des écarts-types d'une variable sur un profil mais à deux profondeurs différentes nous permet également de différencier les horizons en termes d'hétérogénéité. Celle-ci est en effet plus marquée en profondeur. Par ailleurs, rappelons que la précision des mesures est $\pm 0,07$ mm$^2 \cdot$g^{-1} pour Σ_a et $\pm 1,58$ mm$^2 \cdot$g^{-1} pour Σ_d.

La variabilité spatiale ne sera mise en évidence que si elle est supérieure à ces seuils. Ainsi, dans le tableau II, pour Σ_a, π_2, 30–60 cm, la variabilité n'est pas assez marquée pour être apparente. Par contre, pour les autres horizons ou profils, c'est tout à fait possible. Afin de conclure sur l'isotropie du site, nous avons eu recours à deux tests statistiques: le test de Welch permet de comparer les moyennes de deux populations normales sans imposer de conditions particulières sur les variances; le test de Ficher permet de comparer les variances de deux populations normales. Pour que le milieu puisse être considéré comme isotrope, il faut donc que ces deux tests soient non significatifs. Les valeurs $\overline{\Sigma}_a$ et $\overline{\Sigma}_d$ ainsi que σ_{Σ_a} et σ_{Σ_d} sont respectivement testées par horizon selon les

TABLEAU II. VALEURS MOYENNES ET ECART-TYPES CALCULES
SUR LES SERIES DE MESURES NEUTRONIQUES Σ_a ET Σ_d, SUR LES
PROFILS π_1 ET π_2 AUX PROFONDEURS 0–30 ET 30–60 cm

Profils, profondeurs	moyennes $mm^2 \cdot g^{-1}$	écarts-types $mm^2 \cdot g^{-1}$	coefficient de variation %
π_1, 0-30 cm	$\overline{\Sigma}_a = 0,976$	$\sigma_{\Sigma_a} = \pm\, 0,089$	9,1
	$\overline{\Sigma}_d = 21,90$	$\sigma_{\Sigma_d} = \pm\, 3,23$	14,7
π_1, 30-60 cm	$\overline{\Sigma}_a = 0,897$	$\sigma_{\Sigma_a} = \pm\, 0,098$	10,9
	$\overline{\Sigma}_d = 21,22$	$\sigma_{\Sigma_d} = \pm\, 3,68$	17,3
π_2, 0-30 cm	$\overline{\Sigma}_a = 0,937$	$\sigma_{\Sigma_a} = \pm\, 0,057$	6,1
	$\overline{\Sigma}_d = 20,42$	$\sigma_{\Sigma_d} = \pm\, 2,64$	12,9
π_2, 30-60 cm	$\overline{\Sigma}_a = 0,826$	$\sigma_{\Sigma_a} = \pm\, 0,076$	9,2
	$\overline{\Sigma}_d = 17,92$	$\sigma_{\Sigma_d} = \pm\, 1,177$	6,6

deux directions π_1 et π_2, puis par profil selon les deux profondeurs 0–30 cm et
30–60 cm. Les résultats sont les suivants:

— horizon de surface homogène en Σ_a, Σ_d car on ne décèle pas de différences
significatives;

— en profondeur, les moyennes sont significativement différentes sur π_1 et
π_2, le test sur les variances traduisant toutefois une variabilité comparable;

— les mêmes tests effectués pour la comparaison entre horizons sont
significatifs pour les moyennes mais pas pour les variances. On admet donc la
différenciation statistique des couples (π_a et π_d) selon l'horizon.

L'isotropie en surface se conçoit facilement puisque nous étudions une
parcelle cultivée. Le remaniement cultural périodique provoque en effet une
homogénéisation du sol au cours du temps. La différenciation des horizons est

TABLEAU III. EQUATIONS D'ETALONNAGE D'UNE SONDE A NEUTRONS SOLO, POUR LE SOL DE CADARACHE ET UNE DENSITE APPARENTE DE 1,5 g·cm^{-3}

Profil	équation de la courbe
π_1 et π_2 (0-30 cm)	$N = 10,6\ \Theta_v + 48$
π_1 (30-60 cm)	$N = 10,9\ \Theta_v + 50$
π_2 (30-60 cm)	$N = 11,1\ \Theta_v + 38$

sans conteste due au lessivage, et l'anisotropie en profondeur est liée au fait que cette migration a une composante préférentielle selon π_1.

Trois couples moyens ($\overline{\Sigma}_a$, $\overline{\Sigma}_d$) nous conduisent à la détermination de 3 courbes d'étalonnage représentatives chacune d'un horizon et d'une direction. Un programme de calcul nous a donné les résultats suivants pour une sonde de type Solo et d'une densité sèche $\rho_s = 1,5$ g·cm^{-3} (tableau III). On constate que l'hétorogénéité moyenne du sol conduit à une erreur de ±2,3% sur le bilan, et de ±0,5 point sur l'humidité du sol déduite d'une mesure neutronique de 350 impulsions. Ces chiffres sont tout-à-fait satisfaisants, compte tenu des performances des appareils et des besoins agronomiques dans le domaine de l'irrigation.

Il est important aussi de tester la sensibilité du modèle à l'hétérogénéité constatée sur le terrain en matière de Σ_a et Σ_d.

En considérant l'intervalle d'incertitude dû à la précision des mesures et à la variabilité spatiale (écart-type expérimental de l'échantillon) sur π_1 (0–30 cm), nous calculons la courbe d'étalonnage pour les quatre cas de variations extrêmes à comparer à l'étalonnage calculé sur les valeurs moyennes (tableau IV). Nous constatons que l'incidence de la variabilité spatiale sur l'étalonnage est de:

— ±4,2% en matière de bilan d'eau;

— ±2,5 points d'humidité sur la détermination de Θ_v (soit ±10% en valeur relative pour une teneur en eau du sol de 25% et d'autant plus forte que le sol est plus sec).

Ce sont ces chiffres que nous retiendrons en insistant sur l'incidence particulière de la variabilité spatiale sur la mesure in situ des valeurs absolues de Θ_v.

Pour l'échantillonnage, afin de définir le nombre n de prélèvements (soit la taille de l'échantillon) nécessaires pour l'estimation d'une moyenne à une précision donnée et sous un seuil de confiance donné, nous appliquons la méthode suivante.

TABLEAU IV. EQUATIONS D'ETALONNAGE DU SOL ET ECARTS
MAXIMUM RESULTANT D'UNE VARIATION DE ± 1 σ DE Σ_a ET Σ_d

Σa, Σd couple utilisé	équation de la courbe
MOYEN Profil π_1, 0 - 30 cm	$N = 10,5\ \Theta_v + 50$
$(\overline{\Sigma}_a + \sigma_{\Sigma_a},\ \overline{\Sigma}_d)$ ①	$N = 10,1\ \Theta_v + 32$
$(\overline{\Sigma}_a - \sigma_{\Sigma_a},\ \overline{\Sigma}_d)$ ②	$N = 11,0\ \Theta_v + 54$
$(\Sigma_a,\ \Sigma_d,\ + \sigma_{\Sigma_d})$ ③	$N = 10,7\ \Theta_v + 64$
$(\Sigma_a,\ \Sigma_d - \sigma_{\Sigma_d})$ ④	$N = 10,4\ \Theta_v + 37$

Connaissant la précision en absolu sur l'une quelconque des mesures σ^*, et l'écart-type d'une population σ_Σ, on forme le rapport $\delta = \sigma^*/\sigma_\Sigma$. La résolution d'une formule faisant intervenir δ et n nous donne le nombre d'échantillons permettant d'obtenir la précision voulue [8]. En appliquant cette formule à l'estimation des couples $(\overline{\Sigma}_a, \overline{\Sigma}_d)$ de chacun des profils, en imposant la précision maximale σ^*, on trouve pour un intervalle de confiance à 95% les valeurs n du tableau V.

    On constate que, du fait d'une plus grande hétérogénéité spatiale en Σ_d, il faut en moyenne plus d'échantillons pour cette mesure que pour Σ_a (22 contre 12 pour la même précision).

CONCLUSIONS

    La mesure directe des constantes neutroniques d'échantillons de sol du point d'essais de Cadarache, en vue de la détermination de la courbe d'étalonnage d'un humidimètre à neutrons, montre que:

    — il y a une assez grande variabilité spatiale des paramètres Σ_a et Σ_d du sol, avec des coefficients de variation de 9 et 13% respectivement; cette hétérogénéité

TABLEAU V. NOMBRE D'ECHANTILLONS A PRELEVER EN VUE DES
MESURES NEUTRONIQUES Σ_a, Σ_d

Profils	$\overline{\Sigma}_a$	$\overline{\Sigma}_d$
π_1, 0-30 cm	13	26
π_1, 30-60 cm	16	37
π_2, 0-30 cm	8	19
π_2, 30-60 cm	11	7
MOYEN	12	22

affecte les mesures neutroniques: ±4% sur le bilan en eau et ±10% sur la déter-
mination des valeurs absolues de teneur en eau du sol;

— il n'y a pas d'autocorrélation entre échantillons même lorsque l'intervalle
de prélèvement n'est que de 2 m;

— il n'y a pas d'anisotropie de distribution dans la couche de sol arable, mais
il y en a une dans l'horizon sous-jacent;

— pour que l'échantillon de sol soumis à l'analyse neutronique soit représentatif
du point d'essais, il doit résulter d'un nombre de prélèvements qui, dans notre cas,
varie de 12 à 22 selon que l'on considère Σ_a ou Σ_d.

REFERENCES

[1] VAN BAVEL, C.H.M., et al., Calibration and characterization of two neutron moisture
probes, Soil Sci. Soc. Am., Proc. 25 (1961) 329.
[2] HOLMES, J.W., Calibration and field use of the neutron scattering method for measuring
soil water content, Austr. J. Appl. Sci. 7 (1955) 45.

[3] OLGAARD, P.L., On the theory of the neutronic method for measuring water content in soil, Danish Atomic Energy Commission, Risø report n° 97 (1965).

[4] COUCHAT, Ph., «Détermination de la courbe d'étalonnage de l'humidimètre à neutrons à partir de l'analyse chimique des sols», Isotope and Radiation Techniques in Soil Physics and Irrigation Studies (C.R. Coll. AIEA, Istamboul, 1967) AIEA, Vienne (1967) 67.

[5] COUCHAT, Ph., CARRE, C., MARCESSE, J., LE HO, J., «The measurement of thermal neutron constants of the soil; application to the calibration of neutron moisture gauges and to the pedological study of soil», Nuclear Cross Sections and Technology, NBS SP 425 (SCHRACK, R.A., BOWMAN, C.D., Eds), (1975) 516.

[6] COUCHAT, Ph., MOUTONNET, P., L'incidence de l'absorption par les sols des neutrons thermiques sur la mesure neutronique de l'humidité volumique, Terre Malgache 12 (1971) 17.

[7] COUCHAT, Ph., Mesure neutronique de l'humidité des sols, Thèse de Doctorat èssciences, Toulouse (1974).

[8] PERROCHET, P., Variabilités spatiales des paramètres Σ_a et Σ_d dans un sol brun calcaire à profil homogène (application à la mesure de l'humidité volumique par la sonde à neutrons), Mémoire de fin d'étude de l'EPFL (Suisse), décembre 1982.

[9] NIELSEN, D.R., BIGGAR, J.W., ERH, K.T., Spatial variability of field-measured soil water properties, Hilgardia 42 7 (1973) 215.

[10] WARRICK, A.W., NIELSEN, D.R., «Spatial variability of soil physical properties in the field», Applications of Soil Physics (HILLEL, D., Ed.), Academic Press (1980) 319.

Invited Paper

CHARACTERIZATION OF FIELD-MEASURED SOIL-WATER PROPERTIES

D.R. NIELSEN
Department of Land, Air and
    Water Resources,
University of California,
Davis, California,
United States of America

K. REICHARDT
Joint FAO/IAEA Division,
International Atomic Energy Agency, Vienna

P.J. WIERENGA
Department of Agronomy,
New Mexico State University,
Las Cruces, New Mexico,
United States of America

Abstract

CHARACTERIZATION OF FIELD-MEASURED SOIL-WATER PROPERTIES.
    As part of a five-year co-ordinated research programme of the International Atomic
Energy Agency, the Use of Radiation and Isotope Techniques in Studies of Soil-Water Regimes,
soil physicists examined soil-water properties of one or two field sites in 11 different countries
(Brazil, Belgium, Cyprus, Chile, Israel, Japan, Madagascar, Nigeria, Senegal, Syria and Thailand).
Within each field site of approximately 1 hectare, experimental plots (5 X 5 m) free of vege-
tation were established to measure the redistribution of soil water to a depth of 2 m following
steady-state infiltration. Each plot was instrumented with tensiometers placed at 15 or 30 cm
depth intervals and with neutron moisture gauge access tubes. The number of plots within each
field site ranged from 1 to 8. The procedure was to pond water on each plot until steady-state
flow was established, as indicated by stable tensiometer readings. When infiltration was complete,
as indicated by the ponded water level receding to the soil surface, the plot was covered with
plastic to prevent evaporation. Neutron moisture gauge data and tensiometer readings were
taken frequently and eventually once every day during later stages of redistribution. Soil-water
content θ and soil-water pressure head h data obtained through redistribution time t for all depths
z were used to derive soil-water properties by smoothing the temporal relationships and
plotting a range of simultaneous θ and h values [θ(h)] for each soil depth.
The smoothed temporal data [θ(t), h(t)] were also used in the calculation of hydraulic
conductivity $K(\theta)$ by the instantaneous profile method, the flux and θ methods of Libardi et al.,
and the Chong, Green, and Ahuja method. Values of the soil-water diffusivity $D(\theta)$ were

55

obtained from the product $K(\theta)$ and $dh/d\theta$ derived from the field-measured values of $\theta(h)$. An examination of several empirical models of the field-measured $\theta(h)$ revealed that the function

$$\theta = \theta_s/[1 + |\alpha h|^n]^m$$

best described all data where θ_s is the field-measured saturated soil-water content, and α, n, and m are constants. With the exception of two sandy soils, the functional relation $K(\theta)$ was described by

$$K = K_0 \exp[\beta(\theta - \theta_0)]$$

where K_0 and θ_0 are those values of K and θ, respectively, corresponding to steady-state infiltration conditions. Values of K_0 and θ were found to be log-normally and normally distributed, respectively. For a given field site, the standard deviation of θ_0 (or θ) was sufficiently large to render estimates of K to be uncertain by an order of magnitude. Sources of errors in the redistribution method are those associated with the placement and reading of the instrument, the calibration and functioning of the instrument and the spatial and temporal variability of the soil. Smoothing and interpolating procedures give rise to additional errors. The experiment reported here was not designed to examine error propagation but was undertaken to use the commonly reported redistribution method as a routine technique to measure soil-water properties on a wide range of soils. The results indicate that the redistribution method yields values of soil-water properties that have a large degree of uncertainty, and that this uncertainty is not necessarily related to the kind of soil being analysed. Regardless of the fundamental cause of this uncertainty (experimental and computational errors versus natural soil variability), the conclusion is that further developments of field technology depend upon stochastic rather than deterministic concepts.

1.   INTRODUCTION

More than one-half century has passed since Richards [1] suggested that the Darcy equation could be combined with the equation of mass conservation to describe the movement and retention of water within unsaturated soils. Portable, lightweight, dependable neutron moisture gauges have been available for 30 years [2]. Tensiometers are commonplace after being popularized by Richards and are now easily and accurately read with a portable transducer. Analytic and numeric solutions of the Richards' equation are virtually unlimited with today's computer technology. And yet, the application of these solutions to important, practical problems dealing with the transport of water through field soils remains undeveloped, despite the tremendous need to more effectively manage and conserve water for crop production and to protect and enhance the quality of water resources. There are at least three reasons why the development of a field technology has been slow. First, the value of the hydraulic conductivity is extremely sensitive to small changes in soil-water content, and it

is also affected by the concentration and composition of the soil
solution. Moreover, the soil-water characteristic at a given
location depends not only upon the composition of the soil solu-
tion but also upon whether the soil is wetting or drying. Second,
field soils are inherently temporally and spatially variable.
They vary vertically owing to the extent of profile development
and horizontally owing to their relative position upon the land-
scape and to their cultivation and other disturbances caused by
people and animals. Third, soil scientists have not taken advan-
tage of stochastic concepts and equations but have remained
steadfast with their propensity to continue to treat Richards'
equation in a strictly deterministic manner.

The purpose of this presentation is to summarize the results
of a cooperative effort to measure soil-water properties of
several agriculturally important soils and to interpret the
findings relative to present-day and future soil-water management
technology. The effort was part of a five-year Coordinated
Research Program of the International Atomic Energy Agency, the
Use of Radiation and Isotope Techniques in Studies of Soil-Water
Regimes, whereby soil physicists examined soil water properties of
one or two field sites in 11 different countries (Brazil, Belgium,
Cyprus, Chile, Israel, Japan, Madagascar, Nigeria, Senegal, Syria,
and Thailand).

2. THEORETICAL

Throughout this study it is assumed that Richards' equa-
tion describes the vertical redistribution of soil water in
profiles that have been ponded with water sufficiently to
establish initial, steady-state condition to a depth of 1 or 2
meters. Richards' equation is

$$\frac{\partial \theta}{\partial t} = \frac{\partial}{\partial z}\left[K \frac{\partial H}{\partial z}\right] \tag{1}$$

where θ is the soil-water content (cm^3/cm^3), H the hydraulic
head (cm), K the hydraulic conductivity (cm/day), z the ver-
tical coordinate (cm) measured vertically downward and t the
time (day). The hydraulic conductivity is assumed to be a
unique function of θ while H is assumed to be $(h - z)$ where h
is the soil-water pressure head (cm) that is uniquely related
to θ for monitomically decreasing values of θ. The soil-water
diffusivity is defined by

$$D = K \frac{dh}{d\theta} \tag{2}$$

which is also assumed to be a unique function of θ for decreasing values of θ.

Integrating equation (1) from $z = 0$ to soil depth L yields

$$\int_0^L \frac{\partial \theta}{\partial t} \, dz = K \left. \frac{\partial H}{\partial z} \right|_L \tag{3}$$

where the flux at $z = 0$ is assumed nil. Values of K for depth L are calculated from experimental observations of the remaining terms in the above equation using four different methods. Method 1 is the classical redistribution method where $\partial H/\partial z$ is estimated from tensiometers data $h(z,t)$, and the above integral is estimated from neutron moisture gauge data $\theta(z,t)$. Equation (3) rewritten for Method 1 becomes

$$L \frac{\partial \bar{\theta}}{\partial t} = K \left[\frac{\partial h}{\partial z} - 1 \right] \tag{4}$$

where $\bar{\theta}$ is the average soil-water content to depth L and $\partial h/\partial z$ is the gradient of the soil-water pressure head at depth L. Methods 2 and 3 are those of Libardi et al. [3] based upon the assumptions that K is defined as

$$K = K_o \exp \left[\beta(\theta - \theta_o) \right] \tag{5}$$

where K_o, β and θ_o are constants, and $\partial h/\partial z$ is zero. Method 2, the θ-method, yields

$$\theta_o - \theta = \frac{1}{\beta} \ell n t + \frac{1}{\beta} \ell n \, (\beta K_o/az) \tag{6}$$

where $\underline{a}$ is the slope of the linear regression $\bar{\theta} = a\theta + b$ at depth L. Method 3, the flux-method, yields

$$\ell n \left[L \left| \frac{\partial \bar{\theta}}{\partial t} \right| \right] = \beta(\theta_o - \theta) + \ell n \, K_o \tag{7}$$

With Methods 2 and 3 for a measured value of θ_o, values of K and β are found from regression using equations (6) and

(9), respectively. Method 4, the CGA-method reported in [3], based upon the assumption that

$$\bar{\theta} = At^B \tag{8}$$

where A and B are found by regression. Using equation (8) in (4) and assuming that $\partial h/\partial z$ is zero and that $(\theta_o - \theta)$ is small, leads to the formulae

$$K_o = -zA^{1/B} \ B \bar{\theta}_o^{1-1/B} \tag{9}$$

and

$$\beta = a(B-1)/B\bar{\theta}_o \tag{10}$$

Hence, the above four methods can be used to ascertain values of K_o and β whenever equation (5) holds. For sandy soils, as will be shown, K is better described by

$$K = K_o' \exp \{1 - \exp [\beta'(\theta - \theta_o)]\} \tag{11}$$

For such soils, the latter three methods would have to be modified.

The soil-water characteristic is a soil property that relates soil water content and the energy status of the soil water. In this effort, neutron moisture gauge readings and tensiometer readings taken at the same time and soil depth were used to measure the soil-water characteristic. Published literature is replete with empirically derived analytical expressions of $\theta(h)$ for a wide variety of soils and soil materials based upon both laboratory and field observations. We refer the reader to those of Mualem [4] and van Genuchten [5] and those cited by them. Two closed-form analytical expressions were selected for $\theta(h)$. The first is

$$(\theta - \theta_r)/(\theta_s - \theta_r) = [1 + |\alpha h|^n]^{-m} \tag{12}$$

where s and r indicate saturated and residual values of θ, respectively, and α, n and m are independent constants.

Simple, closed-form expressions of $K(\theta)$ can be derived when certain restrictions are imposed upon the values of n and m. For example, when m depends upon n such that $m = i - 1/n$ where i is an integer, $K(\theta)$ can be calculated analytically using equation (12). A second closed-form expression of $\theta(h)$ that was selected is

$$(\theta - \theta_r)/(\theta_s - \theta_r) = (h/h_b)^{\lambda} \quad h < h_b$$
$$= 1 \quad h > h_b \quad (13)$$

where h_b is the so-called "bubbling" soil-water pressure head. This expression has been attractive to some investigators owing to its simplicity and its use by Brooks and Corey [6] to derive an equally simple expression of $K(\theta)$, namely

$$K = K_s [(\theta - \theta_r)/(\theta_s - \theta_r)]^{3+2/\lambda} \quad (14)$$

The relative success of the above as well as other expressions of $\theta(h)$ and $K(\theta)$ has usually been judged upon limited numbers of field observations or upon data that do not adequately represent the full range of θ between oven-dry and water saturation. In this effort, the above expressions were examined in light of field-measurements associated with values of h greater than about -200 cm.

3.   EXPERIMENTAL

Within each field site of approximately 1 hectare, experimental plots (5 x 5 m) free of vegetation were established to measure the redistribution of soil water to a depth of 2 m following steady-state infiltration. Each plot was instrumented with tensiometers placed at 15- or 30-cm depth intervals and with neutron moisture gauge access tubes. The number of plots within each field site ranged from 1 to 8.

The procedure was to pond water on each plot until steady-state flow was established, as indicated by stable tensiometer readings. When infiltration was complete as indicated by the ponded water level receding to the soil surface, the plot was covered with plastic to prevent evaporation. Neutron moisture gauge data and tensiometer readings were taken frequently and eventually once every day during later stages of redistribution.

FIG.1.   Soil-water characteristic at the 75-cm depth of plot 1 from Belgium using Eqs (12) and (13).
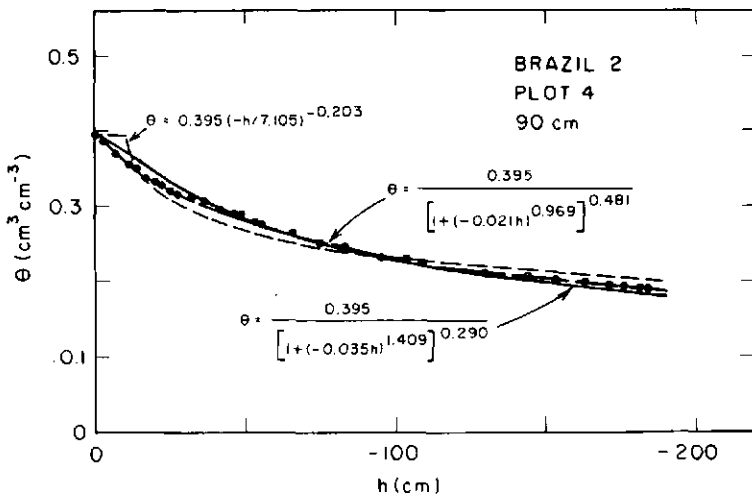
FIG.2.   Soil-water characteristic at the 90-cm depth of plot 4 from Brazil (site 2) using Eqs (12) and (13).
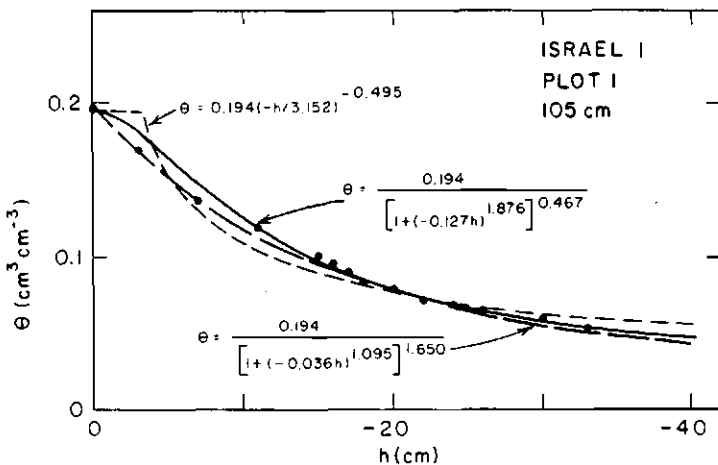
FIG.3. *Soil-water characteristic at the 105-cm depth of plot 1 from Israel using Eqs (12) and (13).*
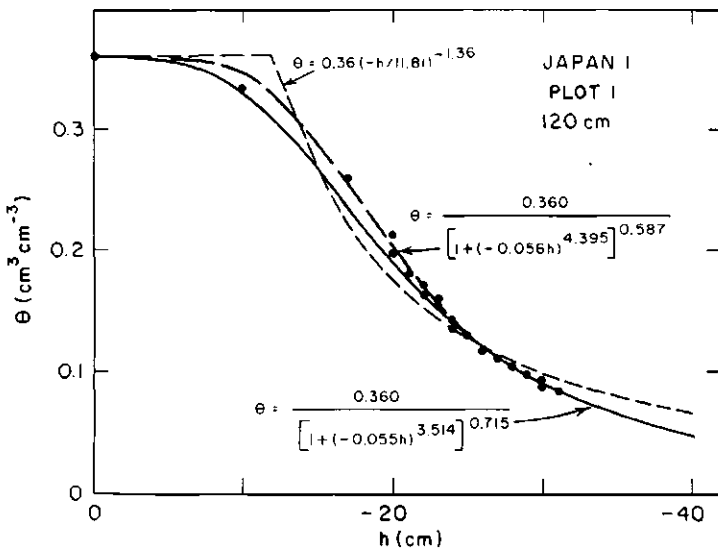
FIG.4. *Soil-water characteristic at the 120-cm depth of plot 1 from Japan using Eqs (12) and (13).*
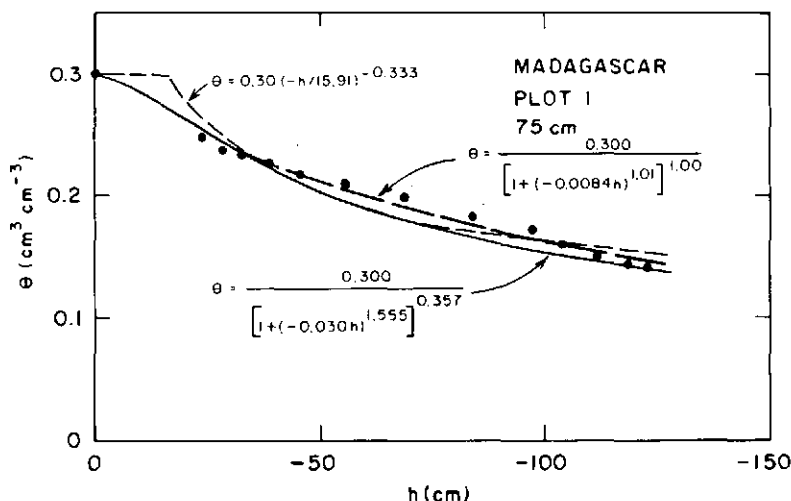
FIG.5. Soil-water characteristic at the 75-cm depth of plot 1 from Madagascar using Eqs (12) and (13).
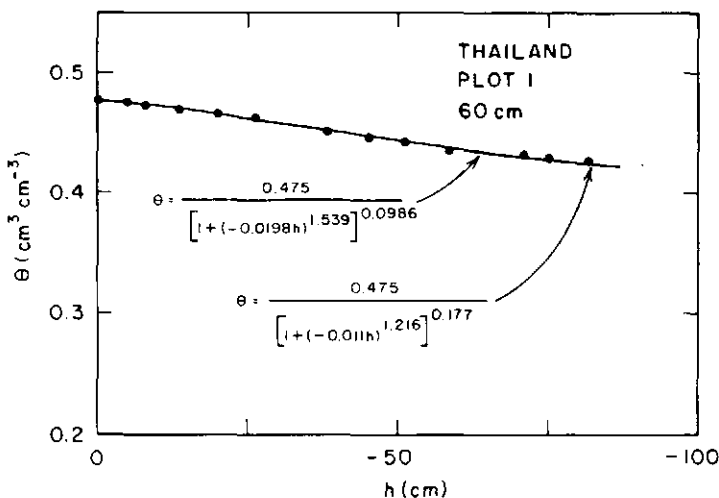
FIG.6. Soil-water characteristic at the 60-cm depth of plot 1 from Thailand using Eq. (12).

TABLE 1. FIELD-MEASURED VALUES OF THE AVERAGE SATURATED WATER CONTENT θ_s, AVERAGE SOIL-WATER CHARACTERISTIC PARAMETERS α AND n, AND THE AVERAGE SOIL-WATER PRESSURE HEAD $h(\theta_s - 0.01)$ FOR BRAZIL PLOTS 4 THROUGH 6

Depth	θ_s	s_{θ_s}	α	s_α	n	s_n	$h(\theta_s - 0.01)$	s_h	N
15	0.409	0.009	0.05684	0.00371	1.372	0.021	3.2	0.2	3
30	0.427	0.023	0.03373	0.00451	1.325	0.020	5.4	1.0	3
45	0.426	0.009	0.03624	0.00208	1.372	0.010	4.8	0.4	3
60	0.450	0.020	0.03210	0.00489	1.406	0.008	5.3	0.9	3
75	0.417	0.009	0.03811	0.00263	1.452	0.008	4.7	0.4	3
90	0.400	0.018	0.03769	0.00798	1.402	0.013	5.0	1.1	3
105	0.399	0.013	0.03565	0.00532	1.414	0.013	5.2	0.8	3
120	0.406	0.003	0.02863	0.00157	1.452	0.010	6.3	0.4	3
135	0.409	0.011	0.03637	0.00357	1.415	0.006	5.0	0.6	3
Mean	0.416	0.020	0.03726	0.00846	1.401	0.040	5.0	1.0	27

TABLE 2. FIELD-MEASURED VALUES OF THE AVERAGE SATURATED WATER CONTENT θ_s, AVERAGE SOIL-WATER CHARACTERISTIC PARAMETERS α AND n, AND THE AVERAGE SOIL-WATER PRESSURE HEAD $h(\theta_s - 0.01)$ FOR CYPRUS PLOTS 1 THROUGH 8

Depth	θ_s	s_{θ_s}	α	s_α	n	s_n	$h(\theta_s - 0.01)$	s_h	N
30	0.521	0.024	0.02138	0.00535	1.200	0.052	9.2	3.5	8
60	0.528	0.034	0.02808	0.00401	1.236	0.059	5.5	1.0	8
90	0.497	0.027	0.02387	0.00736	1.253	0.097	8.6	4.2	8
120	0.484	0.017	0.01724	0.00835	1.181	0.090	16.4	12.6	8
150	0.486	0.030	0.01496	0.00650	1.157	0.071	22.7	18.8	8
Mean	0.503	0.031	0.02111	0.00776	1.223	0.094	12.5	11.7	40

TABLE 3. FIELD-MEASURED VALUES OF THE AVERAGE SATURATED WATER CONTENT θ_s, AVERAGE SOIL-WATER CHARACTERISTIC PARAMETERS α AND n, AND THE AVERAGE SOIL-WATER PRESSURE HEAD $h(\theta_s -0.01)$ FOR MADAGASCAR PLOTS 1 THROUGH 4

Depth	θ_s	s_{θ_s}	α	s_α	n	s_n	$h(\theta_s -0.01)$	s_h	N
45	0.335	0.024	0.03793	0.00844	1.606	0.059	6.0	2.0	4
75	0.305	0.010	0.03827	0.01041	1.525	0.053	6.2	1.5	4
105	0.343	0.022	0.04513	0.01222	1.582	0.092	5.0	1.5	4
135	0.333	0.030	0.03936	0.00779	1.534	0.064	5.6	1.5	4
165	0.363	0.033	0.03734	0.01056	1.542	0.087	5.7	1.7	4
Mean	0.336	0.029	0.03960	0.00936	1.558	0.072	5.7	1.5	20
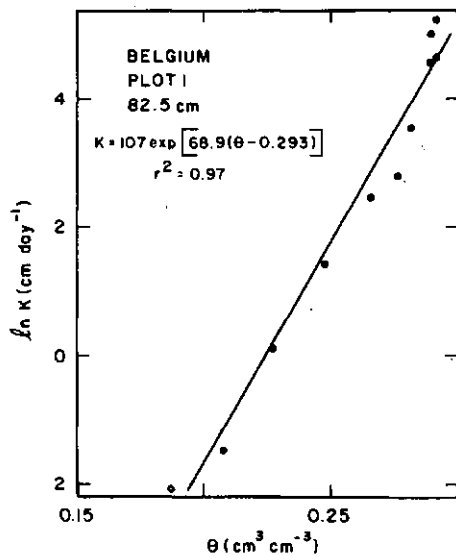
FIG.7. Hydraulic conductivity versus soil-water content for Method 1 at the 82.5-cm depth of plot 1 from Belgium using Eq. (5).
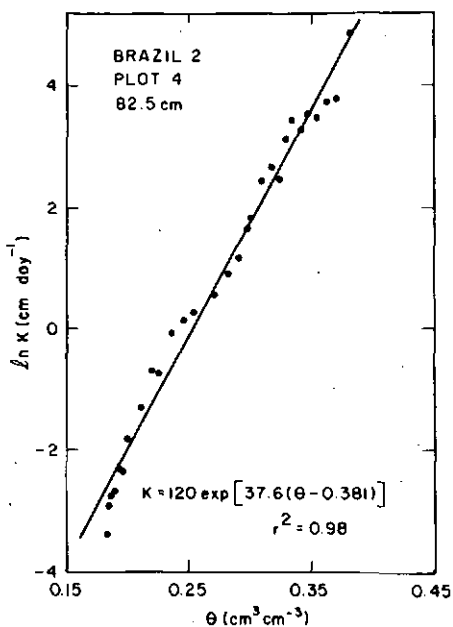
FIG.8. Hydraulic conductivity versus soil-water content for Method 1 at the 82.5-cm depth of plot 4 from Brazil (site 2) using Eq. (5).
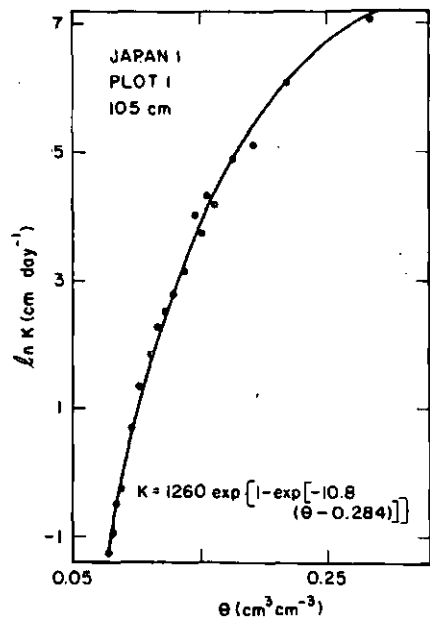
FIG.9.   Hydraulic conductivity versus soil-water content for Method 1 at the 105-cm depth
of plot 1 from Japan using Eq. (11).
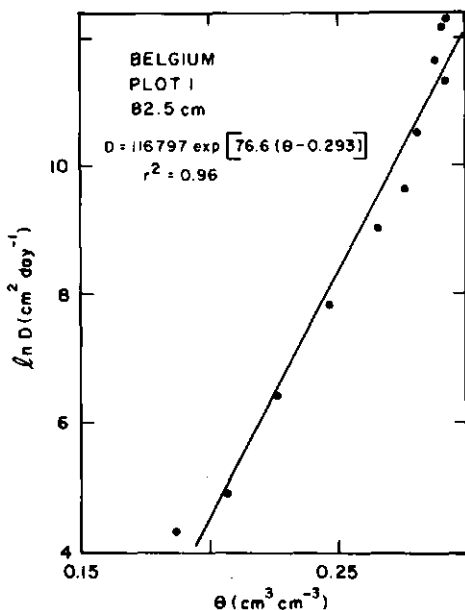
FIG.10.   Soil-water diffusivity versus soil-water content at the 82.5-cm depth of plot 1 from
Belgium using Eq. (2).
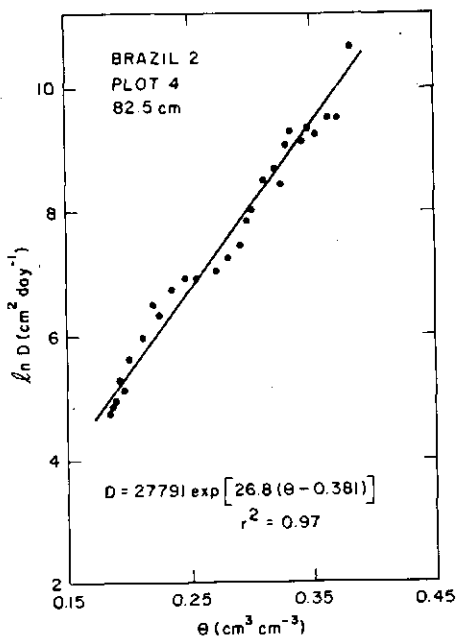
FIG.11. Soil-water diffusivity versus soil-water content at the 82.5-cm depth of plot 4 from Brazil (site 2) using Eq. (2).
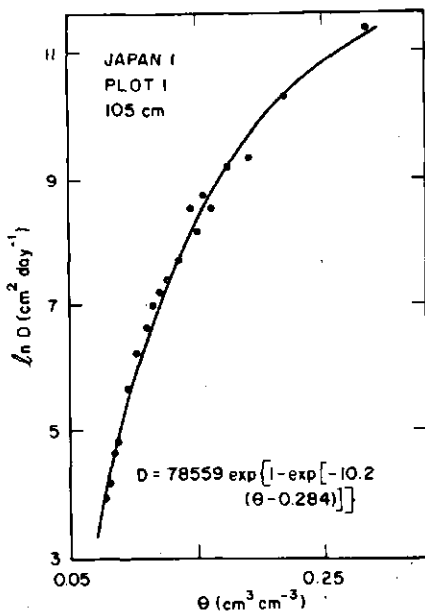
FIG.12. Soil-water diffusivity versus soil-water content at the 105-cm depth of plot 1 from Japan using Eq. (2).

TABLE 4. FIELD-MEASURED VALUES OF THE AVERAGE STEADY-STATE INFILTRATION WATER CONTENT θ_0, THE AVERAGE FINAL SOIL-WATER CONTENT θ_f, AVERAGE VALUES OF K_0 AND $\ell n K_0$, AVERAGE VALUES OF β, AVERAGE VALUES OF D_0 AND $\ell n D_0$ AND AVERAGE VALUES OF δ FOR CHILE PLOTS 1 THROUGH 5

Depth	θ_0	s_{θ_0}	θ_f	s_{θ_f}	K_0	s_{K_0}	$\ell n K_0$	$s_{\ell n K_0}$	β	s_β	D_0	s_{D_0}	$\ell n D_0$	$s_{\ell n D_0}$	δ	s_δ	N
22.5	0.454	0.006	0.422	0.007	0.21	0.14	-1.74	0.75	54.8	32.2	468	220	6.02	0.64	52.5	22.7	5
45	0.455	0.011	0.420	0.007	2.38	1.31	0.72	0.64	40.2	19.2	3705	1554	8.14	0.47	32.3	20.1	5
75	0.457	0.008	0.421	0.006	2.48	1.36	0.80	0.48	14.8	14.5	3264	1371	8.00	0.51	14.4	7.01	5
105	0.455	0.006	0.420	0.015	14.0	11.7	2.29	1.05	50.8	37.2	24612	35272	9.38	1.34	45.6	34.4	5
135	0.433	0.009	0.404	0.012	3.04	1.32	1.03	0.48	53.4	22.7	3661	1056	7.83	0.36	51.0	22.1	5
165	0.444	0.012	0.393	0.012	15.7	13.8	2.45	0.88	42.2	16.8	10831	7950	9.01	0.89	42.6	17.1	5
mean	0.452	0.010	0.413	0.015	6.30	9.21	0.92	1.55	42.7	26.8	7590	15862	8.06	1.30	39.7	24.1	30

TABLE 5. FIELD-MEASURED VALUES OF THE AVERAGE STEADY-STATE INFILTRATION WATER CONTENT θ_0, THE AVERAGE FINAL SOIL-WATER CONTENT θ_f, AVERAGE VALUES OF K_0 AND ℓnK_0, AVERAGE VALUES OF β, AVERAGE VALUES OF D_0 AND ℓnD_0 AND AVERAGE VALUES OF δ FOR THAILAND PLOTS 1 TROUGH 4

Depth	θ_0	s_{θ_0}	θ_f	s_{θ_f}	K_0	s_{K_0}	ℓnK_0	$s_{\ell nK_0}$	β	s_β	D_0	s_{D_0}	ℓnD_0	$s_{\ell nD_0}$	δ	s_δ	N
45	0.481	0.030	0.407	0.009	29.1	21.5	3.05	1.04	82.5	17.4	21239	13252	9.74	0.86	78.6	18.2	4
75	0.508	0.030	0.429	0.009	133	187	4.00	1.67	72.5	9.95	152575	244850	10.88	1.67	68.6	11.8	4
105	0.522	0.021	0.436	0.014	248	215	4.90	1.62	64.5	12.3	281863	284363	11.71	1.84	61.7	11.2	4
135	0.527	0.027	0.442	0.004	263	272	5.05	1.57	68.0	22.7	265636	214451	11.85	1.73	64.4	20.9	4
165	0.512	0.023	0.446	0.012	468	543	5.29	1.70	88.0	15.7	764857	1136694	12.28	2.05	84.5	13.5	4
mean	0.510	0.029	0.432	0.017	228	295	4.46	1.61	75.1	17.0	297234	547971	11.29	1.75	71.6	16.4	20

TABLE 6. FIELD-MEASURED VALUES OF THE AVERAGE STEADY-STATE INFILTRATION WATER CONTENT θ_0, AVERAGE HYDRAULIC CONDUCTIVITY K_0, AVERAGE ρ, AVERAGE SOIL-WATER DIFFUSIVITY D_0 AND AVERAGE δ FOR SEVERAL EXPERIMENTAL SITES

	θ_0	S_{θ_0}	K_0	S_{K_0}	β	S_β	D_0	S_{D_0}	δ	S_δ	N
Belgium	0.295	0.037	59.5	75.9	90.2	56.2	64105.	77559.	97.3	56.1	35
Brazil 1	0.355	0.026	8.57	17.1	110.	53.9	4952.	8155.	98.8	57.8	15
Brazil 2	0.387	0.012	253.	175.	44.6	7.78	64728.	41512.	33.7	7.01	24
Chile	0.452	0.010	6.30	9.21	42.7	26.8	7590.	15862.	39.7	24.1	30
Cyprus 1	0.459	0.016	21.2	46.9	70.5	50.0	9430.	14358.	58.0	47.9	32
Cyprus 2	0.403	0.015	27.1	41.6	67.8	46.6	11164.	14230.	62.2	44.7	12
Israel 1	0.178	0.019	90.7	44.8	43.3	6.12	8351.	4094.	29.5	5.67	25
Israel 2	0.167	0.037	96.0	89.1	84.3	29.0	18124.	12369.	74.7	29.3	24
Israel 3	0.310	0.015	20.3	27.7	92.6	25.0	33648.	34068.	89.1	27.1	14
Japan 1	0.268	0.018	653.[1/]	343.	11.4[1/]	1.22	46071.[1/]	22379.	10.6[1/]	1.22	45
Japan 2	0.210	0.012	144.[1/]	36.8	15.3[1/]	1.60	11686.[1/]	2950.	13.7[1/]	1.80	27
Madagascar	0.271	0.014	32.4	22.8	59.7	9.61	9539.	6109.	48.6	10.4	16
Nigeria	0.260	0.018	12.3	11.6	110.	54.0	9538.	7862.	111.	53.8	15
Senegal 1	0.193	0.024	55.3[1/]	13.5	14.5[1/]	2.17	13177.[1/]	2833.	12.5[1/]	1.69	5
Senegal 2	0.206	0.026	1.63	0.52	37.3	11.6	977.	673.	30.7	8.46	4
Syria	0.338	0.034	11.2	11.1	160.	122.	10702	8116	115.	96.3	10
Thailand	0.510	0.029	228.	295.	75.1	17.0	297234	547971	71.6	16.4	20

[1/] $K = K_0' \exp \{1 - \exp[\beta'(\theta - \theta_0)]\}$ and $D = D_0' \exp \{1 - \exp[\delta'(\theta - \theta_0)]\}$

Soil-water content θ and soil-water pressure head h data obtained through redistribution time t for all depths z were used to derive soil water properties by smoothing the temporal relationships and plotting a range of simultaneous θ and h values [$\theta(h)$] for each soil depth. The smoothed temporal data [$\theta(t)$, $h(t)$] were also used in the calculation of hydraulic conductivity $K(\theta)$ by the four methods described above. Values of the soil-water diffusivity $D(\theta)$ were obtained from the product $K(\theta)$ and $dh/d\theta$ derived from the field-measured $\theta(h)$ fitted to equation (12).

4. RESULTS AND DISCUSSION

Sources of error in this experiment are those associated with the placement and reading of neutron moisture gauges and tensio-

$$\theta = \frac{0.366}{\left[1+(-0.26h)^{1.689}\right]^{0.408}}$$
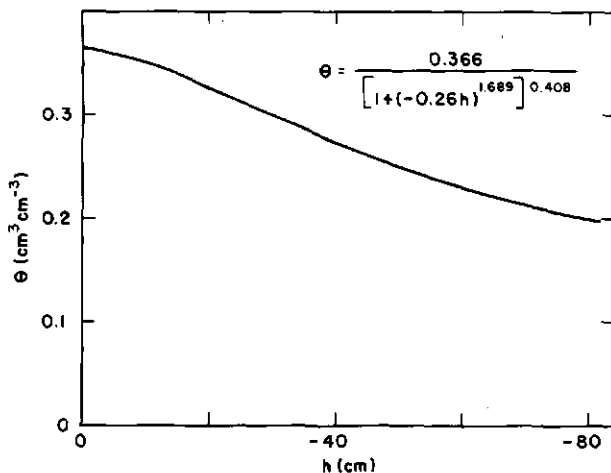
FIG.13.   World average soil-water characteristic.

meters, the calibration and functioning of these instruments and the spatial and temporal variability of the soil. Smoothing and interpolating procedures give rise to additional errors. Within each field site, a field-measured calibration curve for the neutron moisture gauge was established and is being reported elsewhere. The experiment reported here was not designed to examine error propagation (e.g., Vachaud et al. [6] or Flühler et al. [7]) but was undertaken to use the commonly reported redistribution method as a routine technique to measure soil-water properties on a wide range of soils. The following results represent examples of a more complete presentation to be published in a special publication of IAEA, Vienna.

Figures 1-6 are examples of the several hundred soil-water characteristics measured within numerous plots established in the 20 sites throughout the world. Several features are apparent. First, equation (13) fails to describe the shape of the curve for values of h near zero. Second, equation (12) utilizing independent values of α, n and m describe the data best. Third, equation (12) with the assumption that $m = 1 - 1/n$ describes the data better than equation (12). It should be noticed that the value of θ_r in equation (12) was set equal to zero. Although these data are restricted to the tensiometer range of h, our experience leads us to the conclusion that values of θ_r other than zero will not provide better descriptions of field-measured $\theta(h)$ distributions. And equation (12) holds an advantage over equation (13) inasmuch as the slope of equation (13) is unrealistically discontinuous at h_b.
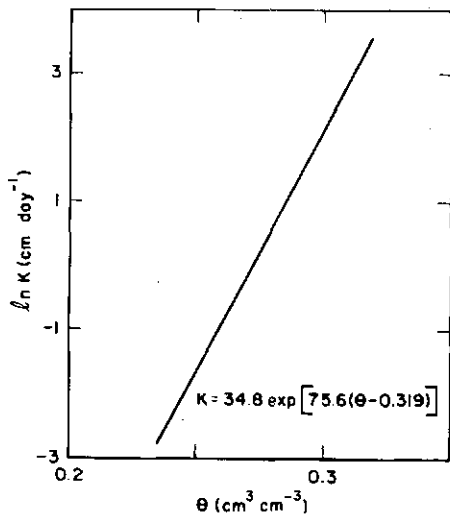
FIG.14.   World average hydraulic conductivity.
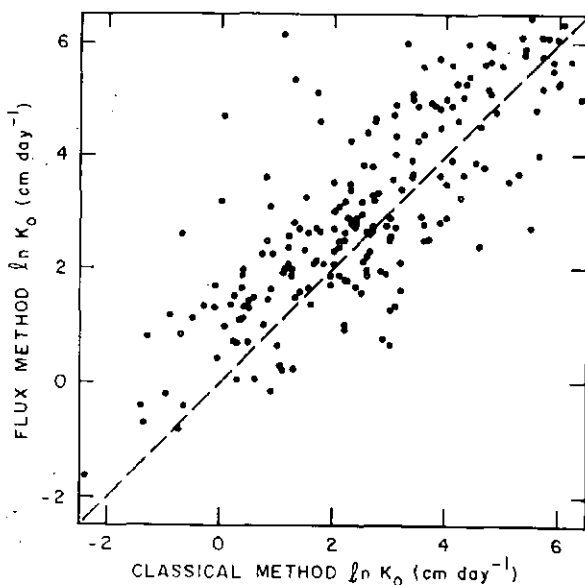
FIG.15.   Values of $\ln K_0$ calculated by Method 3 versus those measured by Method 1 for all depths and plots from all 20 countries except Japan.
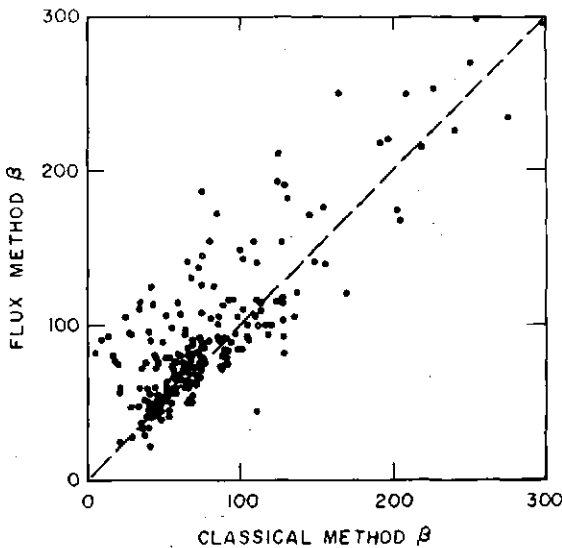
FIG.16.   Values of β calculated by Method 3 versus those measured by Method 1 for all depths and plots from all 20 countries except Japan.

Figures 1-6 indicate the general shapes of the soil-water characteristics. Tables 1-3 indicate the relative precision of describing the soil-water characteristic of a given soil depth within an experimental site of Brazil, Cyprus, and Madagascar using equation (12) where m is assumed equal to (1-1/n). For each site, the standard deviation of θ_s is about 0.02 cm^3/cm^3 or larger. It should also be noticed that the value of h corresponding to a decrease of θ equal to 0.01 cm^3/cm^3 less than θ_s is in the order of only -5 to -10 cm — a further indication that h_b of equation (13) does not exist in naturally occurring field soils. Further, the coefficient of variation of α and n are about 0.25 and 0.05, respectively.

Figures 7 and 8 indicate how well equation (5) describes K(θ) for the 82.5 cm depth of soils from Belgium and Brazil except for sandy soils as depicted in Fig. 9 for Japan. For the sandy Japanese soil, equation (11) was more appropriate. Although not presented here, it was found that equation (14) described the K(θ) data of all 20 soils reasonably well even though equation (13) was not the best fit of the soil-water characteristic data. Figures 10-12 provide soil water diffusivity data that correspond to the K(θ) data given in Figs. 7-9. It should be noticed that the diffusivity data are described by equations of the same form as equations (5) and (11). Tables 4 and 5 indicate the relative

precision of describing $K(\theta)$ and $D(\theta)$ by exponential equations for
a given soil depth within an experimental site of Chile and
Thailand. The standard deviation of θ and θ_f for the two
countries was about 0.01 and 0.03 cm^3/cm^3, respectively. Values
of K_o and D_o manifested large degrees of uncertainty. Table 6
provides values of the soil-water properties from each experi-
mental site averaged over the entire depth of each soil profile.
The coefficients of variation of θ_o range from about 0.02 to
0.15 stemming from standard deviation values that range from 0.01
to nearly 0.04 cm^3/cm^3. Coefficients of variation of K_o are
approximately 1 while those of β range from 0.1 to near unity.
Figures 13 and 14 show the average $\theta(h)$ and $K(\theta)$ for all 20 soils
averaged over all depths.

A comparison of the values of K_o and β obtained by Method 1
with those obtained by the other three methods based upon a unit
hydraulic gradient is illustrated in Figs. 15 and 16 for Method 3.
The data in both figures stem from all depths of almost all
experimental sites. As expected, there is a linear relation with
a large degree of uncertainty. At any one location the hydraulic
gradient may indeed be different than unity giving rise to values
of the soil-water parameters calculated from Method 3 that are
consistently too large (or too small) compared with those from the
classical method. The same results were obtained when comparisons
were made for Methods 2 and 4.

5.   CONCLUSIONS

From all of the above results, a few conclusions are apparent
regardless of the fact that the experimentation was never designed
to examine sources of error and error propagations. First,
equation (12) provided the best description of the soil-water
characteristic inasmuch as none of the field-measured data mani-
fested a well-defined "capillary fringe" or "bubbling" soil-water
pressure head. Owing to the limited range of h for which θ was
measured, it was not possible to ascertain if a potentially useful
functional relation between the parameters m and n exists. Second,
equations (5) and (14) both provided acceptable descriptions of
$K(\theta)$. Equation (5) provides some mathematical convenience owing
to its exponential form while equation (14) provides a description
of $K(\theta)$ when the hydraulic conductivity is not strictly exponen-
tially related to the soil water content. Both equations are
essentially two-parameter models if θ_o is omitted from equation
(5). Third, our analysis indicates that the values obtained for
the soil water parameters $\theta(h)$, $K(P)$ and $D(\theta)$ have a large degree
of uncertainty, and that this uncertainty, regardless of its
fundamental cause, renders solutions of deterministic soil-water
equations and related simulations ineffective in most field
investigations. And, even if soil heterogeneity was minimal, the

strong dependence of K upon θ drastically reduces the accuracy and precision of solutions of Richards' equation applied to field situations. The experimental error of measuring θ regardless of the method (neutron moisture gauge, gravimetric analysis, etc.) is of the order of 0.01 cm^3/cm^3. If this uncertainty is multiplied by the values of β given in Table 6, it yields a nearly two-fold uncertainty in the magnitude of the relative hydraulic conductivity (K/K_o) for a small value of β (e.g., 50), and a greater than five-fold uncertainty for a large value of β (e.g., 150). Thus, we conclude that further developments of field-technology of soil moisture regimes depend upon the explicit use of stochastic rather than strictly deterministic concepts. Several investigations of stochastic problems of water flow through soil have been presented over the past years. Most, but not all of them, have treated steady-state, saturated groundwater flow. Some examples are the efforts of Gutjahr et al. [8], Freeze [9], Delhomme [10], Dagan [11], and Smith and Freeze [12]. Some examples in unsaturated soils include those of Russo and Bresler [13,14], Warrick et al. [15,16], Peck et al. [17], Simmons et al. [18], and Andersson and Shapiro [19].

ACKNOWLEDGMENTS

REFERENCES

[1] RICHARDS, L. A., Phys. 1 (1931) 318.

[2] STONE, J. F., KIRKHAM, D., READ, A. A., Soil Sci. Soc. Proc. 19 (1955) 419.

[3] LIBARDI, P. L., REICHARDT, K., NIELSEN, D. R., Biggar, J. W., Soil Sci. Soc. Am. J. 44 (1980) 3.

[4] MUALEM, Y., Water Resour. Res. 12 (1976) 513.

[5] VAN GENUCHTEN, M. TH., Soil Sci. Soc. Am. J. 44 (1980) 892.

[6] HAVERKAMP, R., VAUCLIN, M., VACHAUD, G., Soil Sci. (in press).

[7] FLÜHLER, H., ARDAKANI, M. S., STOLZY, L. H., Soil Sci. Soc. Am. J. 40 (1976) 830.

[8] GUTJAHR, A. L., GELHAR, L. W., BAKR, A. A., MACMILLAN, J. R., Water Resour. Res. 14 (1978) 953.

[9] FREEZE, R. A., Water Resour. Res. 11 (1975) 725.

[10] DELHOMME, J. P., Water Resour. Res. 15 (1979) 269.

[11] DAGAN, G., Water Resour. Res. 17 (1981) 107.

[12] SMITH, L., FREEZE, R. A., Water Resour. Res. 15 (1979) 1543.

[13] RUSSO, D., BRESLER, E., Soil Sci. Soc. Am. J. 45 (1981) 682.

[14] RUSSO, D., BRESLER, E., Soil Sci. Soc. Am. J. 46 (1982) 20.

[15] WARRICK, A. W., MULLEN, G. J., NIELSEN, D. R., Water Resour. Res. 13 (1977) 355.

[16] WARRICK, A. W., MULLEN, G. J., NIELSEN, D. R., Soil Sci. Soc. Am. J. 41 (1977) 14.

[17] PECK, A. J., LUXMOORE, R. J., STOLZY, J. L., Water Resour. Res. 13 (1977) 348.

[18] SIMMONS, C. S., NIELSEN, D. R., BIGGAR, J. W., Hilgardia 47 (1979) 77.

[19] ANDERSSON, J., SHAPIRO, A. M., Water Resour. Res. 19 (1983) 121.

METHODOLOGIE D'ETUDE
DU BILAN HYDRIQUE D'UNE CULTURE
A L'ECHELLE DE LA PARCELLE[†]

G. VACHAUD*, Z. CHAABOUNI**,
S. EL AMANI**, M. VAUCLIN*

*Institut de mécanique de Grenoble,
Saint-Martin-d'Hères, France

** Centre de recherches du génie rural,
Tunis Ariana, Tunisie

Abstract–Résumé

METHODOLOGY FOR THE STUDY OF THE WATER BALANCE OF A CROP ON A PLOT
SCALE.
    Following an experiment carried out in a one-hectare plot at Mornag (Tunesia), the
authors propose a procedure for establishing sites for measuring the water balance and its
variation in time on the basis of the following criteria: (a) selection of a limited number of
sites (as few as possible) which would enable the mean value and variance of water consumption
to be evaluated in relation to the variability of the soil; (b) no autocorrelation between sites in
order to ensure the relevance of the assumption of conventional statistical analysis; (c) easy
access to the sites to avoid crop deterioration and thereby ensure the representativeness of the
measurements. The procedure comprises the following phases: (1) Surveying of the plot by
taking gravimetric samples with an augur from depths of 0–100 cm at different times over a
20 × 20 m grid and/or along transects in order to define the spatial variability of the textural
components and moisture content; (2) selection of representative sites: Statistical analysis
of the observations shows that moisture content and its variation in time follow a normal law
of distribution, and also indicate the high stability in time of the characteristic points of these
laws (mean value, mean value ± standard deviation); geostatistical analysis shows, apart from
a pronounced anisotropy, an autocorrelation distance of about 20 m for the moisture
measurements; (3) monitoring of the water balance: An analysis of neutron and tensiometric
data obtained at three measurement sites (which are representative of the mean and the mean
plus or minus standard deviation) makes it possible to estimate the different components of
the water balance for a rain-fed crop of wheat.

79

METHODOLOGIE D'ETUDE DU BILAN HYDRIQUE D'UNE CULTURE A L'ECHELLE
DE LA PARCELLE.

A partir d'une expérimentation conduite sur une parcelle de 1 ha située au Mornag
(Tunisie), on propose une méthodologie d'implantation des sites de mesure du bilan hydrique
et de son évolution dans le temps fondée sur les critères suivants: a) choix d'un nombre limité
(et le plus faible possible) de sites permettant d'estimer valeur moyenne et variance de la
consommation hydrique, en relation avec la variabilité du sol; b) absence d'autocorrélation entre
sites afin de garantir la pertinence des hypothèses de l'analyse statistique classique; c) accès
facile aux sites pour éviter la détérioration de la culture et assurer ainsi la représentativité de
la mesure. Cette méthodologie s'appuie sur les phases suivantes: 1) reconnaissance de la
parcelle par prélèvements gravimétriques à la tarière sur 0–100 cm à différents temps aux
noeuds d'une grille 20 X 20 m et/ou le long de transects afin de définir la variabilité spatiale
des composants texturaux et des humidités; 2) choix de sites représentatifs: l'analyse statistique
des observations montre que les humidités et leurs variations temporelles suivent une loi normale
de distribution et met également en évidence la grande stabilité dans le temps des points
caractéristiques de ces lois (valeur moyenne, valeur moyenne ± écart-type); l'analyse géo-
statistique met en évidence, outre une anisotropie marquée, une distance d'autocorrélation de 20 m
environ, pour les mesures d'humidité; 3) suivi du bilan hydrique: l'analyse des données
neutroniques et tensiométriques obtenues en 3 sites de mesures (représentatifs de la moyenne,
de la moyenne augmentée ou diminuée de l'écart-type) permet d'estimer les différentes
composantes du bilan hydrique d'une culture pluviale de blé.

INTRODUCTION

       Grâce notamment à l'aide efficace de la section "Ferti-
lité du sol, Irrigation et Production végétale" de la Division
Mixte "FAO/IAEA", les méthodes de mesure in-situ du bilan hydri-
que, ou de la consommation végétale, à partir de l'utilisation
simultanée d'humidimètre neutronique et de tensiomètres sont main-
tenant bien maitrisées au niveau d'une verticale [1], [2].

Il est toutefois clair que l'aptitude de ces méthodes à caracté-
riser le comportement moyen à l'échelle du champ se heurte à la
prise en compte de la variabilité naturelle du sol et de la cul-
ture [3], [4].

       Durant la dernière décennie, de nombreuses études expé-
rimentales ont porté sur l'étude systématique de cette variabi-
lité spatiale, et sur des tentatives méthodologiques permettant
de l'appréhender. Les résultats essentiels paraissent porter sur
les deux points suivants :

       - d'une part, on a pu définir une certaine cohérence dans
la nature des lois de distribution des variables spatiales, les
variables d'état de type statique (teneur en eau, porosité, indi-
ce textural, etc...) étant dans l'ensemble distribuées selon une

loi normale, alors que les propriétés de type dynamique (perméa-
bilité, flux, coefficient de dispersion) sont très souvent dis-
tribuées log-normalement [5], [6], [7];

        - d'autre part, la variabilité de ces observations doit
être analysée en fonction de la position des points de prélève-
ment dans l'espace pour prendre en compte la possibilité d'auto-
corrélation importante entre mesures, résultant d'une structure
spatiale des variables [8], [9], [10], [11].

        Toutes ces études reposent sur une expérimentation in-
tensive à l'échelle du champ, nécessitant notamment un grand
nombre de points de mesure à petites distances les uns des au-
tres. De ce fait, les méthodes utilisées se heurtent à deux
obstacles essentiels : la lourdeur de leur mise en oeuvre ne per-
met pas une réalisation en pratique dans le cadre d'un essai
agronomique, ni un suivi de l'évolution dans le temps des bilans.

        Cet article se propose de présenter une étude effectuée
à l'échelle d'une parcelle d'un hectare en vue d'obtenir, au coût
minimum, des valeurs représentatives des bilans hydriques à
l'échelle correspondante tenant compte à la fois des lois de dis-
tribution des variables, et des distances d'autocorrélation entre
mesures.

I - PRESENTATION DE L'EXPERIMENTATION

        Le site se situe à environ 20 km au Sud-Est de Tunis sur
la station hydrométéorologique DRES-ORSTOM de MORNAG. Il est amé-
nagé depuis 1981 en vue d'une expérimentation intensive devant
conduire à l'estimation des bilans hydriques à l'échelle d'une
parcelle sous plusieurs types de traitement, et à une étude dé-
taillée des processus de transferts de masse, de chaleur et de
quantité de mouvement à l'interface sol-atmosphère.

        Cette étude est relative à l'expérimentation effectuée
durant l'année 1982 afin d'obtenir des mesures moyennes signifi-
catives du bilan hydrique à l'échelle d'une parcelle de blé.

        La méthodologie développée s'appuie sur les critères
suivants :

        - choix d'un nombre limité de sites de mesure représen-
tatifs de toute la variabilité spatiale du champ,

        - absence d'autocorrélation entre les sites afin d'évi-
ter toute redondance d'information,

        - accès facile aux sites (surtout pour les mesures ef-
fectuées sous culture).
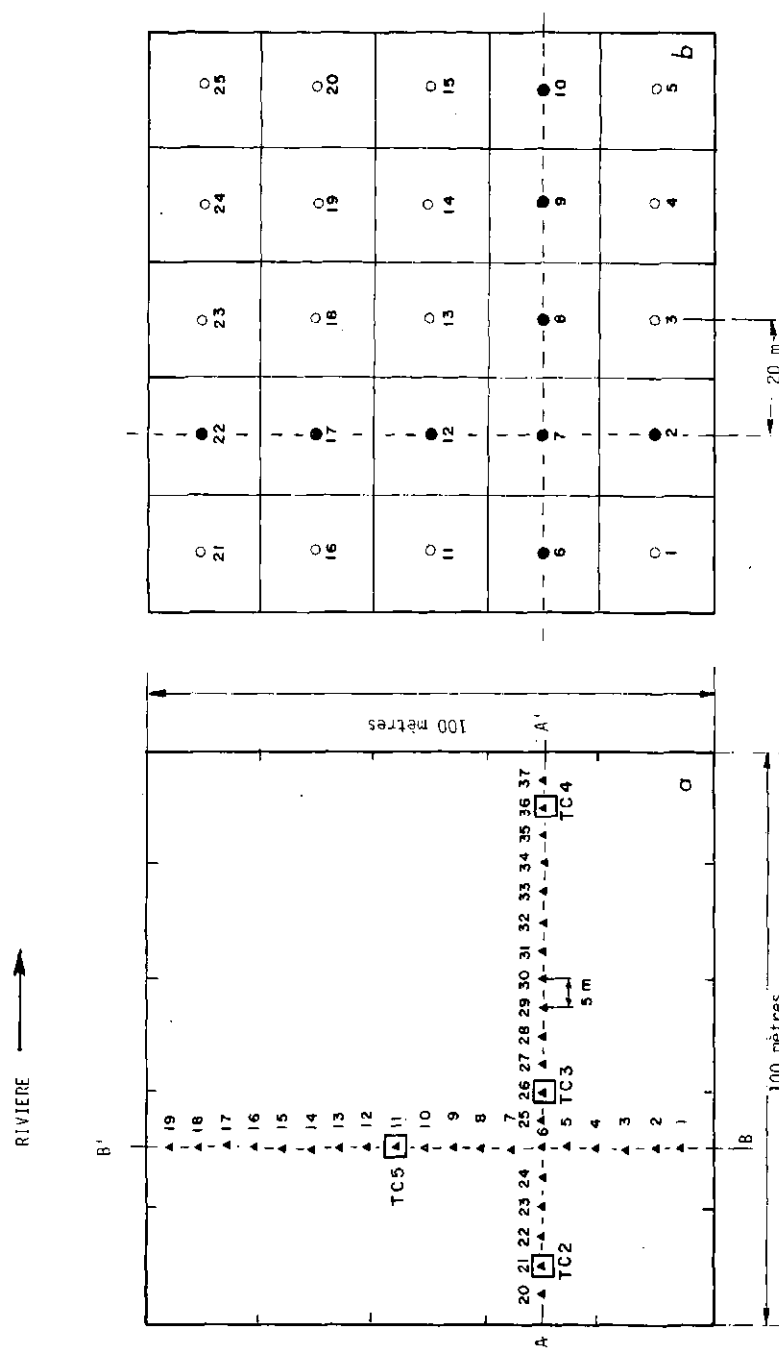
FIG.1.   Schéma des prospections gravimétriques effectuées:
— selon deux transects (1-a), nov. 1981;
— selon un maillage (20 × 20 m) en août 1981, février, avril et juin 1982.   Les points en noir (1-b) sont communs aux deux méthodes d'échantillonnage.

Description du site

La zone d'étude recouvre 18 000 m^2 [12] et se compose
de trois sous-parcelles :

- une parcelle (4000 m^2) laissée en jachère nue, sar-
clée depuis novembre 1981 ; une parcelle de gazon (Kikuyu) irri-
guée, de 4000 m^2 ; une parcelle (10 000 m^2) mise en culture de-
puis plusieurs années qui fait l'objet de cette étude.

Le sol est un dépôt alluvionnaire sur un ancien lit
fluvial. Il représente une assez grande hétérogénéité sur l'é-
paisseur étudiée dans le cadre de cette recherche (zone 0-2 m);
on rencontre globalement une stratification sur deux niveaux :

- une couche argilo-sableuse en surface dont l'épais-
seur varie de 40 à 100 cm,

- une couche plus sableuse en profondeur, avec parfois
présence de lentilles argileuses.

2 - RECHERCHE DE SITES REPRESENTATIFS SUR CULTURE

Compte tenu de la forte variabilité du sol à l'échelle
de la parcelle, la méthodologie utilisée repose sur l'hypothèse
qu'il existe une relation significative entre la quantité d'eau
présente dans le sol et la texture du sol aux mêmes endroits.
On peut penser que cette relation peut induire un certain déter-
minisme au niveau des variations spatiales de l'humidité, à un
instant donné, et surtout dans le temps ; le site le plus humide
devrait se trouver à l'endroit le plus argileux, et rester le
plus humide (relativement) lorsque le sol se dessèche.

Une campagne de mesure a eu lieu le 4 novembre 1981 afin
de définir à cette date :

1) - la loi de distribution caractérisant la variabilité
spatiale de l'humidité,

2) - la distance d'autocorrélation entre mesures d'humi-
dité,

3) - l'emplacement de sites de mesure représentatifs
(spatialement) et non corrélés, permettant des mesures compara-
tives non biaisées.

Cette campagne a porté sur deux transects orthogonaux,
l'un (AA') étant parallèle à la direction de l'oued situé à quel-
ques centaines de mètres du site (fig. 1a). Le long de ces tran-
sects, une distance d'échantillonnage de 5 m a été considérée avec,
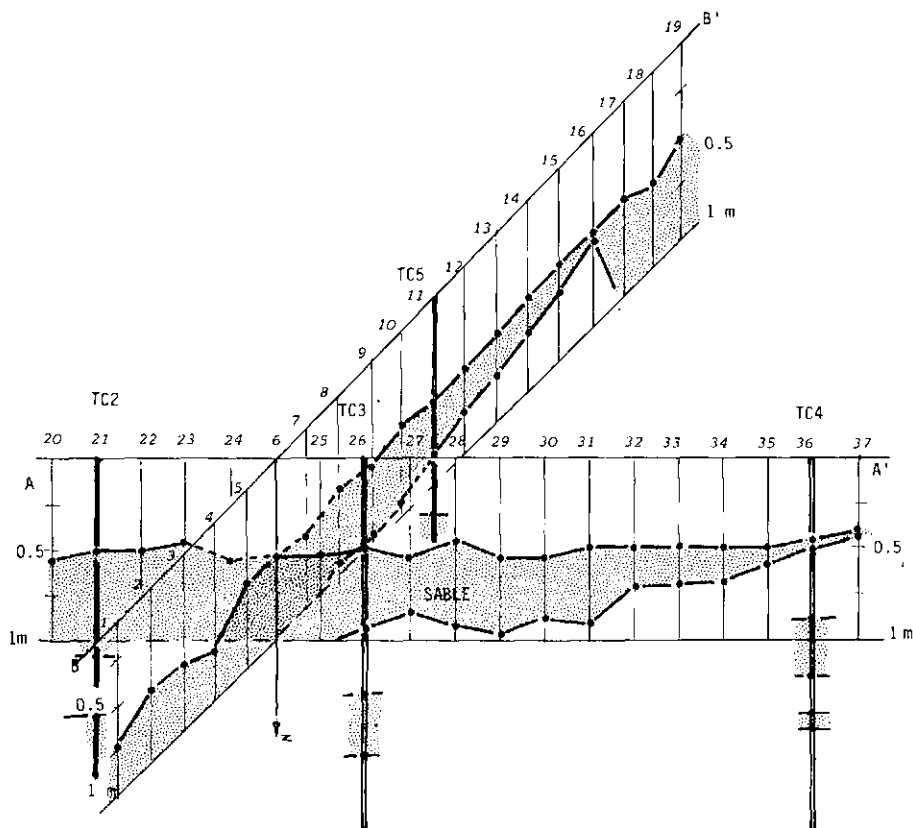
FIG.2. Représentation des profils pédologiques sur les deux transects.

en chaque point, prise d'échantillons à la tarière, par niveau
de 20 cm, jusqu'à la profondeur 100 cm. On dispose de 185 échan-
tillons prélevés le même jour.

On trouvera, fig. 2, une représentation simplifiée des
profils pédologiques selon ces deux directions, et, tableau I, les
valeurs moyennes et les variances des mesures d'humidité ponde-
rale, par tranche de 20 cm d'épaisseur, et pour les deux tran-
sects, pour le premier mètre de sol. Une étude systématique ef-
fectuée par ailleurs à l'aide d'un gamma densimètre de profon-
deur [12] ayant montré que la masse volumique sèche du sol,
toutes profondeurs confondues, ne varie que dans une gamme très
faible (1,63 $\pm$ 0,03 cm^3/cm^3), on a pu obtenir à partir de ces
valeurs les teneurs en eau volumique, et les stocks d'eau sur

TABLEAU I. VALEUR MOYENNE ET VARIANCE DES MESURES
D'HUMIDITE PONDERALE W ET DU STOCK HYDRIQUE LE 4/11/1982

		TRANSECT AA'		TRANSECT BB'	
		Moyenne	Variance	Moyenne	Variance
W g/g	0-20 cm	5,29	0,705	5,98	0,33
	20-40 cm	5,54	0,46	5,95	0,11
	40-60 cm	5,84	0,53	6,07	0,924
	60-80 cm	7,26	3,85	6,79	7,05
	80-100 cm	8,50	10,14	8,43	8,86
Stock 0-100 mm eau		102,5	211,9	103,9	321,3

le premier mètre. La valeur moyenne et la variance du stock sur
chaque transect sont également données tableau I. On trouvera
également, fig. 3, la fonction de distribution en probabilité
cumulée, de toutes les valeurs de stock obtenues en chacun des
37 sites de prélèvement. La loi de distribution peut être vala-
blement approchée par une loi normale.

La recherche d'éventuelles structures spatiales a été
effectuée en considérant dans les directions AA' et BB' la fonc-
tion d'autocorrélation r'(b) et le semi-variogramme γ(b) [10].
Les résultats reportés fig. 4 conduisent aux remarques suivan-
tes :

- il existe une assez grande anisotropie : la variance
du stock hydrique est plus importante dans la direction parallè-
le à la rivière (AA') que dans la direction perpendiculaire (BB'),

- il faut considérer une distance de 20 m environ entre
sites pour que les observations puissent être estimées indépen-
dantes les unes des autres,

- bien que le pas d'échantillonnage retenu (b = 5 m) ne
permette pas de préciser le comportement à l'origine de r'(b) et
γ(b), il semble que la variabilité à courte distance soit plus
importante le long de BB'.

VACHAUD et al.
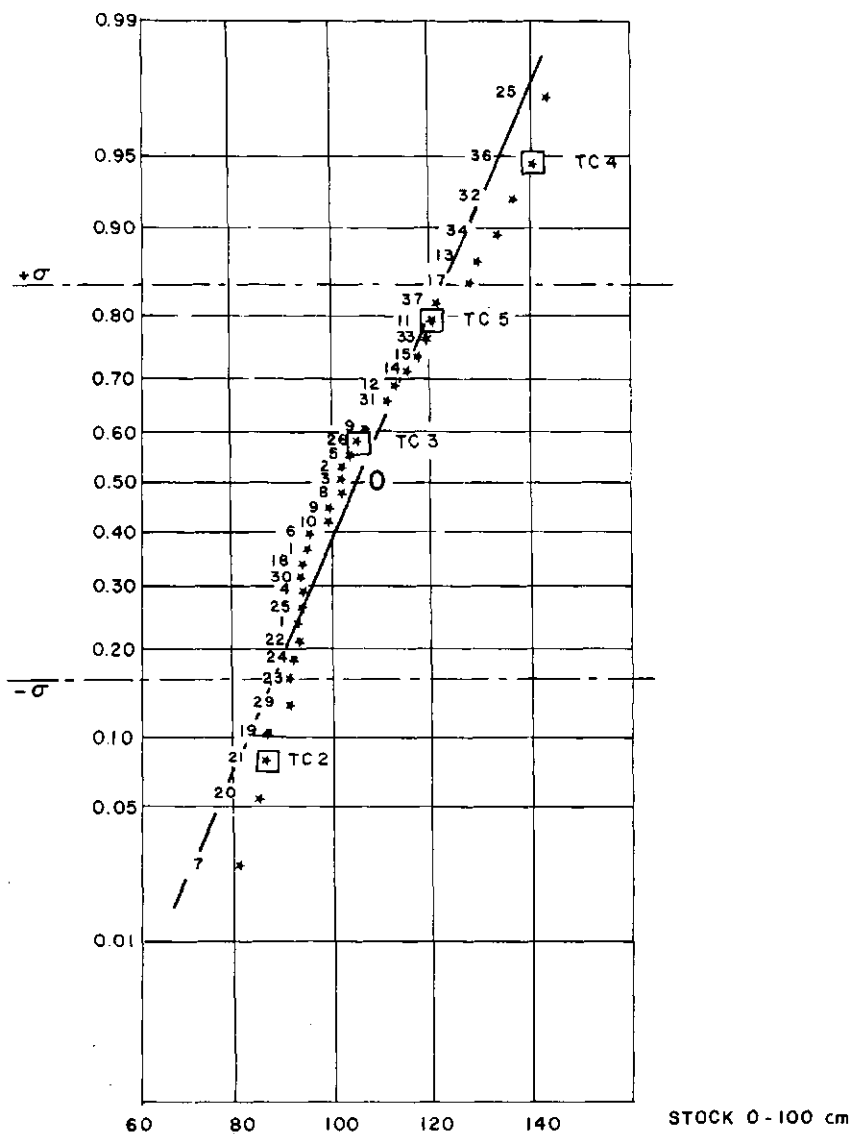
FIG.3. *Loi de distribution (probabilité cumulée) des mesures de stock sur le premier mètre selon les deux transects le 5/11/81.*
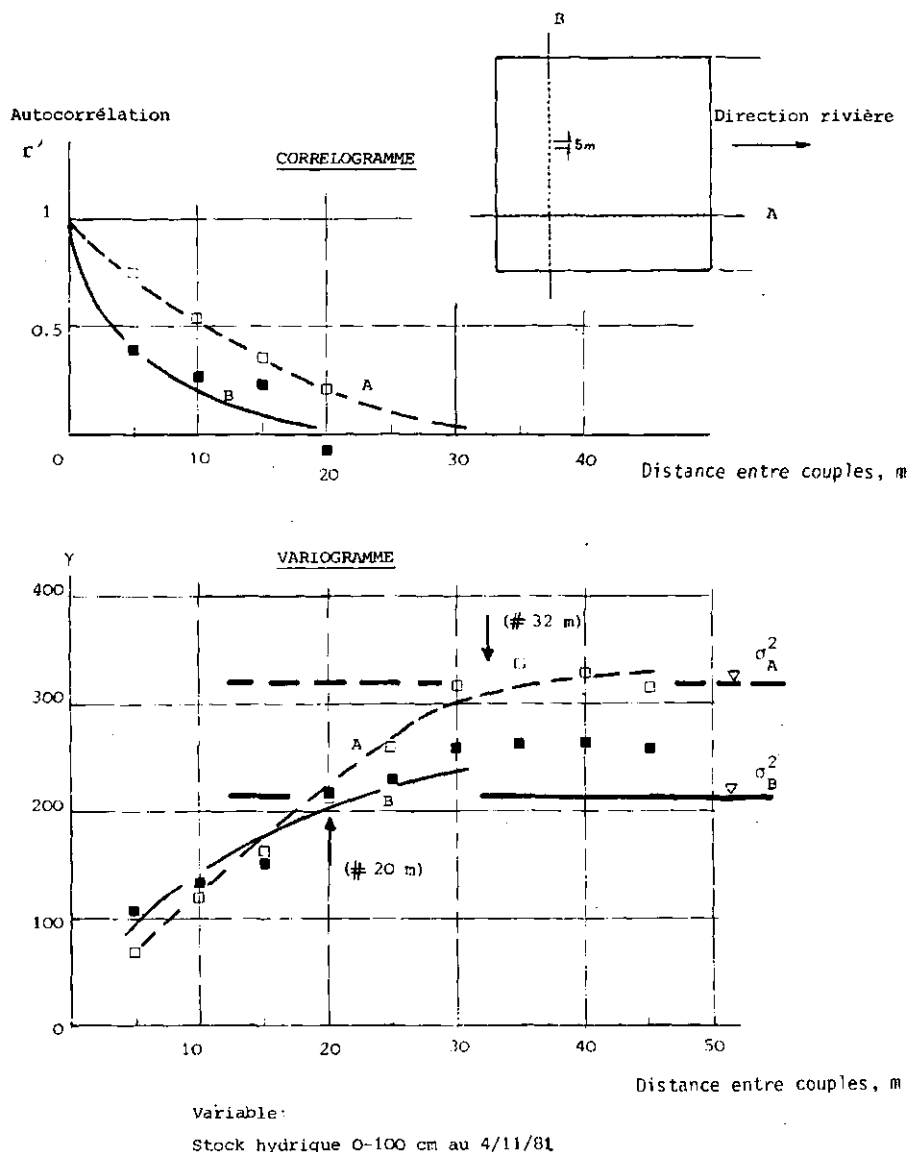
FIG.4.   *Corrélogrammes et variogrammes relatifs à l'estimation du stock sur le premier mètre*
le 4/11/81 selon les deux transects.

Le choix de l'implantation des sites de mesure a finale-
ment été effectué en respectant les critères suivants :

i) - distance entre sites supérieure à 20 m

ii) - accessibilité facile, mais sans effet de bord

iii) - représentativité de valeurs types de la loi de dis-
tribution (moyenne, écart-type ou extrema).

Ces trois critères se sont trouvés être satisfaits simul-
tanément par l'implantation des sites suivants :

- site TC4 sur le point 36 (extrême humide)
- site TC3 sur le point 26 (proche de la moyenne μ)
- site TC5 sur le point 11 (dans la bande $\mu + \sigma$)
- site TC2 sur le point 21 (voisin de $\mu - \sigma$)

Chacun de ces sites a été équipé d'un tube d'accès pour humidimè-
tre neutronique jusqu'à la cote 170 cm, et de tensiomètres aux
niveaux 30, 75, 90 et 130 cm. On y a procédé à l'étalonnage di-
rect d'une sonde type SOLO 20 selon la méthode exposée en [13].
Il est évidemment fondamental de vérifier qu'au cours du temps
chacun de ces sites conserve sa position dans la loi de distri-
bution. C'est ce que nous définirons comme un critère de
stabilité temporelle.

3 - VERIFICATION DE LA STABILITE TEMPORELLE DE LA REPRESENTA-TIVITE DES SITES

Pour valider cette hypothèse, une seconde méthode de
prospection a été utilisée. Elle repose sur l'analyse des me-
sures d'humidité obtenues par prélèvements à la tarière à dif-
férents stades du cycle végétatif, sur une maille régulière cou-
vrant toute la parcelle.

On trouvera, fig. 1b, le schéma de prospection. Les
prélèvements ont été effectués au milieu de chaque maille élé-
mentaire de dimension 20 x 20 m. On dispose de 25 sites de pré-
lèvements.

Les mesures ont eu lieu :

- le 20 août 1981, représentant l'état de sécheresse ex-
trême avant semis;

- le 10 février 1982, après une période de pluie intense
(186 mm en un mois);

- le 27 avril 1982, en pleine épiaison;

- le 3 juin 1982, juste avant la récolte.

TABLEAU II. COEFFICIENT DE
SPEARMAN ENTRE COUPLES DE
MESURES DE STOCK A DIFFERENTES
DATES

Dates de corrélation	RHO
Août 1981-Juin 1982	0,660
Août 1982-Février 1982	0,6357
Février 1982-Juin 1982	0,781

On dispose chaque fois de 25 séries de mesure, avec en chaque point prélèvement chaque 20 cm jusqu'à la profondeur z = 140 cm en août 1981 et février 1982, puis 100 cm par la suite.

La recherche de la stabilité s'appuie essentiellement sur une étude de corrélation de rang entre couples de mesures. Les valeurs des coefficients de Spearman sont données tableau II. Globalement, la probabilité est grande pour qu'un site reste au même rang pour n'importe quelle combinaison.

Dans le but d'obtenir enfin sur toute la période août 1981 à juin 1982 des séries homogènes, incluant les mesures effectuées en novembre sur les 2 transects, on a recherché la représentativité d'un échantillon limite comportant seulement les 9 points communs aux deux méthodes (grille et transect, points noirs, fig. 1b) en comparant les résultats obtenus par cet échantillonnage réduit avec : soit les valeurs résultant des 24 mesures "grilles" en août 1981, février, avril et juin 1982, soit les valeurs résultant des 37 mesures "transects" en novembre 1981.

Les résultats correspondants sont reportés tableau III. Les tests de Fisher (F) et de Student (t) montrent que variances et valeurs moyennes obtenues par les deux modes d'échantillonnage (réduit et complet) ne sont pas statistiquement différentes au seuil α = 0,05.

Il est remarquable de voir que toute la variabilité du sol est prise en compte par ces 9 points sur deux directions orthogonales, sans pertes significatives d'information avec les autres méthodes. Il est clair que, pour des contrôles de routine, cet échantillonnage réduit pourrait être utilisé.

TABLEAU III. COMPARAISON ENTRE ESTIMATIONS MOYENNES DU
STOCK SUR 0–1 m EN FONCTION DE L'ECHANTILLON

DATE	ECHANTILLON REDUIT			ECHANTILLON COMPLET			TESTS	
	N	Moyenne	σ^2	N	Moyenne	σ^2	F	t
AOUT 81	9	95,45	513,22	24	96,30	385,52	1,435	.110
NOV. 81	9	107,32	385,23	37	105,36	278,20	1,515	.298
FEV. 82	9	236,76	1152,89	24	237,30	810,85	1,532	.044
AVR. 82	9	170,50	502,73	24	171,10	526,10	1,030	.065
JUIN 82	9	131,60	524,80	24	129,25	438,72	1,289	.271
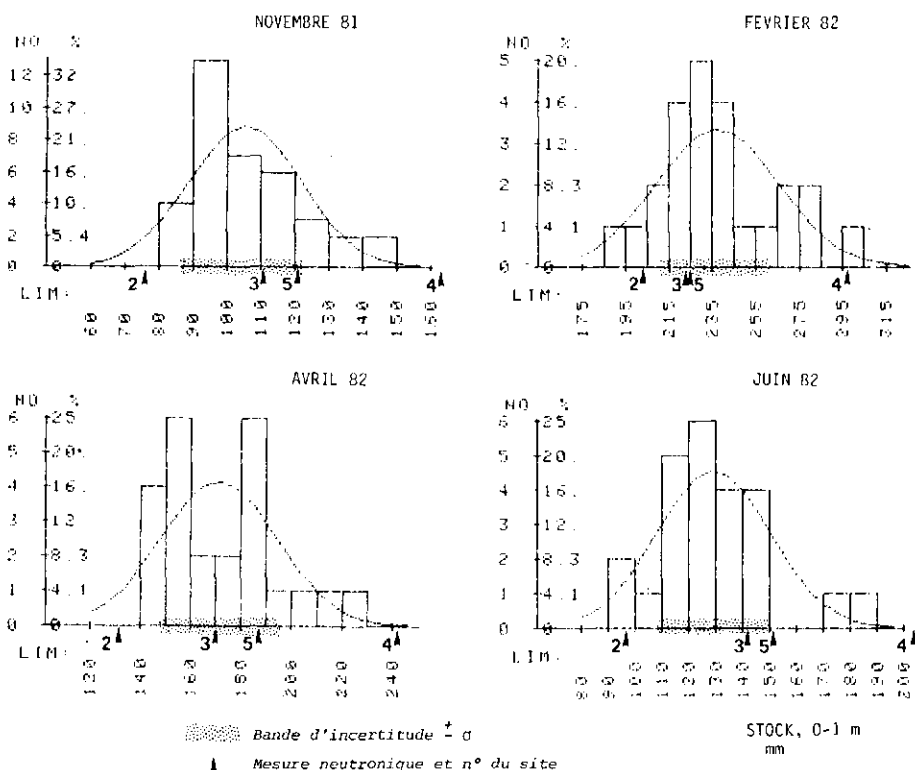
FIG.5.　Histogrammes des fréquences relatives de mesures de stock (0–100) obtenues par
gravimétrie en novembre, février et juin, et comparaison avec les mesures à l'humidimètre
neutronique.

TABLEAU IV. ECART QUADRATIQUE MOYEN ANNUEL
ENTRE MESURES ET VALEUR MOYENNE (μ) OU
MOYENNE A UN ECART-TYPE ($\mu \pm \sigma$) DU STOCK A CHAQUE
DATE DE PRELEVEMENT

	TC2	TC3	TC4	TC5
$\overline{D}_j(\mu)$	1172	101	455	294
$\overline{D}_j(\mu+\sigma)$	3312	645	2089	449
$\overline{D}_j(\mu-\sigma)$	157	582	8032	1165

4 – REPRESENTATIVITE TEMPORELLE DES SITES DE MESURES NEUTRONIQUES

Deux approches ont été utilisées pour juger de la vali-
dité du choix des emplacements des sites de mesure tout au long
du cycle de culture. D'abord une méthode subjective fondée sur
la comparaison des mesures de stock obtenues sur chacun des si-
tes d'accès par rapport aux histogrammes. On trouvera ainsi,
fig. 5, les histogrammes des mesures de stock à la tarière sur
le premier mètre obtenus en novembre 1981 (transects), février
et juin 1982 (ainsi que l'approximation par une loi normale).
On a situé à chaque date les mesures obtenues par humidimétrie
neutronique sur chacun des tubes d'accès TC2, TC3, TC4 et TC5.
On notera les résultats suivants :

        – une grande stabilité d'ordre. Par stock croissant,
on a toujours l'ordre TC2 < TC3 < TC5 < TC4 qui correspond bien
au choix initial;

        – les deux sites TC2 et TC4 restent toujours voisins
des extrêmes, les sites TC3 et TC5 voisins de la moyenne.

        Afin de préciser davantage la représentativité des si-
tes de mesures neutroniques, on a ensuite effectué un test sta-
tistique systématique en vue de caractériser l'écart quadratique
moyen entre les valeurs de stock hydrique estimées par l'humidi-
mètre neutronique $S_{Ni,j}$ en 4 points (TC2, TC3, TC4, TC5) et à
différents temps et des valeurs types obtenues gravimétriquement
X_i aux mêmes temps :

$$D_j(X) = \frac{1}{n} \sum_{i=1}^{n} (X_i - S_{Ni,j})^2 \qquad j = [1,4]$$
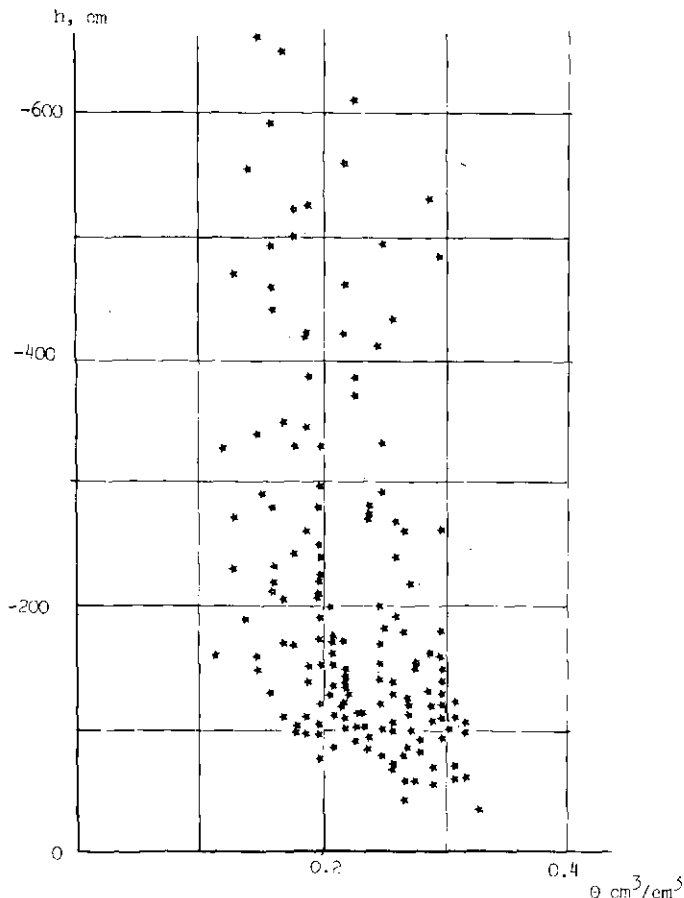
FIG.6. Relation h(θ) tous points de mesure confondus.

On donne à X successivement la valeur moyenne μ, les
valeurs μ+σ et μ-σ des stocks hydriques obtenues par prélèvements
gravimétriques. n est le nombre de répétitions de l'échantillon-
nage à la tarière (n=4).

A l'aide de ce critère, on a recherché systématiquement
quels étaient les sites neutroniques représentatifs de ces va-
leurs. Les résultats sont reportés tableau IV. Il apparaît que
le site TC3 représente bien la valeur moyenne du stock hydrique
sur 0-100 cm ; les tubes TC5 et TC2 représentant μ+σ et μ-σ res-
pectivement. On notera cependant que les résidus sont assez éle-
vés (10 mm pour TC3, 22 mm pour TC5, 12 mm pour TC2) en raison
du faible nombre de répétitions de l'échantillonnage gravimétri-
que [4]. Afin d'augmenter la précision, on a décidé, pour le

TABLEAU V. ESTIMATION DE L'ETR SUR CULTURE DE BLE POUR L'ANNEE 1982

Date	Pluie	TC2		TC3		TC5		ETR par période Moyenne σ		Taux journalier Moyen σ	
		ΔS	ETR	ΔS	ETR	ΔS	ETR				
12/11/81	*mm*	*mm*		*mm*		*mm*		*mm*		*mm/j*	
	44,5	17,2	27,3	16,8	27,6	26,8	17,7	20,9 ± 4,8		0,63 ± 0,14	
15/12/81											
	10,4	-10,4	20,8	- 8,1	18,5	-11,10	21,5	20,2 ± —		0,72 ± —	
12/01/82											
	136,3	140,9	)	100,2	36,3	63,5	72,8	) 46,6 ± 28,9		2,22 ± 1,38	
22/01/82			) 17,0					)			
	41,4	19,8	)	29,7	11,7	39,4	2,0	)			
2/02/82								—		—	
	8,2	-27,0	35,2	-27,8	36,0	-18,5	26,7	32,6 ± 4,2		2,32 ± 0,3	
16/02/82											
	35,2	+ 6,0	29,2	+10,9	24,3	+14,6	20,6	24,7 ± 4,3		1,76 ± 0,3	
2/03/82											
	50,4	-25,8	76,3	-22,3	72,7	- 9,3	59,7	69,6 ± 8,3		2,58 ± 0,31	
29/03/82											
	3,5	-56,1	59,6	-50,5	54,0	-35,6	39,1	50,9 ± 10,2		3,40 ± 0,68	
13/04/82											
	44,4	+ 8,60	35,8	+16,1	28,3	+12,0	32,4	32,1 ± —		2,3 ± -	
27/04/82											
	29,4	-22,1	51,5	-12,4	41,8	- 9,1	38,5	43,9 ± 6,5		3,13 ± 0,46	
11/05/82											
	-	-24,03	24,03	-24,02	24,02	-28,64	28,64	25,56± 2,3		1,82 ± 0,16	
25/05/82											
	-	- 6,8	6,8	-10,5	10,5	-15,65	15,65	10,98± 4,42		0,52 ± 0,21	
15/06/82											
Σ	403,7		383,54		385,60		374,8	378,04			

Note : entre deux mesures, ΔS est toujours défini par $(S_{t=k+1} - S_{t=k})$, et puis entre 0 et 175 cm. Une valeur négative indique une perte de stock sur le profil.

calcul des bilans hydriques moyens à l'échelle de la parcelle, d'effectuer la moyenne des valeurs obtenues sur les sites TC2, TC3 et TC5.

5 - ANALYSE DU BILAN HYDRIQUE

Pour la période étudiée (fin novembre 1981 à juin 1982, soit toute le cycle végétatif), on dispose de mesures hebdomadaires de profils neutroniques et tensiométriques sur chacun des sites. L'ensemble de tous les points de mesures obtenus est reporté fig. 6, sous la forme d'un graphe h(θ). Le grand domaine

de variabilité de cette relation à l'échelle de la·parcelle
-qui a fait par ailleurs l'étude d'une mise en facteur d'échel-
le [5]- montre qu'il serait hasardeux de vouloir estimer le
bilan hydrique par application de la loi de Darcy, avec estima-
tion de la conductivité hydraulique K(θ) en un seul site. L'ana-
lyse du bilan se fondera donc essentiellement sur l'évolution
du stock hydrique.

5.1 - _Evolution du stock hydrique_

        La pluviométrie relative à la période considérée est
donnée tableau V. La culture dispose d'un apport d'eau total
de 403,7 mm, avec une concentration exceptionnelle de 177,7 mm
durant la seconde quinzaine de janvier 1982.

        Globalement, on peut diviser la période de mesure en
3 phases :

        - du semis au 9 février 1982, date correspondant à la
recharge maximum du sol par les pluies d'hiver,

        - du 16 février au 13 avril 1982 (période de faible
pluviométrie et d'extraction racinaire importante),

        - du 27 avril à la récolte (après une forte période de
pluie fin avril).

        Les résultats globaux afférents à ces périodes sont
également présentés fig. 7 sous la forme suivante : évolution
du stock total (0-175 cm), du stock au-dessous de 105 cm et de
la teneur en eau à la cote 170 cm en fonction du temps. Cette
présentation amène aux conclusions suivantes :

        1) - L'essentiel des variations de stock hydrique sur
l'épaisseur de mesure (0-175 cm) a lieu dans le premier mètre,
ce qui justifie l'analyse précédente.

        2) - Il existe de très grandes différences entre les
valeurs absolues du stock hydrique de tube à tube (près de
100 mm d'écart entre les extrêmes, ce qui donne tout son poids
à l'étude spatiale) mais l'allure des courbes, et les variations
relatives (en fonction du temps) sont très voisines.

        3) - Les pluies importantes de fin janvier n'induisent
un écoulement (drainage) au-delà de la cote 160 cm que pour TC4
et à partir du 26 janvier. Sur ce site, les profils hydriques
montrent un comportement très différent de l'ensemble des au-
tres tubes, et la lame d'eau drainée peut être estimée à 25 mm.
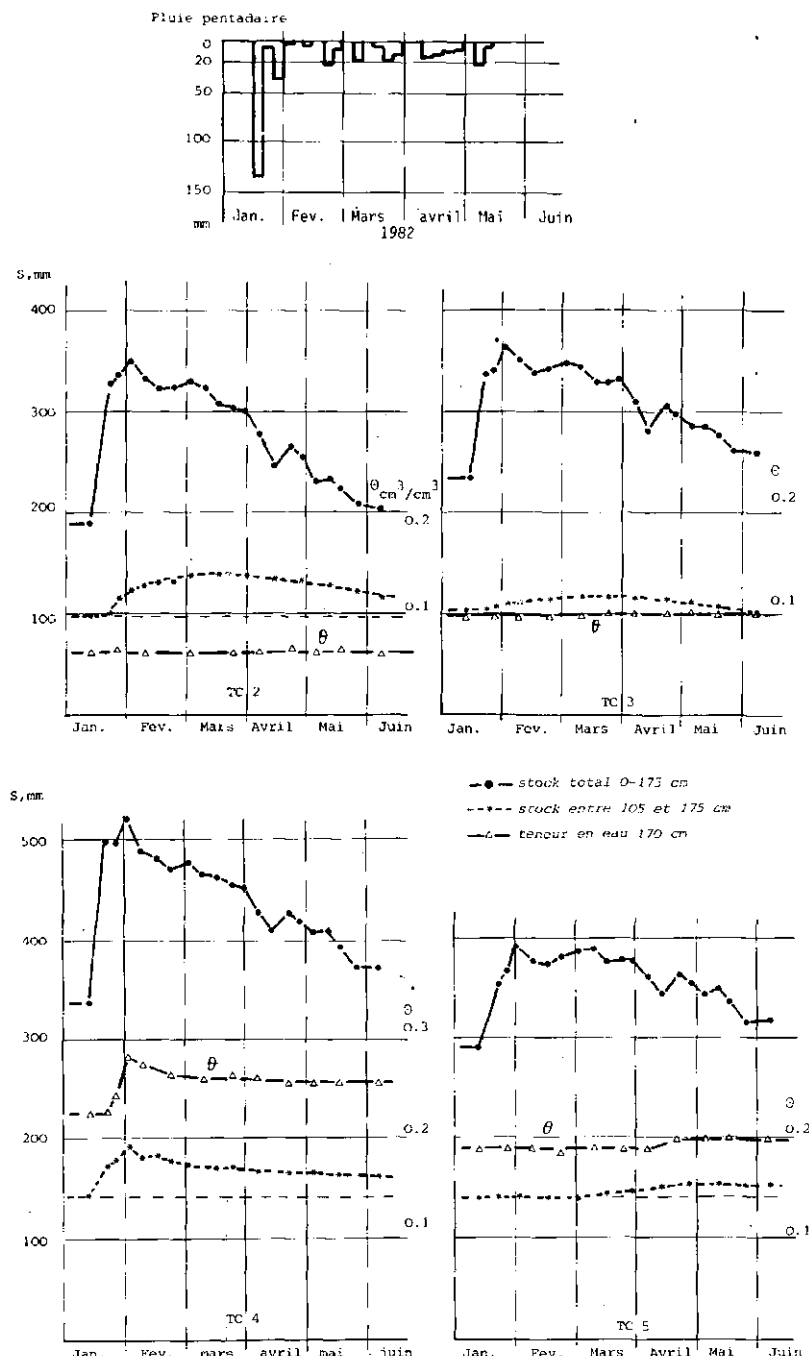
FIG.7. *Variation totale de stock (0–175 cm), variation de stock en-dessous de 1 m, et variation de teneur en eau à 170 cm pour chaque tube.*

VACHAUD et al.

Probabilité cumulée, %
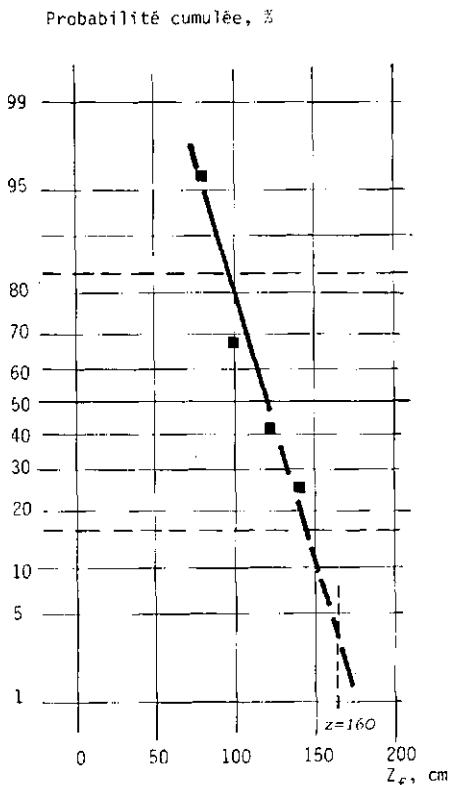
FIG.8. *Loi de distribution (probabilité cumulée) de la profondeur de pénétration de la pluie de janvier obtenue à partir de 24 mesures gravimétriques sur la grille.*

Ce dernier résultat montre qu'il n'est pas possible, a priori, de supposer que le drainage soit nul sur toute la parcelle. Une estimation de cette grandeur s'impose.

La comparaison entre les 24 profils gravimétriques obtenus en août 1981 et février 1982 permet d'avoir une estimation de la profondeur moyenne de pénétration de la pluie de janvier en chacun des sites. Les profils gravimétriques ayant été mesurés jusqu'à la cote 140 cm, on a déterminé la loi de distribution (probabilité cumulée) de pénétration du front d'humidité, en considérant des classes de profondeur 20 cm. La courbe correspondante est donnée fig. 8. La pluie pénètre partout jusqu'à 80 cm au moins. La probabilité de dépasser 120 cm est de 50 % ; sur 25 % seulement de la surface, le front dépasse la cote 140 cm. L'extrapolation de la courbe montre que l'on ne peut

craindre une humidification au-delà de 160 cm (donc une possi-
bilité de drainage) que pour environ 5 % de la surface. Ce ré-
sultat induit à une pondération de l'estimation du drainage sur
TC4 pour la ramener, au niveau de la surface totale de la par-
celle, à une grandeur tout à fait négligeable devant les erreurs
de mesure de stock puisqu'elle correspondrait à un drainage
moyen d'environ 1,25 mm (5 % de 25 mm).

5.2 - *Bilan hydrique. Consommation du blé.*

Compte-tenu de l'analyse précédente, le bilan hydrique
moyen sur les tubes TC2, TC3 et TC5 peut se résumer à :

$$ETR = P - \Delta S$$

où ΔS est la variation de stock hydrique durant la période de
mesure entre 0 et 175 cm (zone de mesure neutronique). P est la
pluviométrie pendant la même période. ETR est l'évapotranspira-
tion réelle, le ruissellement étant négligé.

On trouvera tableau V les résultats des calculs du bi-
lan, obtenus à partir des valeurs de stock par période de 2 à
3 semaines. Les valeurs moyennes et la bande de confiance sont
calculées en fonction des résultats de l'analyse statistique
sur la représentativité des sites.

On a reporté, fig. 9, le taux moyen journalier d'ETR
résultant de ce calcul ainsi que la valeur estimée du taux jour-
nalier d'ETP Penman, obtenue selon la méthode présentée par RIOU
et CHARTIER [14]. Jusqu'au 20/01, la valeur de l'ETR mesurée
correspond au taux d'évaporation sur sol nu. Du 12/01 ou 2/02,
on a une très grande incertitude qui montre une des limites de
cette méthode en cas de fortes pluies, liées probablement à l'as-
pect très local de la mesure qui peut être perturbée par les mo-
difications de structure autour des tubes d'accès. Par contre,
dès le 2 février, on obtient une relative homogénéisation de la
mesure, l'écart-type (estimé) sur le taux d'évapotranspiration
restant en moyenne de 0,3 mm/j. On note une diminution du taux
d'évapotranspiration, en phase de croissance, durant la période
pluvieuse allant du 13 au 27/04/1982. En fin de cycle, il est
enfin important de noter la chute très brutale de la consomma-
tion hydrique.

On a également reporté, fig. 9, la comparaison entre
pluie cumulée et ETR cumulée durant tout le cycle. On notera
que l'alimentation de la culture n'a sûrement pas été satisfai-
sante puisque la consommation moyenne totale n'est que de 370 mm
avec un rendement de 770 kg ; cette valeur est cependant infé-
rieure à la pluie (403,7 mm).
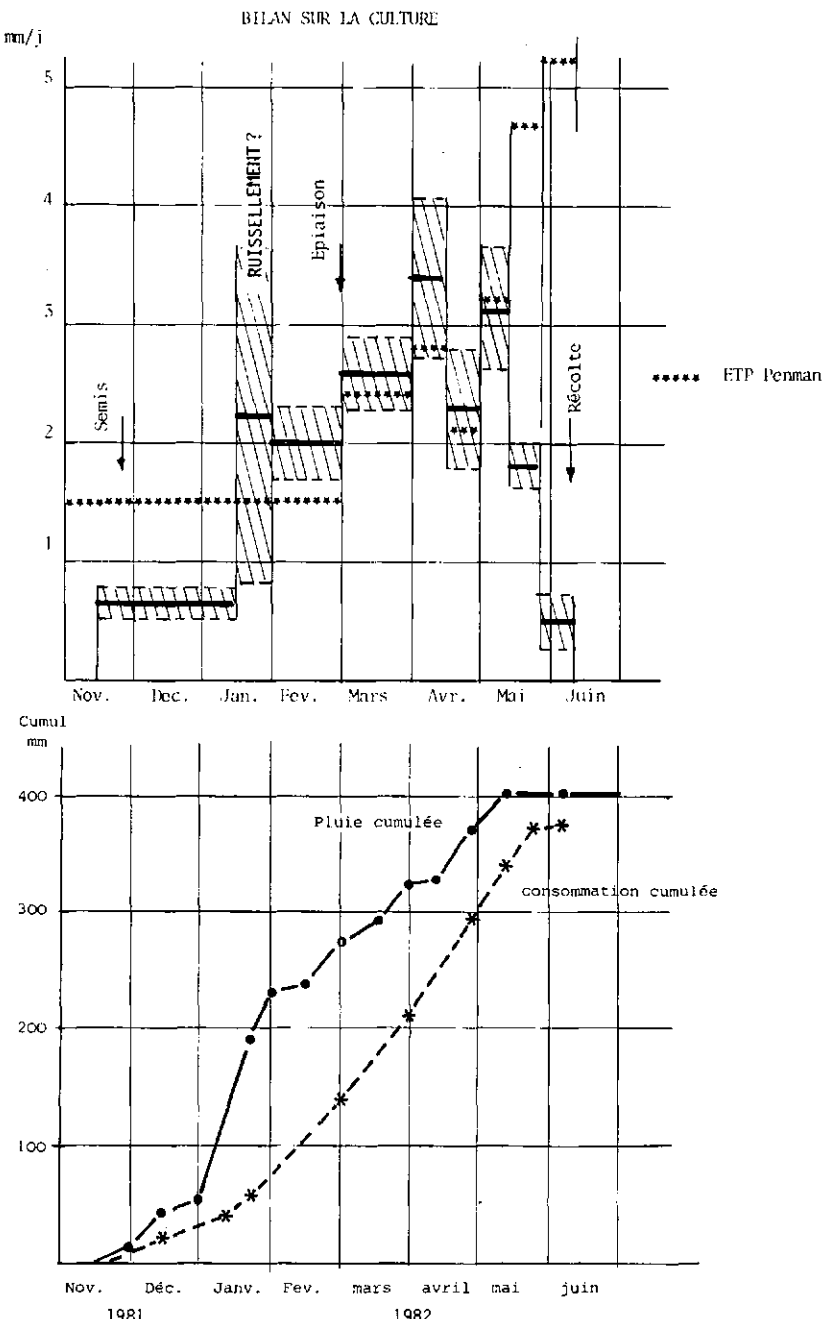
FIG.9. Comparaison entre taux d'évapotranspiration moyen sur la parcelle, et estimé par la formule de Penman, et entre évapòtranspiration cumulée et pluie.

Ce résultat est confirmé par les mesures gravimétriques puisque l'on obtient le bilan suivant :

- stock 0-100 au 4/11/1981   105,35 ± 16,7 mm
- stock 0-100 au 3/06/1981   129,25 ± 21 mm
- pluie 403,7 mm

(sur les 4 sites la variation de stock moyenne en-dessous de 100 cm est de 5 ± 5 mm).

CONCLUSION

Il ne saurait être question de tirer de cette étude des arguments généraux valant pour tout site d'expérimentation. Il nous semble préférable de dégager certaines grandes lignes, ou de suggérer des voies de recherches avec pour but d'approfondir ce type d'étude, de définir ses limites d'application, et de rechercher les possibilités de généralisation.

En premier lieu, il nous paraît indiscutable que, quel que soit l'échantillonnage retenu, une campagne de prospection préalable s'impose avant toute expérimentation de nature spatiale pour caractériser les sites de mesure, définir les distances minimum d'échantillonnage et l'importance du "bruit de fond" lié à l'hétérogénéité spatiale.

Il semble ensuite, au vu de cette étude, et d'autres expérimentations menées en parallèle par ailleurs, que du fait d'une liaison déterministe évidente entre les capacités de rétention, ou de transferts hydriques du sol, et la texture, il peut exister une stabilité temporelle importante dans les lois de distribution spatiale des variables hydriques. Un point dans un domaine pourrait être affecté d'un certain rang dans une loi de distribution, et aurait tendance à le conserver.

La validation de cette hypothèse nécessite cependant un certain nombre de répétition de mesures dans le temps, ce qui induit une limite expérimentale importante, et éventuellement un biais analytique : si les répétitions ne sont pas effectuées au même point, l'analyse peut être biaisée par l'existence d'hétérogénéité à très courte distance. Ceci doit faire au plus tôt l'objet d'une recherche méthodologique.

Pour le site de mesure considéré, la taille de l'échantillonnage représentatif est passé de 24 à 9 sans pertes d'informations, puis à 4 sans qu'il soit toutefois possible de valider complètement le résultat obtenu par ce dernier échantillon. Il ne semble cependant pas illusoire d'espérer définir un point moyen, image du comportement "moyen" de la parcelle.

Si l'on accepte le principe d'analyse ayant conduit aux résultats du tableau V, on notera que,sur le cycle complet, l'erreur quadratique moyenne entre la valeur d'ETR calculée à partir du seul site TC3 (site moyen) et la moyenne sur la parcelle (moyennes des mesures sur TC5, TC2, TC3) vaut 9,3, soit une erreur de ± 3 mm ou 1 % de l'ETR totale.

REFERENCES

[1] DANCETTE, C., HAMON, G., VACHAUD, G., Etude comparée de la dynamique de l'eau en sol sableux nu et cultivé. Isotopes and Radiation in Research on Soil Plant Relationships 1978, (Symposium Colombo) IAEA, Vienne (1979) 213-234.

[2] KALMS, J.M., VACHAUD, G., VAUCLIN, M., Etude méthodologique de l'alimentation hydrique de deux variétés de riz pluvial à l'échelle de la parcelle. Agronomie (1982) 2, 871-883.

[3] VACHAUD, G., Soil Physics Research and Water Management Trans. 12th International Congress of Soil Science (1982), vol. 5 "Whither Soil Research - Panel Discussion Papers" (New Delhi) 32-58.

[4] WARRICK, A.W., NIELSEN, D.R., Spatial variability of Soil Physical Properties in the Field, Chapter 13, p. 319-344 in Hillel D. ed : Application of Soil Physics, Academic Press, N.Y. (1982).

[5] NIELSEN, D.R., BIGGAR, J.W., ERH, K.T., Spatial variability of field measured soil water properties, Hilgardia, 42, (1973) 215-260.

[6] CARVELLO, H.O., CASSEL, D.K., HAMMOND, J., BAUER, A., Spatial variability of in-situ unsaturated hydraulic conductivity of Maddock Silt Loam, Soil Sci., 121, (1976) 1-8.

[7] BIGGAR, J.W., NIELSEN, D.R., Spatial variability of the leaching characteristics of a field soil, Water Resources Research, 13, (1976) 78-84.

[8] WEBSTER, R., CUANALO DE LAC, H.E., Soil transect correlograms of north Oxfordshire and their interpretation, J. of Soil Science, 26, (1975) 176-194.

[9] SISSON, J.B., WIERENGA, P., Spatial variability of steady state infiltration rates as a stochastic process. Soil Sci. Soc. Am. J., 45, (1981) 699-704.

[10] VIEIRA, S.R., NIELSEN, D.R., BIGGAR, J.W., Spatial variability of field measured infiltration rate. Soil Sci. Soc. Am. J., 45, (1981) 1040-1048.

[11] GAJEM, Y.M., WARRICK, A.W., MYERS, D.E., Spatial dependence of Physical properties of a typic torrifluent soil. Soil Sci. Soc. Am. J., 45, (1981) 1040-1048.

[12] VACHAUD, G., LATY, R., VAUCLIN, M., CHAABOUNI, Z., EL AMANI, S., La Station hydroclimatologique du MORNAG, 3, Estimation de la consommation hydrique d'une culture de blé en sec à l'échelle de l'hectare. Rapport DERV-CNRS, Institut de Mécanique de Grenoble, 31 p. (1982).

[13] VAUCLIN, M., HAVERKAMP, R., VACHAUD, G., Error Analysis in estimating soil water content by neutron moisture meters, accepté pour publication, Soil Sci., (1983).

[14] RIOU, C., CHARTIER, R., La Station hydroclimatologique du MORNAG, 1, Description et résultats 1980-81. Evaporation en bac d'eau libre et évapotranspiration potentielle. Rapport DRES-ORSTOM-Tunis, 25 p. (1981).

DESCRIPTION EXPERIMENTALE
ET MODELISATION STOCHASTIQUE
DES TRANSFERTS PAR LA MISE EN ECHELLE
DES PROPRIETES HYDRODYNAMIQUES DES SOLS[†]

M. VAUCLIN*, J. IMBERNON**,
G. VACHAUD*, C. DANCETTE[+]

* Institut de mécanique de Grenoble,
  Saint-Martin-d'Hères, France

** Institut de recherches agronomiques tropicales,
   Montpellier, France

[+] Institut sénégalais de la recherche agricole,
    Bambey, Sénégal

Abstract–Résumé

EXPERIMENTAL DESCRIPTION AND STOCHASTIC MODELLING OF TRANSFERS
USING A SCALING FACTOR FOR THE HYDRODYNAMIC PROPERTIES OF THE SOILS.
    It is well known that natural soils do not have constant hydrodynamic properties on the
plot scale. Experimentally, this means that a water balance obtained in an access tube by means
of a neutron moisture gauge and tensiometers is not necessarily representative of the whole range
studied. For modelling purposes the deterministic aspect of transfers should be associated with
a stochastic description of the hydrodynamic parameters (pressure, water content, hydraulic
conductivity). An experiment was carried out in a one-hectare plot of bare soil at Bambey
(Senegal) in order to characterize its variability: 28 infiltration tests were performed at the
points of a 23 X 23 m grid. At each of these points, the insertion of a neutron access tube to a
depth of 2.0 m, and the positioning of three tensiometers at depths of 100, 110 and 120 cm
made it possible also to monitor the redistribution of water and to derive the pressure-water
content relationships. In addition, internal drainage tests were made in four 1.5 X 1.5 m soil
monoliths so as to find the hydraulic conductivity-water content relationships at different
depths. On the assumption of similarity in porous media (verified in this study) all the results
were analysed in terms of the theory of scaling factors. The data obtained in bare soil were
then used as the basis for solving the stochastic equations for infiltration and drainage. The
results show that, apart from satisfactory agreement, with the experiment, the mean solution
obtained from the mean parameters (deterministic solution) is clearly different from the
mean of the solutions (stochastic solution). These differences, as well as the variance, depend
strongly on the variability of the soil, expressed here as the coefficient of variation of the
scaling factors. This obviously calls in question the concept of equivalent porous media.

DESCRIPTION EXPERIMENTALE ET MODELISATION STOCHASTIQUE DES TRANSFERTS
PAR LA MISE EN ECHELLE DES PROPRIETES HYDRODYNAMIQUES DES SOLS.

Il est bien connu que les propriétés hydrodynamiques des sols naturels ne sont pas
constantes à l'échelle de la parcelle. Cela implique, au plan expérimental, qu'un bilan hydrique
établi sur une verticale par humidimètre neutronique et tensiomètres n'est pas nécessairement
représentatif de tout le domaine d'étude. Au plan de la modélisation, à l'aspect déterministe des
transferts, il convient d'associer une description stochastique des paramètres hydrodynamiques
(pression, teneur en eau, conductivité hydraulique).Une expérience a été conduite sur une
parcelle de sol nu de 1 ha, à Bambey (Sénégal) afin d'en caractériser la variabilité: 28 essais
d'infiltration ont été réalisés aux noeuds d'une grille 23 X 23 m. En chacun de ces points,
l'implantation d'un tube d'accès neutronique jusqu'à 2,0 m et de 3 tensiomètres aux cotes
100, 110 et 120 cm a permis de suivre également la redistribution de l'eau afin d'obtenir les
relations pression-teneur en eau. De plus, des essais de drainage interne ont été réalisés sur 4
monolithes de sol 1,5 X 1,5 m afin d'obtenir les relations conductivité hydraulique-teneur
en eau à différentes cotes. En se fondant sur l'hypothèse de similitude en milieu poreux
(vérifiée dans cette étude), tous les résultats sont analysés en fonction de la théorie de la mise
en facteur d'échelle. Les données obtenues sur le sol nu servent ensuite de base à la résolution
des équations stochastiques de l'infiltration et du drainage. Les résultats montrent, outre un
bon accord avec l'expérience, que la solution moyenne obtenue à partir des paramètres moyens
(solution déterministe) est nettement différente de la moyenne des solutions (solution
stochastique). Ces différences, ainsi que la variance, sont très fortement dépendantes de la
variabilité du sol, exprimée ici par le coefficient de variation des facteurs d'échelle. Cela remet
évidemment en cause le concept de milieu poreux équivalent.

A. INTRODUCTION

Il est bien connu que les transferts isothermes d'eau
dans un milieu poreux non saturé sont décrits à l'échelle macros-
copique par des équations aux dérivées partielles non linéaires.
Il s'agit de modèles conceptuels puisque fondés sur la connais-
sance des processus physiques impliqués. Ces modèles permettent
de connaître l'évolution spatio-temporelle des variables d'état
du milieu poreux, en fonction de conditions initiales et aux
limites imposées par l'intermédiaire de paramètres phénomèno-
logiques. Dans l'hypothèse d'un milieu uniforme et homogène
(au sens défini par FREEZE, [1]) ces modèles conceptuels sont
de type déterministe puisque la connaissance des paramètres en
un point suffit à caractériser l'ensemble du domaine.

De nombreuses études expérimentales de laboratoire,
montrent que cette approche convient pour l'étude des transferts
en milieu poreux non saturé. En revanche, son extension aux con-
ditions naturelles in situ se heurte à de sérieuses limitations :

1) - Un sol n'est jamais uniforme et homogène et ses
propriétés varient d'un point à un autre. Cela impose donc une
description stochastique des paramètres.

2) - L'aspect stochastique n'implique pas nécessaire-
ment que les paramètres et/ou les variables d'état soient aléa-
toirement distribués dans l'espace. Ils (elles) peuvent présen-
ter une structure spatiale horizontale et/ou verticale.

3) - Le caractère aléatoire des conditions aux limites
naturelles (pluie, évaporation) renforce cet aspect stochastique.

Bien que la modélisation des transferts hydriques à
l'échelle de la parcelle ait été l'objet de nombreux développe-
ments, au cours de ces dernières années ([2], [3], [4], [5],
[6], [7], [8]), très peu d'études ([3]) confrontent modèle et
expérience.
On se propose ici de caractériser et d'analyser la va-
riabilité spatiale d'une parcelle de sol nu d'un hectare, de
modéliser les transferts correspondants (infiltration et drai-
nage) à l'aide de la théorie de la mise en facteur d'échelle
des propriétés hydrodynamiques et de comparer les résultats
avec des mesures in situ.

B. THEORIE

1 - APPROCHE CONCEPTUELLE DES TRANSFERTS :

L'écoulement isotherme d'eau, supposée pure et incom-
pressible, dans chaque colonne verticale de sol homogène est
classiquement décrit par l'équation suivante :

$$\frac{\partial \theta}{\partial t} = \frac{\partial}{\partial z} \{K(\theta) \ (\frac{\partial h}{\partial z} - 1)\} \qquad (1)$$

Tous les symboles sont donnés en nomenclature.
En négligeant les effets d'hystérésis et dynamiques
sur h(θ), l'équation (1) peut s'écrire :

$$\frac{\partial \theta}{\partial t} = \frac{\partial}{\partial z} \{D(\theta) \ \frac{\partial \theta}{\partial z} \} - \frac{\partial K(\theta)}{\partial z} \qquad (2)$$

La résolution des équations (1) ou (2), pour des con-
ditions initiales et aux limites définies, permettrait d'obte-
nir θ(z,t) pour un sol uniforme et homogène de caractéristiques
hydrodynamiques (K(θ), D(θ)) données. Leur utilisation pour un
milieu non uniforme nécessite donc la connaissance de la varia-
bilité de ces paramètres.

2 - DESCRIPTION STOCHASTIQUE DES PARAMETRES HYDRODYNAMIQUES :

De nombreuses études expérimentales ([9], [10], [11],
[12], [13]) montrent qu'en s'appuyant sur la théorie de la si-
militude des milieux poreux, la variabilité constatée dans les
propriétés hydrodynamiques d'un sol pouvait être appréhendée

par l'utilisation de facteurs d'échelle, caractéristiques de
chaque point de mesure. Le problème se ramène alors à l'étude
de la variabilité spatiale de ces coefficients.

Rappelons brièvement que l'invariance des coefficients
de tension superficielle et de viscosité cinématique conduit à
écrire pour deux milieux poreux semblables (au sens de MILLER
et MILLER, [14]), la relation suivante :

$$W_r = \alpha_{W,r}^p \, W^{\ast}$$
(3)

où $\alpha_{W,r}$ est le facteur d'échelle relatif à la propriété hydro-
dynamique W_r. Il est défini par le rapport entre les longueurs
caractérisant la géométrie interne des milieux quelconques (r)
et de référence ($\ast$). L'exposant p prend les valeurs suivantes :
p = -1 pour la pression, p = 2 pour la conductivité ou le flux,
p = 1 pour la diffusivité capillaire, $p = \frac{1}{2}$ pour la sorptivité.

On notera que l'hypothèse de similitude implique d'une
part, que la porosité soit constante, d'autre part, que les $\alpha_{W,r}$
en un même point, sont les mêmes quelle que soit la fonction
W considérée.

3 - APPROCHE COUPLEE "STOCHASTICO-CONCEPTUELLE" DES TRANSFERTS :

En admettant l'hypothèse de similitude et en effectu-
ant un changement des échelles d'espace ($z^{\ast} = \alpha z$) et de temps
($t^{\ast} = \alpha^3 t$), on montre aisément que les équations (1) et (2),
compte-tenu de la relation (3), s'écrivent respectivement :

$$\frac{\partial \theta}{\partial t^{\ast}} = \frac{\partial}{\partial z^{\ast}} \{K^{\ast}(\theta) \, (\frac{dh^{\ast}}{dz^{\ast}} - 1)\}$$
(4)

$$\frac{\partial \theta}{\partial t^{\ast}} = \frac{\partial}{\partial z^{\ast}} \{D^{\ast}(\theta) \, \frac{\partial \theta}{\partial z^{\ast}}\} - \frac{\partial K^{\ast}(\theta)}{\partial z^{\ast}}$$
(5)

Pour des conditions initiales et aux limites prescri-
tes, la solution des équations (4) ou (5) est invariante avec
la position, et elle est unique pour un sol fictif dont les
propriétés hydrodynamiques sont assimilées à celles du milieu
de référence. Elle correspond à la solution déterministe du
problème. A titre d'exemple, nous présentons les cas de l'in-
filtration sous charge constante et du drainage gravitaire.

a) *Modélisation stochastique de l'infiltration.*

On s'intéresse ici uniquement à la modélisation de
l'infiltration d'eau sous très faible charge, dans un profil
semi-infini. Le cas de l'infiltration sous flux est traité par
ailleurs [15].

Ainsi pour les conditions initiales et aux limites suivantes :

$$t^{::} < 0 \qquad z^{::} \geqslant 0 \qquad \theta = \theta_n \qquad (6)$$

$$t^{::} \geqslant 0 \qquad z^{::} = 0 \qquad \theta = \theta_S$$

PHILIP [16] donne la solution en série de l'équation (5) qui, limitée aux quatre premiers termes, s'écrit :

$$z^{::}(\theta, t^{::}) = \sum_{q=1}^{4} f_q^{::}(\theta) \cdot t^{::q/2} \qquad (7)$$

où les fonctions $f_q^{::}(\theta)$ sont les solutions d'équations différentielles ordinaires.

L'introduction des facteurs d'échelle dans l'équation (7) donne :

$$z(\theta, t) = \sum_{q=1}^{4} f_q^{::}(\theta) \, \alpha^{(3q/2-1)} \, t^{q/2} \qquad (8)$$

Infiltration cumulée et flux d'infiltration en n'importe quel site sont alors donnés par les relations suivantes :

$$I(t) = \sum_{q=1}^{4} A_q^{::} \, \alpha^{(3q/2-1)} \, t^{q/2} + \alpha^2 \, K^{::}(\theta_n) \, t \qquad (9)$$

$$i(t) = \sum_{q=1}^{4} \frac{q}{2} A_q^{::} \, \alpha^{(3q/2-1)} \, t^{q/2-1} + \alpha^2 \, K^{::}(\theta_n) \qquad (10)$$

où les coefficients $A_q^{::}$ sont estimés par $\int_{\theta_n}^{\theta_S} f_q^{::}(\theta) \, d\theta$.

Il est bien connu que les solutions (8), (9) et (10) ne sont convergentes que pour des temps inférieurs à une valeur critique estimée par :

$$t_c = \frac{1}{\alpha^3} \left\{ \frac{A_1^{::}}{K^{::}(\theta_S)} \right\}^2$$

Au-delà, le régime d'infiltration peut être estimé par l'approximation du profil asymptotique [16] dont les solutions sont les suivantes :

$$(11)$$

$$z = \alpha \int_{\theta_S}^{\theta} \frac{D^{::}(\theta)}{K^{::}(\theta) - K^{::}(\theta_n) - [K^{::}(\theta_S) - K^{::}(\theta_n)][(\theta-\theta_n)/(\theta_S-\theta_n)]} \, d\theta$$

$$I(t) \quad = \alpha^2 \, K^{::}(\Theta_S) t - \frac{a_1}{\alpha a_2} \exp \{-a_2 \alpha^3 t\} + \frac{a_3}{\alpha} \qquad (12)$$

$$i(t) \quad = \alpha^2 \, K^{::}(\Theta_S) + \alpha^2 \, a_1 \exp \{-a_2 \alpha^3 t\} \qquad (13)$$

où les coefficients a_1, a_2, a_3 sont déterminés par continuité des solutions série et asymptotique au temps t_c.

   b) *Modélisation stochastique du drainage.*

        Il s'agit ici de prédire l'évolution dans le temps de l'humidité, et du flux à une cote donnée, au cours d'un processus de ressuyage d'un sol initialement humidifié jusqu'à sa saturation naturelle. Contrairement au cas de l'infiltration on ne dispose pas de solutions quasi-analytiques exactes de ce problème. Il est néanmoins possible, sous certaines conditions d'obtenir une solution approchée. En effet, avec les hypothèses simplificatrices proposées par LIBARDI et al [17], la solution de l'équation (4) donne :

$$\Theta(z,t) = \Theta_S \, \{1 + \alpha^2 \, \frac{b-1}{\Theta_S} \, K_0^{::} \, \frac{t}{z} \}^{1/1-b} \qquad (14)$$

$$q(z,t) = \alpha^2 \, K_0^{::} \, \{1 + \alpha^2 \, \frac{b-1}{\Theta_S} \, K_0^{::} \, \frac{t}{z}\}^{b/1-b} \qquad (15)$$

$$D(z,t) = a\Theta_S z \, \{1 - (1 + \alpha^2 \, \frac{b-1}{\Theta_S} \, K_0^{::} \, \frac{t}{z})^{1/1-b}\} \qquad (16)$$

        On notera que ces équations sont établies ici, avec $K^{::}(\theta) = K_0^{::} \, (\frac{\theta}{\theta_S})^b$ (modèle empirique de BROOKS et COREY [18]).

   c) *Conclusion.*

        Compte-tenu de la variabilité spatiale des propriétés hydrodynamiques du sol, décrite ici par le facteur d'échelle α, les équations de l'infiltration et du drainage apparaissent sous la forme générale suivante :

$$X = g \, (\alpha, \text{paramètres}, t, z) \qquad (17)$$

où les paramètres sont uniques pour toute la parcelle et α est une variable aléatoire. Pour des conditions initiales et aux limites données et supposées ici constantes sur la parcelle, la variable d'intérêt X est donc elle-même une variable aléatoire qui dépend de façon déterministe du temps et de la cote. Supposant connue la loi de distribution des α, il s'agit donc d'inférer les propriétés statistiques (loi de distribution et moments associés) de X satisfaisant aux équations des transferts.

+   % (A + L)
e   Sites d'infiltration
⊞   Monolithes
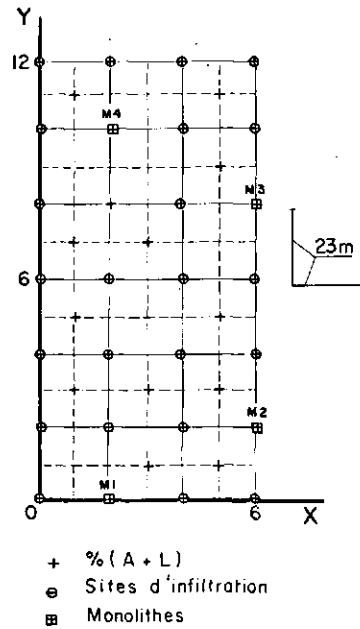
FIG.1. Schéma d'implantation du dispositif expérimental.

         L'aptitude de cette modélisation à prédire la réalité dépend bien évidemment de la validité des hypothèses qui la sou-tendent tant au niveau conceptuel (loi de PHILIP pour l'infiltra-tion, hypothèses du drainage) que stochastique (hypothèse de si-militude des milieux poreux). Il apparaît donc indispensable de confronter les résultats de ce type de modélisation avec l'ex-périence.

C. RESULTATS EXPERIMENTAUX

1 - PROTOCOLE EXPERIMENTAL :

         Une parcelle de 1 ha environ a été considérée sur la station de recherches agricoles de BAMBEY- Sénégal. Le sol, ini-tialement en jachère, a été dénudé et un quadrillage systémati-que avec une maille carré de 23 m de côté a été mis en place (fig.1). En chacun des 28 noeuds ainsi obtenus, le taux d'élé-ments fins (A+L) limités à 20 µm a été déterminé par tranches de sol de 10 cm jusqu'à 20 cm de profondeur, puis de 30 cm jusqu'à 2 m. Des mesures complémentaires ont été effectuées aux centres de 12 mailles (fig.1). En 4 noeuds, M1, M2, M3, et M4, un mono-lithe carré de 1,5 cm de côté isolé latéralement par une feuille de polyane a été équipé d'un tube d'accès neutronique jusqu'à 2m

de profondeur et de 10 tensiomètres implantés verticalement aux
cotes 0,10, 0,20, 0,30, 0,40, 0,50, 0,70, 0,90, 1,10, 1,30 et
1,50m et connectés à des manomètres à mercure. Sur chacun de ces
monolithes, un essai classique de drainage interne ([19], [20])
a été réalisé afin d'obtenir en ces sites les relations K (θ) et
h (θ) à différentes profondeurs [21].

Les 24 autres noeuds (fig.1) ont été équipés d'un tube
d'accès neutronique jusqu'à 2 m de profondeur et de 3 tensiomètres
aux cotes 1,00, 1,10 et 1,20m. En chacun de ces sites, un essai
d'infiltration a été réalisé en utilisant un infiltromètre double
anneaux ($\emptyset_{int}$ = 0,58 m ; $\emptyset_{ext}$ = 0,96 m) alimenté en eau par un
dispositif de type Mariotte afin d'assurer une lame d'eau sensi-
blement constante (3 à 4 cm) à la surface du sol et de mesurer
les volumes infiltrés. Les essais ont duré, en moyenne 60 min.
On notera que sur les 24 essais, 5 ont dû être éliminés en rai-
sont de la présence de "macro-fissures" (trous de rongeurs, et
de serpents) rendant toute mesure impossible.

2 - CARACTERISATION PEDOLOGIQUE DE LA PARCELLE :

Le sol de la parcelle considérée, de dénomination ver-
naculaire "DIOR" est très répandu en zone Centre-Nord du SENEGAL.
Il s'agit d'un sol ferrugineux faiblement lessivé provenant
d'apports éoliens sur un substrat marno-calcaire de l'éocène.
L'observation des profils montre une grande homogénéité verti-
cale, avec prédominance de sable fin et absence d'éléments su-
périeurs à 2 mm. La matière organique est inférieure à 0,5 %.
La masse volumique sèche a pour valeur moyenne 1,45 g/cm^3.
L'analyse statistique des observations du taux d'élé-
ments fins (A+L) limités à 20 μm conduit à une loi de distribu-
tion log-normale dont les paramètres sont :

$$m_{Ln\ (A+L)} = 2,00\ \text{et}\ \sigma_{Ln\ (A+L)} = 0,272.$$

L'analyse géostatistique à l'aide du semi-variogramme
montre que les observations peuvent être considérées comme spa-
tialement indépendantes les unes des autres pour des distances
supérieures à 23 m.

3 - CARACTERISATION HYDRODYNAMIQUE DE LA PARCELLE :

La mesure simultanée des teneurs en eau et des
charges hydrauliques au cours du ressuyage des lames d'eau ap-
portées lors des essais d'infiltration a permis d'obtenir en
23 sites (19 essais d'infiltromètre et 4 monolithes), les re-
lations h$_r$ (θ).

D'autre part, l'analyse des profils hydriques et de
charge hydraulique mesurés lors des essais de drainage interne
sur les 4 monolithes, a permis de déterminer les relations
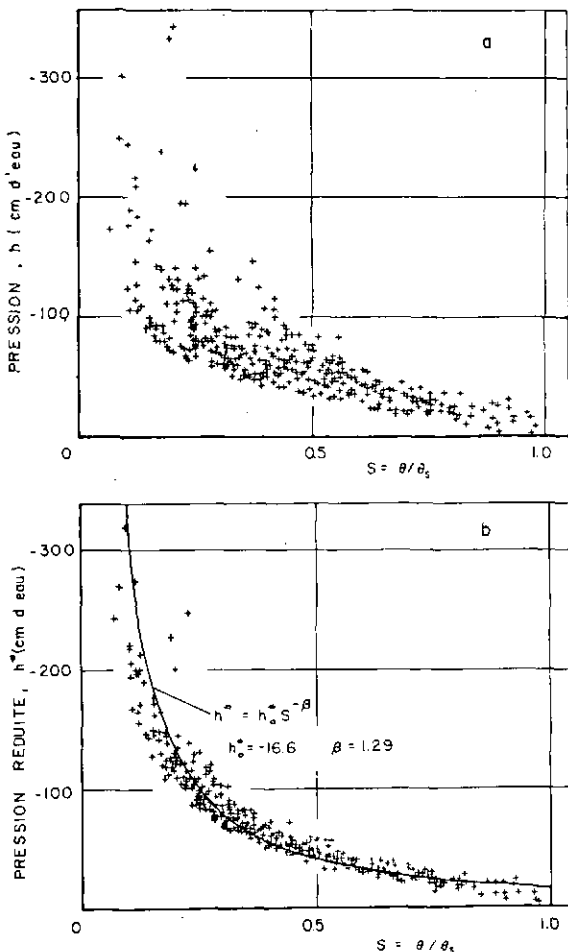
FIG.2.   Relations pression - degré de saturation à z = 110 cm:

a) valeurs brutes

b) valeurs réduites par la mise en facteur d'échelle.

K_r (θ) à différentes cotes. Toutes les données expérimentales h_r (θ) et K_r (θ) où r représente indifféremment un site ou une cote de mesure, ont été lissées par le modèle suivant [18] :

$$h_r \ (S) = h_{or} \ S^{\beta r} \quad ; \quad K_r \ (S) = K_{or} \ S^{br}$$

Les humidités ont été exprimées par le degré de saturation $S = \theta / \theta_S$ afin de s'affranchir des éventuelles variations spatiales de la porosité. A titre d'exemple, les résultats sont reportés fig.2a pour h_r (S) à la cote z = 110 cm et 3a pour K_r (S) aux cotes 30, 50, 90 et 110 cm.
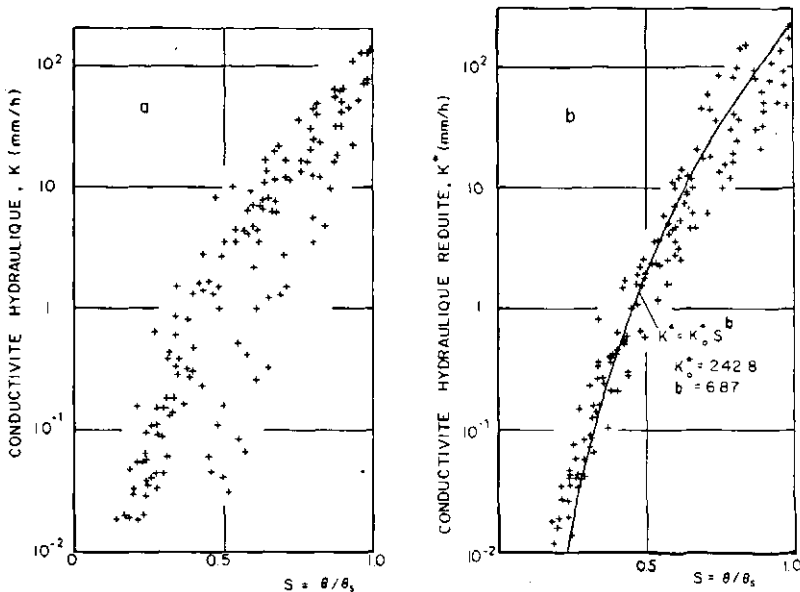
FIG.3.   Relations conductivité hydraulique – degré de saturation:

a) valeurs brutes

b) valeurs réduites par la mise en facteur d'échelle.

4 - <u>DETERMINATION DES FACTEURS D'ECHELLE</u> :

Rappelons qu'il s'agit de trouver les relations moyennes d'échelle :

$$h^{::}(S) = h^{::}_0 S^{\beta} \qquad et \qquad K^{::}(S) = K^{::}_0 S^b \qquad (18)$$

où $h^{::}_0$, β, $K^{::}_0$ et b sont uniques pour toute la parcelle et les facteurs d'échelle définis par la relation (3) sous la contrainte de normalisation : $\frac{1}{n} \sum_{r=1}^{n} \alpha_r = 1$

où n est le nombre de sites de mesure. L'utilisation de la procédure proposée par SIMMONS et al [11] a conduit aux valeurs suivantes : $h^{::}_0$ = - 16,6 cm d'eau ; β = - 1.294 ; $K^{::}_0$ = 242,8mm/h b = 6,87.

La diffusivité capillaire calculée par $D^{::}=K^{::} \frac{dh^{::}}{d\theta}$ se met donc sous la forme suivante :

$$D^{::}(S) = D^{::}_0 S^{\gamma} \quad avec \quad D^{::}_0 = 1,733.10^5 \ mm^2/h \ ; \ \gamma = 4,576 \qquad (19)$$

Les facteurs d'échelle relatifs à la relation pression
teneur en eau calculés pour la cote z = 110 cm (n = 23) suivent
une loi log-normale de moyenne $m_{Ln\alpha}$ = -0,1229 et d'écart-type
$\sigma_{Ln\alpha}$ = 0,5274.

On notera que le semi-variogramme n'a montré aucune
structure spatiale des α, pour l'échantillonnage retenu. La mê-
me procédure a également été utilisée pour les relations h(θ) et
K(θ) déterminées sur les 4 monolithes. La bonne corrélation entre
les facteurs d'échelle de la pression (α_h) et de la conductivité
(α_K) (α_K = 0,97 α_h avec r^2 = 0,85) montre que l'hypothèse de mi-
lieux poreux semblables peut valablement être retenue.

Les valeurs de la pression et de la conductivité mi-
ses en échelle par l'intermédiaire des facteurs α_r sont repor-
tées figures 2b et 3b respectivement, ainsi que les relations
moyennes données par les équations [18].

Il apparaît donc que la procédure de mise en facteur
d'échelle réduit très notablement la dispersion des points ex-
périmentaux autour des courbes moyennes d'échelle. On notera
que la coalescence des points devrait être totale si l'hypo-
thèse de similitude était rigoureusement vérifiée.

5 - RELATION ENTRE LES FACTEURS D'ECHELLE ET LA TEXTURE :

Il est apparu une liaison statistique entre les fac-
teurs d'échelle et le taux d'éléments fins (A+L) à la même co-
te. La recherche de la meilleure corrélation a conduit à :

$$Ln\alpha = - 0,949 \, Ln \, (A+L) + 1,782 \quad (r = - 0,871) \quad (20)$$

On notera que la nature linéaire de la régression
sur les valeurs logarithmiques respecte la loi de distribution
de chacun de ces paramètres.

Cette relation peut servir d'outil pour prédire α en
n'importe quel point de la parcelle, à partir d'une détermi-
nation expérimentale du taux (A+L) plus facile à mettre en
oeuvre, sous les réserves habituelles liées à l'utilisation
des corrélations en prédiction.

D. MODELISATION STOCHASTIQUE DES TRANSFERTS

1 - PRINCIPES DE L'ANALYSE STATISTIQUE DES RESULTATS :

La solution des équations stochastiques de l'infiltra-
tion et du drainage a été obtenue en générant 100 valeurs de α
prises dans sa loi de distribution, selon la procédure décrite
dans [15]. Il est ainsi possible d'inférer la loi de distribu-
tion de X et de calculer ses premiers moments. On notera que
cela revient à simuler numériquement 100 mesures effectuées
sur la parcelle.
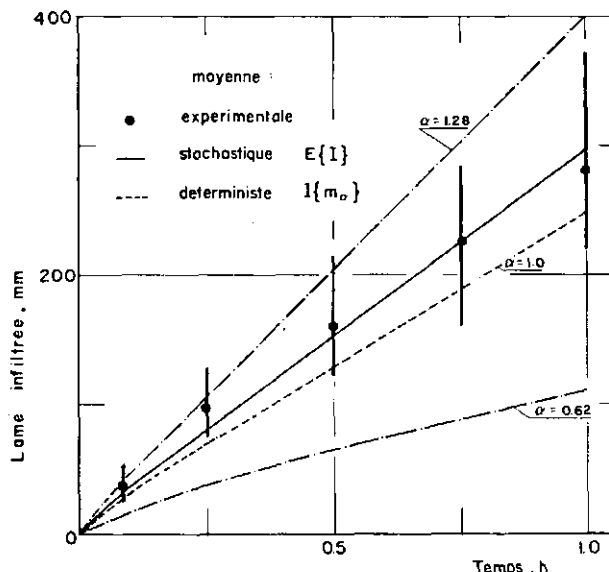
FIG.4. Lame d'eau infiltrée en fonction du temps. Les barres verticales correspondent au domaine de variation des valeurs mesurées sur les 23 sites.

On remarquera qu'une estimation simple de la valeur moyenne E {X} et de la variance var {X} peut s'obtenir directement par développement en série de Taylor de l'équation (17) :

$$E\{ X \} = g(m_\alpha) + \left|\frac{\partial^2 g}{\partial \alpha^2}\right|_{m_\alpha} \cdot \frac{\sigma^2 \alpha}{2} \qquad (21)$$

$$var\{ X \} = \left|\frac{\partial g}{\partial \alpha}\right|^2_{m_\alpha} \cdot \sigma^2_\alpha \qquad (22)$$

où m_α et σ^2_α sont respectivement la valeur moyenne et la variance de α calculées en respectant la loi de distribution. L'équation (21) peut également s'écrire :

$$E \{X\} = g(m_\alpha) \{1 + \varepsilon_X\} \qquad (23)$$

où $\varepsilon_X = \frac{1}{g(m_\alpha)} \left| \frac{\partial^2 g}{\partial \alpha^2}\right|_{m_\alpha} \cdot \frac{\sigma^2 \alpha}{2}$ est l'écart relatif entre l'espérance mathématique de la variable d'intérêt X et la moyenne déterministe $g(m_\alpha)$ calculée avec $m_\alpha = 1$.
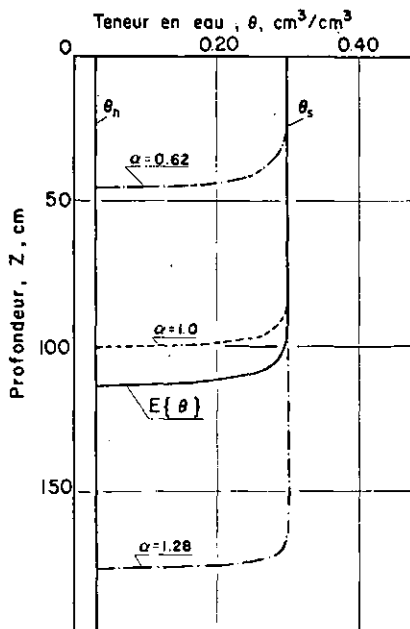
FIG.5. Profils hydriques après 1 heure d'infiltration: $\theta_n = 0,03$ cm^3/cm^3; $\theta_s = 0,30$ cm^3/cm^3.

Bien que cette méthode ne permette pas d'avoir accès à la distribution de la variable X, elle a l'avantage de la simplicité lorsque X est définie analytiquement.

2 - CAS DE L'INFILTRATION.

Les solutions de l'infiltration ont été obtenues ($A_1^{::}$ = 67,74 mmh$^{-1/2}$, $A_2^{::}$ = 82,11 mmh^{-1}, $A_3^{::}$ = 96,92 mmh$^{-3/2}$, $A_4^{::}$ = 86,0 mmh^{-2}, a_1 = 92,83 mmh^{-1}, a_2 = 23,72 h^{-1}, a_3 = 9,63 mm, t_c = 0,08 h) par l'algorithme de calcul donné par VAUCLIN et al [22] avec θ_n = 0,03 cm^3/cm^3 et θ_s = 0,30 cm^3/cm^3 (valeurs mesurées au champ).

a) A titre d'exemple, l'évolution dans le temps de l'infiltration cumulée moyenne, calculée en respectant sa loi de distribution (log-normale) est reportée fig.4 ainsi que les valeurs correspondant aux premier (α = 0,62) et dernier quartiles(α = 1,28) de la loi de distribution des α. Ainsi, après 1 heure d'infiltration, sur 25% de la surface de la parcelle, la lame infiltrée est inférieure à 108 mm et supérieure à 405 mm.

TABLEAU I. PARAMETRES DE LA DISTRIBUTION DU FRONT
D'INFILTRATION

t (h)	$E\{z_f\}$ (cm)	var z_f (cm^2)	CV	Mode (cm)	Médiane (cm)
0,1	14,1	6,86	0,18	7,90	11,6
0,25	29,5	645,6	0,86	12,9	22,4
0,5	55,8	3230,4	1,00	19,7	39,5
1,0	110,0	15376	1,12	32,1	73,0
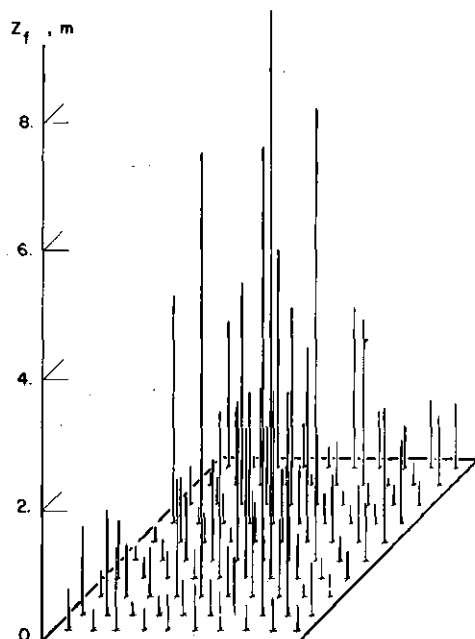
FIG.6. *Répartition spatiale du front d'infiltration au temps t = 1 heure.*
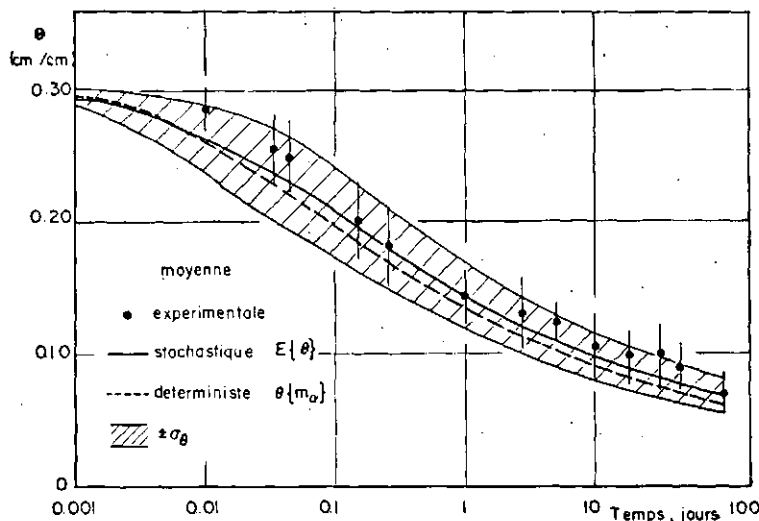
FIG.7.   Teneur en eau volumique en fonction du temps à z = 110 cm; au cours du drainage
les barres expérimentales correspondent aux écarts types expérimentaux.

Les valeurs moyennes expérimentales (calculées à partir des 23 essais) ainsi que les domaines de variation associés sont également reportés. Outre un accord très satisfaisant avec les valeurs prédites, on notera que supposer le sol homogène et uniforme (solution déterministe obtenue avec $\alpha = 1$) reviendrait à sous-estimer de 20% environ la quantité d'eau infiltrée.

b) La figure 5 donne les profils hydriques après 1 heure d'infiltration, correspondant d'une part aux valeurs moyennes déterministe ($\alpha = 1$) et stochastique ($E\{\theta\}$) et d'autre part, aux premier et dernier quartiles de la loi de distribution des α.

c) Les principaux paramètres de la loi de distribution du front d'infiltration défini par :

$$z_f(t) = \frac{1}{\Theta_S - \Theta_n} \int_{\Theta_n}^{\Theta_S} z(\Theta, t) \, d\Theta \qquad (24)$$

sont donnés tableau I à différents temps.

Le caractère fortement asymétrique et aplati de la fonction de répartition $z_f(t)$ implique que les valeurs les plus probables (Mode) sont très différentes des valeurs moyennes.

TABLEAU II. PARAMETRES DE LA FONCTION DE REPARTITION DE
L'HUMIDITE A z = 110 cm, LORS DU DRAINAGE GRAVITAIRE.

t (h)	E {Θ} (cm^3/cm^3)	var {Θ} $(cm^3/cm^3)^2$	CV	Mode (cm^3/cm^3)	Médiane (cm^3/cm^3)
1	0,2340	$1,26.10^{-3}$	0,153	0,230	0,2310
24	0,1434	$6,55.10^{-4}$	0,178	0,1420	0,1425
120	0,1093	$3,85.10^{-4}$	0,180	0,1092	0,1095
240	0,0972	$3,05.10^{-4}$	0,180	0,098	0,100
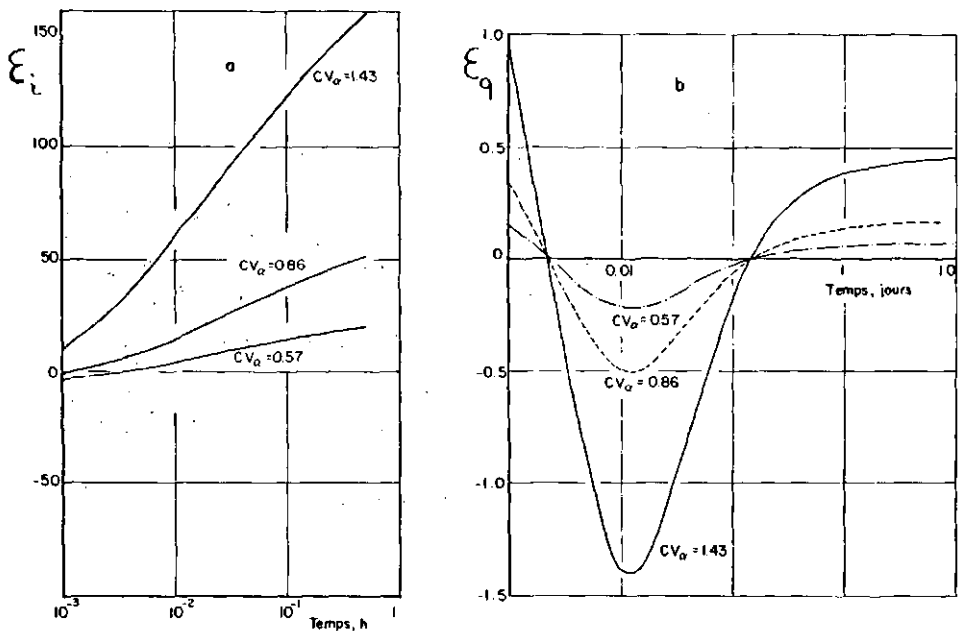
FIG.8.   Ecart relatif entre moyennes stochastique et déterministe en fonction du temps.
$CV_\alpha = 0,57$ correspond à la variabilité observée ($\sigma^2_{Ln\alpha} = 0,2782$); $CV_\alpha = 0,86$ et $CV_\alpha = 1,43$
correspondent à $2\sigma^2_{Ln\alpha}$ et $4\sigma^2_{Ln\alpha}$ respectivement.

a) flux d'infiltration
b) flux de drainage à z = 110 cm.

TABLEAU III. COMPORTEMENT AU VOISINAGE DE t = 0.

	ε_X	var(X)
INFILTRATION		
Flux (i)	$-\dfrac{1}{8} CV_\alpha^2$	$\dfrac{1}{16} A_1^2 \dfrac{m_\alpha}{t} CV_\alpha^2 \to \infty$
Lame (I)	$-\dfrac{1}{8} CV_\alpha^2$	$\dfrac{1}{4} A_1^2 m_\alpha t CV_\alpha^2 \to 0$
DRAINAGE		
Teneur en eau (θ)	$-\dfrac{K_o''}{a\Theta_S} m_\alpha^2 \dfrac{t}{z} CV_\alpha^2 \to 0_-$	$4 K_o''^2 \left(\dfrac{t}{z}\right)^2 m_\alpha^4 CV_\alpha^2 \to 0$
Flux (q)	CV_α^2	$4 m_\alpha^4 K_o''^2 CV_\alpha^2$
Lame (D)	$\dfrac{K_o''}{a\Theta_S} \dfrac{t}{z} m_\alpha^2 CV_\alpha^2 \to 0_+$	$4 K_o''^2 t^2 m_\alpha^4 CV_\alpha^2 \to 0$

La répartition spatiale des fronts après une heure d'infiltration est visualisée figure 6. Des valeurs supérieures à 350 cm bien que rares (3% environ) peuvent paraître néanmoins surprenantes. On notera cependant qu'en 6 points de la parcelle la grande vitesse d'infiltration n'a pas permis la mesure des volumes infiltrés et l'analyse correspondante. De plus, au cours de l'hivernage 1980 des humidifications très significatives ont été observées sous condition de pluie naturelle à 350 cm de profondeur (dernier point de mesure neutronique). Ces faits expérimentaux accréditent donc la possibilité d'infiltration profonde prédite par le modèle et permettent d'envisager la faisabilité de recharger artificiellement les nappes à surface libre en voie de tarissement dans cette région.

3 - CAS DU DRAINAGE :

La figure 7 donne les évolutions en fonction du temps de la teneur en eau à la cote z = 110 cm calculées pour $\alpha = 1$ (solution déterministe), $\alpha = 0{,}624$ (premier quartile) et $\alpha = 1{,}28$ (dernier quartile) ainsi que la valeur moyenne. Les valeurs moyennes expérimentales obtenues par humidimétrie neutronique en 23 sites sont également reportées ainsi que les écarts-types associés. Outre un bon accord entre moyennes expérimentales et numériques, on remarque que là encore la modélisation déterministe ne convient pas.

Les principaux paramètres de la fonction de répartition des humidités à z = 110 cm sont donnés tableau II pour différents temps.

TABLEAU IV. COMPORTEMENT AU VOISINAGE DE $t \to \infty$

	ε_X	var(X)
INFILTRATION		
Flux (i)	CV_α^2	$4 \, K_0^{*2} \, m_\alpha^4 \, CV_\alpha^2$
Lame (l)	CV_α^2	$4 \, K_0^{*2} \, t^2 \, m_\alpha^4 \, CV_\alpha^2 \to \infty$
DRAINAGE		
Teneur en eau (θ)	$\dfrac{b+1}{(b-1)^2} \, CV_\alpha^2$	0
Flux (q)	$\dfrac{b+1}{(b-1)^2} \, CV_\alpha^2$	0
Lame (D)	$-\dfrac{b+1}{(b-1)^2} \, CV_\alpha^2$	0

Il apparaît que les teneurs en eau à une cote donnée
suivent une loi normale de distribution, comme le suggèrent
de nombreuses études expérimentales. On notera que la même ana-
lyse effectuée sur les flux de drainage montre que la loi de
distribution d'abord log-normale tend à devenir normale au fur
et à mesure du processus de drainage.

4 - INFLUENCE DE LA VARIABILITE SPATIALE :

L'utilisation des formules (22) et (23) permet d'étu-
dier aisément la sensibilité des processus d'infiltration et
de drainage à l'hétérogénéité de la parcelle. Les expressions
de ε_X et var (X) pour toutes les variables d'intérêt s'obtien-
nent par simple dérivation des fonctions $g(\alpha)$. A titre d'exem-
ple, les figures 8a et 8b présentent l'évolution en fonction
du temps des écarts relatifs entre moyenne stochastique $E\{X\}$
et déterministe $X(m_\alpha)$ correspondant aux flux d'infiltration et
de drainage pour 3 valeurs de coefficient de variation α. Il
apparaît que pour des sols certes fortement non uniformes
($CV_\alpha = 1,43$) mais non rares, comme le montrent diverses études
([10], [11]): les écarts ε_X peuvent atteindre 150% !
Les tableaux III et IV donnent le comportement de ε_X
et var (X) au voisinage de $t = 0$ et pour $t \to \infty$ dans le cas
de l'infiltration et du drainage.

Ils appellent les commentaires suivants :

a) Les valeurs limites de ε_X et var (X) s'expriment toutes en fonction de CV_α^2.

b) Alors que la modélisation déterministe de l'infiltration surestime la solution réelle aux temps initiaux (ε_i et ε_I sont négatifs), elle la sous-estime aux temps longs (ε_i et ε_I sont positifs). Pour une variabilité observée, la sorptivité $A_1^{::}$ influence la variance du flux et de la lame infiltrée aux instants initiaux (effets capillaires prépondérants), alors qu'aux temps longs elle est affectée par la perméabilité à saturation $K_0^{::}$ (effets gravitaires prépondérants). On notera également les limites non finies des var (i) pour (t → 0) et de var (I) pour (t → ∞).

c) Les limites nulles de ε_θ et ε_D pour t → 0 ainsi que les variances correspondantes proviennent du caractère déterministe de la condition initiale (θ_S est constant sur toute la parcelle) imposée dans la modélisation du drainage. Aux temps longs, l'approche déterministe sous-estime teneur en eau et flux de drainage et surestime la lame écoulée à une cote donnée. De plus, les écarts ε_θ, ε_q et ε_D seront d'autant plus élevés que le coefficient b sera petit ; donc que le sol sera plus sableux, toute chose étant égale par ailleurs. Ecart ε_q et variance var (q) pour t → 0 sont finis et indépendants de la cote considérée. Ils sont d'autant plus grand que le sol sera plus hétérogène et plus perméable (pour la variance seule).

d) On notera la cohérence des résultats suivants :

. $\lim\limits_{t \to 0} \varepsilon_q = \lim\limits_{t \to \infty} \varepsilon_i$

. $\lim\limits_{t \to 0} \{var(q)\} = \lim\limits_{t \to \infty} \{var (i)\}$

. $\{var (D)\}_{t=0}$ et $var\{(I)\}_{t \to \infty}$ ont mêmes équivalents.

E. CONCLUSIONS

A la faveur de ces quelques résultats, il est possible de dégager les conclusions suivantes :

1) - L'utilisation de la théorie de la mise en facteur d'échelle des propriétés hydrodynamiques couplée aux équations classiques des transferts hydriques, a permis une modélisation

relativement simple de l'infiltration et du drainage à l'échelle d'une parcelle de un hectare. Le bon accord entre les valeurs expérimentales et numériques montre l'adéquation de ce type de modélisation.

2) - La comparaison entre les solutions déterministes et stochastiques montre que l'approche déterministe est inadéquate pour modéliser les transferts hydriques in-situ, en sol non uniforme puisque la moyenne spatiale des solutions est différente de la solution moyenne qui serait obtenue en considérant des paramètres moyens. Cela remet en cause le concept de milieu poreux uniforme équivalent, déjà mis à mal en hydrogéologie [1] pour les milieux saturés.

3) - L'approche utilisée ici suppose implicitement que les variations spatiales des propriétés du sol sont totalement aléatoires. On notera que l'absence d'autocorrélation entre les observations distantes de 23 m, mise en évidence ici par le semi-variogramme, n'implique pas nécessairement l'indépendance en-deça. En cas de structure spatiale, une approche de type simulation conditionnelle [23] doit alors être envisagée.

LISTE DES PRINCIPAUX SYMBOLES

CV	: coefficient de variation
$D(\theta)$	: diffusivité capillaire $(L^2 T^{-1})$
D	: lame drainée (L)
$E\{X\}$	: espérance mathématique de X
$h(\theta)$	: pression effective de l'eau (L)
i	: flux d'infiltration (LT^{-1})
I	: lame infiltrée (L)
$K(\theta)$	: conductivité hydraulique (LT^{-1})
q	: flux de drainage (LT^{-1})
S	: degré de saturation (θ/θ_S)
t	: temps (T)
t_c	: temps critique (T)
var(X)	: variance de X
W	: propriété hydrodynamique quelconque
X	: variable aléatoire quelconque
z	: profondeur (L)
z_f	: profondeur du front d'infiltration (L)
α	: facteur d'échelle
εX	: écart relatif entre moyennes stochastique et déterministe
θ	: teneur en eau volumique $(L^3 L^{-3})$
θ_n	: teneur en eau initiale $(L^3 L^{-3})$
θ_S	: teneur en eau saturation $(L^3 L^{-3})$

L'indice r correspond au site de mesure.

$\tilde{}$: représente une valeur moyenne d'échelle.

REFERENCES

[1] - FREEZE, R.A., A stochastic-conceptual analysis of one-
       dimensional ground-water flow in nonuniform homogeneous
       media, Water Resour. Res. 11 5 (1975) 725

[2] - RAO, P.S.C., RAO, P.V., DAVIDSON, J.M., Estimation of the
       spatial variability of the soil-water-flux, Soil Sci.Soc.
       Am. J. 41 (1977) 1208

[3] - WARRICK, A.W., MULLEN, G.J., NIELSEN, D.R., Predictions
       of the soil water flux based upon field-measured soil
       Water properties, Soil Sci. Soc. Am. J. 41 (1977) 14

[4] - PECK, A.J., LUXMOORE, R.J., STOLZY, J.L., Effects of spa-
       tial variability of soil hydraulic properties in water
       budget modelling, Water Resour. Res. 13 (1977) 348

[5] - WARRICK, A.W., AMOOZEGAR-FARD, A.A., Infiltration and
       drainage calculations using spatially scaled hydraulic
       properties, Water Resour.Res. 19 (1979) 348

[6] - SMITH, R.E., HEBBERT, R.H.B., A Monte Carlo analysis of
       the hydrologic effects of spatial variability of infil-
       tration. Water Resour. Res. 15 (1979) 419

[7] - LUXMOORE, R.J., SHARMA, M.L., Runoff responses to soil
       heterogeneity : experimental and simulation comparison
       for two contrasting watersheds, Water Resour.Res. 16
       (1980) 675

[8] - RUSSO, D., BRESLER, E., A univariate versus multivariate
       parameter distribution in a stochastic-conceptual analy-
       sis of unsaturated flow, Water Resour.Res. 18 (1982) 483

[9] - NIELSEN, D.R., BIGGAR, J.W., ERH, K.T., Spatial variabili-
       ty of field-measured soil-water properties. Hilgardia 42
       (1973) 215

[10] - WARRICK, A.W., MULLEN, G.J., NIELSEN, D.R., Scaling field-
       measured soil hydraulic properties using a similar media
       Concept, Water Resour.Res. 13 (1977) 355

[11] - SIMMONS, C.S., NIELSEN, D.R., BIGGAR, J.W., Scaling of
       field-measured soil-water properties, Hilgardia 47 (1979)
       77

[12] - SHARMA, M.L., GANDER, G.A., HUNT, C.G., Spatial variabi-
       lity of infiltration in a watershed, J. of hydrol, 45
       (1980) 101

[13] - RUSSO, D., BRESLER, E., Scaling soil hydraulic properties
       of a heterogeneous field, Soil Sci.Soc. Am.J.44 (1980)
       681

[14] - MILLER, E.E., MILLER, R.D., Physical theory for capillary
       flow phenomena, J. Appl. Phys. $\underline{27}$ (1956) 324

[15] - BOULIER, J.F., VAUCLIN, M., More on the flux-concentra-
       tion based solution of constant flux infiltration equa-
       tion II. Stochastic modeling - Soumis à publication dans
       Soil Sci.Soc. Am.J. (1983)

[16] - PHILIP, J.R., Theory of infiltration, Adv.Hydros.$\underline{5}$
       (1969) 215

[17] - LIBARDI, P.L., REICHARDT, K., NIELSEN, D.R., BIGARRE, J.W.,
       Simple field methods forestimating soil hydraulic con-
       ductivity, Soil Sci.Soc. Am.J. $\underline{44}$ (1980) 3

[18] - BROOKS, R.H., COREY, A.T., Hydraulic properties of porous
       media, Hydr.paper $\underline{3}$ (1964), Fort Collins, USA

[19] - HILLEL, D., KRENTOS, V.D., STYLIANOU, Y., Procedure and
       test of an internal drainage method for measuring soil
       hydraulic characteristics in-situ, Soil Sci.$\underline{114}$ (1972)
       395

[20] - VACHAUD, G., DANCETTE, C., SONKO, S., THONY, J.L., Métho-
       des de caracterisation hydrodynamique d'un sol non saturé.
       Application à deux types de sol du Sénégal. Ann.Agron. $\underline{29}$
       (1978) 1

[21] - IMBERNON, J., Variabilité spatiale des caractéristiques
       hydrodynamiques d'un sol du Sénégal. Application au cal-
       cul d'un bilan sous culture. Doctorat 3ème cycle. Univer-
       sité Scientifique et Médicale et Institut National Poly-
       technique de Grenoble, (1981) 152 p.

[22] - VAUCLIN, M., HAVERKAMP, R., VACHAUD, G., Résolution nu-
       mérique d'une équation de diffusion non linéaire. Appli-
       cation à l'infiltration de l'eau dans les sols non saturés.
       Presses universitaires de Grenoble, (1979) 1983

[23] - DELHOMME, J.P., Spatial variability and uncertainty in
       ground water flow parameters. A geostatistical approach,
       Water Resour.Res.$\underline{15}$ (1979) 269

ANALYSE DE COURBES
POTENTIEL MATRICIEL – TENEUR EN EAU
OBTENUES IN SITU
LORS D'UN ESSAI D'IRRIGATION

C. ISBERIE
Centre national d'étude du machinisme
  agricole, de génie rural et des eaux
  et forêts (CEMAGREF),
Aix-en-Provence, France

Abstract–Résumé

ANALYSIS OF THE MATRIX POTENTIAL – WATER-CONTENT CURVES OBTAINED
IN SITU DURING AN IRRIGATION EXPERIMENT.
     The follow-up of an irrigation experiment may afford an opportunity to learn more
about the water behaviour of a soil and its characteristics when neutron and tensiometric
measurements are performed simultaneously. Thus, on the basis of measurements of water
diffusion in the soil during localized irrigation in an orchard using water from the Bas-Rhône-
Languedoc system, the primary objective of which was to analyse the variation in time of the
soil moisture content and water potential as a function of different treatments, it was possible,
by relating these two types of data, to correlate the curves for the matrix potential versus soil
humidity in situ. In spite of certain approximations stemming from the practical measurement
conditions, analysis of the curves obtained shows a variability associated with the heterogeneity
of the various soil layers and the intensity of the drying and rewetting phenomena. The possible
practical consequences (monitoring of irrigation) of these observations are considered.

ANALYSE DE COURBES POTENTIEL MATRICIEL – TENEUR EN EAU OBTENUES
IN SITU LORS D'UN ESSAI D'IRRIGATION.
     Le suivi d'un essai d'irrigation peut donner l'occasion, lorsque sont réalisées conjointement
des mesures neutroniques et tensiométriques, d'obtenir une meilleure connaissance du comporte-
ment hydrique d'un sol et de ses caractéristiques. C'est ainsi qu'à partir de mesures sur la
diffusion de l'eau dans le sol en irrigation localisée, système Bas-Rhône-Languedoc sous verger,
dont l'objectif premier était l'analyse de l'évolution de l'humidité du sol et du potentiel hydrique
au cours du temps en fonction de différents traitements, nous avons pu, en mettant en relation
ces deux types de données, approcher les courbes potentiel matriciel-humidité du sol en place.
Malgré un certain nombre d'approximations résultant des conditions pratiques de mesure,
l'analyse des courbes obtenues montre une variabilité liée à l'hétérogénéité des diverses couches
de sol et à l'intensité des phénomènes de dessèchement et de réhumectation. Les conséquences
pratiques éventuelles (pilotage de l'irrigation) de ces observations sont envisagées.

INTRODUCTION

L'amélioration de la conduite de l'irrigation, quel qu'en soit le système, passe par un meilleur contrôle des flux hydriques dans le sol (1) et/ou de sa disponibilité en eau pour la culture (2). Elle nécessite donc l'utilisation d'appareils mesurant le *potentiel matriciel* de l'eau du sol. Parmi ceux-ci le tensiomètre s'avère être un appareil d'un coût modéré, facile et rapide d'emploi, pouvant être mis en oeuvre par des agriculteurs (2). Or le pilotage de l'irrigation consiste en décisions concernant les dates et modalités d'apports de *volumes* d'eau au sol. La connaissance de la relation potentiel matriciel-teneur en eau volumique peut offrir au pilotage tensiométrique des indications complémentaires pour sa mise en oeuvre. Cependant cette relation varie en fonction du sol, et n'est ni linéaire, ni unique (hystérésis). Par ailleurs les mesures effectuées au laboratoire sur échantillons s'avèrent souvent peu représentatives des propriétés du sol en place (3).

Nous présentons ici les relations observées in situ au cours d'un essai d'irrigation. L'obtention de ces courbes n'était pas l'un des objectifs primitifs de l'essai ; elles ont pu être cependant réalisées grâce d'une part à la lenteur et à l'uniformité des processus de dessèchements et de réhumectation aux profondeurs étudiées, et d'autre part à la régularité des mesures effectuées sur une longue période (13 mois). La méthode utilisée n'a demandé aucun moyen supplémentaire par rapport à l'essai primitif. Ceci présente un intérêt évident lorsque l'on veut pouvoir multiplier des expérimentations sans trop les alourdir, tout en acquérant suffisamment de connaissances relatives au sol pour permettre la généralisation de leurs résultats. Un certain nombre d'objections pourront être faites, que nous nous efforcerons d'examiner pour pouvoir juger de la validité et de l'utilité des courbes obtenues.

MATERIELS ET METHODES

Des mesures en parallèle de teneur en eau volumique à l'aide d'une sonde de profondeur gamma-neutronique (NEA), et de potentiel matriciel, à l'aide de tensiomètres à manomètre Bourdon (Irrometer, $z = 75, 105, 135$ et 165 cm),ou à mercure (Neyrtec, $z = 215$ cm) ont été réalisées pendant 13 mois (juillet
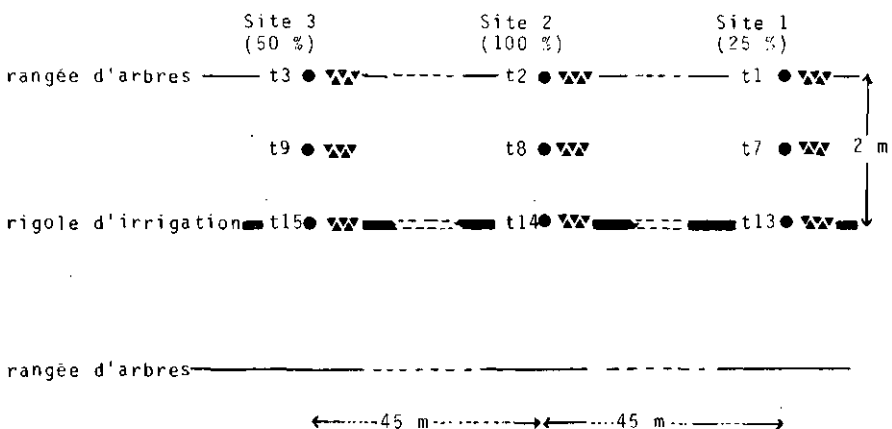
FIG.1. Schéma d'implantation du matériel de mesure.

78 à août 79) à 5 profondeurs, sur 9 emplacements d'une même parcelle, un verger de poiriers irrigué par le système Bas-Rhône-Languedoc. Celui-ci était composé de rigoles divisées en biefs de 5 m de long, situées au milieu de chaque interligne, à 2 m des rangées d'arbres. Les 9 emplacements étudiés étaient répartis sur 3 sites, 1, 2, 3, correspondant à 3 traitements irrigation (25 %, 100 % et 50 % d'une ETP estimée), espacés de 45 m les uns des autres. Chacun des 3 emplacements de mesure d'un site était constitué d'un tube d'accès pour la sonde et de tensiomètres associés situés à une distance de 50 à 80 cm du tube, et se trouvait sous la ligne d'arbres, sous la rigole, ou entre ligne et rigole (4) (fig.1). Le sol est de type alluvial, avec une alternance de couches à texture plus fine (Limon fin) et plus grossière (Limon sableux) (fig. 2). Les profils de densités sèches ont été obtenus avec la sonde gamma-neutronique (fig. 3). Ils traduisent eux aussi l'hétérogénéité verticale du sol. Enfin il existe une nappe de profondeur variable (2,30 à 3,30 m).
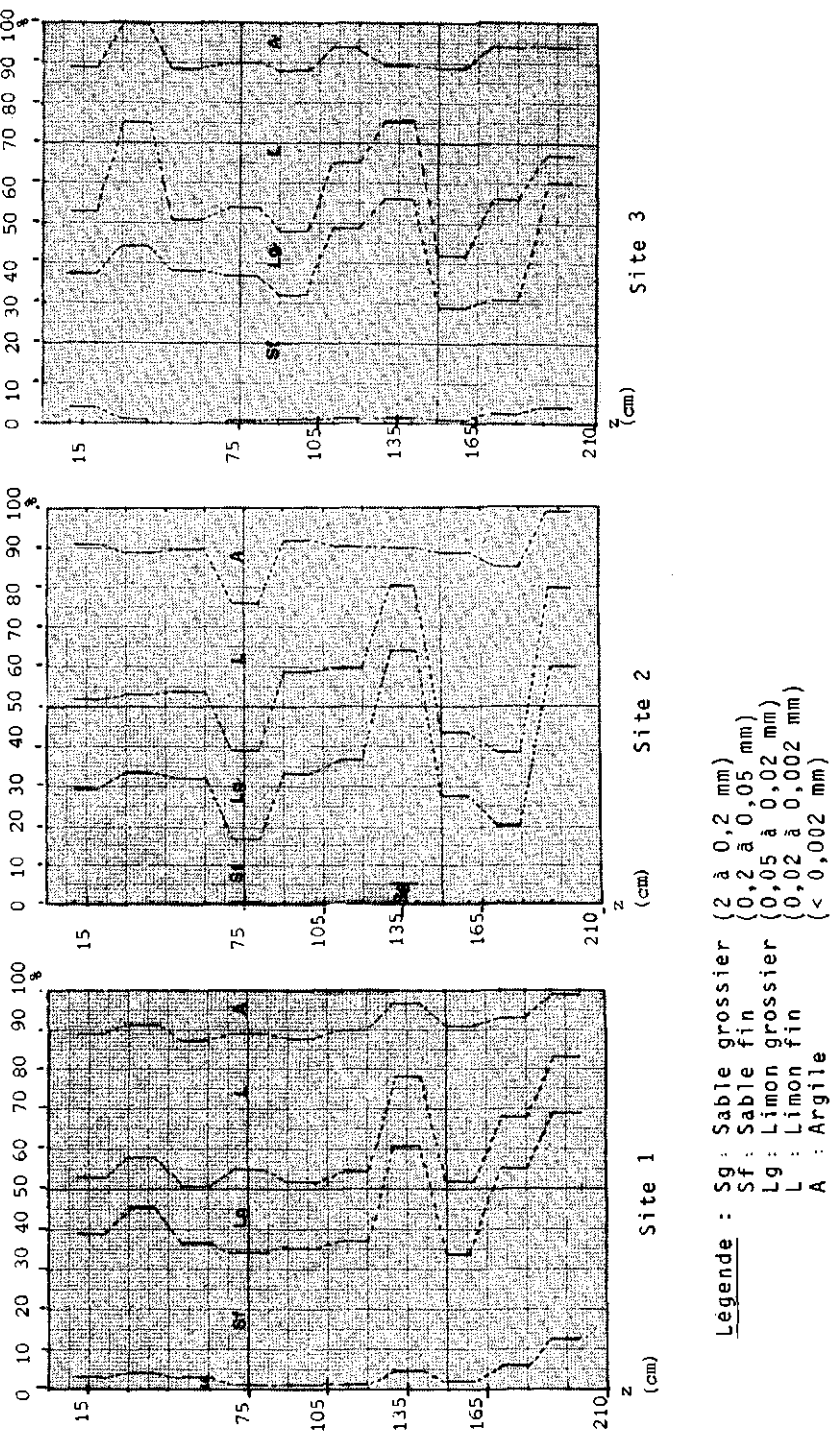
FIG.2. *Profils de textures.*

Légende : Sg : Sable grossier (2 à 0,2 mm)
           Sf : Sable fin   (0,2 à 0,05 mm)
           Lg : Limon grossier (0,05 à 0,02 mm)
           L : Limon fin   (0,02 à 0,002 mm)
           A : Argile   (< 0,002 mm)
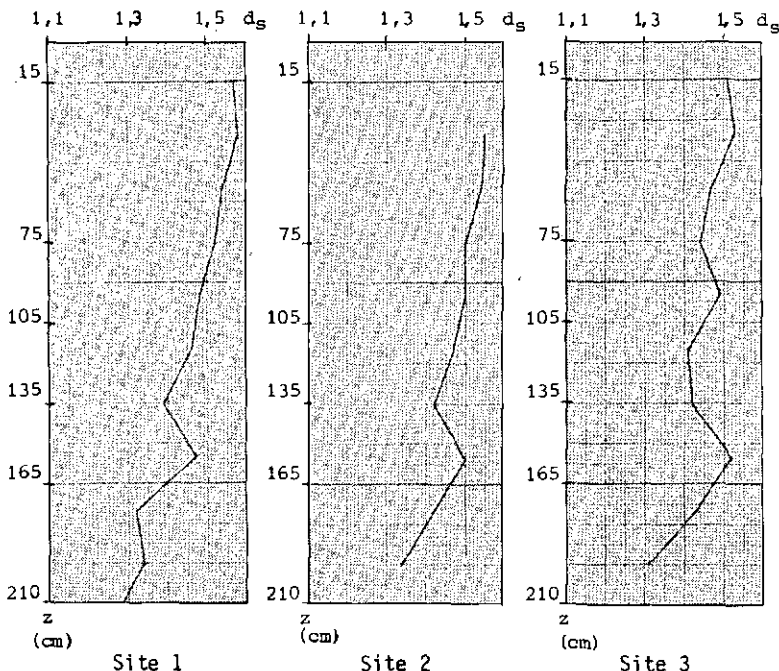
FIG.3. *Profils de densités sèches.*

        L'étalonnage de la sonde a été réalisé à
l'aide de la méthode développée par NORMAND (5), en
adoptant un seul faisceau d'étalonnage par tube.
Nous avons vérifié en assimilant à des droites les
courbes d'étalonnages sur la gamme allant de 10 à
40 points d'humidité volumique (r^2 = 0,998) que
l'erreur due à l'hétérogénéité du sol ne dépassait
pas 2 points d'humidité volumique en ordonnée à
l'origine, et 8 % au maximum (tube 1, z = 215 cm)
sur la pente, soit 1,6 points pour 20 points d'humi-
dité, représentant l'ordre de grandeur des variations
maximales d'humidité étudiées.
        Les relevés tensiométriques étaient effec-
tués tous les 4 ou 5 jours, et neutroniques tous
les 14 jours environ. L'observation des courbes de
potentiel et de teneur en eau en fonction du temps
a permis de mettre en évidence trois processus prin-
cipaux d'évolution : dessèchement du sol de juillet-
août ou septembre (selon le traitement irrigation) à
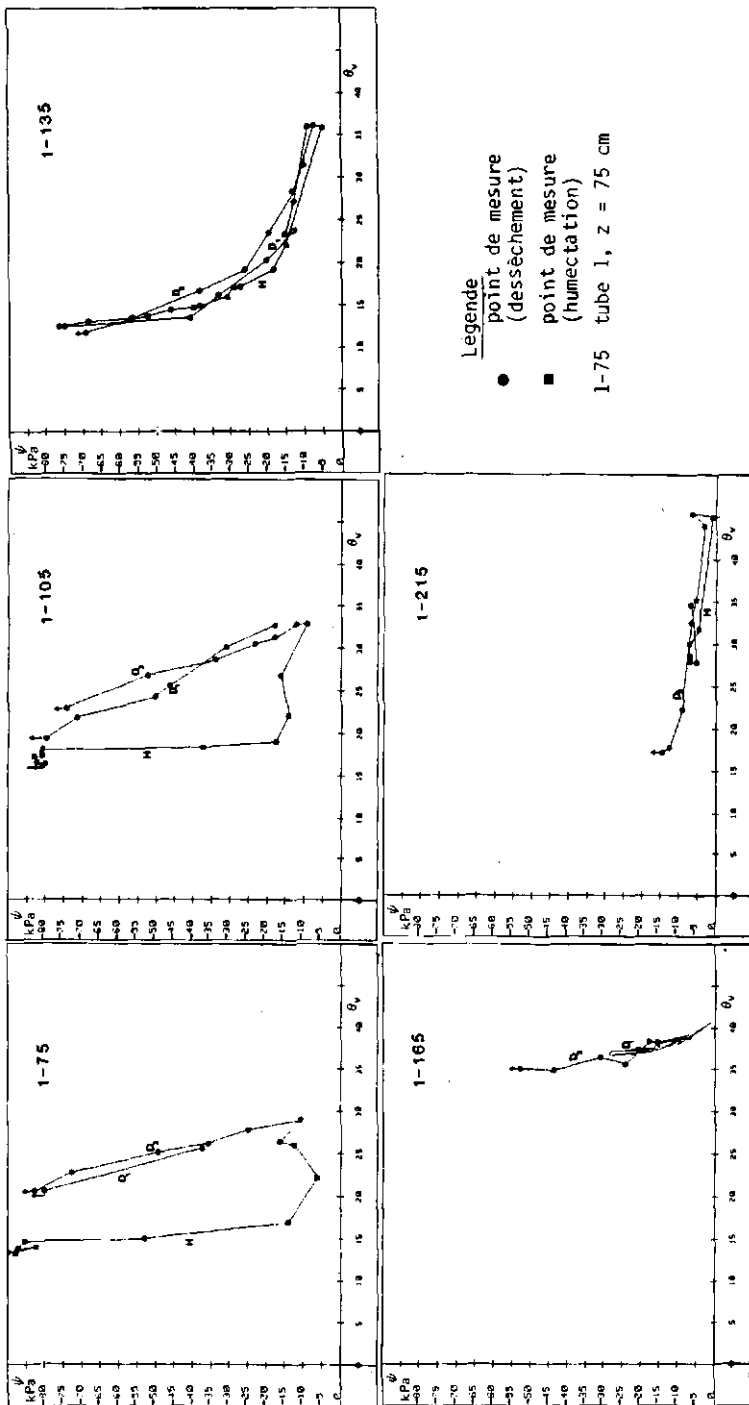
FIG.4.   Courbes potentiel matriciel-teneur en eau à cinq profondeurs pour le tube 1.

octobre 78, réhumectation de novembre 78 à février-
mars 79, nouveau dessèchement d'avril à juillet [4]
Ces processus étaient suffisamment lents, même pour
l'horizon étudié le plus haut (z = 75 cm),et prolongés
pour pouvoir tracer des courbes reliant le potentiel
matriciel et la teneur en eau (fig. 4 et 5) à diverses
profondeurs et souvent sur l'ensemble du domaine cou-
vert par le tensiomètre (0 à -80 kPa). De plus, même
si 14 jours séparent deux points de mesure consécutifs
sur les courbes, on peut vérifier la régularité et
l'univocité des processus grâce à l'existence de
mesures tensiométriques plus rapprochées dans le
temps. Par ailleurs la limite de fonctionnement des
tensiomètres ayant été vérifiée avant leur mise en
place (ainsi que les origines de ceux à manomètre
Bourdon), on a pour le tracé convenu d'éliminer les
points ultérieurs à l'obtention de cette limite en
dessèchement, tant que la teneur en eau continuait
à décroître. Le tracé n'est repris que lorsque le
processus de réhumectation est nettement amorcé
(θ augmente régulièrement) et que l'on a de nouveau
atteint le domaine de mesure du tensiomètre.

RESULTATS ET DISCUSSION

        Compte tenu de l'ensemble des remarques ci-
dessus, nous avons pensé qu'il était intéressant de
présenter les courbes brutes obtenues en reliant
point par point les mesures effectuées, ce qui permet
non seulement d'observer l'évolution au cours du temps
des processus individualisés de dessèchement et
d'humectation et leur éventuelle répétabilité (dessè-
chement), mais également de juger de l'intérêt de
résultats de terrain obtenus sans traitement parti-
culier.
        On a obtenu ainsi une quarantaine de courbes
$\psi(\theta)$. Nous n'en présentons ici qu'une partie.

        1) Analyse pour un tube (1) des courbes
obtenues aux diverses profondeurs (fig. 4) : on note
une forte hétérogénéité verticale, liée aux variations
de texture. D'une part les pentes des courbes en
fonction des gammes d'humidité sont très différentes
(on peut opposer les courbes 1-75, 1-105, des couches
de limon fin aux courbes 1-135 et 1-215 correspondant
au limon sableux). Par ailleurs, on observe aux hori-
zons 75 et 105 un phénomène d'hystérésis marqué. Les
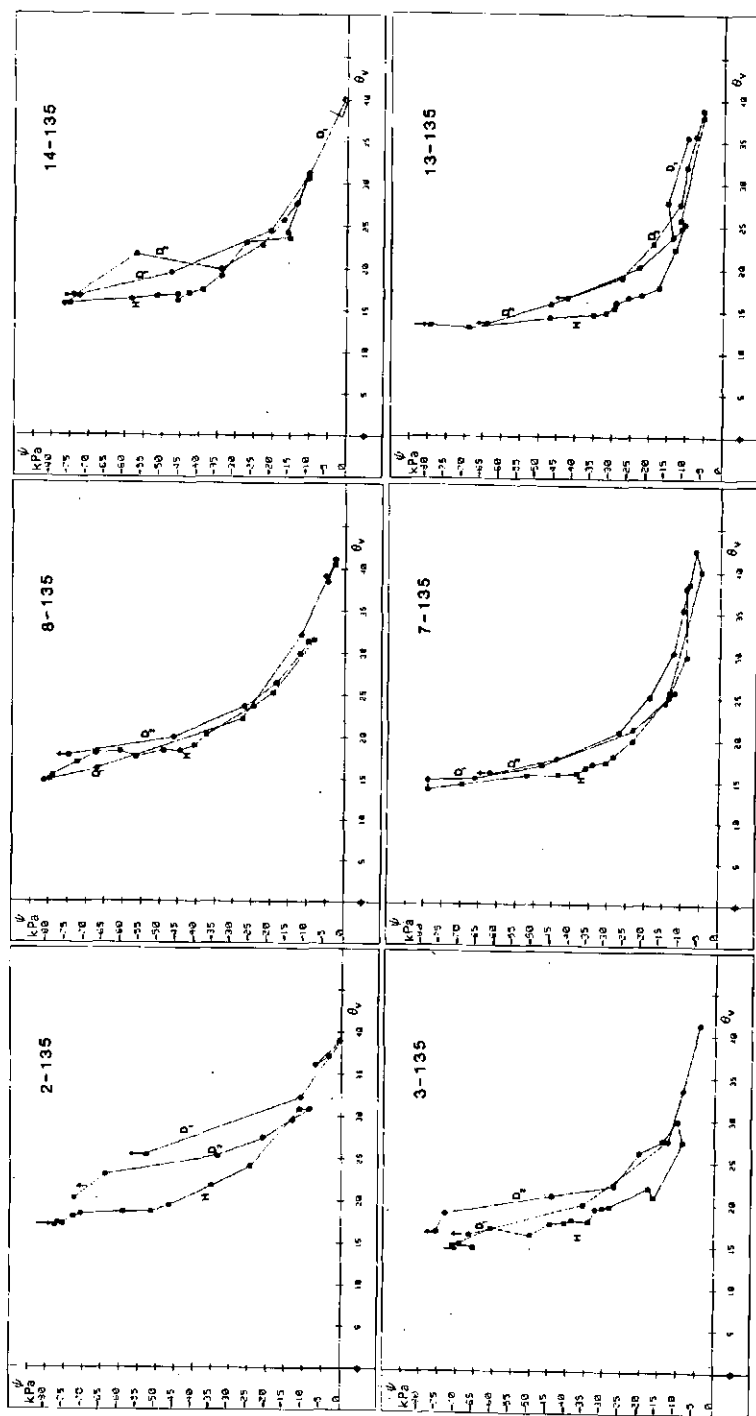
FIG.5. Courbes potentiel matriciel-teneur en eau obtenues à la profondeur z = 135 cm sur les 3 sites (même légende que FIG.4).

mesures effectuées lors des deux processus de dessèche-
ment se superposent bien, ce qui confirme leur vali-
dité. Quant aux fortes pentes constatées en réhumecta-
tion, on peut leur reprocher de n'être obtenues qu'à
partir de 3 points de mesure. En fait, la variation
apparemment brusque de ψ se déroule sur 15 jours (75)
à 2 mois (105), période pendant laquelle θ n'a varié
que peu et où l'on dispose de l'évolution de ψ,
mesuré tous les 4-5 jours. L'obtention de points sup-
plémentaires en multipliant les mesures de sonde à
neutrons n'aurait pas apporté une plus grande précision
à ces courbes. Ainsi l'hystérésis observée correspond
bien à un phénomène réel sur le terrain. A la profondeur
135, au contraire, l'hystérésis n'apparaît pas, malgré
les faibles humidités atteintes. On peut mettre en
cause non seulement la texture plus grossière du sol,
mais également le fait que dans cette zone plus profonde
on n'a pas atteint de potentiel matriciel très faible
(les tensiomètres n'ont pas "décroché") : or le point
de départ de la réhumectation conditionne l'importance
de l'hystérésis (6), qui, même à sol identique, serait
donc plus faible à z = 135 qu'à z = 75 ou 105 où ψ
atteint probablement des valeurs très faibles (non
mesurables à l'aide du tensiomètre) avant la réhumec-
tation.

        Enfin la comparaison des courbes z = 75,
105, et 165, montre un décalage vers les fortes teneurs
en eau quand la densité du sol diminue, pour des
textures proches.

        2) Comparaison des courbes obtenues à une
même profondeur (z = 135) aux divers emplacements
(fig. 5) : les diverses courbes se superposent assez
bien, avec parfois un décalage de 2 à 3 points pour θ
(problème d'étalonnage de la sonde ?). Sur le site 2,
traitement le plus irrigué, on observe à certaines
dates, en dessèchement, un décalage des courbes qui
pourraient être causé par la teneur en eau élevée de
la couche immédiatement sous-jacente et son incidence
sur les mesures réalisées à la sonde à neutrons (sphère
d'influence). Enfin, en réhumectation, pour laquelle
on dispose de beaucoup de mesures, on observe une
homogénéité dans la variation de ψ en fonction du
temps, même sur des mesures rapprochées, qui paraît
meilleure que celle obtenue pour les variations de
teneur en eau sur la plupart des courbes. Ce phénomène
est, lui aussi, probablement imputable à la sphère
d'influence de la sonde à neutrons, dans cette couche
de sol très différente de ses voisines (fig. 2 et 3).

Ceci peut être rapproché des constatations de
MOUTONNET et al. (7) sur sol d'alluvions fluviatiles,
selon lesquelles l'hétérogénéité de mesures tensiomé-
triques sur le terrain apparaît moindre que celle des
mesures de teneur en eau, les premières paraissant,
quoique très ponctuelles, mieux adaptées à la gestion
des irrigations. Il faut cependant remarquer que la
réhumectation suivie ici est due en grande partie à
des remontées hydriques à partir de la nappe (rééqui-
librage des profils de potentiels), l'automne 78 ayant
été peu pluvieux. Par conséquent, on n'avait que peu
à craindre de phénomène d'emprisonnement d'air dans le
sol (à partir d'une humectation provenant de la sur-
face) qui aurait pu perturber les mesures de potentiel.

    3) Conclusions pratiques sur la méthode
utilisée
         En résumé, on peut constater qu'un certain
nombre d'éléments qui auraient pu constituer des
obstacles à l'établissement des courbes n'ont pas
semblé présenter d'inconvénient majeur :
         - en ce qui concerne la *localisation des
appareils*, on notera : la possibilité d'effectuer des
mesures même sous une rigole d'irrigation, en sol non
gonflant et à condition de réaliser une bonne mise en
place du matériel ;
              . l'absence de perturbation par les racines
des arbres environnants (enracinement atteignant
1m40 environ),
              . le fait que l'écartement entre tensio-
mètres et tube neutronique n'est pas apparu comme une
cause d'erreur, dans la mesure où leurs distances aux
zones d'apport d'eau (rigole d'irrigation, nappe, sur-
face du sol) sont égales,
              . l'existence de quelques anomalies liées
aux différences de volumes de mesure concernés par
les mesures tensiométriques et neutroniques,pour des
couches de sol assez fines;
         - en ce qui concerne le *matériel*, on remar-
quera le bon fonctionnement des tensiomètres à mano-
mètre Bourdon, qui n'ont posé aucun problème parti-
culier pendant 15 mois d'utilisation, et dont la
précision (± 1 cbar) est apparue largement suffisante
ici.(De plus ils n'ont causé aucune gêne au travail
de l'agriculteur). La bonne reproductivité des courbes
(superposition) de dessèchement d'une année sur l'autre
montre l'absence de dérive notable de l'ensemble du
matériel utilisé ;

- par ailleurs, les décalages (2 à 3 points
de teneur en eau) entre certaines courbes, peut-être
dus à des problèmes d'étalonnage de sonde au départ
(dates différentes d'installation des tubes), n'ont
pas eu d'incidence sur les formes (pentes) de ces
courbes (tube 1 et 7 voisins, z = 135). Or dans la
pratique de l'irrigation ce sont les variations de la
teneur en eau plus que sa valeur absolue qui importent.
Les courbes obtenues en un emplacement sont donc uti-
lisables telles quelles, et la confusion de l'ensemble
des points d'emplacements voisins pour une "courbe
moyenne" n'aboutirait qu'à une perte d'information sur
les pentes ($\Delta\psi/\Delta\theta$) tout en faisant apparaître une
dispersion importante des teneurs en eau.
        Quant à l'ensemble des résultats, on notera
que,sans travail de mesure supplémentaire,on a obtenu
des courbes :
        . qui couvraient toute la gamme de mesure du
tensiomètre,
        . en atteignant des teneurs en eau volumiques
relativement faibles (qu'il aurait fallu beaucoup de
temps pour atteindre, dans la phase de redistribution
d'un essai de drainage interne [8]).
        Enfin les points de départ de certaines
courbes de dessèchement (z = 135, z = 215), ou d'hu-
mectation (z = 75, 105) peuvent laisser penser que ces
courbes se rapprochent des branches principales des
courbes d'hystérésis, d'autant plus que les phénomènes
suivis étaient lents . Elles sont donc caractéristiques
des couches de sol concernées : on constate sur la
parcelle étudiée une forte hétérogénéité verticale,
avec d'importantes différences entre des points situés
à 30 cm l'un de l'autre sur une verticale, qui s'oppose
à une relative homogénéité horizontale, entre des points
situés à 45 ou 90 m l'un de l'autre.

        4) Applications éventuelles au pilotage de
l'irrigation par tensiomètres
        Très souvent, les méthodes de pilotage par
tensiomètres font appel à la notion de "seuil" de dé-
clenchement et parfois d'arrêt des arrosages, défini
en valeur absolue [9], [10], ou relative par rapport
à des valeurs enregistrées précédemment [2]. Nous
avons pu constater sur un même terrain la variabilité
de la relation $\psi(\theta)$, qu'il s'agisse de l'hystérésis
ou des pentes des courbes pour une même gamme d'humidité.
Or ces dernières peuvent donner des indications sur le
choix des valeurs de seuil à adopter en fonction de la
texture : en dessèchement, quand $|\Delta\psi/\Delta\theta|$ est faible,

peu de risque du décrochement rapide du tensiomètre,
jusqu'à une limite plus ou moins nette où $|\Delta\psi/\Delta\theta|$
devient élevé. Quant à l'hystérésis, pour éviter qu'une
même valeur de seuil de potentiel matriciel ne corres-
ponde à des valeurs de teneurs en eau volumiques très
différentes, avec les conséquences que cela peut
entraîner en sur -ou sous- irrigation, on peut
conseiller:

        .soit de ne plus utiliser un tensiomètre
qui a "décroché" pour le pilotage et de se reporter
par exemple à un tensiomètre plus profond (2), on
évite ainsi de commencer la réhumectation à partir
d'un point de très faible potentiel et de se retrou-
ver sur des courbes présentant une forte hystérésis
par rapport à celle du premier dessèchement;

        .soit de ne réutiliser un tel tensiomètre
qu'après une réhumectation importante, ayant permis
de retrouver approximativement la teneur en eau
initiale du sol (ce qui ne sera pas forcément souhai-
table).

        En définitive, pour le pilotage de l'irri-
gation, si la connaissance de la relation $\psi(\theta)$ ne
s'avère pas indispensable, -une bonne connaissance
du profil de texture du sol étant de toute façon for-
tement conseillée-, elle apporte cependant des infor-
mations sur :

        - la variation de teneur en eau volumique
(à comparer aux volumes d'eau apportés par l'irriga-
tion ou la pluie) correspondant à la gamme des poten-
tiels matriciels couverte par le tensiomètre;

        - les risques de désarmorçage plus ou moins
rapide d'un tensiomètre, en fonction du seuil de dé-
clenchement choisi et de sa localisation.

        Si le pilotage est basé sur le contrôle des
directions de flux dans le sol (1) ces informations
restent également utiles.

CONCLUSION

        La mise en relation de données tensiométriques
et humidimétriques obtenues simultanément lors d'une
expérimentation sur le terrain peut fournir, comme
dans le cas étudié, un supplément d'information sans
que ne soient mis en oeuvre de moyens supplémentaires.
Cette information peut permettre de préciser les
modalités de pilotage de l'irrigation par tensiomètres,
et aider à la généralisation des essais entrepris dans

cet objectif ou à d'autres fins. Quelques précautions préliminaires permettent de l'améliorer :

.localisation des mesures réalisées en parallèle pour obtenir des processus lents et prolongés, ou au contraire décrire les dessèchements et réhumectations rapides successifs consécutifs à des irrigations fréquentes (éviter aussi les couches trop fines pour lesquelles la discrimination verticale de la sonde n'est pas suffisante, etc...),

.choix de la fréquence des mesures neutroniques (surveillance de l'évolution des courbes).

Il apparaît donc possible et souhaitable, dans des essais mettant en oeuvre la tensiométrie et l'humidimétrie neutronique, et sans trop les alourdir, d'envisager dès le départ la quête possible de cette information dans le protocole expérimental.

LISTE DES SYMBOLES OU ABREVIATIONS

ETP   évapotranspiration potentielle

θ_v teneur en eau volumique (donnée en "point", ou %)

ψ potentiel matriciel (en kPa)

z   profondeur (en cm)

REFERENCES

[1] STREUTKER, A., Tensiometer-controlled medium frequency topsoil irrigation: A technique to improve agricultural water management, Water SA 4 3 (1978) 134.

[2] PEYREMORTE, P., Des tensiomètres pour améliorer la conduite des arrosages, Perspectives agricoles 67 (1983) 42.

[3] POULOVASSILIS, A., «Soil water properties of a layered soil determinated in situ», Isotope and Radiation Techniques in Soil Physics and Irrigation Studies 1973 (C.R. Coll. Vienne, 1973), AIEA, Vienne (1974) 205.

[4] ISBERIE, C., ROUQUIER, F., Influence de diverses modalités d'irrigation sur la mobilisation des ressources en eau naturelles, C.R. de recherche DGRST, CEMAGREF (1978).

[5] NORMAND, M., «Méthode d'étalonnage d'un humidimètre à neutrons utilisant les mesures de densité du densimètre gamma associé», Isotope and Radiation Techniques in Soil Physics and Irrigation Studies 1973 (C.R. Coll. Vienne, 1973), AIEA, Vienne (1974) 53.

[6] VACHAUD, G., THONY, J.L., Hysteresis during infiltration and redistribution in a soil
     column at different initial water contents, Water Resour. Res. 7 1 (1971) 111.

[7] MOUTONNET, P., BRANDY-CHERRIER, M., Possibilité d'utilisation des tensiomètres
     pour l'automation de l'irrigation, Plant Soil 59 (1981) 335.

[8] HILLEL, KRENTOS, STYLIANOU, Procedure and test of an internal drainage method
     for measuring soil hydraulic caracteristics in situ, Soil Sci. 114 5 (1972) 395.

[9] ROULOT, D., VILLEMIN, P., MARINI, P., JOURDAN, O., Déclenchement automatique
     de l'irrigation à partir de données tensiométriques ou climatiques, Bull. GFHN 8 (1981).

[10] MOUTONNET, P., Un système d'irrigation automatique des cultures: principe et
     simulation théorique, Agr. Meteorology 20 (1979) 25.

FIELD METHODS FOR STUDYING SOIL MOISTURE REGIMES AND IRRIGATION PRACTICES IN CLAY SOILS

J. BOUMA
Netherlands Soil Survey Institute (STIBOKA),
Wageningen, Netherlands

Abstract

FIELD METHODS FOR STUDYING SOIL MOISTURE REGIMES AND IRRIGATION
PRACTICES IN CLAY SOILS.
   Characterization of water flow through swelling clay soils with macropores ("cracks")
requires special techniques because these soils are not isotropic and homogeneous as required
by standard flow theory. The techniques should preferably be rapid and inexpensive to allow
applications in the field. Three experimental techniques, which were recently developed at the
Netherlands Soil Survey Institute, are discussed. The measure: (i) vertical and horizontal K_{sat} in
a gympsum-covered cube of soil which is carved out in situ (the cube method); (ii) the K_{unsat} near
saturation down to pressure heads of about −15 cm by determining fluxes through a series
of crusts and the associated negative pressure heads below the crusts (the crusts test); and
(iii) short-circuiting, which is the preferential movement of free water along vertical macropores
in unsaturated soil, by applying sprinkling irrigation to large, undisturbed cores. In addition,
three examples are discussed whereby soil morphological field data are used for simulation models
which characterize soil moisture regimes of clay soils. These examples cover: (i) the effect
of horizontal cracks on upward unsaturated flow; (ii) infiltration of sprinkling irrigation in
a cracked clay soil; and (iii) ponded infiltration of water in a clay soil with worm channels.

1. INTRODUCTION

   Moisture regimes in clay soils are difficult to characterize because the porous
system is constantly changing, owing to processes of swelling and shrinking,
following wetting and drying of the soil. Large pores, such as shrinkage cracks,
have a profound effect on patterns of water movement, particularly when clay
soils are moist or dry. But preferential flow patterns may also occur under
wet conditions after complete swelling. Bouma et al. [1] demonstrated preferential
movement of water along small cracks in a clay soil that had been saturated for
several months. Rapid downward flow of free water through vertical cracks in
moist or dry clay soils ("short-circuiting") results in very heterogeneous patterns
of wetting during irrigation or natural rainfall. Surface soil is poorly wetted as
water moves rapidly downwards to the subsoil [2, 3]. The occurrence of horizontal
cracks strongly inhibits the upward movement of water in unsaturated soil from

the water table to the root zone. This phenomenon explains abrupt changes in moisture content with depth, which are observed in many clay soils during the growing season [4].

Soil physical methods for studying soil moisture regimes and irrigation practices, are based on Darcy-type flow theory which is presented in many current soil physical text books.

The occurrence of heterogeneous flow patterns in clay soils, as broadly described above, does not allow the use of classical flow concepts which assume the presence of a homogeneous, non-swelling porous medium (e.g. Klute [5], Beven and Germann [6]). The question regarding which procedure should be followed in clay soils is complex and only some aspects can be discussed. Implications for selection procedures of soil physical methods to be applied in clay soils, have already been discussed elsewhere [7]. This paper broadly describes four field methods for studying water movement in clay soils. Reference is made to more specific publications for more details. These methods were developed at the Netherlands Soil Survey Institute.

2.   METHODS

Four methods are discussed by describing the procedures involved and by suggesting the context in which the methods should be applied. The first two methods deal with saturated and very wet soil, the third is used in dry or moist soil, and the fourth uses morphological data for flow models. Reference is made to more detailed publications (e.g. Bouma [8]).

2.1. The cube method for measuring K_{sat}

Measurement of K_{sat} in clayey soils with large natural aggregates ("peds") presents the following problems: (i) smearing of the walls of bore-holes may yield unrealistically low K_{sat} values for the auger-hole method, which are in any case an undefined mixture of K_{sat} (hor) and K_{sat}(vert); (ii) small samples give poor results because of unrepresentative large-pore continuity patterns (e.g. [9]); and (iii) water movement occurs only along some pores which occupy less than 1% by volume [1]. These pores can be easily disturbed by compaction which may occur when sampling cylinders are pushed into the soil.

The cube method [10] avoids these problems and uses a cube of soil (25 cm × 25 cm × 25 cm) which is carved out in situ and encased in gypsum on four vertical walls (Fig.1). First, the K_{sat} (vert) is measured by determining the flux leaving the cube while a shallow head is maintained on top. Next, the cube is turned 90°. The open surfaces are closed with gypsum and the new upper and lower surfaces are exposed. Again, a K_{sat} is measured which now represents the K_{sat} (hor) of the soil in situ.
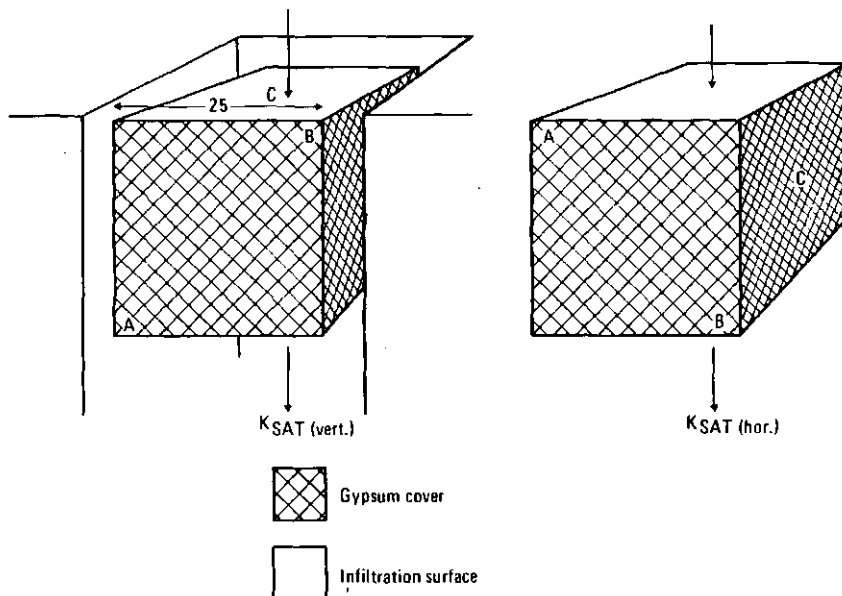
FIG.1.   The cube method for measuring K_{sat} (vertical) and K_{sat} (horizontal) in a large, undisturbed block of soil that is encased in gypsum.

2.2. The crust test for measuring K near saturation

Non-steady-state methods, which are widely used to measure K_{unsat}, are not suitable to obtain K values near saturation in all soils, in the range h = 0 cm to, say, h = −15 cm. These values are particularly relevant for describing water flow in clay soils with continuous macropores ("cracks"). In these soils there is a strong drop of K upon desaturation owing to emptying of the macropores [11]. Again, very large samples are needed to obtain representative results. The cube method can be extended to provide K_{unsat} data near saturation. This procedure represents a version of the crust test [12–14]. Two tensiometers are placed about 2 and 4 cm below the surface of infiltration, which is covered by a series of crusts, composed of mixtures of sand and quick-setting cement (Fig.2) [15]. Earlier, the crust test used gypsum but this may dissolve too rapidly. Dry sand and cement are thoroughly mixed, water is applied and a paste is formed which is applied as a 0.5 to 1 cm thick crust on top of the cube. The crust, which has perfect contact with the underlying soil because of the application method, hardens within 15 minutes. Light crusts (5 to 10% of cement by volume) induce pressure heads (h) near saturation and relatively high fluxes. Heavier crusts (20% cement and more) induce lower h values and fluxes. These fluxes, when steady, are equal to K_{unsat}
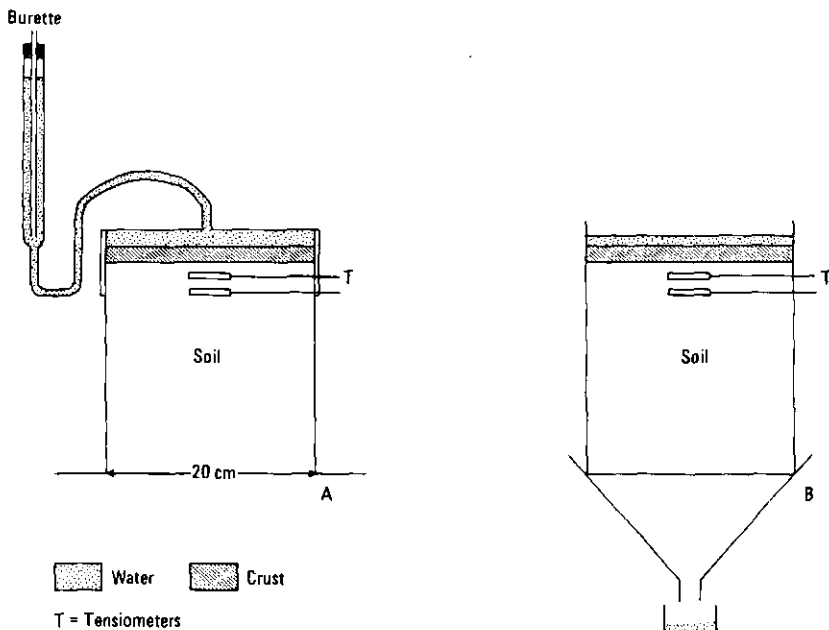
FIG.2.   The crust test for measuring K_{unsat} near saturation by monitoring fluxes through a series of surface crusts and corresponding negative pressure heads in subcrust soils.

at the measured sub-crust h value. Of course, sub-crust h values can never be lower than equilibrium values dictated by the height of the cube. Fluxes are measured as outflow rates from the cube (Fig.2B). Cylinders with soil can also be used and inflow rates can be measured rather than outflow rates by using cylinder-infiltrometers with a Mariotte device [16] (Fig.2A).

2.3. Measurement of short-circuiting

Irrigation of dry, cracked clay soils presents problems because much of the applied water may rapidly disappear into the subsoil, following vertical cracks of root- and worm-channels which are continuous up to the soil surface. As a result, the bulk of the soil between the cracks is hardly wetted or leached (relevant in saline soils), and surface-applied fertilizers and pesticides may rapidly move beyond rooting depth. Downward movement of "free" water along the walls of continuous macropores in unsaturated soil has been called short-circuiting [2, 4]. Short-circuiting can be measured by using large undisturbed cores of surface soil with a height that is equal to rooting depth [17] (Fig.3). For Netherlands conditions in heavy clay soils, cylinders are used with a height and diameter of 20 cm. These
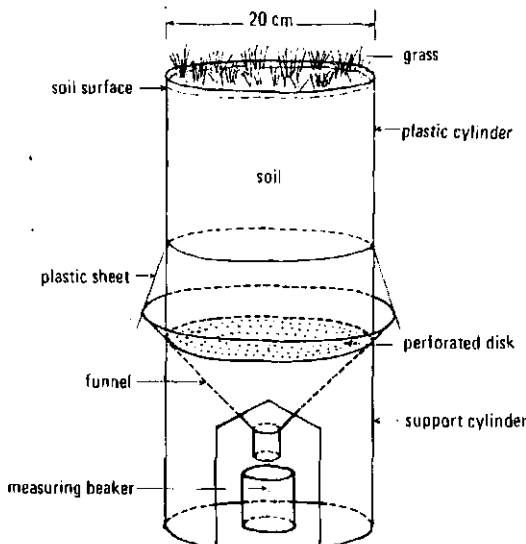
FIG.3. Field apparatus to measure short-circuiting in large cores by monitoring outflow during sprinkling irrigation.

cores include the soil surface with grass, which is closely cropped. The cores are placed in the path of a spraying gun in the field which is commonly used for sprinkling irrigation. In general, sprinkling conditions should correspond to local practices. The mass of the soil-filled cylinder is determined before and after sprinkling and the stove-dry mass is measured at the end, thus allowing calculation of physical constants such as bulk density and moisture contents. Sprinkling intensities and duration should be measured independently. The volume of water that leaves the column is measured as a function of time, thus allowing an estimate of short-circuiting which can be expressed as a percentage of the applied quantity of water. Many measurements can be made in a short time and the effects of using different sprinkling rates of different durations can be easily evaluated. Thus, irrigation efficiencies can be improved because movement of water beyond the root zone often presents a loss of precious irrigation water and surface-applied chemicals.

3.   USE OF SOIL MORPHOLOGY IN FLOW MODELS FOR CRACKED SOIL

Computer simulation models are available for characterizing soil moisture regimes. However, soils with continuous, large pores are difficult to model by using the standard flow theory, as was demonstrated in Section 2.3. We have

obtained good simulation results for water regimes in clay soils by using the
traditional (sand) models for the soil matrix only and by defining the effect of
cracks and other large soil pores in terms of boundary conditions for the overall
flow system. These boundary conditions are defined from morphological
observations, using dyes and gypsum to define flow patterns. Bouma and
De Laat [4] used methylene blue to stain continuous air-filled horizontal cracks
in a clay soil at various moisture contents. The stained area increases at decreasing
moisture contents owing to further opening of the cracks upon drying of the
soil. Air-filled horizontal cracks have a strongly impeding effect on upward
unsaturated flow of water from the water table to the root zone. Using the
staining test, a K curve could be defined which allowed independent prediction
of upward flux densities in a heavy clay soil.

Hoogmoed and Bouma [3] used sprinkling irrigation, with methylene blue
in water, to show infiltration patterns in cracked clay soil. These consisted of
the band on vertical pedfaces ("the contact area") occupying only approximately
2% of the total vertical surface area of the peds. Thus, little lateral absorption
of water into the peds could occur and the water (with solutes) reached a great
depth in a short time. Bouma et al. [18] simulated ponded infiltration of water
in a soil with large, vertical worm channels. Steady infiltration rates into individual
channels were measured and were used to calculate ponding times for the entire
soil, including soil between the channels. The number of channels per unit
horizontal area, to be obtained by a morphological count, is crucial for
estimating these ponding times. The simulation cannot be made without such
morphological observations. A similar conclusion can be reached for the
two other examples discussed earlier, referring to the count of stained horizontal
planes and to the contact area.

REFERENCES

[1] BOUMA, J., JONGERIUS, A., SCHOONDERBEEK, D., Calculation of saturated hydraulic
     conductivity of some pedal clay soils using micromorphometric data, Soil Sci. Soc. Am. J.
     43 (1979) 261.

[2] BOUMA, J., DEKKER, L.W., A case study on infiltration into dry clay soil. I. Morpho-
     logical observations, Geoderma **20** (1978) 27.

[3] HOOGMOED, W.B., BOUMA, J., A simulation model for predicting infiltration into
     cracked clay soil, Sci. Soc. Am. J. **44** (1980) 458.

[4] BOUMA, J., De LAAT, P.J.M., Estimation of the moisture supply capacity of some
     swelling clay soils in the Netherlands, J. Hydrol. **49** (1981) 247.

[5] KLUTE, A., The determination of the hydraulic conductivity and diffusivity of unsaturated
     soil, Soil Sci. **113** (1972) 264.

[6] BEVEN K., GERMANN, P., Macropores and water flow in soils, Water Resour. Res. **18**
     (5) (1982) 1311.

[7]   BOUMA, J., Use of soil survey data to select measurement techniques for conductivity,
      Agric. Water Manage. 1983 (in press).
[8]   BOUMA, J., Soil morphology and preferential flow along macropores, Agric. Water
      Manag. 3 (1981) 233.
[9]   BOUMA, J., Field measurement of soil hydraulic properties characterizing water move-
      ment through swelling clay soils, J. Hydrol. 45 (1980) 149.
[10] BOUMA, J., DEKKER L.W., A field method for measuring the vertical and horizontal
      K_{sat} of clay soils above the water table, Soil Sci. Soc. Am. J. 45 (1981) 662.
[11] BOUMA, J., Measuring the hydraulic conductivity of soil horizons with continuous
      macropores, Soil Sci. Soc. Am. J. 46 (1982) 438.
[12] BOUMA, J., HILLEL, D.I., HOLE, F.D., AMERMAN, C.R., Field measurement of
      unsaturated hydraulic conductivity by infiltration through artificial crusts, Soil Sci. Soc.
      Am Proc. 35 (1971) 362.
[13] BOUMA, J., DENNING, J.L., Field measurement of unsaturated hydraulic conductivity
      by infiltration through gypsum crusts, Soil Sci. Am. Proc. 36 (1972) 846.
[14] BAKER, F.G., Factors influencing the crust test for in situ measurement of hydraulic
      conductivity, Soil Sci. Soc. Am. J. 41 (1977) 1029.
[15] BOUMA, J., BELMANS, C., DEKKER, L.W., JEURISSEN, W.J., Assessing the suitability
      of soils with macropores for subsurface liquid waste disposal, J. Environ. Qual. (in press).
[16] BOUMA, J., Soil survey and the study of water in unsaturated soil, Soil Survey Paper 13,
      Soil Survey Institute, Wageningen (1977).
[17] BOUMA, J., DEKKER, L.W., Van MUILWIJK, K., A field method for measuring short
      circuiting in clay soils, J. Hydrol. 52 (1981) 347.
[18] BOUMA, J., BELMANS, C., DEKKER, L.W., Water infiltration and redistribution in a
      silt loam soil with vertical worm channels, Soil Sci. Soc. Am. J. 46 (1982) 917.

CHARACTERIZATION OF FIELD SOILS: WATER QUALITY AND SALT-AFFECTED SOILS

(Sessions 3 and 4)

Chairman (Session 3)

I. P. ABROL
India

Chairman (Session 4)

G. VACHAUD
France

INTERPRETATION MATHEMATIQUE ET PHYSIQUE DU TRANSFERT DE PESTICIDES MARQUES DANS LES SOLS NON SATURES EN EAU
Exemples d'application[†]

Sylvia GASPAR-DAUTREBANDE*, J.P. AGNEESSENS*,
A. COPIN**, R. DELEU**, Ph. DREZE[+]

* Chaire d'hydraulique agricole

** Chaire de chimie analytique

[+] Chaire de chimie physique

Faculté des sciences agronomiques de l'Etat,
Gembloux, Belgique

Abstract—Résumé

MATHEMATICAL AND PHYSICAL INTERPRETATION OF THE TRANSFER OF LABELLED PESTICIDES IN WATER-UNSATURATED SOILS: EXAMPLES OF APPLICATION.
Studies were carried out for the purpose of predicting the behaviour of pesticides currently used in agriculture and their derivatives in the soil-water system. These studies are being continued with a view to gaining a more thorough knowledge of the quantities to be applied and the contribution they make as a function of climatic conditions. With the use of radioisotope-labelled products on top of a laboratory soil column under controlled conditions we can more easily monitor the variation in product concentrations in the percolation water as a function of time and the fate of those products in the soil. Experiments were performed in soil columns exposed to average climatic conditions with various pesticides (Neburon, Metoxuron, Chlortoluron and Nitrofene) applied at rates similar to those employed in agriculture. The results are compared with field data for the same products. The measurements (chemical concentrations and radioactivity of the percolating water) are interpreted. In the case of the pesticides used, it was found that the derivatives (little or none of the initial product) accumulated ultimately in the surface layers and that activity stemming from the derivatives migrated into the percolation water.

INTERPRETATION MATHEMATIQUE ET PHYSIQUE DU TRANSFERT DE PESTICIDES MARQUES DANS LES SOLS NON SATURES EN EAU: EXEMPLES D'APPLICATION.
Le but des études réalisées est la prédiction du comportement de pesticides couramment utilisés en agriculture et de leurs dérivés dans le système sol-eau du sol. Le prolongement de telles études s'inscrit dans le contexte d'une meilleure maîtrise des doses d'application et de leur apport en fonction des conditions climatiques. L'emploi de produits marqués radio-activement appliqués sur un matériel de laboratoire en conditions contrôlées permet de suivre plus aisément l'évolution des concentrations en produits dans les eaux de percolation en

---

[†] Recherche effectuée sous les auspices de l'Institut pour l'encouragement de la recherche scientifique dans l'industrie et l'agriculture (IRSIA).

fonction du temps, et leur devenir dans le sol. Des expériences sur colonnes de sol placées
en conditions climatiques moyennes ont été réalisées avec divers pesticides (Néburon, Méto-
xuron, Chlortoluron, Nitrofène) à partir d'applications semblables à celles pratiquées en
agriculture. Les résultats sont comparés avec ceux obtenus sur le terrain pour les mêmes
produits. Les mesures (concentrations chimiques et radioactivité des eaux de percolation)
font l'objet d'une interprétation. On constate, pour les produits utilisés, une accumulation
finale dans les horizons superficiels de produits dérivés (peu ou pas de produit initial) ainsi
qu'une migration d'activité correspondant à des dérivés dans les eaux de percolation.

1.   INTRODUCTION

Les difficultés d'interprétation de la migration de produits phytosanitaires
en plein champ sont liées au fait que l'on ne peut suivre aisément l'évolution
des produits migrants au cours du temps. De plus, les conditions climatiques
et les caractéristiques du sol et de la végétation sont très variables.

Une approche de compréhension des phénomènes a été réalisée par une
simulation sur colonnes de sol à l'aide de produits marqués radioactivement. Il
est possible de suivre, au cours du temps, la migration des produits utilisés (ou
de dérivés) dans les eaux de percolation.

Les analyses chimiques et radiochimiques des horizons du substrat ont fourni
les données complémentaires relatives à la migration des produits ou de leurs
dérivés.

On a opté pour le maintien de conditions moyennes (pluviométrie, température,
luminosité, humidité) en cours d'expérimentation, en vue de la comparaison avec
les essais sur le terrain.

Les produits appliqués correspondent à des formulations similaires aux pratiques
culturales.

2.   DISPOSITIF EXPERIMENTAL

Le diamètre des colonnes de sol est de 30 cm, afin de minimiser les effets
de parois susceptibles de modifier le processus.

L'utilisation d'un matériel en verre permet d'éviter la plupart des interférences
recontrées lors du dosage chimique des éluats.

La hauteur efficace des colonnes est de 50 cm. Ce fait résulte d'essais
préalables réalisés avec des pesticides de la famille des urées pour lesquels on a
constaté le stockage dans les niveaux supérieurs.

Le montage réalisé au laboratoire est indiqué en figure 1 et les caractéristiques
pédologiques du sol sont indiquées dans le tableau I.
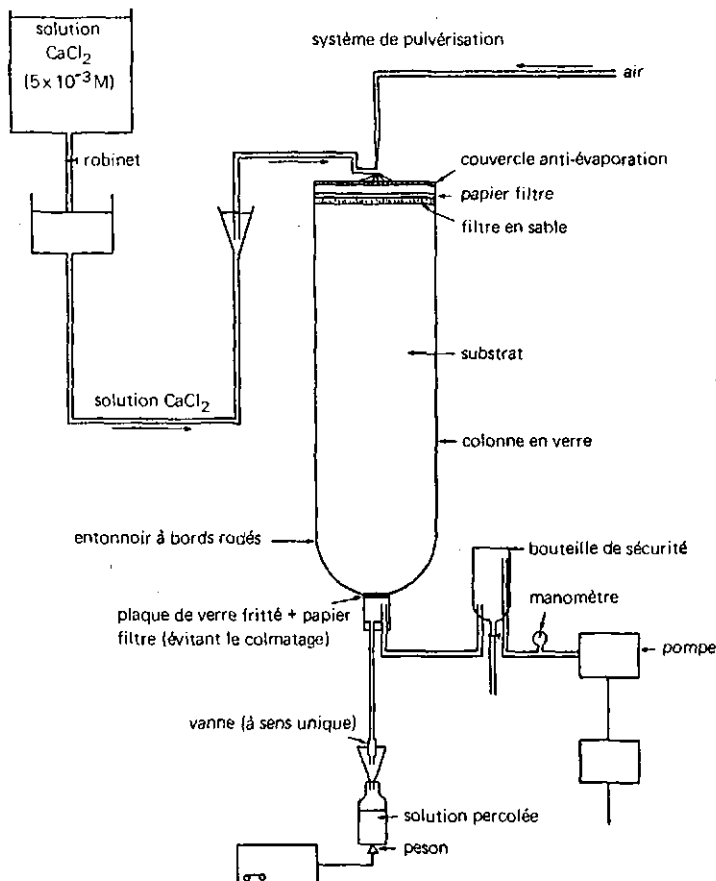
FIG.1. Schéma de montage.

Le remplissage des colonnes est effectué avec du sol tamisé à 2 mm, à l'état humide, par couches successives de plus ou moins 10 cm. Chaque couche est humidifiée par pulvérisation d'une solution aqueuse de chlorure de calcium.

Une expérimentation détaillée a permis de constater que ce mode d'application confère à la colonne une structure homogène et stable. De plus, elle porte le sol à une teneur en eau correspondant à une valeur moyenne normale pour nos régions.

La pluviométrie correspondant à $1-1,5$ mm par jour est obtenue par pulvérisation de la solution de chlorure de calcium $5 \cdot 10^{-3}$ molaire.

L'application intermittente d'une dépression d'un mètre d'eau en bas de colonne permet une percolation aisée évitant la formation de zones saturées en eau. La récolte des percolats se fait une fois par semaine.

TABLEAU I. CARACTERISTIQUES PEDOLOGIQUES DU SOL

Phosphore soluble eau (mg/100 g)	0,5
Acide phosphorique (mg/100 g)	2
Potasse échangeable (mg/100 g)	16
pH au KCl	7,25
Teneur en chlorure (mg/100 g)	5,85
Teneur en humus (%)	0,72
Azote total (mg/100 g)	112
Carbone/azote	3,21
Calcium (mg/100 g)	500
Sodium (mg/100 g)	9
Magnésium (mg/100 g)	25
Fer (mg/100 g)	4

Granulométrie: $< 50 \, \mu m$, 84%; $> 50 \mu m$, 16%.

La température est maintenue entre 15 et 17°C. Les colonnes sont tenues dans l'obscurité.

3. EXPERIMENTATION

Les mesures ont débuté dès que les éluats ont présenté une concentration constante en $CaCl_2$ (environ quatre mois). La stabilité du système est ainsi acquise.

3.1. Migration de l'eau tritiée

Quatre colonnes ont reçu une impulsion d'eau tritiée en surface. Ces essais visent à caractériser les paramètres hydrodynamiques du système (vitesse moyenne et coefficient de dispersion) et à vérifier l'indentité de fonctionnement des colonnes.

La mesure de la quantité d'eau tritiée est effectuée par scintillation liquide.

En fin d'expérimentation, le sol des colonnes est découpé (0–10, 10–30, 30–50 cm).

3.2. Migration des pesticides

Deux colonnes ont reçu en surface une formulation de Chlortoluron tritiée à des doses doubles de la pratique agricole.

L'utilisation conjointe de la scintillation liquide et de la chromatographie en phase gazeuse a permis de dissocier la migration des molécules initiales des éventuels métabolites et produits de dégradation.

Une colonne a reçu une application de Nitrofène marqué au carbone 14.

Le sol en fin d'essai est découpé en trois horizons et analysé chimiquement et radiochimiquement.

4.   MODELISATION MATHEMATIQUE

Dans les modèles de simulation pour mouvements unidimensionnels de solutés dans les sols, on considère en général que le sol comprend une phase d'eau mobile, une phase d'eau immobile et que les équilibres d'adsorption sont instantanés.

Des solutions analytiques sont disponibles [1].

Il existe également des solutions numériques qui consistent à remplacer les équations par des expressions en différences finies via un choix judicieux des pas de temps et de longueur [2].

Dans le cas de nos expérimentations, on peut se limiter à l'utilisation de l'équation aux dérivées partielles suivante [1] :

$$\frac{\delta C}{\delta t} = D \frac{\delta^2 C}{\delta x^2} - U \frac{\delta C}{\delta x} \tag{1}$$

expression dans laquelle:

X et t sont les coordonnées d'espace et de temps, C est la concentration en soluté dans la phase liquide par unité de volume d'eau, U est le flux d'eau en volume par unité de surface et par unité de temps, D est le coefficient de dispersion longitudinale, en cm^2 par unité de temps.

La solution analytique dans le cas d'une impulsion (injection instantanée d'une quantité de traceur) est donnée par l'équation suivante [1] :

$$C = \frac{M_o x}{U t \sqrt{4 \pi D t}} \exp - \frac{(x - U t)^2}{4 D t} \tag{2}$$

Pour un échelon (alimentation en continu d'un traceur) la solution s'écrit [2] :

$$C = \frac{C_o}{2} \operatorname{erfc} \frac{x - Ut}{\sqrt{4\,Dt}} + \exp \frac{xU}{D} \cdot \operatorname{erfc} \frac{x + Ut}{\sqrt{4\,Dt}} \qquad (3)$$

où M_o est la quantité de traceur injectée par unité de surface, C_o est la concentration du traceur injecté, erfc est l'erreur fonction complémentaire.

5.   RESULTATS ET INTERPRETATION

5.1. L'eau tritiée

Les modèles analytiques précités fournissent, par le biais de l'ajustement automatique, les valeurs des paramètres caractéristiques du transfert par convection et dispersion, soit la vitesse de parcours et le coefficient de dispersion.

L'ajustement du modèle (2) aux percolats d'eau tritiée aboutit aux résultats suivants:

Colonne	Vitesse (cm/jour)	Coefficient de dispersion (cm^2/jour)
Eau tritiée 1	0,37	0,39
Eau tritiée 2	0,42	0,83
Eau tritiée 3	0,43	0,79
Eau tritiée 4	0,39	0,76

Les vitesses sont très semblables d'une colonne à l'autre, également les coefficients de dispersion (fig. 2).

5.2. Les pesticides

Rappelons que deux colonnes ont reçu une dose de Chlortoluron en formulation marquée au tritium. Une autre a reçu du Nitrofène marqué au carbone 14. Les essais ont duré 11 à 12 mois.

Pour le Nitrofène, aucune trace de carbone 14 n'a été trouvée dans les éluats. Une quantité appréciable de produit s'est retrouvée dans le sol. Il s'agit d'une adsorption irréversible.

La figure 3 représente l'évolution de l'activité en tritium résultant du Clortoluron en fonction du temps dans les percolats de colonnes Chlortoluron 1 et 2.

On constate la symétrie relative des courbes ascendante et descendante et l'atteinte d'un palier.
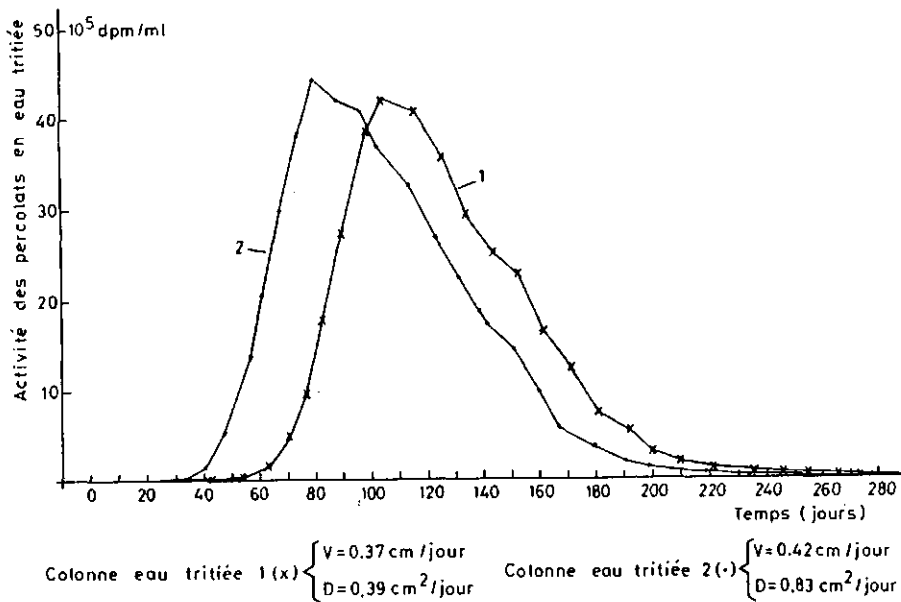
FIG.2. Evolution de l'activité en fonction du temps (eau tritiée).
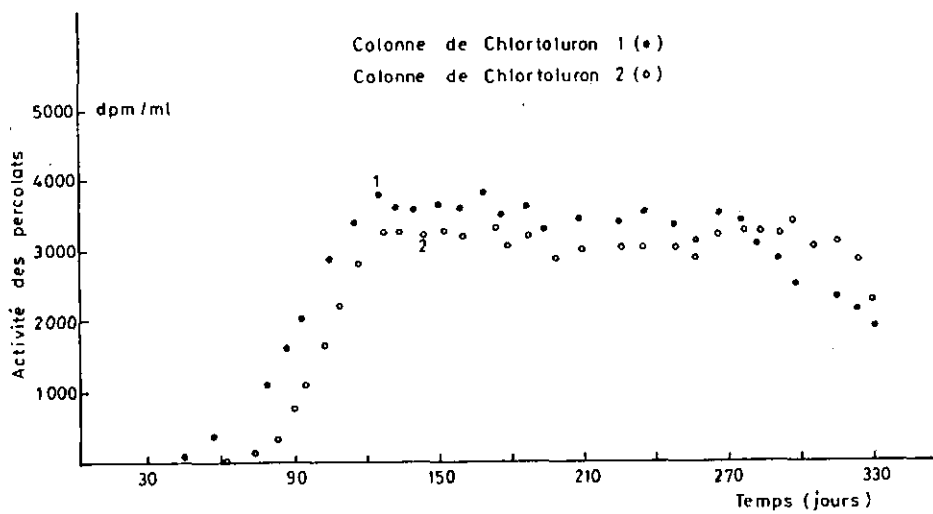
FIG.3. Evolution de l'activité en fonction du temps (Chlortoluron).

L'application de la théorie des systèmes linéaires paraît dès lors autorisée et la réponse du système tel que représenté en figure 3 correspond aux conditions d'injection d'un produit, d'ailleurs de nature inconnue, tel que le temps depuis l'apparition du produit jusqu'à la fin du palier correspondrait à la durée de l'injection du produit inconnu libéré (dérivé du Chlortoluron), en l'occurrence ±250 jours.

L'ajustement du modèle (3) fournit les valeurs optimalisées reportées ci-dessous:

Colonne	Vitesse (cm/jour)	Coefficient de dispersion $(cm^2/jour)$
Chlortoluron 1	0,52	0,86
Chlortoluron 2	0,51	0,40

La similitude remarquable des résultats liés au comportement de l'eau tritiée et aux dérivés du Chlortoluron permet d'avancer l'hypothèse que les dérivés ont un comportement similaire à l'eau.

La découpage final du sol montre qu'un tiers du produit marqué sous forme dérivée est resté fixé en surface. Le pourcentage estimé de l'activité dans les percolats est de 35%.

6.   CONCLUSIONS

L'eau tritiée utilisée comme traceur permet de caractériser le mouvement de l'eau dans un sol. Par le biais de l'utilisation d'un modèle mathématique adéquat, on définit les paramètres hydrodynamiques de la migration verticale en milieu non saturé.

En ce qui concerne les pesticides étudiés (Chlortoluron, Nitrofène), ils se fixent partiellement dans les couches supérieures de sol; la migration de produits dérivés, quand constatée (cas du Chlortoluron), présente un comportement hydrodynamique similaire à celui de l'eau tritiée. En outre on constate que le produit dérivé se comporte comme s'il était libéré à partir des couches supérieures de sol, à vitesse constante et dans une proportion déterminée et quantifiable.

Rappelons qu'ils s'agit d'essais sur colonnes de sol en laboratoire.

REFERENCES

[1]   SINE, L., AGNEESSENS, J.P., Modélisation de la migration d'éléments dans les sols, «I. Théorie mathématique en absence de réactions d'échange», Bulletin de la Société belge de pédologie 3 (1978) 349, et «III. Solutions analytiques générales» 3 (1980) 359.
[2]   Rapport d'activité 1980–1982 du CRUPA, Chaire d'Hydraulique agricole, Faculté des Sciences agronomiques de l'Etat, Gembloux (Belgique).

DETERMINATION OF THE UNSATURATED HYDRAULIC CONDUCTIVITY FROM A WATER-TABLE DRAINAGE EXPERIMENT

F. DE SMEDT, P. STEVENS
Laboratory of Hydrology,
Free University Brussels,
Brussels, Belgium

Abstract

DETERMINATION OF THE UNSATURATED HYDRAULIC CONDUCTIVITY FROM A
WATER-TABLE DRAINAGE EXPERIMENT.

An approximate solution is presented for drainage of a porous medium in the presence
of a water-table. It is shown that the unsaturated hydraulic conductivity versus water content
relation can be calculated from observations of the amount of water drained in a function of
time. The method was tested in the laboratory on a 140 cm long sand column. The results
agree with those of classical methods. This new technique can also be used in the field in the
case of the drainage of a previously saturated soil profile with a shallow water-table present.
In this case, the unsaturated hydraulic conductivity versus water content relation can be
calculated from observations of the water-content profiles only.

1. INTRODUCTION

Darcy's law for water movement in an unsaturated porous medium is

$$q = - K(\Theta)\partial h/\partial z \tag{1}$$

where q is the flux, h the total water potential, z the depth (only vertical flow is
considered), and K the unsaturated hydraulic conductivity, a function of the
water content, Θ. Many methods exist for measuring the $K(\Theta)$ relation [1]. In
general, laboratory methods consist of establishing steady flow through an
unsaturated sample, and simultaneously measuring the hydraulic gradient $\partial h/\partial z$,
the flux q and the water content Θ. A very popular field technique is the
instantaneous profile method, consisting of the drainage of a previously saturated
soil profile. The $K(\Theta)$ relation is calculated from measurements of water potential
and water-content profiles.

Recent developments [2–4] have concentrated on the so-called unit gradient
approximation. It is assumed that for a deep water-table, drainage occurs by
gravity forces only, i.e. the hydraulic gradient is equal to one. The $K(\Theta)$ relation
can be obtained from measurements of the water-content profiles only. Theoretical

contributions to this problem of gravity drainage have recently been
published [5, 6].

The present study intends to expand the theory to drainage experiments
where a shallow water-table is present.

2.   THEORY

2.1. Gravity drainage

The total water potential is given by

$$h = \Psi(\Theta) - z \tag{2}$$

where $-z$ represents the gravity potential and Ψ is the pressure potential, which
is negative in unsaturated media and depends upon the water content Θ. The
hydraulic gradient is

$$\partial h/\partial z = \partial \Psi/\partial z - 1 \tag{3}$$

To solve the drainage problem, Darcy's law has to be combined with the equation
of continuity

$$\partial \Theta/\partial t = - \partial q/\partial z \tag{4}$$

In the case of gravity drainage, the term $\partial \Psi/\partial z$ can be neglected, and the flow
equation becomes

$$\partial \Theta/\partial t = - \partial K/\partial z \tag{5}$$

The solution has been presented [5] as

$$k(\Theta) = z/t \text{ for } z/t \leqslant k(\Theta_s) \tag{6}$$

$$\Theta = \Theta_s \qquad z/t > k(\Theta_s) \tag{7}$$

where $k = dK/d\Theta$, and Θ_s is the saturated water content. The unsaturated
hydraulic conductivity can be calculated [6] as

$$K = (\Theta z - W)/t \tag{8}$$

where $W(z,t)$ is the amount of water stored in the profile above depth z. This
amount can be calculated from observations of the water-content profiles.
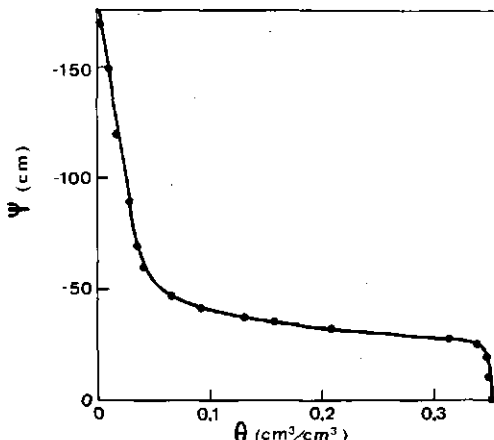
FIG.1.   The pressure potential versus water content relationship in the case of drainage for the sand used in this study.

2.2. Drainage to a shallow water-table

In the case of drainage of a previously saturated profile in the presence of a shallow water-table, $\partial \Psi/\partial z$ cannot be neglected. However, an approximation is possible. The $\Psi(\Theta)$ relation often shows a flat part, where Ψ does not vary much with the water content. The average value of Ψ in that part of the curve is equal to the average capillary pressure h_c of the larger pores of the medium

$$\Psi = - h_c \tag{9}$$

For instance, Fig.1 shows the $\Psi(\Theta)$ relation of the sand used in this study, with $h_c \approx 40$ cm. Hence, during the initial stage of the drainage, the water pressure at the soil surface remains approximately equal to $-h_c$. The average pressure potential gradient in the profile can be approximated by

$$\partial \Psi/\partial z = h_c/z_0 \tag{10}$$

where z_0 is the depth of the water-table.

The flow equation becomes

$$\partial \Theta/\partial t = (h_c/z_0 - 1) \partial K/\partial z \tag{11}$$

The solution is

$$k(\Theta) = z/t(1 - h_c/z_0) \tag{12}$$

for $\quad z/t(1 - h_c/z_0) \leqslant k(\Theta_s)$ $\qquad\qquad$ (13)

and $\quad z \leqslant z_0 - h_c$ $\qquad\qquad\qquad\qquad$ (14)

otherwise

$\qquad$ $\Theta = \Theta_s$ $\qquad\qquad\qquad\qquad$ (15)

Condition (14) results from the fact that only the zone between the surface to a height of h_c above the water-table is able to drain. The unsaturated hydraulic conductivity can be calculated from observations of the water-content profiles by

$\qquad$ $K = (\Theta z - W)/(1 - h_c/z_0)t$ $\qquad\qquad$ (16)

for $\quad z \leqslant z_0 - h_c$ $\qquad\qquad\qquad\qquad$ (17)

Hence, only measurements of the water-content profiles are needed for calculating K.
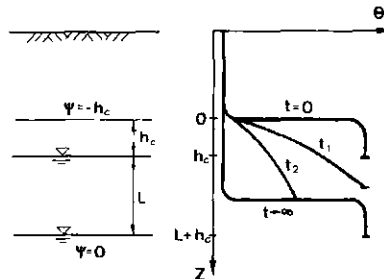
FIG.2. Schematic representation of drainage of a sand medium, induced by a lowering of the water table.

2.3. Drainage induced by a water-table decline

Consider a soil profile with a water-table in equilibrium. If the water-table is suddenly lowered over a distance L, drainage will occur. This situation is schematically shown in Fig.2. The average pressure potential gradient can be estimated as

$\qquad$ $\partial\Psi/\partial z = L/(L + h_c)$ $\qquad\qquad$ (18)

The flow equation is

$$\partial\Theta/\partial t = - (L/L + h_c)\partial K/\partial z \qquad (19)$$

The *solution* is

$$k(\Theta) = z(L + h_c)/Lt \qquad (20)$$

$$\text{for} \quad z(L + h_c)/Lt \leqslant k(\Theta_s) \qquad (21)$$

$$\text{and} \quad z \leqslant L \qquad (22)$$

otherwise

$$\Theta = \Theta_s \qquad (23)$$

The total amount of water drained, V, is

$$V = (\Theta_s - \Theta)L + LKt/(L + h_c) \qquad (24)$$

where Θ and K are taken at $z = L$, the positions at a height h_c above the water-table. The drainage rate is

$$dV/dt = LK/(L + h_c) \qquad (25)$$

With Eqs (24) and (25) K and Θ can be calculated as

$$K = (1 + h_c/L)\,dV/dt \qquad (26)$$

$$\Theta = \Theta_s - V/L + (t/L)(dV/dt) \qquad (27)$$

Hence, the $K(\Theta)$ relation can be calculated from observations of the total amount of water drained as a function of time.

3.   EXPERIMENTAL

A plexiglass column, 6 cm in diameter and 140 cm long, was filled with sand with grain diameters ranging from 120 to 1000 μm. The average bulk density was 1.67 g/cm^3.

The $\Psi(\Theta)$ relation, as shown in Fig.1, was determined with a hanging water column experiment [7]. The saturated water content was 0.354 cm^3/cm^3.
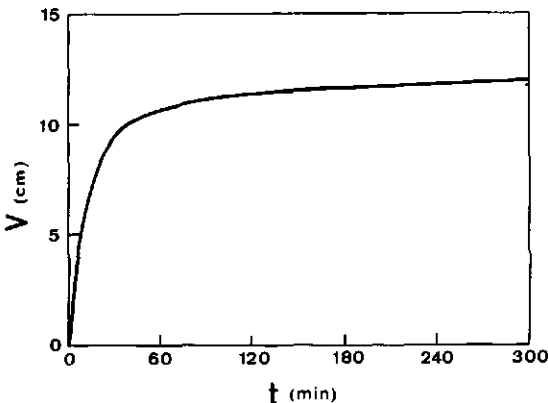
FIG.3. Observed total drainage versus time.

The column was saturated from below and allowed to drain for several days with a water-table fixed at 40 cm above the lower end. After equilibrium was established, the drainage experiment was started by suddenly lowering the water-table to the bottom of the column. The outflow was collected and weighed on a balance. The time was recorded for every 2 g water drained from the column. The experiment lasted for about 5 h.

4.   DISCUSSION AND CONCLUSION

The resulting total amount of water drained as a function of time is shown in Fig.3. The K and Θ values were calculated with Eqs (26) and (27). The time derivative of the total outflow was evaluated with a three-point finite difference approximation. The resulting K versus Θ values are represented in Fig.4 by the dots.

To verify these results, the $K(\Theta)$ relation was also determined by a classical method, in this case the infiltration method [8]. The details of this experiment can be found elsewhere [9]. Much more effort, equipment and time (several weeks) were required in comparison with the drainage experiment. The resulting $K - \Theta$ values are represented in Fig.4 by stars.

Agreement between the results of the drainage experiment and those of the infiltration experiment is generally good, although the drainage method seems to predict somewhat lower K values for the higher water contents. Since the drainage experiment is fast and the calculation of the $K(\Theta)$ relation requires only very simple observations, it can be concluded that this new technique for determining the $K(\Theta)$ relation is very useful.
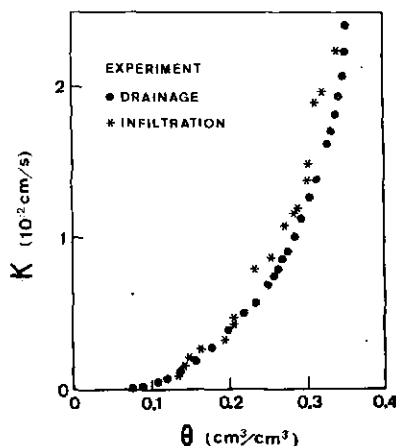
FIG.4. *Calculated unsaturated hydraulic conductivity versus water-content values.*

In fields where the gravity drainage technique cannot be used because of a shallow water-table, Eq.(16) is proposed for calculating the K(Θ) relation with observation of water-content profiles only. Also, this technique requires little data and can be considered as very promising. However, the method has not been tested yet. Verification of this drainage technique in the field will be the subject of future investigations.

REFERENCES

[1] KLUTE, A., The determination of the hydraulic conductivity and diffusivity of unsaturated soils, Soil Sci. 113 (1972) 264.

[2] BLACK, T.A., THURTELL, C.W., TANNER, C.B., Hydraulic load-cell lysimeter, construction, calibration, and tests, Soil Sci. Soc. Am. Proc. 32 (1968) 623.

[3] DAVIDSON, J.M., STONE, L.R., NIELSEN, D.R., LA RUE, M.E., Field measurements and use of soil water properties, Water Resour. Res. 5 (1969) 1312.

[4] LIBARDI, P.L., REICHARDT, K., NIELSEN, D.R., BIGGAR, J.W., Simple field methods for estimating soil hydraulic conductivity, Soil Sci. Soc. Am. J. 44 (1980) 3.

[5] SISSON, J.B., FERGUSON, A.H., VAN GENUCHTEN, M.Th., Simple method for predicting drainage from field plots, Soil Sci. Soc. Am. J. 44 (1980) 1147.

[6] RAATS, P.A.C., Implications of some analytical solutions for drainage of soil water, Agric. Water Manag. (in press).

[7] WAUTERS, F., Experimentele studie van de stroming van een polluent in een kunstmatige zandbodem, Hydrology Thesis, Free University Brussels, 1980, 124 pp.

[8] YOUNGS, E.G., An infiltration method of measuring the hydraulic conductivity of unsaturated porous materials, Soil Sci. 97 (1964) 307.

[9] STEVENS, P., Bepaling in het laboratorium van de hydraulische geleidbaarheid van een onverzadigde zandbodem, Hydrology Thesis, Free University Brussels, 1982, 103 pp.

STUDIES ON THE MOBILITY OF SOME HEAVY METALS AND TRANSURANIC RADIONUCLIDES IN MAJOR INDIAN SOIL TYPES

T.J. D'SOUZA, B.N. VYAS, V.V. ATHALYE,
V. RAMACHANDRAN, K.B. MISTRY
Biology and Agriculture Division,
Bhabha Atomic Research Centre,
Trombay, Bombay,
India

Abstract

STUDIES ON THE MOBILITY OF SOME HEAVY METALS AND TRANSURANIC RADIONUCLIDES IN MAJOR INDIAN SOIL TYPES.
    Studies on the mobility of the heavy metals, chromium, lead, zinc and transuranic radionuclides plutonium and americium in three major Indian soils, namely a vertisol-pellustert (black soil), an oxisol (laterite soil) and an entisol-haplaquent (alluvial soil), indicated that more than 98% of the surface-deposited pollutants were retained in the top 0 to 2.5 cm layer when leached with rain-water. In general, the mobility of these elements was either unaffected or marginally reduced at high doses of added organic matter as compared with controls. However, leaching with dilute solutions of (10^{-4}M) EDTA, EDDHA and DTPA resulted in enhancement of the mobility of all these pollutants with a high degree of chelate specificity for individual ions, depending upon the soil type. Rapid formation of stable soluble Cr-EDDHA, Pu-DTPA and Am-DTPA complexes facilitated the leaching of these pollutants from the contaminated soils.

1. INTRODUCTION

    Chromium, lead and zinc are among the heavy metals which are considered as important soil and water pollutants. They are known to be present in sewage sludges, waste waters, phosphatic fertilizers as well as in emissions from automobile exhausts, smelters and related industries [1, 2], and there is growing concern that these elements may enter the food chain in toxic amounts. Trivalent as well as hexavalent forms of chromium may be present in soils and reports exist on the rapid conversion of soluble Cr to insoluble forms in soils of widely varying pH [3–5] as well as the oxidation of Cr^{3+} to Cr^{6+} resulting in the prevalence of soluble anion [6]. Chromium accumulated in soils is also toxic to plants, the toxic limits depending upon the soil type [7, 8]. Since the anti-detonating substances

containing lead additives in petrol are burnt and released in the ambient atmo-
sphere through automobile exhaust gas which contains several compounds of lead,
the accumulation of lead in the top layers of soil alongside highways is a well-
established phenomenon [9, 10]. Zinc pollution from sewage sludge and in
areas surrounding zinc smelters has also gained importance in recent years
[11, 12], though zinc is generally considered as a plant micronutrient.

There has also been an increase in the inventory of transuranic radionuclides
in the environment over the past few years, either because of nuclear weapon
tests or accidental and planned releases from installations associated with the
expanding nuclear power industry. Among these, ^{239}Pu and ^{241}Am are of
considerable environmental significance owing to their long half-lives and extremely
high radiotoxicity.

Studies on the contamination of 'toxic' heavy metals and transuranic radio-
nuclides in soils and plants have so far been restricted to highly industrialized
temperate regions [11–18] and hardly any quantitative data are available on
the fate of these pollutants in soils of subtropical and tropical regions. The
accelerated growth of various industries, including nuclear industry, in India, the
potential use of sewage sludges and municipal composts as organic fertilizers,
and the increasing application of phosphate rocks as fertilizer material, raise
the question that Indian soils and soil-crop systems could be subjected to contamina-
tion from these pollutants. As a part of our continuing programme aimed at
understanding the behaviour of heavy metals and transuranics in subtropical and
tropical soils and the soil-plant system, studies were undertaken on the mobility
of these pollutants in contrasting Indian soil types. This paper reports on the
mobility of chromium, lead, zinc, ^{239}Pu and ^{241}Am in three contrasting soils
representing three major Indian soil groups, namely, a vertisol-pellustert (black),
an oxisol (laterite) and an entisol-haplaquent (alluvial), as affected by rain-water
organic matter addition, and synthetic chelating agents like EDTA, EDDHA and
DTPA. In these studies ^{51}Cr, ^{65}Zn and ^{210}Pb were used as tracers for Cr, Zn and
Pb, respectively.

2.   MATERIALS AND METHODS

As the mobility studies for individual heavy metals and transuranic radio-
nuclides were carried out at different periods, the soils used in the experiments,
though belonging to the same class, were not identical. The range of values of the
important physico-chemical characteristics of the soils used in the studies are
presented in Table I.

Surface soil samples (0–20 cm) passed through a 2 mm sieve were transferred
to glass leaching columns (2.5 cm dia.) so that after compaction a depth of 15 cm
and a bulk density of 1.36, 1.27 and 1.56 were provided for pellustert, oxisol

TABLE I. IMPORTANT CHARACTERISTICS OF THE SOILS USED IN THE INVESTIGATION

Soil characteristics	Vertisol-Pellustert (black)	Oxisol (laterite)	Entisol-haplaquent (alluvial)
pH (1:2.5)	8.0−8.5	5.1−5.9	7.0−7.4
Moisture equivalent (%)	31.2−37.4	29.6−34.2	23.0−25.9
Electrical conductivity (mmho/cm)	0.20−0.28	0.12−0.20	0.30−0.71
Cation exchange capacity (meq/100 g)	48.8−60.7	10.5−14.6	15.9−28.4
Organic carbon (%)	0.39−1.32	0.52−1.80	0.51−1.65
Predominant clay mineral	Montmorillonite/illite	Kaolinite	Degraded illite
Texture	Clay loam	Sandy loam	Loamy sand

and haplaquent, respectively. The soils were packed with a packing block similar to that described for measuring hydraulic conductivity [19]. Organic matter treatments comprised an addition of either vegetable compost (C/N = 21.1) or sewage sludge (C/N = 7.24) or municipal compost (C/N = 8.67) at 5 or 10% levels corresponding to 50 t/ha and 100 t/ha, respectively. The addition of organic matter did not result in significant variations in bulk density of the soil profiles. The soils were maintained at field capacity moisture status for one week after which the top surface of each soil was labelled with 1480 kBq (40 μCi) of $^{51}Cr^{3+}$ and 74 kBq (2 μCi) each of ^{210}Pb, ^{65}Zn, ^{239}Pu and ^{241}Am in separate sets of soil columns using solutions of $^{51}CrCl_3$, $^{210}Pb(NO_3)_2$, $^{65}ZnCl_2$, $^{239}Pu(NO_3)_4$ and $^{241}Am(NO_3)_3$, respectively. The labelling was done by adding the radioactive solution in two instalments of 1 mL each to the top of the soil column; the second instalment was added only after the disappearance of standing liquid on top of the column. Glass wool was packed on the surface to reduce the disturbance of soil when the leaching liquids were applied.

Two days after contamination, control and organic-matter-treated soil columns were leached with rain-water (de-ionized) while each synthetic chelate, namely ethylenediaminetetraacetic acid (EDTA), ethylenediamine di(o-)hydroxyphenylacetic acid (EDDHA) and diethylene triaminepentaacetic acid (DTPA) was used at $10^{-4} M$ concentration. The pH of all the leaching solutions was

adjusted to 7 and the solutions were in ammoniacal form. The leaching volumes consisted of 100 cm, 250 cm and 75 cm for pellustert, oxisol and haplaquent soil columns, respectively, which correspond to the mean annual precipitation at the site of soil collection. The leaching solutions were applied to the top of the soil column in instalments of 5 cm (25 mL) at a time. Each 5 cm aliquot was allowed to leach completely before the next aliquot was applied. The time taken for each 5 cm aliquot to pass through the column depended upon the soil type (one to five days), the leaching being comparatively faster in the initial stages. In some treatments, leaching could not be continued to the mean annual precipitation level, owing to the formation of an impervious layer in the soil, and the quantity of solution leached is indicated in the respective tables. The possibility of breakthrough of the radionuclides from the soil columns was checked daily by monitoring the leachates for radioactivity, and leaching was discontinued on occurrence of a breakthrough to prevent the overrun of the radionuclide out of the column.

On completion of leaching and after about one week (drying period), the soil columns were sliced, either in 2.5 cm segments (^{51}Cr and ^{210}Pb) or in 1 cm segments (^{65}Zn, ^{239}Pu and ^{241}Am) by gently pushing the column downwards using a rubber stopper attached to a thick glass rod on to a Petri dish. This procedure did not alter the physical dimensions of the original soil column contained in the glass leaching container and was found to be very convenient for accurate partitioning of the soil column into different segments. The individual segments were further air dried and 2 g of the soil from each segment was packed in test tubes for assay of ^{51}Cr, ^{210}Pb, ^{65}Zn and ^{241}Am through gamma-ray spectrometry using a well-type 7.5 cm × 7.5 cm NaI(Tl) crystal integral line assembly, and a Nuclear Data 512-Channel pulse-height analyser attached to an oscilloscope and a computer readout typewriter. The gamma photopeak of 325 keV for ^{51}Cr, 47 keV for ^{210}Pb, 1110 keV for ^{65}Zn and 60 keV for ^{241}Am was used for a quantitative estimation of the radionuclides.

In the case of the ^{239}Pu-treated soil columns, the dried 1 cm segments were digested in 8M HNO$_3$ for 30 min, centrifuged and the clear extracts were taken for plutonium assay by planchetting on to a stainless-steel planchet and alpha counting using a low-background ZnS(Ag) scintillation counter.

3.   RESULTS

3.1. Chromium

Data on the mobility of ^{51}Cr presented in Table II indicate that in both soil types more than 99% of the surface-applied ^{51}Cr^{3+} was retained in the top contaminated layer with very little downward movement when leached with rain-water. Incorporation of organic matter at 5% level and leaching with water also did not result in ^{51}Cr breaking through from the soil columns in both soil types.

TABLE II. MOBILITY OF ^{51}Cr ($^{51}CrCl_3$) IN TWO SOIL TYPES AS
INFLUENCED BY RAIN-WATER, ORGANIC MATTER (5%) AND
SYNTHETIC CHELATES ($10^{-4}\underline{M}$ conc.)

Distribution of radionuclide in soil columns (% of total)

Depth (cm)	Control	Organic matter	EDTA	EDDHA	DTPA
Pellustert	(50 cm)	(40 cm)	(50 cm)	(10 cm)[a]	(50 cm)
0–2.5	99.88	99.59	99.08	99.40	99.50
2.5–5.0	0.12	0.17	0.42	0.18	0.30
5.0–7.5	–	0.13	0.30	0.13	0.10
7.5–10.0	–	0.06	0.20	0.11	0.10
10.0–12.5	–	0.05	–	0.09	–
12.5–15.0	–	–	–	0.09	–
Oxisol	(250 cm)	(250 cm)	(250 cm)	(15 cm)[a]	(250 cm)
0–2.5	99.82	99.19	99.56	99.90	94.45
2.5–5.0	0.14	0.59	0.15	0.04	2.70
5.0–7.5	0.03	0.15	0.13	0.02	1.40
7.5–10.0	0.01	0.05	0.11	0.02	0.70
10.0–12.5	–	0.02	0.05	0.01	0.49
12.5–15.0	–	–	–	0.01	0.26

[a] Breakthrough of ^{51}Cr from the soil column.

A rapid breakthrough of ^{51}Cr occurred in both soil types after passage of
10 cm and 15 cm of $10^{-4}\underline{M}$ EDDHA solution in the pellustert and oxisol, respectively.
No breakthrough of ^{51}Cr occurred in both soils when they were leached with
$10^{-4}\underline{M}$ EDTA or DTPA solution. EDDHA was therefore most effective in
complexing and leaching out ^{51}Cr from both soils. A downward movement of
^{51}Cr to a small extent was also observed with DTPA and EDTA; DTPA was more
effective than EDTA in inducing mobility of ^{51}Cr, especially in the oxisol.

TABLE III. MOBILITY OF ^{210}Pb IN THREE SOIL TYPES AS INFLUENCED BY RAIN-WATER, ORGANIC MATTER (10%) AND SYNTHETIC CHELATES ($10^{-4}\underline{M}$ conc.)

Distribution of radionuclide in soil columns (% of total)

Depth (cm)	Control	Organic matter	EDTA	EDDHA	DTPA
Pellustert	(100 cm)	(60 cm)	(100 cm)	(100 cm)	(100 cm)
0--2.5	99.41	99.91	96.66	99.98	99.97
2.5−5.0	0.35	0.04	2.71	0.01	0.01
5.0−7.5	0.13	0.02	0.51	0.01	0.01
7.5−10.0	0.07	0.01	0.10	−	0.01
10.0−12.5	0.02	0.01	0.01	−	−
12.5−15.0	0.02	0.01	0.01	−	−
Oxisol	(250 cm)	(250 cm)	(250 cm)	(250 cm)	(250 cm)
0−2.5	99.85	99.82	85.43	99.93	99.53
2.5−5.0	0.05	0.08	9.27	0.04	0.43
5.0−7.5	0.03	0.05	2.16	0.02	0.01
7.5−10.0	0.03	0.02	1.08	0.01	0.01
10.0−12.5	0.03	0.02	1.52	−	0.01
12.5−15.0	0.01	0.01	0.54	−	0.01
Haplaquent	(75 cm)	(75 cm)	(75 cm)	(75 cm)	(75 cm)
0−2.5	99.90	99.80	56.43	99.98	99.76
2.5−5.0	0.01	0.06	24.74	0.01	0.12
5.0−7.5	0.01	0.04	12.60	0.01	0.05
7.5−10.0	0.03	0.04	4.73	−	0.03
10.0−12.5	0.03	0.03	1.21	−	0.02
12.5−15.0	0.02	0.03	0.29	−	0.02

3.2. Lead

Data on the mobility of ^{210}Pb presented in Table III indicate that nearly all (>99%) applied Pb was retained in the surface-deposited layer of the three soil types. Incorporation of organic matter at a high level of 10% also did not induce mobility of Pb in any of the three soils; on the contrary, a slight reduction in the mobility of Pb, especially in the pellustert, was observed.

No breakthrough of ^{210}Pb was recorded in the pellustert, oxisol and haplaquent soils with leaching volumes of 100, 250 and 75 cm, respectively, of any of the three synthetic chelating agents (Table III). EDDHA in particular was ineffective in including mobility of ^{210}Pb in all three soil types, which is in contrast with the observation in the case of $^{51}Cr^{3+}$ (Table II) where EDDHA was most effective in inducing mobility of $^{51}Cr^{3+}$. Among the remaining two chelates, EDTA was relatively more effective in enhancing the mobility of ^{210}Pb than DTPA in all three soil types, as revealed from the comparatively larger fraction of ^{210}Pb retained in the surface layer of soils leached with DTPA solution. Moreover, ^{210}Pb was more mobile in the haplaquent, followed by oxisol and pellustert, when these soils were leached with EDTA solution as indicated by the greater fraction of ^{210}Pb found in the lower layers of these soils.

3.3. Zinc

Data on the influence of sewage sludge, municipal compost and synthetic chelating agents on the mobility of ^{65}Zn in the three soils are presented in Table IV. Data indicate that 99.9% of the applied ^{65}Zn in the three soil types was retained in the surface layers (0–2 cm) when leached with rain-water. Incorporation of high doses (10%) of either sewage sludge or municipal compost did not result in any significant movement of ^{65}Zn in the three soil types; mostly all (>99.8%) ^{65}Zn was located in the surface zone of the soil column.

Application of $10^{-4}M$ EDTA or DTPA solutions caused a variable movement of ^{65}Zn in all the three soils (Table IV). Although no breakthrough of the nuclide occurred in any of the three soils studied, the ^{65}Zn movement beyond a depth of 6 cm in the pellustert was 40.92% and 23.54% of applied ^{65}Zn with 100 cm leaching with EDTA or DTPA, respectively, indicating thereby that EDTA was more effective than DTPA in enhancing the mobility of ^{65}Zn in the pellustert. Comparatively reduced mobility of applied ^{65}Zn to the lower depths was observed in the oxisol, the movement being almost negligible beyond 8 cm depth when the soil was leached with 105 cm of the chelating solution; no differences were observed between the two chelating agents. In the haplaquent, the leaching was greatly impeded owing to the formation of an impervious layer in the soil column at 2–3 cm depth and hence only 10 cm of the leaching liquids could be passed.

TABLE IV. MOBILITY OF ^{65}Zn IN THREE SOIL TYPES AS INFLUENCED BY SEWAGE SLUDGE (10%), MUNICIPAL COMPOST (10%) AND SYNTHETIC CHELATES (10^{-4} M conc.)

Distribution of radionuclide in the soil columns (% of total)

Depth (cm)	Pellustert					Oxisol					Haplaquent				
	Control (100 cm)	Sludge (55 cm)	Compost (100 cm)	EDTA (100 cm)	DTPA (100 cm)	Control (105 cm)	Sludge (105 cm)	Compost (105 cm)	EDTA (105 cm)	DTPA (105 cm)	Control (25 cm)	Sludge (15 cm)	Compost (25 cm)	EDTA (10 cm)	DTPA (10 cm)
0–1	99.94	99.96	99.92	3.50	3.22	99.15	99.64	99.90	9.80	8.64	99.99	99.99	99.76	85.08	80.23
1–2	0.06	0.04	0.04	7.63	13.47	0.78	0.25	0.10	14.35	18.45	0.01	0.01	0.15	13.29	19.11
2–3	–	–	0.04	13.31	17.03	0.07	0.11	–	21.35	19.27	–	–	0.09	1.52	0.65
3–4	–	–	–	13.20	16.58	–	–	–	21.84	21.48	–	–	–	0.09	0.01
4–5	–	–	–	11.70	14.34	–	–	–	19.52	16.55	–	–	–	0.01	–
5–6	–	–	–	9.73	11.83	–	–	–	8.96	10.14	–	–	–	–	–
6–7	–	–	–	8.26	9.17	–	–	–	3.39	4.44	–	–	–	–	–
7–8	–	–	–	7.83	6.45	–	–	–	0.65	0.96	–	–	–	–	–
8–9	–	–	–	6.17	4.00	–	–	–	0.11	0.07	–	–	–	–	–
9–10	–	–	–	4.73	2.28	–	–	–	0.01	–	–	–	–	–	–
10–11	–	–	–	4.62	0.83	–	–	–	–	–	–	–	–	–	–
11–12	–	–	–	3.41	0.50	–	–	–	–	–	–	–	–	–	–
12–13	–	–	–	2.55	0.21	–	–	–	–	–	–	–	–	–	–
13–14	–	–	–	1.75	0.10	–	–	–	–	–	–	–	–	–	–
14–15	–	–	–	1.60	–	–	–	–	–	–	–	–	–	–	–

Nevertheless, there was considerable movement of ^{65}Zn even with 10 cm leaching with the chelating solution, and in this case DTPA was slightly more effective in enhancing the mobility of Zn than EDTA.

3.4. Plutonium

Data on the mobility of ^{239}Pu presented in Table V indicate that nearly 98% of the applied ^{239}Pu was retained in the surface-deposited layer of the three soils when leached with rain-water. Incorporation of organic matter at 5% level in the soils did not significantly affect the mobility of ^{239}Pu except in the pellustert where a slightly enhanced movement was detected at lower depths, i.e. at 10 cm compared with controls where plutonium was detected only up to 5–6 cm depth.

A breakthrough of ^{239}Pu was recorded on leaching with 10 cm volumes of $10^{-4}\underline{M}$ DTPA in the pellustert and in the haplaquent, and with 45 cm in the case of oxisol soil profiles (Table V). It is noteworthy that, despite variation in soil characteristics (Table I), DTPA was highly effective in enhancing the mobility of plutonium through columns of all the three soils. Leaching with $10^{-4}\underline{M}$ EDTA solution showed that this chelate was less effective than DTPA in enhancing ^{239}Pu mobility in the three soils. However, EDTA induced greater mobility of ^{239}Pu compared with that in controls and the organic-matter-treated soil column.

3.5. Americium

Data on the mobility of ^{241}Am presented in Table VI indicate that more than 99% of the applied ^{241}Am was retained in the top 2 cm (surface deposited) layer of the three soil types when leached with rain-water. Incorporation of 5% organic matter in these three soils appeared to decrease the mobility of ^{241}Am as compared with the controls.

The behaviour of ^{241}Am when leached with chelating solution (Table VI) was similar to that of ^{239}Pu (Table V). A breakthrough of ^{241}Am was obtained when the soils were leached with $10^{-4}\underline{M}$ DTPA solution (10 cm solution in the pellustert and haplaquent, and 45 cm solution in the oxisol). However, EDTA solution was less effective than DTPA in enhancing the mobility of ^{241}Am, although the radionuclide moved to 10 cm depth.

4.   DISCUSSION

The retention of the heavy metals Cr, Pb and Zn, and the transuranics, Pu and Am, in the surface-deposited layers of the contrasting tropical soils used in this investigation suggests that ions of these elements are held at the adsorption

TABLE V. MOBILITY OF ^{239}Pu IN THREE SOIL TYPES AS INFLUENCED BY RAIN-WATER, ORGANIC MATTER (OM) (5%) AND SYNTHETIC CHELATES (10^{-4} $\underline{M}$ conc.)

Distribution of radionuclide in soil columns (% of total)

Depth (cm)	Pellustert				Oxisol				Haplaquent			
	Control (100 cm)	OM (100 cm)	EDTA (100 cm)	DTPA (10 cm)[a]	Control (250 cm)	OM (250 cm)	EDTA (250 cm)	DTPA (45 cm)[a]	Control (35 cm)	OM (75 cm)	EDTA (40 cm)	DTPA (10 cm)[a]
0–1	99.4	95.9	97.3	94.1	98.2	97.8	84.1	1.1	98.4	97.8	97.6	97.1
1–2	0.2	1.4	1.5	1.6	1.1	1.0	14.4	1.4	1.3	1.7	1.7	2.3
2–3	0.1	1.3	0.6	0.8	0.3	0.6	0.9	1.4	0.3	0.2	0.3	0.3
3–4	T	0.6	0.3	0.5	0.2	0.3	0.7	93.3	T	0.1	0.1	0.1
4–5	T	0.3	0.2	0.6	0.1	0.1	0.3	1.0	T	T	T	T
5–6	T	0.1	0.1	0.5	T	T	0.1	0.7	–	T	T	T
6–7	T	0.1	T	0.5	T	T	T	0.5	–	T	T	T
7–8	–	0.1	T	0.6	–	T	T	0.2	–	T	T	T
8–9	–	T	–	0.4	–	T	T	0.2	–	T	T	T
9–10	–	T	–	0.2	–	T	T	T	–	T	T	T
10–11	–	–	–	0.1	–	–	T	T	–	–	T	T
11–12	–	–	–	T	–	–	–	T	–	–	T	T
12–13	–	–	–	T	–	–	–	T	–	–	T	T
13–14	–	–	–	T	–	–	–	T	–	–	–	T
14–15	–	–	–	T	–	–	–	T	–	–	–	T

[a] Breakthrough of the radionuclide from the column. T = trace.

TABLE VI. MOBILITY OF ^{241}Am IN THREE SOIL TYPES AS INFLUENCED BY RAIN-WATER, ORGANIC MATTER (OM) (5%) AND SYNTHETIC CHELATES (10^{-4} $\underline{M}$ conc.)

Distribution of radionuclide in soil columns (% of total)

Depth (cm)	Pellustert				Oxisol				Haplaquent			
	Control (100 cm)	OM (100 cm)	EDTA (100 cm)	DTPA (10 cm)[a]	Control (250 cm)	OM (250 cm)	EDTA (250 cm)	DTPA (45 cm)[a]	Control (75 cm)	OM (75 cm)	EDTA (45 cm)	DTPA (10 cm)[a]
0–1	99.9	99.9	88.4	60.7	99.6	99.9	59.1	43.4	96.5	99.5	77.7	74.7
1–2	T	T	10.0	5.7	0.3	T	16.5	9.1	2.9	0.4	14.2	3.9
2–3	T	–	1.4	2.8	T	T	11.8	8.2	0.5	T	5.5	1.3
3–4	T	–	0.1	1.6	T	–	9.3	9.7	T	T	1.6	1.1
4–5	–	–	T	1.6	T	–	2.3	10.0	T	–	0.7	1.0
5–6	–	–	T	1.5	T	–	0.9	7.7	T	–	0.2	1.7
6–7	–	–	T	1.7	–	–	0.1	5.0	T	–	T	1.0
7–8	–	–	–	1.7	–	–	T	2.1	–	–	T	1.3
8–9	–	–	–	1.9	–	–	–	2.0	–	–	T	1.3
9–10	–	–	–	2.1	–	–	–	1.3	–	–	T	1.4
10–11	–	–	–	2.5	–	–	–	0.8	–	–	–	2.3
11–12	–	–	–	2.9	–	–	–	0.3	–	–	–	2.5
12–13	–	–	–	3.1	–	–	–	0.2	–	–	–	2.3
13–14	–	–	–	3.8	–	–	–	0.1	–	–	–	2.0
14–15	–	–	–	6.1	–	–	–	0.1	–	–	–	2.0

[a] Breakthrough of the radionuclide from the column.   T = trace.

sites of the exchange complex of the soils and the strong bonding potential of the soils prevented the movement of these pollutants to lower depths under normal conditions of rain-water leaching. A similar high degree of retention and immobilization of heavy metals and transuranics has been reported for chromium [2, 20], lead [21–24], zinc [25–28] and ^{239}Pu [29–31] in temperate soils. Further, very rapid hydrolysis of Pu and Am, when added to soils, resulting in the formation of highly insoluble hydroxides, is another important factor responsible for their fixation in soils [32, 33].

Soluble organic complex formation has been attributed as one of the factors involved in the movement of inorganic ions in soils [34, 35]. In our present experiments, however, the mobility of ^{210}Pb^{2+}, ^{65}Zn^{2+}, ^{51}Cr^{3+}, ^{241}Am^{3+} and ^{239}Pu^{4+} in soils was in general either unaffected or marginally reduced at high doses of organic matter as compared with controls. This is probably due to an increase in the fixing capacity or complexation for metals in soil owing to organic matter addition [36, 37]. It has been reported that the humic acid component of organic matter in soils forms many multiple bonds with di- and trivalent metals, and these metals in turn would be chelated and not readily released, and the complex would usually not be soluble [38]. In our other studies, organic matter has been found to reduce the solubility of both Pu and Am in soils over extended periods of up to 400 days [32, 33]. It is likely, therefore, that the formation of insoluble larger molecular weight complexes with constituents of compost and sewage sludge, such as fulvates and humates [mol.wt.: 30 000 to 50 000], could result in the immobilization of Pb, Zn, Cr, ^{241}Am and ^{239}Pu in the surface layer of soils.

In general, low molecular weight synthetic chelating agents EDTA (mol.wt. 292), EDDHA (mol.wt. 359) and DTPA (mol.wt. 393) at concentrations of 10^{-4} $\underline{M}$ were quite effective in inducing the mobility of the heavy metals and transuranics in soils; however, these chelates exhibited a high degree of specificity for complexing individual heavy metal or transuranic radionuclide depending upon the soil type. The occurrence of ^{51}Cr^{3+} breakthrough from columns of pellustert and oxisol on leaching with 10^{-4}M EDDHA was suggestive of the rapid formation of stable, soluble Cr-EDDHA complexes compared with the slower formation of Cr-EDTA or Cr-DTPA complexes where no breakthrough of ^{51}Cr occurred. The formation of Cr^{3+} complexes in the soils may be similar to the formation of high stable chelates of Fe^{3+} with EDTA, DTPA and EDDHA [39]. By contrast EDDHA was ineffective in inducing mobility of added ^{210}Pb in all the three soils. EDTA was the most effective enhancing mobility of Pb, followed by DTPA, suggesting the formation of stable and soluble Pb-EDTA and Pb-DTPA complexes that persist in soils over extended periods.

EDTA appeared to be more effective in enhancing the mobility of ^{65}Zn as compared with DTPA in the pellustert which may again be due to the more rapid formation and/or greater stability of soluble Zn-EDTA complexes than Zn-DTPA complexes. As EDDHA was not used in this experiment, it is not possible to

predict the formation or behaviour of Zn-EDDHA complexes. In the oxisol, however, both EDTA and DTPA were more or less equally effective; and in the haplaquent, DTPA was slightly more effective in enhancing the mobility of Zn than EDTA. These findings again suggest that leaching with solutions of EDTA and DTPA results in the formation of soluble stable Zn-EDTA and Zn-DTPA complexes in soils over extended periods, thereby enhancing the mobility of zinc. Earlier studies [40, 41] have also reported transformation of solid-phase soil Zn into soluble Zn-EDTA complexes, thereby increasing the concentration gradient of total diffusable zinc and its mobility in soils.

DTPA was highly effective in enhancing the mobility of the transuranic radionuclides through columns of all three tropical soils examined. These findings are suggestive of the formation of stable and soluble Pu-DTPA and Am-DTPA complexes that are stable in soils over extended periods [42] and are more mobile and available for plant uptake [15, 43]. The effect of DTPA in increasing the solubility of ^{241}Am in Hacienda loam [44], Burbank sandy loam [45] and Dothan sandy clay loam [46] soils of the United States of America has been reported earlier. EDTA was less effective than DTPA in inducing the mobility of the transuranic radionuclides in the three soil types.

It is noteworthy that the formation of complexes of the heavy metals and transuranics with low molecular weight synthetic chelating agents resulted in generally enhanced mobility of these elements in soils. In contrast, the compost and sewage sludge treatments, which may have led to the likely formation of relatively large molecular weight complexes with these elements, either marginally reduced or had no significant influence on their mobility in the soil types examined. The present results have practical implications in terms of distribution of heavy metals and transuranics in different tropical and subtropical soils and the development of practices for leaching Cr, Zn, Pb, ^{239}Pu and ^{241}Am below the active root zone of crop plants grown in contaminated soils.

REFERENCES

[1] MERTZ, W., Fed. Proc. Fed. Am. Soc. Exp. Biol. 26 (1967) 186.

[2] LISK, D.J., Adv. Agron. 24 (1972) 290.

[3] BARTLETT, R.J., KIMBLE, J.M., J. Environ. Qual. 5 (1976) 379.

[4] BARTLETT, R.J., KIMBLE, J.M., J. Environ. Qual. 5 (1976) 383.

[5] CARY, E.E., ALLAWAY, W.H., OLSEN, O.E., J. Agric. Food Chem. 25 (1977) 305.

[6] BARTLETT, R., JAMES, B., J. Environ. Qual. 8 (1979) 31.

[7] TURNER, M.A., RUST, R.H., Proc. Soil Sci. Soc. Am. 35 (1971) 755.

[8] MORTVEDT, J.J., GIORDANO, P.M., J. Environ. Qual. 4 (1975) 170.

[9] NRIAGU, J.C., The Biogeochemistry of Lead in the Environment. Part A. Ecological Cycles, Elsevier/North-Holland Biomedical Press (1978).

[10] FERGUSSON, J.E., HAYES, R.W., TAN, S.Y., SIM, H.T., N.Z. J. Sci. 23 (1980) 293.

[11] Council for Agriculture Science and Technology (CAST) Rep. No. 83, Ames, Iowa (1980).

[12] HINESLY, T.D., ZIEGLER, E.L., BARRETT, G.L., J. Environ. Qual. 8 (1979) 35.

[13] NRIAGU, J.C., The Biogeochemistry of Lead in the Environment. Part B. Biological Effects, Elsevier/North-Holland Biomedical Press (1978).

[14] MILBERG, R.P., LAGERWERF, J.V., BROWER, D.L., BIERSDORF, G.T., J. Environ. Qual. 9 (1980) 6.

[15] ROMNEY, E.M., MORK, H.M., LARSON, K.H., Health Phys. 19 (1970) 487.

[16] ROMNEY, E.M., DAVIS, J.J., Health Phys. 22 (1972) 551.

[17] FRANCIS, C.W., J. Environ. Qual. 2 (1973) 67.

[18] PRICE, K.R., J. Environ. Qual. 2 (1973) 62.

[19] United States SALINITY LABORATORY STAFF, Diagnosis and Improvement of Saline and Alkali Soils, US Dept. Agriculture Handbook 60 (1954) 160.

[20] SHEWRY, P.R., PETERSON, P.J., J. Ecol. 64 (1976) 195.

[21] HASSETT, J.J., Commun. Soil Sci. Plant Anal. 5 (1974) 499.

[22] CZUBA, M., HUTCHINSON, T.C., J. Environ. Qual. 9 (1980) 566.

[23] CARTWRIGHT, B., MERRY, R.H., TILLER, K.G., Aust. J. Soil.Res. 15 (1977) 69.

[24] LITTLE, P., WIFFEN, R.D., Atmos. Environ. 12 (1978) 1331.

[25] BROWN, A.L., KRANTZ, B.A., MARTIN, P.E., Proc. Soil Sci. Soc. Am. 26 (1962) 167.

[26] JURINAK, J.J., THORNE, D.W., Proc. Soil Sci. Soc. Am. 19 (1955) 446.

[27] NAVROT, J., JACOBY, B., RAVIKOVITCH, S., Plant Soil 27 (1967) 141.

[28] SINGH, B.R., Plant Soil 41 (1974) 619.

[29] CLEVELAND, J.M., The Chemistry of Plutonium, Gordan and Breach Science Publishers, Inc., New York (1970) 653.

[30] BONDIETTI, E.A., REYNOLDS, S.A., SHANKS, M.H., in Transuranium Nuclides in the Environment (Proc. Symp. Vienna, 1976), IAEA, Vienna (1976) 273.

[31] GLOVER, P.A., MINER, F.J., POLZER, W.L., USERDA Rep. BNWL-2117 (1976) 225.

[32] VYAS, B.N., Studies on the behaviour of some transuranic radionuclides in typical Indian soils and soilplant systems, Ph.D. Thesis (Chemistry) Gujarat University (1981).

[33] VYAS, B.N., MISTRY, K.B., Science of the Total Environment, in press.

[34] HODGSON, J.F., Adv. Agron. 15 (1963) 119.

[35] SAAS, A., GRAUBY, A., in Environmental Behaviour of Radionuclides Released in the Nuclear Industry (Proc. Symp. Aix-en-Provence, 1973), IAEA, Vienna (1973) 255.

[36] KIRKHAM, M.B., Compost Sci. 18 (1977) 18.

[37] HOYT, G.D., ADRIANO, D.C., J. Environ. Qual. 8 (1979) 393.

[38] ALLISON, F.E., Soil Organic Matter and its Role in Crop Production, Elsevier Scientific Publishing Co., New York (1973) 637.

[39] NORVELL, W.A., "Equilibria of metal chelates in soil solution", Micronutrients in Agriculture (MORTVEDT, J.J., GIORDANO, P.M., LINDSAY, W.L., Eds), Soil Sci. Soc. Am. Inc., Madison, Wisconsin (1972) Chap.6.

[40] JACKSON, M.L., "Chemical composition of soils", Chemistry of the Soil (BEAR, F.E., Ed.), Am. Chem. Soc., Monograph Series, Reinhold (1956) Chap. 2.

[41] ELGAWHARY, S.M., LINDSAY, W.L., KEMPER, W.D., Proc. Soil Sci. Soc. Am. 34 (1970) 66.

[42] WILDUNG, R.E., GARLAND, T.R., USERDA Rep. BNL-245 (1977) 45.

[43] LIPTON, W.V., GOLDIN, A.S., Health Phys. 31 (1976) 425.

[44] WALLACE, A., Health Phys. 22 (1972) 559.

[45] BALLOV, J.E., PRICE, K.R., GIES, R.A., DOCTOR, P.G., Health Phys. 34 (1978) 445.

[46] ADRIANO, D.C., J. Agric. Food Chem. 27 (1979) 1371.

Invited Paper

SOIL PHYSICAL PROPERTIES OF SALINE AND ALKALI VERTISOLS

M. KUTÍLEK
Soil Science Laboratory,
Department of Irrigation and Drainage,
Technical University,
Prague, Czechoslovakia

Abstract

SOIL PHYSICAL PROPERTIES OF SALINE AND ALKALI VERTISOLS.

Soil samples with variation in exchangeable sodium percentage (ESP) were selected from vertisols in Gezira in the Sudan. In one sample the study was conducted with a substantial increase of electrical conductivity (EC). Using free and confined samples, the moisture retention curves $H(\theta)$ and saturated hydraulic conductivities K_S were determined. The diffusivity $D(\theta)$ was evaluated from the horizontal infiltration together with sorptivity S. The unsaturated conductivity $K(\theta)$ was obtained by the outflow method, from $D(\theta)$ and $H(\theta)$ values. The functional relationships of $D(\theta)$ are extremely dissimilar when the ESP changes. Since the $D(\theta)$ of alkali samples is very low, it is concluded that alkalization leads to a substantial reduction of the water flux to the roots of plants. In high ESP samples, the $D(\theta)$ remains at values lower than D, corresponding to a wilting of the majority of plants. Saturation of alkali vertisols with Ca^{2+} leads to a substantial increase of both $D(\theta)$ and $K(\theta)$. This increase is higher than the rise of $D(\theta)$ and $K(\theta)$ because of the increased solute concentration up to EC = 8.4 mmho/cm. The self-mulching process in the vertisol topsoil has a positive influence upon the substantial increase of $D(\theta)$ and $K(\theta)$. Sorptivity is an order of magnitude lower owing to the high ESP and it can be ignored when the rainfall infiltration problem is solved. The three calculation models, $K_r(\theta) = K(\theta)/K_S$ from $H(\theta)$, are not applicable to soils with an increased ESP value with or without high EC.

1. INTRODUCTION

The accumulation of salts and the alteration in the composition of exchangeable cations because of salinization and alkalization, induce a change of physical properties in irrigated soils. In addition to the alteration of the soil-water regime, this change affects the water regime of plants and the intensity of the salinization itself [1]. Among the physical properties of the soil, the saturated and unsaturated hydraulic conductivities, K_S and $K(\theta)$, the soil-water diffusivity $D(\theta)$, and the

moisture retention curve $H(\theta)$, are considered the most important characteristics from the practical aspect. Here, θ denotes the soil moisture, and H the pressure head (moisture potential).

The retention and flow of water in soils are affected by factors such as swelling and dispersion of clay, and these phenomena are the result of (i) the nature of clay mineralogy; (ii) the concentration of the percolating solution, characterized here by the electric conductivity, EC; (iii) the sodium adsorption ratio (SAR); and (iv) the exchangeable sodium percentage (ESP) of the soil. Many studies have shown (e.g. Ref.[2]) that an increase in ESP results in a decrease of K_S. The increase of EC has a buffer effect upon this change. More experimental data with model soil, and discussion on some threshold values, can be found in Ref.[3]. The applicability of these findings to the texturally and mineralogically different soils, as for example to vertisols, is still questionable. Russo and Bresler [4] tested the effects of mixed Na-Ca solutions on D and K of a loamy soil. They have demonstrated that $D(\theta)$ and $K(\theta)$ are independent of solution concentrations in Ca soil. In mixed Ca-Na systems, both $D(\theta)$ and $K(\theta)$ depend upon the composition and concentration of the solution. The influence is similar to that acting upon K_S. Dane and Klute [2] conducted experiments with one soil subjected to variation of concentration and SAR values, and they found that the decrease of $K(\theta)$ with the decrease of EC and the increase of SAR is to some extent irreversible. Their soil consisted of 43% clay in which 60% was formed by montmorillonite. It was reported earlier [5, 6] that an increase in ESP results in increasing the retention of water in soil. In irrigation practice, the difference between field capacity and wilting point is denoted as available water capacity (AWC) and this value is widely used. The value of AWC in soils of high ESP is either higher than, or roughly equal to, the AWC of soils of low ESP value or of soils saturated with Ca^{2+}. Kutílek [7] and Varallyay [6] have proved that the concept of AWC is misleading in salt-affected soils since the availability of water to plants should be evaluated according to the flux of water to the roots of plants. In alkali soils the flux is very low judging from the low values of $K(\theta)$ and $D(\theta)$ in the range of "available" water, and the wilting point does not correspond to 15 bar pressure head.

Our practical knowledge in soil physics has been deduced mainly from sandy and silty soils of the temperate zone where, for example, the concept of AWC is acceptable provided that the field capacity is an appropriate approximation. However, the extrapolation to soils occurring in regions of different ecological conditions on different substrates could be false. It is important to check our assumptions for these soils. The study of soils' principal physical characteristics such as $K(\theta)$ and $D(\theta)$ is considered to be the prime starting point for such an investigation.

In arid, semi-arid and semi-humid tropical zones, vertisols belong to soils of high potential productivity which are frequently the dominant soil type in

irrigation agriculture. Vertisols are typified by their high montmorillonitic clay content, and by intensive swelling and shrinkage and, partly due to these processes, they have extremely high bulk density. When irrigated they are subjected to accelerated salinization and alkalization. It is not yet clear to which extent the resulting change of physical properties can be deduced from model experiments conducted on texturally less extreme samples, nor is the range of values known. Experimental soil samples were therefore selected from vertisols in Gezira in the Sudan and the $D(\theta)$ and $K(\theta)$, as determined by various methods on samples with variations in EC and ESP, are discussed.

2.   MATERIALS AND METHODS

Experimental samples for this study are from Gezira vertisols in the Sudan. See Table I for the basic information on their properties. Sample Nos 1 and 2 are from one profile, Nos 3, 4 and 5 are from different profiles. Dissimilarity between both groups is in the clay content of the samples. The range of clay content of samples is probably the maximum range existing in Gezira vertisols. Sample Nos 3, 4 and 5 have about 47% fine clay ($< 0.2~\mu m$) and this value is very high, even in vertisols. A detailed study of clay mineralogy [5] has shown that the content of montmorillonites was about 82% in fine clay and the remaining part was formed by kaolinites and chlorites. Illites were absent. Sample Nos 1 and 3 are from the typical self-mulching top layers of vertisols and are characterized by high aggregate stability despite the relatively high ESP value (10.5 and 13). The process of self-mulching in the thin surface layer of vertisols has not yet been sufficiently explained, but the favourable physical properties of the self-mulch are well known. As an alternative sample No.4 was saturated with a solution resulting in EC = 8.4 mmho/cm and is denoted by No.4 c. Also, as an alternative sample, No.5 was saturated with Ca^{2+} and it is described as No.5a.

For sample Nos 3, 4 and 5, adsorption isotherms were determined by the desiccator method and for their evaluation the BET procedure was applied; the results are in Table I. As no appropriate technique was available at the time of experimentation to obtain all the entry data needed for applying theories on flow in swelling materials, the samples were used either as free, unconfined soil and the moisture was recalculated with regard to the actual volume, or the samples were confined at bulk densities corresponding to field values (with the exception of the self-mulching layer) and the eventual volumetric change was neglected.

Saturated hydraulic conductivity was determined by constant water head, the hydraulic gradient was 60 and Darcy's law was taken as at least a working approximation despite the fact that there were indications of deviations from Darcy's linearity between the flux and the gradient.

TABLE I. GENERAL DESCRIPTION OF SOILS USED IN EXPERIMENT

Sample No.	Depth (cm)	Clay (%)	CaCO₃ (%)	CEC (meq.%)	EC (mmho/cm)	ESP (%)	A (m²/g)	C_BET (arb. units) water vapour adsorption
1	0−5	33	5.8	31	1.1	10.5		
2	5−30	35	6.0	36	0.74	19.5		
3	0−2	59	5.7	57	1.05	13	125	25.5
4	10−35	62	3.8	54	0.96	21.5	115	31.5
5	55−90	68	5.8	62	0.75	27.5	135	29

A = specific surface.
C_{BET} = constant in the BET equation describing adsorption phenomena.

The moisture retention curves $H(\theta)$ were determined on the samples with
(a) unlimited swelling (free samples), and (b) samples of field bulk density when
the swelling at the water saturation was hindered (confined samples). Details
about $H(\theta)$ are discussed in Ref.[5]; generally, the retention curve of a free
sample is close to the straight line in the semi-log paper.. The confined samples
keep the saturated (or very near to saturated) moisture at a relatively high
pressure head, H_R, and the first release of water occurs at the value of H_R depend-
ing upon the confined bulk density. In most cases the H_R rose to more than
100 cm. The release of water is linked with shrinkage and the value of H_R should
not be confused with the air-entry value. The availability of water to plants as
deduced from $H(\theta)$ was discussed in Section 2.

H(θ) was used to compute the hydraulic conductivity $K(\theta)$ according to
Refs [8 - 10]. In the procedure of Ref.[9] the retention curve was fitted by
spline function; in Refs [8, 10] the expression of Ref.[11] was used for minimum
square fitting.

$D(\theta)$ was determined from horizontal infiltration of water into soil columns
packed to field bulk density. Distilled water was used for samples 1, 2, 3, 4 and 5
while for 4c and 5a the appropriate concentrations of chloride solutions were
prepared. For evaluation, the method described in Ref.[11] was applied. From
$D(\theta)$ and $H(\theta)$, the $K(\theta)$ relations were obtained and are referred to as experimental
K of confined samples. These data are compared with $K(\theta)$, computed from $H(\theta)$
according to Refs [8 – 10]. From the recorded cumulative infiltration in time,
sorptivity S was also obtained.
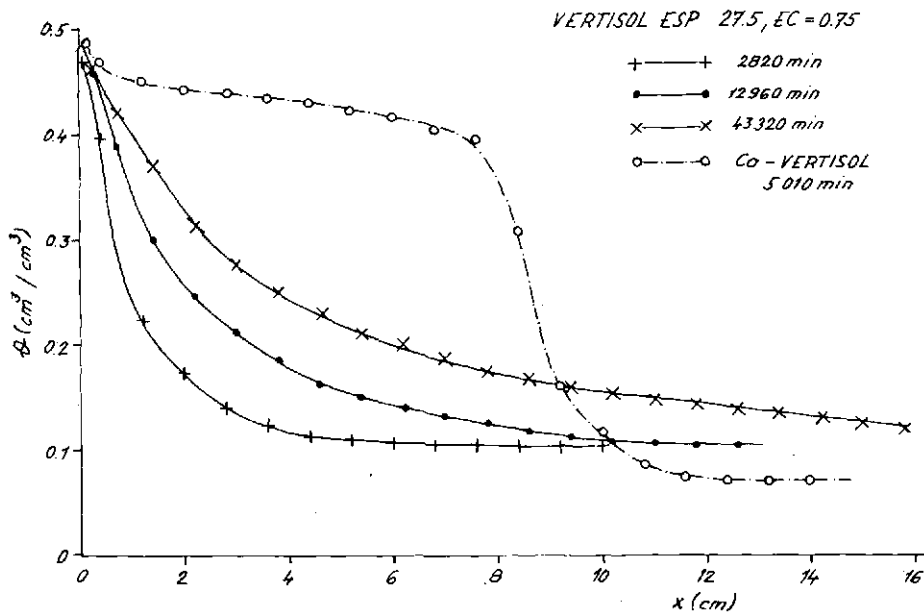
FIG.1. Moisture profiles θ (χ) of the horizontal infiltration of water in alkali vertisol (No.5) at three time intervals, and the results of the same type of experiment when the soil was saturated with Ca^{2+} (sample No.5a).

The $K(\theta)$ of free unconfined samples was determined by the outflow method [12]. The corresponding volumetric moisture was recalculated with reference to the actual sample volume. The procedure was approximative.

3. DISCUSSION OF THE RESULTS

3.1. Soil-water diffusivity

An example of the experimental results with horizontal infiltration in soil of extreme alkalinity (sample No.5) is shown in Fig.1, where the moisture θ is plotted against the co-ordinate χ. The shape of the moisture profile $\theta(\chi)$ is different from $\theta(\chi)$ of non-alkali soils and is similar to $\theta(\chi)$ for D = const. In the same figure, the substantial change in both the infiltration rate and in the change of moisture profile is demonstrated when the original sample No. 5 was saturated with Ca^{2+} (sample No.5a).
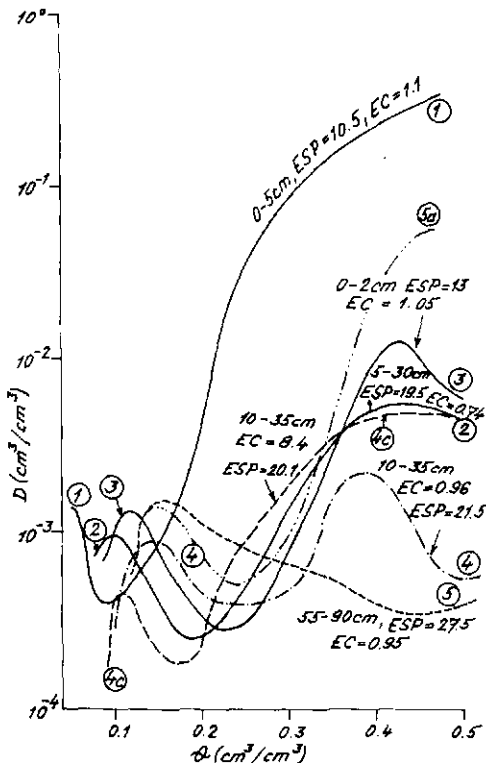
FIG.2. Dependence of the soil-water diffusivity D upon the moisture θ as determined from
the horizontal infiltration of water in vertisols of various degrees of salinity and alkalinity.

The computed values of D(θ) are plotted for all samples in Fig.2. With the
exception of the self-mulching sample No.1, the D(θ) of all samples is substantially
lower in the wet part of the curve when compared with non-alkali, non-vertisol
soils. The functional relationships of D(θ) are changed. From the practical
point of view, the scaling technique is not applicable when the profile is affected
by alkalization.

The increase of ESP leads to the decrease of D(θ) in the wet part and for
ESP > 20% the D(θ) of the wet part tends to keep D values below the peak
values of the dry part of the curve and, in practice, below the value corresponding
to the permanent wilting of plants. In soil with ESP = 27.5 the D decreases with
the increase of θ, starting from the peak at θ = 0.16. The strong D peaks in ranges
of θ = 0.1 to θ = 0.16, correspond to the values of relative vapour pressure above
0.94, and this is not in accordance with D peaks of water vapour flux in mont-
morillonites (p/p_0 ≤ 0.4) and in clay soils (p/p_0 ≤ 0.6).
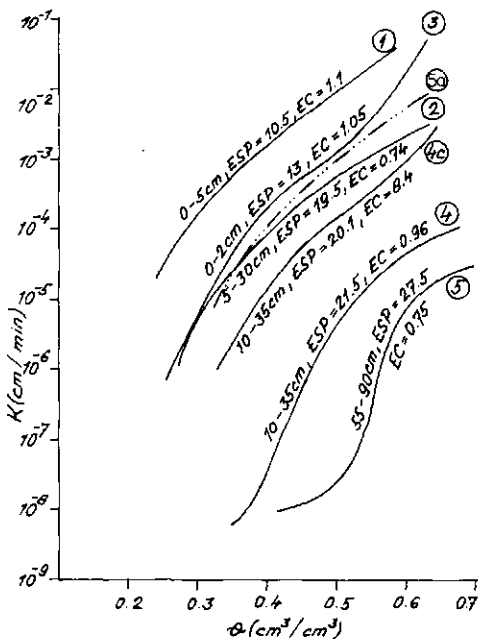
FIG.3. Dependence of the unsaturated conductivity K upon the moisture θ as determined from the outflow of water from the unconfined samples of vertisols placed in the pressure apparatus.

If $D = 2 \times 10^{-3}$ cm/min is taken as a critical value when permanent wilting of plants starts, we get as critical moisture θ_c:

In soil Nos	1	2	3	4	5	4c	5a
θ_c	0.18	0.30	0.32	all ranges		0.31	0.33

Since, with the exception of Nos 1 and 5a, D is by 1.5 – 2.0 orders of magnitude below the values of D reported for non-alkali non-vertisols, we can conclude that the alkalization of vertisols leads to a substantial reduction of the water flux to the roots and the reduced consumption of water has a direct result on the reduced photosynthesis even when the moisture is kept above θ_c.

The self-mulching effect increases the D values substantially in soils of moderate clay content (33%), while in soils of high clay content (59%) this favourable influence still exists, but is developed to a lower degree. However, self-mulching is restricted to a thin top layer and the positive features of the layer are of less practical importance. On the other hand, compared with hydrophobic

TABLE II. SATURATED CONDUCTIVITY K_S AND SORPTIVITY S

Sample No.	ρ_b (g/cm³)		K_S (cm/min) a	b	S (cm·min$^{-1/2}$)	θ_i (cm³/cm³)
1	conf.	1.34	9E−4	6E−3	1.2E−1	0.05
	free	1.09	5−2	−	−	−
2	conf.	1.31	6−5	−	1.8−2	0.07
	free	0.95	3−3	−	−	
3	conf.	1.30	5−4	−	3.8−2	0.09
	free	0.90	5−2	−	−	
4	conf.	1.36	4−6	2−2	1.1−2	0.09
	free	0.89	1−4	−	−	
4c	conf.	1.31	5−4	4−2	2.6−2	0.09
	free	1.02	3−3	−	−	
5	conf.	1.25	2−6	2−3	8.5−3	0.12
	free	0.75	3−5	−	−	
5a	conf.	1.27	6−4	−	8.5−2	0.09
	free	1.06	1−2	−	−	

a = experimental; b = computed according to Ref.[9].
conf. = confined; θ_i = initial moisture; ρ_b = bulk density.

developments on the surface of some irrigated saline soils, the self-mulching effects of vertisols are still highly positive phenomena.

The saturation of alkali vertisol samples with Ca^{2+} leads to a substantial increase of D values, and in the wet part the increase is up to two orders of magnitude. The increase of the solute concentration also shifts the $D(\theta)$ to higher values, when compared with the original sample No.4. But, surprisingly, this influence is less pronounced than the saturation of clay with Ca^{2+}. At $\theta = 0.4$, the D value of Ca vertisol is already by one order of magnitude higher than D of the vertisol sample of EC = 8.4 mmho/cm. The more positive effect of exchangeable Ca^{2+} gradually diminishes with decrease of θ. Similar differences between two treatments of soil samples are in $K(\theta)$ — see Fig.3. The results are not fully consistent with model experiments [3], but they can be simply explained when the electrokinetic phenomena, as induced by the extremely large specific surface of vertisols, are considered.

The very low values of sorptivity S of soils with high ESP agree well with the $D(\theta)$ relations – see Table II. In field situations, the sorptivity into the soil matrix is negligible when the rainfall situation is considered, and the cumulative infiltration at the ponding time represents the volume of free macropores. Let us remember that the ponding time equations contain the term with S^2 in addition to the characteristics of the macroporous system where the S term is absent [13]. The contribution of S to the value of the ponding time is therefore negligible in soils of increased ESP.

3.2. Hydraulic conductivity

The results of measurements with free, unconfined samples when the outflow method [12] was applied are plotted in Fig.3. Similar tendencies, as found for $D(\theta)$ are also distinct in $K(\theta)$ relations. The increase of ESP causes the decrease of $K(\theta)$ and in the range of ESP = 13 to ESP = 27.5 the decrease of $K(\theta)$ is more than two orders of magnitude greater. The general run of $K(\theta)$ for variations in ESP is less dissimilar than in $D(\theta)$ for variations in ESP, and when the self-mulched samples 1 and 3 are not considered, a good similarity between $K(\theta)$ of individual natural samples exists, and the difference in $K(\theta)$ between various samples does not change substantially. The scaling of $K(\theta)$ therefore looks to be applicable to soils of various degrees of alkalization, and only surface self-mulched soil could be an exception. The saturation of alkali vertisol with Ca^{2+} leads again to a more distinct increase of $K(\theta)$ than that of $K(\theta)$ due to the high EC. The relatively high values of $K(\theta)$ in Ca vertisol allow the conclusion that the irreversibility of K in Na vertisol is either of little importance or it does not exist at all. This conclusion is also supported by the results on the $D(\theta)$ relations.

The moisture retention curves of confined samples were used to calculate $K(\theta)$ and these values were compared with $K(\theta)$ obtained from $D(\theta)$ and $d\theta/dH$. The starting point of $K(\theta)$ computation is the value of K_S. The computed K_S was compared with experimental K_S – see Table II. The difference is in various orders of magnitude but generally the computed K_S values differ substantially from the experimental K_S values. Experimental K_S was therefore used as the correction factor for the computed $K(\theta)$ and the relative conductivities K_r were compared, where $K(\theta)_r = K(\theta)/K_S$ – Table III and Fig.4. The computational models of $K(\theta)_r$ fit relatively well to the experimental data of samples from the self-mulched top layer where the capillary phenomena are supposed to exist because of micro- and macroaggregation. When ESP increases, the computed K_r values differ again in orders of magnitude with a tendency for an increased difference between the computed K_r and the experimental K_r when θ decreases. It can therefore be concluded that the computation of $K(\theta)$ from $H(\theta)$ does not offer reliable data on saline-alkali and alkali vertisols and preference should be given to the directly measured values.

TABLE III. COMPARISON OF THE EXPERIMENTAL AND COMPUTED RELATIVE CONDUCTIVITIES K_r, WHERE $K_r = K(\theta)/K_S$ IN CONFINED SAMPLES

Sample No.	θ (cm^3/cm^3)	Exper.	K_r computed according to Ref		
			[10]	[8]	[9]
1	0.338	4.5E−2	1.9E−2	2.3E−2	6.0E−3
	0.149	2.2−6	7.7−7	1.6−6	3.1−5
2	0.316	2.1−2	5.5−3	7.6−3	−
	0.169	2.3−5	3.5−7	8.6−7	−
3	0.34	1.0−3	2.5−4	3.1−4	1.8−3
	0.259	8.9−6	7.5−7	1.1−6	1.3−5
4	0.363	1.5−1	2.8−3	3.3−3	7.2−3
	0.254	1.1−3	2.6−6	3.9−6	6.0−6
4c	0.335	1.7−2	6.8−4	8.5−4	5.1−4
	0.218	7.3−5	4.8−7	7.5−7	2.3−6
5	0.352	1.2−2	2.2−4	2.8−4	2.2−3
	0.258	9 −4	4.6−7	6.8−7	9.1−5

Later, additional core samples were taken from the soil corresponding to sample No.2 from a depth of 3 − 6 cm after the rainy season when the cracks in the moist soil disappeared and the surface had a homogeneous appearance. The position of the original cracks was marked earlier and one set of six samples was taken there. Another set of six samples was taken from the place where the cracks did not open in the dry season. The mean value of K_S was as follows: In the position of earlier crack $\overline{K}_S = 8.8 \times 10^{-4}$ cm/min; in the position without crack $\overline{K}_S = 7.2 \times 10^{-5}$ cm/min. It follows from this measurement that a steady heterogeneous system can be expected in vertisols even in wet soil, owing to the earlier existence of cracks.
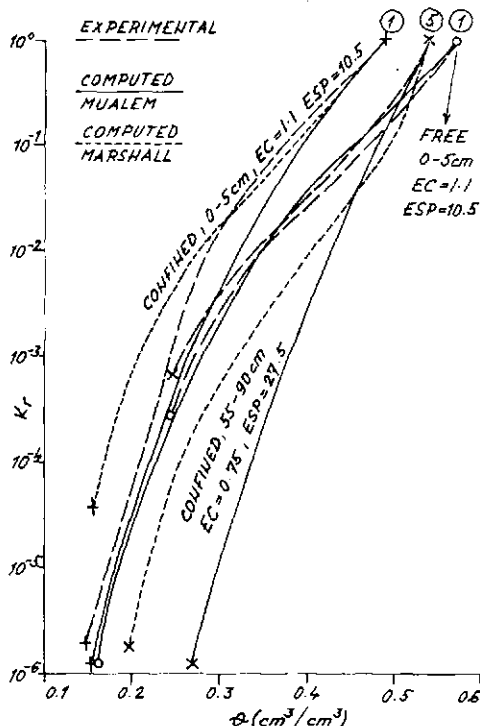
FIG.4. Comparison of the results of the computation of the relative conductivity K_r depending upon the moisture θ when two different methods were applied: (a) K_r computed from the soil-water diffusivity and from the retention curve, denoted by "experimental"; (b) K_r computed from the retention curve either by Marshall's [9] or by Mualem's [10] procedure.

ACKNOWLEDGEMENT

REFERENCES

[1] KOVDA, V.A., SZABOLCS, I., Modelling of soil salinization and alkalization, Agrokémia es talajtan **28** Budapest (1979).

[2] DANE, J.H., KLUTE, A., Soil Sci. Soc. Am. J. **41** (1977) 1043.

[3] SHAINBERG, I., RHOADES, J.D., PRATHER, R.J., Soil Sci. Soc. Am. J. **45** (1981) 273.

[4] RUSSO, D., BRESLER, E., Soil Sci. Soc. Am. J. **41** (1977) 713.

[5]   KUTILEK, M., SEMOTAN, J., "Soil water properties of Gezira soils", New Development
      in the Field of Salt-affected Soils (Proc. Int. Symp. UAR, Cairo), Agric. Res. Establishment
      Egypt (1975) 299.
[6]   VÁRALLYAY, G., "Soil factors limiting optimum water supply of plants", Physical
      Factors of Soil Environment, Polish Acad. Sciences, Warsaw (1979) 373.
[7]   KUTÍLEK, M., "The influence of clay minerals and exchangeable cations on soil moisture
      potential", Physical Aspects of Soil Water and Salts in Ecosystems (HADAS, A.,et al.,
      Eds.) Springer Berlin-New York (1973) 153.
[8]   CHILDS, E.C., COLLIS-GEORGE, N., Proc. R. Soc. Ser. A 201 (1950) 392.
[9]   MARSHALL, T.J., J. Soil Sci. 9 (1958) 1.
[10] MUALEM, Y., Water Resour. Res. 12 (1976) 513.
[11] BROOKS, R.H., COREY, A.T., Hydraulic properties of porous media, Hydrology 3,
      Colorado State University (1964).
[12] GARDNER, W.R., Soil Sci. Soc. Am. Proc. 20 (1956) 317.
[13] KUTÍLEK, M., NOVÁK, V., "The influence of soil cracks upon infiltration and ponding
      time", Water in Heavy Soils Proc. (KUTÍLEK, M., ŠÚTOR, J., Eds), Int. Commission on
      Irrigation and Drainage (ICID), Int. Soil Science Soc. (ISSS) Bratislava (1976) 126.

Memoria encargada

SISTEMA INTEGRADO
AGUA-CULTIVO-SUELO-MANEJO
PARA EVALUAR LA CALIDAD
DE AGUA PARA RIEGO

I. PLA-SENTIS
Instituto de Edafología,
Facultad de Agronomía,
Universidad Central de Venezuela,
Maracay, Venezuela

Abstract—Resumen

INTEGRATED WATER-CROP-SOIL-MANAGEMENT SYSTEM FOR EVALUATING THE
QUALITY OF IRRIGATION WATER.
　　The authors make use of an independent balance of the salts and ions present in the water
available for irrigation, based on the residence times in the soil solution that are allowed by
solubility limits and drainage conditions, to develop an efficient system for evaluating the
quality of such water which combines the factors: water, crop, soil and management. The
system is based on the principle that such quality depends not only on the concentration and
composition of the salts dissolved in the water, but also on existing possibilities and limitations
in using and managing it in respect of the soil and crops, with allowance for the crop's tolerance
of salinity, drainage conditions and hydrological properties of the soils, climate and current
or potential practices for the management of the irrigation. If this system is used to quantify
approximately the time behaviour of the concentration and composition of the salts in the
soil solution, it is possible not only to predict the effects on soil, crops and drainage water,
but also to evaluate the various combinations of irrigation water, soil, crops and management
and to select the most suitable. It is also useful for fairly accurately diagnosing current problems
of salinity and for identifying alternatives and possibilities for reclamation. Examples of its
use for these purposes in Venezuela are presented with particular reference to the diagnosis
of the present and future development of "salino-sodic" and "sodic" soils by means of low-
salt irrigation water spread over agricultural soils with very poor drainage in a sub-humid
or semi-arid tropical climate. The authors also describe the use of radiation techniques for
gaining an understanding of the relations between the factors making up the system and for
improving the quantitative evaluations required to diagnose problems and to select the best
management methods for the available irrigation water.

SISTEMA INTEGRADO AGUA-CULTIVO-SUELO-MANEJO PARA EVALUAR LA CALIDAD
DE AGUA PARA RIEGO.
　　Se utiliza un balance independiente de las sales e iones presentes en las aguas disponibles
para riego, basado en sus posibilidades de permanencia en la solución del suelo de acuerdo
a los límites de solubilidad y condiciones de drenaje, con el fin de desarrollar un sistema

191

racional de evaluación de la calidad de dichas aguas, en el que se integran los factores agua, cultivo, suelo y manejo. Se basa en el principio de que dicha calidad no depende solamente de la concentración y composición de las sales disueltas en el agua, sino de las posibilidades y limitaciones para su uso y manejo en relación a suelos y cultivos, para lo cual se toman en cuenta la tolerancia del cultivo a la salinidad, las condiciones de drenaje y propiedades hidrológicas de los suelos, el clima y las prácticas actuales o potenciales para manejo del riego. La utilización del sistema para cuantificar en forma aproximada la evolución de la concentración y composición de las sales en la solución del suelo permite no solo prever los efectos sobre suelos, cultivos y aguas de drenaje, sino también evaluar las diferentes combinaciones de agua de riego, suelo, cultivos y manejo, y seleccionar las más convenientes. Asimismo es útil para realizar diagnósticos bastante precisos de problemas actuales de salinidad, y para establecer las alternativas y posibilidades de recuperación. Se presentan ejemplos de su uso para dichos fines en Venezuela, haciendo hincapié en el diagnóstico del desarrollo actual y potencial de suelos "salino-sódicos" y "sódicos" con aguas de riego de bajo contenido de sales en suelos agrícolas con drenaje muy deficiente, y con clima tropical subhúmedo o semiárido. Se señala la utilidad que podrían tener el uso de técnicas de radiación en el entendimiento de las relaciones entre los factores incluídos en el sistema, y en el mejoramiento de las evaluaciones cuantitativas requeridas para el diagnóstico de los problemas y la selección del mejor uso y prácticas de manejo del agua de riego disponible.

1.   INTRODUCCION

Los problemas de salinización de suelos revisten particular importancia, especialmente en agricultura de regadío, por su acción sobre las propiedades fisicoquímicas de los mismos, sobre los cultivos y sobre los animales y personas que los consumen. Dichos problemas han sido más estudiados en zonas áridas, donde tienen características específicas, ya que la agricultura bajo riego convencional se ha aplicado tradicionalmente en dichas áreas, mientras que en otros climas el riego se ha usado más que todo para el cultivo de arroz bajo inundación, condiciones bajo las cuales el problema de salinidad es menos frecuente. Al irse expandiendo el riego como fuente suplementaria de agua a zonas con climas semiáridos o subhúmedos, con distribución estacional de las lluvias, especialmente en suelos con drenaje restringido y en latitudes tropicales con altas tasas de evapotranspiración, se han presentado problemas de salinización de mayor complejidad [1--3], difíciles de detectar a corto plazo y, por ello, menos analizados. Sin embargo, por provocar efectos aún más permanentes y difíciles de resolver, estos casos deben estudiarse cuidadosamente, determinándose las prácticas que resulten convenientes para su prevención.

Aunque es de gran interés conocer el contenido y composición de sales en el agua desde el punto de vista de salinización de los suelos a los cuales va a aplicar con el riego, es necesario tener en consideración que, de acuerdo a las condiciones del clima, propiedades hidrológicas del perfil del suelo y facilidades del drenaje, dicha concentración y composición pueden variar mucho en la solución del suelo

resultante. Es por ello que la calificación de salinidad de aguas de riego no puede hacerse en forma aislada, sin tomar en cuenta los demás factores que inciden sobre las concentraciones finales de la solución del suelo. En el proceso de salinización revisten particular importancia los cambios que pueden ocurrir en la composición de la solución del suelo por la precipitación de ciertas sales de solubilidad limitada, tales como carbonatos de Ca y Mg y sulfatos de Ca. En cualquier caso, condiciones que favorezcan dicho proceso, como predominio de bicarbonatos y sulfatos en el agua, pérdidas de CO_2, mal drenaje, etc., contribuirán a un enriquecimiento relativo de Na en la solución del suelo y concurrentemente en el complejo de intercambio, aunque se presentará una disminución en el contenido total de sales en la solución.

2.   REQUERIMIENTOS DE LIXIVIACION Y DRENAJE PARA CONTROL DE LA SALINIZACION DE LOS SUELOS

Las plantas no toman las sales en la misma proporción con que absorben agua y por ello las aportadas con el riego tienden a acumularse en la solución del suelo. Esto puede evitarse aplicando un exceso de agua de riego por encima del uso consuntivo del cultivo para lixiviar esas sales y evitar su acumulación en la zona crítica del suelo. Cuando este contiene originalmente una cantidad excesiva de sales en solución, será necesario aplicar también un exceso de agua para lixiviarlas. En cualquier caso, la cantidad de agua a aplicar en exceso dependerá del contenido y tipo de sales en el agua de riego [4], del contenido original de sales en la solución del suelo, del clima, y de la efectividad de la lluvia lixiviando sales en la estación húmeda [2]. El exceso de agua de riego requerido para el control de sales en el suelo ha sido llamado "requerimiento de lixiviación" [5].

Cuando el exceso de agua de riego o lluvia que penetra en el suelo no se elimina debido a déficits en el drenaje interno, su efecto sobre la salinización puede ser contraproducente, al provocar en algunos casos un incremento más acelerado de élla y, en otros, el ascenso de sales acumuladas en el subsuelo hasta el suelo superficial. Ambas situaciones son originadas por ascenso del nivel freático general, o por formación de mesas de agua colgantes cuando el déficit en drenaje interno se debe más que todo a la baja permeabilidad de algún estrato en el perfil del suelo. Para evitar que eso suceda, es necesario proveer un sistema de drenaje capaz de eliminar el exceso de agua, cuyo diseño y posibilidades prácticas y económicas dependerá tanto del "requerimiento de lixiviación" como de las propiedades hidrológicas del perfil del suelo.

Se ha planteado [6, 7] la posibilidad de reducir los requerimientos de lixiviación de sales del suelo utilizando métodos de riego que por su frecuencia y control preciso permitan, por un lado, que gran parte de las sales se acumulen y precipiten en zonas profundas del suelo y, por el otro, provoquen un mayor desarrollo y

actividad radicular, con la mayor absorción de agua, en zonas más superficiales
libres de excesos de sales. Ello reduce los requerimientos de agua para riego y
de drenaje, pero sólo es aplicable en situaciones donde sean económicos y prácticos
la utilización y control preciso de dichos sistemas de riego. Además, no está claro
ni probado si dicho sistema de control de sales puede mantenerse a largo plazo
sin un incremento progresivo de la salinización en suelo cada vez más superficial.
En climas donde en una parte del año hay aportes no controlables de agua de lluvia,
sería sumamente peligroso adoptar este criterio de control de salinidad.

3.   ESTIMACION DE LA CALIDAD DE AGUAS PARA RIEGO

Desde el punto de vista cuantitativo, para establecer el balance de sales en
el suelo es necesario considerar algunos factores fijos o poco controlables, a saber:

a) Suelo (propiedades físicas e hidrológicas)
b) Clima (precipitación y uso consuntivo)
c) Agua (cantidad y sales en solución)
y de otros, controlables hasta cierto límite, como:

a) Cultivos
b) Drenaje artificial
c) Manejo del riego
los cuales permiten atenuar, evitar o escapar de los problemas de afectación
por sales o sodio derivados de los factores fijos.

En todas las aguas usadas para irrigación existen en forma predominante los
iones bicarbonato, cloruro, sulfato, calcio, magnesio y sodio. Para calificarlas,
generalmente se ha tomado en cuenta la salinidad total, sus contenidos de sodio
y de bicarbonatos y, ocasionalmente, sus contenidos de ciertos elementos tóxicos
como B, Li, etc. En cualquier caso, su calificación está determinada por el peligro
potencial de causar problemas ya sea en cuanto a reducciones en rendimiento o
calidad de los cultivos, o al requerimiento de prácticas especiales de manejo. Hoy
en día existe la tendencia a definir cuantitativamente las posibilidades de uso de
un agua de riego en base a las condiciones específicas en que dicha agua va a ser
usada, incluyendo propiedades del suelo, clima, cultivos y manejo del riego [1, 8--11].

Usando un agua determinada, la acumulación de sales y sodio en el suelo
dependerá de la fracción del agua infiltrada que pase a través y hacia abajo de la
zona radicular y de las posibilidades de precipitación de sales poco solubles como
carbonatos de Ca y Mg y en algunos casos sulfatos de Ca en el suelo [1, 4, 12, 13].
También dependerá de la eficiencia con que dicha agua infiltrada actúe lixiviando
las sales, la cual está determinada fundamentalmente por el tipo de suelo y la
forma de aplicación del agua de lixiviación. Esta eficiencia es menor en suelos
pesados con tendencia a agrietarse, cuando el agua para lixiviación se aplica en

grandes cantidades de una sola vez, y es mayor en suelos livianos, con aplicaciones frecuentes y pequeñas de agua de lixiviación. Pla [1] demostró que en suelos con permeabilidad lenta, pero con escasa tendencia a agrietarse, situación típica de suelos aluviales limosos, la eficiencia de lixiviación de sales del suelo superficial aumentaba cuando se permitía un agotamiento mayor del agua utilizable o aprovechable antes del riego.

Los límites máximos de sales y sodio en el suelo, determinantes de la fracción del agua infiltrada que debe pasar a través de la zona radicular (requerimiento de lixiviación), dependerán de la tolerancia del cultivo a las sales y de las propiedades del suelo, respectivamente. La cantidad de agua de riego aplicada, además de la requerida para satisfacer el uso consuntivo del cultivo, debe proveer un exceso para cumplir con dichos requerimientos de lixiviación. Estos a su vez determinarán las necesidades de drenaje y la intensidad del sistema de drenaje artificial en el caso de que sea necesario corregir deficiencias en los drenajes naturales.

En conclusión, un esquema de clasificación para aguas de riego o cualquier ecuación para predecir sus efectos en el suelo debe tomar en cuenta las posibilidades o necesidades de lixiviación. Utilizando la relación que existe entre lixiviación y acumulación de Na y Ca + Mg en la solución del suelo, es posible predecir aproximadamente la concentración total de sales y la "Relación de Adsorción de Sodio" en dicha solución cuando nos acercamos a condiciones de equilibrio. Para ello es necesario considerar las solubilidades de las diferentes sales de Na, Ca y Mg bajo las condiciones prevalecientes en el suelo. Como los valores de "Relación de Adsorción de Sodio" en el extracto de saturación (RASES) pueden ser usados como índice bastante preciso de la acumulación de Na intercambiable en el suelo en el rango de 5-30 correspondiente a los límites de procentajes de sodio inter-cambiable en la mayoría de los suelos afectados por Na, pueden establecerse valores límites de RASES [9] dependiendo del suelo, cultivo, etc., en la misma forma que se ha hecho hasta ahora para salinidad total.

La predicción de las concentraciones de sales e iones en la solución del suelo cuando se alcance equilibrio es importante para clasificar las aguas de riego en relación a los requerimientos y posibilidades de lixiviación y, por lo tanto, con referencia a las condiciones de drenaje existentes o requeridas en áreas bajo riego. Ello es indispensable para una determinación general de las demandas de riego y drenaje de un área que va a ser regada con un agua específica. Para esto, conjunta-mente con los requerimientos de lixiviación deben tomarse en cuenta los aportes de agua por lluvia o filtraciones subterráneas y el uso consuntivo de los cultivos en el área. La selección de las prácticas de manejo y cultivo más apropiados para cumplir con las necesidades así establecidas dependerá de consideraciones prácticas y económicas.

Uno de los sistemas de calificación más utilizado en las últimas décadas, y aún hoy en día, es el propuesto por el Laboratorio de Salinidad del Servicio de Investigaciones Agrícolas del Departamento de Agricultura de Estados Unidos [14],

desarrollado para condiciones promedio en la región árida del SO de Estados
Unidos. La sencillez del sistema ha conducido a un uso general e indiscriminado
en situaciones muy diferentes y con alcances más allá de los previstos cuando fue
desarrollado. Ello ha provocado y está provocando muchos errores en los
diagnósticos de problemas de salinización, y en las recomendaciones de prácticas
de manejo para prevenirlos. En fechas más recientes, y por iniciativa de investiga-
dores de la misma Institución, se han establecido criterios y desarrollado sistemas
de evaluación de calidad de aguas para riego que tratan de precisar y ampliar el
rango de condiciones para su utilización [10, 15], los cuales se recogen en publica-
ciones de la FAO [16, 17], proponiéndose guías para su uso. Al establecer dichos
criterios de calificación, se incurre en la utilización de ecuaciones empíricas basadas
en resultados experimentales obtenidos bajo condiciones muy particulares de clima,
suelos, drenaje, cultivos, y manejo de riego.

El hecho de que las diferentes ecuaciones propuestas sean de naturaleza
eminentemente empírica, y las muy particulares condiciones asumidas o experi-
mentadas para su formulación, hace que la utilización sea restringida a situaciones
similares a ellas, y que aun ahí se puedan presentar desviaciones de lo predicho
[18] por factores asumidos, difíciles de controlar en la práctica. Todo ello hace
que el sistema no tenga aplicación universal, especialmente en los muy particulares
problemas de salinización que pueden presentarse en zonas tropicales con clima
semiárido o subhúmedo [3].

4.   SISTEMA INTEGRADO AGUA-CULTIVO-SUELO-MANEJO PARA LA
     CALIFICACION DE AGUAS PARA RIEGO

El sistema de calificación que aquí presentamos ha sido desarrollado en base a
numerosas evidencias experimentales y a observaciones de campo antes citadas,
y evaluado bajo las más variadas situaciones en zonas de riego [19]. Se basa en
un balance independiente de los iones más comunes en las aguas de riego y en
la solución del suelo, de acuerdo a la fracción de lixiviación efectiva (LF) y a
las solubilidades máximas de las sales bajo diferentes condiciones. Con ello, y al
no asumir "a priori" condiciones particulares para su uso, no hay restricciones
en cuanto al empleo del sistema para el diagnóstico de problemas potenciales de
salinización bajo las más variadas condiciones de clima, suelo, cultivos y manejo
del riego. Además, por la flexibilidad del sistema es posible establecer las combi-
naciones más apropiadas de suelos, cultivos y manejo del riego que conduzcan
a los balances de sales e iones más adecuados para prevenir dichos problemas.
Las bases teóricas del sistema y su desarrollo detallado aparecen en publicaciones
previas [1, 4, 9, 20, 21]. Para facilitar su aplicación en la práctica se hacen algunas
simplicaciones, basadas en deducciones teóricas y mediciones a nivel experimental
y de campo, después de comprobar que no afectan apreciablemente la precisión

CUADRO I. ECUACIONES PARA CALCULAR L(ST)F Y L(NA)F PARA CADA
GRUPO DE CONDICIONES Y EN FUNCION DE LOS VALORES MAXIMOS
PREESTABLECIDOS DE STES Y RASES

CONDICIONES	L(ST)F	L(NA)F
BR $\leqslant$ CAR BR $\leqslant$ 10xLF CASR $\leqslant$ 30xLF	(NAR + CAR)/STES	$2 \times NAR^2 / RASES^2 \times CAR$
BR $\leqslant$ CAR BR $>$ 10xLF CASR $\leqslant$ 30xLF	(NAR+CAR-BR)/(STES-10)	$\dfrac{\left[RASES^2 \times (CASR+CACLR)^2 + 80NAR^2\right]^{1/2}}{20\ RASES} - \dfrac{(CASR+CACLR)}{20}$
* BR $\leqslant$ CAR BR $\leqslant$ 10xLF CASR $>$ 30xLF	(NAR+CAR-CASR)/STES-30)	------
BR $\leqslant$ CAR BR $>$ 10xLF CASR $>$ 30xLF	(NAR+CAR-BR-CASR)/STES-40	$\dfrac{\left[RASES^2 \times CACLR^2 + (320 \times NAR^2)\right]^{1/2}}{80 \times RASES} - \dfrac{CACLR}{80}$
BR $>$ CAR	NAR/(STES-CAR)	$NAR/RASES \times (CAR/2)^{1/2}$

B: Bicarbonatos; S: Sulfatos; CL: Cloruros; CA: Ca + Mg; NA: Na; ST: Sales totales; RAS: Relación de
adsorción de sodio; ES: Extracto de saturación del suelo; R: Agua de riego; L: Requerimiento de lixiviación
para control de (ST) o (NA); F: Eficiencia de lixiviación; CACLR= CAR-BR-SR; CASR= CAR-BR-CACLR.
(* Situación poco frecuente).

de los diagnósticos. Como máxima concentración de bicarbonatos de Ca y Mg (CAB)
en la solución del suelo, cuando en el agua de riego la concentración de Ca + Mg (CAR)
es igual o mayor que la concentración de bicarbonatos (BR) se toma un valor fijo
de 10 meq/L. Cuando BR es mayor que CAR, se espera que la máxima concentra-
ción de CAB en la solución de suelo se aproxime a CABR. En el caso del sulfato
de Ca (CAS) se toman 30 meq/L como la máxima concentración en la solución
del suelo. Aunque esta concentración puede subir apreciablemente en soluciones
muy salinas, con alto contenido de cloruros, dentro de los rangos de salinidad
permisible en la gran mayoría de los suelos para uso agrícola, las desviaciones a
partir de ese valor no afectan en forma apreciable los diagnósticos. En el caso de
los bicarbonatos de Ca y Mg, las desviaciones son aún menores y dependientes de
la presión de CO_2 y de la proporción Ca/Mg en la solución.

Aunque en base a valores reportados por numerosos investigadores y a nuestra
propia experiencia se propone el uso de valores de infiltración básica como índices
de la permeabilidad del perfil del suelo (alta >5 cm/h; mediana $0,5-5$ cm/h; baja
$0-1-0,5$ cm/h; muy baja $<0,1$ cm/h) y determinados valores límite de concentra-
ción de sales (STES) y de índices de Na (RASES) en el extracto de saturación,

CUADRO II. CLASIFICACION DE AGUAS DE RIEGO DE ACUERDO AL PELIGRO DE ACUMULACION DE SALES TOTALES (ST) O DE SODIO (NA) EN EL SUELO (L(ST)F y L(NA)F calculados con ecuaciones del Cuadro I)

PERMEABILIDAD DEL SUELO (Infiltración básica)	STES MAXIMO (meq/l)	RASES MAXIMO	L(ST)F (para ST) – L(NA)F (para NA)						
			< 0,01	0,01–0,02	0,02–0,05	0,05–0,10	0,10–0,20	0,20–0,30	> 0,30
ALTA (>5 cm/hora)	40	20	ST_{11} NA_{11}	ST_{11} NA_{11}	ST_{11} NA_{11}	ST_{11} NA_{11}	ST_{21} NA_{21}	ST_{31} NA_{31}	ST_{41} NA_{41}
	80	30	ST_{12} NA_{12}	ST_{12} NA_{12}	ST_{12} NA_{12}	ST_{12} NA_{12}	ST_{22} NA_{22}	ST_{32} NA_{32}	ST_{42} NA_{42}
	160	40	ST_{13} NA_{13}	ST_{13} NA_{13}	ST_{13} NA_{13}	ST_{13} NA_{13}	ST_{23} NA_{23}	ST_{33} NA_{33}	ST_{43} NA_{43}
MEDIANA (0,5–5 cm/hora)	40	15	ST_{11} NA_{11}	ST_{11} NA_{11}	ST_{21} NA_{21}	ST_{21} NA_{21}	ST_{31} NA_{31}	ST_{41} NA_{41}	ST_{51} NA_{51}
	80	20	ST_{12} NA_{12}	ST_{12} NA_{12}	ST_{22} NA_{22}	ST_{22} NA_{22}	ST_{32} NA_{32}	ST_{42} NA_{42}	ST_{52} NA_{52}
	160	30	ST_{13} NA_{13}	ST_{13} NA_{13}	ST_{23} NA_{23}	ST_{23} NA_{23}	ST_{33} NA_{33}	ST_{43} NA_{43}	ST_{53} NA_{53}
BAJA (0,1–0,5 cm/hora)	40	10	ST_{11} NA_{11}	ST_{11} NA_{11}	ST_{21} NA_{21}	ST_{31} NA_{31}	ST_{41} NA_{41}	ST_{51} NA_{51}	ST_{51} NA_{51}
	80	15	ST_{12} NA_{12}	ST_{12} NA_{12}	ST_{22} NA_{22}	ST_{32} NA_{32}	ST_{42} NA_{42}	ST_{52} NA_{52}	ST_{52} NA_{52}
	160	20	ST_{13} NA_{13}	ST_{13} NA_{13}	ST_{23} NA_{23}	ST_{33} NA_{33}	ST_{43} NA_{43}	ST_{53} NA_{53}	ST_{53} NA_{53}
MUY BAJA (<0,1 cm/hora)	40	5	ST_{11} NA_{11}	ST_{21} NA_{21}	ST_{31} NA_{31}	ST_{41} NA_{41}	ST_{51} NA_{51}	ST_{51} NA_{51}	ST_{51} NA_{51}
	80	10	ST_{12} NA_{12}	ST_{22} NA_{22}	ST_{32} NA_{32}	ST_{42} NA_{42}	ST_{52} NA_{52}	ST_{52} NA_{52}	ST_{52} NA_{52}
	160	15	ST_{13} NA_{13}	ST_{23} NA_{23}	ST_{33} NA_{33}	ST_{43} NA_{43}	ST_{53} NA_{53}	ST_{53} NA_{53}	ST_{53} NA_{53}

ST_{xy} NA_{xy}

x: 1 = Muy buena calidad
2 = Regular calidad
3 = Mala calidad
4 = Muy mala calidad
5 = No utilizable

y: 1 = Cultivo sensible a las sales (STES 40 meq/l)
2 = Cultivo tolerante a las sales (STES 40–80 meq/l)
3 = Cultivo muy tolerante a las sales (STES 80–160 meq/l)

CUADRO III. EJEMPLOS DE CLASIFICACION DE CUATRO AGUAS DE RIEGO UTILIZADOS EN SUELOS DE LAS ZONAS DELIMITADAS EN EL MAPA DE LA FIG.1

AGUA DE RIEGO (N° Mapa)*	meq/litro						PERM. DEL SUELO	STES MAX. meq/L	L(ST)F	RASES MAX.	L(NA)F	SALES PRECIP.	CLASIFICACION	
	CAR	NAR	BR	CLR	SR	CASR								
(6)	16,9	10,5	4,3	8,3	14,8	12,6	ALTA	40	0,69	20	0,12	---	ST_{51}	NA_{21}
								80	0,26	30	0,08	CAC,CAS	ST_{32}	NA_{12}
								160	0,09	40	0,06	" "	ST_{13}	NA_{13}
							MEDIANA	40	0,69	15	0,16	---	ST_{51}	NA_{31}
								80	0,26	20	0,12	CAC,CAS	ST_{42}	NA_{32}
								160	0,09	30	0,08	" "	ST_{23}	NA_{23}
(15)	15,4	1,8	3,1	1,2	12,9	12,3	BAJA	40	0,43	10	0,04	---	ST_{51}	NA_{21}
								80	0,04	15	0,03	CAC,CAS	ST_{22}	NA_{22}
								160	0,02	20	0,02	" "	ST_{13}	NA_{13}
(17)	5,4	0,5	5,2	0,2	0,5	0,2	BAJA	40	0,02	10	0,02	CAC	ST_{21}	NA_{21}
								80	0,01	15	0,01	"	ST_{12}	NA_{12}
								160	0,01	20	0,01	"	ST_{13}	NA_{13}
							MUY BAJA	40	0,02	5	0,04	CAC	ST_{21}	NA_{31}
								80	0,01	10	0,02	"	ST_{12}	NA_{22}
								160	<0,01	15	0,01	"	ST_{13}	NA_{13}
(18)	3,7	0,7	4,0	0,2	0,2	--	MUY BAJA	40	0,02	5	0,10	CAC	ST_{21}	NA_{51}
								80	<0,01	10	0,05	"	ST_{12}	NA_{42}
								160	<0,01	15	0,03	"	ST_{13}	NA_{33}

CAC: Carbonatos de Ca y Mg; CAS: Sulfato de Ca.

Interpretación del Cuadro III

(6): Problemas de salinización predominando sobre los de sodificación en todas las situaciones. De muy mala, mala y buena calidad respectivamente para cultivos sensibles, tolerantes y muy tolerantes a las sales en suelos de alta permeabilidad, mientras que en suelos de mediana permeabilidad y para los mismos cultivos en orden creciente de tolerancia a las sales resulta ser no utilizable, de muy mala y de regular calidad. En el proceso de acumulación de sales precipitan carbonatos de Ca y Mg y sulfato de Ca en el suelo.

(15): El problema de salinización predomina sobre el de sodificación en todas las situaciones. En suelos de baja permeabilidad el agua pasa de ser no utilizable para cultivos sensibles, a ser de regular a buena calidad para cultivos tolerantes y muy tolerantes a las sales respectivamente. En el proceso de salinización precipitan tanto carbonatos de Ca y Mg, como sulfato de Ca en el suelo.

(17): El problema de sodificación predomina en suelos con muy baja permeabilidad, y anda asociado al de salinización en suelos de baja permeabilidad. En suelos de baja permeabilidad el agua es regular a buena calidad de acuerdo al nivel de salinidad tolerado por el cultivo, pero en suelos de muy baja permeabilidad, debido al peligro de sodificación, pasa a ser de mala calidad en el caso de niveles máximos de salinidad para cultivos sensibles.

(18): El problema de sodificación predomina sobre el de salinización en todas las situaciones, siendo el agua no utilizable de muy mala y de mala calidad respectivamente para niveles máximos de salinidad correspondientes a cultivos sensibles, tolerantes y muy tolerantes en suelos de muy baja permeabilidad.
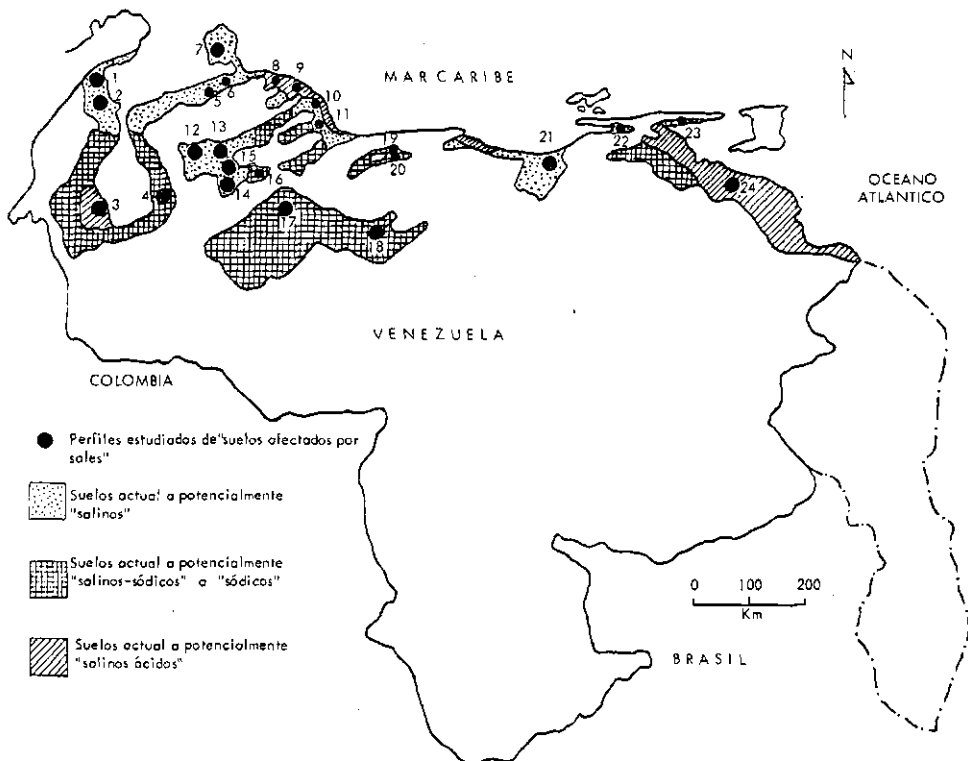
FIG.1.   Zonas con suelos actual o potencialmente afectados por sales en Venezuela.

de acuerdo a cultivos y suelos, la flexibilidad del sistema permite que, en casos donde la experiencia y condiciones lòcales así lo justifiquen, se modifiquen dichos límites sin alterar su uso.

Los índices utilizados para calificar las aguas de riego son los valores de lixiviación efectiva requerida para control de sales totales (L(ST)F) o sodio (L(NA)F) calculados con las ecuaciones del Cuadro I, para cada combinación de condiciones dadas. Su deducción puede facilitarse a través del uso de nomogramas desarrollados al efecto [21]. Con los valores de L(ST)F y L(NA)F se pueden encontrar las clases de agua para riego en el Cuadro II. En ese Cuadro las clases se basan en los valores de requerimientos de lixiviación para controlar la acumulación de sales y Na en la zona radicular, dentro de valores límites determinados por dificultades derivadas de tasas de percolación bajas, y altos requerimientos de drenaje. Los valores máximos de STES y RASES son presentados como valores de referencia para seleccionar cultivos, suelos y prácticas de manejo de riego para prevenir problemas potenciales de salinidad y permeabilidad.

En el Cuadro III se dan algunos ejemplos de clasificación, empleando el sistema aquí propuesto (véanse los Cuadros I y II), de cuatro aguas de riego utilizadas en suelos de las zonas delimitadas en el mapa de la Fig.1.

5.   APLICACIONES DEL SISTEMA

Una vez establecidos los requerimientos de lixiviación efectiva (L(ST)F o L(NA)F) para un determinado suelo (valores límites de RASES) y cultivo (valores límites de STES), pueden determinarse las posibilidades prácticas y económicas de aplicarlos, tomando en cuenta las diferentes alternativas. Las posibilidades prácticas dependerán fundamentalmente de la disponibilidad de agua para aplicar el exceso requerido para la lixiviación, y de las propiedades hidrológicas del suelo que permitan infiltrar y drenar ese sobrante en un período de tiempo razonable, sin causar problemas al cultivo. Las posibilidades económicas están supeditadas fundamentalmente a los requerimientos de drenaje artificial para eliminar el exceso de agua sin que ascienda el nivel freático y, en algunos casos, a los costos extra derivados de un control más preciso del riego y de la cantidad de agua y tiempo extra para aplicarla.

Los factores fundamentales a ser considerados serían, además del valor de L (el que resulta mayor entre L(ST) y L(NA)) y F, la tasa de infiltración básica, el uso consuntivo del cultivo, y la capacidad de almacenamiento del agua aprovechable para el cultivo del suelo, los cuales determinarán los requerimientos de riego (duración e intervalos) y drenaje.

La duración del riego tiene un máximo determinado por el suministro de agua, el costo de aplicación y el tiempo durante el cual el cultivo puede estar sometido a condiciones de mucha humedad y baja aireación, mientras se lleva a cabo. Se puede reducir la duración del riego bajando el intervalo entre riegos.

El requerimiento de drenaje puede resultar muy alto, en el sentido de exigir períodos de tiempo demasiado largos para la aplicación de los riegos, o sistemas de drenaje artificial imprácticos o antieconómicos. Si ese alto requerimiento de drenaje se debe a valores altos de L(ST), se puede recurrir a varias alternativas, de acuerdo a las circunstancias:

a) Utilización de un cultivo más tolerante a las sales, con lo que subirá el valor de STES, y con ello bajará L(ST).

b) Utilización de cultivos que no sufran deterioro con riegos prolongados.

c) Aplicación del agua de lixiviación, no en forma constante con cada riego, sino de manera intensiva, sin cultivos, cada cierto período de tiempo, cuando se alcancen niveles críticos de sales en el suelo.

CUADRO IV. CONDICIONES PARA EL DESARROLLO DE DIFERENTES TIPOS DE "SUELOS AFECTADOS POR SALES" DE ACUERDO A LOS CRITERIOS DEL SISTEMA INTEGRADO DE CALIFICACION AQUI PRESENTADO

(véanse los Cuadros I-III)

AGUA		DRENAJE	CLIMA	SUELO "AFECTADO POR SALES"				
STR (meq/l)	Composición iónica	Infiltración básica (cm/hora)	P > ETP (meses/año)	STES (meq/l)	Composición iónica	Sales precipitadas	Clasificación	No. en Mapa*
<10	B>S>CL CA>NA	<0,5	<2	>40	S>CL>B NA>>CA	CAC CAS	SALINO	21
>10	S>CL>B NA<CA	0,5-5,0	<2	>40	S>CL>>B NA>CA	CAC (CAS)	SALINO	5, 6, 7
		<0,5	<2 (2-4)	>40	S>CL>>B (CL>S>>B) NA>CA (NA<CA)	CAC CAS	SALINO	1, 2 10, 11, 12 13, 14 15, 22, 23
<10	B>S>CL CA>NA	<0,5	4-6	>40	S>CL>B NA>>CA	CAC	SALINO -SODICO	4, 16 17, 19
				(Lixiviación. Condiciones de anaerobiosis) $(2Na^+ + SO_4^= + 2C + 2H_2O \longrightarrow S^= + 2NaHCO_3)$				
				<40	B>S>CL NA>>>CA	CAC	SODICO	19
<10	B>S>CL NA>CA B>CA	0,5-5,0	<2	20-40	B>S>CL	CAC	SODICO	18, 20
		<0,5	2-4	<40	NA>>CA			
		<0,5	<2	>40	S>CL>B NA>>>CA	CAC	SALINO -SODICO	
				(Lixiviación)				
				<40	B>S>CL NA>>>CA	CAC	SODICO	

STR: Sales totales en el agua de riego; STES: Sales totales en el extracto de saturación del suelo.
P: Precipitación; ETP: Evapotranspiración potencial; (): Ocasionalmente; * Mapa en FIG. 1.

Si el alto requerimiento de drenaje se debe a L(NA), se puede recurrir a:

a) Uso del suelo para cultivos que puedan ser manejados en condiciones de riego prolongados o por inundación continua.

b) Uso de enmiendas en el suelo que al mejorar las condiciones hidrológicas logren bajar L(NA).

c) Uso de enmiendas (generalmente yeso) en el agua de riego [20]. Esta alternativa, que permite bajar el valor de L(NA), puede resultar efectiva y práctica cuando las condiciones naturales de drenaje son muy pobres y difíciles de mejorar con drenes artificiales y cuando las aguas de riego tienen una baja concentración total de sales con alta proporción de bicarbonatos.

Ejemplos de estas aplicaciones para aguas, suelos y cultivos en zonas bajo riego en Venezuela, con evaluaciones positivas a nivel de campo, se han presentado en publicaciones previas [21]. Asimismo, el sistema ha sido utilizado para el establecimiento de criterios cuantitativos para regular el uso de aguas salinas en agricultura [22] y para determinar las alternativas de recuperación y manejo de suelos salino-sódicos [23] y salinos [24] con cultivos bajo riego en Venezuela.

La utilización del sistema en forma más general, y tomando en consideración los posibles efectos del clima sobre el régimen hídrico de los suelos ha permitido elaborar los esquemas de desarrollo del Cuadro IV. Estos, conjuntamente con estudios directos de perfiles de suelos y aguas, a nivel de campo y de laboratorio, se han utilizado para establecer el origen, distribución y diagnóstico de suelos afectados por sales en Venezuela [25], y delimitar las áreas con problemas actuales y potenciales de salinidad en sus diferentes manifestaciones (Fig.1).

Entre los suelos actual o potencialmente "salinos" se incluyen aquellos cuya concentración, composición y distribución de sales en el perfil del suelo, asociado a condiciones climáticas, de drenaje y de composición y concentración de sales en las aguas disponibles, provoquen o puedan provocar al introducir el riego problemas en los cultivos derivados de la concentración total de sales en la solución del suelo. Según este criterio cualitativo, entran como "suelos salinos" aquellos que acumulan sulfato de sodio en climas áridos, o cloruro de sodio en climas áridos o semiáridos, independientemente de si los valores de relación de adsorción de sodio (RAS) de la solución son altos, ya que en ambos casos dicha acumulación va acompañada generalmente de precipitación de yeso, lo que unido a la baja hidrólisis del Na en ambas sales, en especial en el NaCl, permite su lixiviación del perfil del suelo sin un deterioro marcado en las propiedades físicas del suelo.

Los suelos actual o potencialmente "salino-sódicos" incluyen aquellos cuya concentración, composición y distribución de sales en el perfil del suelo, asociado a condiciones de drenaje, clima y de composición y concentración de sales en las aguas de uso potencial para riego, provoquen o puedan provocar al introducir el riego problemas de deterioro físico del suelo derivados de la acumulación de Na intercambiable. El desarrollo de suelos "sódicos" a partir de suelos salino-sódicos ricos en sulfato de Na parece ser un proceso común en áreas con drenaje muy deficiente donde se acumula materia orgánica y se mantienen condiciones de exceso de agua por períodos prolongados en la estación de lluvias, e incluso en la estación seca cuando el agua se aplica en forma de riego. Este proceso, de escasa significación en climas templados [26], parece ser la fuente actual y puede ser la fuente potencial de sodificación de grandes áreas de Venezuela donde se da la combinación de aguas, drenaje y clima señalados en el Cuadro IV. En los otros casos, la existencia aún en pequeñas cantidades de excesos de bicarbonato sobre Ca + Mg en las aguas aplicadas, llevarían en climas áridos, o en suelos con drenaje deficiente en otros climas, a la formación de suelos sódicos, en los cuales el Ca y Mg prácticamente desaparecen de la solución. Al airearse el suelo, y cerca de la superficie, parte

de esos bicarbonatos de Na se transforma en carbonato de Na, intensificando
el problema.

Incluídos en el mapa, y no en los esquemas del Cuadro IV, están los suelos
que hemos calificado como actual o potencialmente "salino-ácidos", los cuales
son aquellos que conservando niveles, tipo y localización de sales totales que los
ubicarían como salinos, presentan sin embargo pequeñas cantidades de Al (o mejor
dicho, hidroxialuminio) en solución, lo que hace que su reacción sea ácida, con
pH generalmente inferior a 5. Aunque este tipo de suelos aparece en muy escasas
ocasiones en zonas templadas, en Venezuela ha sido detectado en zonas relativa-
mente extensas [27], cuyos suelos se formaron aparentemente por procesos naturales
de mejora de drenaje en sedimentos y suelos sulfato-ácidos. Las zonas donde
aún las condiciones de drenaje mantienen los niveles freáticos altos en forma
continua, son consideradas como potencialmente salino-ácidas. El proceso de
desarrollo inicial de este tipo de suelos parece corresponder a la formación de
suelos sulfato-ácidos [28, 29], acompañado de condiciones de clima árido a
semiárido y drenaje deficiente.

6.   USO DE ISOTOPOS Y TECNICAS DE RADIACION

La evaluación y utilización precisas de un sistema integrado como el propuesto
requiere de un conocimiento continuo y detallado del balance de agua e iones
específicos tanto en el suelo como en la planta, para las muy variables combinaciones
de suelos, cultivos, clima y manejo del riego. Ello es particularmente importante,
y a su vez difícil, en el caso menos estudiado y conocido del desarrollo de suelos
salino-sódicos y sódicos en zonas tropicales semiáridas y subhúmedas, con suelos
mal drenados, regados en la estación seca con aguas relativamente bajas en contenido
de sales. Por lo lento y complejo del proceso, y la dificultad de detectar a corto
plazo los efectos por otros procedimientos, se hace necesaria y conveniente la
utilización de isótopos y técnicas de radiación que permitan detectar y precisar
desde un comienzo la tendencia al desarrollo de dicho tipo de suelos afectados por
sales, y su relación con el régimen hídrico del suelo tanto en la estación de
lluvias como en la seca. Esto reviste particular importancia ya que, por la
naturaleza prácticamente irreversible del problema, es indispensable un diagnóstico
precoz que permita tomar a tiempo las medidas correctivas en cuanto a utilización
y manejo de aguas y suelos para agricultura de riego en esas condiciones.

REFERENCIAS

[1] PLA-SENTIS, I., "Evaluation of the quality of irrigation waters with high carbonate
content in relation to the drainage conditions", Trans. 9th Int. Congr. Soil. Sci. Adelaide,
Australia, Vol. 1 (1968) 357.

[2]   PLA-SENTIS, I., Evaluación de la influencia de factores naturales y artificiales en la
      recuperación y prevención de desarrollo de suelos afectados por sales, Agronomía
      Tropical 21 5 (1971) 431.
[3]   PLA-SENTIS, I., "Salt and water balances in irrigated soils under tropical conditions",
      New Developments in the Field of Salt Affected Soils, Proc. Symp. Cairo (1972).
[4]   PLA-SENTIS, I., Evaluación cuantitativa de los efectos de los bicarbonatos en el agua
      de riego sobre las propiedades químicas y físicas de los suelos y factores que influyen
      sobre la magnitud de tales efectos, Rev. Fac. Agron., Maracay, Venezuela (1967).
[5]   REEVE, R.C., "The relation of salinity to irrigation and drainage requirements",
      Trans. 3rd. Congr. Int. Commission on Irrigation and Drainage, San Francisco (1957)
      10.175.
[6]   BERNSTEIN, L., FRANCOIS, L.E., Leaching requirements studies: Sensitivity of
      alfalfa to salinity of irrigation and drainage waters, Soil Sci. Soc. Am. Proc. 37 (1973) 931.
[7]   RHOADES, J.D., et al., Minimizing the salt burdens of irrigation drainage water,
      J. Environ. Qual. 3 (4) (1974) 311.
[8]   PLA-SENTIS, I., "Calidad de aguas de riego y requerimientos de drenaje" (Memoria
      V Seminario Latinoamericano de Irrigación y III Jornadas Venezolanas de Riego, Caracas)
      Venezuela (1968) 85.
[9]   PLA-SENTIS I., "Calidad de aguas de riego como fuente de salinización y sodificación"
      (Actas VIII Reunión Latinoamericana de Fitotecnia, Bogotá) Colombia (1971) 213.
[10] RHOADES, J.D., Quality of water for irrigation, Soil Sci. 113 (1972) 277.
[11] SHALHEVET, J., Aspects of soil salinity and sodicity in relation to irrigation and
      reclamation (Symp. Israel-France, Bet Dagan, Israel), Publ. Sp. 39 (1974) 117.
[12] DONEEN, L.D., Salinization of soil by salts in the irrigation water, Trans. Am. Geophys.
      Union 35 (1954) 943.
[13] BOWER, C.A., OGATA, G., TUCKER, J.M., Sodium hazard of irrigation waters as influenced
      by leaching fraction and by precipitation of calcium carbonate, Soil Sci. 106 (1968) 29.
[14] US SALINITY LABORATORY STAFF, Diagnosis and Improvement of Saline and Alkali
      Soils, US Dept. of Agriculture Handbook No. 60 (1954).
[15] BERNSTEIN, L., Quantitative assessment of irrigation water quality, Am. Soc. Test. Mater.,
      Spec. Tech. Publ. 416 (1967) 51.
[16] FOOD AND AGRICULTURE ORGANIZATION (Ed.), Water Quality for Agriculture,
      Irrigation and Drainage, Paper No. 29, FAO, Rome (1976).
[17] FOOD AND AGRICULTURE ORGANIZATION (Ed.), Prognosis of Salinity and
      Alkalinity, FAO Soil Bull. No. 31, FAO, Rome (1976).
[18] BINGHAM, F.T., MAHLER, R.J., SPOSITO, G., Effects of irrigation water composition
      on exchangeable sodium status of a field soil, Soil Sci. 127 (4) (1976) 248.
[19] PLA-SENTIS, I., DAPPO, F., "Field testing of a new system for qualifying irrigation
      waters", Managing Saline Water for Irrigation (Proc. Int. Conf. Lubbock, Texas)
      (1977) 376.
[20] PLA-SENTIS, I., Calcium required as an amendment for irrigation waters with high
      bicarbonate content in relation to the drainage conditions, Agrokém. Talajtan 18
      Budapest (1969) 183.
[21] PLA-SENTIS, I., DAPPO, F., Sistema Racional para la Evaluación de Calidad de Aguas
      para Riego, Suplemento Técnico No. 12, FUDECO, Barquisimeto, Venezuela (1974).
[22] PLA-SENTIS, I., DAPPO, F., "Criterios para regular el uso de aguas salinas en Agricultura",
      Annales Juris Aquarum (Conf. Int. sobre Derecho y Administración de Aguas, Caracas)
      Vol. 2 II, Venezuela (1975) 1085.

[23] ALVAREZ, J.R., Requerimientos de lixiviación y alternativas de recuperación de un suelo salino-sódico en el Sistema de Riego El Cenizo, Tesis M.S., CIDIAT, Mérida, Venezuela, 1974.

[24] SUCRE, R.E., Requerimientos de lixiviación y alternativas de recuperación de tres suelos afectados por sales en la depresión de Quíbor, Edo. Lara, Tesis M.S., UCV, Maracay, Venezuela (1982).

[25] PLA-SENTIS, I., Origin, distribution and diagnosis of salt-affected soils in Venezuela, Experts Consultation Meeting, FAO, Rome (1977).

[26] WHITTIG, L.D., JANITZKY, P., Mechanisms of formation of sodium carbonate in soils: I. Manifestation of biological conversions, J. Soil Sci. 14 (1963) 322.

[27] PLA-SENTIS, I., FLORENTINO, A., "Diagnóstico de problemas de salinidad en suelos "salino-ácidos" de las llanuras costeras al norte de los Estados Falcón y Anzoátegui" (Memorias VII Congreso Venezolano de la Ciencia del Suelo, San Cristóbal, 1982) Venezuela (1982).

[28] PONS, L.J., "Outlines of the genesis, characteristics, classification and improvement of acid sulphate soils", Proc. Int. Symp. on Acid Sulphate Soils, Wageningen Vol. 1 (1973) 3.

[29] FLORENTINO, A., PLA-SENTIS, I., "Características físico-químicas y mineralógicas de suelos "salino-ácidos" de las llanuras costeras del Estado Falcón" (Memorias VII Congreso Venezolano de la Ciencia del Suelo, San Cristóbal, 1982) Venezuela (1982).

Invited Paper

SALINE-SODIC SOILS AND THEIR MANAGEMENT IN PAKISTAN

S.H. Mujtaba NAQVI
Nuclear Institute for Agriculture
    and Biology (NIAB),
Faisalabad, Pakistan

Abstract

SALINE-SODIC SOILS AND THEIR MANAGEMENT IN PAKISTAN.
    This paper gives a short review of the soil salinity problem in Pakistan and discusses briefly
the measures that have been taken to tackle it. It describes a biological approach of the economic
utilization of salt-affected lands by plant succession through initial colonization with salt-tolerant
plant species, and describes results of the practical application of this approach and the role of
nuclear techniques in these studies.

INTRODUCTION

Salinity and waterlogging of good lands in Pakistan has become a problem
of gigantic proportions. It has its origins in seepage from the Indus Basin river
system and the irrigation canals taken from the rivers. The largest canal irrigation
network in the world suffers from the fact that a drainage system was not built
along with it.

Pakistan has a total of 145 million acre feet (MAF)[1] of surface waters. The
rivers that originate in the Himalayas, the Karakorams and the Hindu Kush
mountains, form the Indus Basin, and carry this water south to the Arabian Sea.
Of the total surface waters, 102 million acre feet are diverted through dammed-up
reservoirs and barrages into over 23 000 miles of irrigation canals and the main
distributaries[2].

Recent studies have shown that, of the 102 MAF of water diverted, only
60 MAF reaches the farm gate; the rest is lost because of seepage and evaporation.
The water that seeps out of the rivers and canals has raised the groundwater table;
at places where it was 100 feet below the surface a hundred years ago, it is now
only a few feet below, and sometimes even above the surface. The water has
brought a large amount of salts which is left on the surface. As a result the

---

[1] 1 acre foot = ca. 2331.5 m^3/ha.
[2] 1 mile = 1.609 km.
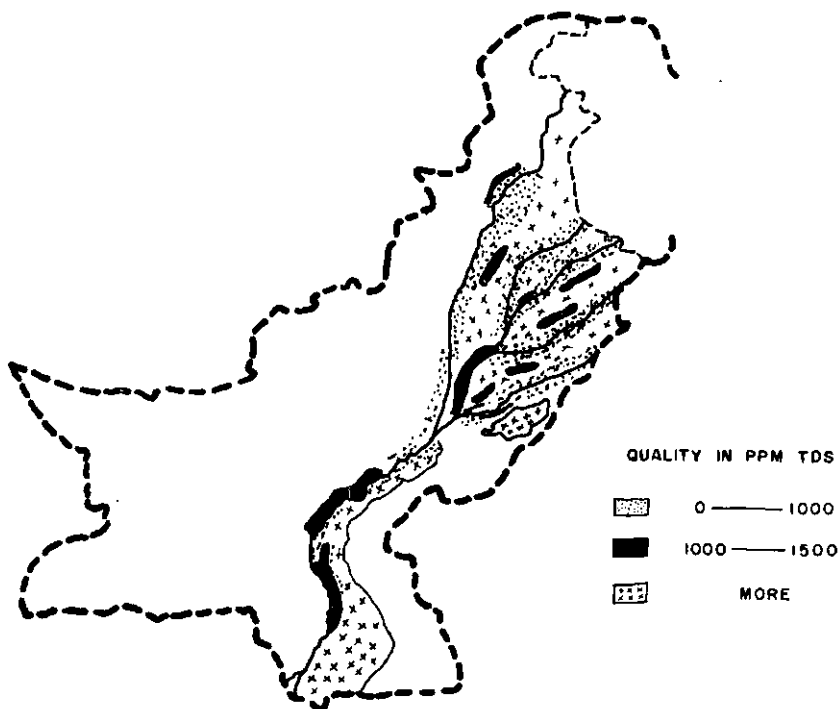
FIG.1. Map of the Indus river system showing the groundwater quality.

physical, chemical and biological characteristics of the soil have been changed leaving little or no vegetation. A total of 11 million acres of land has been affected with moderate to high salinity and sodicity.

It can be seen from Fig. 1 that the groundwater is more saline in the middle of the *doabs* (the area between two rivers).

MODEL STUDIES ON THE ORIGINS OF GROUNDWATERS IN THE INDUS PLAINS

To investigate the origins of the accumulated groundwater and the causes of salinity, our institute analysed the chemical contents and isotopes such as hydrogen, deuterium, tritium, ^{18}O and ^{14}C of the surface and groundwaters from a depth of down to 600 feet in a small area around the city of Faisalabad. The Faisalabad area faces an acute problem of waterlogging and salinity and, situated
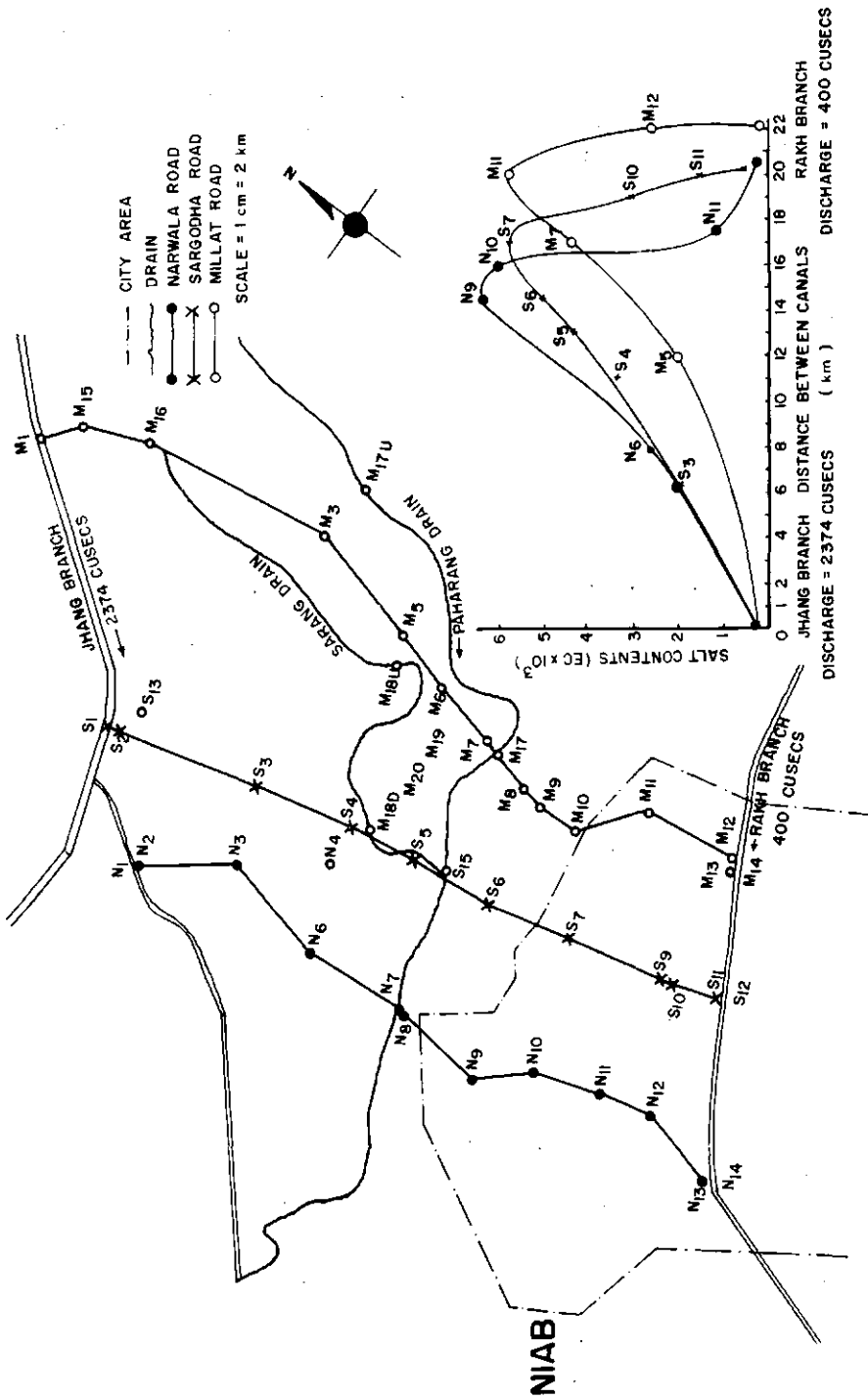
FIG.2.   Water sampling points between two irrigation canals and the salinity profile of the area.
Also indicated is an outline of the city of Faisalabad.   (1 cusec = 1 ft^3/s, i.e. 0.0283 m^3/s).

between two canals, it can serve as a model for a *doab* (Fig. 2). The area, 600 miles from the sea, is almost flat, like most of the Indus Basin, and the height above sea level varies from 597 to 626 feet. Water samples were collected from open wells/bore holes, hand pumps and tube-well/motor pumps. Surface water samples were collected from canals, drains and rain-water to determine the isotopic load of these sources. Chemical analysis was done at NIAB and the stable and radio-isotopes were studied at PINSTECH, Islamabad and the Institute of Radio-hydrometry, Munich.

The results show that there is no rapid groundwater movement in the area and the residence time of the groundwater above the pre-irrigation water table is around some tens of years. Near canals is a larger amount of actual groundwater. A definite drainage pattern in the groundwater cannot be seen. The salinity of the water does not seem to be due to an admixture of sweet water with connate waters of marine origin. Rather it may be due to the dissolution of salts from the sediment itself, or local enrichment of salt content owing to heavy evaporation of groundwaters.

In the groundwater of the irrigated areas no response was seen in the form of an isotopic variation, indicating that infiltration from irrigated areas is low compared to that from canals and their distributaries. Studies with a neutron moisture probe supplemented by isotopic analyses also indicate that, except in case of sandy soils, the irrigation water seeps down only about three feet and as the top gets dried it evaporates and does not, perhaps, make any significant contribution to the groundwater.

These studies indicate that the rise in groundwater levels in the irrigated plains in the Indus Basin is mainly due to seepage from rivers and irrigation canals. The seepage water washes the sediment and carries the salt away towards the middle of the *doabs* where it becomes concentrated through evaporation (Fig. 2).

EFFORTS AT RECLAMATION OF SALT-AFFECTED LANDS

A permanent solution to the problem seems to be to provide a comprehensive drainage system throughout the irrigated areas which is a tall order indeed. Therefore, efforts have been made by the Water and Power Development Authority (WAPDA) of Pakistan, in the worst affected areas to provide vertical drainage through pumping the groundwater and lowering the water-table so that surface salts could be leached back into the soils. The WAPDA have completed 28 such schemes, and constructed drains and tube-wells in an area of eight million acres while 13 schemes in progress will benefit another seven million acres. Though these efforts have no doubt met with temporary success they have not solved the problem. The procedure is energy intensive and expensive, it creates the

problem of the disposal of pumped saline water, and also does not work well in the case of sodic soils where the excess of sodium has changed the soil structure to make it impermeable. For such cases the application of an excess of calcium in the form of powdered gypsum has been recommended. However, again, this treatment is expensive.

While efforts at more durable solutions of the salinity and waterlogging problems may take a while, immediate steps are required to live profitably with the existing situation. Our institute has been examining the possibility of colonizing the saline and sodic lands with salt-tolerant crops. A few highly salt-tolerant grasses and other crops were selected after many salt-tolerant species were screened.

The aim of introducing salt-tolerant crops is not necessarily to produce cereals or other routine crops but to produce better quantities of biomass with the lowest possible inputs and to improve the sodic soils. The biomass can then be used for various purposes.

The salt-affected soils, particularly the sodic soils, have a preponderance of sodium ions on the soil complex which results in compaction, decreased permeability to water and exclusion of air from the soil pores − conditions inimical to the growth of plants and other organisms. These soils also have a high pH which influences nutrient transformation and uptake. Numerous secondary effects of the sodic condition of the soil adversely affect the ecology.

THE BIOLOGICAL APPROACH

Numerous soils in Pakistan are calcareous and have large amounts of insoluble calcium. If this calcium could be dissolved in situ, the exchangeable sodium could be reduced. This is possible through acidification of the soil. But, again, to add acid is expensive. Therefore, it was felt that acidic conditions could be created through green manuring. The biological approach for utilizing and ameliorating these soils thus consisted of introducing highly salt-tolerant plant species followed by lesser salt-tolerant crops and green manuring.

Initial experiments showed that *Diplachne fusca* (Kallar grass) could be introduced on highly saline sodic soils and would flourish even when irrigated with sodic groundwaters (sodium absorption ratio (SAR), 7−10) and without the addition of nitrogen. Studies with disturbed soils in glass or teflon columns or cement lysimeters, and irrigation/leaching with different quality waters, indicate that growth of the grass resulted in increasing permeability and leaching, and resulted in an increase in soluble $Ca^{2+} + Mg^{2+}$ and reduction in exchangeable sodium (Fig. 3). Green manuring further increased these parameters.

This grass was found to grow on highly saline lands for years without the application of nitrogenous fertilizers. Investigations were made on the rhizosphere,
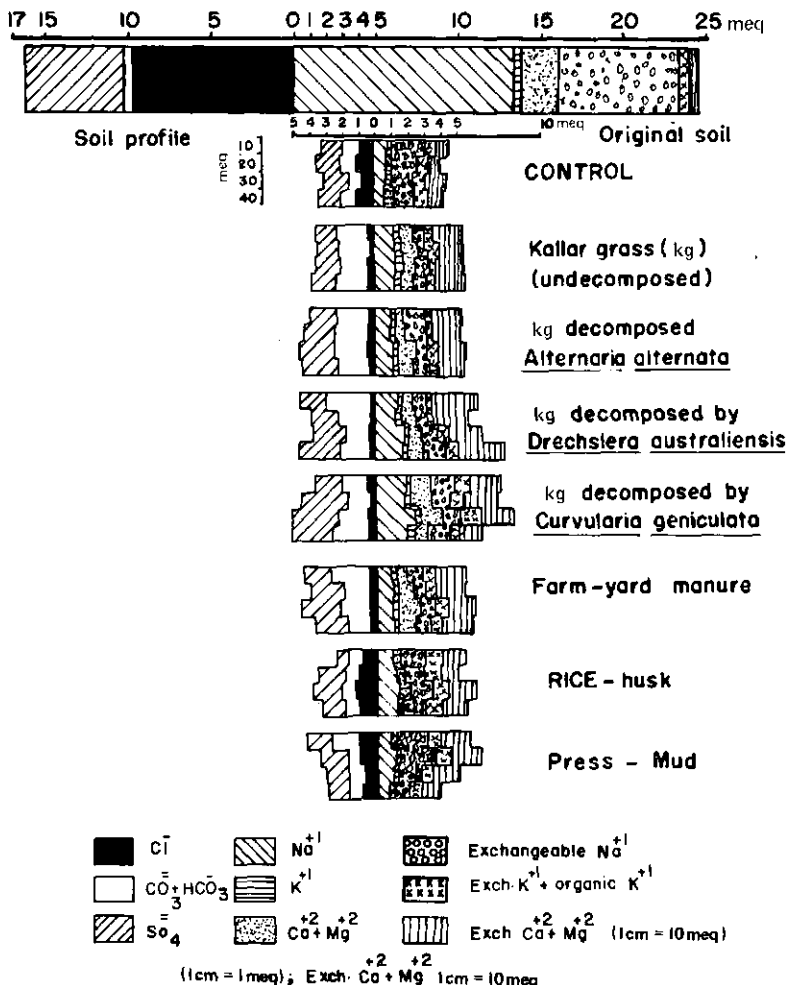
FIG.3. *Lysimeter studies indicating the effects of different organic amendments on the anions and cations in the soil solution.*

rhizoplane (root surface) and histoplane (root tissue) for the presence of nitrogen-
fixing bacteria. Rhizospheres along with intact plants, soil cores and excised roots,
all indicated nitrogenase activity by the acetylene reduction method. In soil cores
the activity decreased with depth, and the washed and unwashed roots showed
higher activity. Microorganisms responsible for nitrogen fixation were isolated
and rechecked for nitrogenase activity and have now been identified as *Azospirillum
brazilense* (SST 22), *Klebsiella* sp. (NIAB-1), *Beijerinckia* sp. (C-2), Isolate-2

(unidentified). By extrapolating the acetylene reduction assay values it is estimated that this system can fix up to 127 kg N/ha per 100 days. This is only an estimate based on extrapolations. The correct figure will be obtained through further studies.

Studies on the limits of its salt tolerance indicate that it can survive under extremely high salinity conditions, (EC 40 mmho) but to remain an economical crop (50% reduction in yield compared with normal soil conditions) it can tolerate saline conditions very well up to EC 22 mmho.

It was observed that at higher salinities the plant expelled salt from its leaf, which could be seen as a layer on both surfaces of the leaf, and dropped off with wind. By using radioisotope-labelled (^{22}Na, ^{36}Cl) salts, investigations on the mechanism of its salt tolerance indicated that there was no rejection mechanism at the root level. Rather, the salts were transported to the top and excluded through the leaf, and also through phloem transport and exclusion through the root. The plant thus does not retain very high amounts of salt and is palatable to animals.

The grass was found to have a C-4 photosynthetic pathway. The carbon dioxide compensation point was found to be around 10 ppm while for C-3 plants the value is in the range of 70 to 100 ppm. By the natural isotopic abundance method, the C-13 value was −15.9‰ confirming the C-4 photosynthetic pathway and thus showing that the plant is a better converter of solar energy.

The laboratory investigations thus conclude that Kallar grass is a highly salt-tolerant grass, has associative nitrogen fixation, is a better converter of solar energy, has a reasonable fodder value, and when grown on saline-sodic lands it opens up the soil physically and reduces exchangeable sodium, resulting in effective leaching of surface salts.

Kallar grass as green manure

It was initially thought that once the sodic soil had been improved through the cultivation of Kallar grass, a legume and a common green manuring crop in Pakistan, *Sesbania aculeata,* could be introduced and green manured for further improvement of the soil. Sesbania is very succulent and would be a better fodder as well as manure.

The decomposition rate of organic matter and humus formation is greatly dependent on the active mycoflora of the soil. Saline-sodic soils have a low biological activity and scanty mycoflora, making green manuring less effective. However, once the soil has been colonized by Kallar grass, the biological activity is restored. To compare the green manuring qualities of Kallar grass and Sesbania, both were uniformly labelled with ^{14}C by being grown in a growth chamber provided with a ^{14}C-labelled CO_2 atmosphere.

Using the labelled plant material for decomposition studies it was found that Sesbania, which contains easily degradable carbon compounds and harbours
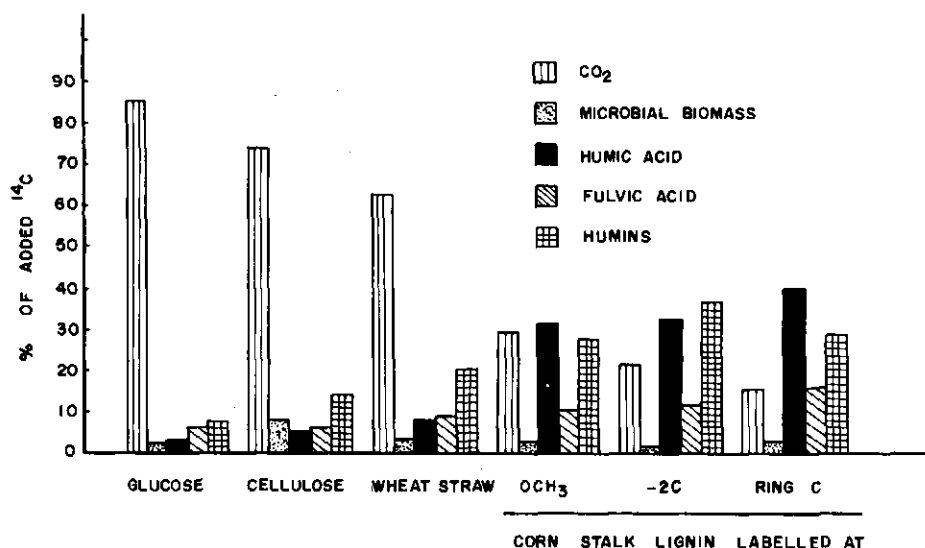
FIG.4.   Transformation of ^{14}C-labelled plant components in soil after 12 weeks of incubation.

TABLE I. CRUDE PROTEIN, LIPID AND TRACE ELEMENT CONTENT OF
WASHED KALLAR GRASS SHOOT GROWN AT DIFFERENT ROOT
SALINITIES AND MINIMUM DIETARY REQUIREMENTS[a]

Root medium salinity EC (mmho/cm)	% Dry matter (DM)		Trace element content (μg/g DM)			
	Protein	Liquid	Zn	Fe	Cu	Mn
3	17	2.8	46	390	11	60
5	17	2.8	44	330	9	64
10	14	2.2	42	250	11	78
20	12	1.8	47	270	14	150
30	11	1.5	96	310	16	230
40	12	1.8	63	230	11	210
			Minimum dietary requirements[a]			
			50	30	5–10	40

[a] Estimated minimum dietary requirements (Agricultural Research Council, 1965) for the
four micronutrient elements.
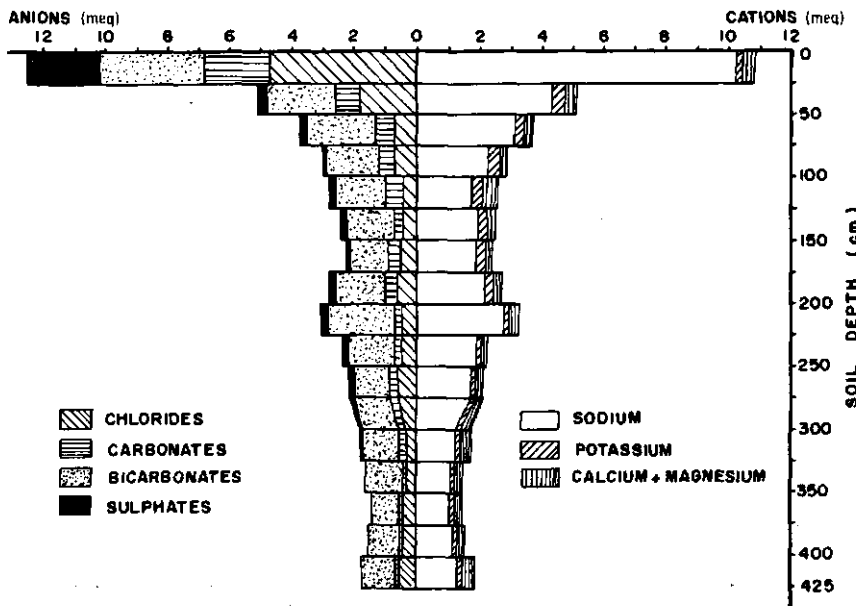
FIG.5.   Analysis of soil solutions of a soil core of saline-sodic experimental land.
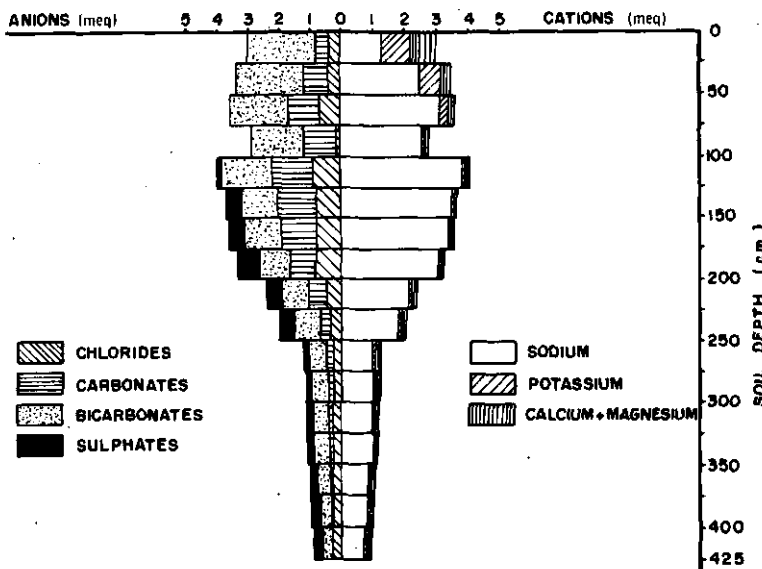
FIG.6.   Analysis of soil solutions of a soil core of saline-sodic land after cultivation of Kallar grass for 18 months.
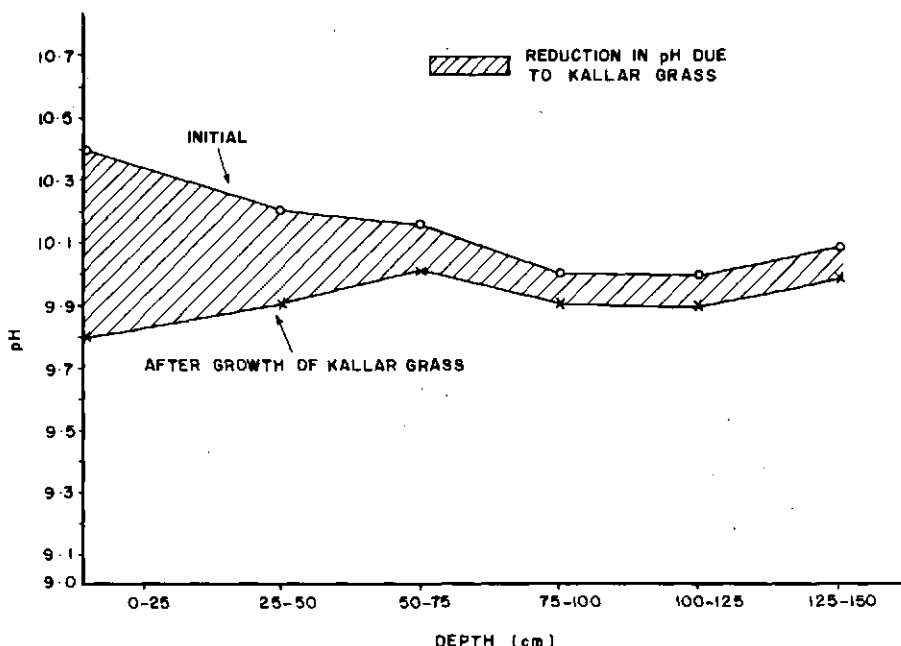
FIG. 7. pH of the saline-sodic land before and after cultivation of Kallar grass.

hyaline fungi including species of *Aspergillus* that are good cellulose decomposers, but inefficient in producing humic compounds, decomposed rapidly. On the other hand, *Diplachne fusca*, which has a high lignin content and is attacked mainly by melanoid fungi found to be less efficient cellulose decomposers, decomposed slowly but made a fairly high contribution to stable organic matter fraction (Fig. 4). It is thus clear that even as a green manure Kallar grass is not a bad choice.

After initial field observations and laboratory experiments the procedure was tried on 150 acres of highly saline sodic land (EC 40), using sodic groundwaters (TSS 1000; RSC 9—10; SAR 7—9) for its irrigation. Kallar grass was introduced through spreading small cuttings of the grass in an irrigated field, and regular irrigation was done using sodic groundwater. The grass thrives in the summer months from March to October (air temperatures ranging from a minimum of $15°C$ to a maximum day temperature of $45°C$) and reaches the peak of its photosynthetic activity at the height of the summer months. During this period it grows to a height of 4—5 ft and four such cuttings can be obtained, giving a total of 40 tons biomass per hectare. Its associative nitrogen fixation is also at a maximum during this period. In winter months (air temperatures ranging from a minimum of $2°C$ at night to a maximum of $25°C$ during the day) the grass dries up but if irrigation is maintained some growth does take place.
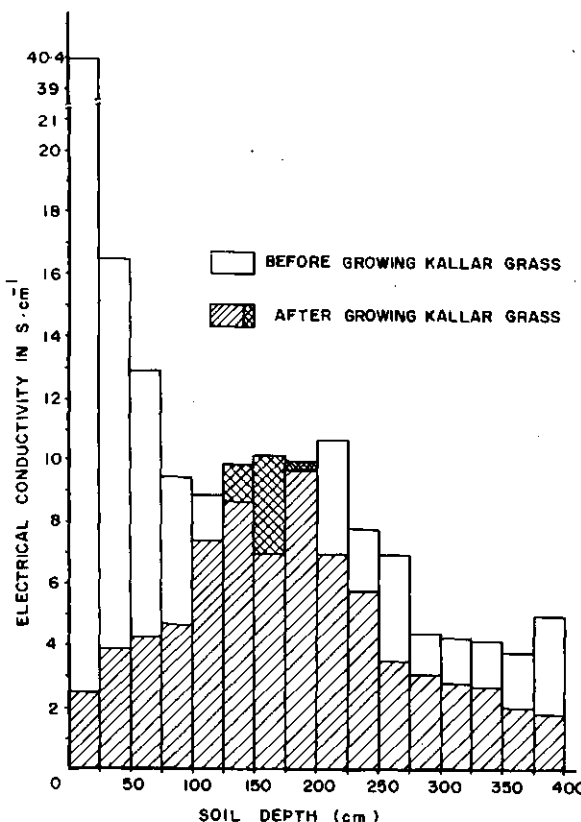
FIG.8. Electrical conductivity of the saline-sodic land before and after cultivation of Kallar grass.

Table I gives the fodder value of the grass. It has an acceptable palatability. In the presence of a more succulent fodder, however, the cattle, buffalo or goats do not prefer it. However, long-term feeding of buffalo with this grass by some farmers has not shown any adverse affects on their health.

The grass can be used for pulp making. Results from a factory-making packing material were encouraging.

Figures 5–8 show the effects of cultivation of this grass on the various soil parameters. An analysis of the soil core for anions and cations before the cultivation of the grass (Fig. 5) shows a large amount of sodium in the top 25 cm. Figure 6 shows a similar analysis after 18 months while the grass was growing in the field. It is clear that leachability of the soil has increased and most of the sodium has been leached into lower horizons.

Figure 7 shows the initial pH of the soil core and also the pH values after the growth of the grass; it has helped to lower the pH in the top soil from 10.4

TABLE II. TOTAL ENERGY OBTAINED FROM KALLAR GRASS WHEN USED FOR LIVESTOCK OR FOR PRODUCTION OF METHANOL

I.   Utilization of Kallar grass for fuel production

Green-matter production	40 t/ha
Dry matter	16.8 t/ha
Total digestible nutrients (TDN) (proteins, cellulose; hemicellulose, lignin)	7.88 t/ha
Potential for methane production (0.18 m^3/kg dry matter)	3024 m^3/ha per year
Sludge (0.72 kg/kg dry matter)	12 t
Nitrogen in the sludge	240 kg
Total energy yield from Kallar-grass-derived fuel	15×10^6 kcal/ha

II.   Utilization of Kallar grass for meat/milk production

Total buffalos	3
Total milk	4320 L
Calorific value of milk	2.86×10^3 kcal/ha
Calorific value of meat	0.28×10^5 kcal/ha
Calorific value of biogas from dung	2.64×10^6 kcal/ha
Total energy yield from buffalos	2.9×10^6 kcal/ha

to 9.8. Similarly, the effects on electrical conductivity indicate reduction of salt load on the surface (Fig. 8).

The ameliorative effects of the cultivation of the grass on the sodic soil are thus clear. The entire ecology of the area has shown a great overall improvement.

Keeping in view the better photosynthetic ability of Kallar grass because of its C-4 pathway, and its capability to provide a reasonable amount of biomass per hectare, it could be considered as a good energy crop.

If the energy yielded by Kallar grass, when used for livestock, is compared when it is directly converted to methane gas, the direct conversion would yield nearly six times more energy (Table II). Efforts have therefore been made for the microbial degradation of its biomass into methane gas or alcohol.

Anaerobic methanogenic organisms were isolated from water sediments, decomposing biomass, biogas plant effluents, etc. and a few gave positive results. Similarly, a mutant strain of cellulomonas and a couple of cellulolytic fungi are being explored for degradation of biomass from Kallar grass to ethanol. An enzyme preparation was obtained which gives encouraging results.

CONCLUSIONS

The problem of saline and sodic soils is a threat to good agriculture in the Indus plains. For a durable solution of this problem a drainage system has to be provided in the irrigated areas. Salinity in the irrigated areas is mainly due to seepage of water from the irrigation system and washing of salt from the sediment. This seepage should be minimized so that the main cause of salinity is plugged and more surface water becomes available for leaching salt-affected lands and for irrigation.

Lowering of the water-table through vertical pumping in the badly affected areas is unavoidable but has its problems.

While a durable solution may take time, efforts are needed to be able to live profitably with the salinity/sodicity situation. The biological approach described here shows great promise for economic utilization of saline-sodic lands, not only in the Indus Basin but also elsewhere where the conditions are similar.

Invited Paper

SALT-AFFECTED SOILS IN INDIA
AND THEIR MANAGEMENT

I.P. ABROL
Central Soil Salinity Research Institute,
Karnal, India

Abstract

SALT-AFFECTED SOILS IN INDIA AND THEIR MANAGEMENT.

Excess salts reduce the productivity of an estimated 7×10^6 hectares of otherwise productive soils. Of these, nearly 2.5×10^6 hectares are spread in the Indo-Gangetic plains, and are characterized by the presence of measurable quantities of sodium carbonate which impart to these soils a high exchangeable sodium percentage (ESP) and a high pH. These, in turn, cause the physical properties to deteriorate. A high pH also influences the availability and transformation of several plant nutrients and affects other physico-chemical phenomena independent of high ESP. Together these factors are responsible for the unproductivity of these soils. Apart from losses in crop production, alkali soil areas cause large runoffs which are hazardous for areas downstream. The paper summarizes research efforts to develop appropriate technologies for reclaiming and managing alkali soils. Field and laboratory investigations have been concerned with defining the optimum needs of drainage, crops and cropping sequences, amendments, nutrients, water management, etc. It has been shown that conventional subsurface tile drainage is not feasible in these soils because of their poor transmission characteristics. Vertical drainage, on the other hand, has proved to be effective for controlling the groundwater table. Rice is tolerant of sodicity, and growing rice considerably enhances reclamation. Karnal *(Diplachne fusca)* and para grasses *(Brichiaria mutica)* are among the grasses that are highly tolerant. Gypsum proved to be an effective amendment. The best results were obtained when gypsum was only surface mixed. Crops in alkali soils responded to higher doses of applied nitrogen fertilizers but did not respond to phosphorous and potassium fertilizers, while fertilization with zinc was very beneficial in the initial years. Reduced soil-water storage and its availability, restricted root penetration and low water transmission rates in alkali soils require irrigation to be applied frequently and in small quantities at a time. The technology of alkali soil reclamation was tested in farmers' fields and found economically feasible for being undertaken on a large scale. Research areas, where the use of isotope and radiation techniques can assist in better management of these soils, have been indicated.

INTRODUCTION

Our overall efforts to increase agricultural production must include measures to reclaim soils that have gone out of cultivation because of the accumulation of excess salts in the root zone, and to prevent the soils from becoming salinized

in the future. It is estimated [1] that at present about 7×10^6 hectares of salt-affected soils produce very little or practically no crops of economic significance. It is also feared that large areas of productive soils are going out of cultivation in irrigated areas owing to a rise in the groundwater table and consequent salinization of the root zone, or to the use of highly saline waters for irrigation. This paper summarizes our research efforts to develop acceptable technologies for reclaiming an estimated 2.5×10^6 hectares of alkali soils spread throughout the Indo-Gangetic plains of India.

SALT-AFFECTED SOILS IN INDIA

Climatic differences, soil characteristics including the nature of salts, available water resources and associated features require a different approach to the management of salt-affected soils occurring in different regions (Fig.1).

From a physico-chemical standpoint salt-affected soils occurring in different regions can be grouped into two categories — (a) Saline soils; and (b) Alkali or sodic soils [2, 3].

Saline soils

Saline soils are those which contain excess neutral soluble salts, chiefly chlorides and sulphates of sodium, magnesium and calcium, in quantities sufficient to affect plant growth adversely. Sodium chloride is most often the dominant soluble salt. Plant growth in saline soils is adversely affected, chiefly because of the osmotic effects of excess salts on soil-water availability, but the toxic effect of specific ions, e.g. Cl, SO_4, B, etc., is often an additional factor influencing plant growth relationships in saline soils. For purposes of definition saline soils are those whose water-saturated paste extract has an electrical conductivity of more than 4 dS/m at 25°C. The pH of water-saturated paste of saline soils is less than 8.2.

Alkali soils

Also termed sodic, alkali soils are those which contain measurable quantities of the salt, sodium carbonate. Plant growth in alkali soils is adversely affected, chiefly because of excess exchangeable sodium and the accompanying high pH on the soil's physical and physico-chemical properties including the availability and transformation of some essential plant nutrients. The toxic effect of specific ions, e.g. Na, B, etc., is often an additional factor determining plant growth relationships in alkali soils. Alkali soils are those which have an exchangeable sodium percentage (ESP) of more than 15, and pH of saturation
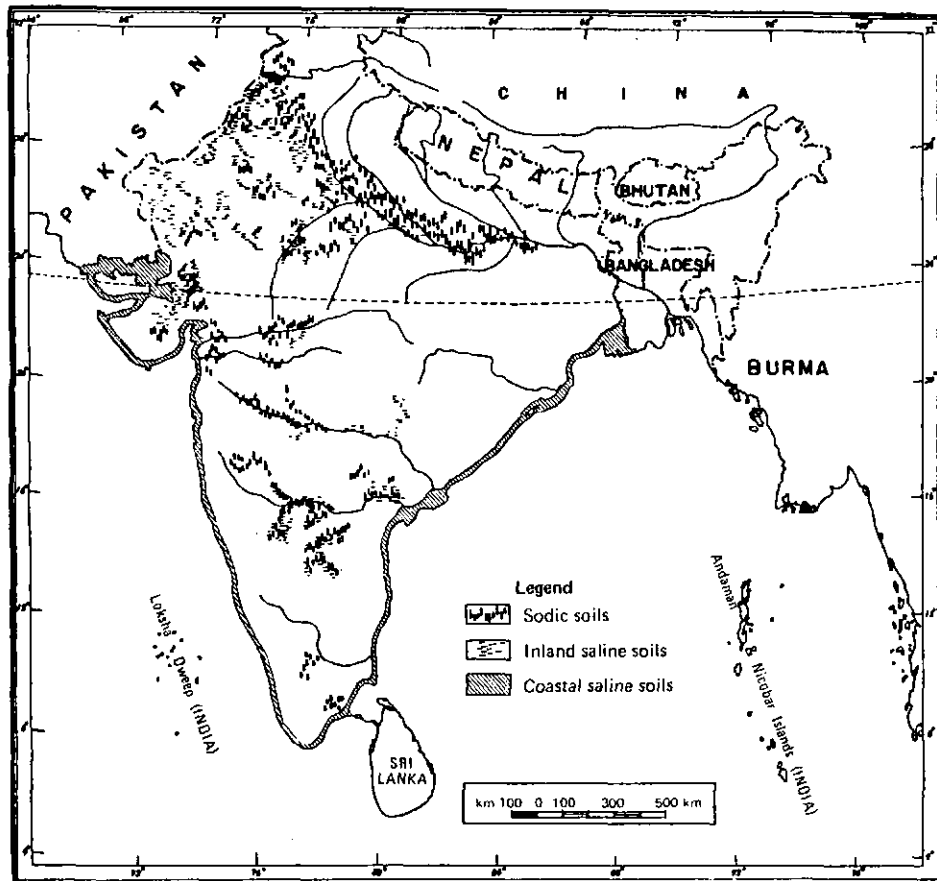
FIG.1.   India — salt-affected soils.

paste in water above 8.2 [2, 4]. Our recent studies [5, 6] have shown that
soils' physical properties and the physico-chemical behaviour of nutrient ions
in alkali soils are strongly influenced by soil pH, independent of the effect of
exchangeable sodium. For this reason we feel that pH should form an integral
part of the definition of alkali soils.

    Although, in nature, various sodium salts do not occur absolutely separately,
in most cases either the neutral sodium salts or salts capable of alkaline
hydrolysis, exert a dominating influence. The two kinds of salt-affected soils
tend to occur in distinct geographic and geochemical zones and require different
approaches to their management and reclamation. Both saline and alkali soils
occur extensively in India (Fig.1) and in other parts of the world.

TABLE I. PHYSICO-CHEMICAL CHARACTERISTICS OF A TYPICAL ALKALI SOIL PROFILE[a]

| Horizon | Depth (cm) | Mechanical composition: | | | Organic carbon (%) | CaCO$_3$ (72 mm) (%) | pH[b] | CEC (meq/100 g) | Exch. Na (%) |
		Sand (2–0.05) (%)	Silt (0.05–0.02) (%)	Clay (<0.002) (%)					
A$_{11}$	0–5	43.4	34.6	22.0	0.3	0.5	10.3	10.2	97
A$_{12}$	5–24	33.4	37.6	29.0	0.3	0.9	10.3	12.8	94
B$_{21t}$	24–56	30.6	36.2	33.2	0.2	1.4	9.8	14.8	90
B$_{22t}$	56–85	26.0	42.6	31.4	0.2	3.3	9.8	14.6	85
B$_{3Ca}$	85–118	33.2	40.0	26.8	0.1	12.4	9.6	11.2	68
C$_{Ca}$	118–140	45.0	32.0	23.0	0.1	20.5	9.2	9.8	39

| Depth (cm) | Composition of saturation extract | | | | | | |
| | EC (ds/m) | (Ca+Mg)$^{2+}$ | Na$^+$ | K$^+$ | CO$_3^{2-}$ | HCO$_3^-$ | Cl$^-$ | SO$_4^{2-}$ |
							(meq/L)	
0–5	8.2	0.4	85.3	0.2	30.0	36.5	12.5	5.5
5–24	8.0	0.4	83.9	0.1	27.0	40.5	14.5	5.5
24–56	1.9	0.6	18.0	0.1	2.5	8.5	5.5	3.0
56–85	1.4	0.5	13.5	0.1	2.2	7.6	2.5	2.0
85–118	1.0	0.8	10.0	0.1	2.2	4.5	2.5	1.0
118–140	0.9	1.0	9.2	0.1	1.5	5.0	2.5	1.0

a　Source: Dr. G.P. Bhargava, personal communication.

b　Measured in 1:2 soil-water suspension.

CEC = cation exchange capacity.

ALKALI SOILS OF INDO-GANGETIC PLAINS

In the Indo-Gangetic plains alkali soils are generally confined to areas
with a mean annual rainfall of between 550 and 1000 mm. In areas with a
mean annual rainfall above 1000 mm, salt-affected soils generally do not occur
extensively, and in areas with a mean annual rainfall of less than 550 mm the
dominant soluble salts are chlorides and sulphates which impart a saline
character to the soils rather than an alkali one [7, 8]. Alkali soils occur inter-
spersed with normal soils and may sometimes occupy a few thousand hectares
at a stretch. The soils usually occupy a somewhat lower elevation in the
otherwise flat terrain and are subject to flooding in the rainy season by waters
containing the weathering products of alumino silicate minerals including alkali
bicarbonates. In the ensuing dry season the soil solution is concentrated,
resulting in an increase of the sodium adsorption ratio (SAR) of soil solution
which results in an increased adsorption of sodium ions on the soil exchange
complex and soil pH. The introduction of canal irrigation and other develop-
mental activities has accentuated the problem through restricting surface
drainage, and the rise in the groundwater table resulting in reduced natural
leaching. In other cases the use of groundwaters with a high sodic hazard for
irrigation has increased the problems of alkali soils.

Soil characteristics

Table I gives the physico-chemical characteristics of a typical alkali soil
profile. Illite is the dominant clay mineral in these soils. Based on chemical,
physical and morphological features many such soils have been classified as
Typic Natrustlfs according to soil taxonomy. The soils owe their unproductivity
to a high ESP, accompanied by high pH and a low organic-matter content.
The soils often have a zone of accumulation of calcium carbonate nodules
at around 1 m depth which may act as a physical barrier to root penetration.
The dispersed nature of these soils makes them highly impermeable to water
and air resulting in an almost complete loss of rainfall as runoff. The runoff
produced by storms of even a five-year return period can be very high. The
measured peak runoff values reported [9] from these catchments range from
13 to 26 $m^3 \cdot s^{-1} \cdot km^{-2}$. Fluctuations in the groundwater table are associated
with the rainfall patterns. In many alkali-affected areas the groundwater table
comes to within 1 m of the soil surface in the rainy season, and this is followed
by a gradual recession in the post-rainy season. Groundwaters generally have a
low total salt content although in some areas the proportion of sodium to
divalent cations may be high enough to be a source of sodicity hazard.

TABLE II. MAXIMUM STORM RAINFALL AND DRY SPELLS OF
DIFFERENT RETURN PERIODS IN A TYPICAL ALKALI SOILS AFFECTED
AREA [10]

Duration of event	Return period in years					
	1.01	2.33	5	10	25	100
Maximum 1-day rainfall (mm)	41	120	152	183	221	282
Maximum 2-day rainfall (mm)	51	155	201	238	285	355
Maximum 4-day rainfall (mm)	67	179	228	268	318	394
Maximum dry spell in monsoon season (days)	15	28	34	39	45	54

Climate

The climate of alkali soil areas is characterized by hot summers and cool
winters. The monsoon rains fall from July to September. These climatic
features give rise to two distinct cropping seasons in a year, viz. *kharif* (summer,
i.e. June to October) and *rabi* (winter, i.e. November to April). The average
annual rainfall is about 700 mm and nearly 90% of this falls during the south-
west monsoon from June to September. The average open-pan evaporation
value is approximately 1900 mm, thus giving a net annual water deficit of
about 1200 mm. Generally this water deficit is evident in all months except
July and August. The maximum two-day rainfall and the length of the dry
spell of a five-year return period, were estimated [10] to be 201 mm and 34 days,
respectively (Table II). Such a situation calls for greater emphasis on the
conservation of rainfall, not only from the drainage aspect, but also to meet
the water requirements of crops during the dry spells in the growing season.

MANAGEMENT OF ALKALI SOILS

Reclamation of alkali soils basically requires that excess sodium on the
soil exchange complex be replaced by calcium through amendments, and the
exchanged sodium leached out of the root zone. The socio-economic conditions
of farmers further necessitate crop production from these soils to have the
highest priority during the reclamation phase to enable them to recover the
cost of input. A brief description of appropriate management practices
evolved over the past few years is presented below.

Drainage

Narayana et al. [11] concluded that tile drains or open ditches were ineffective in lowering the groundwater table because of the extremely poor water transmission characteristics of alkali soils. Vertical drainage, involving pumping underlying water through a bore-hole, on one hand, and using pumped water for irrigation on the other, proved to be an effective and promising measure for groundwater table control. The conditions for successful vertical drainage, i.e. the presence of a favourable aquifer within 10–20 m and favourable quality of groundwaters, are met with in most areas which have an alkali soil problem.

Amendments

Since it is the cheapest and is abundantly available, gypsum ($CaSO_4 2H_2O$), is the most commonly used amendment for reclaiming alkali soils. The quantity of gypsum required depends on the quantity of exchangeable sodium that must be replaced and the depth to which soil improvement is desired. For soils containing soluble carbonates the usual laboratory procedure [12] for estimating the gypsum needs of soils, estimates both the gypsum required to neutralize the soluble carbonates and that required to replace exchangeable sodium. Our studies [13, 14], however, showed that when gypsum was surface-applied and alkali soils leached, only a small fraction of the applied calcium reacted with soluble carbonates while most carbonates leached did not react. Based on these studies it was suggested that the existing procedure overestimated the gypsum requirement and that a modified procedure suggested by Abrol et al. [14] was more realistic. It was further shown [15] that if a correct choice of crops was made it was sufficient to add gypsum to improve only the surface 15 cm soil, thereby reducing the reclamation cost considerably. Further soil improvement is accomplished through continuous cropping with rice as one of the crops [16].

Because a good correlation exists between the pH and ESP of alkali soils [4], for advisory purposes a graphical relationship between the pH and gypsum requirements of soils was prepared [17] for routine recommendations. The results of field and laboratory studies [18, 19] also helped to define the optimum gypsum fineness and application method for alkali soils.

Crops

Growing crops tolerant of excess exchangeable sodium can ensure reasonable returns during the initial years of reclamation. In Table III important crops and some grasses are listed according to their relative tolerance to soil sodicity, based on results of several field studies [15, 20–23]. In general, crops that are able

TABLE III. RELATIVE TOLERANCE OF SOME CROPS AND GRASSES TO EXCHANGEABLE SODIUM

Tolerant[a]	Semi-tolerant	Sensitive
Karnal grass *(Diplachne fusca)*	Wheat *(Triticum vulgare)*	Cowpeas *(Vigna sinensis)*
Rhodes grass *(Chloris gayana)*	Barley *(Hordeum vulgare)*	Gram *(Cicer arietinum)*
Para grass *(Brachiaria mutica)*	Oats *(Avena sativa)*	Groundnut *(Arachis hypogaea)*
Bermuda grass *(Cynodon dactylon)*	Raya *(Brassica juncea)*	Lentil *(Lens esculenta)*
Rice *(Oryza sativa)*	Senji *(Melilotus parviflora)*	Mash *(Phaseolus mungo)*
Sugarbeet *(Beta vulgaris)*	Berseem *(Trifolium alexandrinum)*	Mung *(Phaseolus aureus)*
	Sugarcane *(Saccharum officinarum)*	Peas *(Pisum sativum)*
	Bajra *(Pennisetum typhoides)*	Maize *(Zea mays)*
	Cotton *(Gossypium hirsutum)*	Cotton at germination *(Gossypium hirsutum)*

[a] Crop yields are seriously affected if the ESP is more than about 55, 35 and 10 in respect of tolerant, semi-tolerant and sensitive crops, respectively. Tolerance in each column decreases from top to bottom. The grasses listed are highly tolerant and some, like Karnal grass, will grow even in soils of ESP 80 to 90.
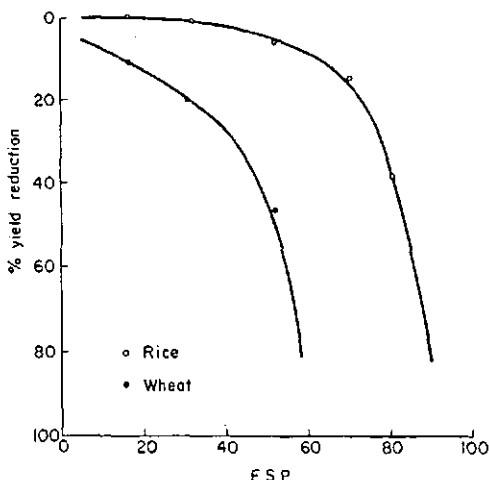
FIG.2.   Effect of soil sodicity on the relative yield of rice and wheat crops.

to withstand excess moisture conditions are also more tolerant of sodic conditions.
Deep-rooted crops generally perform poorly because of sodic sub-layers. The
relative tolerance of rice and wheat (Fig.2) shows that at an ESP of 55, while
the yield of rice was reduced by only 10%, wheat completely failed to grow. The
high tolerance of rice to sodic conditions is due to its ability to withstand (and,
in fact, its need for) a layer of water in the field throughout the growing season.
During rice growth there is a marked reduction in soil ESP [15, 16] making rice
an ideal crop during reclamation.

Field and greenhouse studies [24, 25] have shown that some grasses, e.g.
Karnal grass *(Diplachne fusca)*, Rhodes grass *(Chloris gayana)*, para grass
(Brichiaria mutica) and Bermuda grass *(Cynodon dactylon)*, are highly tolerant
of sodic conditions and can be successfully grown where most crops will fail
to yield satisfactorily. Growing tolerant grasses will provide not only the much-
needed forage but will also improve the soils, resulting in increased absorption
of rain-water and reduced runoff. Efforts are also currently under way to evolve
suitable agrotechniques for growing trees in these soils. The auger-hole
technique [26], where the tree seedlings are planted in 15 cm diameter and
150 cm deep auger holes filled with an appropriate mixture of original soil,
gypsum and farmyard manure, appears promising for large-scale plantation
of trees. Success in growing trees along with grasses will provide an alternative
land use for these marginal lands.

Nutrients

Low organic-matter content, poor air-water relationships and high soil pH influence the transformation and availability of applied and native nutrients in alkali soils.

Nitrogen

A number of field studies have shown that crops grown in alkali soils respond to higher levels of applied nitrogen compared with crops grown in non-alkali soils. Conditions for nitrogen losses through volatilization and denitrification are ideal in alkali soils because of their high pH and poor physical conditions. For this reason it is recommended that crops grown in alkali soils be fertilized with 20% more nitrogen than the recommended rates for normal soils.

Phosphorus and potassium

Chhabra et al. [27] reported that alkali soils have high amounts of Olsen's extractable P and that a significant fraction of this was leached to lower depths following the application of amendments and ponding. Field studies further showed that P application was not required for rice and wheat crops in the initial years of reclamation [28]. Similarly, the crops did not respond to applied potassium because of sufficient release from the soil minerals [29].

Micro-nutrients

Among the micro-nutrients, zinc deficiency is most common in alkali soils. Several studies [30–32] have clearly high-lighted the need for applying zinc to soils in the initial years of reclamation to obtain optimum yields.

Water management

For crops other than rice, irrigation management presents major difficulties in obtaining optimum crop yields in alkali soils. The gypsum applications recommended are generally sufficient to reduce sodicity of only the upper 15 cm so that the deeper soil layers continue to be sodic and to influence soil-water behaviour and therefore the irrigation management needs of these soils. Being structurally unstable the soils are prone to spontaneous slaking and crust formation upon irrigation which impedes water intake and therefore the storage capacity of soils [33]. Effective water storage is further reduced owing to the restriction of roots only in the upper few centimetres of soil (Fig.3), depending on the extent of soil improvement. The movement of stored water
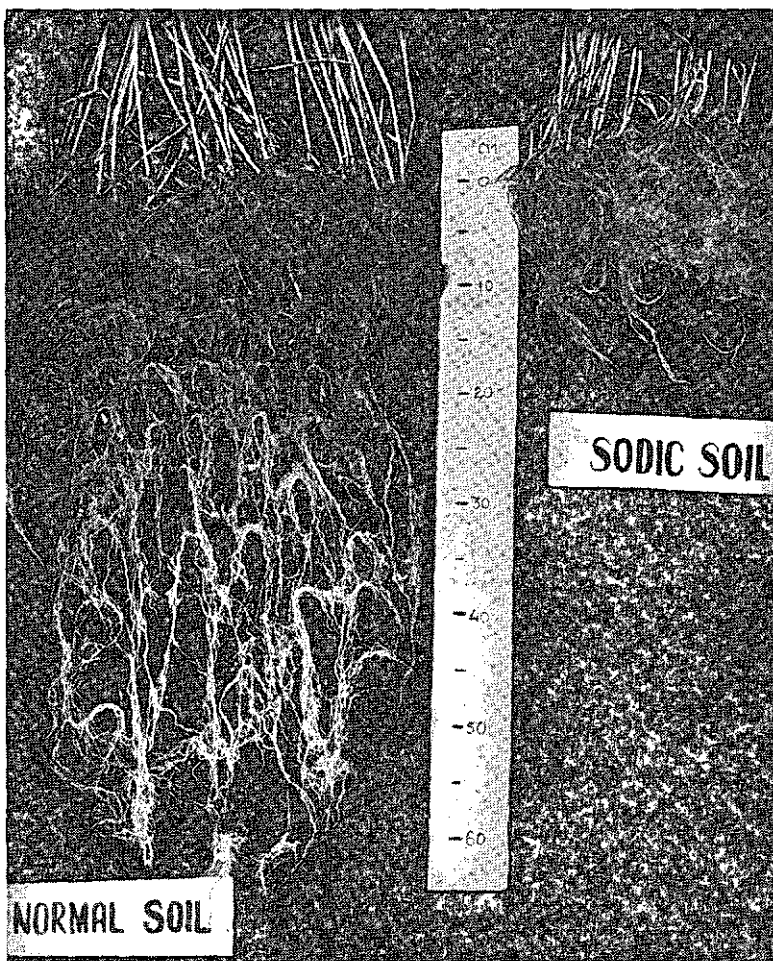
FIG.3.   Growth of wheat roots in a normal and in a partially reclaimed sodic soil.

to plant roots is restricted because of the low hydraulic conductivity of alkali soils. A number of studies [34–38] have shown that the contribution of subsoil layers to meet the water demands of growing crops is negligible. These studies have shown that, in alkali soils, limited root penetration, a lowered capacity to store water in an available form and poor transmission characteristics, require that irrigation is applied at small depths and more frequently than would be required for crops grown under normal soil conditions.

ISOTOPE AND RADIATION TECHNIQUES IN RESEARCH ON BETTER MANAGEMENT

This paper has stressed that the whole range of management practices suitable for alkali soils are different from practices adopted in normal soils. Our ability to optimize production from such soils will ultimately depend on how accurately we can describe various processes that influence soil-plant relationships quantitatively so that the relevant management practices have a sound base. Thus, it is known that considerable losses of N in alkali soils may occur through volatilization/denitrification, and of P and other elements through leaching — but, to what extent? What is the influence of different sodicities on these losses? How could these be minimized? What are the alternative management practices for obtaining higher efficiencies of applied nutrients? Sodicity strongly influences water absorption, redistribution within the soil and movement in response to different gradients. Root growth in these soils is markedly influenced owing to the chemical and physical effects of high ESP. A quantitative evaluation of these processes will form a basis for sound irrigation management practices for these soils and for controlling sodicity. The management of rain-water in a land use involving trees and grasses is a challenging task. Any research towards this must include complete monitoring of components of the water-balance equation. In all these and in basic studies involving exchange behaviour of soils, measurements of exchange capacity, nutrient transformations, and isotope and radiation techniques, will be extremely helpful in finding appropriate solutions.

REFERENCES

[1]   ABROL, I.P., BHUMBLA, D.R., FAO World Soil Resources Rep. **41** (1971) 42.
[2]   ABROL, I.P., CHHABRA, R., GUPTA, R.K., "A fresh look at the diagnostic criteria for sodic soils", Salt Affected Soils (Int. Symp. Karnal, 1980) 142.
[3]   BHUMBLA, D.R., ABROL, I.P., "Saline and sodic soils", Soils and Rice, Int. Symp. Int. Rice Research Institute, Los Banos, Phillipines (1977) 719.
[4]   GUPTA, R.K., CHHABRA, R., ABROL, I.P., Soil Sci. **131** (1981) 215.
[5]   GUPTA, R.K., CHHABRA, R., ABROL, I.P., Soil Sci. **133** (1982) 364.
[6]   GUPTA, R.K., BHUMBLA, D.K., ABROL, I.P., Soil Sci. (1983) in press.
[7]   BHARGAVA, G.P., ABROL, I.P., BHUMBLA, D.R., J. Indian Soc. Soil Sci. **24** (1976) 81.
[8]   ABROL, I.P., BHUMBLA, D.R., "Some comments on terminology relating to salt affected soils", Dryland Saline Seep, Int. Symp. Edmonton, Alberta, Canada (1978) 6.
[9]   SHARMA, R.P., SEHGAL, S.R., "Design criteria for drainage projects in Punjab", Waterlogging: Causes and Measures for its Prevention, C.B.I.P. Publication **118** (1972) 111.

[10] NARAYANA, V.V.D., ABROL, I.P., "Effect of reclamation of alkali soils on water balance", Tropical Agricultural Hydrology (LAL, R., RUSSEL, E.W., Eds), John Wiley (1981) 283.

[11] NARAYANA, V.V.D., PANDEY, R.N., GUPTA, S.K., J. Indian Assoc. Hydrologists 1 (1977) 21.

[12] RICHARDS, L.A., USDA Agricultural Handbook No.60.

[13] ABROL, I.P., DAHIYA, I.S., Geoderma 11 (1974) 1.

[14] ABROL, I.P., DAHIYA, I.S., BHUMBLA, D.R., Soil Sci. 120 (1975) 30.

[15] ABROL, I.P., BHUMBLA, D.R., Soil Sci. 127 (1979) 79.

[16] CHHABRA, R., ABROL, I.P., Soil Sci. 124 (1977) 49.

[17] ABROL, I.P., DARGAN, K.S., BHUMBLA, D.R., Reclaiming alkali soils, Bull. No.2, Division of Soils and Agronomy, Central Soil Salinity Research Institute, Karnal (1973) 58.

[18] KHOSLA, B.K., DARGAN, K.S., ABROL, I.P., BHUMBLA, D.R., Indian J. Agric. Sci. 43 (1973) 1024.

[19] CHAWLA, K.L., ABROL, I.P., Agric. Water Manag. 5 (1982) 41.

[20] CHHABRA, R., SINGH, S.B., ABROL, I.P., Soil Sci. 127 (1979) 242.

[21] SINGH, S.B., CHHABRA, R., ABROL, I.P., Agron. J. 71 (1979) 767.

[22] SINGH, S.B., CHHABRA, R., ABROL, I.P., Indian J. Agric. Sci. 50 (1980) 852.

[23] SINGH, S.B., CHHABRA, R., ABROL, I.P., Indian J. Agric. Sci. 51 (1981) 885.

[24] ASHOK KUMAR, ABROL, I.P., Forage Res. 5 (1979) 101.

[25] ASHOK KUMAR, ABROL, I.P., Indian J. Agric. Sci. 49 (1979) 473.

[26] SANDHU, S.S., ABROL, I.P., Indian J. Agric. Sci. 51 (1981) 437.

[27] CHHABRA, R., ABROL, I.P., MAHAVIR SINGH, Soil Sci. 132 (1981) 319.

[28] DARGAN, K.S., CHHILLAR, R.K., Indian J. Agron. 23 (1978) 14.

[29] PAL, D.K., MONDAL, R.C.J., Indian Soc. Soil Sci. 28 (1980) 347.

[30] DARGAN, K.S., GAUL, B.L., ABROL, I.P., BHUMBLA, D.R., Indian J. Agric. Sci. 46 (1976) 535.

[31] TAKKAR, P.N., RANDHAWA, N.S., Fertilizer News 23 (1978) 1.

[32] SINGH, M.V., CHHABRA, R., ABROL, I.P., Soil Sci. (1983) in press.

[33] ABROL, I.P., ACHARYA, C.L., in Proc. 2nd World Congr. 1, Int. Water Resources Assoc. New Delhi (1975) 335.

[34] ACHARYA, C.L., ABROL, I.P., Soil Sci. 125 (1978) 310.

[35] ACHARYA, C.L., SANDHU, S.S., ABROL, I.P., Soil Sci. 127 (1979) 56.

[36] ACHARYA, C.L., SANDHU, S.S., ABROL, I.P., Agron. J. 71 (1979) 936.

[37] SANDHU, S.S., ACHARYA, C.L., ABROL, I.P., J. Indian Soc. Soil Sci. 29 (1981) 148.

[38] SANDHU, S.S., ACHARYA, C.L., ABROL, I.P., J. Indian Soc. Soil Sci. 30 (1981) 6.

Invited Paper

PRINCIPLES OF ROOT WATER UPTAKE, SOIL SALINITY AND CROP YIELD FOR OPTIMIZING IRRIGATION MANAGEMENT

C. DIRKSEN
Department of Soil Science and
    Plant Nutrition,
Agricultural University,
Wageningen, Netherlands

Abstract

PRINCIPLES OF ROOT WATER UPTAKE, SOIL SALINITY AND CROP YIELD FOR OPTIMIZING IRRIGATION MANAGEMENT.
    The paper reviews the principles of water and salt transport, root water uptake, crop salt tolerance, water quality, and irrigation methods which should be considered in optimizing irrigation management for sustained, viable agriculture with protection of the quality of land and water resources. In particular, the advantages of high-frequency irrigation at small leaching fractions with closed systems are discussed, for which uptake-weighted mean salinity is expected to correlate best with crop yields. Optimization of irrigation management depends on the scale considered. Non-technical problems which are often much harder to solve than technical problems, may well be most favourable for new projects in developing countries.

1. INTRODUCTION

In many parts of the world lack of water is the major cause of less than optimal crop production. Elimination of this limiting factor by means of irrigation usually leads to crop yields that are much higher than on nonirrigated land, while often also per year two or three crops can be grown. While quantities and composition vary, irrigation water always contains salts. Plant roots normally take up water with only a negligible fraction of the dissolved salts, and only pure water evaporates from the soil surface. The remaining soil solution becomes more and more concentrated, which has a detrimental effect on crop yields. For sustained irrigation agriculture the salts dissolved in the irrigation water may not accumulate in the rootzone, but must be leached out of the rootzone.

In humid regions with supplemental irrigation, leaching occurs naturally by excess rainfall in the wet season. In arid and semi-arid regions, however, this natural leaching process is

not sufficient, and the salts must be removed by supplying
irrigation water in excess of the amounts transpired by the
plants. If there is plenty of water available this presents
no problem, unless excessive irrigation leads to waterlogging
and a high groundwater table. This, in turn, may lead to yield
reductions due to poor aeration and salt accumulation at the
soil surface due to capillary rise from the groundwater.

In many areas all the good land and water are being used and
crop production can be increased only by bringing marginal land
into cultivation with a limited supply of poor quality water.
Maintaining viable agriculture under such adverse conditions
requires good understanding of the principles of irrigation
water quality, salt and water movement in soil, the influence
of salt and water distributions on root water uptake and crop
yields, and the possibilities for improving crop yields and
land and water resources by irrigation management. All this
must be done within acceptable economic, social, and political
limits. In this paper I will review some recent developments in
this area, with heavy emphasis on experience gained while working
at the U.S. Salinity Laboratory, Riverside, Ca, USA.

2. SOIL WATER POTENTIALS

Irrigation water quality can affect crop yields in three
different ways; directly as a result of
- osmotic potential of the soil solution, or
- specific ion toxicity (e.g., chloride, boron), indirectly
- via the effect of the composition of the dissolved salts
  on soil structure, infiltration rate, aeration, etc.
I will deal mostly with the first effect, and make only a few
remarks with respect to the last.

Root membranes exclude virtually all salts dissolved in
water being taken up, making the osmotic component of the soil
water potential (energy per mass, J/kg) fully effective in
reducing the rate of water uptake. The latter is then proporti-
onal to the gradient of the total soil water potential

$$\psi_t = \psi_o + \psi_p + \psi_g, \tag{1}$$

where the subscripts stand for total, osmotic, pressure, and
gravitational, respectively [1].
The osmotic potential depends on the total dissolved solids
(TDS), which is expressed often in milligrams of salt per liter
of solution, or parts per million (ppm). Usually the salinity
of soil solution or irrigation water is measured as electrical
conductivity and expressed in mmho/cm at 25 $^{\circ}$C. The SI unit
for EC is S/m (mmho/cm = dS/m). The relationship between
osmotic potential and EC, which depends somewhat on the compo-
sition and concentration of the salt solution, for most soil

solutions with EC values up to about 30 dS/m is described
adequately by [2] :

$$h_o \text{ (m)} \simeq - 4.0 \times EC \text{ (dS/m)} \tag{2}$$

Here, the osmotic potential is expressed in meter head of
water (energy per weight, J/N) [1] . This form can be compared
directly to the gravitational head (ψ_g/g), which is the
elevation above a reference level, and the pressure head (h_p or h)
of the solution, which can be measured directly with a tensio-
meter. The sum of the three components is the total head h_t.

3. SOIL WATER SALINITY AND CROP YIELDS

Transpiration is basically a physical process in which
plants play a rather passive role. The driving force for the
transpiration stream is the difference in total head of the
water in the soil and that in the atmosphere. When the total
head of the soil water decreases due to a decrease in water
content, increase in salinity, or both, the leaf water potential
will decrease. If the latter drops below a certain range of
values, depending on evaporative demand, crop, etc, the stomates
in the leaves close to prevent dessication of the plant. How-
ever, the diffusion of CO_2 through the stomates, required for
photosynthesis, is then also blocked. Thus there is a relation-
ship between crop yields and transpiration and, therefore,
also between crop yields and soil water salinity.

Salt tolerance of crops has been evaluated mostly under
rather uniform salinity in the rootzone, by growing plants
either in salt solutions or in excessively irrigated soil columns.
Under field conditions, water contents and salinities in root-
zones vary in space and time, and plants interact with and
adjust to these varying conditions. The actual water uptake
distribution for a given root distribution, evaporative demand,
etc., depends on the prevailing osmotic and pressure potential
distributions. These, in turn, change as a result of the water
uptake, irrigation management, etc. If irrigation exceeds
transpiration, the soil solution moves down the rootzone while
being concentrated. Considering only the concentrating effect
of root water uptake, and starting with a given amount of
irrigation water and dissolved salts, the concentration of this
water is doubled each time the volume is halved. For instance,
the uptake required for changing the EC from 8 to 16 dS/m is
only 1/8 -th of that which was required earlier to change it
from 1 to 2 dS/m. Thus, very little uptake is involved in
concentrating the soil solution to the higher salinities in
the lower part of the rootzone. The maximum salinity depends
on the quality of the irrigation water and the leaching
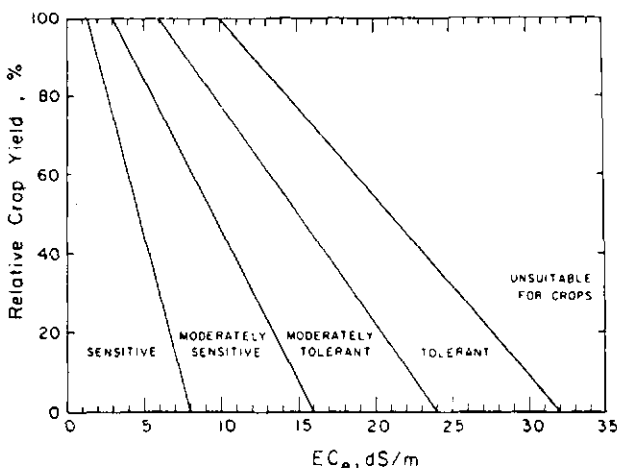
FIG.1.   Divisions for classifying crop tolerance to salinity.

fraction, L, which is the fraction of the irrigation water that
drains beyond the root zone.

The soil water salinity distribution may be affected
further by diffusion, dispersion, precipitation, and dissolu-
tion of salts, and by cation exchange. Water uptake is compli-
cated further by a growing root system and different demands
by the plant at various growth stages. Also, roots do not
penetrate readily into highly saline soil layers, but once
established, subsequent salination usually does not change root
distributions appreciably. It is not surprising, in view of this
complex situation, that the literature reports best correlations
with yields for variously averaged rootzone salinities, ranging
from the least saline to the most saline zone [3] . Maas and
Hoffman [4] compiled crop salt tolerance data from the litera-
ture by listing the threshold salinity level below which crop
yields are not affected, and the rate of decrease of yields with
increasing salinity beyond the threshold. This provided a
classification of crops according to their salt tolerance
(Fig. 1). The salinities are expressed as EC of the saturation
extract, EC_e. EC_e values are about half the EC values at field
capacity and are commonly used because they are measured easily
and with good reproducebility.

Bernstein and Francois [5] found that as long as roots had
access to water of low salinity, they were able to take up water
of higher salinity in the bottom of the rootzone without adverse
effects on alfalfa yields. They believed crop yields to be
related to the uptake-weighted mean salinity (see Equation 8).

From the preceding discussion it should be clear that this mean
is heavily biased towards the lower salinities. If this has
general validity, leaching requirements based on crop salt
tolerance data under uniform salinity conditions can be
reduced up to a factor four [6] . If there are no other growth-
limiting factors, the uptake-weighted mean salinity, integrated
over time and adjusted according to growth stages, theoretically
can be expected to correlate best with crop yield. This hypothesis
will be explored further, in particular for high-frequency
irrigation.

4. WATER FLOW THEORY FOR HIGH-FREQUENCY IRRIGATION

The concentration of the soil solution may increase con-
siderably towards the bottom of the rootzone, but additional
salts dissolved in the irrigation water must be carried beyond
the rootzone by a net downward flux of water. This water flux
can be very small and may even be intermittent. From a water
conservation point of view, leaching fraction should be as
small as possible, as low as 0.05. Such high irrigation effi-
ciencies cannot be achieved with conventional flood irrigation
methods. Saturated hydraulic conductivities may vary over an
order of magnitude and, as long as a field is flooded, this
soil property determines how much water infiltrates into the
soil at a given site. Spatially uniform infiltration requires
spatially uniform application of water at rates which do not
cause ponding of water at the soil surface. Thus, for minimum
leaching the control must be shifted from the soil to the
irrigation system. This can be done most easily with closed
irrigation systems which deliver water at low rates to relatively
small areas, and which can be switched on and off on demand.
Then there is no minimum amount of water that must be applied
per irrigation, and there is no fixed cost per application.
Technically and economically, such systems can be operated at
high frequencies, and can even be automated with several
applications per day [7] .

High-frequency irrigation[8] approaches a steady state
situation in which, at each depth, the soil water content is
established which corresponds with the hydraulic conductivity
required to accommodate the water flux density according to
Darcy's Law:

$$q = -k(\theta) \frac{dH}{dz} = -k(\theta) \left(\frac{dh}{dz} - 1\right) \qquad (3)$$

Here q   = water flux density, $m^3 \, m^{-2} \, s^{-1}$
     θ = volume fraction of water, $m^3 \, m^{-3}$
     $k(\theta)$ = hydraulic conductivity function, $m \, s^{-1}$
     z   = vertical coordinate, positive downward, m
     H   = hydraulic head = h-z, m

The water flux density varies between the irrigation rate at the soil surface and the drainage rate out of the bottom of the rootzone, the ratio being the inverse of the leaching fraction, L. Since $k(\theta)$ varies very rapidly with θ, the θ values and, according to the soil water characteristic $h(\theta)$, also the h values will vary only moderately from top to bottom of the rootzone. As a result, the waterholding capacity (field capacity) of soil is unimportant for high-frequency irrigation. It can be used even on coarse sandy soils, without excessive drainage. Soil water contents and pressure heads can be maintained at values somewhat higher than those at field capacity, such that the drainage flux density is just sufficient for salinity control.

5. UPTAKE-WEIGHTED MEAN SALINITY

Under high-frequency irrigation there is always water available of essentially irrigation water quality near the soil surface. Therefore, most of the water uptake will occur in the regularly replenished surface layer, and roots tend to prolife- rate in this layer. Water uptake in the lower, more saline zone is small and probably occurs only during periods of highest evaporative demand. As a result of the shallow water uptake, salinity will increase rapidly with depth. Generally, root zone salinity increases with increasing irrigation frequency.

While the average rootzone salinity depends on the water uptake distribution and thus on irrigation frequency, the uptake-weighted mean salinity is insensitive to the water uptake distribution. This is shown easily for steady state conditions [9, 10] . The mass balance for steady, one-dimensional, vertical flow of water in soil is

$$dq/dz = - \lambda (z) \tag{4}$$

where $\lambda(z)$ is the rate of water uptake $(m^3 \cdot m^{-3} \cdot s^{-1})$ as function of depth. Neglecting salt precipitation, dissolution, diffusion, and dispersion, the mass balance for steady, vertical salt transport in the rootzone is

$$d(cq)/dz = 0 \tag{5}$$

where c is the local salt concentration $(mol \cdot m^{-3})$. Integration of Eq. (5), with subscript 0 standing for values at the soil surface (z=0), yields

$$q = c_o q_o /c \tag{6}$$

Substitution of Eq. (6) into Eq. (4) yields

$$\lambda(z) = - c_o q_o \ d/dz(c^{-1}) \tag{7}$$

Thus, under the stated conditions, the rate of water uptake is proportional to the slope of the dilution profile and the salt flux density at the soil surface. This relationship can be used to derive $\lambda(z)$ from salinity data. The uptake-weighted mean soil salinity can be defined as:

$$<c> = \frac{1}{T} \int_0^\infty \lambda c \, dz \qquad (8)$$

where T is the rate of transpiration. Substitution of Eq. (7), which is valid for any uptake distribution, into Eq. (8) yields

$$\frac{<c>}{c_o} = \frac{1}{1-L} \ln(\frac{1}{L}) \qquad (9)$$

Equation (9) shows that for steady irrigation and purely convective, vertical salt transport, the ratio of uptake-weighted mean salinity and irrigation water salinity is only a *function of the leaching fraction*, independent of the root water uptake distribution. In fact, this ratio increases only slowly with decreasing L. For L = 0.3, 0.2, 0.1 and 0.05, its value is 1.72, 2.01, 2.56, and 3.15, respectively. This suggests that for irrigation with fixed water quality at high frequency, which approaches steady state conditions, crop yields will not decrease with leaching fraction until a certain salinity threshold is reached, and will decrease only moderately with leaching fraction beyond that threshold. This can be expected because under high-frequency irrigation soil water contents and pressure potentials are always high and, therefore, play a minor role in root water uptake. In contrast, under traditional low-frequency irrigation total soil water potentials vary from very high immediately after irrigation to very low at the end of the irrigation interval. These low potentials may be very detrimental to crop yields.

The concept of high-frequency irrigation at low leaching fraction while maintaining crop yields was tested on a field scale with citrus and alfalfa using Colorado river water with EC = 1.35 dS/m [11] . During the first four years leaching fraction showed no effect on citrus yield and quality; during the fifth and last year, only 5% leaching caused substantial yield reduction. The leaching requirement for alfalfa appeared to be less then 5%.

6. SALINITY DISTRIBUTIONS AND SALT BALANCE

The four main factors determining soil water salinity distributions mentioned so far, are:
- quality of irrigation water
- leaching fraction
- irrigation frequency
- water uptake distribution

The first three factors are externally dictated by irrigation
management and can be varied independently. The fourth factor
is partly determined by the plant-specific characteristics of
the root system, but also adjusts itself to the first three
factors. The salt concentration of the irrigation water has a
large effect, but can be treated mostly as a simple scaling or
multiplication factor. The effect of the other three factors
is illustrated in Fig. 2, 3, and 4.

Substitution of an exponential water uptake distribution in
Eq. (7) and integration yields the concentration profile:

$$c/c_o = \{L + (1-L)\ e^{-z/\delta}\}^{-1} \tag{10}$$

where δ is a characteristic length of the water uptake distri-
bution [9] . Figure 2 shows salinity profiles according to
Eq. 10 for various leaching fractions. Hoffman and Van Genuchten
[12] presented dimensionless concentration profiles for L=0.1
according to Eq. (10), and for a trapezoidal and a "40-30-20-10"
water uptake distribution (Fig. 3; c_1/c_0, c_2/c_0, and c_3/c_0,
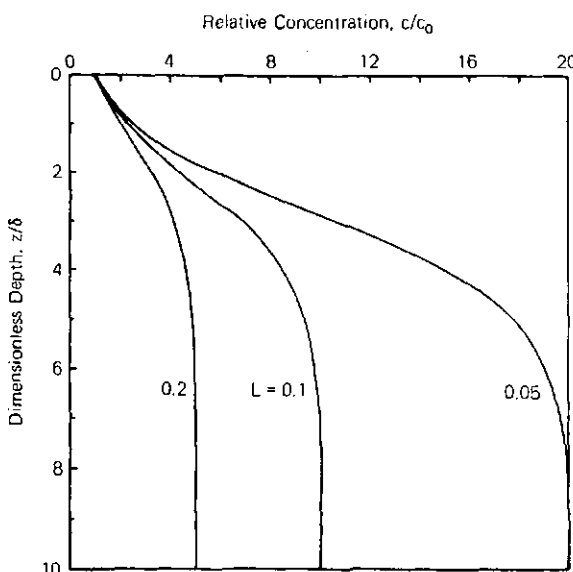
FIG.2.   Salinity profiles as function of leaching fraction.

Relative Concentration, c/c_0
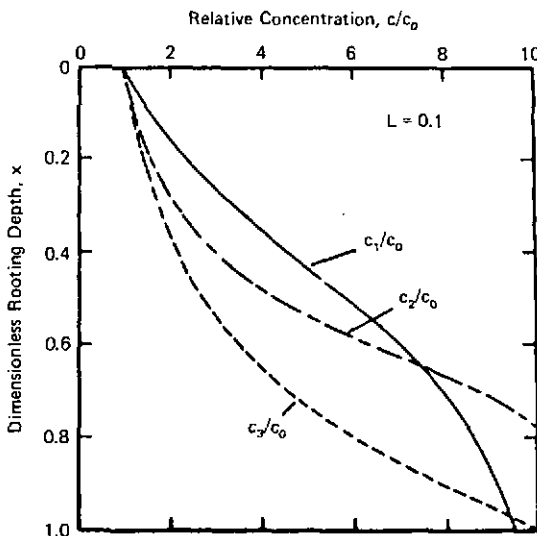
FIG.3. Salinity profiles as function of water uptake distribution.
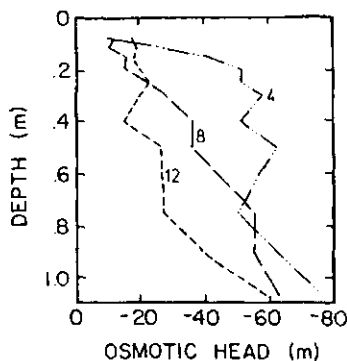
FIG.4. Salinity profiles as function of irrigation interval.

respectively). Jury, et al. [13] also found a large sensitivity
of salinity distributions for water uptake distributions by
numerical simulation. Figure 4 shows salinity distributions I
obtained in laboratory soil columns by irrigating alfalfa with
the same total amounts of water of h_0 = -12.0 m, but applied at
intervals of 4, 8, and 12 days, respectively. Salinity profiles
for daily irrigation were similar to that for the 4-day interval.

TABLE 1. Salt burdens of applied waters (V_w/C_{iw}) and drainage waters ($V_{dw}C_{dw}$), differences (SB), and potential for reducing salt return, metric tons/hectare per year.

River	EC_{iw} dS/m	leaching fraction						Reduction in salt return [*]
		0.1			0.3			
		$V_{iw}C_{iw}$	$V_{dw}C_{dw}$	SB	$V_{iw}C_{iw}$	$V_{dw}C_{dw}$	SB	
Feather	0.10	0.13	0.25	+0.12	0.17	0.67	+0.50	0.41
Grand	0.94	1.22	0.89	-0.33	1.57	1.65	+0.08	0.76
Missouri	0.91	1.17	1.08	-0.09	1.51	1.66	+0.15	0.58
Salt	1.56	2.02	1.84	-0.18	2.60	2.94	+0.34	1.10
Colorado	1.27	1.65	1.24	-0.41	2.12	2.10	-0.02	0.86
Sevler	2.03	2.63	2.15	-0.47	3.39	3.52	+0.13	1.36
Gila	3.14	4.05	3.73	-0.33	5.22	5.54	+0.31	1.81
Pecos	3.26	4.22	2.57	-1.65	5.43	4.94	-0.49	2.37

[*] difference between leaching fractions of 0.3 and 0.1, assuming consumptive use of 91 cm/year.

The salinity distributions of Fig. 2 and 3 represent only the concentration process of the soil solution as a result of root water uptake assuming piston flow. In reality, diffusion and dispersion tend to increase concentrations towards the soil surface, while some plants decrease concentrations by taking up appreciable amounts of salt. The salt balance is also affected by dissolution of highly soluble salts, such as NaCl, present in the soil, the amounts being roughly proportional to the volume of water passing through the soil. Therefore, minimizing the amount of water diverted from a river or pumped from groundwater minimizes this salt pick-up. On the other hand, at low leaching fractions the plant roots may concentrate the soil solution to the point where poorly soluble salts, such as $CaCO_3$ and $CaSO_4$, precipitate. Whether the overall salt balance of the irrigation water on its way through the rootzone, due to dissolution and precipitation, is positive or negative depends on the chemical composition of the irrigation water and the leaching fraction, as illustrated in Table 1 [14]. The benefit on a larger scale in terms of reduced salt load for downstream users also depends on the presence or absence of special salt deposits in the area and on the chemical composition of the river water.

The loss of porosity and reductions in hydraulic conductivity as a result of salt precipitation in the bottom of the rootzone are negligible, even if it is continued for hundreds of years. Another effect is potentially more hazardous. Since Ca-salts precipitate while Na-salts stay in solution, salt precipitation increases the sodium adsorption ratio, SAR, of the soil solution. This may lead to large reductions in hydraulic conductivity of soils with high contents of swelling clay, if the high salt concentrations are not enough to prevent swelling.

7. OPTIMISATION OF IRRIGATION MANAGEMENT

The higher water use efficiencies of closed, high-frequency irrigation methods save not only water, but also energy for pumping and fertilizers due to reduced leaching. They also reduce the chance for water logging and salt accumulation at the soil surface due to capillary rise from a high groundwater table. Closed system irrigation can be used on land that is unsuitable for other forms of irrigation because it does not require landleveling and the restrictions on the soil hydraulic properties are minimal. Closed systems such as trickle, sprinkler, and center pivot irrigation, require energy for pressurisation. This is a distinct disadvantage over open systems. Rawlins [15] developed a low pressure bubbler system for tree cultures which does not require pressurisation and still has essentially all the advantages and possibilities of high-frequency irrigation at low leaching fraction. It would be a major step forward if low pressure closed systems were also developed for field crops.

Optimal irrigation management depends on the scale that one considers, who are the beneficiaries, who pays for improvement costs, etc. For an individual farmer it is most beneficial to irrigate at a large leaching fraction, especially if he pays the same for the last unit water as for the first and there is no danger for a high groundwater table. However, excess leaching increases the salt load in the return flow. For a downstream user it would be better that the first user would divert as little water as possible and would not discharge the return flow back into the river. Then he would be able to irrigate with nearly the same quality water as the first user. Therefore, optimal use of land and water resources on a larger scale could well be that as little water as possible is diverted for irrigating the most salt-sensitive crops and that the drainage water is not returned to the river. Instead, it should be used for irrigating less salt-sensitive crops. On an experimental scale, cotton was irrigated with drainage water of EC = 8.0 mmho·cm^{-1} without essential yield reduction[16]. The drainage water from the second irrigation could possibly be used for irrigating even more salt-tolerant crops or halophytes suitable for energy production from biomass. When no beneficial use can be made of the remaining small volume of very saline drainage water, it should either be discharged in sea or evaporated in a pond.

8. NON-TECHNICAL FACTORS AFFECTING OPTIMISATION

Optimisation of irrigation management as outlined above is possible only when institutional, legal, and political obstacles can be removed. Especially in established irrigation districts, this is often not the case. Water rights and water pricing policies usually do not enhance efficient water use. Optimal water delivery systems are often thwarted by existing boundaries of irrigation districts. In some areas discontinuing irrigation agriculture altogether would be the most economical solution. Obviously, this requires political decisions. Van Schilfgaarde [17] gives a review of these non-technical aspects of irrigation agriculture for four irrigation districts in the western USA.

In general, non-technical problems are much harder to solve then technical problems. They tend to be less of an obstacle for optimizing new irrigation projects than existing irrigation management practices. Also, capital investments in existing conventional irrigation projects usually are such that additional investment in closed irrigation systems are out of the question. In contrast, the necessary high initial investments in newly established closed irrigation systems are offset by initial savings in canal lining, landleveling, turn-outs, etc., as well as savings in water, fertilizers, energy, and labor with every irrigation. Therefore, new irrigation projects in

developing countries may well present the most favorable con-
ditions for bringing into practice the principles outlined
in this paper.

REFERENCES

[1] KOOREVAAR, P., MENELIK, G., DIRKSEN, C., "Elements of Soil
Physics", Elsevier Science Publishers, Amsterdam, The
Netherlands (1983, in press).

[2] U.S. Salinity Laboratory Staff, "Diagnosis and Improvement
of Saline and Alkali Soils", Agriculture Handbook No. 60,
USDA, Washington, D.C., USA (1954).

[3] INGVALSON, R.D., RHOADES, J.D., PAGE, A.L., Soil Sci. 122
3 (1976) 145.

[4] MAAS, E.V., HOFFMAN, G.J., J. Irrig. Drain. Div., ASCE,
103 IR2 (1977) 115.

[5] BERNSTEIN, L., FRANCOIS, L.E., Soil Sci. Soc. Amer. Proc.
37 6 (1973) 931.

[6] VAN SCHILFGAARDE, J., et.al., J. Irrig. Drain., Div., ASCE,
100 IR3 (1974) 321.

[7] HOFFMAN, G.J., et.al., Agric. Water Mgmt 1 (1978) 233,

[8] RAWLINS, S.L., RAATS, P.A.C., Science 188 (1975) 604.

[9] RAATS, P.A.C., Soil Sci. Soc. Amer. Proc. 38 5 (1974) 717.

[10] RAATS, P.A.C., Proc. Second Internat. Drip Irrig. Congr.
San Diego, Ca. USA (1974) 222.

[11] U.S. Salinity Laboratory Staff, "Minimizing Salt in Return
Flow through Irrigation Management", Final Report. U.S.
Environmental Protection Agency, ADA, OK., USA (1981).

[12] HOFFMAN, G.J., VAN GENUCHTEN, M.Th. In "Efficient Water
Use in Crop Production". Amer. Soc. Agron. Madison, Wis.
USA (in press).

[13] JURY, W.A., FLUHLER, H., STOLZY, L.H. Water Resour. Res.
13 3 (1977) 645.

[14] RHOADES, J.D., et.al., J. Environ. Qual. 3 4 (1974) 311.

[15] RAWLINS, S.L., Agric. Water Mgmt 1 (1977) 167.

[16] RHOADES, J.D., RAWLINS, S.L., PHENE, C.J., Amer. Soc. Civ.
Eng. Preprint 80-119 (1980).

[17] VAN SCHILFGAARDE, J., Trans. ASAE 22 2 (1979) 344.

Invited Paper

MANAGEMENT OF SALINE SOILS
IN ISRAEL

E. RAWITZ
The Faculty of Agriculture,
The Hebrew University of Jerusalem,
Rehovot, Israel

Abstract

MANAGEMENT OF SALINE SOILS IN ISRAEL.
    The main soil salinity problem in Israel is the danger of gradual salinization as a result
of excessively efficient water management. Aquifer management is aimed at preventing flow
of groundwater into the ocean, causing a creeping salinization at a rate of about 2 ppm per
year. Successful efforts to improve irrigation efficiency brought with them the danger of
salt accumulation in the soil. A ten-year monitoring programme carried out by the Irrigation
Extension Service at 250 sampling sites showed that appreciable salt accumulation indeed
occurred during the rainless irrigation season. However, where annual rainfall is more than
about 350 mm this salt accumulation is adequately leached out of the root zone by the
winter rains. Soil salinity in the autumn is typically two to three times that in the spring, a
level which does not affect yields adversely. In the drier regions of the country long-term
increasing soil salinity has been observed, and leaching is required. This is generally
accomplished during the pre-irrigation given in the spring, whose size is determined by the
rainfall amount of the preceding winter. The increasing need to utilize brackish groundwater
and recycled sewage effluent requires special measures, which have so far been successful.
In particular, drip irrigation with its high average soil-water potential regime and partial
wetting of the soil volume has achieved high yields under adverse conditions. However, the
long-term trend of water-quality deterioration is unavoidable under present conditions, and
will eventually necessitate either major changes in agricultural patterns or the provision of
desalinated water for dilution of the irrigation water.

1. INTRODUCTION

    Salts may be present in the soil as weathering products of
the parent material, as a result of marine inundation, or due to
anthropogenic factors, e.g. irrigation with water containing
soluble salts. While all three types of soil salinity are
found in Israel soils, only the latter factor is a cause of
major concern. The soil properties and the composition of the
salts make leaching of the soil entirely feasible. The clima-
tic zones of Israel range from the subhumid Mediterranean zone,
with mean annual rainfall of 500-700 mm, to extreme desert with
a mean annual rainfall of 25 mm.

The major agricultural areas of the country are located in
the Mediterranean and in the semi-arid zones, and are supplied for
the most part with irrigation water of good to moderate quality.
Since water supply is the limiting factor, there has been very
strong emphasis on efficient irrigation since the inception of
modern agriculture. Thus virtually no surface irrigation is prac-
ticed, and the dominant irrigation methods are sprinkling and
drip irrigation. Careful determination of crop water require-
ments and technologically sophisticated control of actual water
application resulted in a high water application efficiency, the
average probably being better than 75% for sprinkled areas, and
close to 100% under drip irrigation. At present over 90% of
available water resources are being utilized. The laudable con-
sciousness of the need for water conservation brought with it,
however, the real danger that soluble salts deposited in the
soil even by good quality irrigation water would eventually lead
to soil salinization, especially in areas with relatively low
rainfall.

Equally great efforts were made to obtain maximum exploita-
tion of groundwater resources by preventing flow into the ocean
[1]. This has resulted in the aquifers being essentially closed
systems, with any salts leached into the aquifers becoming per-
manent additions to the groundwater reservoir.

2. MANAGEMENT APPROACHES

2.1. Water supply

All water resources are essentially nationalized by law.
Water is pumped from the Sea of Galilee into a short canal,
and from an operational reservoir enters a pressurized 108-in.*
pipeline extending some 250 km, to the south of Beer Sheba,
interconnecting along its route with numerous secondary net-
works. Planning and monitoring of the system are entru-
sted to a government corporation, "Tahal"; water is allocated
to consumers by the Water Commissioner's Office of the Ministry
of Agriculture, and the system is operated by "Mekorot", a
public water company. The entire system is managed as a single
unit, making it possible to pump water from wells into the main
pipeline, to discharge water to consumers, or into recharge
wells during periods of low demand. Thus free aquifer capacity
is utilized for temporary storage, also making possible modifi-
cations in the chemical quality of either the groundwater or
the water in the distribution system by mixing water from
various sources.

---

* 1 inch = 2.54 cm.

The optimal design and operation of a system supplied by two major aquifers and the Jordan River watershed, serving thousands of delivery points with a total annual discharge of approximately 1,500 million cubic meters of water is a task of enormous complexity. This was facilitated by design and construction by stages, but based on an initial integrated concept [1]. The lack of complete technical information was taken into acount by incorporating the required flexibility into the design process. The required information was and still is being generated by research departments of the abovementioned authorities as well as by the Agricultural Research Organization, institutions of higher learning, and the Irrigation Extension Service of the Ministry of Agriculture.

Rapid development of irrigated agriculture in the 1950's led to the decision to construct a national water system and to supply local systems eventually to be integrated into the national system, from local groundwater wells as an interim measure. This required deliberate overpumping for a certain period, and measures had to be taken to minimize damage due to seawater intrusion. This led to the initiation of very intensive activity in "Tahal" combining survey and description of all water resources, monitoring of their quantity and quality, and research aimed at understanding the processes taking place in the aquifers and watersheds. By the mid-1970's a large body of geohydrological and hydrochemical knowledge contained in various progress reports and scientific publications could be summarized in major reports which included conclusions and operational recommendations [2,3,4]. While during the work water sources were analyzed by standard methods for all the important anions, cations, total soluble salts and SAR, the criterion adopted was chloride concentration expressed as ppm. Firstly, high correlation coefficients were found between the above criteria in the major water sources. Secondly, citrus groves were the major agricultural consumer of water and are known to be particularly sensitive to chlorides. A maximum concentration of 170 ppm Cl^- was adopted for the orange-growing area of the northern and central coastal plain. For the inland valleys, the southern coastal plain and the northern Negev, where citrus does not occupy such a large portion of the area and the main variety is the more salt-tolerant grapefruit, an upper limit of 250 ppm Cl^- was set. The surface water quality nevertheless fluctuates within fairly wide limits depending on the winter rainfall of a particular year, and thus maintenance of the water quality in the distribution system requires constant monitoring and dilution with groundwater of appropriate amount and quality. Simulation models [5,6] have been developed for the main aquifers, and an operational model is used by the Mekorot water company for monitoring and control of the complex distribution network.

A number of presently known and possible future changes of
conditions will undoubtedly require further adjustments both in
the models and in operating procedures. For example, creeping
salinization of 0.5-2.0 ppm/year has been found in large parts
of the inland Cenomanian aquifer, with rates of up to 5 ppm/
year in certain parts [3], and the same process is even more
pronounced in the coastal aquifer; anticipated urbanization and
groundwater recharge with treated municipal effluent have led
to the prediction of an eventual increase of 100 ppm CI^- in the
coastal aquifer. The salinity-yield function is so far known
in detail only for citrus, and as more information becomes
available on additional crops, criteria may change. Changing
cropping patterns will affect quality criteria, as for example
the increasing area under avocado at the expense of citrus;
avocado varieties presently grown are thought to tolerate no
more than 70-100 ppm Cl^-, but new rootstocks or scion varieties
may be more tolerant. The management of the aquifers as a
closed system, resulting in their gradual but virtually irrever-
sible salinization, will ultimately necessitate upgrading of
the water quality by industrial processes such as desalinization
by distillation or reverse osmosis, whose present cost would
entail drastic reduction of water use by agriculture.

2.2. SOIL MANAGEMENT

2.2.1. Soil properties

The interrelation between present climate, and soil parent
material and climate during the soil forming process is the
dominant factor determining the salinity status of unirrigated
soils in Israel. The soils of the central mountain spine are
mainly well-structured, well-drained terra rossa clay-loams
receiving 400-1,000 mm annual rainfall. They are thus thoroughly
leached, and even if supplied with poor quality water the sali-
nity hazard would be minimal.
At the other extreme, the desert soils of the country are
for the most part unarable and unirrigable desert lithosols
(lithic xerothents) and reg soils (calciorthids and haplargids)
[7], and these are the soils mainly affected by pedogenic
salinity. The soils which potentially require salinity manage-
ment are located in the semi-arid and sub-humid plains and
valleys of the northern Negev, the coastal plain, the
Esdraelon Valley, and the three parts of the Jordan Rift Valley
known as the Jordan and Bet Shean valleys and the Arava, bet-
ween the Dead Sea and the Red Sea . Rainfall ranges from
less than 50 mm per year in the Arava, to about 200 mm in the
Beer Sheba plain, 400-600 mm in the coastal plain and the

Esdraelon Valley, and 200-400 mm in the Jordan and Bet Shean valleys. Soils range from sands and sandy loams (psamments) through soils of loessial origin with high silt and lime content (torrifluvents, argids and xerolls), rendzinas (rendolls), to highly montmorillonitic vertisols (Fig. 2). Soils above about the 350mm isohyetal are not saline, and saline desert soils with the exception of playas are generally easy to leach.

2.2.2. The salinity survey as a basis for management decisions

2.2.2.1. Background and methods

As the National Water Carrier system went into operation in the early 1960's, concern arose both with respect to the possible effect of the water quality on sensitive citrus groves, and to the danger of salt accumulation in the soil. The Irrigation Extension Service of the Ministry of Agriculture initiated the salinity survey in 1963 and intensive monitoring continued for a decade [8]. A total of 250 observation plots were chosen throughout the country, of which 190 were under citrus, with the remainder including deciduous fruit trees, avocado, vineyards, various field crops and a number of unirrigated plots as control. Total water application, rainfall and yield were determined annually, soil properties were determined initially, and soil samples were taken every spring and fall at 30 cm depth intervals to a depth of 150 cm to be analyzed by standard methods [9]. Irrigation water samples were also taken periodically each year. Numerous correlations were determined between various indices of soil and water salinity and the yield of several citrus varieties.

2.2.2.2. Principal findings

The survey confirmed that the high *irrigation application* efficiencies attained by good water management caused an accumulation of salts in the 0-150 cm soil profile during the irrigation season. Yaron and Shalhevet [10] report on six sites with soils including sandy loams, loess silty loam and vertisol, receiving roughly 650 mm of irrigation water with an electrical conductivity ranging from 0.7 to 4.0 dS m^{-1}, finding increases in the conductivity of the saturation extract ranging from zero to three times the salinity in the spring, depending on soil type, water quality and depth layer. There was a tendency for greatest increase in the 60-90 cm layer. In all the plots of the salinity survey the average salinity of the saturation extract in the autumn was approximately equal to that of the irrigation water, representing a 2½-fold increase in soil salinity over the season, since the saturated paste water content was roughly 2.5 times that at field capacity [11].

It was also found that the sandy soils of the coastal plain were completely leached each winter, even during relatively dry years. The heavier soils of the inland valleys and the loessial soils of the South, where annual rainfall is also lower, were leached by the winter rains to depths varying between 30 and 120 cm, depending mainly on the amount and distribution of rainfall in a particular winter.

The long-term trend was that the soils of the coastal plain with rainfall over 400 mm/year were not being salinized, while the heavier soils of the inland valleys were gradually accumulating salts below the 90-cm depth. Likewise, in the South, those soils with a finer-textured horizon in the deeper layers and some sodic properties, showed a long-term trend of salinization. A gradual rise in ESP was also noted in these soils.

Yield response to salinity was found to be a function of the combination of citrus variety and rootstock, as well as of soil texture as expressed by the saturation water content. In view of the very high correlation found between the various soil and water salinity indices, only one salinity index was sufficient for interpretation of results. On the whole, roughly half of the yield depression due to salinity was explained by either Na or Cl, while 90% of the variation was explained by the combined effect of either ion and the value of the saturation percentage. Overall, yield of the most sensitive variety-rootstock combination decreased by about 5 t/ha for each increase of 50 ppm Cl^-, and 10 t/ha for each 50 ppm of Na^+, with variations due to age of the trees and their yield potential. General yield levels were in the range of 35-50 t/ha.

While it is not implied that water quality rather than soil salinity is the determining factor on yield, the high correlation between them and the lower variability of the water quality data led to the choice of the latter in determining practical recommendations [11]. The following limiting values were recommended for irrigation water on the basis of response of the most sensitive variety combination:

Cl^- :   200 ppm
Na^+ :   100 ppm
EC   :   1.0 $dS \cdot m^{-1}$
SAR   :   2.0-2.5

A more detailed analysis between yield and yield potential, soil texture and water salinity is given by Shalhevet et al. [11]. While detailed yield functions have not been developed for all other crops, critical salinity values are known for most of the important ones and are used to avoid unfavorable combinations of water quality and crop.

2.3.. The utilization of brackish water for irrigation

2.3.1. Sources and scope of utilization

In Israel water is classified as brackish between chloride
concentrations of 400 and 4,000 ppm (approximately 1,000 to
10,000 ppm total soluble salts) [12], and it has been estimated
by Michaeli [13] that some 300 million m^3/year of brackish
groundwater are available for exploitation, an appreciable per-
centage of the total water resources. A similar amount will
ultimately be abstracted from the fresh water supply and recycled
as lower quality sewage effluent. The main sources of brackish
groundwater are in the Esdraelon and Bet Shean valleys in the
North, in the Beer Sheba plain and northwestern Negev, and in the
Arava. In the North, the brackish water is generally diluted
with better quality water and thus does not represent a special
problem. It must be noted that among the salt-tolerant crops
according to the U.S. Salinity Laboratory [9], the only major
crop grown on a large scale in Israel is cotton, with minor
areas under date palms and Rhodes grass. Among the moderately
tolerant crops, cantaloupes, grapes, vegetable crops and wheat
are of economic importance. Cotton has become the most impor-
tant single field crop in the country, while winter vegetables
are the economic mainstay of farmers in the Arava valley.
Brackish water has assumed rather unique importance in the cotton
growing area of the northwestern Negev, and in the Arava. In
the first instance, a highly brackish and sodic aquifer has been
successfully utilized for cotton irrigation, utilizing water
which is outside of and in addition to the rationed water allo-
cation. In the Arava, the brackish water is the only available
source. This water has an electrical conductivity of 3 $dS \cdot m^{-1}$,
and contains 600 ppm of chlorides and 700 ppm of sulfates.
Winter vegetables are the major agricultural products, and
include peppers, tomatoes, cucumbers, melons and sweet corn.
Yields obtained under sprinkler irrigation were generally low,
and in many cases complete crop failure resulted from leaf burn
caused by wetting with the saline water. Goldberg and coworkers
have shown that in this situation drip irrigation is the critical
requirement for successful crop production [14,15,16]. Compari-
sons between sprinkler, furrow and drip irrigation and between
different irrigation water qualities showed that drip irrigation
roughly doubled yields, and brought them to the level attainable
with non-saline water (EC of 0.1 $dS \cdot m^{-1}$).
The dramatic success of the drip method with the highly
brackish water under extreme desert conditions is due to the
following factors:

1. In contrast to sprinkling, plant leaves are not wetted
    by the irrigation water, thus preventing leaf burn.

2. The adaptability of drip irrigation to the frequent
    application of small amounts of water facilitates the
    continuous maintenance of a high matric water potential
    in the root zone, thus limiting the total water poten-
    tial essentially to the osmotic potential of the
    irrigation water.
3. The radial pattern of water movement in the soil away
    from the drip emitter leaches soluble salts to the
    periphery of the wetted soil volume, thus preventing
    salt accumulation in the root zone.

The brackish water of the coastal aquifer in the northern
Negev contains 2,000-6,000 ppm of dissolved salts, has an elec-
trical conductivity of 4.5-5.5 $dS \cdot m^{-1}$, and its SAR ranges bet-
ween 15 and 26 [17]. This water is used exclusively for the
irrigation of cotton, both by sprinkler and by drip irrigation,
but principally by the drip method. In addition to the possible
salinity effect on the crop, the extremely high SAR value poses
a serious soil management problem. Twersky et al. [18], using
sprinkler irrigation, found that the brackish water actually
produced somewhat higher yields than did good quality irrigation
water (EC = 0.98 $dS \cdot m^{-1}$, SAR = 3.4), with the average yield over
four years being around 5,000 kg of seed cotton per hectare,
which is considered a good yield in this area. Similar results
have been obtained by Meiri and a group of coworkers at the
Volcani Institute (personal communication), and by the growers
of the region. Some fields yield up to 7,000 kg/ha. The suc-
cessful use of brackish water is attributed to the favorable
effect of some stress on the cotton plant in limiting excessive
vegetative growth at the expense of fiber formation.

The high SAR of the water is cause for concern about the
maintenance of soil structure, which is inherently unstable,
tends to crust, and has a low infiltrability [19]. Due to the
high electrolyte concentration of the soil solution, reasonably
good soil structure and infiltrability are maintained during
the irrigation season, but all the expectable problems appear
as the soil surface is wetted by winter rains. The problems
can be alleviated by application of gypsum, and runoff prevented
by the method of basin tillage [20]. While the soil properties
appear to be at equilibrium over at least an 8-year period [19],
the higher residual soil moisture at tillage time is a cause of
compaction and structure deterioration to which no solution has
yet been found, and is presently being investigated.

While long-term trends of water quality deterioration, soil
salinization in certain regions, and the danger of soil struc-
ture degradation are discernible and predictably will continue,
a strategy for response to these processes has not been deve-
loped as yet. The present response is an effort to optimize
water management by adding a minimum of water and thus salts to

the soil, principally by expanding use of drip irrigation, and
to develop less aggressive tillage practices and high-value
crops. Future developments may include a shift of emphasis
from agriculture to industry, a process already under way, and,
with the hoped-for development of cheaper energy sources, allo-
cation of some desalinated water to agriculture. In any event,
continuing efforts to attain maximum water utilization effi-
ciency are certain to be required.

REFERENCES

[1] WIENER, A., The development of Israel's water resources,
     Am. Scientist 60 4 (1972) 466.
[2] KANFI, Y., RONEN, D., The Chemical Quality of Groundwater
     in the Aquifers of the Coastal Plain of Israel, Ministry of
     Agriculture, Water Commission, Water Polution Control Unit
     Rep. 76/1 (1976) 155 pp.
[3] YATIR, Y., AVRON, M., MERCADO, A., The Chemical Quality of
     the Aquifers of the Mountains and the Interior Valleys,
     TAHAL - Water Planning for Israel Ltd., Dep. of Research
     and Preliminary Design Prog. Rep. 01/78/06 (1978) 111 pp.
[4] SALITERNIK, C. (Ed), Water Quality in Israel (Report of the
     committee on water quality), The Israel National Com. on
     Biosphere and Environment, The National Council for Research
     and Development Rep. NCRD-7-73 (1973) 266 pp.
[5] MERCADO, A., The kinetics of mineral dissolution in carbo-
     nate aquifers as a tool for hydrogeological investigations
     II, Hydrogeochemical models, J. Hydrol. 35 (1977) 365.
[6] AVRON, M., A Salinity and Flow Model of the Coastal Aquifer
     Using the Amended Aquifer Simulator "MASS", TAHAL - Water
     Planning for Israel Ltd. Project on Groundwater Salinity in
     the Coastal Plain Prog. Rep. 3, (Tahal 01/77/86) (1977).
[7] DAN, J., YAALON, D.H., KOYUMDJISKY, H., RAZ, Z., Soils and
     soil association map of Israel, Min. of Agric. and Hebrew
     Univ. of Jerusalem 1962.
[8] HAUSENBERG, Y., POZIN, Y., BOAZ, M., Salinity Survey, Min.
     of Agric. Irrig. Extension Service Summary Rep. 1963-1973
     (1974) 78 pp.
[9] U.S. SALINITY LABORATORY STAFF, Diagnosis and Improvement
     of Saline and Alkali Soils, USDA Agric. Handbook 60 (1954)
     160 pp.
[10] YARON, B., SHALHEVET, J., "Quality of irrigation water",
     FAO/UNESCO International Sourcebook of Irrigation and
     Drainage, Ch. VII (1965).
[11] SHALHEVET, J., YARON, D., HOROWITZ, U., Salinity and citrus
     yield - an analysis of results from a salinity survey,
     J. Hort. Sci. 49 (1974) 15.

[12] BONNE, J., GRINWALD, Z., "Source, consumption and use of brackish water in Israel", Brackish Water as a Factor in Development (A. ISSAR, Ed.), (Proc. Int'l. Symp. on Brackish Water, Ben-Gurion Univ. of the Negev, Beer Sheba) (1975) 77.

[13] MICHAELI, A. "Brackish water resources in Israel", Proc. Ninth Israel Symposium on Desalination - Utilization of Brackish Water, National Council for Research and Development (1972) 25.

[14] GOLDBERG, D., GORNAT, B., SHMUELI, M., BEN-ASHER, I., RINOT, M., Increasing the agricultural use of saline water by means of trickle irrigation, Water Resources Bul. $\underline{7}$ 4 (1971) 802.

[15] GOLDBERG, D., SHMUELI, M., Drip irrigation - a method used under arid and desert conditions of high water and soil salinity, Trans. ASAE $\underline{13}$ 1 (1970) 38.

[16] SHMUELI, M., GOLDBERG, $\overline{D}$., Sprinkle, furrow and trickle irrigation of muskmelon in an arid zone, HortScience $\underline{6}$ 6 (1971) 557.

[17] FRENKEL, H., SHAINBERG, I., "Irrigation with brackish water - chemical and hydraulic changes in soils irrigated with brackish water under cotton rotation", Brackish Water as a Factor in Development (A. ISSAR, Ed.), (Proc. Int'l. Symp. on Brackish Water, Ben-Gurion Univ. of the Negev, Beer Sheba), (1975) 175.

[18] TWERSKY, M., PASTERNAK, D., BOROVIC, I., "Effects of brackish water irrigation on yield and development of cotton", Ibid. 135.

[19] HADAS, A., FRENKEL, H., Infiltration as affected by long-term use of sodic-saline water for irrigation. Soil Sci. Soc. Am. J. $\underline{46}$ 3 (1982) 524.

[20] RAWITZ, E., $\overline{\text{MO}}$RIN, J., HOOGMOED, W.B., MARGOLIN, M., ETKIN, H., Tillage practices for soil and water conservation in the semi-arid zone I., The management of fallow during the rainy season preceding cotton, Soil and Tillage Res. (1983) In Press.

Memoria encargada

AVANCES EN LA REHABILITACION
DE SUELOS SALINOS EN EL PERU

J.A. ESTRADA
Universidad Nacional Agraria
"La Molina",
Lima, Perú

Abstract—Resumen

PROGRESS WITH THE RECLAMATION OF SALINE SOILS IN PERU.
    The present report is the result of five years' experimental work at the Costa Regional
Development Institute (IRD-Costa), based in Cañete, Lima, Peru, on the reclamation of land
affected by salts and hence of seriously limited agricultural value (production lower than 50%).
A reclamation method combining surface and at depth washing with artificial drainage of excess
water has been tried out and a method of nutrition has been developed which is based on
tonification of the seeds before sowing. The results obtained are rather encouraging, so the
method looks very promising, especially as it also makes for considerable savings in fertilizers
(some 20% less) and for better yields per unit area. Once the ionic behaviour of this method
has been studied by means of radioisotopes a large contribution will have been made towards
alleviating the problem of saline soils.

AVANCES EN LA REHABILITACION DE SUELOS SALINOS EN EL PERU.
    El presente informe es el fruto de 5 años de trabajos experimentales en el Instituto Regional
de Desarrollo de Costa (IRD-Costa), con sede en Cañete, Lima, Perú, y trata de la rehabilitación
de un suelo afectado por sales, con serias limitaciones para la actividad agrícola (producción
inferior al 50%). Se ha ensayado una metodología combinada de rehabilitación, mediante el
lavado superficial y en profundidad, evacuando el exceso de agua a través de drenaje artificial.
Asimismo se ha desarrollado una metodología nutricional, comenzando desde la tonificación
de la semilla previamente a la siembra. Los resultados obtenidos son bastante halagadores, lo cual
hace muy promisoria la metodología ensayada. Además, permite una economía considerable en
el uso de fertilizantes (cuando menos alrededor del 20%), así como un mayor rendimiento por
unidad de área. De comprobarse el comportamiento iónico de esta metodología, mediante el uso
de radisótopos, se habrá logrado un gran aporte para eliviar la problemática de los suelos afectados
por sales.

1. INTRODUCCION

    La rehabilitación de suelos afectados por sales es una práctica que puede
variar mucho en su manejo debido a su complejidad física, química, fisicoquímica
y bioquímica. Esta complejidad aparece como consecuencia de la relación y

proporcionalidad existente entre el plasma, el esqueleto del suelo y la micro-
biología del suelo. El grado de complejidad estará en función de la calidad y
cantidad de los coloides inorgánicos y orgánicos presentes en el substrato. De
ahí que la práctica de la rehabilitación puede aparecer como muy simple (suelos
ligeros) o muy compleja (en suelos pesados, montmoriloníticos).

2.   METODOLOGIA COMBINADA DE REHABILITACION

En vista de esto, y considerando la actividad agrícola como un todo integral
dentro de un ecosistema en particular, se ha ideado un sistema combinado de
rehabilitación. Este contempla tanto la mecánica simple del lavado superficial,
mediante el empleo de surcos y del auxilio de un sistema de drenaje entubado,
como el aspecto sanitario y nutricional del cultivo; este último empieza desde la
tonificación de la semilla, instantes antes de la siembra, y uno o dos refuerzos
foliares a partir de los 15 ó 20 días después de la emergencia.

La sustentación básica de esta metodología se apoya, en general, en la
problemática de los cuatro parámetros siguientes:

— Suelo-agua
— Planta contra adversidad
— Cultivo-sanidad
— Economía.

2.1.   Suelo-agua

Siendo el problema principal la acumulación de agua y sales, fue lógico
considerar el establecimiento de un sistema de drenaje para evacuar el exceso de
agua y el de sales removidas por el lavado. Se planeó una evacuación rápida del
exceso de agua, tanto de la napa freática como de la proveniente del lavado.

Como el suelo experimental es de origen aluvial, deficiente en materia
orgánica (1% o menor), con presencia de arcillas montmoriloníticas e ilíticas, fue
necesario aplicar materia orgánica en cantidad adecuada (alrededor de 10 a 20 t/ha),
especialmente en las áreas más afectadas (40 a más de 100 mmho/cm). Además
se contempló aplicar de 1 a 1,5 t de yeso en mezcla conjunta con el estiércol y/o
paja de cebada previamente triturada con un rotavator.

La aplicación de estiércol-paja y yeso tuvo por finalidad: a) evitar la
orientación del sodio en el espacio interbasal de las arcillas vía solvatación, lo
cual hace que el ion sodio quede atrapado y se prolongue el período de lavado
2, 3 o más años; y b) influenciar el parámetro SAR de manera que la presión
osmótica no alcance valores muy altos y las semillas y las plantas puedan absorber
agua adecuadamente, al aliviarse la magnitud de agua disponible en cuanto a la
relación capacidad de campo-punto de marchitez. Además, el yeso se hace

necesario en una práctica de lavado, pues al disolverse las sales salubles, éste tiende a aumentar su solubilidad (de 2,04 g/L en ausencia de NaCl, puede elevarse a 7,1 g cuando hay 358 g/L de NaCl).

El agua empleada fue del río Cañete, con una fluctuación en conductividad eléctrica de 0,2 a 0,6 mmho/cm. La calidad del agua juega un papel muy importante, no solo en cuanto a la cantidad de sal removida sino en cuanto a la estabilidad estructural del sistema suelo.

2.2. Planta contra adversidad

En suelos afectados por sales, la planta encontrará un medio ambiente adverso tanto para su germinación como para su crecimiento posterior. En un medio no apropiado para la germinación, la semilla agotará todas sus reservas al incrementar su metabolismo y al generar un gran potencial energético en un gran intento para adaptarse a un medio adverso. El gran consumo de azúcar-fosfato dará lugar a un desgaste intensivo del fósforo, lo que originará una deficiencia que perjudicará el vigor de crecimiento meristemático. La semilla se agotará y la plántula no logrará emerger; las plantitas que lleguen a salir sobre la superficie serán individuos débiles y propensos a las plagas y enfermedades.

Bajo este criterio se decidió tonificar la semilla utilizando su poder de imbibición (un 20% en este caso) y empleando concentraciones variables de fósforo y zinc, y concentraciones constantes de Fe, Cu, Mn y Mo, este último donde sea menester (ejemplo: leguminosas, oleaginosas, etc.).

En la presente experiencia se han utilizado las siguientes concentraciones:

P	de 200 a 1500 ppm
Zn	de 100 a 700 ppm
Fe	de 20 a 40 ppm
Cu	10 ppm
Mn	10 ppm

Los iones de elementos menores fueron aplicados en forma de sulfatos o $MnCl_2$. El fósforo fue extraído del superfosfato de calcio simple; puede utilizarse el ácido fosfórico, cuando al frente de esta experiencia se cuente con un professional especializado.

2.3. Cultivo-sanidad

Las acciones contempladas bajo este concepto estuvieron orientadas hacia la sincronización y oportunidad de las operaciones culturales, así como de la prevención de plagas y enfermedades, sin sacrificar el equilibrio del control biológico natural del cultivo.

CUADRO I. RESULTADOS OBTENIDOS EN EL CULTIVO EXPERIMENTAL DE ALGODON

Campaña	Rendimiento promedio por ha[a]	
	qq[b]	kg
78/79	60	2760
79/80	70	3220
80/81	77	3542
81/82	86	3956

[a] Promedios sobre una extensión de 28 a 30 ha.
[b] Quintales.

2.4. Economía

Este es un aspecto crítico en el éxito de la empresa agrícola, el cual se agudiza cada vez más debido al alto costo generado por el aumento de precio de los insumos y al incremento en el costo de la mano de obra.

Se ha encontrado que la tonificación de la semilla permite economizar, cuando menos, un 20% del fertilizante que se aplica al suelo, de acuerdo con la formulación recomendada por el análisis del suelo. Esta economía en fertilizantes es sumamente atractiva si se compara con el gasto ocasionado por la tonificación de la semilla para una ha de terreno (de 1 a 2 dólares).

El terreno utilizado en este experiencia fue un franco arcillo limoso, con pH 7,8 y una conductividad eléctrica muy variable (alrededor de 8 a más de 100 mmho/cm). El 40% del área total (30,84 ha) era improductivo, con una salinidad de 40 a más de 100 mmho/cm. La napa freática era alta y muy oscilante, apareciendo sobre la superficie en la parte baja del terreno, especialmente en época de riego del valle.

Los cultivos experimentales han sido: algodón, papa, maíz verde y forraje, cebada. De éstos, el algodón se ha cultivado en forma continuada durante cuatro campañas. Los resultados sobre el rendimiento promedio de estas cuatro campañas se exponen en el Cuadro I.

Las otras plantas fueron cultivadas una sola vez; la papa rindió 32 t/ha en 1981, el maíz forrajero 50 t/ha en 1978, el promedio del valle fue de 35 t/ha, y

la cebada alrededor de 4 t/ha en una extensión de 22 ha. El tratamiento (11 ha)
superó en un 20% al testigo.

Los rendimientos del cultivo del algodón demuestran claramente que la
rehabilitación ha sido positiva, ya que se encuentran muy por encima del promedio
del valle (65 qq/ha o 2990 kg/ha), e igual o superior al rendimiento de un suelo sin
problemas de sales (75 a 80 qq/ha o 3450 a 3680 kg/ha). Experimentalmente,
en parcelas de 10 × 4,8 m se han obtenido rendimientos de alrededor de 120 qq
o 5520 kg/ha.

La bondad de esta metodología de tonificar la semilla, especialmente para
suelos afectados por sales, fue probada en una condición muy adversa, en la
localidad de Chilca, en alrededor de 3 ha de la Villa Hozanan, organizada y
administrada por la Sociedad San Vicente de Paul. Esta villa alberga niños en
abandono moral y material.

El suelo de Chilca fue un franco arenoso, con pH 7,6 y una salinidad
fluctuante entre 15 a más de 60 mmho/cm, pobre en fósforo (2 ppm) y en yeso
(0,15%). El agua es no recomendable para la agricultura (de 10 a 12 mmho/cm).
El algodón nunca llega a producir más de 20 qq/ha. Gracias a la colaboración de
algunas familias alemanas, se logró la financiación para este cultivo en los suelos
de la Villa, alcanzándose un rendimiento de alrededor de 40 qq/ha o 1840 kg/ha.
Esto quiere decir que muy pronto se podría contar con una metodología que
permita lograr una productividad eficiente en suelos afectados por sales, convivir
con las sales, y utilizar aguas de drenaje de 2 a 5 mmho/cm, especialmente en
suelos arenosos desérticos (costa del Perú y de otros países con zonas áridas).
Posiblemente pueda ayudar a cultivar suelos desérticos sin necesidad de ir a la
formación previa de suelo, etapa que puede llevar más de dos años.

3. CONCLUSIONES

En conclusión se puede decir que:

1) El método de rehabilitación combinada, lavado superficial y en profundidad
    a través de surcos fue muy eficiente. En menos de 4 años hubo una respuesta
    positiva.
2) La tonificación de la semilla con los elementos críticos de cada cultivo y para
    cada suelo en particular se presenta como una técnica suplementaria muy
    importante.
3) La aplicación de materia orgánica en mezcla con el yeso permitió una
    evacuación racional de sales solubles, dando lugar a una rápida rehabilitación.
4) Se hace necesario profundizar la investigación de esta metodología mediante
    el uso de radisótopos, especialmente para el Na, P y Zn. Esto permitirá
    aceptar o rechazar los criterios propuestos.

BIBLIOGRAFIA

ESTRADA, J.A., "La tecnología edáfica en el agro peruano: Situación actual y perspectivas",
Situación Actual y Perspectivas del Problema Agrario en el Perú, Edit. Eguren F., (1982) 535.
ESTRADA, J.A., Avances de la Investigación: Suelos y Fertilización, Segunda Jornada Técnica
del Algodonero del Sur Medio, Colegio de Ingenieros del Perú, Ica (1982).
KHAN, A.A., The Physiology and Biochemistry of Seed Dormancy and Germination, North
Holland Publishing Company (1977).
LINDSAY, W.L., Chemical Equilibria in Soils, A. Wiley-Interscience Publication, John Wiley & Sons
(1979) 449.
PIZARRO, F., Drenaje Agrícola y Recuperación de Suelos Salinos, Editorial Agrícola Española,
S.A., Madrid (1978) 521.

Invited Paper

EFFECT OF SUBSURFACE DRAINAGE ON SALT MOVEMENT AND DISTRIBUTION IN SALT-AFFECTED SOILS*

A.T.A. MOUSTAFA, M.H. SELIEM, H.K. BAKHATI
Soils and Water Research Institute,
Agricultural Research Center,
Ministry of Agriculture,
Giza, Egypt

Abstract

EFFECT OF SUBSURFACE DRAINAGE ON SALT MOVEMENT AND DISTRIBUTION
IN SALT-AFFECTED SOILS.
    This study was carried out to evaluate different subsurface drainage treatments (com-
binations of depth and spacing) on salt movement and distribution. The soil is clay and the
drainage was designed according to the steady-state condition (Hooghoudt's equation).
Three spacings and two depths resulted in six drainage treatments. Soil samples represented
the initial state of every treatment and after 14 months they (cotton followed by wheat)
were analysed. The data show that drain depth has its effective role in salt leaching, while
drain spacing has its effect on salt distribution in the soil profile. The leaching rate of each
specific ion is also affected by the different drainage treatments. In general, the salt movement
and distribution should be taken into consideration when evaluating the design of drainage
systems.

INTRODUCTION

    In arid and semi-arid regions cultivated lands under perennial irrigation
tend to deteriorate, especially in the absence of adequate drainage. Drainage
systems are engineering structures that remove water according to the principles
of soil physics and hydraulics.
    Subsurface drainage (tile drainage) is defined as the removal of excess
groundwater below the ground surface [1].
    It is well established that a rise of the groundwater table is considered to
be one of the major causes of salinity. El-Leboudi et al. [2] and Anter et al. [3]

265

have discussed the effect of drainage on salt accumulation and leaching in the soils of Egypt.

In general, Bouwer [4] stated that perhaps the most effective way to evaluate drainage criteria for a given climatic region would be to observe systems of different drainage intensities, farm as well as experimental systems.

This work aims to study the effect of different subsurface drainage treatments (combinations of depth and spacing) on salt movement and distribution in salt-affected soils to help in evaluating these treatments.

MATERIALS AND METHODS

This study is part of a research project entitled Criteria for Design of Field Drainage Systems. The design and performance of the experimental layout [5], based on Hooghoudt's formula [6] ,resulting in six treatment as combinations of three spacings and two depths of the subsurface lateral drains. The spacings were 25 m (calculated), 12.5 m (half the calculated), and 50 m (double the calculated), while the depths were the normal one which started at 120 cm, and the shallow depth which started at 90 cm. Each subsurface lateral drain was 300 m long with an inclination of 10 cm/100 m. The test subsurface lateral drain for each treatment was between two other guard drains.

Soil samples from twelve soil profiles were taken to represent the six treatments. The two profiles of each treatment were one on both sides of the lateral test drain at midpoint spacing, and at a half-way point along the length. The soil samples were taken at arbitrary successive depths of 0—15, 15—30, 30—60, 60—90, 90—120 and 120—150 cm, then air dried, crushed and sieved through a 2 mm sieve. This sampling process was carried out at first immediately after installation of the tiles and before cotton planting in March 1977, and repeated again after 14 months (cotton followed by wheat) in June 1978 after wheat harvesting. All drainage treatments underwent identical agricultural preparations including irrigation water.

All soil samples were analysed for total soluble salts as well as soluble cations and anions in 1:5 soil:water extract [7]. Sulphate was calculated by the difference between the sum of cations and anions. The averages of the data of the two profiles representing each treatment are given in Figs 1—6.

RESULTS AND DISCUSSION

The soil of the experimental site is clay soil (about 50% clay) containing 3.5% $CaCO_3$ on an average. The soil is saline [7], but its salinity differs from place to place since the area was not under correct agricultural development and
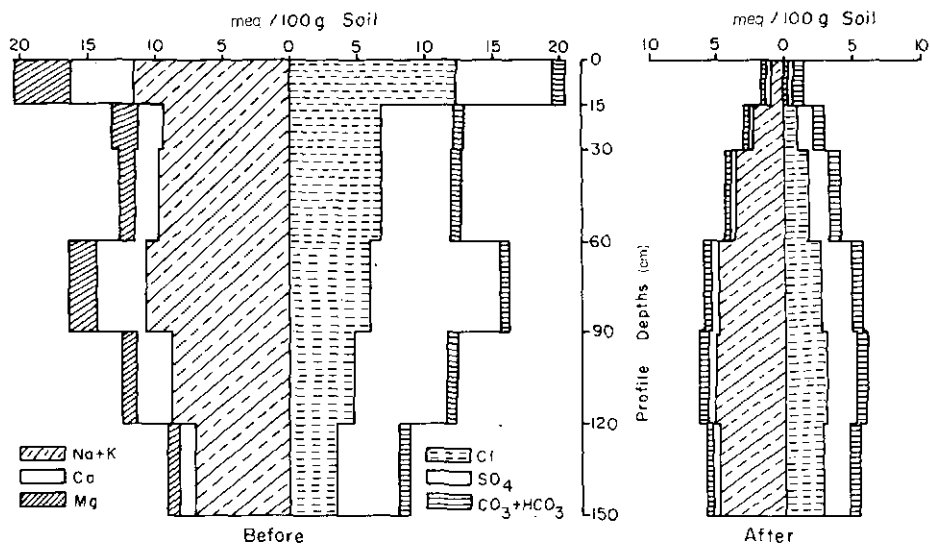
FIG.1.   Composition and distribution of soluble salts in the soil profile before and after
field drainage: at 120 cm depth and 12.5 m spacing.
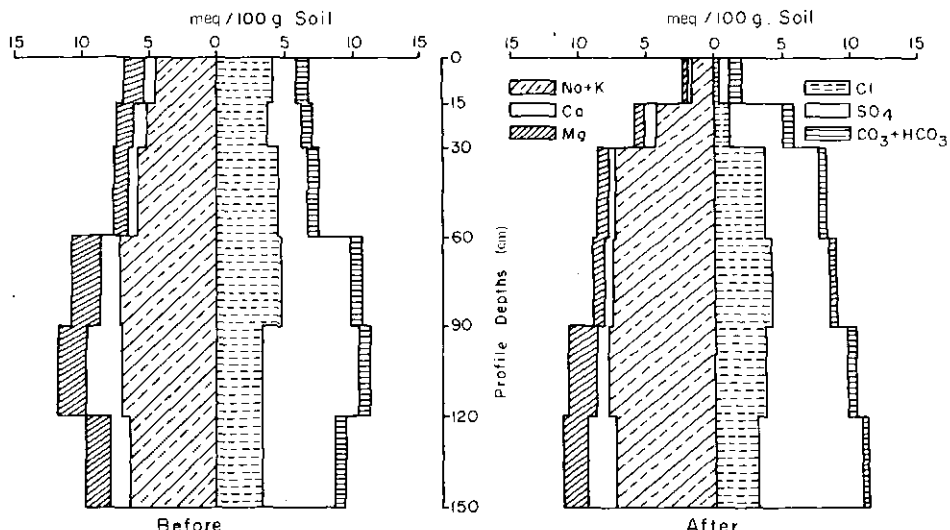
FIG.2.   Composition and distribution of soluble salts in the soil profile before and after field
drainage: at 120 cm depth and 25 m spacing.
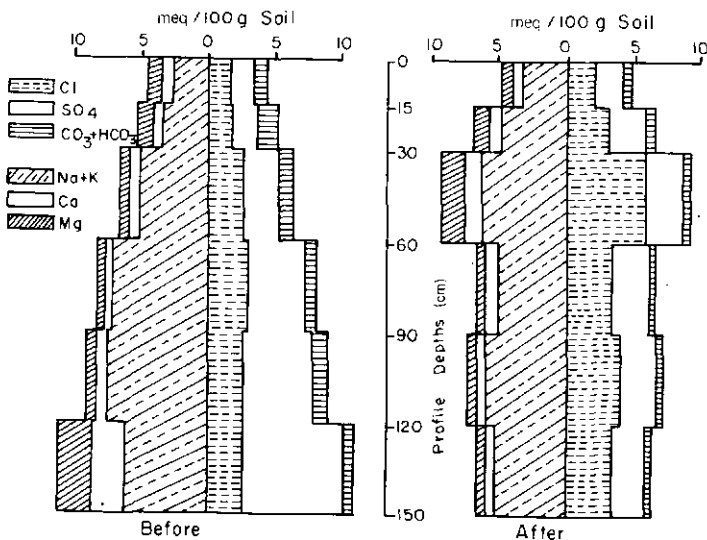
FIG.3.   Composition and distribution of soluble salts in the soil profile before and after field drainage: at 120 cm depth and 50 m spacing.
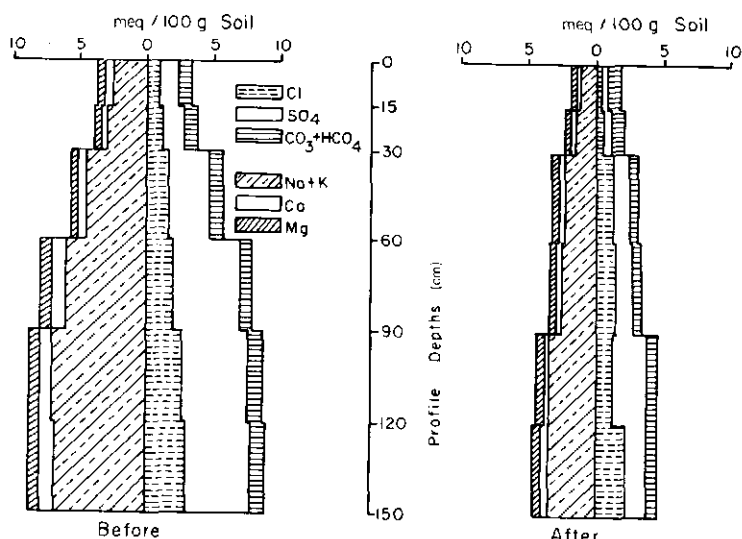

FIG.4.   Composition and distribution of soluble salts in the soil profiles before and after field drainage: at 150 cm depth and 12.5 m spacing.
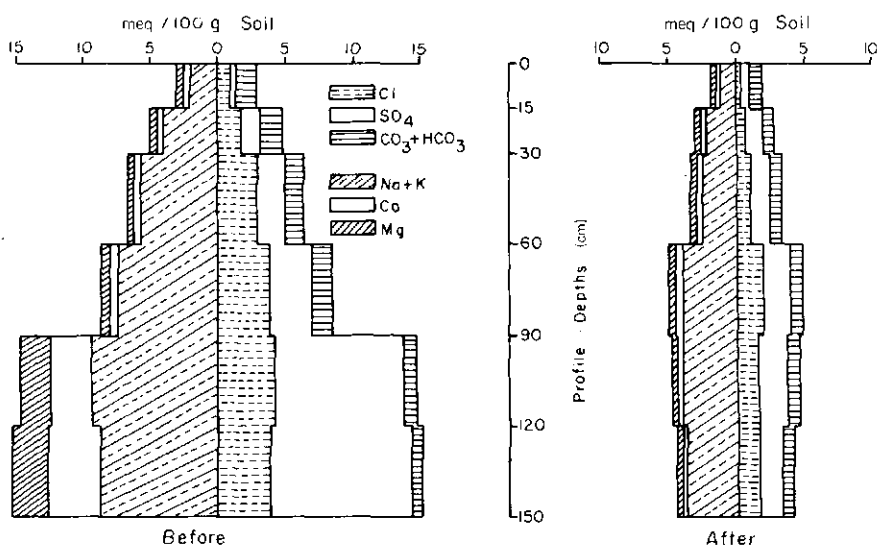
FIG.5.   Composition and distribution of soluble salts in the soil profile before and after field drainage: at 150 cm depth and 25 m spacing.

weeds and grasses of saline soils dominated the grown crop plants. The ground-water salinity was about 10 000 ppm.

Figures 1—6 (indicating "before" and "after" field drainage) show, in the "before" part, the salinity status (initial salinity) for each drainage treatment just after the subsurface lateral drains were installed and before cotton planting in March 1977. The general observation from these figures is that salt content increases by depth except in the case of Fig.1 where there is an accumulation of salts in the soil surface. Also, there is a salt accumulation at the 60—120 cm depth in Figs 1 and 2. Considering that the average soluble K^+ is about 0.05 meq/100 g soil, it could be stated that soluble Na^+ is the dominant soluble cation, amounting to more than 70% of the soluble cations. Soluble Ca^{2+} and soluble Mg^{2+} are almost at a ratio of 1:1. On the other hand, soluble CO_3^{2-} is almost nil with some traces in some soil samples, and soluble HCO_3^- is generally constant in amount through each soil profile with a tendency in some cases to increase in the surface layers. Soluble SO_4^{2-} and soluble Cl^- are the dominant soluble anions with a general trend for soluble SO_4^{2-} to increase with depth to become the dominant soluble anion in most cases.

The "after" parts of Figs 1—6 show the salinity status 14 months after installation where two crops, i.e. cotton followed by wheat, were planted in
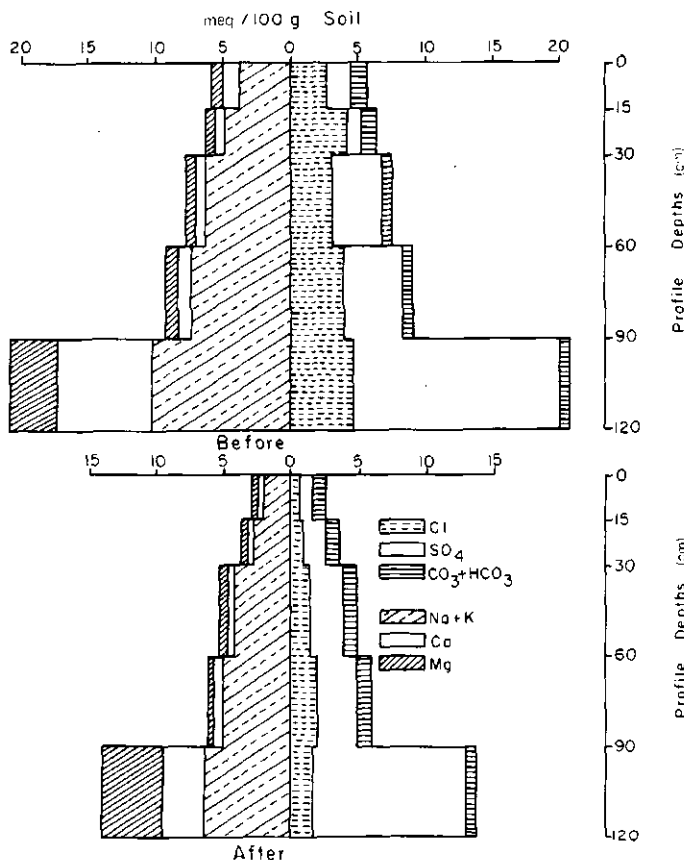
FIG.6.   Composition and distribution of soluble salts in the soil profile before and after field drainage: at 150 cm depth and 50 m spacing.

this period. The effects of the drainage treatments on salt content and distribution, as observed from these figures, are as follows:

(1)   The depth of subsurface lateral drains has an effective role in leaching salts out of the soil profile where the normal depth resulted in a higher leaching of salts than the shallow depth. As an example, the mean averages of the profiles for the initial soil salinity of the 25 m spacing were 9.29 and 9.80 meq/100 g soil for shallow and normal depths, respectively. After wheat harvesting it became 8.74 and 3.91 meq/100 g soil in the same order. In other words the salts leached out were 5.92 and 60.10% for shallow and normal depths, respectively. This could be because the deeper the drain depth the higher the discharge rates and amounts [8], and consequently the leaching of salts.

TABLE I. REMOVAL PERCENTAGES[a] OF SOLUBLE ANIONS AND
SOLUBLE CATIONS FROM THE DIFFERENT LAYERS OF THE SOIL
PROFILE[b] (120–150 cm depth treatment)

Spacing treatment (m)	Depth (cm)	Soluble anions (%)			Soluble cations (%)		
		HCO_3^-	Cl^-	SO_4^{2-}	Ca^{2+}	Mg^{2+}	$Na^+ + K^+$
12.5	0–15	6.32	61.47	69.23	61.67	32.61	50.79
	15–30	8.70	53.39	50.31	9.09	12.50	49.83
	30–60	21.43	17.50	60.58	23.08	2.17	48.37
	60–90	19.28	32.21	75.74	50.93	61.18	59.27
	90–120	37.25	52.61	50.60	60.36	32.93	50.00
	120–150	23.53	26.35	67.51	55.00	30.99	49.12
25	0–15	39.22	63.27	+15.38	33.33	40.43	38.35
	15–30	48.78	55.56	+2.96	+14.29	33.33	43.43
	30–60	38.28	61.92	32.56	+15.56	25.00	54.08
	60–90	42.66	52.48	33.66	27.54	32.00	46.72
	90–120	16.33	58.94	77.70	89.14	83.12	57.91
	120–150	+11.69	56.68	83.88	91.88	86.09	58.90
50	0–15	7.26	74.10	53.85	61.86	64.84	48.45
	15–30	6.09	78.72	+74.00	44.19	47.44	41.19
	30–60	+22.73	51.89	33.97	37.33	40.00	34.18
	60–90	+22.35	51.64	33.49	36.46	68.82	31.97
	90–120	8.54	64.15	25.79	55.87	+17.55	37.49
	120–150	+88.57	57.31	76.02	92.68	90.93	43.09

[a] From initial amounts.

[b] Average of two profiles for each treatment.

   (2)   The spacing affects both the leaching of the salts and their distribution
where it is found that even surface layers were leached to be non-saline, but
there is a new pattern of salt distribution, which is that the depth of the layer
where the relatively higher salt accumulation is to be found is at 90 cm, 60 cm
and 30 cm, respectively, for 12.5 m, 25 m and 50 m spacings.

   At the same time, this is accompanied by the salts being leached out of
the soil profile for the three spacings of normal depth, and 12.5 m spacing of
the shallow depth. In the other two spacings, i.e. 25 m and 50 m of the shallow

TABLE II.   REMOVAL PERCENTAGES[a] OF SOLUBLE ANIONS AND
SOLUBLE CATIONS FROM THE DIFFERENT LAYERS OF THE SOIL
PROFILE[b] (90–120 cm depth treatment)

Spacing treatment (m)	Depth (cm)	Soluble anions (%)			Soluble cations (%)		
		HCO_3^-	Cl^-	SO_4^{2-}	Ca^{2+}	Mg^{2+}	$Na^+ + K^+$
12.5	0–15	5.49	98.29	91.96	92.84	94.63	90.59
	15–30	+22.86	86.84	78.37	85.34	81.25	75.11
	30–60	+11.59	73.46	66.05	77.05	69.42	62.53
	60–90	+10.45	53.69	75.57	83.56	81.86	53.96
	90–120	1.37	37.53	66.57	79.64	54.37	42.57
	120–150	6.49	18.82	54.86	58.04	53.57	30.76
25	0–15	+24.71	89.63	62.30	56.67	85.92	64.06
	15–30	5.13	69.27	+51.15	13.68	43.10	20.08
	30–60	+12.70	15.87	+82.19	29.76	3.66	+24.83
	60–90	17.33	11.83	24.11	54.09	60.54	+3.10
	90–120	15.87	+6.80	13.51	58.85	2.51	+10.33
	120–150	28.57	4.64	+43.25	+49.67	+19.08	+14.74
50	0–15	31.68	+9.60	+16.67	9.09	25.96	+18.38
	15–30	50.34	+72.13	+40.69	+23.38	15.04	+40.94
	30–60	53.27	+117.71	1.42	+114.29	+101.23	+20.39
	60–90	51.22	+9.51	34.70	+76.79	+11.76	29.71
	90–120	43.62	+49.26	48.86	5.63	16.67	19.89
	120–150	14.49	+25.27	66.40	73.68	76.64	12.87

[a]   From initial amounts.

[b]   Average of two profiles for each treatment.

depth, it was confirmed that there is only a redistribution of the initial salinity.
This shows how the interaction between depth and spacing affects salt leaching
and distribution.

These effects could be explained by the fact that the narrower the spacing
the higher the discharge rates and amounts of drainage water [8].

When dealing with soluble cations and anions it has been found that there
is no effect on the soluble cation ratios between each other where Na^+ is still the
dominant soluble cation, and soluble Ca^{2+}:soluble Mg^{2+} has a ratio 1:1 — this

despite the fact that the removal percentages of the soluble cations from the different layers under the different treatments (Tables I and II) are not the same. On the other hand, it has been observed that leaching of soluble SO_4^{2-} (removal percentage — Tables I and II) is higher under those treatments where there is a higher salt leaching (mainly 12.5 m spacing at both depths). This is because SO_4^{2-} is less than Cl^- in leaching [9]. Consequently, SO_4^{2-} will not be removed from the soil profile by higher percentages except when, under these conditions, the leaching process is encouraged. Its removal percentages (leaching) under these conditions could easily exceed those of Cl^- (Tables I and II, 12.5 m spacing treatments) and then SO_4^{2-} will not be a dominant soluble cation. At the same time soluble CO_3^{2-} and HCO_3^- have still the same size, to be almost constant along the depth of the soil profile.

In general it could be concluded that salt leaching and salt distribution, either as total salt content or as soluble cations and soluble anions, are greatly affected by the different combinations of depth and spacing of subsurface lateral drains. An accurate evaluation should take this point into consideration when designing drainage systems.

REFERENCES

[1]   UNITED STATES DEPARTMENT OF AGRICULTURE, Soil Conservation Service, "Drainage of Agricultural Land", Water Information Center, Inc., Huntington, NY (1973).

[2]   EL-LEBOUDI, A., SHAABAN, K., EL-DAMATY, A.H., IBRAHIM, M.M., Desalinisation of soils of Menoufeya Governorate put under tile drainage, Egypt J. Soil Sci. 14 (2) (2) (1974) 167–76.

[3]   ANTER, F., OMAR, M., EL-HADY, O., The influence of water table levels on some chemical properties and plant growth, Egypt J. Soil Sci. 17 (2) (1977) 169–82.

[4]   BOUWER, H., "Developing drainage design criteria", Drainage For Agriculture (VAN SCHILFGAARDE, J., Ed.), No.17 Series Agronomy Am. Soc. Agron. Inc., Madison, Wisconsin, USA (1974) 67–79.

[5]   MOUSTAFA, A.T.A., BAKHATI, H.K., et al., Criteria for design of field drainage systems: Depth and spacing requirements of subsurface drains, for proper soil drainage. 1. Design and performance, Agric. Res. Rev. Min. Agric. ARE 58 (4) (1980) 59–68.

[6]   VAN BEERS, W.F.J., Some Nomographs for the Calculation of Drain Spacings, Int. Inst. for Land Reclamation and Improvement, Wageningen, Netherlands, Bull. 8 (1965).

[7]   United States Salinity Laboratory Staff, Diagnosis and Improvement of Saline and Alkali Soils, US Dept. Agric. Handbook No.60 (1954).

[8]   MOUSTAFA, A.T.A., BAKHATI, H.K., ABASSERI, M.A., HERMSMEIER, L.F., Criteria for design of field drainage systems: Depth and spacing requirements of subsurface drains, for proper soil drainage. 2. Effect of depth and spacing on discharge of tiles and fluctuation of water-table level, at Mahallet-Mousa farm, Agric. Res. Rev. Min. Agric. ARE 58 (4) (1980) 69–80.

[9]   HABIB, I.M., Removal of salts from saline soils with reference to salt solubility, diffusion and micromorphological studies, Ph.D. Thesis, Faculty of Agric. Cairo University, Egypt (1962).

FERTILIZER NITROGEN LEACHING IN RELATION TO WATER REGIME AND THE FERTILIZER PLACEMENT METHOD*

A.T.A. MOUSTAFA, M.S. KHADR
Soils and Water Research Institute,
Agricultural Research Center,
Ministry of Agriculture,
Giza, Egypt

Abstract

FERTILIZER NITROGEN LEACHING IN RELATION TO WATER REGIME AND THE
FERTILIZER PLACEMENT METHOD.
    A field experiment was conducted at the farm of Sids Experimental Station, Ministry
of Agriculture, Middle Egypt, to evaluate the effect of the water regime and fertilizer placement
method on the leaching of urea fertilizer under field conditions. Ordinary and heavy irrigations
were the water regimes, while side-banding and surface broadcasting were the fertilizer place-
ment methods. Wheat (Giza 158, local variety) was planted, and urea labelled with ^{15}N at
the rate of 100 kg N/ha was added at planting. The data obtained showed that in general the leaching
process of urea fertilizer, as evaluated from the amounts of fertilizer nitrogen residues, is
not uniform even within replicates. This is despite the fact that the average total amount of
fertilizer nitrogen residues in the soil profile to a depth of 125 cm is almost the same in the
different treatments. Data also show that the bulk of fertilizer nitrogen residues is accumulated
in the surface soil layers, especially at 0–25 cm. Only 10% of the fertilizer nitrogen is
detected below 75 cm and up to 125 cm depth of the soil profile. It could be concluded that
urea leaching (amount and depth) under these conditions is affected mainly by the soil
characteristics, namely soil pores. This is in addition to some other factors that cause variable
concentrations in the soil solution leaving the root zone.

INTRODUCTION

    Fertilizer nitrogen levels, timing, placement and types interact with
irrigation and crop management in affecting fertilizer nitrogen leaching and
the distribution of its residues through the soil profile. Good management of
these items will help in pollution control, especially with intensive nitrogenous
fertilizer application.
    Bauder and Schneider [1] found that N leaching occurred following each
urea application. Their results indicate marked NO_3-N movement from urea

---

under excessive irrigation. Oza and Subbiah [2] mentioned that the bulk of
the residual fertilizer nitrogen remained in a 0—20 cm layer.

The objective of this study is to evaluate the effect of water regime
(irrigation) and fertilizer placement methods on the leaching of urea fertilizer
under field conditions.

MATERIALS AND METHODS

A field experiment was conducted at the farm of Sids Experiment Station,
Middle Egypt. The treatments were a combination of the following:

(a)   Two methods of fertilizer nitrogen placement, namely side-banding
(Ba) in which bands were 5 cm apart to the side of the wheat row and
5 cm below seed level; and surface broadcasting (Br).

(b)   Two water regimes, namely ordinary irrigation (M1) and heavy
irrigation (M2).

This resulted in four treatments — M1Ba, M1Br, M2Ba and M2Br.

The design was a split plot of eight randomized whole plots corresponding
to four replications of the two water regimes. The whole plots were divided
into two sub-plots (3 X 3.5 m each) for the two fertilizer placement methods.
In each sub-plot there was an area of 0.75 X 2 m for the ^{15}N-labelled fertilizer.

Wheat (Giza 158, local variety) was planted on 28 November 1976 and
harvested on 17 May, 1977. Phosphorus at the rate of 36 kg P_2O_5/ha as super-
phosphate, and nitrogen at the rate of 100 kg N/ha in the form of urea, were
added at planting. The areas of ^{15}N-labelled fertilizer received ^{15}N-labelled
urea while the rest of the sub-plot received regular urea. The urea was added
as either side-banded (Ba) or surface broadcast (Br), depending on the treatment.
Common agronomic practices were applied to the experiment.

Soil samples from the ^{15}N-labelled areas in each replicate to the depth of
125 cm were taken depth-wise at 25 cm intervals after wheat harvest with a
tube auger 2.5 cm in diameter. These soil samples represent depths of 0—25,
25—50, 50—75, 75—100 and 100—125 cm. The soil samples were analysed for
total nitrogen using the modified Kjeldahl method [3]. Samples were sent
to the IAEA Laboratory, Seibersdorf, for ^{15}N determinations. Soil bulk density,
using a core sampler [4], was determined for each depth. Its average values
were used for the whole experiment.

TABLE I. SOME PHYSICAL AND
CHEMICAL CHARACTERISTICS
OF SOIL

Clay content	38%
pH	8.3
CaCO$_3$	4%
Total soluble salts	0.15%

RESULTS AND DISCUSSION

The data in Table I indicate that the soil is clay loam, non-saline and
non-alkali. The soil profile is almost homogeneous with an increase in soil bulk
density with depth (Table II).

The data of the total nitrogen in ppm (Table II) show great variability,
despite the fact that the average total nitrogen as t/ha to the depth of 125 cm
is almost identical in the four treatments. The general trend is that the highest
amount of total nitrogen (t/ha) is in the surface layer (0—25 cm) followed by
the 25—50 cm layer, while the lowest amount is in the deeper layers of the
soil profile (below 75 cm depth). The 50—75 cm layer is in between with an
almost constant value of 1.78 t N/ha. The differences between the soil layers
could be explained on the basis that the upper layers of the soil profile (0—50 cm)
are those affected by fertilization and root growth.

Table III gives the per cent ^{15}N excess and the per cent N derived from
fertilizer (%Ndff), while Table IV gives the fertilizer nitrogen residues (kg/ha)
which are based on the data of Tables II and III.

When taking the amounts of fertilizer nitrogen residues (kg/ha — Table IV)
as an indication of the leaching of the fertilizer nitrogen through the soil
profile, it seems that there is great variability in the leaching process. This
variability is either in amounts or depths. Calculating the average amounts of
fertilizer nitrogen residues (kg/ha) for the four treatments shows that there is
only a little variation between these average amounts, where they are 42.94,
40.25, 40.85 and 48.67 kg/ha to the depth of 125 cm, for M1Ba, M1Br,
M2Ba, and M2Br, respectively. Moustafa et al. [5] showed that no significant
differences exist between the same treatments concerning fertilizer nitrogen
uptake or fertilizer use efficiency. This means that the total amount of
fertilizer nitrogen residues under these conditions are not affected by the
experimental treatments.

TABLE II. TOTAL NITROGEN (ppm) AND TOTAL NITROGEN (t/ha)
AFTER WHEAT HARVESTING

Treatment	Depth (cm)	Bulk density (g/cm^3)	Total nitrogen (ppm) Replicates				Total nitrogen[a] (t/ha)
			1	2	3	4	
M1Ba	0–25	1.16	665	788	595	784	2.05
	25–50	1.20	665	468	438	595	1.67
	50–75	1.30	578	595	385	630	1.78
	75–100	1.35	560	420	333	490	1.52
	100–125	1.40	508	455	350	455	1.55
M1Br	0–25	1.16	910	945	508	665	2.20
	25–50	1.20	648	700	665	560	1.93
	50–75	1.30	613	525	490	560	1.78
	75–100	1.35	490	473	420	543	1.63
	100–125	1.40	455	455	420	455	1.56
M2Ba	0–25	1.16	718	875	590	840	2.19
	25–50	1.20	718	665	630	560	1.93
	50–75	1.30	770	560	490	350	1.77
	75–100	1.35	438	490	455	350	1.46
	100–125	1.40	420	490	438	385	1.52
M2Br	0–25	1.16	490	963	893	1138	2.05
	25–50	1.20	525	665	665	665	1.67
	50–75	1.30	490	525	490	543	1.78
	75–100	1.35	600	263	455	578	1.52
	100–125	1.40	473	490	438	455	1.55

M1 = Ordinary irrigation   M2 = Heavy irrigation
Ba = Side-banding   Br = Surface broadcasting

[a]   Each figure represents the average value of the four replicates.

TABLE III. THE PER CENT ^{15}N EXCESS AND THE PER CENT NITROGEN
DERIVED FROM FERTILIZER (% Ndff) AS AFFECTED BY IRRIGATION
AND FERTILIZER PLACEMENT TREATMENTS

Treatment	Depth (cm)	% ^{15}N excess Replicates				% Ndff Replicates			
		1	2	3	4	1	2	3	4
M1Ba	0−25	0.06	0.03	0.05	0.03	2.00	1.00	1.67	1.00
	25−50	0.01	0.01	0.01	0.01	0.33	0.33	0.33	0.33
	50−75	0.01	−	0.01	0.01	0.33	−	0.33	0.33
	75−100	−	0.01	0.01	−	−	0.33	0.33	−
	100−125	0.01	−	0.01	−	0.33	−	0.33	−
M1Br	0−25	0.01	−	0.02	0.04	0.33	−	0.67	1.33
	25−50	−	0.01	0.02	0.01	−	0.33	0.67	0.33
	50−75	−	−	0.01	0.01	−	−	0.33	0.33
	75−100	−	0.02	0.01	−	−	0.67	0.33	−
	100−125	−	−	0.01	0.01	−	−	0.33	0.33
M2Ba	0−25	[a]	0.04	0.03	0.04	−	1.33	1.00	1.33
	25−50	0.02	0.02	0.02	0.02	0.67	0.67	0.67	0.67
	50−75	0.02	−	−	0.03	0.67	−	−	1.00
	75−100	0.01	−	−	0.01	0.33	−	−	0.33
	100−125	0.01	−	−	−	0.33	−	−	−
M2Br	0−25	0.05	0.05	0.01	0.03	1.67	1.67	0.33	1.00
	25−50	0.01	0.01	0.01	0.02	0.33	0.33	0.33	0.67
	50−75	−	−	−	0.01	−	−	−	0.33
	75−100	−	−	−	0.01	−	−	−	0.33
	100−125	−	−	−	0.01	−	−	−	0.33

M1 = Ordinary irrigation   M2 = Heavy irrigation
Ba = Side-banding   Br = Surface broadcasting

[a]   The sample contained little nitrogen.

TABLE IV. FERTILIZER NITROGEN RESIDUE (kg/ha) DISTRIBUTION
IN THE SOIL PROFILE (125 cm depth) AS AFFECTED BY IRRIGATION
AND FERTILIZER PLACEMENT TREATMENTS

Treatment	Depth (cm)	Fertilizer nitrogen residues (kg/ha) Replicates			
		1	2	3	4
M1Ba	0–25	38.57	22.85	28.82	22.74
	25–50	6.58	6.58	4.34	5.89
	50–75	6.20	–	4.13	6.76
	75–100	–	4.68	3.71	–
	100–125	5.87	–	4.04	–
M1Br	0–25	8.71[a]	–[a]	9.87	25.65
	25–50	–	6.93	13.37	5.54
	50–75	–	–	5.26	6.01
	75–100	–	10.70	4.68	–
	100–125	–	–	4.85	5.26
M2Ba	0–25	–	33.75	17.11	32.40
	25–50	14.43	13.37	12.66	11.26
	50–75	16.77	–	–	11.38
	75–100	4.88	–	–	3.90
	100–125	4.85	–	–	–
M2Br	0–25	23.73	46.60	8.55[a]	33.00
	25–50	5.20	6.58	6.58	13.37
	50–75	–	–	–	5.82
	75–100	–	–	–	6.44
	100–125	–	–	–	5.26

M1 = Ordinary irrigation   M2 = Heavy irrigation
Ba = Side-banding   Br = Surface broadcasting

[a] Replicate excluded from average fertilizer nitrogen residue calculation.

Based on the findings of Stewart [6], who stated that the amounts of water moving through the soil profile determine the rate and extent of fertilizer movement, and from the patterns of fertilizer nitrogen residue distribution (Table IV) it could be concluded that soil pores, which vary in shape, width and direction, are responsible for these distribution patterns. Hillel [7] mentioned that the liquid flow depends on the geometric properties of the pore channels through which flow takes place. Taking into consideration the relatively small diameter of the sampling auger (2.5 cm), it could be accepted that fertilizer nitrogen residues are not found in some soil profile layers in some cases, and that these residues are distributed through the whole soil profile in other cases.

Many other factors affect fertilizer nitrogen leaching. Walter et al. [8] indicated that immobilization, ammonification and nitrification all interacted significantly to affect N leaching. Tables III and IV show that there is a relation between total nitrogen (t/ha) distribution and fertilizer nitrogen residue (kg/ha) distribution. Both follow the same pattern where it could be stated that total nitrogen in soil to some extent affects the leaching of the fertilizer nitrogen.

REFERENCES

[1] BAUDER, J.W., SCHNEIDER, R.P., Nitrate-nitrogen leaching following urea fertilization and irrigation, Soil Sci. Soc. Am. J. 43 (1979) 348–52.

[2] OZA, A.M., SUBBIAH, B.V., "A study on the residual fertilizer nitrogen in the soil under multiple cropping conditions using ^{15}N", Use of Isotopes and Radiation in Agriculture Biology and Animal Sci., Chandigarh, 1–2 Jan. 1973 (1973) 55–56.

[3] JACKSON, M.L., Soil Chemical Analysis, Prentice-Hall of India Ltd., New Delhi (1973).

[4] UNITED STATES SALINITY LAB. STAFF, Diagnosis and Improvement of Saline and Alkali Soils, US Dept. Agric. Handbook No.60 (1954).

[5] MOUSTAFA, A.T.A., HAMISSA, M.R., KHADR, M.S., Effect of method of nitrogen fertilizer placement and water regime on wheat yield and fertilizer use efficiency, Agric. Res. Rev., Min. Agric., Agric. Res. Estab. 57 (5) (1979) 227–32.

[6] STEWART, B.A., "A look at agricultural practices in relation to nitrate accumulations", Nutrient Mobility in Soils: Accumulations and Losses (ENGELSTAD, O.P., Ed.), Soil Sci. Soc. Am. Sp. Pub. No.4, Madison (1970) 47–60.

[7] HILLEL, D., Introduction to Soil Physics, Academic Press, New York, London (1982).

[8] WALTER, M.F., BUBENZED, G.D., CONVERSE, J.C., Predicting vertical movement of manurial nitrogen in soil, Trans. Am. Soc. Agric. Engrs. 18 (1975) 100–105.

SOIL WATER

(Session 5)

Chairman

Ph. COUCHAT
France

ECONOMIE D'EAU EN IRRIGATION DE CULTURES FAMILIALES DANS LES ZONES ARIDES

A. MHIRI, M.J. ELLOUMI, M. LAOUINI
Institut national agronomique de Tunisie,
Tunis, Tunisie

Abstract–Résumé

WATER ECONOMY IN THE IRRIGATION OF FAMILY FARMLAND IN ARID ZONES.
   A simple irrigation technique based on the use of polyethylene bags was developed and tested so as to achieve maximum water economy in family-scale farming in arid zones. It simulates localized irrigation and eliminates water losses due to evaporation and drainage. The method was tried out in the cultivation of tomatoes in glasshouses. In comparison with the control experiment in the field with furrow irrigation, the saving of water was 60%, with a 30% drop in production. There was thus a net improvement in efficiency in the utilization of the irrigation water.

ECONOMIE D'EAU EN IRRIGATION DE CULTURES FAMILIALES DANS LES ZONES ARIDES.
   Une technique simple de culture irriguée en sacs de polyéthylène est conçue et expérimentée en vue de réaliser le maximum d'économie d'eau en cultures familiales dans les zones arides. Elle simule une irrigation localisée et permet d'annuler les pertes d'eau par évaporation et drainage. Essayée sur la tomate sous serre, en comparaison avec une culture témoin en place et irriguée à la raie, elle a permis d'économiser 60% d'eau avec une chute de production de 30% par rapport au témoin. Il en résulte une amélioration nette de la productivité de l'eau d'irrigation.

1. INTRODUCTION

L'économie d'eau en agriculture dans les régions arides prend de plus en plus une dimension particulière. Depuis longtemps, diverses techniques sont utilisées pour valoriser les moindres ressources en eau dans la production végétale. De nos jours, en irrigation, les techniques qui permettent d'économiser le maximum d'eau sont celles qui réduisent le plus les pertes d'eau par évaporation et percolation. Celle du goutte à goutte réalise ces conditions. Néanmoins ce mode d'irrigation étudié par Chaabouni [1, 2] présente deux inconvénients majeurs qui empêchent son adoption en cultures familiales dans les zones arides:
— selon Benzarti [3], son coût reste encore élevé pour les petits périmètres familiaux;
— il n'est réalisable qu'en présence de ressources d'eau suffisantes et continues.

Pour les situations où l'on ne dispose que de ressources en eau très limitées (petits puits, eaux pluviales de ruissellement récoltées sur des impluviums ou sur les toits des serres), la recherche d'une technique d'arrosage simulant l'irrigation localisée s'est avérée nécessaire. Cette simulation consisterait à réduire l'évaporation à une quantité négligeable, et à réduire le volume du sol irrigué.

Le but de ce travail est de concevoir et d'expérimenter une technique répondant à ces exigences.

2.   MATERIEL ET METHODE

La technique proposée consiste à arroser manuellement une culture installée sur un volume de sol réduit contenu dans un sac en plastique.

2.1. Matériel

2.1.1. Le sol

La terre utilisée est prélevée dans l'horizon de surface d'un sol alluvial peu évolué. Ses caractéristiques sont portées au tableau I.

2.1.2. La culture

L'expérimentation a porté sur la tomate (*Lycorpersicum esculentum* var. Vemone).

2.1.3. L'eau d'irrigation

Les résultats d'analyse de cette eau sont portés au tableau I.

2.2. Méthode

L'expérimentation a été conduite sous serre en culture de primeur dans la région de Tunis. Deux modes d'irrigation ont été comparés: l'irrigation localisée en sac (T1) et l'irrigation traditionnelle à la raie (T2). Chaque traitement comporte 120 plants de tomate disposés en trois lignes espacées de 1 m. Dans le traitement T1, la culture a été réalisée comme suit: dans des sacs en polyéthylène basse densité laiteux (PEBD) de 50 L, 35 kg de terre sèche enrichie en NPK ont été logés. Les sacs fermés sont couchés en ligne dans des fossés et couverts de 2 cm de terre. Sur la face supérieure des sacs, trois trous alignés sont aménagés: le trou central sert à l'arrosage, les latéraux à loger deux plants de tomate.

TABLEAU I.   ANALYSES DU SOL ET DE L'EAU D'IRRIGATION

Sol	Argile (%)	Limon (%)	Sable (%)	pH	Matière organique (%)	T$^+$
	33,3	27,7	38	8,1	1,48	23,7

Eau	Résidu sec (mg/L)	Conductivité électrique (mmho/cm)	pH	Taux d'absorption du sodium
	340	0,52	8,2	1,85

Note: T$^+$ = capacité totale d'échange des cations en meq/100 g.

La culture a démarré le 17 février 1982 et chaque traitement a reçu une fumure fractionnée totalisant, avec la dose initiale, l'équivalent de 250 kg/ha de N_2, 100 kg/ha de P_2O_5 et 180 kg/ha de K_2O. Les plants de tomate ont été taillés sur une seule tige et palissés, la fréquence d'arrosage a été en moyenne de 15 fois par mois pour T1 et 4 fois par mois pour T2.

La récolte a été arrêtée le 30 juin 1982. Au cours de l'expérience, plusieurs observations ont été faites, et en particulier, la consommation d'eau et les récoltes ont été enregistrées.

3.   RESULTATS ET DISCUSSION

Notons en premier lieu que la culture en sac (T1) a réussi sans poser de problème particulier ni au niveau du système racinaire ni à celui de la partie aérienne. Dans le sol qui passe tous les deux ou trois jours par deux états hydriques extrêmes (humidités à la capacité au champ et point de flétrissement temporaire), nous n'avons enregistré ni échauffement excessif ni manifestation d'anaérobiose. Néanmoins, la partie aérienne des plants de T1, comparée au témoin T2, a manifesté une réduction de croissance (surface des feuilles et diamètre moyen des fruits). Aussi, une légère précocité de la maturation des fruits a été notée au traitement T1 par rapport au T2. Ces résultats traduiraient l'effet d'un stress hydrique en T1. Les figures 1 et 2 rapportent respectivement les consommations d'eau et les productions de fruits cumulées des traitements. Le tableau II résume les principaux résultats obtenus.
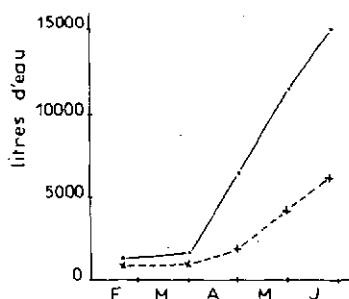
FIG.1.   *Consommation cumulée d'eau par 120 plants (— culture témoin; ----- culture en sac).*
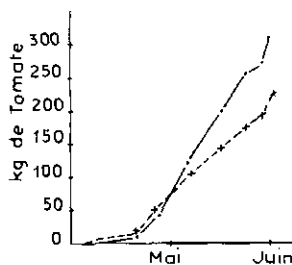

FIG.2.   *Production cumulée de tomate par 120 plants (- — culture témoin; ------ culture en sac).*

       La méthode proposée a donc permis de réaliser une réduction de la consommation d'eau de l'ordre de 59% par rapport au témoin, au prix d'une perte de production de 28%. Mais le bilan reste positif, et il se traduit par une amélioration nette de la productivité de l'eau. Exprimée en kg de tomate par m^3 d'eau, cette productivité est de 34,5 pour la culture en sac contre 20,1 pour la culture témoin. Ces résultats vont dans le sens de ceux de Hammami [4]: en comparant la productivité de différentes doses d'irrigation à la raie d'une autre variété de tomate cultivée dans le même sol en place sous serre, il trouvait une productivité de 21,1 pour la dose maximale couvrant les besoins de la culture, et 33 pour la dose couvrant 60% de ses besoins. Selon nos propres résultats, il suffirait de 154 mm d'eau pour réussir une culture de primeur de tomate sous serre par la méthode proposée, contre 375 mm par la méthode témoin. Pour les zones arides, cela représente une économie considérable d'eau et ouvrirait une perspective nouvelle pour la valorisation des faibles ressources hydriques au profit des cultures familiales. En effet, en l'absence de toute ressource classique d'eau, il serait possible de récupérer les eaux pluviales qui tombent sur des impluviums ou sur les toits des serres, et de la stocker pour arroser des cultures de primeur.

TABLEAU II. RECAPITULATION DES RESULTATS ENREGISTRES DANS
LES DEUX TRAITEMENTS

	Culture en sac (T1)	Culture in situ (T2)
Consommation d'eau (litres/plant)	51,3	124,8
Production de fruits (kg/plant)	1,8	2,5
Diamètre moyen des fruits (cm)	4,4	5,2
% de fruits de $\phi < 4$ cm	14	3
Matière sèche de la partie aérienne (g/plant)	78,5	86,3
Productivité de l'eau (kg de tomate/m^3)	34,5	20,1

4.   CONCLUSION

La culture de tomate sur un substrat de terre enrichie en NPK en sac est
possible dans les conditions de notre expérimentation. Elle permet d'économiser
environ 60% d'eau par rapport à la culture en place irriguée à la raie, et améliore
la productivité de l'eau. La technique proposée est réalisable en cultures familiales
dans les régions arides. Si on escompte une récupération de 70% des eaux pluviales
à partir des impluviums, cette technique de culture en sac serait envisageable dans
les régions à pluviosité annuelle supérieure à 220 mm/an. Dans les autres régions
plus sèches, le déficit hydrique pourrait être compensé par un accroissement de la
surface réceptrice des pluies, ou éventuellement par la dessalinisation d'eau salée
dans des bacs solaires.

REFERENCES

[1]   CHAABOUNI, Z., «Besoins hydriques des cultures et des arbres», Système d'irrigation et
économie d'eau (Actes des Journées d'études sur l'utilisation économique des eaux en
agriculture, Bougrara, Sfax, Tunisie, 1980), CRGR, Ministère de l'Agriculture, Tunis (1980).

[2]   CHAABOUNI, Z., «Economie de l'eau et systèmes d'irrigation sur olivier dans les
       conditions arides de la Tunisie» (Actes du séminaire international sur l'utilisation des eaux
       chargées en oléïculture, Tunis, 1982), CRGR, Ministère de l'Agriculture, Tunis (1982).
[3]   BENZARTI, J., L'irrigation localisée en Tunisie, Bulletin d'information de l'INRAT
       (Tunis) 14 (1982).
[4]   HAMMAMI, M., Evapotranspiration sous serre, Mémoire du cycle de spécialisation,
       Département Aménagement et Equipement, INA, Tunis (janvier 1982) 143.

EVAPOTRANSPIRATION REELLE, EXTRACTION RACINAIRE, REGIME HYDRIQUE ET PRODUCTION DE CULTURES DE LUZERNE

S. RAMBAL, A. BERGER, J.M. PARISOT
Centre d'études phytosociologiques et écologiques,
Centre national de la recherche scientifique,
Montpellier, France

Abstract–Résumé

ACTUAL EVAPOTRANSPIRATION, ROOT EXTRACTION, WATER REGIME AND
PRODUCTIVITY IN THE CASE OF LUCERNE.
Measurements were made of the actual evapotranspiration, root extraction and above-
ground yield in the case of two varieties of lucerne *Medicago sativa* L. – Du Puits and Polder –
and mixtures of them in equal parts. The daily kinetics of the water potential of the leaves
and the collar show that the water regimes of the two varieties are identical in a first approxima-
tion. The root systems are different. Polder has the deeper system. The regime of the binary
mixture is not simply a juxtaposition of the regimes of the constituents. Two types of
non-linearity were found. The first relates to water flow and the second to productivity. It is
postulated that the root systems of the two varieties constituting the mixture undergo plastic
deformation, leading to a more efficient resultant system. A system of this type needs, on the
other hand, an allocation of photosynthates that would affect its productivity.

EVAPOTRANSPIRATION REELLE, EXTRACTION RACINAIRE, REGIME HYDRIQUE
ET PRODUCTION DE CULTURES DE LUZERNE.
Nous avons mesuré l'évapotranspiration réelle, l'extraction racinaire et la production
aérienne de deux variétés de luzerne *Medicago sativa* L. Du Puits et Polder et de leur mélange
à part égale. Des cinétiques journalières de potentiel hydrique foliaire et du collet montrent
qu'en première approximation les fonctionnements hydriques des deux variétés sont identiques.
Les systèmes racinaires sont différents. Polder possède le système le plus profond. Le
fonctionnement du mélange binaire n'est pas la simple juxtaposition des fonctionnements des
constituants. Nous avons mis en évidence deux types de non-linéarité. Les premières con-
cernent les flux hydriques et les secondes, la productivité. Nous faisons l'hypothèse d'une
déformation plastique des systèmes racinaires des deux variétés constitutives du mélange,
conduisant à un système résultant plus efficace. En contrepartie, un tel système a besoin d'une
allocation de photosynthétats telle que sa productivité s'en trouve pénalisée.

MATERIELS ET METHODES

Le dispositif expérimental a été mis en place sur les terrains d'expériences
du Centre d'études phytosociologiques et écologiques du CNRS. Il comprend
trois parcelles adjacentes, de 10 X 10 m implantées en 1981, avec deux variétés

de luzerne (*Medicago sativa* L.), Polder et Du Puits, et de leur mélange à part égale. La densité de plantation est de 25 pieds par mètre carré.

Le sol argilo-limoneux dans l'horizon $0-50$ cm (30% d'argile) devient progressivement argileux en profondeur. La teneur moyenne en argile dans l'horizon $150-200$ cm est de 55%. Au centre de chaque parcelle, un tube d'accès en duralumin permet la mesure de la teneur volumique en eau jusqu'à 150 cm de profondeur. L'humidimètre à neutrons utilisé possède une source de 100 mCi d'^{241}Am-Be au centre d'un détecteur BF_3 de 18 cm de longueur active; sa droite d'étalonnage est obtenue par gravimétrie. Chaque tube d'accès est entouré d'une batterie de 6 tensiomètres aux profondeurs respectives de 15, 30, 60, 90, 120 et 150 cm. Le relevé des tensiomètres est journalier, celui des profils hydriques bi-hebdomadaire, avec un pas de mesure de 10 cm, à partir de 10 cm de la surface du sol. Pour cette première mesure, un réflecteur hémisphérique en polyéthylène est utilisé. Lors de précédentes expérimentations, ce sol a été caractérisé du point de vue hydrodynamique en quelques points de cette parcelle [1].

Ainsi, nous possédons un ensemble de couples de relations pression (h) – teneur en eau (θ) et conductivité hydraulique (K) – teneur en eau (θ). Dans le cas présent, nous affectons, à chaque point d'observation tensiométrique, une relation $K(\theta)$ telle que, à l'échelle de notre parcelle, tout les niveaux de mesure qui possèdent des relations h (θ) identiques ont, par hypothèse, la même relation $K(\theta)$.

Au niveau du régime hydrique de la végétation, les paramètres concernés par la mesure sont les suivants: le potentiel foliaire, dont la valeur maximale ou potentiel d'équilibre sol-plante est atteinte, avant le lever du soleil, lorsque la transpiration est nulle; le potentiel au niveau du collet, obtenu à la base d'une tige dont la transpiration a été bloquée 30 à 45 minutes par une enceinte obscure et humide. Toutes ces mesures sont faites à la chambre à pression [2]. Elles ne concernent que les parcelles pures car il n'a pas été possible de repérer les constituants de la parcelle mélange. Douze cinétiques journalières ont été réalisées au cours des deux cycles de culture, compris entre trois coupes successives, du 10 mai au 3 juin et du 10 juin au 12 juillet 1982. A la fin de chaque cycle, la phytomasse épigée est estimée sur un échantillon de 3 X 1 m. L'indice foliaire du couvert est calculé à partir du poids moyen d'une unité morphologique (tige + feuilles) et de sa surface foliaire. Une estimation de la phytomasse racinaire des deux cultures pures, présente dans le premier mètre, a été réalisée à partir de 5 carottages manuels.

Les précipitations journalières et les paramètres climatiques nécessaires au calcul de l'évapotranspiration potentielle (ETP) Penman sont enregistrés à proximité du dispositif expérimental.

RESULTATS

Bilan hydrique

Au début des mesures, les réserves hydriques du sol sont reconstituées par des apports différentiés aux trois parcelles, afin que dans chacune d'elles les profils de charge hydraulique soient voisins de profils gravitaires. Les deux cycles de culture sont marqués par la faiblesse des précipitations: 9 mm de pluie durant les 24 jours du premier cycle et 13 mm durant les 32 jours du second cycle. Entre ces deux cycles, du 3 au 10 juin, la hauteur de précipitation est de 11 mm.

Lors du premier intervalle de temps (tab. I), l'efficacité de Polder à consommer l'eau du sol, à des pressions de l'eau du sol voisines de zéro, est plus grande (ETR/ETP = 1), que celle des deux autres parcelles (ETR/ETP = 0,75 à 0,78). Pour ces dernières, le maximum de consommation est déphasé d'un intervalle de temps (ETR/ETP = 0,93 à 0,96). Simultanément, Polder réduit sa consommation (ETR/ETP = 0,67). Cette réduction traduit une diminution plus rapide de la charge hydraulique dans cette parcelle que dans les deux autres (fig.1). Au total, pour l'ensemble de cette période, les niveaux de réalisation de l'ETP sont assez voisins. Ils se situent à 85, 82 et 81% pour Du Puits, Polder et le mélange.

Lors du deuxième cycle, la végétation profite, dans la première période, de 10 mm de précipitation, ce qui permet de situer son évapotranspiration réelle (ETR) à un niveau assez satisfaisant (ETR/ETP = 0,73 à 0,94). En l'absence de renouvellement des réserves hydriques, nous observons ensuite une réduction importante de l'ETR dans les cultures pures; le rapport ETR/ETP se situe, du 23 au 30 juin, entre 0,51 et 0,60. Ce schéma classique de réduction de l'évapotranspiration ne s'applique que partiellement au mélange. En effet, la réduction de son évapotranspiration n'a pas l'amplitude observée pour les 2 autres parcelles. Le rapport ETR/ETP qui se situe, dans la première période, au départ à 0,82, se maintient à ce niveau la période suivante (ETR/ETP = 0,83), puis passe à 0,77, avant de chuter à un niveau moyen de 0,23 pour les deux dernières périodes. Ce niveau moyen est respectivement de 0,31 et 0,25 pour Du Puits et Polder. Pour l'ensemble du cycle, les rapports ETR/ETP sont respectivement égaux à 0,54, 0,49 et 0,59 pour Du Puits, Polder et le mélange.

Extraction racinaire

Dans le premier cycle de culture, les profils d'extraction racinaire sont assez voisins. Du 10 au 24 mai, ils donnent une bonne image de la distribution des racines en profondeur, car la résistance rhizosphérique aux transferts d'eau est négligeable aux teneurs en eau élevées (fig.2). Nous pouvons les superposer aux répartitions relatives de la biomasse racinaire (tab. II). Polder a la capacité d'extraction en profondeur la plus importante, comme l'a déjà montré la variation

TABLEAU I. BILAN HYDRIQUE DES TROIS PARCELLES PENDANT LES DEUX CYCLES DE CULTURE

PERIODE	Δt (j)	P (mm)	ETP (mm)	ETR (mm) Du Puits	Polder	Mélange
10/05 – 18/05	8	0	32	24	33	25
18/05 – 24/05	6	2,5	27	26	18	25
24/05 – 03/06	10	7,5	39	33	29	29
TOTAL	24	10,0	98	83	80	79

PERIODE	Δt (j)	P (mm)	ETP (mm)	ETR (mm) Du Puits	Polder	Mélange
10/06 – 16/06	6	10	33	31	24	27
16/06 – 23/06	7	1	36	23	21	30
23/06 – 30/06	7	1	35	18	21	27
30/06 – 07/07	7	1	36	11	9	6
07/07 – 12/07	5	0	29	9	7	9
TOTAL	32	13	169	92	82	99
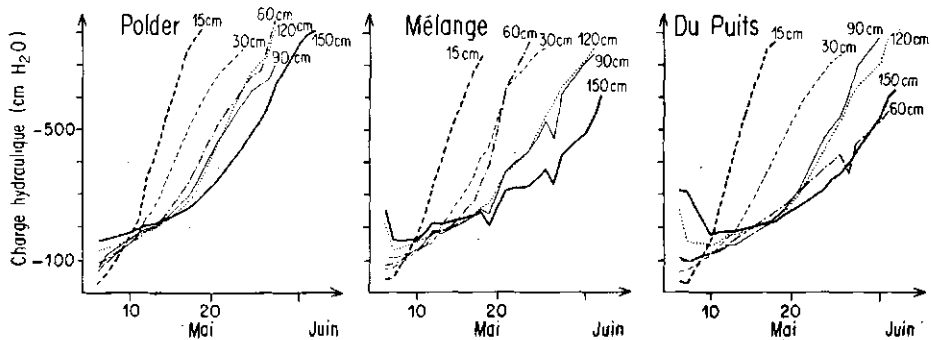
FIG. 1. Évolutions temporelles des charges hydrauliques aux profondeurs 15, 30, 60, 90, 120 et 150 cm.
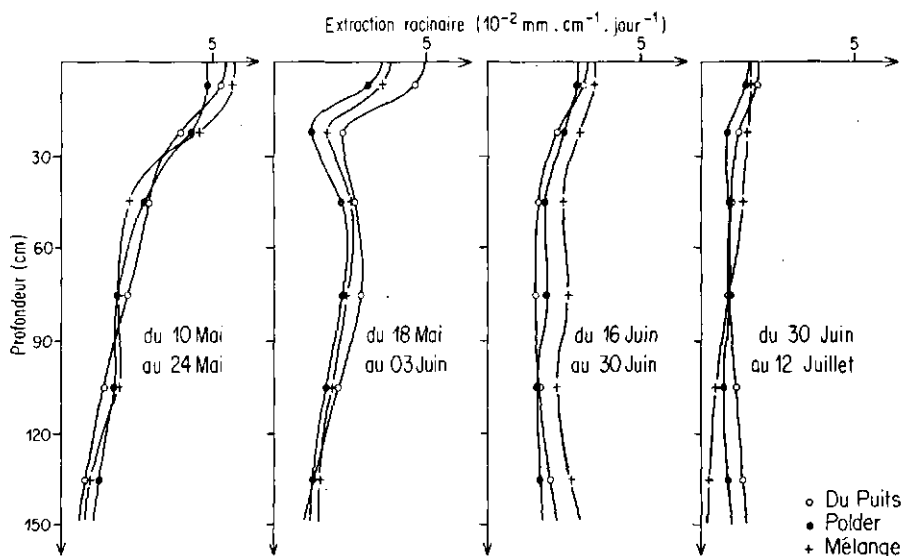

FIG.2. Évolution temporelle de l'extraction racinaire pour Du Puits, Polder et le mélange.

temporelle de la charge hydraulique à la profondeur 150 cm. Lors du dessèche-ment, le pic d'extraction, localisé initialement dans les horizons de surface, se déplace en profondeur selon un schéma bien connu. Au début du deuxième cycle de culture, le mélange extrait plus d'eau que ses deux constituants, comme l'ont déjà montré les résultats relatifs au bilan hydrique. Ce supplément d'extraction est distribué d'une manière uniforme dans tous les horizons du sol. En fin de période, les 150 premiers centimètres du sol sont desséchés. Les niveaux d'extraction sont faibles, sans localisation précise dans le profil.

TABLEAU II. REPARTITIONS RELATIVES DE LA BIOMASSE RACINAIRE
DU PUITS ET POLDER, ET ECARTS-TYPES DES ESTIMATIONS

	Du Puits		Polder	
	$\bar{x}$ (%)	s_x (%)	$\bar{x}$ (%)	s_x (%)
0 - 20 cm	46	18	39	26
20 - 40 cm	17	11	19	11
40 - 60 cm	19	18	17	16
60 - 80 cm	13	11	11	6
80 - 100 cm	5	7	14	8
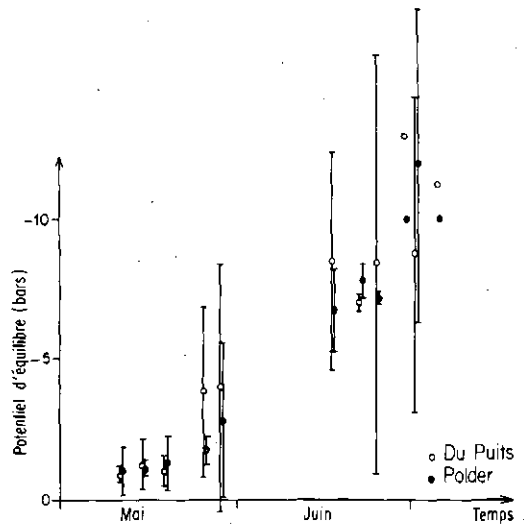
FIG.3. Evolution temporelle du potentiel d'équilibre pour Du Puits et Polder. Les résultats
sont affectés de leurs intervalles de confiance à 95%.
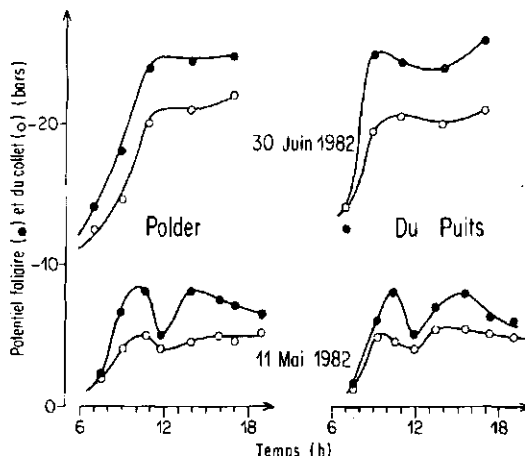
FIG.4. Cinétiques des potentiels hydriques et du collet les 11 mai et 30 juin pour Du Puits et Polder.

Régime hydrique

Jusqu'au 20 mai, les potentiels d'équilibre des deux variétés sont très voisins de −1 bar (fig.3). Ensuite, ce potentiel évolue pour atteindre, à la fin du premier cycle, −4 bars (coefficient de variation CV = 0,55) chez Du Puits et −2,8 bars (CV = 0,49) chez Polder. Un écart, de l'ordre de 1 à 2 bars, se maintient tout au long du second cycle. Il traduit une différence d'enracinement. Polder a le système racinaire le plus profond. Les potentiels d'équilibre sont inférieurs à −10 bars à la fin du cycle.

Le potentiel d'équilibre est le potentiel foliaire obtenu après la récupération hydrique de la plante, lorsque la transpiration est nulle. Dans ces conditions, la plante atteint un niveau de potentiel voisin de celui de la couche la plus humide exploitée par le système racinaire. Si nous reportons le potentiel d'équilibre en fonction du potentiel de la couche la plus humide observée dans les 150 premiers centimètres, la relation présente deux parties distinctes. Jusqu'à la mi-juin, cette relation est linéaire, comme l'observent Sala et al. [3] pour une graminée. Ensuite, le potentiel de la couche la plus humide décroît beaucoup plus rapidement que le potentiel d'équilibre, démontrant que nous ne contrôlons pas la couche la plus humide, c'est-à-dire que notre profondeur d'investigation est insuffisante.

Nous avons reporté sur la figure 4 les cinétiques journalières des potentiels foliaires et du collet des 11 mai et 30 juin. La première date concerne une période pendant laquelle la réserve hydrique du sol est maximale, la seconde la fin de la période sèche. La différence de potentiel entre le collet et les feuilles est proportionnelle à la transpiration car nous pouvons faire l'hypothèse que, à

l'échelle journalière, la résistance à la circulation de l'eau dans le trajet collet-feuilles est constante. Cette hypothèse n'est pas transposable au cas de la différence entre le potentiel d'équilibre et le potentiel foliaire, car la résistance rhizosphérique varie tout au long du jour.

Le 11 mai, nous avons une augmentation progressive de la différence de potentiel donc de la transpiration. Puis, à partir de 11 h, les variations du potentiel foliaire traduisent une réduction puis un retour de la transpiration à son taux initial. Trois hypothèses de fonctionnement peuvent être proposées. Dans la première, les variations de la transpiration sont consécutives à celles de l'extraction racinaire. Ces dernières sont provoquées par l'augmentation puis, après réhydratation du sol autour des racines, la diminution de la résistance rhizo-sphérique. Dans la seconde, l'extraction racinaire n'est pas modifiée, la transpi-ration est réduite par une fermeture hydroactive des stomates. La différence entre l'extraction racinaire et la transpiration réalimente les réserves hydriques du végétal qui, ensuite, recouvre son taux initial de transpiration. Dans ce cas, le flux n'est pas conservatif, contredisant Katerji et al. [4] qui observent que la variété Du Puits ne mobilise ses réserves hydriques que pour des potentiels foliaires inférieurs à −8,5 bars. La troisième hypothèse est la plus vraisemblable: elle suppose une fermeture des stomates provoquées par la forte sensibilité des jeunes feuilles à l'air sec [5].

Le 30 juin, les potentiels foliaires descendent jusqu'à −25 bars. Leurs cinétiques ne présentent pas le «creux» discuté précédemment. Les différences de potentiel entre les feuilles et le collet sont du même ordre de grandeur que celles observées le 11 mai. Nous nous situons, comme nous l'avons vu au niveau du bilan hydrique, dans une période à transpiration réduite. Nous pouvons conclure à une augmentation de la résistance collet-feuilles.

Les deux variétés ne présentent pas de dissemblance importante dans le fonctionnement hydrique. Les nuances que nous avons mises en évidence ne peuvent pas être interprétées à partir des seules mesures effectuées. En première approximation, nous ferons l'hypothèse d'une identité de fonctionnement. Les différences que nous discuterons seront en grande partie dues aux enracinements.

DISCUSSION ET CONCLUSION

Le premier cycle est caractérisé par l'absence de stress hydrique. L'ETR dépasse 80% de l'ETP, assurant aux trois parcelles une production végétale satisfaisante. La biomasse épigée atteinte en fin de cycle est de 652 ± 41; 530 ± 57 et 546 ± 6 g de matière sèche (MS) par m^2 pour Du Puits, Polder et le mélange. Les indices foliaires correspondants sont de 5,0, 4,5 et 4,4 m^2 de feuilles par m^2 de sol. Au niveau de la production, le mélange se comporte plutôt comme Polder. Le déficit de production aérienne de ce dernier s'explique par l'importance

de sa biomasse souterraine. Le rapport Polder/Du Puits est estimé à 3,7 pour les 100 premiers centimètres du sol: 1500 g MS·m⁻² pour Du Puits et 4100 g MS·m⁻² pour Polder. Ces chiffres ne sont pas en contradiction avec ceux de la bibliographie [4, 6]. Une allocation substantielle de photosynthéthats est nécessaire pour l'entretien du système racinaire de Polder. Elle explique sans doute les différences de productivité.

Lors du second cycle, l'alimentation en eau est réduite. L'efficacité de l'eau pour la production végétale est divisée par 5. La biomasse épigée atteint en fin de cycle 127 ± 12; 130 ± 2 et 109 ± 14 g MS·m⁻² pour Du Puits, Polder et le mélange. Les indices foliaires correspondants sont de 1,0; 1,1 et 0,9 m² de feuilles·m⁻² sol. L'ETR du mélange est la plus élevée. Ses profils d'extraction montrent une activité importante pour toutes les strates du sol, comme l'observent Martin et al. [7] en étudiant l'extraction du lithium par un mélange orge-vesce. Nous pouvons faire l'hypothèse d'une déformation plastique des systèmes racinaires des deux variétés constitutives du mélange, conduisant à un système résultant plus efficace du point de vue de l'extraction racinaire. En contrepartie, un tel système nécessite une ration d'entretien telle que la productivité de cette parcelle est la plus faible.

Nous avons mis en évidence deux types de non-linéarité dans le fonctionnement du mélange. Les premières concernent les flux hydriques et les secondes la productivité. Cependant, la présence dans les cultures de proportions différentes d'individus ayant des racines pivotantes et d'autres des racines fasciculées introduit une variabilité dans les comportements impossible à maîtriser et a rendu les interprétations hasardeuses. La relativité de nos conclusions est augmentée par le fait que nous n'avons pas contrôlé l'intégralité de la zone racinaire.

REFERENCES

[1] MAHBOUBI, A.A., Etude in situ du bilan hydrique pour quelques graminées: extraction de l'eau par le système racinaire et résistance à la sècheresse, Thèse USTL, Montpellier (1980).

[2] RITCHIE, G.A., HINCKLEY, T.M., Advances in Ecological Research 9 (1975) 165.

[3] SALA, O.E., LAUENROTH, W.K., PARTON, W.J., TRLICA, M.J., Oecological (Berl) 48 (1981) 327.

[4] KATERJI, N., HALLAIRE, M., PERRIER, A., DURAND, R., Acta Oecologica, Oecologia Plantarum (1983) (à paraître).

[5] FARQUHAR, G.D., Aust. J. Plant Physiol. 5 (1978) 787.

[6] LIPPS, R.C., FOX, R.L., Soil Sci. 97 (1964) 4.

[7] MARTIN, M.P.L.D., SNAYDON, R.W., DRENAN, R.S.H., Plant and Soil 64 (1982) 203.

USE OF EXPANDED VERMICULITE AS A SOIL CONDITIONER IN THE TROPICS

P.L. LIBARDI, E. SALATI
Centro de Energia Nuclear na
    Agricultura (CENA),
Piracicaba, S.P., Brazil

K. REICHARDT
Joint FAO/IAEA Division,
International Atomic Energy Agency, Vienna

Abstract

USE OF EXPANDED VERMICULITE AS A SOIL CONDITIONER IN THE TROPICS.
     Expanded vermiculite is used as a soil conditioner to improve soil-water retention and
cation exchange properties of poor tropical soils (alfisols and oxisols). Results show that fresh
laboratory mixtures of soil and expanded vermiculite increase the amount of water retained,
the process being affected by the rate of application, origin and granule size of the vermiculite.
Pot experiments show that the incorporation of vermiculite into the soil increases soil-water
storage capacity without affecting evapotranspiration rates. This indicates that crops grown
in soils conditioned with vermiculite lose the same quantities of water through evapotranspiration,
but support plants for longer periods without water addition. Diminishing irrigation frequency
raises the possibility of irrigating larger areas and/or using irrigation equipment more rationally.
Field experiments have been developed to examine the potential use of vermiculite, at low
application rates, in extensive agriculture. Encouraging results have been obtained regarding
crop resistance to drought spells, and yield in vermiculite conditioned soils. This new manage-
ment practice seems to be one solution for semi-arid agriculture and for areas of soil with poor
water retention properties subjected to irregular rainfall patterns. Experiments show also that
vermiculite addition improves root growth and affects soil nutrient ratios. This depends again
on soil type, vermiculite origin and granule size, application rates, form of incorporation into
the soil and type of crop. It affects Ca/K, Ca/Mg and Mg/K ratios in soil extracts and the
availability of micronutrients. Tracers were used to study some aspects of the dynamics of
N and P.

1.   INTRODUCTION

     Vermiculite, being a secondary mineral which is formed during the genesis
of the soil, can be found as a natural substance in soils. It is a 2:1 lattice clay
mineral, with variable interlaminar spacing. The specific surface area is very high
and possesses excellent cation exchange and water-holding capacities. Soils rich
in 2:1 clay minerals, especially in vermiculite, exhibit very good physico-chemical
properties and, therefore, in general support high crop productivity.

Vermiculite can also be found as a primary mineral, as a major constituent over large areas, close to or at the soil surface. It consists of macroscopic crystals formed of an enormous number of 2:1 layers held together by electrochemical forces, with water molecules and ions strongly adsorbed between the layers. When these crystals or plates are suddenly subjected to temperatures of around 700 to 800°C they expand and liberate the water in vapour form and then become elongated, curved and sometimes spiral-shaped. The name vermiculite is derived from Latin (vermicularis = worm-shaped). The thermally expanded vermiculite has properties similar to the clay mineral vermiculite found in soils. An extensive study of Brazilian vermiculites was carried out by Souza Santos and Navajas [1]. Its use as a soil conditioner for soils poor in 2:1 clay minerals, is a practice known for a long time.

The addition of expanded vermiculite to soils in order to improve their physico-chemical properties and also crop growth, is a known technology but is only used in intensive cash-crop agriculture, mainly horticulture. In Brazil, because of peculiar conditions, the extension of this technology to more extensive agriculture might be successful. The country is among those that have large vermiculite reserves which, according to Meisinger [2], are around 15 million tons; they are located within problematic agricultural areas, which are mainly the *cerrado* in the central part and the semi-arid areas in the north-east. Most of the soils located in these areas are old soils (oxisols and alfisols) with deep profiles, highly weathered and therefore very poor in 2:1 clay minerals, with low fertility and frequently high aluminium saturation. For agricultural use they are limited by extremely low cation exchange and water-holding capacities.

Cerrado soils, which cover approximately 180 million hectares, have been proved productive under correct management. The use of vermiculite as a conditioner in this situation would be recommended. The economic aspects of this technology are, of course, important. Today's price of vermiculite is mainly a reflection of transport costs over long distances and energy inputs for thermal expansion. Should distances be shortened by expanding the vermiculite close to application sites, and should the expansion be done more efficiently, the costs would certainly decrease. Application rates must be kept low and incorporation should be localized (bands, strips, hills, in pits, etc.). Successive applications of vermiculite could also be considered cumulative owing to its stability in the soil system, resulting in a gradual improvement of soil properties related to crop production. An increase in soil-water holding capacity can increase the irrigation interval, and the irrigation equipment could be used more efficiently over large areas. This increase in water-holding capacity is also very important when rainfall is low and not well distributed, which is the case in the above-mentioned areas.

The answer to most of these questions is being sought in a programme on the efficient use of vermiculite as a soil conditioner under tropical conditions, which is being carried out in Brazil. This paper reviews the latest achievements of this project.

2.   SOIL-WATER RELATIONSHIPS

Laboratory results obtained by Salati et al. [3] with homogeneous fresh mixtures of soil and vermiculite indicate a significant increase of soil-water retention as compared with untreated soil. Two oxisols from the *cerrado* area were used to obtain mixtures containing different proportions of two types of vermiculite (0 to 10% of soil weight). The increase in water-holding capacity is greater in the high moisture content range (between saturation and "field capacity") than in the dry range (around "wilting point") so that the so-called "available water" is increased. Similar results were also obtained by Choudhury [4], using different soils of semi-arid regions.

The above-mentioned results depend on soil type, origin (type) of vermiculite and vermiculite granule size. When the results were extrapolated to a field condition, receiving a homogeneous vermiculte application over the total area down to a given depth, the rates to apply were found to be economically unrealistic. As an example, for a soil with a 50 mm capacity for available water in the 40 cm top layer, and vermiculite added in the proportion of 5% by weight of the top 15 cm soil, the water storage capacity increases to 80 mm. The amount of vermiculte, however, reaches a value over 500 m^3/ha, depending on its bulk density.

On the other hand, for homogeneous application rates that are too low the response is not significant. If, however, consecutive applications at low rate are made over several years, a cumulative effect could be expected. This fact is now under investigation. On the other hand, the localized application of vermiculite in bands, strips or pits, decreases overall rates significantly. As an example, with pits of 30 × 30 × 30 cm for coffee trees spaced 1.5 × 1.5 m apart, if vermiculite is applied at a rate of 10% of volume, the total application rate will be 12 m^3/ha. Strips of 15 × 15 cm, with a spacing of 1.5 m, also at 10% volume, will give a total application rate of 15 m^3/ha.

Galbiati [5] in a later study evaluated the influence of vermiculite granule size on soil-water retention, saturated hydraulic conductivity and water redistribution after irrigation. Three soils and five granule sizes were used in this study. Results show that the addition of vermiculite at a rate of 10% by volume of soil affects soil-water retention, saturated hydraulic conductivity, water content at saturation and redistribution patterns. Vermiculite with finer granules was more effective for water retention. In all soils a direct relation was found between vermiculite granule size and saturated hydraulic conductivity. Redistribution patterns show that the advance of the wetting front is slower for vermiculite-treated soils, which is a result of a greater water storage capacity.

3.   PLANT-WATER RELATIONSHIPS

Salati et al. [3] also reports results of a pot experiment with corn (*Zea mays* L.) which show that the addition of vermiculite to the soil increases its water storage capacity without affecting evapotranspiration. This means that crops grown on vermiculite-conditioned soil, although losing the same quantity of water through evaportranspiration, resist wilting for a longer period without water addition. As already stated, if the irrigation frequency is decreased, irrigation equipment can be used more efficiently.

The addition of vermiculite to the soil also promotes root growth. The extent of it depends on types of crops and soil, and on vermiculite application rate. Reichardt [6] reports very significant root weight increases for corn (*Zea mays* L.) as a function of vermiculite content in soil. Other unpublished work carried out at the Centre for Nuclear Energy in Agriculture, Piracicaba, S.P., Brazil, shows no significant differences for root patterns, for rice (*Oryza sativa* L.) and beans (*Phaseolus vulgaris* L.) grown in pots.

Under field conditions, however, in which the root system is not restricted to pot size, there may be a positive effect of vermiculite on plant root development. It is, however, difficult to separate the effects of vermiculite on soil-water availability, root growth and nutrient uptake. A larger and deeper root system allows a better exploitation of the soil profile. This might be the explanation of many positive results obtained under field conditions, using very low vermiculite application rates.

A field study was carried out by Reichardt et al. [7] to evaluate the effect of vermiculite application on rice yield under water-deficient conditions. A water deficit was imposed at flowering stage by covering experimental plots with transparent plastic sheets. Considering 100% as the yield of the water-stressed plots without vermiculite, the yield of plots which received 2 and 10% (volume) vermiculite were 126 and 129%, respectively. The plot without water deficit, and without vermiculite had a yield of 144%. It can be seen that the drought treatment reduced the yield by 44% and that vermiculite reduced these losses by 18% for the 2% application and 15% for the 10% application. During this study the authors observed visually, through differences in leaf curling during water-stress periods, that soil conditioning with vermiculite gives a greater drought resistance to the crop.

In the latest study, Stone [8] carried out a ^{15}N isotope pot experiment with rice in order to learn about nitrogen dynamics in soil/plant systems, as affected by drought and vermiculite application. This study showed no effect of vermiculite application on water use efficiency and grain yield. Vermiculite was applied at a rate of 10% by volume.

4.   SOIL/PLANT-NUTRIENT RELATIONSHIPS

The addition of vermiculite affects many crop nutrient relationships, also
depending on soil type, vermiculite type, application rate and the crop. In soil
extracts it changes Ca/K, Ca/Mg and Mg/K ratios, which in turn may affect micro-
nutrient availability. Nitrogen dynamics are affected by changing N quantities
taken up from soil and fertilizer. The cation exchange capacity is increased,
a fact that could diminish ion losses by leaching. The available information on
nutrient relationships is, however, partial, and not sufficient for a definition of
the problem. Although Reichardt et al. [9] in their review state that, at normal
fertilizer rates, losses of N by leaching are not a problem, this statement cannot
be extended to other nutrients and evidence shows that, under particular conditions
of irregular rainfall pattern, fertilizer losses can be significant.

Freitas [10] carried out a ^{15}N and ^{32}P isotope-aided pot experiment to study
water and nutrient availability to beans (*Phaseolus vulgaris* L.) as affected by
vermiculite application. He showed a significant decrease in the Ca/Mg ratio with
a corresponding increase in the Mg/K ratio, owing to the liberation of Mg by the
vermiculite. This fact decreased manganese availability to the plants. Stone [8],
in a similar study with rice, concluded that the incorporation of vermiculite into
the soil caused favourable effects in some chemical characteristics of the soil:
it increased pH, the cation exchange capacity, the exchangeable cation (Ca, Mg
and K) concentrations and decreased exchangeable aluminium concentration. It
also increased the above-ground dry-matter yield and affected the dynamics of
nitrogen in the soil/plant system. It reduced plant nitrogen concentration. Under
conditions of water stress imposed gradually for a long period, the use of ^{15}N
showed a reduction of nitrogen in plants derived from fertilizer, and the nitrogen
fertilizer utilization efficiency; this was probably due to ammonium fixation
by vermiculite. Grain yield was not affected by vermiculite addition.

Yield increases of various crops (rice, beans, corn, carrots and lettuce), owing
to soil conditioning with vermiculite, were reported by Aquino et al. [11] and
Santos et al. [12]. The latter authors, however, point out that the favourable
effects of using vermiculite were only verified under good soil moisture conditions
and with the application of high doses of vermiculite. They are of the opinion
that the application of vermiculite has more positive effects on soil chemical
properties than on physical properties. They observed that under field conditions
the addition of vermiculite did not significantly alter soil-water retention. Aquino
et al. [11], however, suggest that by using vermiculite as a soil conditioner,
it would be possible to reduce chemical fertilizer maintenance application levels
in successive cropping, and reduce liming levels. This is presumably because of
nutrient retention by vermiculite. In contrast to Santos et al. [12] they also
report a positive influence of vermiculite on soil-water retention during short
periods of water deficit (up to three days). The increased yields reported should,

therefore, be related to the cumulative effects of vermiculite on nutrition and water retention during short periods of drought owing to irregular rainfall patterns.

5.   CONCLUSION

Information available to date still does not give a clear picture on the use of vermiculite as a soil conditioner for extensive agriculture. Published results show positive, non-significant and sometimes negative results of the use of vermiculite in pot, laboratory or field experiments. More research is therefore needed to confirm these results. Most of the available information, however, indicates positive responses which would recommend this soil conditioner mainly for intensive agriculture and, in some special cases, even in more extensive agriculture. As pointed out in the paper, one of the major constraints is the cost of this management practice. All efforts should be made to minimize the cost of vermiculite, and research should be oriented to low application rates, localized application practices, and to the use of vermiculite as a fertilizer carrier as suggested by Castoll [13] in the early 'sixties.

REFERENCES

[1] SOUZA SANTOS, P., NAVAJAS, R., Estudos sobre a piroexpansão de vermiculitas brasileiras – uma revisão, Ceramica **27** (1981) 423.

[2] MEISINGER, A.C., Vermiculite, mineral facts and problems, Washington, US Dept. of Irrigation, Bureau of Mines, Bull. **671** (1980) 9.

[3] SALATI, E., REICHARDT, K., URQUIAGA, C.S., Efeitos da adição de vermiculita na retenção e armazenamento de agua por latossolos, Rev. Bras. Cienc. Solo **4** (1980) 125.

[4] CHOUDHURY, E.N., Influencia da vermiculita na retencão de agua e capacidade de troca de cations em latossolo vermelho amarelo, National Irrigation and Drainage Congress, Belo Horizonte 1982, in press.

[5] GALBIATI, J., Influencia da gramulometria de vermiculita nas relaçoes solo agua, Ph.D. Thesis, University of São Paulo, Piracicaba, 1983.

[6] REICHARDT, K., "Soil physico-chemical conditions and the development of roots", The Soil/Root System in Relation to Brazilian Agriculture, (SCOTT RUSSEL, R., IGUE, K., METHA, Y.R., Eds), Fundação Instituto Agronômico do Parana (IARAR), Londrina (1981).

[7] REICHARDT, K., LIBARDI, P.L., URQUIAGA, C.S., SARAIVA DA COSTA, A.C., "Effects of vermiculite in the control of water deficits in rice crop", Regional Seminar, Use of Nuclear Techniques in Soil-Plant-Atmosphere Studies, Centro di Energia na Agricultura (CENA) Piracicaba, 1981, in press.

[8] STONE, L.F., Produtividade do arroz (*Oriza sativa* L.) e dinamica do nitrogenio no sistema solo/planta: efeitos de cultivares, vermiculita e deficiencia hídrica, Ph.D. Thesis, University of São Paulo, Piracicaba, 1983.

[9] REICHARDT, K., LIBARDI, P.L., URQUIAGA, S.C., "Fate of fertilizer nitrogen in soil-plant systems with emphasis on the tropics", Agrochemicals: Fate in Food and the Environment (Proc. Symp. Rome, 1982), IAEA, Vienna (1982) 277–90.

[10] FREITAS, E., Efeitos da vermiculita na disponibilidade de agua e de nutrientes en feijoeiro (*Phaseolus vulgaris*, L.) cultivar "carioca comum", Ph.D. Thesis, University of São Paulo, Piracicaba, 1982.

[11] AQUINO, A.R.L., SANTOS, A.B., STEINMETZ, S.L., CHAGAS, J.M., SILVEIRA, P.M., MAH, M.G.C., CARVALHO, J.R.P., COUTO, A.J., Utilização da vermiculita no aumento da produtividade de solos do cerrado, Tech. Rep. EMBRAPA-CNPAF (Empresa Brasileira de Pesquisa Agropecuária – Centro Nacional de Pesquisas do Arroz e Feijão), Goiânia (1981) 22.

[12] SANTOS, A.B., STEINMETZ, S., SILVEIRA, J.M., BARBOSA, M.P., FAGERIA, N.K., Comentarios sobre resultados obtidos em estudos com vermiculita na agricultura, Tech. Rep. EMBRAPA-CNPAF (Empresa Brasileira de Pesquisa Agropecuária – Centro Nacional de Pesquisas do Arroz e Feijão), Goiânia (1982) 19.

[13] CASTOLL, L.A., Vermiculite as a chemical carrier in agriculture, Can. Farm Impl. Winnipeg (1963) 25.

INFLUENCE OF SOIL SURFACE STRUCTURE ON SIMULATED INFILTRATION AND SUBSEQUENT EVAPORATION

H. VERPLANCKE, R. HARTMANN, M. DE BOODT
Laboratory of Soil Physics, Soil Conditioning
   and Horticultural Soil Science,
Faculty of Agricultural Sciences,
State University of Ghent,
Belgium

Abstract

INFLUENCE OF SOIL SURFACE STRUCTURE ON SIMULATED INFILTRATION AND SUBSEQUENT EVAPORATION.

A laboratory rainfall and evaporation experiment was conducted to study the effectiveness of the soil surface structure on infiltration and subsequent evaporation. The stability of the surface layer was improved through the application of synthetic additives such as bituminous emulsion and a prepolymer of polyurea (Uresol). The soil column where the soil surface was treated with a bituminous emulsion shows a decrease in depth of wetting owing to the water repellency of that additive, and consequently an increased runoff. However, the application of Uresol to the surface layer improved the infiltration. The main reason for these differences is that in the untreated soils there is a greater clogging of macropores originating from aggregate breakdown under raindrop impact in the top layer. The evaporation experiment started after all columns were wetted to a similar soil-water content and was carried out in a controlled environmental tunnel. Soil-water content profiles were established during evaporation by means of a fully automatic γ-ray scanner. It appears that in both treatments the cumulative evaporation was less than in the untreated soil. This was due to the effect of an aggregated and stabilized surface layer. Under a treated soil surface the evaporation remains constant during the whole experiment. However, under an untreated soil surface different evaporation stages were recorded. From these experiments the impression is gained that the effect of aggregating the soil surface is an increase of the saturated hydraulic conductivity under conditions near saturation. On the other hand, a finely structured layer exhibits a greater hydraulic conductivity during evaporation in the lower soil-water potential range than a coarsely aggregated layer. So it may be concluded that, to obtain the maximum benefit from the available water. — optimal water conservation — much attention must be given to the aggregation of the top soil and its stability.

INTRODUCTION

The problem under investigation concerns the infiltration and evaporation from bare soils, and the conservation of soil moisture by the suppression of evaporation.

The primary focusing point of water management in the field is the soil surface for it is through this surface that water enters the profile during infiltration and subsequently escapes to the atmosphere during evaporation.

Because of the importance of both processes, efforts have been made to improve and protect the structure of the soil surface to promote infiltration and/or to suppress evaporation through the application of natural additives.

Although several natural materials have been found to improve various soil physical properties they often have disadvantages such as being insufficient in supply, inconvenient to handle and to apply, difficult to remove, or they interfere with succeeding crops.

During the last decade a renewed interest in synthetic soil conditioners, which can profoundly affect the above-mentioned basic processes, has been noticeable [1].

Futher improvements of the formulation and manufacture of soil conditioners, as a substitute for organic matter and laboratory and field experiments to improve the techniques of aggregation, are still required before this valuable technique can be universally introduced.

The object of this study was to investigate whether a stable aggregated surface layer, obtained by applying synthetic soil conditioners (Uresol and bitumen), favourably affects the soil-water balance by its effect on infiltration, evaporation and water distribution. These two chemical treatments of the soil surface were compared under standard conditions in the laboratory.

MATERIALS AND METHODS

The soil used in our experiments was a silt loam, containing 17.3% clay, 69.4% silt and 13.3% sand, with an organic matter content of 0.25% and 4.15% $CaCO_3$.

The soils were treated with two soil conditioners known as Bitumen HP 739 (50% emulsion) and Uresol 336 E (77% solution) which consist of polyalkylene oxide chains with terminal isocyanate groups (polyurea). Bitumen is a well-known hydrophobic soil conditioner and Uresol is a hydrophylic one. The application rates were bitumen 0.4% and Uresol 0.6% active material.

The soil conditioners were diluted with water and sprayed on air-dry soil aggregates (fraction ≤ 8 mm). Afterwards the soil was allowed to dry for at least 24 hours and then passed through an 8-mm sieve. The untreated soil was handled in the same way but without the addition of a soil conditioner.

The water stability of aggregates smaller than 8 mm was determined by wet-sieving according to De Leenheer and De Boodt [2]. The difference between the mean weight diameter of the dry aggregate distribution and the wet stable

aggregate distribution is defined as the instability index. The smaller this index the better the water stability of the aggregates.

The liquid-solid contact angle was measured by the capillary absorption method [3] on the soil fraction smaller than 2 mm. This method is based on the comparison of the penetrability of water and ethylalcohol (the contact angle of ethanol being zero).

For the penetrability and sorptivity, a uniform soil column was made with the soil fraction smaller than 2 mm. After the water infiltration was started the distances of the wetting front and the quantity of infiltrated water were noted.

Air permeability was measured by an air flux through the soil column (8 cm long, 2 cm diameter) under a certain pressure. The soil was then saturated and the water permeability was determined during six weeks, and the ratio of the air and water permeability was calculated.

For the sedimented bulk density, 25 g soil (fraction <0.3 mm) was put into a 100-mL graduated cylinder, which was filled with water to 100 mL, stirred and the sedimented volume was checked and the density of the sedimented soil calculated.

In the water-balance study, air-dry soil (fraction <2 mm) was packed homogeneously in Perspex tubes (internal diameter 5 cm, length 34 cm) up to 2 cm below the top of the tube, and the bulk density was measured every 1 cm by means of the gamma-ray attenuation technique described by Verplancke [4]. The soil was then covered with a 2-cm top layer of the treated and untreated aggregates (≤ 8 mm).

The air-dry soil columns were exposed to a simulated rainfall of 22.9 mm/h, produced for 3 h by the simulator described by Gabriels and De Boodt [5]. The soil columns were covered with parafilm to prevent evaporation and the depth of the wetting front was checked. The soil moisture was measured by the gamma-ray attenuation equipment [4] at certain time intervals until the moisture distribution reached almost equilibrium.

When the soil moisture redistribution was almost in equilibrium the soil surface was subjected to evaporation for about 600 hours in a controlled environment tunnel in which climatic variables could be automatically controlled: temperature, relative humidity and wind speed. In these experiments the temperature was 20°C, the relative humidity 40% and the wind speed 5 km/h.

During the evaporation experiment the evaporation rate was measured regularly by means of the gamma-attenuation technique and the potential evaporation was determined by weighing two water-filled cylinders which were also placed in the climatic tunnel.

The daily potential evaporation was 5 ± 0.05 mm and the total evaporation was 122 mm in 25 days.

Soil erodibility was tested during a simulated rainfall in a soil pan (30 cm $\times$ 29.7 cm) which was filled with a 3-cm soil layer and covered with

TABLE I. EFFECT OF URESOL AND BITUMEN TREATMENT ON THE
STRUCTURE STABILITY OF A SILT LOAM SOIL

	Treatment		
	Untreated	Uresol 0.4%	Bitumen 0.6%
Structure instability index (mm)	3.64	0.36	0.61
Air permeability K'_a (m^2)	9.87×10^{-13}	1.33×10^{-12}	5.55×10^{-13}
Water permeability K'_w (m^2)	1.05×10^{-13}	2.52×10^{-13}	7.99×10^{-14}
K'_a/K'_w	9.4	5.3	6.9
Sedimented bulk density (g/cm^3)	1.04	0.84	0.98

a 2-cm layer of treated and untreated aggregates (< 5.35 mm). The bulk density
of the soil layer was 1.4 g/cm^3 and the bulk density of the layer with aggregates
was 1.3 g/cm^3.

Runoff starting time and runoff rate were checked and the soil loss was
measured by dry weight of the runoff material and finally the erodibility data
were calculated.
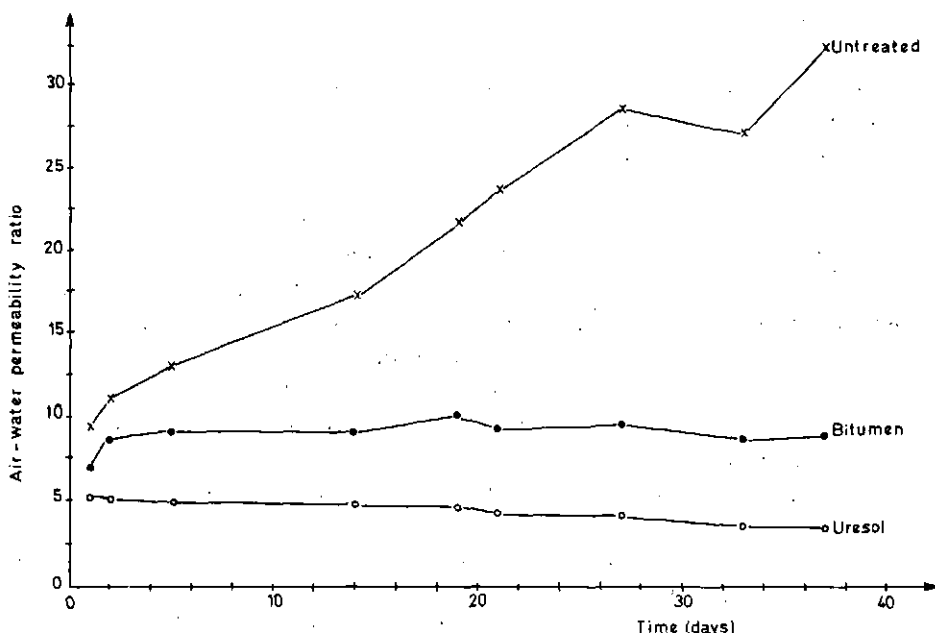
FIG.1.   Changes of the air-water permeability ratio of the treated and untreated silt loam.
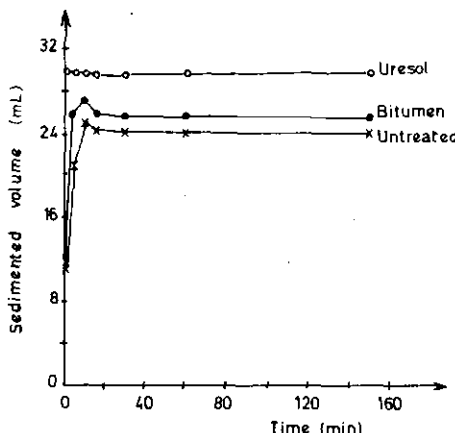
FIG.2. Sedimented volume of the treated and untreated silt loam (fraction <3 mm, 25 g) after stirring in distilled water (in 100-mL cylinders).

RESULTS AND DISCUSSION

1. Effects on the soil physical properties

From Table I it appears that through the addition of Uresol and bitumen the aggregate stability increased substantially. The instability index of untreated silt loam aggregates was 3.64 mm in comparison with only 0.61 mm and 0.36 mm for bitumen- and Uresol-treated aggregates, respectively.

The air-water permeability ratio, which is an index to define the stability, was also decreased by ca. 50% by the soil conditioner treatment (Table I). The air-water permeability ratio K'_a/K'_w of the treated soils was constant until 40 days after saturation, but in the case of the untreated soil the ratio increased (Fig. 1). It means that the water permeability of the untreated soils was gradually decreased by slaking the unstable aggregates, but was constant in treated soils because the aggregates were stable in water for a long period.

The sedimented bulk densities were calculated and presented in Table I. The sedimented bulk density of the untreated soils is greater than that of the bitumen- and Uresol-treated soils. Uresol-treated soil was quickly sedimented (Fig. 2) and had a lower bulk density, because the particles were more stable. These results present good prospects for solving some problems in rice cultivated soils. It is very difficult to transplant the rice seedlings in newly reclaimed marine soil because the soil is structureless and the mechanical compositon is ideal to compact after ploughing. Not only for upland soils but also for poorly drained paddy soils it is necessary to improve the water drainage so as to increase the crop yields and workability.

TABLE II. EFFECT OF URESOL AND BITUMEN TREATMENT ON THE HYDROPHYSICAL PROPERTIES OF A SILT LOAM SOIL

	Treatment		
	Untreated	Uresol 0.4%	Bitumen 0.6%
Liquid-solid contact angle ($^{\circ}$)	68.1	69.4	84.9
Penetrability (cm/min$^{1/2}$)	1.26	1.17	0.59
Sorptivity (cm/min$^{1/2}$)	0.419	0.416	0.186
Saturated hydraulic conductivity (m/s)	1.03×10^{-6}	2.46×10^{-6}	7.8×10^{-7}

TABLE III. EFFECT OF URESOL AND BITUMEN TREATMENT ON THE WATER BALANCE OF SILT LOAM SOIL COLUMNS DURING SIMULATED RAINFALL AND EVAPORATION

		Treatment		
		Untreated	Uresol 0.4%	Bitumen 0.6%
Infiltration (mm)	1	52.5	77.3	12.8
	2	48.1	74.5	11.6
	mean	50.3	75.9	12.2
Evaporation (mm)	1	34.4	20.0	21.0
	2	33.8	24.2	25.4
	mean	34.1	22.1	23.2

Rainfall: 68.7 mm/3 h.
Potential evaporation: 122 mm/25 days.
Wind tunnel: Temperature 20°C.
              Relative humidity 40%.
              Wind speed 5 km/h.

The liquid-solid contact angle of the Uresol-treated soil and the natural silt loam soil showed almost no difference (Table II). The bitumen-treated soil was absolutely water repellent and the wettability was decreased.

The penetrability and the sorptivity of the treated soils were affected in the same way as the liquid-solid contact angle (Table II).
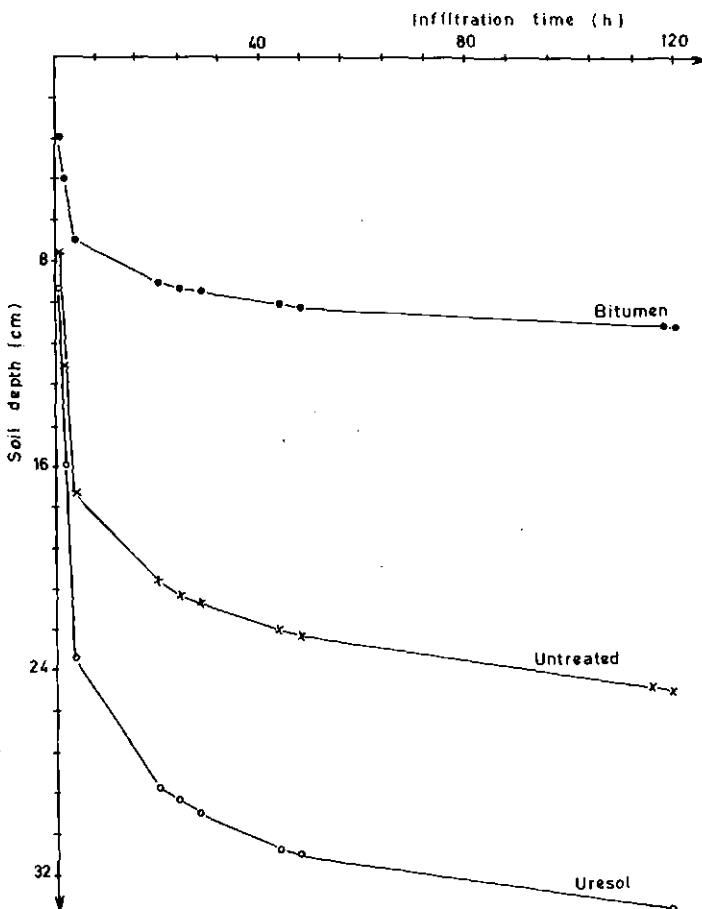
FIG.3. Progress of the wetting front into treated and untreated silt loam soil columns during simulated rainfall.

2.   Effects on the infiltration rate

The results shown in Table III are averages of two replicates.

Progress of the wetting front during simulated rainfall is shown in Fig. 3. The soil column with the Uresol-treated top layer exhibited faster penetration rates than the columns with an untreated top layer. The water infiltration rate was increased with by 50% by the Uresol treatment.

The main reason for this difference is a greater clogging of macropores originating from aggregate breakdown in the untreated top layer. Indeed the untreated aggregate layer is less stable under raindrop impact, resulting in the formation cf a crust with low hydraulic conductivity. In this manner water
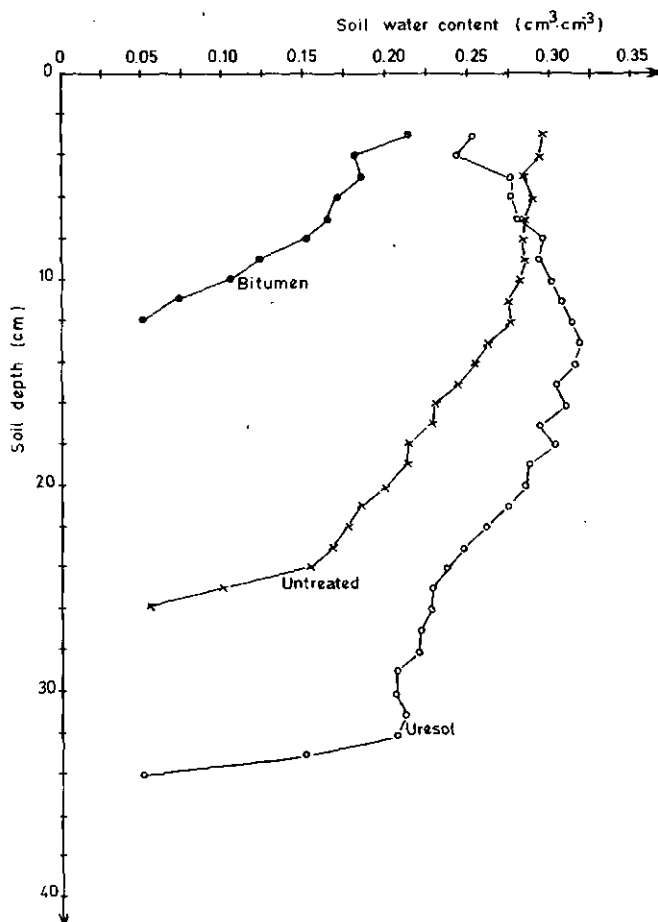
FIG.4.   Soil-water content distribution in treated and untreated silt loam soil columns at 120 h after simulated rainfall.

remained longer on the untreated sealed soil surface which allowed the water to be splashed during simulated rainfall.

The infiltration rates were very low in the soil columns with a bitumen-treated top layer. The infiltration rate decreased to 25% in comparison with the untreated soil columns. The main reason for this difference is the very low wettability of the bitumen-treated aggregates, as was stated in the values of the liquid-solid contact angles, the penetrability and the sorptivity (Table II).

Table III shows the total amount of water infiltrated during three hours of simulated rainfall. In the treated soil columns the amount of water infiltrated was much larger than the total amount of simulated rainfall (68.7 mm). This is

because the splash on the wall of the Perspex column (wall thickness 0.5 cm) allows more water to infiltrate than the total rainfall on the effective soil surface.

The aggregated and stabilized top layer exhibits a high inter-aggregate macroporosity which remains during rainfall and through which most of the flow under or near saturation takes place.

The changes of the water-content profiles in the soil columns obtained during the soil-water redistribution period are shown in Fig. 4.

The small differences in depths of the wetting front between those presented in Fig. 3 are due to internal drainage during the period between the termination of simulated rainfall and the time of soil-water content determination by means of the gamma-attenuation equipment.

The effectiveness of the Uresol treatment is reflected in the water redistribution profiles obtained after simulated rainfall. After the soil-water distribution was equilibrated, the water content of the silt loam soil column with an untreated top layer was high in the upper soil layers and decreased with depth, but in the case of Uresol treatment, the water content was lower in the upper layer and increased with depth until 15 cm. The surface structure of the untreated aggregates was broken and a crust was formed which inhibits the downward water movement; therefore, the data were retained in the upper layers, but the Uresol-treated aggregates were stable enough to keep the rain-water in the deeper soil layers.

This moisture distribution pattern is very important for inhibiting the evaporation and providing good conditions for plant growth.

From Fig. 4 it appears that at the start of the evaporation experiments the soil-water content distribution profiles were nearly identical.

3. Effects of the inhibition of evaporation

During the evaporation period, the potential evaporation was 122 mm in 25 days and the changes of the daily evaporation rate from the soil are shown in Fig. 5. The evaporation rate from the silt loam columns with an untreated aggregate layer on top was much higher than that from the treated top layers. The effect of bitumen and Uresol on the evaporation rate was almost the same.

In Fig. 5 the evaporation rate was plotted versus time, and it is interesting to see that the curves of the untreated and treated soils came together at about the same time (16 days) after evaporation started.

The relationship between the cumulative evaporation versus the evaporation time for the soil columns with the untreated and treated top layers is shown in Fig. 6. For the untreated aggregates these relationships are curvilinear, while for the treated aggregates they are gently linear.

The bitumen treatment suppressed the total evaporation to 68% and the Uresol treatment inhibited the total evaporation to 65% (Table III).
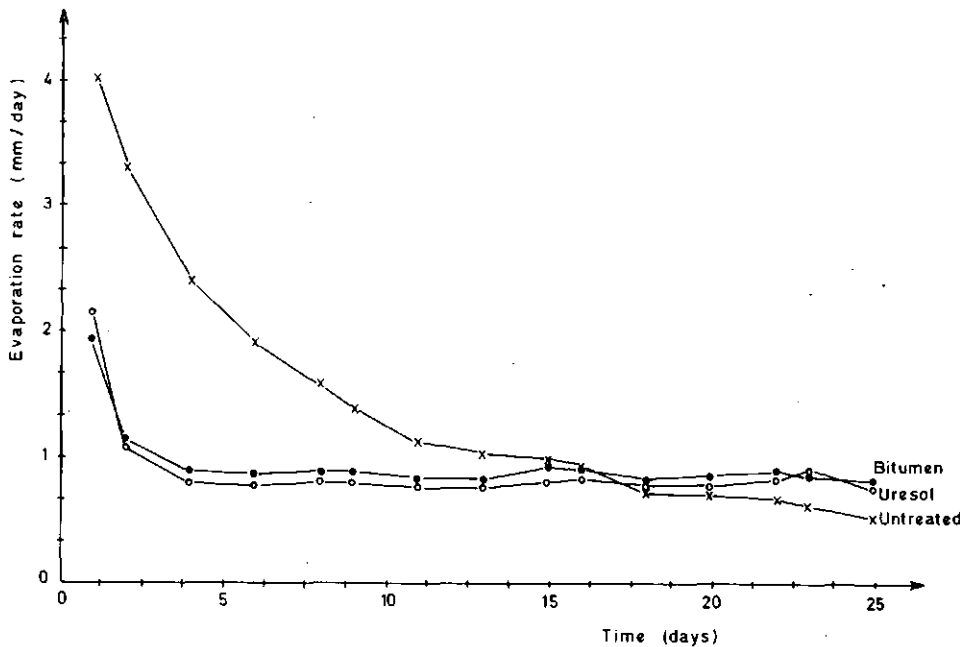
FIG.5.   Changes of evaporation rate from the treated and untreated silt loam soil columns.
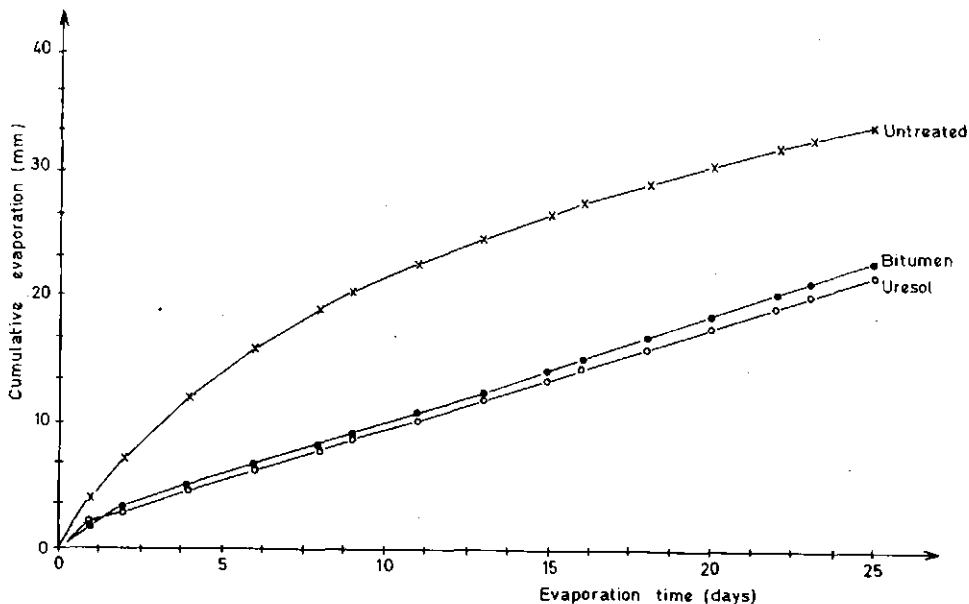
FIG.6.   Cumulative evaporation from treated and untreated silt loam soil columns.

TABLE IV. EFFECT OF URESOL AND BITUMEN TREATMENT ON
EROSION CONTROL UNDER SIMULATED RAINFALL (SILT LOAM SOIL)

	Treatment		
	Untreated	Uresol 0.4%	Bitumen 0.6%
Starting time to runoff (min)	11	31	10
Energy to initiate runoff (J/cm^2)	0.0383	0.1133	0.0348
Runoff rate (mm/h)	11.8	11	15.8
Infiltration rate (mm/h)	36.4	39.3	32.3
Total soil loss $(g/1000 \ cm^2)$	32.2	7.6	17.7
Final soil loss rate $(g/1000 \ cm^2$ per 10 min)	15.0	2.1	5.6

From these experiments the impression is gained that the effect of aggregating
the soil surface lies in increasing the saturated hydraulic conductivity under
conditions of near saturation. On the other hand, it is known that during eva-
poration a finely structured layer exhibits a greater hydraulic conductivity in the
lower soil-water potential range than a coarsely aggregated layer. So it may be
concluded that much attention has to be given to the aggregation of the top soil
and its stability to obtain maximum benefit of the available water.

By Uresol treatment the total water management effects, which combined
the infiltration and the evaporation effects, were increased to 332% compared
with the untreated soils (Table III). Bitumen treatment is also attractive for
inhibiting evaporation but, because of the very low wettability, only for those
soils where subsurface irrigation is applied, or on flat sandy areas.

4.   Effects on erosion control

The runoff starting time of silt loam soil with the Uresol-treated aggregate
top layer was delayed by 31 minutes after rainfall compared to 11 minutes for
the natural, untreated top layer and 10 minutes for the bitumen-treated top
layer (Table IV). The runoff starting from the Uresol-treated soil surface was
about three times longer than from the untreated soil surface.

Runoff rates were reduced by the Uresol treatment, but were increased
by the bitumen treatment. The higher the infiltration rate into the soil profile
(Table III), the less runoff from the soil surface.

The soil loss could be reduced to 75% by a Uresol treatment and to about
50% by a bitumen treatment, compared with an untreated natural silt loam soil.

CONCLUSIONS

(1) The physical properties of the silt loam soil were greatly changed by the bitumen 0.4% and Uresol 0.6% treatments.

(2) Improving the aggregation and stability of the aggregated surface layer with Uresol increased the amount of infiltrated water during simulated rainfall by about 50%. A bitumen treatment, on the other hand, decreased the infiltration to less than 25%.

(3) Under untreated soil surfaces the evaporation rates were initially higher than under treated surfaces. The evaporation from the treated soil columns was clearly inhibited by ca. 65%.

(4) By a Uresol treatment, the beneficial water management effects, which combined the infiltration and the evaporation effects, were almost three times as great as for the untreated silt loam soil.

(5) The soil erosion was reduced by 75% by Uresol treatment and by 50% by bitumen treatment.

REFERENCES

[1]   DE BOODT, M., "Improvement of soil structure by chemical means", Optimizing the
       Soil Physical Environment Toward Greater Crop Yields (HILLEL, D., Ed.), Academic
       Press (1972) 43–45.
[2]   DE LEENHEER, L., DE BOODT, M., "Aggregate stability determination by the change
       in mean weight diameter", West-European Methods for Soil Structure Determination
       (Edited by the West-European Working Group on Soil Structure of the International
       Soil Science Society, Ghent, 6 (1967) 28.
[3]   HAMMOND, L.C., YUAN, T.L., "Methods of measuring water repellency of soils",
       Water Repellent Soils (Proc. Symp. California, 1968), University of California, Riverside,
       (1968) 49–60.
[4]   VERPLANCKE, H., Studie van de wetmatigheid van de infiltratie en de diffusiviteit van
       water in natuurlijke en gekonditioneerde leemgronden, Ph.D. Thesis, Rijksuniversiteit
       Ghent (1973) 137 pp.
[5]   GABRIELS, D., DE BOODT, M., A rainfall simulator for soil erosion studies in the laboratory,
       Pedologie 25 (1975) 80–86.

SAND-RAPG COMBINATION SIMULATING FERTILE CLAYEY SOIL (Parts I to IV)

R. AZZAM
Nuclear Chemistry Department,
Atomic Energy Authority,
Cairo

O.A. EL-HADY, A.A. LOTFY, M. HEGELA
Soils and Water Use Laboratory,
National Research Center,
Dokki, Giza

Egypt

Abstract

SAND-RAPG COMBINATION SIMULATING FERTILE CLAYEY SOIL. (PARTS I to IV).

I. Radiation Preparation of RAPG. Radiation chemical investigation of acrylamide polymerization has revealed conditions for maximum hydrophilicity. Polyacrylamide gel (PAMG) in aggregating sand is explained by co-ordination of the nucleophilic nitrogen with a silicon atom of the soil particles. This is reinforced by hydrogen bonds, possibly formed between the carbonyl and silanol groups. Accordingly, sites of co-ordination and reinforcement are dominated in reclaimer ameliorator polymeric gel (RAPG). It is a modified acrylonitrile base multifunction polymer grafted upon a binder of worthless cellulosic agricultural discard. It varies chemically from non-ionic through anionic and cationic to ampholite. The hydroproperty of the gel is similarly controlled. Thus, RAPG can be tailored for any soil texture under various climatic conditions.

II. Structure Stability and Maintenance. Sinai dune sand is treated with non-ionic and anionic RAPGs at rates varying from 0.05 to 0.2 wt.%. The stability increased with RAPG anionicity and application rate. The structure formed maintained three cycles of complete destruction and re-formation without significant changes in erosion index. The resistance of sand-RAPG combination to breakdown by tillage, as well as to wind and water erosion, is practically proved. This is in addition to the beneficial changes in bulk density, void ratio and micro-porosity, which were also achieved.

III. Water Preservation. Inshas sandy soil treated by RAPG is compared with fertile clayey soil. The water-holding capacity and retention at different suctions are increased. The available water to plants in treated sand has reached 15 times that of the control, and even exceeded clay by 11%. Water losses by evaporation and leaching as well as deep percolation are all reduced to a minimum.

IV. Plantation and Nutritional Status. Pepper seed germination, growth and dry matter are increased in the sand-RAPG combination relative to fertile clayey soil. The optimum rate and anionicity of RAPG are determined. This increases water-use efficiency to twice that of the

fertile clayey soil. Macro- and micro-nutrient uptake have also increased. Thus, fertilizer use efficiency is increased by almost three times over that of clay. These factors lead convincingly to the conclusion that RAPG furnishes adequate conditions for sandy soil plantation.

I. RADIATION PREPARATION OF RAPG

R. Azzam

In 1980 we found that polyacrylamide gel (PAMG) seemed appropriate for conditioning sandy soil [1]. Since then, we have worked on a research programme dealing with methods for preparing and applying acrylamide polymeric gels. This has been financed partly by the International Atomic Energy Agency and supported by the Academy of Scientific Research and Technology.

EXPERIMENTAL

Radiation sources: We used a Canadian ^{60}Co gamma cell No. 220 and spent fuels of the nuclear reactor stored under water. The dosage distribution was calibrated by solid-state TL dosimeters of ^{7}LiF in teflon matrices. The average dose rate was calculated [2]. The integral dose was also determined by Fricke dosimeter of ferrous ammonium sulphate [2].

Monomer solutions were prepared and the polymer was identified, as described elsewhere [3, 4].

The degree of swelling is determined by soaking the gel in excess water for 24 h. It is the weight of water absorbed per unit dry weight of polymer.

RESULTS AND DISCUSSION

1.   Polyacrylamide gel preparation by ^{60}Co radiation, PAMG-1

The dose distribution inside the ^{60}Co irradiation chamber is determined by solid TL dosimeters. The results are shown in Fig. 1.

It can be inferred from the figure that the dose is uniform. The dose rate was calculated [2] to be 519.93 Gy/h. However, the value determined by Fricke dosimeter was 542.7 Gy/h. The difference between those values is attributed to the building-up factor in aqueous media [5].

Acrylamide in aqueous solutions was irradiated with ^{60}Co. The gelation dose is met at an absorbed dose of $\geqslant 2.5$ kGy, which exceeds the dose for complete
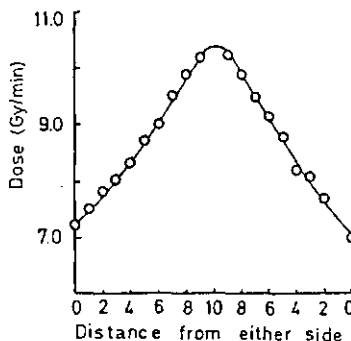
FIG.1.   Dose distribution inside a ^{60}Co irradiation chamber.

TABLE I. VARIATION OF SWELL-
ABILITY OF PAMG-1 WITH ABSORBED
DOSE, D, AT CONSTANT MONOMER
CONCENTRATION OF 1.4$\underline{M}$/L

| D (kGy)	Swelling degree
2.7	25.99
25.7	13.98
61.7	9.57
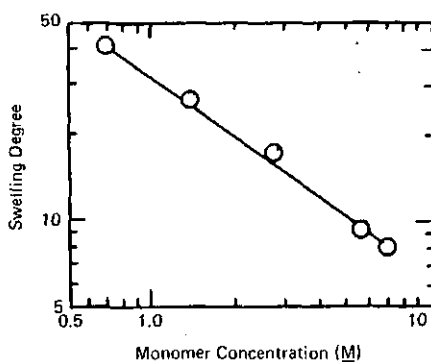
*FIG.2.   Effect of monomer concentration at constant dose of 2.7 kGy on the degree of swelling.*
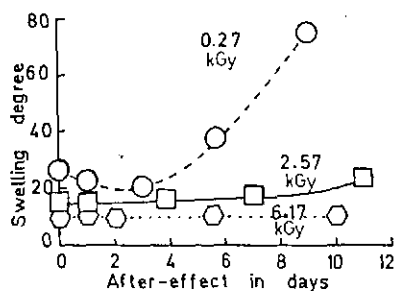
FIG.3. Swellability variation of polymers prepared at varying absorbed dose and constant monomer of 1.4M, within the post-effect.
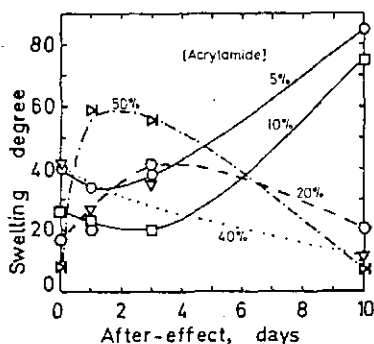
FIG.4. Swellability variation of polymers prepared at varying monomer concentration, but a constant dose of 2.7 kGy, within the post-effect.

conversion. Thus, the influences of dose and monomer concentration on the swellability of the gel were studied. The results are given in Table I and Fig. 2.

Table I shows that swellability decreases with dose. This is mostly considered to create some cross-links, the intensity of which increases with the dose. It is also inferred from Fig. 2 that the swellability decreases with monomer concentration. This may be attributed to compactness of the polymeric gel. Thus, hydrogen bond intensity among the macromolecules increases, which hinders the swelling process. Further evidence is gained by studying post-effects (Figs 3 and 4).

Figure 3 shows that at the lowest dose the degree of swelling increased with the post-effect. This can be due to segmental motion or to function group orientation. As the amide group is hydrophilic by nature its orientation in aqueous media would be towards the water phase. However, with increasing dose the intensity of cross-links increases. This restricts the orientation of macromolecules
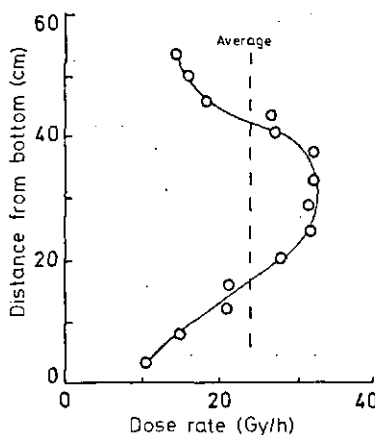
FIG.5.   Dose distribution inside irradiation chamber in the storage of spent reactor fuels under water.

and therefore the change in hydroproperty of the gel. Consequently, at the highest dose no appreciable change in the swelling degree is seen. Moreover, in Fig. 4 two isopiestic points are manifested, and provide corroborating evidence for the structural changes of the macromolecules within the post-effect. However, the swelling degree increases at low monomer concentrations and decreases at high ones. Thus, the effect of gel compactness on decreasing swellability appears to be inevitable.

2.   Gel preparation by spent reactor fuel radiation, PAMG-2

Spent reactor fuel elements are stored under water. In a position surrounded by four elements the dose distribution is determined. The results are shown in Fig. 5.

Figure 5 shows that the radiation dosage is symmetrical in the irradiation position. The average dose rate is determined as being 24 Gy/h. The average energy of gamma radiation is found to approach 0.9 MeV.

Acrylamide in aqueous solutions is polymerized by radiation of the reactor fuel elements. The process behaves similarly to the previous one. Some peculiarities have come to light. The gelation dose is nearly one-fourth that of ^{60}Co while the swelling degree is fourfold the latter. These are attributed to the low dose rate and continuous dissipation of the heat of polymerization. At low dose rates the monomeric segments are aligned almost quantitatively towards the water phase. Macromolecules collapsing by heat effect is avoided in irradiation under water. Thus, the method appears most advantageous.

TABLE II. EFFECT OF DOSE AND MONOMER CONCENTRATION ON
ACRYLAMIDE POLYMERIZATION IN ACETONE-WATER MIXTURE

| D (kGy)	0.59	1.15	1.68	2.81
M ($\underline{M}$/L)		Conversion (q) in %		
2.8137			96.62	100
4.2206	86.30	93.60	99.12	100
7.0343	87.03	94.77	100	100
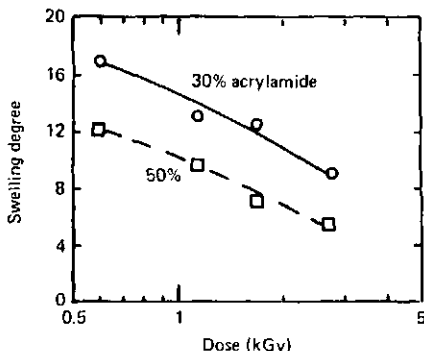
FIG. 6.   *Swellability of gels prepared in an acetone-water system.*

3.   Two-phase polymerization system

Acrylamide polymerization in acetone-water mixture was studied using ^{60}Co radiation. The polymerization medium is at first examined by a varying acetone:water volumetric ratio at constant absorbed dose. The results showed that the conversion stood constant at acetone:water $\geqslant$55 vol.%. Thus, the poly-merization medium employed is composed of 60:40 acetone:water. The effects of the dose and monomer concentration on the conversion are given in Table II.

Table II shows that the conversion increases with absorbed dose and monomer concentration. This is expected from the kinetics of the process [6]. Moreover, the gelation dose is rather low. It is around 0.59 kGy.

The influence of the dose at two monomer concentrations on the swellability of the gel is shown in Fig. 6.
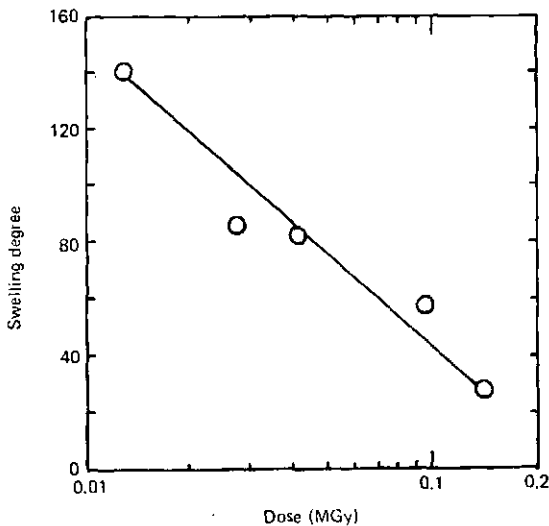
FIG.7. Effect of dose on the swellability of copolymers gelled by solid-state irradiation.

Figure 6 shows that the swelling degree decreases with increasing dose and monomer concentration. This is consistent with previous findings. However, the values of the swelling degree in the present system are much lower than PAMG-1. This may be due to the acetone, which is a poor solvent [7, 8]. When present, the hydrophilic group is mostly oriented into the polymeric matrix far from the environmental medium.

4. Gel preparation by solid-state irradiation of soluble polymer

Water-soluble acrylamide-acrylate copolymer is prepared [2, 3], and irradiated by ^{60}Co under vacuum in the solid state. The gelation dose is found to be greater than 10 kGy. The variation of the swelling degree with the dose is shown in Fig. 7.

Figure 7 shows that the swellability decreases with the dose, as previously noted. However, the values of the degree of swelling are much higher than PAMG-1. This is mostly attributed to the presence of the carboxylic group. It may substantially increase or fortify hydrogen bonding. Thus, the hydrophilicity of the gel is increased.

Accordingly, the hydrophilicity of polyacrylamide gel is presumably dependent on the structure of the macromolecule.
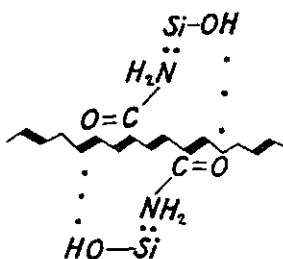
FIG.8.   The mechanism of soil co-ordination with PAMG.
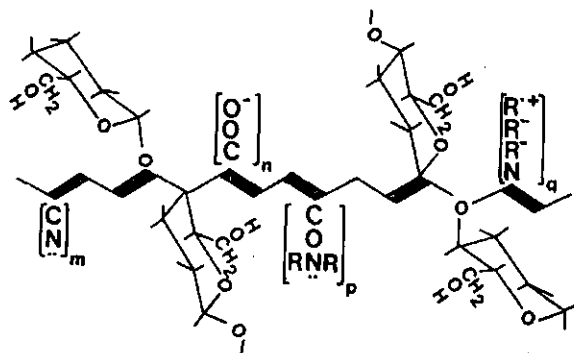
FIG.9.   Structural representation of RAPG.
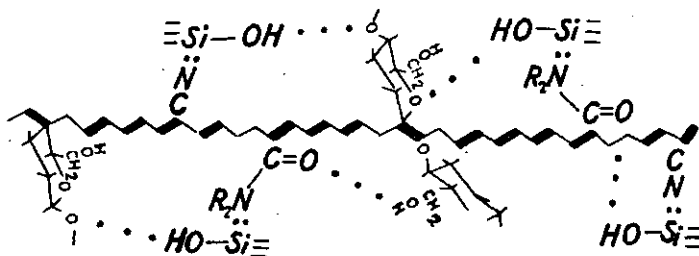
FIG.10.   The mechanism of soil stabilization with RAPG.

MECHANISM OF SOIL STABILIZATION WITH PAMG

There is ample evidence that polyacrylamide gel stabilizes sandy soil [9—11].
It is a truism that it does not follow either the adsorption or adhesion mechanisms.
It is surmised that the nucleophilic nitrogen of the amide group co-ordinates with
one silicon atom of soil particles. This may be geminated or fortified by hydrogen
bond formation between the carbonyl and silanol groups. Figure 8 shows the
proposed mechanism of soil stabilization with PAMG, which may be supported
by the findings of Griot and Kitchener [12] that PAM was adsorbed by newly
exposed silica surfaces. Immediately, the ignited silicas showed a similar
adsorbability [13].

Accordingly, the co-ordination and reinforcement sites are increased in the
reclaimer ameliorator polymeric gel — RAPG. It is a multi-functional acrylonitrile
base polymer grafted upon worthless cellulosic agricultural discards [14]. The
versatility of RAPG is evident from its structure (Fig. 9). The OH-rich binder
grows water-trees besides fortifying the co-ordination bonds. However, the co-
operative effect of function groups with the binder may be envisaged to increase
hydrogen bond induction. This explains the increase in soil stability and water
abstraction synergistically. The proposed mechanism is shown in Fig. 10. Also,
the swelling degree reached 750 times the dry weight of the gel. Moreover, the
cationic exchange capacity reaches 650 meq/100 g. This implies efficient
abstraction of cations by the acidic group while the basic one forms adducts with
the anions. Furthermore, there is recent evidence of increasing population of
bacterium rhizobia.

REFERENCES

[1] AZZAM, R., Commun. Soil Sci. Plant Analysis 11 8 (1980) 767.
[2] AZZAM, R., Sandy Soil Plantation in Semi-Arid Zones by Polyacrylamide Gel Conditioner
     Prepared by Ionizing Radiation, IAEA Contr. No. 2596/RB Progr. Rep., IAEA, Vienna
     (1981).
[3] AZZAM, R., SINGER, K., in Proc. 5th IUPAC Int. Conf. Modified Polymers 1,
     Bratislava (1979) 143.
[4] AZZAM, R., SINGER, K., Polym. Bull. 2 (1980) 147.
[5] LEIPUNSKII, O.I., NOVOZHILOV, B.V., SAKHAROV, V.N., The Propagation of
     Gamma Quanta in Matter, Pergamon Press, Oxford (1965).
[6] AZZAM, R., "Radiation Chemical Polymerization I. Theoretical Treatment", in Proc. 4th
     Int. Meeting Radiation Processing, Dubrovnik, Yugoslavia (1982).
[7] WADA, T. et al., J. Polymer Sci. A-1 Polym.Chem. 13 (1975) 2375.
[8] GROMOV, V.F. et al., Europ. Poly. Chem. 13 (1975) 2375.
[9] AZZAM, R., SIYAM, T., Ann. Agric. Sci. Moshtohor 13 (1980) 215.
[10] EL-HADY, O., AZZAM, R., Egypt. J. Soil Sci. 23 (1983) 2.

[11] AZZAM, R., Polymeric conditioner gels for desert soils, Commun. Soil Sci. Plant Analysis
      (1983) in press.

[12] GRIOT, O., KITCHENER, J.A., Trans. Faraday Soc. 61 (1965) 1026.

[13] GREENLAND, D.J., Med. Fak. Landbouww. State Univ. Ghent 37 3 (1972) 897.

[14] AZZAM, R., Egypt. Pat. Appl. No. 311, 7 June, 1981.

II. STRUCTURE STABILITY AND MAINTENANCE

R. Azzam and O.A. El-Hady

INTRODUCTION

Sand-dune fixation is an international objective. A long-lasting stable structure against wind and water erosion — with adequate inter- and intra-aggregate voids — is of supreme importance, which would enable beneficial cropping.

In this work, the stabilization of Sinai dune sand with reclaimer and ameliorator polymeric gel (RAPG), is studied. Maintenance of the structure formed is further determined.

EXPERIMENTAL

1. Soils: (a) Sinai dune sand from the Quantra — El-Arish road (99.9% fine sand); and (b) Fertile clayey soil from Belbis, Sharkia Governorate (46.2% clay and 0.63% organic matter (OM)).

2. RAPG application: RAPG dispersed in water is homogeneously mixed with sand, dried and passed through an 8-mm sieve.

3. Indices applied for structure evaluation:
    (a) Mechanical stability using a rotating "soil test" dry-sieving machine [1];
    (b) Water-stable aggregate size distribution by wet sieving; time of sieving 10 min [2]; and erosion index [3];
    (c) Hydraulic conductivity of 2–1 mm fractions after percolation for three hours under a constant water head;
    (d) Bulk density, pore size distribution and volume expansion [4, 5].

4. Maintenance of structure is revealed by three cycles of destruction of the formed structure to ≤1 mm and re-forming it again by wetting and drying. The water-stable aggregates >0.5 mm and erosion index were determined.

TABLE III. DE-AGGREGATION CHARACTERISTICS OF SINAI DUNE SAND
TREATED WITH RAPG

Treatment (%)	A_0 %	$\frac{1}{2}$ %	SP $\times 10^2$	R_D $\times 10$	W_∞	t_∞
Untreated	0.05	0.01	5.365	1.341	----	----
Non-ionic						
0.05	7.4	3.6	1.975	0.494	217	1.45
0.1	12	8.4	1.890	0.472	271	1.81
0.2	21	11	1.815	0.454	297	1.98
10% anionic						
0.05	9.6	5.4	1.928	0.482	243	1.62
0.1	26	14	1.757	0.439	321	2.14
0.2	50	24	1.563	0.391	395	2.63
20% anionic						
0.05	19	10	1.834	0.458	289	1.93
0.1	42	20	1.650	0.412	363	2.42
0.2	78	34	1.497	0.374	436	2.91
30% anionic						
0.05	22	12	1.782	0.445	308	2.05
0.1	62	31	1.523	0.381	422	2.81
0.2	85	52	1.247	0.312	557	3.71
40% anionic						
0.05	23	13	1.770	0.443	314	2.09
0.1	76	32	1.519	0.380	425	2.83
0.2	96	64	1.169	0.292	612	4.08

RESULTS AND DISCUSSION

1.   Mechanical stability against wind erosion

Different criteria used to evaluate the conditioning process are presented
in Table III. These are the total (A_0) and the most stable (Y_2) structural units
> 0.84 mm, the relative values of either instability parameter (SP) and
deaggregation rate (R_D), and the destructive mechanical action expressed by the
number of rotations (W_∞), or the time of dry sieving in minutes (t_∞) needed to
return the conditioned soil to its original state, i.e. the control [1].

Data reveal that the soil structure was improved with an increasing degree of anionicity and with the amounts of conditioners applied. Since soils with a content of non-erodible particles > 0.8 mm exceeding 60% were increased as soil resistant to wind erosion [6], RAPGs of 0.2% from 20% anionic, 0.1 and 0.2% from both 30 and 40% anionic, seem to be the most stable treatments. They show the highest values of Y_2, W_∞ and t_∞ and the lowest values of both SP and R_D.
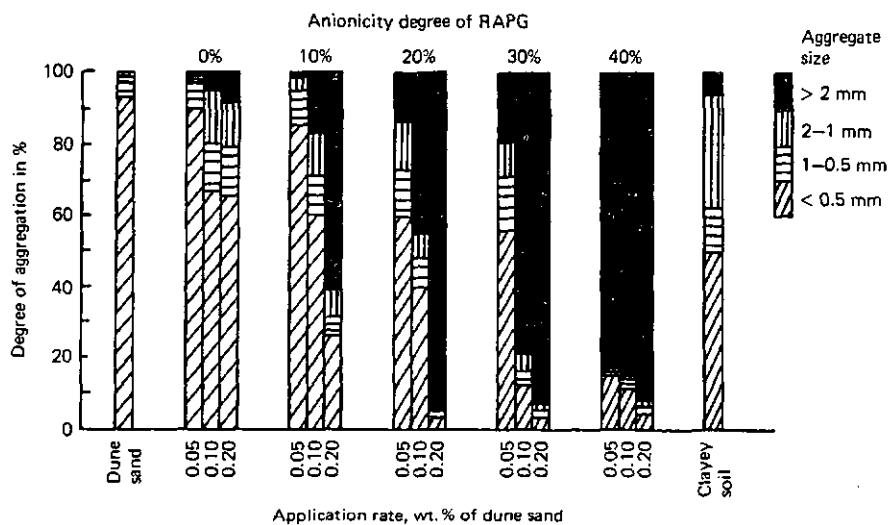

FIG.11.   Water-stable aggregate size distribution.

TABLE IV. MAXIMUM HYDRAULIC CONDUCTIVITY
(cm/h) OF 2−1 mm AGGREGATES

Gels rate (%)	Anionicity degree (%)				
	0	10	20	30	40
0.05	12.94	17.91	24.81	28.05	36.03
0.1	14.67	21.57	29.13	34.52	43.15
0.2	16.40	29.13	32.36	45.31	49.62

NB. Relevant value of the untreated dune sand is 10.14 cm/h.

TABLE V. WATER-STABLE AGGREGATES > 0.5 mm AND EROSION INDEX
DURING THREE CYCLES OF DESTRUCTION OF, AND RE-FORMING,
THE STRUCTURE BY SOIL WETTING AND DRYING

Treatment (%)	Water-stable aggregates > 0.5 mm			Erosion index		
	1st cycle	2nd cycle	3rd cycle	1st cycle	2nd cycle	3rd cycle
Untreated	6.8	6.1	6.0	0.290		
Non-ionic						
0.05	9.9	7.7	7.1	0.361	0.292	0.289
0.1	33.1	10.0	9.6	0.713	0.328	0.320
0.2	34.2	14.7	13.8	0.853	0.371	0.358
10% anionic						
0.05	13.9	9.8	8.6	0.400	0.323	0.317
0.1	40.3	28.6	25.3	1.239	0.972	0.877
0.2	74.8	50.7	46.7	3.257	2.113	1.812
20% anionic						
0.05	39.8	28.9	24.8	1.104	0.900	0.765
0.1	59.6	41.7	36.2	2.504	2.017	1.670
0.2	96.8	90.7	78.0	4.778	4.399	3.613
30% anionic						
0.05	44.2	33.8	29.6	1.359	1.205	1.073
0.1	88.2	77.8	73.2	4.102	3.661	3.184
0.2	97.4	90.4	86.9	4.727	4.044	3.494
40% anionic						
0.05	84.1	83.9	77.0	4.227	4.135	3.489
0.1	89.4	87.4	82.3	4.316	4.311	3.862
0.2	96.2	91.8	88.4	4.662	4.402	4.132
Clayey soil	49.8			0.99		

2. Water stability

The water-stable aggregate size distribution (Fig. 11) and the maximum
hydraulic conductivity values (Table IV) indicate that the structure of sand
treated by RAPGs is stable in the wet state. This is also revealed from data pre-
sented in Table V (1st & 4th columns) where the water-stable aggregates > 0.5 mm
reached more than 95% and the erosion index reached its maximum, while those
of clayey soil were < 50% and < 1.0, respectively.

TABLE VI. CHANGES[a] IN BULK DENSITY, VOID RATIO AND
SOIL POROSITY

Treatment (%)	Decrease in bulk density (g/cm^3)	Increase in void ratio	Increase in soil porosity	
			Micro [b]	Total
Non-ionic				
0.05	11.05	39.22	69.43	23.81
0.1	11.93	42.67	176.77	25.71
0.2	14.42	53.23	307.52	31.07
10% anionic				
0.05	13.37	48.71	114.42	28.81
0.1	19.61	76.94	233.07	42.26
0.2	23.15	95.04	317.26	49.88
20% anionic				
0.05	20.5	81.47	119.68	44.17
0.1	28.34	124.78	241.23	61.01
0.2	34.86	168.97	346.72	75.18
30% anionic				
0.05	26.52	113.79	169.40	57.11
0.1	31.77	146.98	325.68	68.51
0.2	38.45	197.20	471.43	82.81
40% anionic				
0.05	17.90	68.75	138.36	38.57
0.1	27.96	122.41	270.43	60.24
0.2	35.19	171.34	363.04	75.77

[a] Calculated as % relative to the untreated sand.
[b] For separating the macro from micro pores a radius of 14.5×10^{-3} mm, corresponding to
100 cm water suction, was used [5].

3.   Inter- and intra-aggregate voids

Beneficial changes in bulk density, void ratio, total porosity and micro-
porosity were achieved by conditioning sand (Table VI). These changes are
mostly related to the swelling degree of the gel. Moreover, the changes in the
parameters under study increased when the application rate was increased. This
is plausible. The maximum vertical swelling (Table VII) ranges between 2.7 and
35.0% for the untreated sand, and 0.4% of 30% anionic RAPG, respectively. This
can be compared with 20.5% for the clayey soil. No appreciable changes in the
volume of sandy soil were noticed during drying, while clayey soil showed high
shrinkage (17%) with cracking.

TABLE VII. VOLUME EXPANSION (%) OF SANDY SOIL AS
AFFECTED BY RAPGs

Anion-icity (%)	Rate of application (%)					Sandy soil	Clayey soil
	0.025	0.05	0.1	0.2	0.4		
0	4.0	4.7	5.2	5.9	8.7		
10	5.0	5.3	8.2	9.9	15.2		
20	6.2	8.3	13.3	20.2	25.2	2.7	20.5
30	9.1	11.5	17.5	28.7	35.0		
40	6.6	7.8	13.4	20.5	22.6		

4.   Maintenance of structure

The structure obtained is highly maintained after complete destruction within
the studied cycles. Table V shows that the water-stable aggregates > 0.5 mm and
erosion index are greater as the application rate and anionicity of RAPG become
higher. Insignificant changes within the three cycles are noticed at anionicity
⩾ 20% and rates ⩾ 0.1%. This indicates the resistance of structured sand to break-
down by tillage.

CONCLUSIONS

This work verifies the mechanism envisaged in Part I. The advantage of the
present bonded structure is that it is self-dependant. Its formation requires no
external chemicals or environmental conditions, which is why it is restored
instantaneously.

REFERENCES

[1]   EL-HADY, O.A., Criteria to evaluate soil conditioners for aggregate formation and wind
      erosion control, Egypt. J. Soil Sci. 24 (1) (1984) in press.
[2]   KEMPER, W.D., "Aggregate stability", Methods of Soil Analysis Part I (BLACK, C.A. et al.,
      Eds) Agronomy 9, Am. Soc. Agron., Madison (1965) 511−19.
[3]   VANDEVELDE, R., DE BOODT, M., GABRIELS, D., Determination of an erosion index
      for conditioned soils in accordance with data of the rainfall simulator, Pedologie 24 (1)
      (1974) 5−16.
[4]   BLACK, C.A. et al. (Eds), Methods of Soil Analysis Part 1, Am. Soc. Agron., Madison (1965).
[5]   LOVEDAY, J., Methods for Analysis of Irrigated Soils, Tech. Commun. No. 54, Common-
      wealth Bureau of Soils, Commonwealth Agricultural Bureaux (1974).
[6]   PASÀK, V., "Determination of the potential wind erosion of soil", in Trans. 10th Int.
      Congr. Soil Science 6, Moscow (1974) 80.

III. WATER PRESERVATION

R. Azzam and O.A. El-Hady

INTRODUCTION

Deserts suffer from droughts, and rainfall distribution is poor in semi-arid zones. Therefore, the improvement of water preservation in sandy soils is profoundly important, and this is the aim of the present work.

EXPERIMENTAL

1.   Soils and gels examined

These are presented in Table VIII. The application rates for sandy soil varied from 0.0 to 4 g/kg soil.

2.   Moisture characteristics

Soil-moisture equilibrium values were determined over a range from 0.0 to 15 atm, using a pressure cooker and pressure membrane. A biological method to determine wilting percentage was also carried out [1, 2].

3.   Evaporation

Soil aggregates < 4 mm were carefully packed in plastic columns to simulate the bulk density of each treatment. These were saturated and exposed to an evaporation process under the climatic conditions of Inshas. The water loss through evaporation was periodically determined by weight. The first evaporation cycle was finished when the control lost all its water content. This cycle was repeated six times, each cycle lasting eight to ten days.

4.   Intrinsic permeability and mean pore diameter

The hydraulic conductivity was measured [2]; data were corrected to avoid variation in temperature; and intrinsic permeability and mean soil pore diameter were calculated [3].

TABLE VIII. SOME ANALYTICAL PROPERTIES OF THE SOILS AND
GELS STUDIED

Soil type	Coarse sand 2000– 200 μm	Fine sand 200– 20 μm	Silt 20– 2 μm	Clay <2 μm	CaCO$_3$ (%)	OM (%)	TSS (%)	pH	CEC (meq/ 100 g)
Inshas sandy soil	86.2	10.5	1.1	0.9	0.45	0.02	0.11	8.0	0.91
Clayey soil	2.7	18.2	31.3	46.2	2.33	0.63	0.14	7.9	41.60

Studied gels	Non-ionic	10% anionic	20% anionic	30% anionic	40% anionic
Swellability	190	370	450	750	400
CEC (meq/100 g soil)	150	189	263	445	650

CEC = cation exchange capacity.
TSS = total soluble salts.

RESULTS AND DISCUSSION

Figure 12 illustrates the moisture characteristics of sandy Inshas soil as
affected by RAPG treatments. These were compared with those of clayey soil.
The applied conditioners increased the soil-water holding capacity and water
retained in soil at different suctions. A greater increase was obtained by increasing
gel concentrations. Although the total water-holding capacity of sand treated
with 0.2% of the 30% anionic RAPG is only about three times that of the untreated
sand it can retain, at its field capacity, over nine times the amount of water
retained under the same conditions by sand alone. The available moisture was
more than 15 times that of the untreated sand and exceeded that of fertile clay
by 11%.

RAPG also reduces water evaporation from the soil (Fig. 13). Moreover, at
the end of the evaporation cycle the evaporation adjusted to unity for the control
decreased to 0.67 and 0.61 for the 0.2% of 30% anionic RAPG and clay, respect-
ively (Table IX, first column). Therefore, a corresponding increase in water
retention in soil is evident. Under Inshas agroclimatological conditions ($E_0 = 5.1$
and 6.5 mm/d during March and April, respectively), while the clayey soil reached
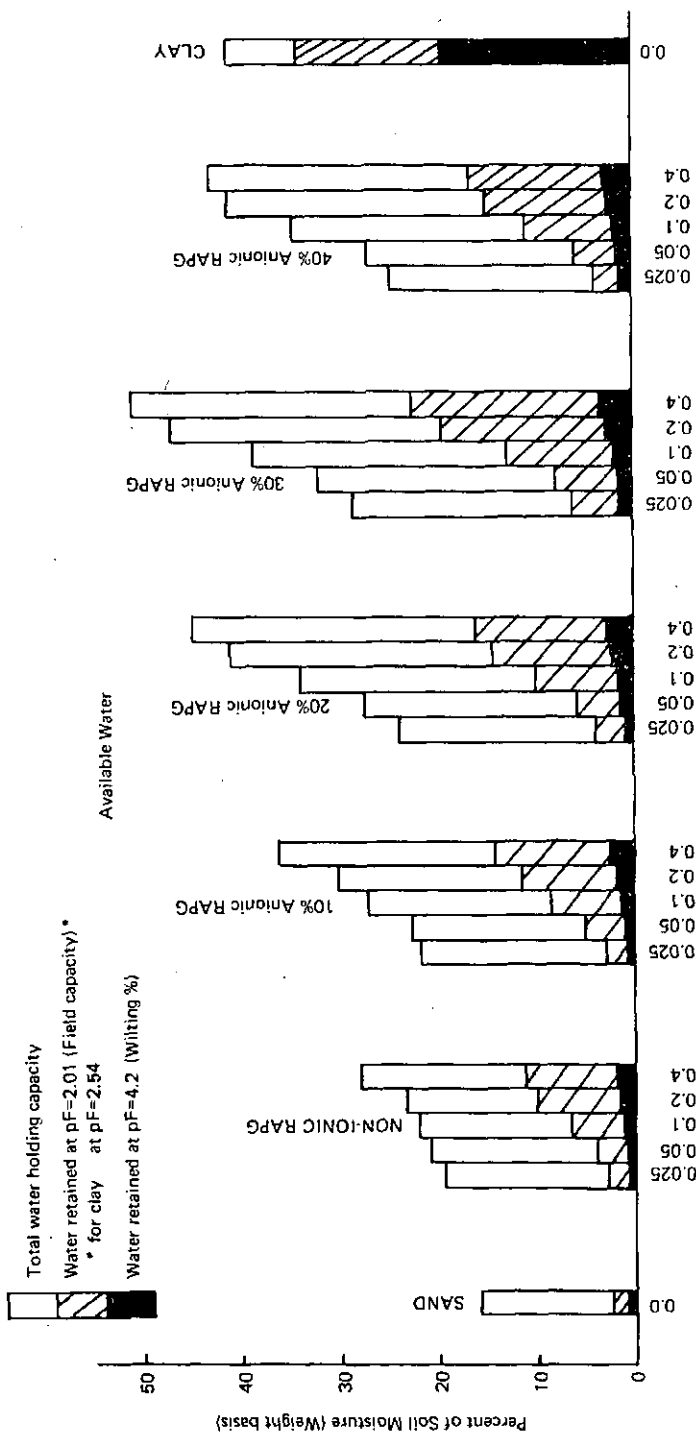
FIG. 12. Available water as affected by treating Inshas sandy soil with RAPG, compared with that of clayey soil.
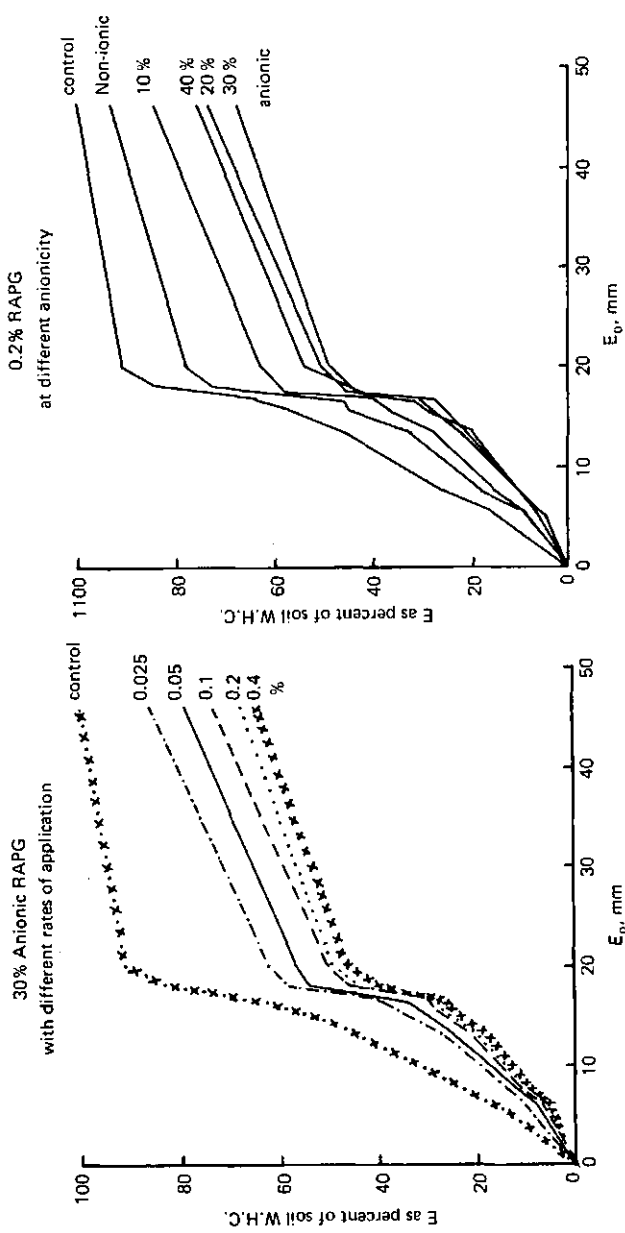
FIG.13.   Effect of RAPG on water evaporation from Inshas sandy soil (F = evaporation from soil (mm); E₀ = evaporation from the free water surface (mm)).

TABLE IX. ADJUSTED WATER EVAPORATION[a] FROM SANDY SOIL TREATED WITH RAPG DURING SIX CYCLES OF WETTING AND DRYING

Treatment conc. (%)	Cycle number:					
	1st	2nd	3rd	4th	5th	6th
Control	1.00	1.00	1.00	1.00	1.00	1.00
Non-ionic RAPG						
0.025	0.999	0.983	0.985	0.990	0.996	0.995
0.05	0.984	0.971	0.979	0.975	0.982	0.967
0.10	0.972	0.939	0.917	0.937	0.921	0.909
0.20	0.940	0.922	0.913	0.931	0.906	0.901
0.40	0.909	0.879	0.882	0.876	0.834	0.805
10% anionic RAPG						
0.025	0.987	0.963	0.971	0.965	0.970	0.944
0.05	0.982	0.939	0.963	0.946	0.952	0.913
0.10	0.921	0.874	0.905	0.911	0.900	0.895
0.20	0.885	0.839	0.896	0.873	0.865	0.832
0.40	0.873	0.775	0.783	0.778	0.770	0.726
20% anionic RAPG						
0.025	0.953	0.904	0.933	0.940	0.962	0.802
0.05	0.886	0.809	0.835	0.843	0.802	0.776
0.10	0.856	0.779	0.801	0.790	0.782	0.751
0.20	0.813	0.721	0.783	0.766	0.700	0.666
0.40	0.796	0.670	0.672	0.653	0.619	0.598
30% anionic RAPG						
0.025	0.875	0.843	0.864	0.853	0.869	0.789
0.05	0.792	0.771	0.789	0.772	0.783	0.732
0.10	0.749	0.719	0.711	0.703	0.698	0.710
0.20	0.670	0.662	0.662	0.651	0.646	0.633
0.40	0.596	0.631	0.583	0.576	0.534	0.530
40% anionic RAPG						
0.025	0.864	0.868	0.883	0.879	0.890	0.861
0.05	0.830	0.816	0.801	0.836	0.821	0.788
0.10	0.795	0.788	0.763	0.782	0.756	0.745
0.20	0.755	0.741	0.710	0.721	0.698	0.648
0.40	0.699	0.701	0.672	0.633	0.596	0.573
Evaporation from free surface water						
	47.2	46.5	46.8	48.1	47.9	49.4

[a] $E_{adj.} = (E_{tr}/WHC_{tr}) \cdot (WHC_s/E_s)$ where E and WHC are the cumulative evaporation and total water-holding capacity, respectively, while tr and s are the treated soil and control, respectively.

TABLE X. INTRINSIC PERMEABILITY (K')
AND MEAN PORE DIAMETER (ϕ) OF
INSHAS SAND TREATED WITH RAPG

Treatment (%)	K' (m²)	ϕ (μm)
Untreated	8.69	16.7
Non-ionic		
0.05	6.40	14.3
0.1	4.83	12.4
0.2	4.26	11.7
10% anionic		
0.05	5.58	13.4
0.1	4.62	12.2
0.2	3.94	11.3
20% anionic		
0.05	5.44	13.2
0.1	4.11	11.5
0.2	3.52	10.6
30% anionic		
0.05	5.26	13.0
0.1	3.40	10.4
0.2	2.79	9.5
40% anionic		
0.05	5.12	12.8
0.1	3.76	10.9
0.2	3.36	10.4

its wilting percentage after one week, the sand treated with 0.2% of 30% anionic
RAPG can remain with enough available moisture for plants for about two weeks.
Moreover, water loss through evaporation was nearly constant over six successive
cycles of wetting and drying (Table IX). This reveals that RAPG remained fully
effective in soil during the period of study and indicates the stability of the
structure formed and the slow biodegradability of the prepared gels.

Also, to a great extent RAPG decreased the vertical water movement under
saturated conditions and the mean diameter of soil pores (Table X), indicating
decreasing water and nutrient losses by leaching or by deep percolation.

REFERENCES

[1]   BLACK, C.A., EVANS, D.D., ENSMINGER, L.E., WHITE, J.L., CLARK, F.E. (Eds),
       Methods of Soil Analysis, Part I, Am. Soc. Agron., Madison (1965).
[2]   LOVEDAY, J., Methods for Analysis of Irrigated Soils, Tech. Commun. No. 54, Common-
       wealth Bureau of Soils, Commonwealth Agricultural Bureaux (1974).
[3]   DIELMAN, P.J., DE RIDDER, N.A., Elementary groundwater hydraulics. Drainage
       Principles and Applications. Publ. No. 16, ILRI, Wageningen (1972) 1–153.

IV. PLANTATION AND NUTRITIONAL STATUS

O.A. El-Hady, R. Azzam, A. Lotfy, M. Hegela

INTRODUCTION

Arid zones furnish inadequate environmental conditions for germination and
nursery agriculture. So, considerable failure is expected, especially with sandy
soils. This work aims to find out the proper sand/RAPG combination for growing
sensitive plants.

EXPERIMENTAL

Greenhouse experiments with pepper *(Capsicum Frutescens* Var. California
Wonder) were carried out using Inshas sandy soil. The sand is treated by RAPGs with
different anionicity at different rates up to 0.4%. A fertile clayey soil was chosen
for comparison. The data of the original soils and gels are given elsewhere [1].
Thirty seeds were planted in < 4 mm aggregates uniformly packed in pots to
simulate bulk density of each treatment. All pots were adjusted to the same
moisture percentage, i.e. 60% soil-water holding capacity, twice a week. After
12 days the plants were thinned to 10 per pot. Complex fertilizer containing both
macro- and micro-nutrients was used at the normal rates. Forty days after sowing
the transplants were investigated [2–4].

RESULTS AND DISCUSSION

Figure 14 illustrates the germination percentage of pepper seeds 12 days after
sowing. It shows that 100% germination lies at 0.1% of 30% anionic RAPG. The
corresponding values for untreated sand and clayey soil were 51.5 and 77%,
respectively.
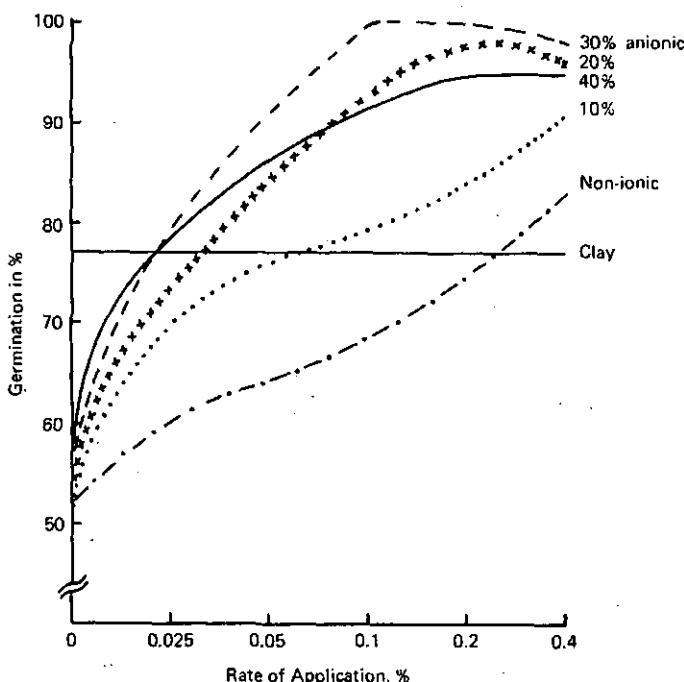
FIG.14. Germination of pepper seeds in Inshas sandy soil as affected by RAPG additions.

Similarly, growth continued, going significantly higher in conditioned sand than in the control. Moreover, the increase in the transplant's height for the treated sand exceeded that for clay by 38—55% according to the degree of RAPG anionicity and application rates (Fig. 15).

The dry weight of pepper transplants 40 days after planting is given in Table XI. This implies a further advantage of the conditioned sand. The recorded decrease in dry weight with high rates of conditioners could be attributed to gels' swellability, and consequently the high moisture retention of the treated sand over the needs of transplants. The effect of the anionicity degree on the retention and release of plant nutrients may be another reason.

Regarding the relation between the dry-matter production and evapotrans-piration, data in Table XII indicate the beneficial effect of the gels studied on water-use efficiency by plants. This could be explained on the basis of decreasing evaporation [1] and the increase in dry-matter production relative to the evapo-transpired water. In other words, RAPG can convert soil-water evaporation into plant transpiration.
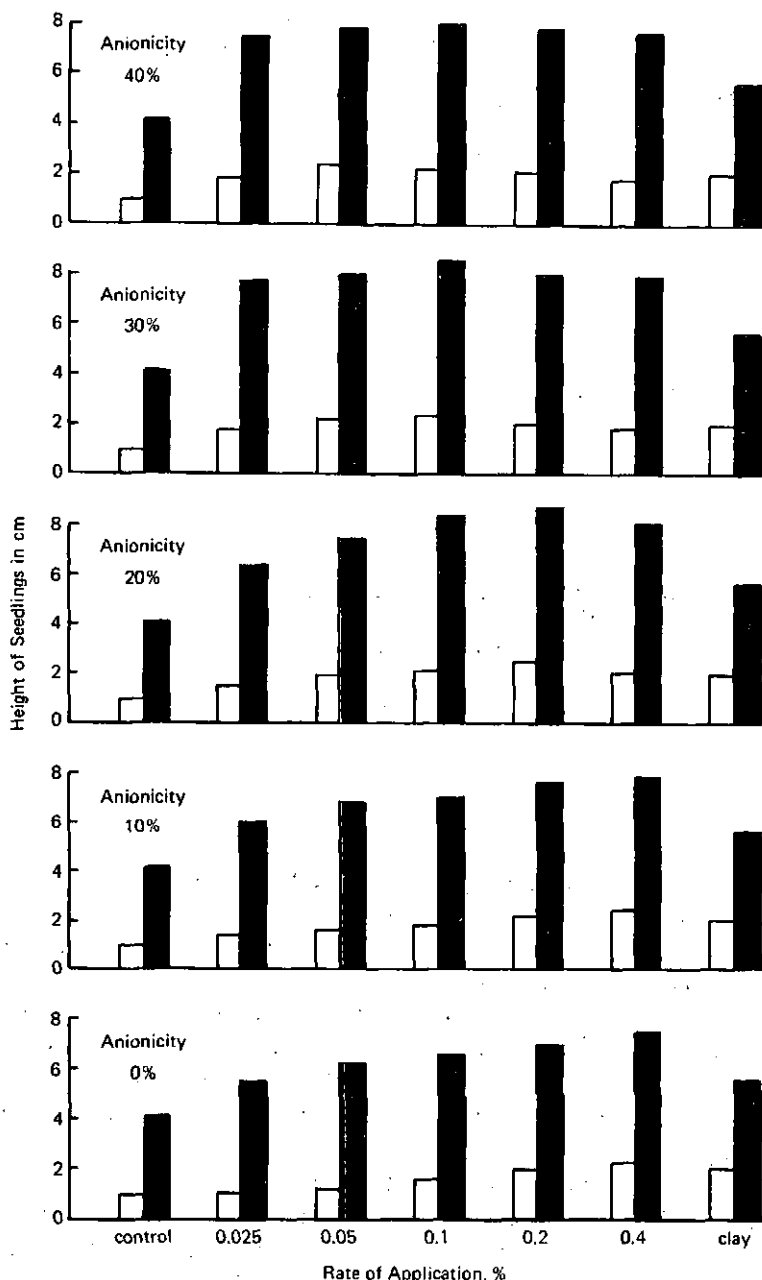
FIG.15. Height of pepper seedlings 20 days (white) and 40 days (black) after plantation as affected by anionic RAPG additions.

TABLE XI. EFFECT OF RAPG ON DRY WEIGHT OF SEEDLINGS (40 DAYS)
(mg/plant)

Application rate (%)	Anionicity of RAPG				
	0%	10%	20%	30%	40%
0.025	15.42	17.78	20.76	23.65	22.65
0.05	17.72	20.97	24.61	26.58	25.03
0.1	22.48	24.15	28.18	29.32	28.00
0.2	25.20	26.00	28.86	28.15	26.05
0.4	27.77	28.61	27.32	26.34	24.31

TABLE XII. EFFECT OF TREATING INSHAS SANDY SOIL WITH RAPG
ON WATER-USE EFFICIENCY[a] BY PEPPER TRANSPLANTS
(40 days after sowing)

Application rate (%)	Anionicity degree				
	Non-ionic	10%	20%	30%	40%
0.025	0.5535	0.5988	0.6850	0.7326	0.6793
0.05	0.5698	0.6491	0.7765	0.8172	0.7603
0.10	0.6887	0.7536	0.8132	1.1237	0.8367
0.20	0.7921	0.8197	0.9464	1.0078	0.9311
0.40	0.8362	0.8834	0.9078	0.9431	0.8985

[a] g dry matter/kg water.
Water-use efficiency for untreated sandy soil = 0.5410.
Water-use efficiency for fertile clayey soil = 0.7509.
Each figure is the mean of four replicates.

The uptake of macro-nutrients by pepper transplants is illustrated in
Fig. 16. It shows that N, P and K uptake generally increases with RAPG appli-
cation rates. Nitrogen uptake reached 225.5 and 270.1% of the untreated sand
at rates of 0.1 and 0.2%, respectively. This is twice that of the fertile clayey soil.
The phosphorus uptake was more than five times that of the control by treating
sand with 30% anionic RAPG at the rate of 0.2% or more. The increase in P uptake
reached 250% of that of the clayey soil. On the other hand, the increase in
K uptake reached 146% compared with the untreated sand at the 0.4% of 30%
anionic RAPG. This is more or less 2.5 times that of clayey soil.
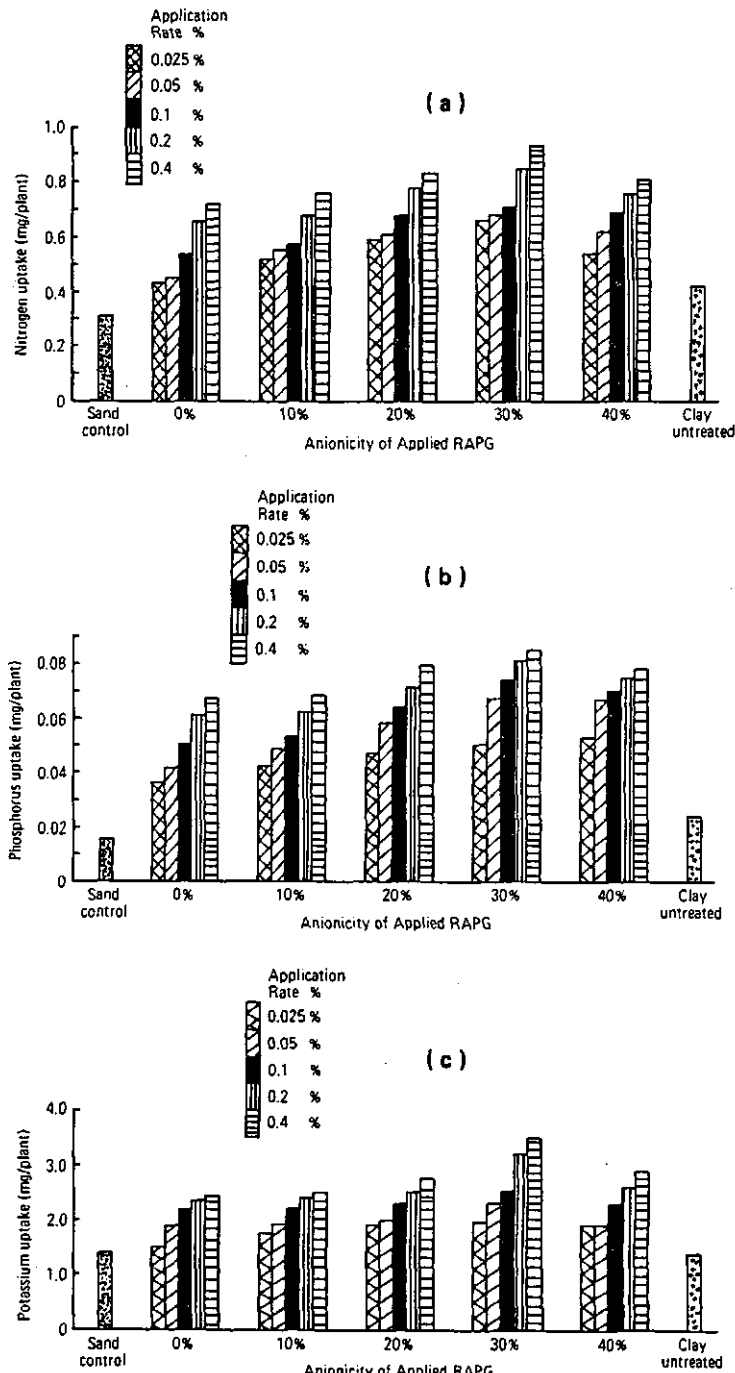
FIG.16.   *Uptake of (a) nitrogen, (b) phosphorus, (c) potassium in mg/plant, by pepper plants as affected by RAPG.*
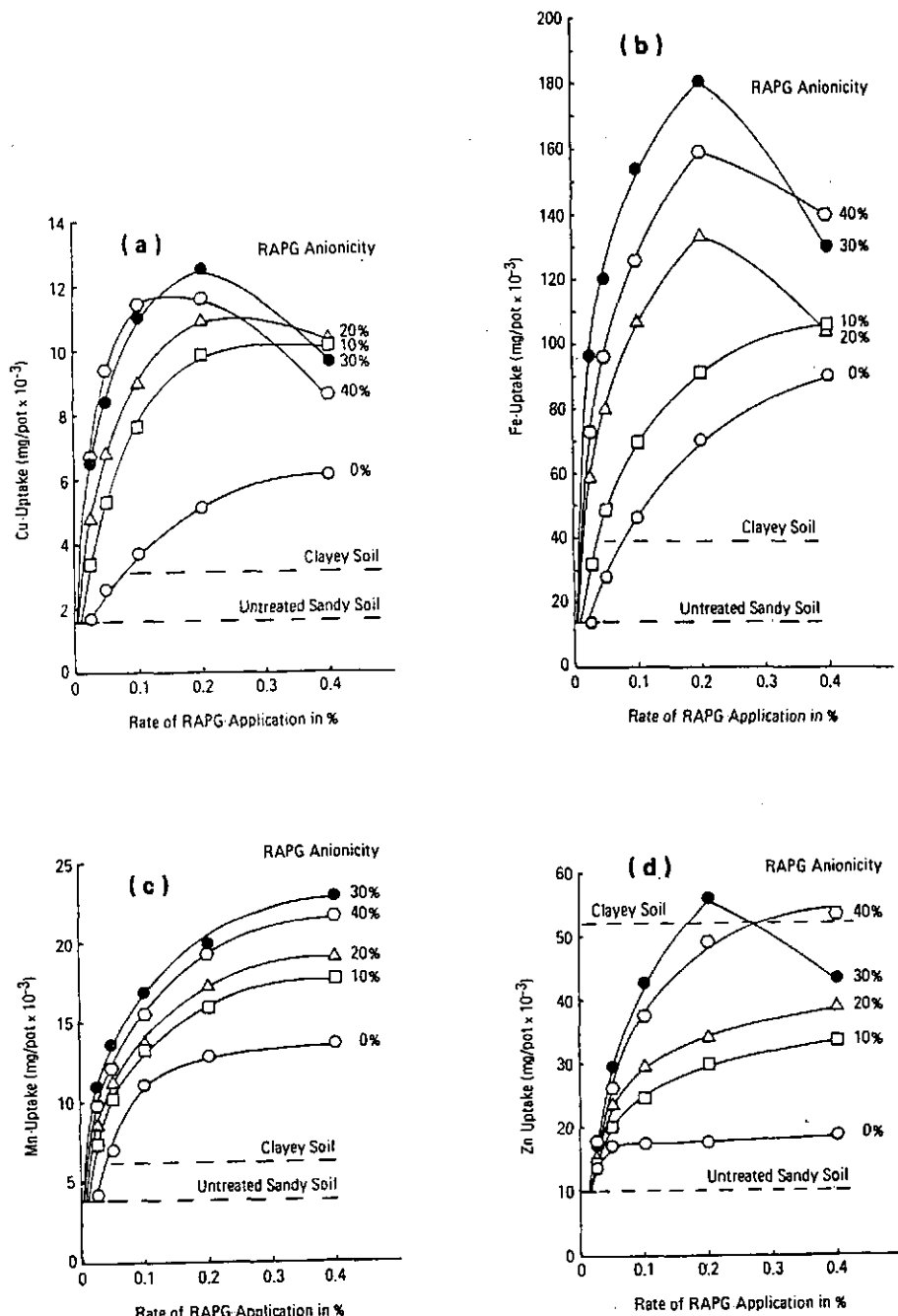
FIG.17. Micro-nutrient uptake (mg/pot) by pepper transplants as affected by RAPG treatment.
(a) Copper; (b) Iron; (c) Manganese; (d) Zinc.

TABLE XIII. FERTILIZER-USE EFFICIENCY BY PEPPER TRANSPLANTS AS AFFECTED BY RAPG ADDITION

Treat-ment & concen-tration	N	P	K	Fe $\times 10^{-2}$	Zn $\times 10^{-3}$	Mn $\times 10^{-2}$	Cu $\times 10^{-3}$	% increase over control
Control, sand	8.60	9.00	11.13	51.23	27.82	48.60	24.89	
Non-ionic RAPG (%):								
0.025	9.35	9.78	12.10	55.68	30.24	52.82	27.06	8.7
0.05	10.74	11.24	13.90	63.98	34.75	60.70	31.09	24.9
0.1	13.62	14.26	17.63	81.14	44.07	76.98	39.43	58.4
0.2	15.27	15.98	19.77	90.98	49.41	86.31	44.21	77.6
0.4	16.83	17.61	21.78	100.25	54.45	95.10	48.72	95.7
10% anionic RAPG (%):								
0.025	10.78	11.28	13.95	64.19	34.86	60.89	31.19	25.3
0.05	12.71	13.30	16.45	75.71	41.12	71.83	36.79	47.8
0.1	14.64	15.32	18.94	87.19	47.36	82.71	42.37	70.2
0.2	15.76	16.49	20.39	93.85	50.97	89.03	45.61	83.2
0.4	17.34	18.14	22.44	103.27	56.09	97.97	50.19	101.6
20% anionic RAPG (%):								
0.025	12.58	13.17	16.28	74.95	40.71	71.10	36.42	46.3
0.05	14.91	15.61	19.30	88.83	48.25	84.27	43.17	73.4
0.1	17.08	17.87	22.10	101.74	55.26	96.51	49.44	98.6
0.2	17.49	18.31	22.64	104.20	56.59	98.84	50.64	103.4
0.4	16.56	17.33	21.43	98.61	53.56	93.55	47.92	92.5
30% anionic RAPG (%):								
0.025	14.34	15.00	18.55	85.40	46.38	81.01	41.50	66.7
0.05	16.11	16.86	20.85	96.68	52.11	91.02	46.63	87.3
0.1	17.77	18.59	22.99	105.84	57.48	100.40	51.43	106.6
0.2	17.06	17.86	22.08	101.63	55.20	96.41	49.39	98.4
0.4	15.96	16.70	20.66	95.08	51.64	90.19	46.20	85.6
40% anionic RAPG (%):								
0.025	13.73	14.36	17.76	81.76	44.41	77.56	39.73	59.6
0.05	15.17	15.88	19.63	90.36	49.08	85.72	43.91	76.4
0.1	16.97	17.76	21.96	101.07	54.90	95.88	49.12	97.3
0.2	15.79	16.52	20.43	94.05	51.08	89.22	45.71	83.6
0.4	14.73	15.42	19.07	87.75	47.66	83.25	42.64	71.3
Fertile clayey soil	6.75	7.07	8.74	40.22	21.84	38.15	19.54	

Micro-nutrient uptake is given in Fig. 17. Generally, at low rates of RAPG application the uptake increases with the degree of anionicity, though at higher rates both 30 and 40% anionic RAPG may change positions. This behaviour goes in parallel with the change in the swellability of the polymeric gels, and consequently the water content of the treated soil. The increase in micro-nutrient uptake in treated sand with 0.2% of the 30% anionic RAPG reached 7.7, 222.6, 358.4 and 303.2% over that of the fertile clayey soil for Zn, Mn, Fe and Cu, respectively.

Fertilizer use efficiency data (dry matter produced by a unit of added nutrients) are presented in Table XIII, which also indicates the beneficial effects of RAPGs for sand conditioning. It is obvious that the highest efficiency lies at 0.1% of the 30% anionic RAPG treatment. This is about three times that of the fertile clayey soil.

CONCLUSIONS

Germination process, plant growth and dry-matter production are increased owing to the improvement in both soil structure and water regime. Moreover, the beneficial effect of RAPGs is evident from increasing nutrient uptake and efficiencies of both water and fertilizer use. At the rate of 0.1% of 30% anionic RAPG was superior compared with the others. This was applied successfully in field scale experiments [5].

REFERENCES

[1] AZZAM, R., EL-HADY, O.A., Part III of this paper.
[2] JACKSON, M.L., Soil Chemical Analysis, Prentice Hall (1967).
[3] BLACK, C.A. et al. (Eds), Methods of Soil Analysis, Part II, Am. Soc. Agron., Madison (1965).
[4] CHAPMAN, H.D., PRATT, P.F., Methods of Analysis for Soil, Plant and Water, University of California, Division of Agric. Sci. (1961).
[5] EL-HADY, O.A., AZZAM, R., LOTFY, A., Sand-RAPG combination simulating fertile clayey soil. V: Field application. To be published.

SOIL WATER: MANAGEMENT CONSIDERATIONS
(Session 6)

Chairman

J.A. ESTRADA
Peru

EFFECT OF SOIL-MOISTURE STRESS ON NITROGEN UPTAKE AND FIXATION BY PLANTS

M.M. MITROSUHARDJO
Center for the Application of
    Isotopes and Radiation,
Jakarta, Indonesia

Abstract

EFFECT OF SOIL-MOISTURE STRESS ON NITROGEN UPTAKE AND FIXATION BY
PLANTS.
    The effect of four levels of soil moisture, namely 25, 30, 35, and 40% (g/g) on nitrogen
uptake and fixation by plants was studied in a greenhouse experiment. Soybean and wheat
were used in this experiment. Both crops were grown in pots containing 7 kg loamy
alluvial soil. *Rhizobium japonicum* was used as an inoculant for soybean, one week after
planting. Nitrogen-15 labelled urea with 10% atom excess was applied to each pot with a dose
rate of 70 mg N/pot (20 kg N/ha) two weeks after planting. Soil moisture was regularly
controlled with porous-cup mercury tensiometers, and the amount of water consumed by plants
was always recorded. Water was applied to each pot with a distribution pipe which was laid
down in the centre of the soil depth, horizontally in a circular form, and was connected with
a smaller pipe to the soil surface. The result obtained showed that the amount of water
consumed by plants grown in a higher level of soil moisture was increased until soil aeration
problems arose. A different amount of water consumption between soybean and wheat was
observed at least until a certain period of growing time. Fertilizer nitrogen taken up by both
crops varied with the different levels of soil moisture. Generally, greater fertilizer nitrogen
was taken up by both crops grown in a higher level of soil moisture. The symbiotic fixation
of nitrogen was reasonable, although no clarification has been found about the role of the
four levels of soil-moisture treatment on it. A similar effect of soil-moisture stress on nodule
dry matter and acetylene reduction was found.

INTRODUCTION

Water is one of the most essential things for plant growth. During the growing
period of crops much water may be lost to the atmosphere through evapotranspi-
ration. Several hundred kilograms of water are lost from the aquatic herbaceous
plants by evapotranspiration for each kilogram of dry matter produced; however,
plants still contain water up to about 4--8 times their dry matter [1].
    The amount of soil-water storage in the soil profile does not always have
good effects on plant growth. When its availability is abundant, a bad effect will

occur because of aeration problems, while a lack of water will inhibit the evapo-transpiration rate; therefore, for these reasons the control of soil water is extremely necessary [2].

The presence of soil water allows the plant to absorb soil nutrient smoothly, including soil nitrogen, but not under conditions where there is a lack of soil water.

Generally, the amount of soil nitrogen is insufficient for plant growth, so that an additional input should be made, either through fertilizer nitrogen application or through biological dinitrogen fixation [3].

To measure the efficiency of fertilizer nitrogen taken up by plants, ^{15}N-labelled nitrogen fertilizer is applied so as to differentiate between fertilizer nitrogen and soil nitrogen taken up by plants. On the other hand, legume and non-legume crops (non-nodulated) are needed for measuring dinitrogen symbiotic fixation [3, 4].

The stress effect of soil moisture on the availability of soil nutrient has commonly been recognized; however, detailed information is still needed. It seems that the availability of soil nitrogen for plant growth is higher when there is sufficient soil water.

MATERIAL AND METHODS

A pot experiment to study the effect of soil-moisture stress on nitrogen uptake and fixation by plants was carried out in a greenhouse of the IAEA Seibersdorf Laboratory, Vienna, during the winter of 1981/1982. The temperature inside the greenhouse ranged from 20 to 30°C, while the intensity of solar radiation varied widely.

A completely randomized design was used in this experiment. Four levels of soil moisture were tested, namely 25, 30, 35, and 40% (g/g), and replicated three times. Soybean and wheat were used as experimental crops.

Each pot was filled with 7 kg air-dried loamy alluvial soil, and three plants (either soybean or wheat) were grown. *Rhizobium japonicum* was used as an inoculant for soybean one week after planting. ^{15}N-labelled urea with 10% atom excess was applied to each pot with a dose rate of 70 mg N/pot (20 kg N/ha), two weeks after planting, in soluble form to several locations in about 3–4 cm soil depth.

Water was applied to each pot by a distribution pipe which was laid down in the centre of the soil depth, horizontally in a circle, and connected by a smaller pipe to the soil surface. The soil moisture was regularly controlled with a porous-cup mercury tensiometer, and the amount of water consumed by plants was regularly recorded. A calibration curve was prepared before the experiment started. Both crops were harvested 79 days after planting.

Parameters used in this experiment were dry weight of plants, dry weight of nodules, acetylene reduction measurement, total nitrogen, fertilizer nitrogen uptake, and dinitrogen fixed by soybean crop [3--5].

RESULT AND DISCUSSION

Stress effect of soil moisture on total water consumption

The amount of water consumed by plants per pot varied among the four levels of soil-moisture treatment. Significant differences were found between 25, 30, and 35% soil moisture. It was observed that plants grown in a higher level of soil moisture consumed a higher amount of water. It could be explained that it took place owing to the effects of evaporation, transpiration and soil conditions, which influenced the consumption of soil water. Water might be easily evaporated under conditions of less soil retention or higher soil-water content. Plants grown in 35 and 40% soil moisture consumed a similar amount of total water. It could be explained that water might be transpired more from larger plants grown in a higher level of soil moisture (see Table I). By contrast, soil aeration would be a serious problem in excessive soil water, which could inhibit the rate of plant growth. It was observed that, with soil moisture higher than 35%, the problem of aeration occurred. A significant total water consumption in plants started at an earlier stage of growth up till the harvest time, might support these findings (see Table II and Fig. 1).

Total water consumption

The total water consumed by plants (lost by evapotranspiration) varied from 5.1 to 11.3 L/pot for soybean and from 4.5 to 9.2 L/pot for wheat grown in the four levels of soil moisture tested (see Table I and Fig. 2). A significantly higher water consumption was found in soybean than in wheat, namely at the moisture levels of 30, 35, and 40%, begun three weeks after planting until harvest time. It is clearly understood that soybean has a larger plant performance, particularly in leaf area index. The other aspect, that the generative growth stage of wheat started later than soybean, might also support this result.

To produce each kilogram dry matter of plant several hundred litres of water were lost by evapotranspiration (Fig. 3 and Table I). Both crop species released a similar quantity of water — 982 and 917 litres for soybean and wheat, respectively. This result was similar to the amount of water lost by evapotranspiration from aquatic herbaceous plants [1]. Of all the water treatments less

TABLE I. AVERAGE OF TOTAL WATER CONSUMED BY PLANTS PER POT (7 kg soil) UP TO HARVEST (79 days)

Level of soil moisture	Crops	Dry matter (g)	Total water consumption/pot (L)	Total water consumption/kg of dry matter (L)
25% (g/g)	Soybean	7.0	5.135	753.433
	Wheat	6.1	4.520	750.592
30% (g/g)	Soybean	7.8	8.718	1197.376
	Wheat	8.0	7.539	958.240
35% (g/g)	Soybean	12.4	11.307	966.730
	Wheat	10.1	9.211	917.844
40% (g/g)	Soybean	10.7	10.313	1011.517
	Wheat	8.7	9.001	1039.530
% CV		26.13	8.64	20.55
LSD(0.05) soil moisture		4.414	1.357	372.747
HSD(0.05) soil moisture		5.401	1.661	456.183
LSD(0.05) crops		–	1.160	–
HSD(0.05) crops		–	1.230	–

HSD = higher significant difference; LSD = lower significant difference; CV = coefficient variation.

TABLE II. AVERAGE CUMULATIVE TOTAL WATER CONSUMED BY PLANTS PER POT

Level of soil moisture	Crops	Weekly cumulative total water consumed by plants per pot										
		1 (L)	2 (L)	3 (L)	4 (L)	5 (L)	6 (L)	7 (L)	8 (L)	9 (L)	10 (L)	11 (L)
25% (g/g)	Soybean	0.097	0.334	0.515	0.779	1.093	1.453	1.914	2.656	3.358	4.003	4.905
	Wheat	0.107	0.341	0.529	0.781	1.048	1.316	1.680	2.236	2.784	3.384	4.260
30% (g/g)	Soybean	0.132	0.527	0.942	1.373	1.880	2.674	3.517	4.580	5.707	6.907	8.341
	Wheat	0.129	0.551	0.915	1.253	1.633	2.271	2.880	3.560	4.376	5.320	6.942
35% (g/g)	Soybean	0.156	0.699	1.182	1.672	2.258	3.259	4.224	5.407	6.884	8.501	10.542
	Wheat	0.133	0.641	1.064	1.474	1.933	2.675	3.326	4.137	5.122	6.730	8.318
40% (g/g)	Soybean	0.179	0.682	1.163	1.672	2.241	3.143	4.003	5.068	6.412	7.939	9.713
	Wheat	0.175	0.603	1.029	1.510	2.005	2.748	3.408	4.210	5.193	6.474	8.294
% CV		9.85	10.32	9.08	8.42	8.80	10.20	10.04	10.22	9.81	9.38	8.78
$LSD_{(0.05)}$	s. moist.	0.026	0.108	0.159	0.211	0.296	0.480	0.598	0.778	0.932	1.095	1.286
$HSD_{(0.05)}$	s. moist.	0.032	0.132	0.195	0.259	0.362	0.587	0.732	0.952	1.141	1.340	1.574
$LSD_{(0.05)}$	crops	—	—	—	0.181	0.253	0.410	0.511	0.665	0.797	0.936	1.099
$HSD_{(0.05)}$	crops	—	—	—	0.192	0.268	0.435	0.542	0.705	0.845	0.993	1.116
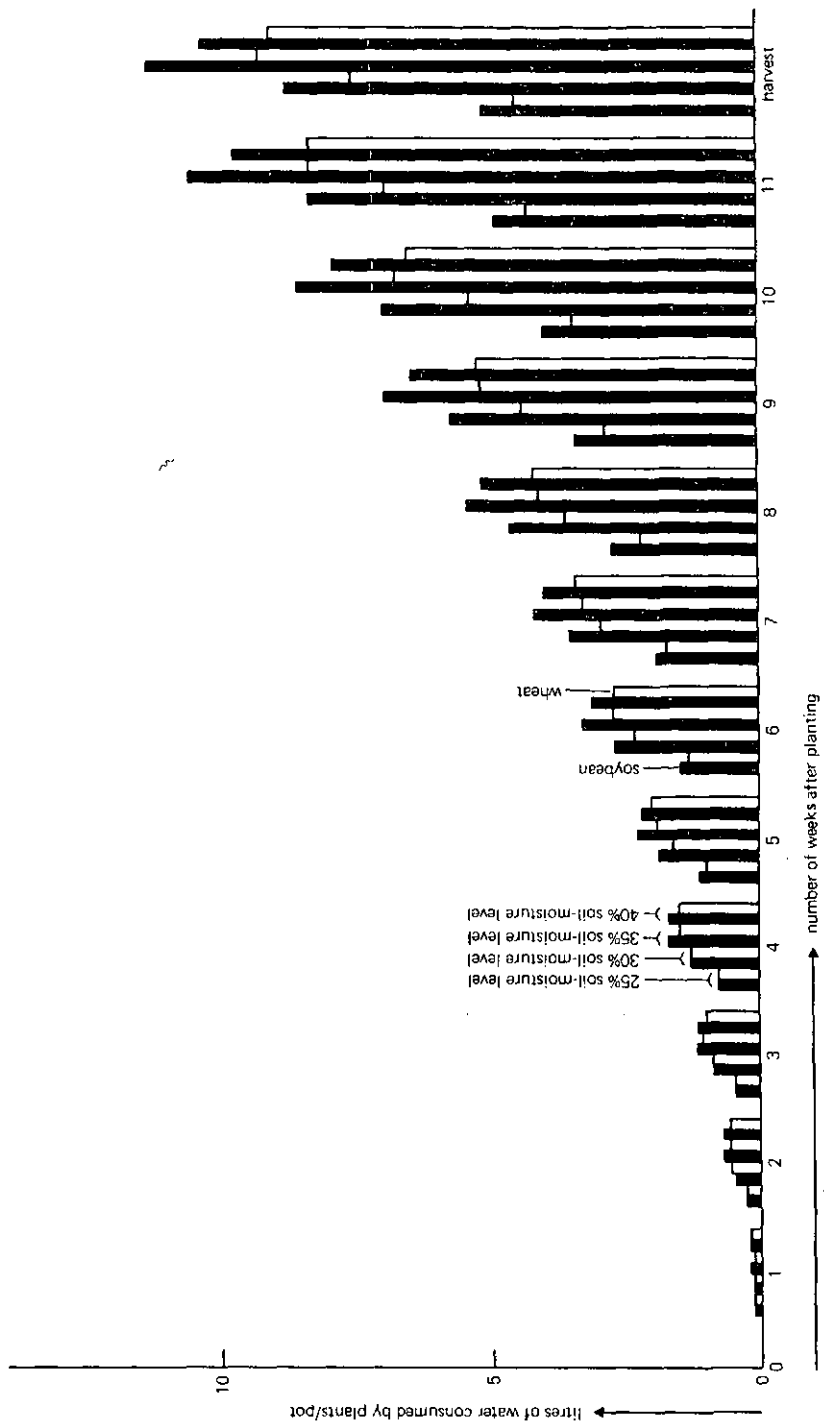
FIG.1. Average cumulative total water consumed by plants per pot.
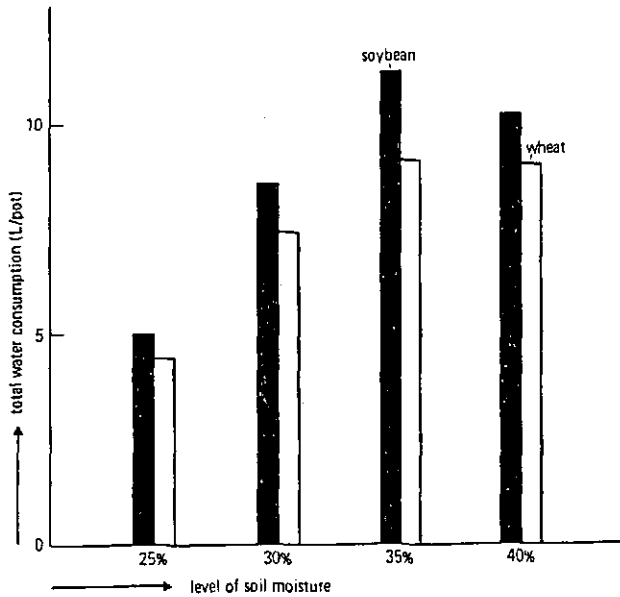
FIG.2. Average of total water consumption (L/pot).
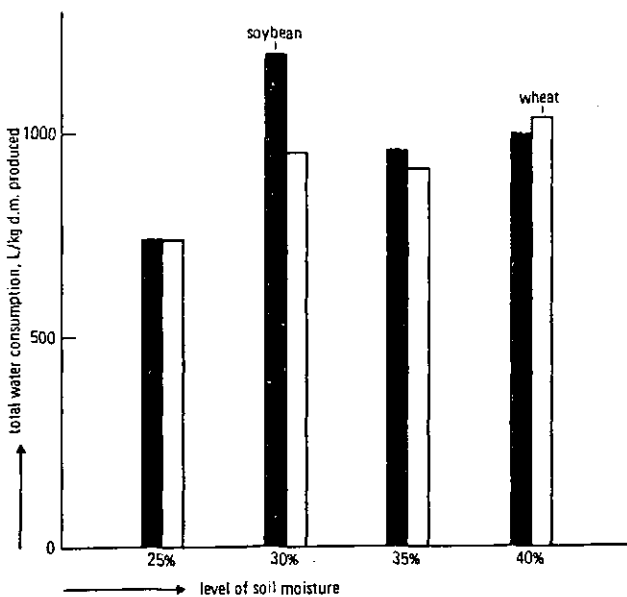
FIG.3. Average of total water consumption per kg dry matter produced. (d.m. = dry matter).

TABLE III. AVERAGE OF NITROGEN TAKEN UP AND FIXED BY PLANTS

Level of soil moisture	Crops	Dry matter (kg/ha)	% N	Total N (kg/ha)	Ndff (%)	Ndff (kg/ha)	%N fixed	Fixed N (kg/ha)
25% (g/g)	Soybean	1990	3.35	66.3	0.68	0.456	60.5	39.7
	Wheat	1752	2.85	50.9	1.71	0.877	–	–
30% (g/g)	Soybean	2219	3.24	72.6	0.68	0.480	44.8	36.8
	Wheat	2295	3.03	69.4	0.97	0.680	–	–
35% (g/g)	Soybean	3543	3.03	105.2	0.95	1.081	53.4	48.2
	Wheat	2876	3.13	90.1	1.49	1.350	–	–
40% (g/g)	Soybean	3048	3.33	100.5	1.56	1.649	44.6	42.1
	Wheat	2476	3.20	79.3	2.83	2.233	–	–
% CV		25.94	7.8	22.84	27.98	45.47	24.16	20.77
LSD$_{(0.05)}$ soil moisture		1251	–	34.6	0.72	0.956	–	–
HSD$_{(0.05)}$ soil moisture		1352	–	42.4	0.89	1.171	–	–
LSD$_{(0.05)}$ crops		–	0.397	–	–	–	–	–
HSD$_{(0.05)}$ crops		–	0.421	–	–	–	–	–
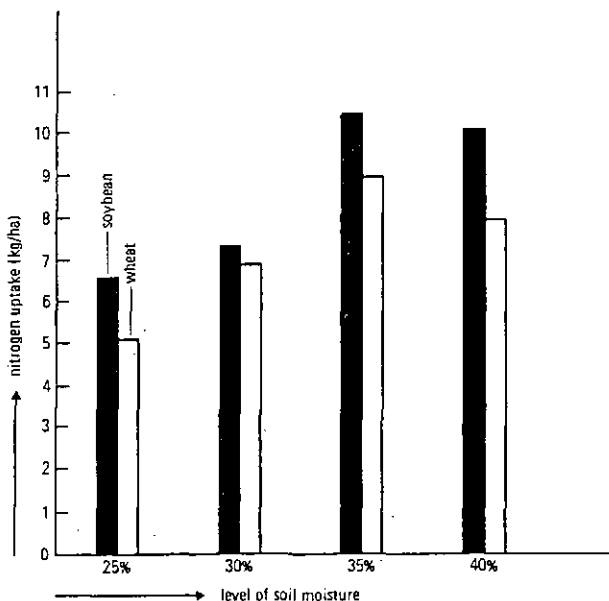
FIG.4. *Average of total nitrogen uptake.*

water was released from 25% soil moisture. This performance was affected by water firmly held in the soil particle which could inhibit the evapotranspiration rate.

Total nitrogen uptake

The stress effect of soil moisture on the total nitrogen uptake was observed in this experiment. Significant differences were found among the four levels of soil-moisture treatments, with the exception of between 25 and 30% and between 35 and 40%. A higher amount of total nitrogen uptake was observed at a higher level of soil moisture (see Table III and Fig.4). The result was supported by the general concept of nutrient solubility. No differences in the total nitrogen uptake in both crops were observed between 25% and 30% soil moisture. Under both conditions the soil-moisture stress on soybean as well as on wheat crops still existed. The insignificant differences between the 35% and 40% soil-moisture levels might be due to a sufficient water supply to plant growth, so that no difference in soil nitrogen absorption was observed. It seemed that an aeration problem occurred in soil with a moisture content higher than 35%.
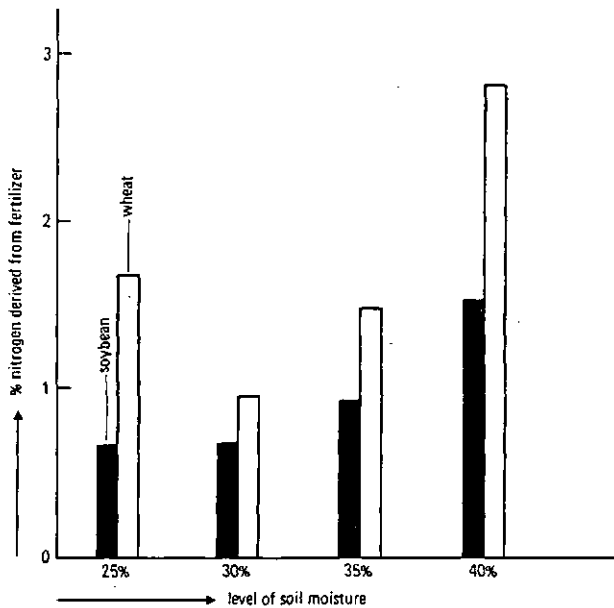
FIG.5.   Average of nitrogen derived from fertilizer in plants.
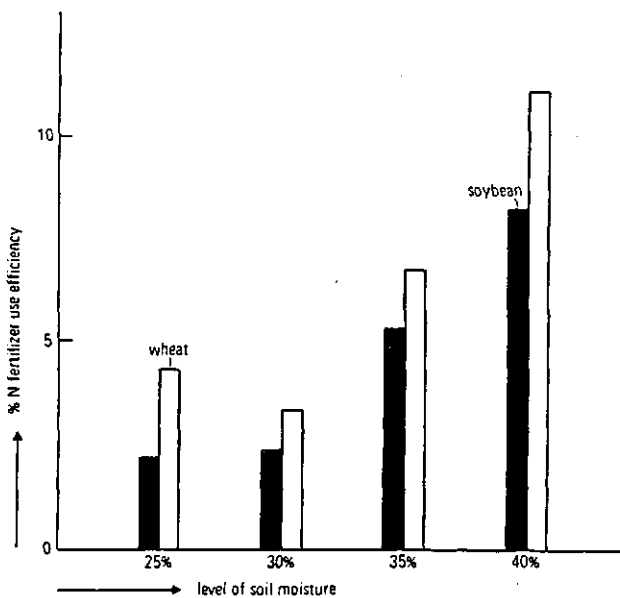
FIG.6.   Average of nitrogen fertilizer use efficiency.

TABLE IV. AVERAGE OF NITROGEN FERTILIZER USE EFFICIENCY

Level of soil moisture	Crop	% of N fertilizer use efficiency
25% (g/g)	Soybean	2.28
	Wheat	4.39
30% (g/g)	Soybean	2.40
	Wheat	3.40
35% (g/g)	Soybean	5.41
	Wheat	6.75
40% (g/g)	Soybean	8.25
	Wheat	11.17

Fertilizer nitrogen absorption

The amount of fertilizer nitrogen absorbed by plants varied with the levels of soil moisture where the plants grew. A higher amount of fertilizer nitrogen was absorbed by plants grown in a higher level of soil moisture (Figs 5 and 6 and Tables III and IV). Soybean absorbed less fertilizer nitrogen than wheat. The amount of fertilizer nitrogen absorbed by both crops was definitely low (see Table III and Fig.5). This result would be supported by the relatively dry conditions at the place where nitrogen fertilizer was applied. It is important to mention that nitrogen fertilizer was applied at 3—4 cm below the soil surface, while the water was applied at a depth of 7.5—10 cm, so that the problem of such a stress effect could not be eliminated, particularly in the low level of soil moisture. This condition could inhibit the absorption of nitrogen fertilizer, but not affect the soil nitrogen in the deeper layer where the moisture was still greater. A large amount of soil nitrogen will easily provide uptake to the plants. These conditions might support the results of this experiment which showed a higher total nitrogen, but a lower fertilizer nitrogen, uptake by plants. On the other hand, a higher amount of fertilizer nitrogen was taken up by wheat compared with that taken up by soybean, but relatively lower total nitrogen was absorbed by wheat than that absorbed by soybean, which indicated the obvious existence of symbiotic dinitrogen fixation by soybean.

TABLE V. DRY MATTER OF NODULES AND ACETYLENE REDUCTION AT HARVEST TIME
(79 days after planting)

Level of soil moisture	Crops	Dry matter (g)	Dry matter of nodules/pot (g)	Acetylene reduction per plant per hour (nmol)
25% (g/g)	Soybean	7.3	80	154
		5.5	20	–
		8.1	60	–
30% (g/g)	Soybean	5.8	30	–
		10.8	40	–
		6.7	40	21
35% (g/g)	Soybean	8.1	30	17
		12.3	146	1276
		16.8	161	765
40% (g/g)	Soybean	14.0	150	891
		10.2	50	59
		7.8	20	24
% CV		32.43	75.2	141.20
LSD(0.05)		–	–	–
HSD(0.05)		–	–	–

Dinitrogen symbiotic fixation

Dinitrogen fixed by soybean through symbiosis with *Rhizobium japonicum* took place to a reasonable degree, although no clarification has been given for the different stress effects of the four levels of soil moisture on its process. The insignificantly different effects of the four levels of soil moisture on symbiotic dinitrogen fixation might be due to the condition surrounding the soybean roots, which was still suitable for the activity of *R. japonicum*. The suitable amount of dinitrogen fixation might be obtained at the mid-pod filling stage where the activity of *R. japonicum* was increased to fix dinitrogen from the atmosphere, while at the same time the light intensity was gradually improving (weather changing from deep winter to spring). These results were in line with results obtained in other experiments [6].

Dry matter of nodule production

Observation on the dry matter of nodules usually supports well the symbiotic dinitrogen fixation. The same trends were also observed in this experiment, but were not very clearly shown from the data obtained (see Table V). In this case, it might come from a relatively wide coefficient variation (CV) of the dry matter of nodules. It is necessary to mention that during winter a heterogeneity of light and temperature was found, although the temperature inside the greenhouse was adjusted to between 20 and 30°C. This condition will cause *R. japonicum* to grow heterogeneously (in low light intensity and low temperature, *R. japonicum* grows under normal conditions and also in low light intensity and high temperature).

Acetylene reduction

Data of acetylene reduction showed the activity of nodule bacteria in fixing dinitrogen when the observation was made, but did not directly reflect the amount of dinitrogen fixed by the legume crop.

The trend of acetylene reduction of the data obtained was similar to that of the dry matter of nodule bacteria obtained in this experiment, although it was less valuable owing to its high variability (see Table V). The high variability in the data obtained might be due to the heterogeneity of plant maturity. At the time of harvesting, several plants were still green (mid-pod filling stage).

CONCLUSION

From the data obtained, some conclusions can be made:

(1) The amount of water lost by evapotranspiration is higher in higher soil-water content, unless soil aeration problems inhibit the rate of plant growth.

(2) It seems that 35% (g/g) soil-water content is an optimal condition for both crops in terms of total water consumption and total nitrogen taken up by plants in loamy alluvial soil.

(3) A higher amount of fertilizer nitrogen was taken up by both crops (soybean and wheat) from soil with a higher soil-water content.

(4) Fertilizer nitrogen uptake was relatively low in both crops. Lower fertilizer nitrogen uptake was observed from soil with relatively dry conditions.

(5) Soybean crop fixed a reasonable amount of dinitrogen through symbiotic process, although no clarification was found about the effect of different levels of soil-moisture treatment on it. This result was supported by the data of the dry matter of nodules and acetylene reduction.

ACKNOWLEDGEMENTS

REFERENCES

[1] BLACK, C.A., "Water", Soil-Plant Relationships, John Wiley & Sons (1968) 70.

[2] BAVER, L.D., "Soil water", Soil Physics, John Wiley & Sons (1956) 224.

[3] ZAPATA, F., The Use of N15 Tracer Techniques in the Quantitative Estimate of Symbiotic Nitrogen Fixation by Legume Crops under Field Condition, Experimental Guidelines, IAEA Seibersdorf Laboratory (1981).

[4] FAUST, H., in ZFI-Mitteilungen, Akademie der Wissenschaften der DDR Zentralinstitut für Isotopen und Strahlenforschung, Leipzig 38 (1981) Appendix 2, 131.

[5] SUBBA RAO, N.S., "The acetylene reduction techniques", Recent Advances in Biological Nitrogen Fixation, Oxford & IBH Publishing Co. (1979) 8.

[6] HANDAWELLA, J., A Report on the Use of Isotopes in Studies on Biological Dinitrogen Fixation, Progr. Rep. to the Joint FAO/IAEA Division 1981/1982.

WATER-MOVEMENT STUDIES IN A SOIL BY USING A NEUTRON GAUGE

J. SALGADO, C. OLIVEIRA
Physics Department,
Laboratório Nacional de Engenhariae
    Tecnologia Industrial,
Sacavém

C. ARRUDA PACHECO
Instituto Superior de Agronomia,
Lisbon

Portugal

Abstract

WATER-MOVEMENT STUDIES IN A SOIL BY USING A NEUTRON GAUGE.
    This paper describes the studies of water movement in a Vertisols Chromiques (FAO), under field conditions, using a neutron gauge. Small areas of soil surface centred on each access tube were irrigated using the double-cylinder infiltrometer. The water profiles taken at different positions, depths,and times enabled a study of field capacity, macroporosity, vertical and horizontal movement of water during redistribution and the kinetics of the redistribution. The drainage is interpreted by using the model proposed by Marcesse. For the soil studied, the field capacity values range from 35 to 50% moisture by volume. Redistribution curves show the superposition of a fast process, which occurs only at depths lower than 40 cm, with a period of one or two hours, and a slow process with a longer period lying between 200 and 300 days. The constancy of water content below 40 cm during infiltration suggests that the drainage is not significant at these layers.

INTRODUCTION

The determination of hydrodynamic soil characteristics, i.e. infiltrability, drainage, hydraulic conductivity in saturated and unsaturated soils, and field capacity, is one of the rpime objectives of hydrological and agronomical research.
    Neutron gauges are particularly suitable for studying water movement in soils, under different conditions, since they can measure repeatedly the same soil sample, with little soil disturbance. It is easy to follow the moisture changes at different depths, locations and times. Field capacity and the kinematics of water redistribution can be deduced from these measurements.
    This paper examines some aspects of water redistribution into a saturated swelling soil – a Vertisols Chromiques (FAO) [1]. The textural class of this soil

TABLE I.   SOIL CHARACTERISTICS

Profile type (cm)	Size and shape of compound peds	Porosity [3]		Bulk dens. (g/cm³)[a]	
		class	diameter	clods[b]	cylinder method
Ap-1 (0—26)	Fine, med. gran. and fine subang. blocky	V P	VF, F Med.	1.19	1.13
Ap-2 (B1) (26—49)	Very coarse ang. blocky and med. prismatic	S P	VF, F	1.33	1.30
(B2) (49—82)	Medium and coarse, prismatic	VSP	VF	1.36	1.34
C1 (82—120)	Very coarse, prismatic	VSP	VF	1.40	1.37
C2 (120—165)	Massive			1.41	1.38
C3 > 230	Basaltic rock, very weathered				

[a]   At field capacity.
[b]   Paraffin method.

is a clay (A > 50%). The clay contains fundamentally a mineral belonging to the iron montmorillonite group (nontronite), showing a variable degree of crystallization [2]. Table I gives the soil characteristics.

EXPERIMENTAL PROCEDURES

We installed several PVC tubes 1.7 m long in the soil, as illustrated in Fig. 1. The soil was ploughed in July 1982 with a moldboark plough. Tubes 7 and 8 were used for calibration purposes.

The measurements were carried out during two periods: (a) Oct/Nov 1982, and (b) Jan/Feb 1983.
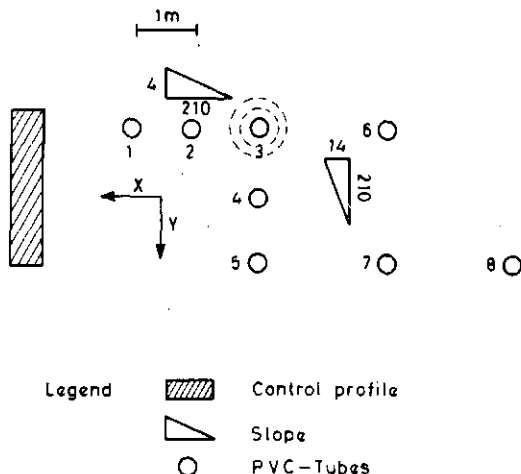
FIG.1.   Schema of experimental set-up.

In the first period, small portions of circular-shaped soil centred on access tubes 3, 5 and 6 were limited by stainless-steel cylinders ($\sim$ 50 cm in outer diameter) resting on the soil surface. The tank wall penetrated in the soil to a depth of 5 cm. The water poured on these circular portions of soil surface was as follows:

Tube	3	5	6
Water supplied (cm)	96	156	126

In the second period we supplied water within a double ring (ϕ_1 = 55 cm, ϕ_2 = 94 cm) centred on tube 3. The irrigation was divided into three phases:

Time	35 min	4 h	106 min	24 h	44 min
Water supplied (cm)	65		66		38
	1st irrig.		2nd irrig.		3rd irrig.

Figure 2 shows the time dependence of the cumulative infiltration and of the infiltration rate. The soil surface was covered with straw and polyethylene
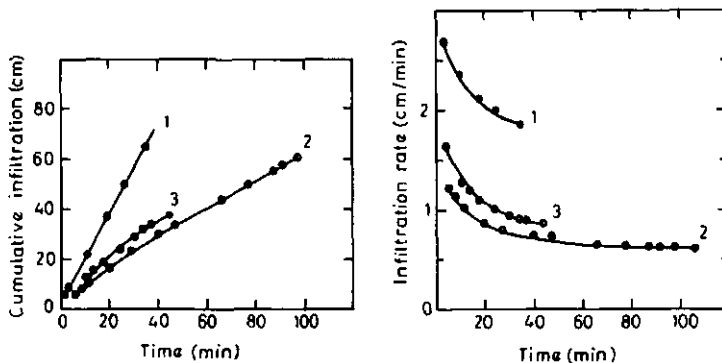
FIG.2. Dependence of the cumulative infiltration and of the infiltration rate on time.
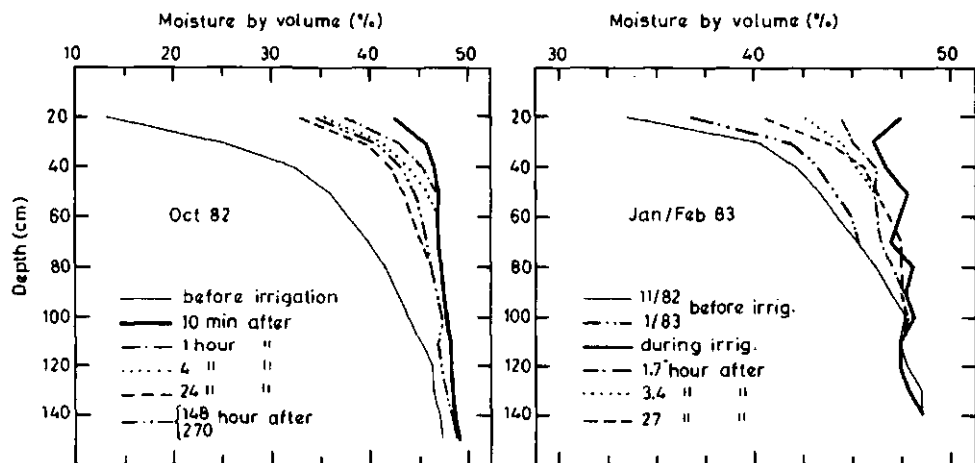
FIG.3. Soil-water profile before and after irrigation.

sheet to prevent evaporation and condensation. During both periods the water precipitation was zero. The moisture profiles were taken at different times with a neutron gauge developed at Sacavém [4].

RESULTS AND DISCUSSION

Figure 3 represents the water profiles taken at different times after irrigation. In both periods we observe a faster rate of moisture decrease in the 20–40 cm depth zone. This fact is related to the high structural porosity [5] of this upper
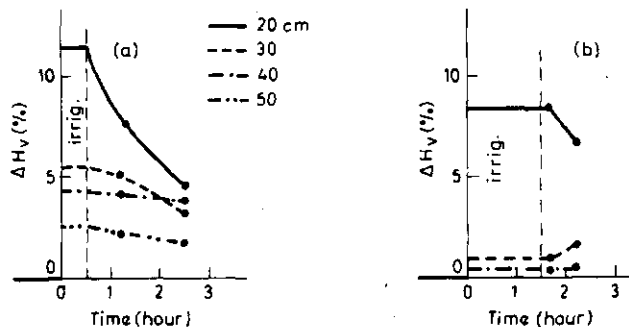
FIG.4.   Variation of water content during and after irrigation:
         (a) In the irrigation tube;
         (b) In a tube 1.1 m from the irrigated tube.

layer and to the strong gradient of bulk density (1.19/1.32) in the ploughed zone,
associated with the soil slope — there is a strong horizontal component of water
movement.

To illustrate the infiltration rate of water, Fig. 4 shows the variation of the
soil-water content with time in the second measurement period:

(a)   In the irrigated tube during and after the 1st irrigation; and
(b)   In a tube 1.1 m from the irrigated tube during and after the 3rd irrigation.
      From Fig. 4 we conclude that the water rapidly reaches the 20 cm layer.

The horizontal movement of water is displayed in Fig. 5, where the variation
of soil moisture — (a) 30 min and (b) 2 h 30 min after the end of infiltration — is
expressed as a function of the distance from the irrigated region.

The decrease of soil moisture during the water redistribution after the
saturation can be interpreted by using the model proposed by Marcesse [6], in
which the water movement is explained by the assumption of two exponential
kinematic processes — a fast process due to gravity and a slower process related
to capillary forces. Accordingly, at each depth, the moisture variation with time
is described by a combination of two exponentials:

$$H_v(t) = H_{01} \exp(-0.693t/T_1) + H_{02} \exp(-0.693t/T_2) \tag{1}$$

where T_1 and H_{01} are, respectively, the period and moisture at the origin for the
fast process and T_2 and H_{02} are the corresponding quantities for the slow process.
H_{02} can be interpreted as the field capacity. $H_{01} + H_{02}$ is the moisture at saturation
at the end of infiltration.

The water movement at a given depth (20 cm) is depicted in Fig. 6 where the
two kinetic processes are clearly apparent.
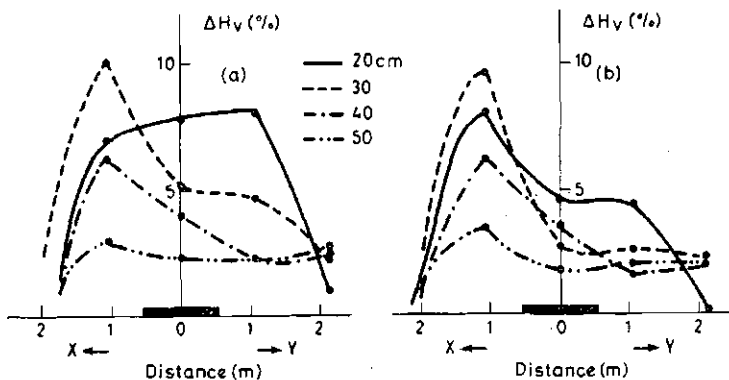
FIG.5. Variation of soil moisture with distance from the irrigated region:
(a) 30 min;
(b) 2h 30 min after the end of infiltration.
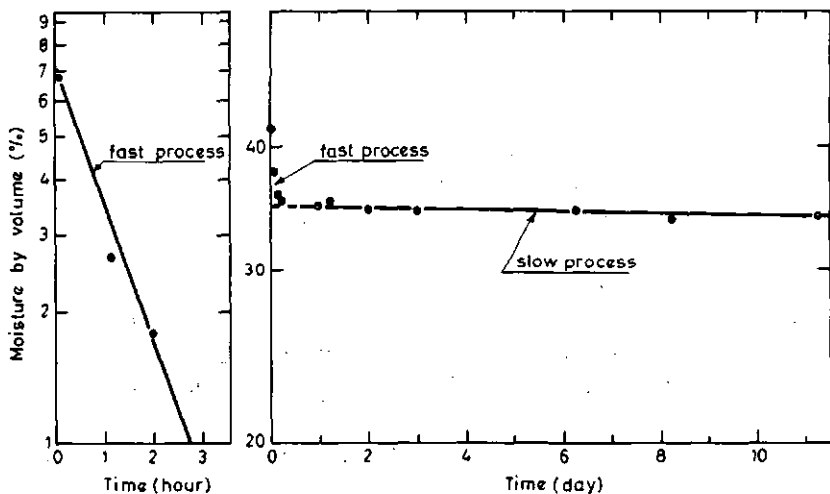
FIG.6. Water redistribution after infiltration at a depth of 20 cm.

The field capacity at different depths was calculated using Eq. (1) — see Fig. 7.
The results show:

(a) No significant differences in field capacity for the two periods at
     depths greater than 50 cm;

(b) Significant differences at depths between 20 and 50 cm. The increase of
     field capacity in Jan/Feb can be explained as due to the natural evolution
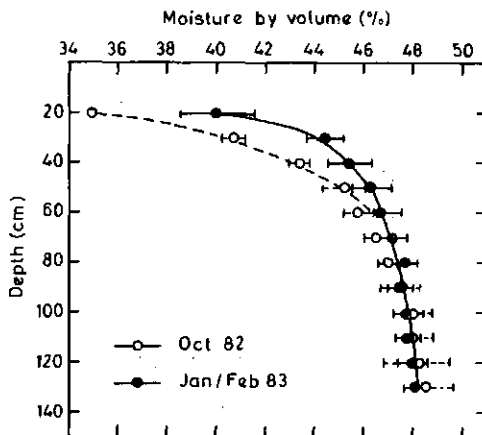
FIG.7. Field capacity at different depths.
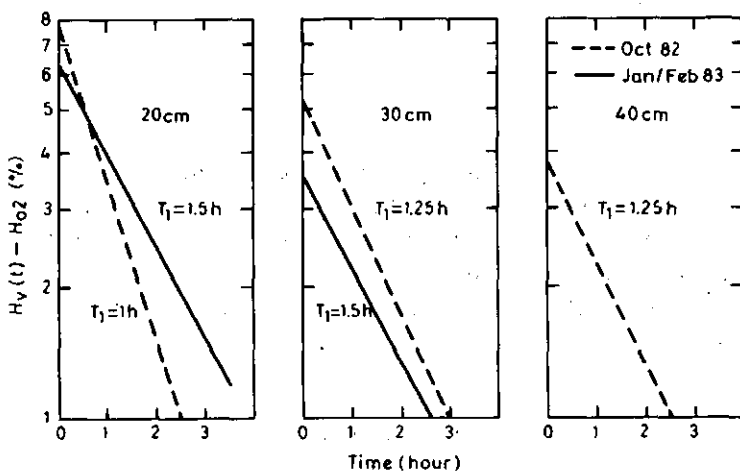
FIG.8. Variation of the fast process with time at different depths.

of the bulk density of the upper layers, with the decrease of macro-porosity.

Since the time interval of each measurement is limited to a few weeks, we cannot calculate the period of the slow process. However, we can estimate that this value lies between 200 and 300 days.

Figure 8 shows the fast process for different depths. We observe that the drainage is slower during the second period of measurement. This fact reveals once again the variation of macroporosity between both experiments. The same
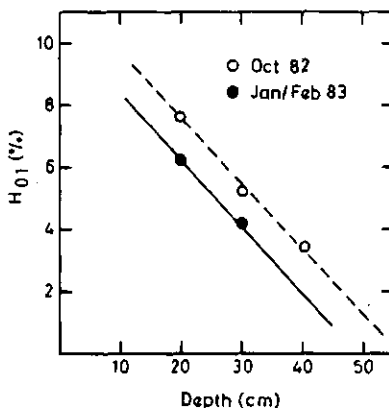
FIG.9. *Variation of H_{01} with depth.*

effect is also illustrated in Fig. 9, which presents H_{01} versus depth. The period of the fast process lies between one and two hours.

CONCLUSIONS

This work shows once again the advantages of a neutron gauge for measuring soil-water content. These results show that the infiltration in the saturated soil does not take place through vertical cracks and macrovoids, but laterally in the layers with a strong gradient of bulk density.

The morphological observation of the pedological profile confirms these assumptions.

REFERENCES

[1]   BOULAINE, J., in Sols, No. 8, INA — Paris (1982).
[2]   FURTADO, A.F.S., "Mineralogia de barros castanho-avermelhados derivado de rochas do complexo basáltico de Lisboa", An. Inst. Superior de Agronomia, Vol. 33 (1972).
[3]   HODGSON, J.M., in Soil Survey Field Handbook, Tech. Monograph No. 5, Harpenden (1976).
[4]   SALGADO, J., et al., "Nuclear depth probe for moisture and bulk density measurements", Industrial Application of Radioisotopes and Radiation Technology (Proc. Conf. Grenoble, 1981), IAEA, Vienna (1982) 470.
[5]   STENGEL, P., Utilisation de l'analyse des systèmes de porosité pour la charactérisation de l'état physique du sol in situ, Ann. Agron. 20 (1) (1979) 27−51.
[6]   MARCESSE, J., "Détermination in situ de la capacité de retention d'un sol au moyen de l'humidimètre à neutrons", Isotope and Radiation Techniques in Soil Physics and Irrigation Studies (Proc. Symp. Istanbul, 1967), IAEA, Vienna (1967) 137.

STUDY OF THE DOWNWARD MOVEMENT OF SOIL WATER IN AN UNSATURATED ZONE BY USING ISOTOPIC TECHNIQUES

M.I. HAQ, M.I. SAJJAD, KAUSER A. MALIK
Nuclear Institute for Agriculture and Biology,
Faisalabad, Pakistan

Abstract

STUDY OF THE DOWNWARD MOVEMENT OF SOIL WATER IN AN UNSATURATED ZONE BY USING ISOTOPIC TECHNIQUES.
Experiments carried out to study the contribution of infiltration from irrigated fields to the water-table have shown that the normal delta of irrigation water does not seem to have any appreciable effect on the water-table through heavy textured soil. However, the chemical analysis and isotopic contents of the sandy loam profile showed that the normal delta of irrigation water and rainfall does have some effect on the water-table.

INTRODUCTION

The irrigation system in Pakistan has raised the water-table and introduced the problems of water-logging and salinity. To get a better insight into the groundwater recharge, one has to distinguish the infiltration from canals and their distributaries; monsoon rains; and irrigated fields.

While the line infiltration from canals and their distributaries is considered to be the most important, the monsoon infiltration may not be so. There is no precise knowledge on the infiltration from the irrigated fields [1]. The present study is, therefore, intended for investigating the process of infiltration in detail with the help of isotopic and chemical methods to get a better insight into the seepage, especially from the irrigated fields.

Area of study

Two fields (designated as fields No. 2 and No. 3), each measuring 170 m², located at Faisalabad, were selected for carrying out experimental work during the first year of the study period. Faisalabad is situated in Rechna Doab (land between the rivers Ravi and Chenab) and is badly hit by the problem of water-logging and salinity. The water-table in the area is 1−4 m below the ground surface. At some places it also appears on the ground surface.

375

Geology

The Faisalabad area forms part of the Punjab plains which are an extension of the upper Indus plains. The area was originally a sea bed, and formed part of the extension of the Aravali mountain ranges of northern India. The area is filled by recent flood deposits comprising unconsolidated clay, silt and fine- to medium-grained sand. These sediments are irregularly interconnected. Fine-grained sediments prevail in the upper 3–5 m depth while medium-grained sands are predominant below 5 m. The mountains are buried under alluvium, with some hill-tops still exposed as out-crops in the vast flat Indus plains. The average height of the area is about 215 m above sea level. The alluvial deposits are about 450 m thick in the project area.

Climate

The project area goes from arid to semi-arid zones. For most of the winter months (November to January) the weather is characterized by dry air and bright sun during the day. Some of the climatological features are discussed below.

Temperature: January is the coldest month in winter and June is the hottest month in summer. The maximum temperature during January is 20°C and the minimum is 5°C.

From February to June the temperature shows a rising trend and June becomes the hottest month. The maximum temperature is 47°C, while the minimum is 32°C.

In July and August the temperature falls to some extent owing to the onset of monsoons. The annual maximum temperature is 32°C and minimum is 17°C.

Humidity: May and June are the driest months of the year, with 17% mean relative humidity. The relative humidity during July and August is about 70%. The wet bulb temperature is about 23°C in these months, making the weather more uncomfortable.

Rainfall: Rainfall occurs mainly in summer because of the monsoon. The area also receives winter showers of lesser intensity. The monsoon takes place during July–September, whereas in winter the showers occur during December–February. The average annual rainfall is about 40 cm [2, 3].

Isotopes used in the study

The environmentally stable isotopes, namely deuterium (D), ^{18}O and the radioactive isotope tritium (H^3), were studied. All these isotopes are produced

in nature, form a part of water molecules and are transported through precipitation. Further, these isotopes do not react with the aquifer and therefore serve as conservative tracers in the study of groundwater movement.

The principal heavy stable isotopic components of water are $HD^{16}O$ and $H_2^{18}O$. They occur in natural waters in concentrations of about 320 ppm and 2000 ppm, respectively. Systematic investigations over many years have revealed that the proportions of $H_2^{18}O$ and $HD^{16}O$ fluctuate within ranges of 1880 to 2010 and 180 to 340 ppm, respectively [4, 5]. This is essentially because of the lower vapour pressures of $H_2^{18}O$ and $HD^{16}O$, as a result of which the isotopic fraction takes place during every transformation phase, i.e. condensation and evaporation. Isotopic exchange, diffusion and dispersion ensure that isotopic fluctuation, which initially takes place at the phase boundaries, becomes a measurable volume effect in a water sample.

The varying proportions of these components in terrestrial waters can be measured by a mass spectrometer with a precision of 1.0% for deuterium and 0.1‰ for ^{18}O.

The analysis of precipitation and waters, which have not been subjected to evaporation, shows a good linear relationship of the general type:

$$\delta D = 8 \, \delta^{18}O + Y$$

where

$$S = \frac{R_{sample} - R_{SMOW}}{R_{SMOW}} \times 1000, \quad R = {}^{18}O/{}^{16}O \text{ or } D/H$$

The excess of deuterium (Y) may vary, but is normally +10. However, waters which have been subjected to evaporation are found to fall off the general line of slope 8. In these cases, lines with a slope between 4 and 6 have been observed [7].

The tritium in precipitation originates from two causes. The first, a neutral one, is production by interaction of cosmic high-energy radiation with atmospheric components. Estimates of the concentration of tritium in precipitation resulting from this source vary, but seem to be around 10 TU. The second source is man-made and since 1952 has been derived principally from the detonation of thermonuclear devices. This production has swamped the former by injecting periodic pulses into the atmosphere, with the result that precipitation has been labelled with an amount of tritium which can be relatively easily measured. The occurrence of tritium in precipitation results in an overall labelling of water in the hydrological cycle. The tritium is, therefore, found in varying degrees, not only in precipitation but also in surface waters, groundwaters and the oceans [6].

TABLE I. VARIATION OF SAND, SILT AND CLAY WITH DEPTH IN
FIELD No. 2

Depth (cm)	% Sand	% Silt	% Clay	Soil class [8]
0–25	55	26	19	Clay loam
26–50	57	24	19	Sandy clay loam
51–75	57	24	19	Sandy clay loam
76–100	58	24	18	Sandy clay loam
101–125	64	23	13	Loam
126–150	61	26	13	Loam
151–175	55	32	13	Loam
176–200	47	35	18	Clay loam
201–255	62	23	15	Sandy clay loam
226–250	78	14	8	Sandy loam
251–275	84	8	8	Sandy loam
276–300	88	8	4	Loamy sand
301–325	90	8	2	Loamy sand
326–350	94	4	2	Loamy sand
351–375	93	4	3	Loamy sand
376–400	92	5	3	Loamy sand

EXPERIMENTAL

Each experimental field was ploughed and levelled before starting the
experiment. By using an auger a background soil core sample was taken before
the field was irrigated. About 75 mm (3 in.) irrigation, which is the normal
irrigation level in the area, was applied. Post-irrigation core samples were
collected at proper time intervals. It was ensured that the auger hole was at least
1 m away from the position of the previous core. The soil core sections, each
25 cm long, were taken down to a depth of 4 m below the ground surface. These
core samples were properly sealed in thick polythene bags or in PVC tubes
and transported to the laboratory.

Samples of irrigation water standing in the experimental field were taken
at different times to see the effect of evaporation on the isotopic composition
of the infiltrating water.

TABLE II. VARIATION OF SAND, SILT AND CLAY WITH DEPTH IN
FIELD No. 3

Depth (cm)	% Sand	% Silt	% Clay	Soil class [9]
0–25	64	26	10	Loam
26–50	66	22	12	Sandy loam
51–75	66	22	12	Sandy loam
76–100	68	21	11	Sandy loam
101–125	70	20	10	Sandy loam
126–150	72	21	7	Sandy loam
151–175	75	18	7	Sandy loam
176–200	68	24	8	Sandy loam
201–225	73	22	5	Sandy loam
226–250	67	25	8	Sandy loam
251–275	60	30	10	Loam
276–300	70	24	6	Sandy loam
301–325	83	15	2	Sandy loam
326–350	91	9	–	Loamy sand
351–375	94	6	–	Loamy sand

The moisture extraction from the soil cores was done in a vacuum distillation assembly with four units. To check the performance of the system, water of known isotopic composition (^{18}O) was added to dry soil samples, and then these wet soil samples were processed in the vacuum-distillation units and isotopic contents of extracted water compared with those of the original water. The results were reproducible and well within the acceptable error limits.

The extracted water samples were analysed for ^{18}O and D contents by a mass spectrometer equipped with a double ion collector system and automatic ^3H compensation unit. The tritium (T) content was determined by a Packard Tricarb Liquid Scintillation Spectrometer system. The moisture content of each soil core was also determined by drying it for 24 h in an oven at 105°C and noting the weight loss. The sand/clay/silt percentage was determined by the mechanical method and is presented in Tables I and II.

The first experiment was performed in January/February 1981 in field No. 2, and the second one from April 1981 onwards in field No. 3. The last core sampling of the year was made in September (after monsoon rains) in field No. 3.

Results and discussion

The results from experiments performed in fields No. 2 and 3 are as follows:

Field No. 2:

In the first experiment about 70 soil core samples were taken for analysis of $^{18}O/^{16}O$, D/H, tritium, moisture and chloride determinations, and soil texture analysis. These results have been plotted in Figs 1 and 2. The D-^{18}O plot of irrigation water standing in the field is given in Fig. 6.

The moisture (wt%) and isotopic data (%O) indicate that the penetration of irrigation water is approximately down to 1 m deep for this particular soil.
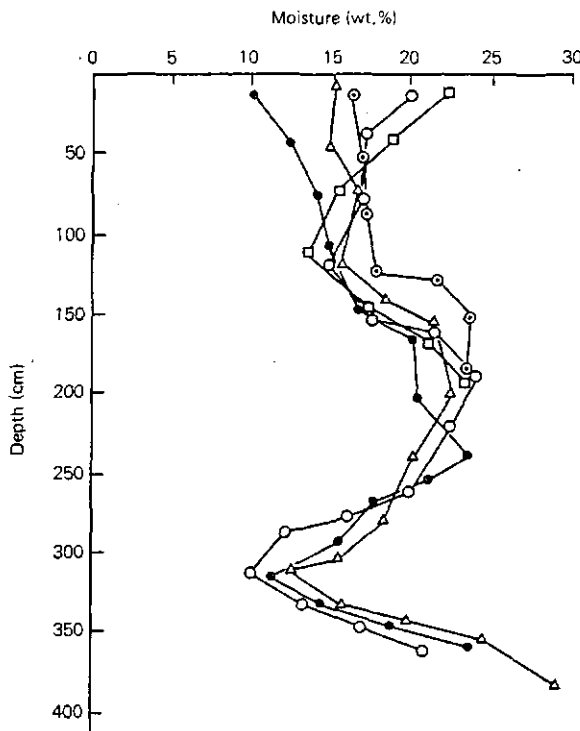
FIG.2.   *Moisture variation with depth. Field 2.*
Key: ● — *25.1.1981*
       □ — *26.1.1981*
       ○ — *28.1.1981*
       ☉ — *4.2.1981*
       △ — *11.2.1981*

The pre-irrigation and post-irrigation ^{18}O and D correlations for various soil cores are:

	Date	Equation	Correlation coefficient: r
Pre-irrigation	25.1.81	$SD = 4.63\ \delta^{18}O - 17.51$	0.95
Post-irrigation	26.1.81	$SD = 5.13\ \delta^{18}O - 13.24$	0.88
	28.1.81	$SD = 5.87\ \delta^{18}O - 8.15$	0.91
	4.2.81	$SD = 5.26\ \delta^{18}O - 9.25$	0.97
	11.2.81	$SD = 4.23\ \delta^{18}O - 16.96$	0.99

The slope for the pre-irrigation soil core is 4.63, which shows the evaporation effect in soil moisture. Even some of the moisture samples below 1 m deep are

Cl (meq/L)
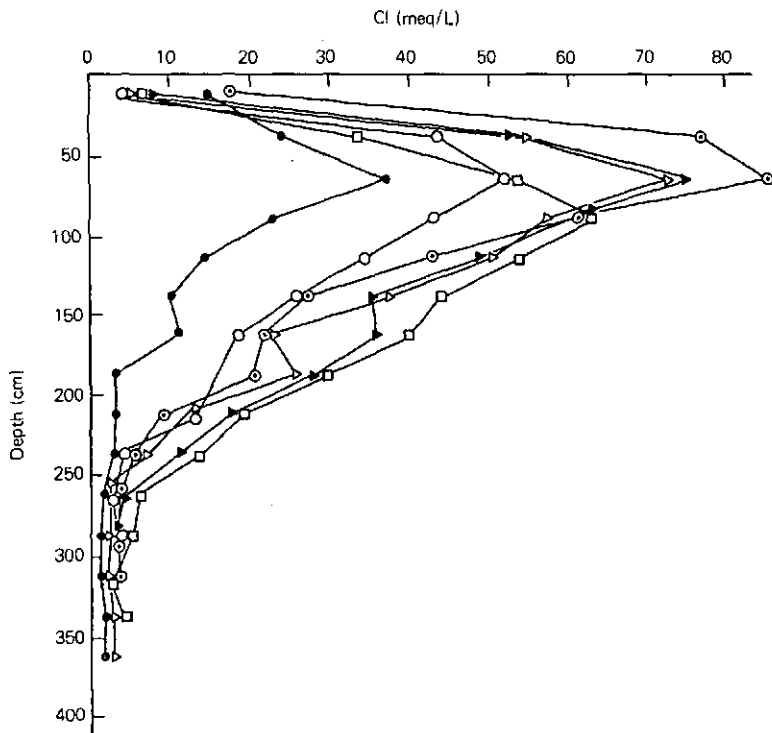
FIG.3.   Variation of chloride with depth. Field 3.
Key: ● —   5.4.1981 pre-irrigation
        ○ —   7.4.1981 post-irrigation
        △ —   9.4.1981
   □ — 11.4.1981
        ▲ — 17.4.1981
        ⊙ — 11.5.1981

displaced to the right of the meteoric water line, indicating isotopic enrichment
of water in the soil because of evaporation.

When water is applied to the field its downward movement under tension
adjustments aided by gravity flow is relatively rapid in the beginning till the
soil reaches its field capacity state. The moisture movement still continues to
take place but its rate is quite slow as at this stage only capillary forces are effective.
During this process the mixing of isotopically enriched soil moisture with the
irrigation water occurs and shifts the isotopic composition towards that of
irrigation water as it moves downwards.

Later on, as the top layers dry out through the loss of water vapour to
atmosphere through diffusion and convection, the soil moisture content is reduced
to below that of the field capacity, and the rate of downward movement is drasti-
cally curtailed. Eventually this downward movement of water also ceases.
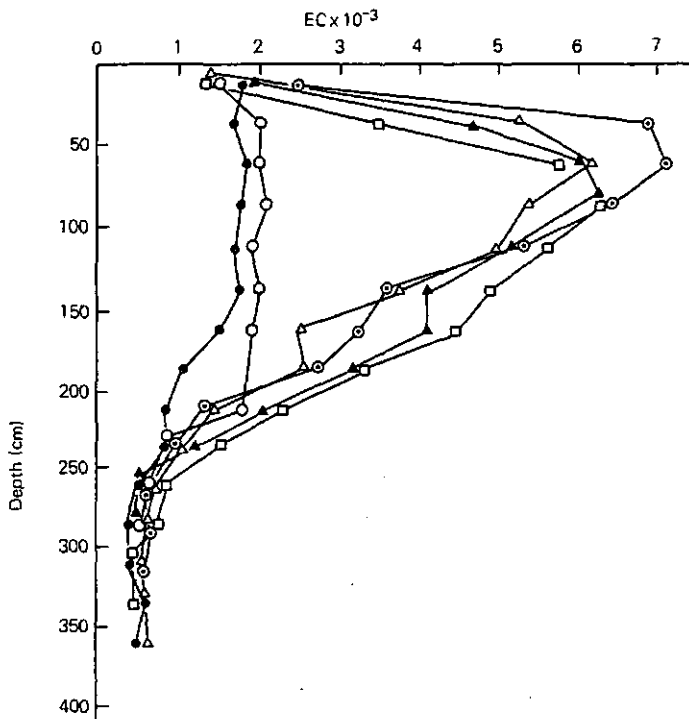
FIG.4.   Variation of EC with depth. Field 3.
Key: ● –   5.4.1981 pre-irrigation
      ○ –   7.4.1981 post-irrigation
      △ –   9.4.1981
      □ – 11.4.1981
      ▲ – 17.4.1981
      ⊙   11.5.1981

    Evaporation at the soil surface creates a region of low tension; consequently
an upward movement of soil moisture through capillary action takes place. During
evaporation process, the soil moisture gets enriched isotopically.

    This back and forth moisture movement is always operating in the soil after
each irrigation. However, the depth of water penetration depends upon the type
of soil (texture and structure), intensity of irrigation, prevailing atmospheric
evaporation rates and many other factors. Isotopic and moisture data of the two
fields under experiment indicate the behaviour of each soil.

Field No. 3

    The soil texture of this field is slightly different from that of the previous
one.

    Altogether nine core samples were taken during approximately six months.
The results are shown in Figs 3 to 5.
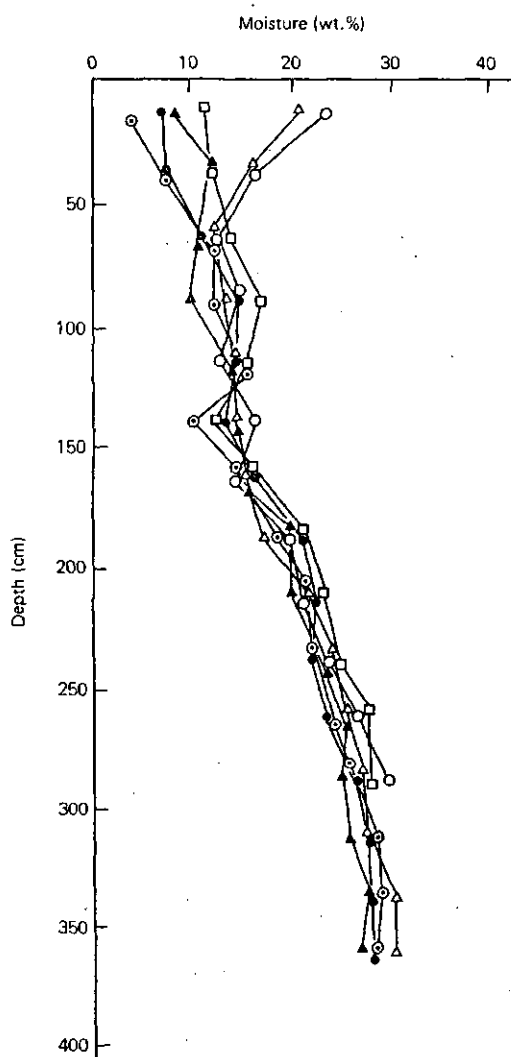
FIG.5.   *Moisture variation with depth. Field 3.*
   *Key:*   ●   —   *5.4.1981   pre-irrigation*
          ○   —   *7.4.1981   post-irrigation*
          △   —   *9.4.1981*
          □   —   *17.4.1981*
          ▲   —   *26.4.1981*
          ⊙   —   *22.6.1981*

δ¹⁸O‰ — shown as $\delta^{18}O‰$

-10.0   -8.0   -6.0   -4.0   -2.0   0.0

-10.0

-20.0

-30.0

δD‰

-40.0

-50.0

-60.0

$\delta D = 8.0\ \delta^{18}O + 10.0$

25-1-81

1200 h

1310 h
1415 h
1715 h
1945 h

1315 h

1515 h

0800 h
0905 h

1400 h

1212 h
28-1-81

Field irrigation water

26-1-81
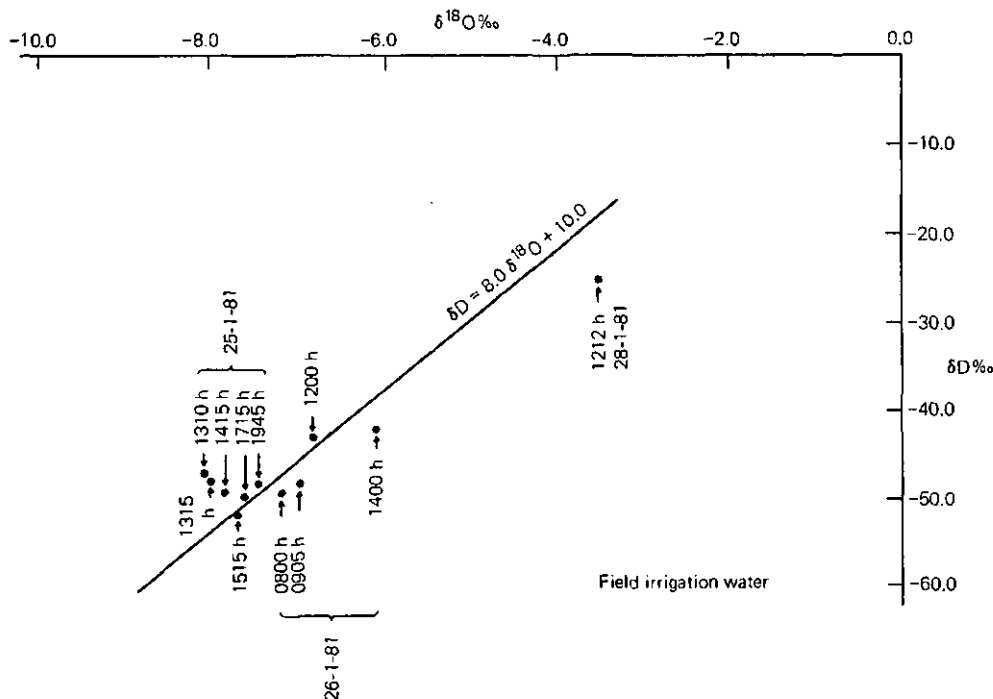
FIG.6. Isotopic enrichment with time. Field 2. Relative humidity : 75−93%; Temp.: 5.5−13°C.

During this experiment, the irrigation water (70 mm) standing in the field showed considerable enrichment in its isotopic composition with time, indicating higher evaporation rates (see Figs 6 and 7) because of prevailing atmospheric conditions of less humidity and higher temperature.

The δD versus depth (Fig. 8) indicates a larger deuterium distribution in the upper soil layers because of intense fluctuations in soil moisture. In lower layers the isotopic transport processes in the soil moisture smooth out the isotopic composition differences of water in different layers during the passage of time. In still deeper soil layers, these isotopic differences are not distinguishable. All these smoothing phases are clearly demonstrated in Fig. 8.

The δD-δ¹⁸O relations of various soil cores indicated that only a few points representing the upper layers deviate from the general meteoric line [7].

$$\delta D = 8.0\ \delta^{18}O + 10.0$$

All other points group around this non-evaporated line showing the least evaporation effect.
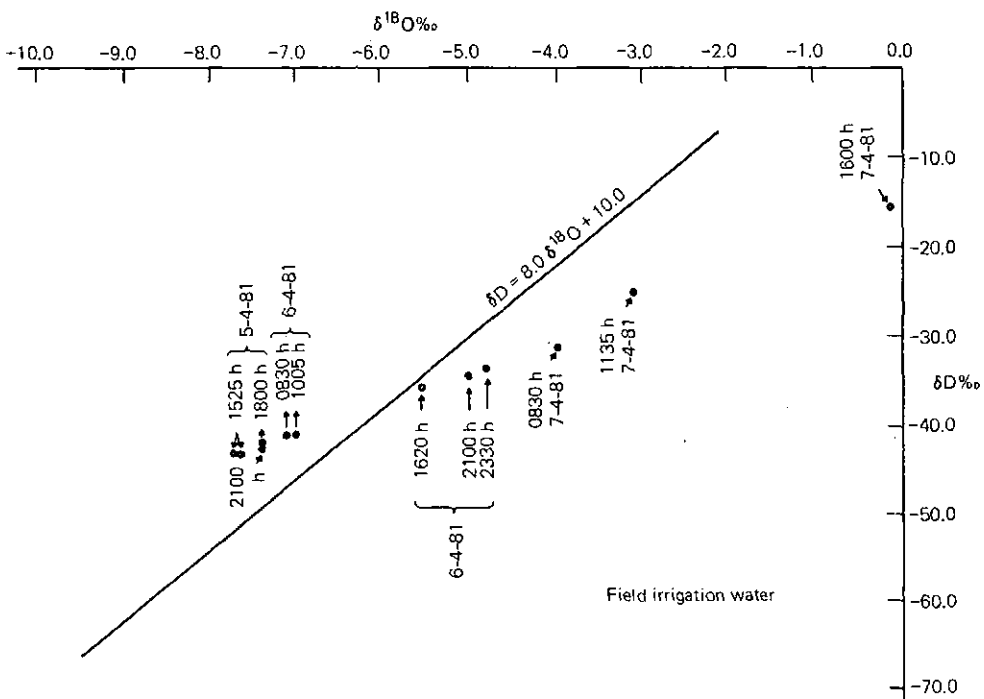
FIG. 7. Isotopic enrichment with time. Field 3. Relative humidity: 23–79%; Temp.: 12–30°C.

The chloride ion (Cl⁻) measurements of the soil moisture in both fields indicate that the accumulation of these ions is limited to the upper soil profile depth of 2.5 m. This is essentially due to prolonged irrigation of the soils, during which the soil salinity increases considerably depending upon the concentration of soil solution present and the chloride content of the irrigation water. A typical case is presented in Fig. 3 where, after irrigation of the field, the chloride content increased from 37 meq/L to 85 meq/L during a period of about one month (5 April to 11 May 1981). The variations of electrical conductivity are shown (2–7 mmho/cm) in Fig. 4.

Despite the high solubility of chloride in water and its ability to move faster through the soil than the average velocity of water molecules[1] available, Fig. 3 shows a peak at a depth of 75–80 cm (its height increasing with time). This shows that the penetration of irrigation water was limited to the upper soil layers

---

[1] The apparent higher velocity of Cl⁻ions is because they are excluded from the immediate vicinity of negatively charged soil particles where the water is relatively immobile, and from narrow pores where solution velocities are slow [9].
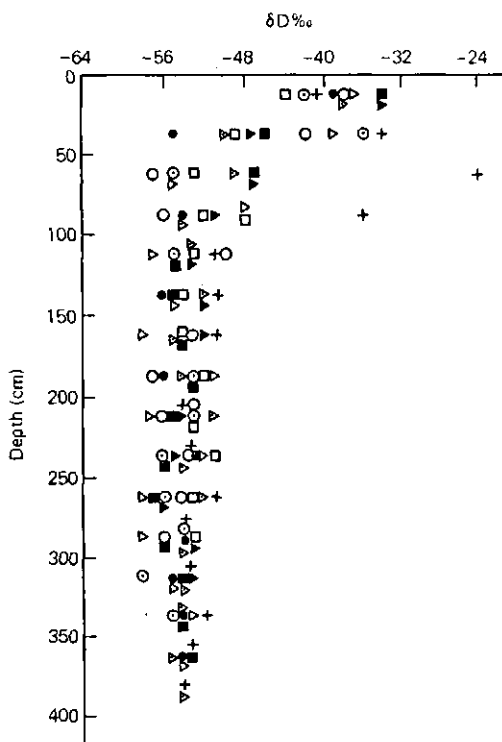
FIG.8.   δD variation with depth.   Field 3.

Key: ● —   5.4.1981 pre-irrigation
       ○ —   7.4.1981 post-irrigation
       △ —   9.4.1981
       ⊙ — 11.4.1981
       □ — 17.4.1981
       ■ — 26.4.1981
       ▲ — 13.5.1981
       ⧆ — 22.6.1981
       + — 27.9.1981

only. As the top soil dries up, the soil moisture starts moving upwards, carrying Cl⁻ with it. Consequently, the previously leached salt profiles shift upwards as indicated by the subsequent core sampling on 11.5.81 (Fig. 3).

The accumulation of salinity in soil can be diluted to some extent by applying a higher delta of irrigation water, or after heavy rains during which the soluble salts leach down to greater depths.

The soil core samples taken on 27 Sep. 1981, after monsoon rains, give evidence that these rains had penetrated down to a depth of one metre by then (Fig. 8).

CONCLUSIONS

The results of first and second experiments in loamy soil and sandy loams indicate that penetration of irrigation water is limited to a maximum of one metre soil depth and most of it remains stored in the upper layers of the soil where it starts evaporating upwards.

The contribution of heavy rains to the underground reservoir seems very possible even through such types of soil. Further work is in progress to establish this phenomena.

ACKNOWLEDGMENTS

REFERENCES

[1]   SEILER, K.P., STICHLER, W., HANIF, M., HUSSAIN, D.I., SAJJAD, I., "Isotopic and hydrochemical studies at Faisalabad/Pakistan", Inter-American Symp. Isotope Hydrology, Bogotá, Colombia, August, 1980.
[2]   WADIA, D.N., Geology of India (1966).
[3]   WYNES, A.B., Records of Geol. Surv. India (1970).
[4]   EPSTEIN, S., MAYEDA, T., Variations of the O^{18} content of waters from natural sources, Geochim. Cosmochim. Acta 4 (1953) 213–24.
[5]   GAT, J.R., Comments on the stable isotope method in regional groundwater investigations, Water Resour. Res. 1 (1971) 980–93.
[6]   INTERNATIONAL ATOMIC ENERGY AGENCY, Guidebook on Nuclear Techniques in Hydrology, Tech. Rep. Series No. 91, IAEA, Vienna (1968).
[7]   CRAIG, H., Isotopic variations in meteoric waters, Science 133 (1961) 1702–03.
[8]   BOUYOUEOS, G.J., Hydrometer method improved for making particle size analysis of soils, Agron. J. 54 (1962) 464–65.
[9]   THOMAS, G.W., SWOBODA, A.R., Anion exclusion effects on chloride movement in soils, Soil Sci. 110 (1970) 163–66.

SUGAR-BEET IRRIGATION SCHEDULING AND THE POSSIBILITIES OF USING A NEUTRON PROBE TO MEASURE SOIL MOISTURE IN NORTHEASTERN YUGOSLAVIA

S. DRAGOVIĆ
Faculty of Agriculture,
Institute of Field and Vegetable Crops,
University of Novi Sad,
Novi Sad, Yugoslavia

Abstract

SUGAR-BEET IRRIGATION SCHEDULING AND THE POSSIBILITIES OF USING A
NEUTRON PROBE TO MEASURE SOIL MOISTURE IN NORTHEASTERN YUGOSLAVIA.
   The paper reviews the results of a study of irrigation scheduling for sugar-beet in
northeastern Yugoslavia – Vojvodina Province – under conditions of a semi-humid climate.
The region has suitable soil and climatic conditions for sugar-beet. The limiting factor for high
and stable yields is an insufficient and unfavourably distributed rainfall which is compensated
for by irrigation. The irrigation in the region under discussion is strictly supplementary. The
crucial problem is the determination of irrigation scheduling. It has been found that four
scheduling methods may be used. The irrigation method based on soil moisture applies
600 m³/ha of water at 65% filled water capacity. This method, made simpler and more
efficient by using a neutron probe, resulted in the highest yields in the experiment. Sugar-beets
increase their water requirements in the course of growth and development. One irrigation is
necessary in the first stage. Two irrigations (1200 m³/ha) suffice for the second stage (1 July –
20 August). At the stage of technological maturity, sugar-beet requirements for water are the
lowest – one irrigation is enough. The level of water provision for sugar-beet may also be
controlled by analysing the concentration of cell sap in the leaf. The marginal values are 7%
till the end of June and 8% in July and August. The bioclimatic method of calculating sugar-beet
requirements for water has certain advantages. It was found that sugar-beet uses 1.8 m³/ha of
water each 1°C mean daily air temperature. As the crop varies so do its water requirements and
the phytobioclimatic coefficient.

INTRODUCTION

   Sugar-beet production is quite intensive in Yugoslavia, especially in the
northeast, the Vojvodina Province. This region is a plain with favourable soil
and climatic conditions for sugar-beet. A limiting factor for high and stable crop
yields is the rainfall, i.e. its shortage and the uneven distribution during the vegetative
season. There is frequently a dry spell in July and August, when the crop needs

the most water. Supplementary irrigation compensates for the lack of rainfall and secures high and stable yields.

Irrigation in the Vojvodina Province is strictly supplementary. To achieve economy in irrigation, maintaining sugar-beet yields at a desired level, it is necessary to pinpoint the irrigation schedule with precision.

A number of methods exist for determining the irrigation schedule for sugar-beet. These methods may be grouped according to the basic principles of their operation.

METHODS

A field trial was conducted from 1970 to 1978 on loamy, slightly calcareous soil with favourable water-physical and chemical properties. We tested four methods of irrigation scheduling for sugar-beet according to (1) soil moisture; (2) stages of plant growth and development; (3) cell-sap concentration in leaf; and (4) bioclimatic indicators.

Soil moisture was determined by the sample drying method. We used a Yugoslav-made neutron probe, working on the principle of fast neutrons (100 mCi ^{241}Am-Be) coupled with a portable PS-4 counter. Soil moisture was determined for depths of 0–25, 25–50, 50–75, and 75–100 cm. Cell-sap concentration was determined refractometrically.

Sugar-beet variety NS-poly-mono, developed at the Novi Sad Institute, was used. The planting density was 50 X 20 cm, and irrigation was done by the sprinkling method.

WEATHER CONDITIONS

The long-term average annual rainfall for the experimental site is 600 mm, i.e. 344 mm or 56% in the April – September period and 256 mm or 44% in the October – March period. Figure 1 shows the water balance calculated after Thornthwaite.

The annual rainfall in the years of the trial ranged from 440 to 751 mm. The variations in the vegetative seasons were even larger, from 196 to 487 mm (Table I). The monthly distribution of rainfall was still more unfavourable. The amount for July varied from 21 to 151 mm. If we add that the monthly distribution was also unfavourable, the necessity of irrigation becomes obvious.

The long-term mean annual temperature is 11.0°C; the summer average is 17.7°C, the winter average 1.5°C. The coldest month is January (−1°C), the warmest is July (21.3°C).
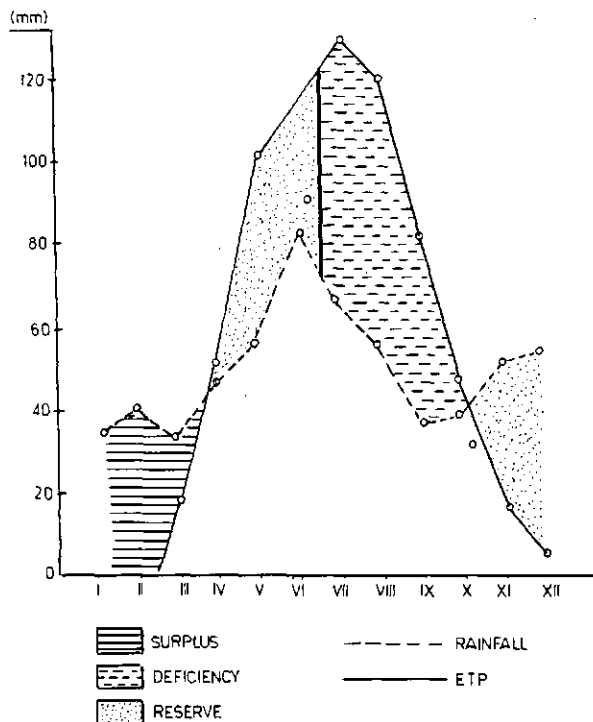
FIG.1.   Water balance of the Vojvodina in the 1948–1978 period, calculated after Thornthwaite [12].

RESULTS

Sugar-beet irrigation schedule and rates depend on climatic, soil and agrotechnical conditions, and the planned yield level. As the annual rainfall and its distribution were variable during the trial, it was not feasible to adhere to a fixed irrigation schedule, but it had to be adapted to specific conditions of each year. The number of irrigations and water rates differed more from year to year than among the tested methods.

Method 1

For Method 1 irrigation schedule and rates were determined on the basis of the water-physical properties of soil and water constants. Knowledge of the relationships in the soil-water-plant system and of the range of optimum moisture and its application via the method ensures high sugar-beet yields and a high irrigation effect. A number of researchers studied the range of optimum soil moisture (Rode [1]; Maksimov [2]). They proposed FWC (filled water capacity) as the

TABLE I. RAINFALL (TOTAL AND DURING VEGETATION) IN THE PERIOD OF EXPERIMENT (mm)

Year	Month						Summer	Winter	Annual
	4	5	6	7	8	9			
1970	49	66	107	91	54	21	388	363	751
1971	26	40	44	21	40	25	196	244	440
1972	56	47	60	151	148	25	487	109	596
1973	90	31	87	38	34	25	305	231	536
1974	57	88	85	60	56	38	362	192	554
1975	47	64	78	119	96	35	439	224	663
1976	39	31	129	48	113	61	421	148	569
1977	59	52	84	49	107	35	386	290	676
1978	36	126	128	26	12	71	399	323	722
40-year average	48	57	84	65	55	36	344	256	600
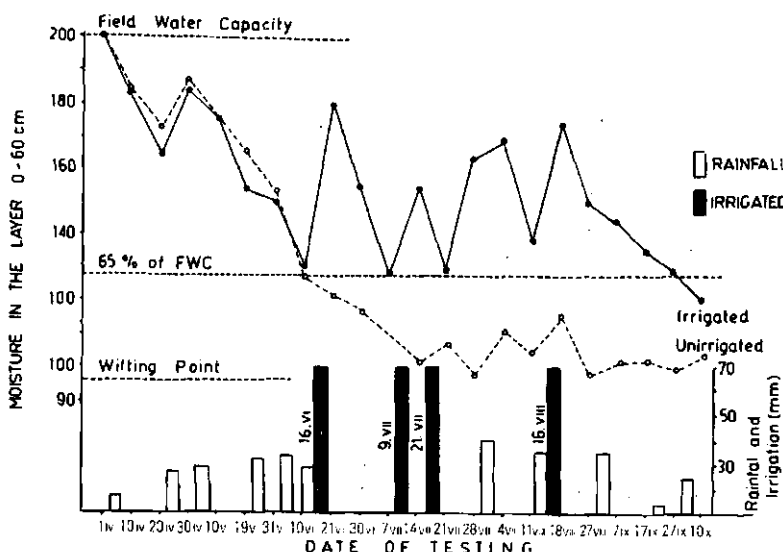
FIG.2. Moisture dynamics in the soil under sugar-beet in 1971.

upper limit and a slightly higher value than the point of permanent wilting as
the lower limit. The latter level of soil moisture was termed lentocapillary
moisture by Widtsoe (see Ref. [3]).

According to our study conducted on loamy soil [4], the lower limit at which
plants start taking up water with difficulty is 65% FWC.

In this trial, irrigation rates were calculated by Kostyakov's formula [5]:

$$M = 100H \ (A-r) \, m^3/ha$$

H = the depth of irrigated soil layer which, in our case, was 0.60 m;
A = the average FWC for that layer was 32% vol.
r = pre-irrigation moisture, as technical minimum, was 22% vol.
   Thus, M = 100 × 0.60 (32−22) = 600 m³/ha.
   The number of irrigations according to Method 1 was:

One irrigation, in 1975: total water added, 600 m³/ha;
Two irrigations, in 1970, 1972, 1974, 1976 and 1977: total water added, 1200 m³/ha;
Three irrigations, in 1973 and 1978: total water added, 1800 m³/ha.
Four irrigations, in 1971: total water added, 2300 m³/ha.

Irrigation dates were determined by charting the values of soil moisture
according to the dates of analysis. To illustrate this, the chart for 1971, when
we had the largest number of irrigations, is given in Fig. 2.

Although Method 1 provides precise data on plant provision with water, the
analytical procedure involved renders the method unsuitable. It is slow and it
requires certain instruments and physical effort. Naturally, simpler and faster
methods are preferred. One of them is soil-moisture determination by a neutron-
scatter probe. Its advantages are that moisture is determined on site quickly without
disturbing the natural soil structure.

Calibration had to be done in order to use the method in our trial. The
calibration curve plotted on the basis of a larger number of analyses (Fig. 3)
had the form of linear regression and a high correlation coefficient (r = 0.735).
A similar curve was plotted by Filipovich [6], who conducted experiments on a
similar soil type.

A tube for inserting the probe was positioned 20−25 cm from the sugar-beet
plants. However, the roots neared the tube as they grew and thickened. Since the
roots have a high water content, the accuracy of moisture readings was affected,
especially in the surface soil layer.

McHenry [7] found that the neutron flux is 10−12 inches (25−30 cm) and
recommended 30−35 cm as a safe distance between plants and the tube to secure
reliable results.
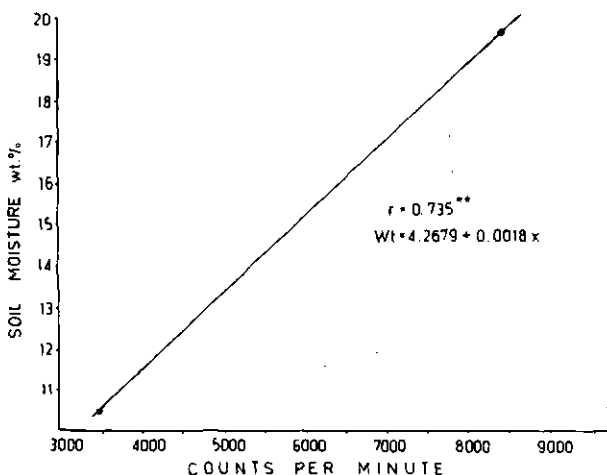
FIG.3.   Calibration curve for neutron measurements of soil moisture.

Method 2

Sugar-beet, like many other agricultural crops, varies in its requirements for
water at different stages of development on account of the degree of development
of roots and foliage and differences in air temperature and other conditions in the
course of the vegetative season.

Sugar-beet requirements for water have been studied intensively and under
different agroclimatic conditions. Orlovskij [8] divided the vegetative period of
sugar-beet into three 50-day stages and found that the transpiration ratio was
1:9:3. In view of the similarities in agroclimatic conditions, we accepted the
above division into three stages but modified their duration.

The first stage lasts from 1 April to 30 June, including the period from planting
to the fuel development of the foliage. During that stage more water is at first
spent on evaporation and later, as the plants grow, for transpiration.

The total water expenditure during that stage was about 200 mm, or 35%
of the total annual expenditure. According to our division of sugar-beet vege-
tation, the stage lasts for 90 days and the water expenditure is correspondingly
high. Similar values were reported by Snitko [9] whereas others, who
limited that stage to 50 days from planting, reported lower values (25 to 30%).
The number of irrigations during that stage varied from zero to two. The irrigation
rate varied from 20 to 40 mm, depending on irrigation date. The average daily
water expenditure was 2.7 mm, with a range of 1 to 4 mm.

The second stage lasts from 1 July to 20 August (50 days). It includes an
intensive growth and thickening of sugar-beet roots and a slow development of the

foliage. The stage is critical regarding sugar-beet requirements for water. One to three irrigations (usually two) with rates of 60 mm were required, the actual number of irrigations depending on the quantity and distribution of rainfall. The total water expenditure was about 240 mm or 40%. The daily expenditure ranged from 4 to 6 mm or 4.6 mm on the average. Half the required amount (120 mm) was usually provided from rainfall and soil reserves and the second half had to be added by irrigation.

The third stage lasts from 21 August to 10 October and includes an intensive accumulation of sugar in the roots. The total water expenditure was about 160 mm or 20–25%. The usual practice was to perform one irrigation with 60 mm water before the end of August because later irrigations tended to reduce the percentage of sugar. The daily water expenditure ranged from 2 to 3 mm or 2.5 mm on an average.

Method 3

This method is also applicable for sugar-beet. In some countries, the USSR for example, the method has been practiced for a long time. Numerous authors, e.g. Shtojko and Andrusenko [10], Lobov [11] etc., pronounce the method as the most appropriate since it deals with the plants themselves. Cell-sap concentration depends on the crop grown and its environment, soil moisture exerting the largest influence.

We performed numerous comparative analyses of cell-sap concentration in the nerve of the seventh leaf of sugar-beet and soil moisture and found high correlations ($r = -0.88$ to -0.92). The processing of the analytical data indicated a square regression (Fig. 4).

Several important parameters had to be determined in order to apply this method. Since cell-sap concentration is greatly affected by leaf age, it was necessary to analyse leaves of the same age. It was found that the seventh or eighth leaf from the centre of the rosette was the most suitable for analysing. Furthermore, better results were obtained by analysing sap taken from the main nerve than from the lamina. Cell-sap concentration depends also on air temperature and relative humidity. Therefore, the analysing was done at the same time of the day, in morning hours (9–10 a.m.)

Cell-sap concentration in sugar-beet leaf increased with plant growth. We found that the limit values, when irrigation becomes necessary, were 7% till the end of June and 8% in the course of July and August.

Method 4

Method 4 balances the uptake and release of water. The latter parameter implies evapotranspiration calculated on the basis of one or several meteorological factors.

$$33.75 - 2.46x + 0.056 x^2$$
$$r = -0.88$$

I. MOISTURE   CONTENT   (% vol)   a. DETERMINATION   OF   TIME
II. MOISTURE   CONTENT   OF FWC   AND QUANTITY OF IRRIGATION
III. WATER   CONTENT   m³/ ha
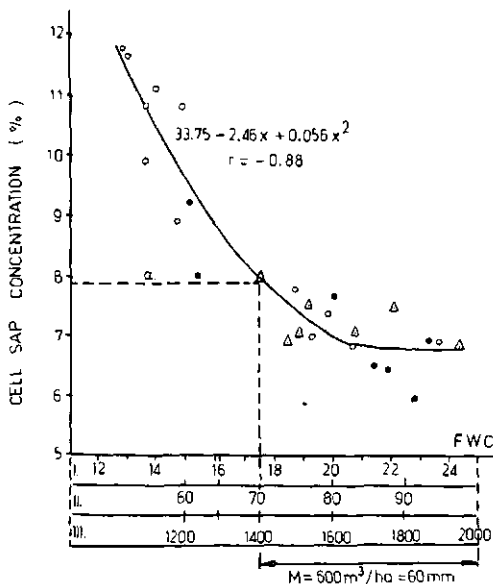
FIG.4.   *Change of cell-sap concentration in the nerve of the 7th leaf of sugar-beet, depending on soil moisture.*

I.   Moisture content (vol. %)   a. Determination of time and quantity of
II.   Moisture content of FWC   irrigation
III.   Water content (m³/ha)

Studies made under different agroclimatic conditions indicated unanimously high correlations between meteorological factors and evapotranspiration. A number of empirical formulas have been proposed. The majority may be expressed by the following equation:

$$e = K \cdot N$$

N = one or several meteorological factors
K = coefficient of total evaporation.

Correlation coefficients, so-called phytobioclimatic coefficients, are used to convert meteorological factors into calculable values. The coefficients are determined for a certain region and a certain crop, experimentally or lysimetrically.

Since evapotranspiration is essentially a thermic process, water expenditure may be approximated on the basis of air temperature. Thornthwaite [12] made
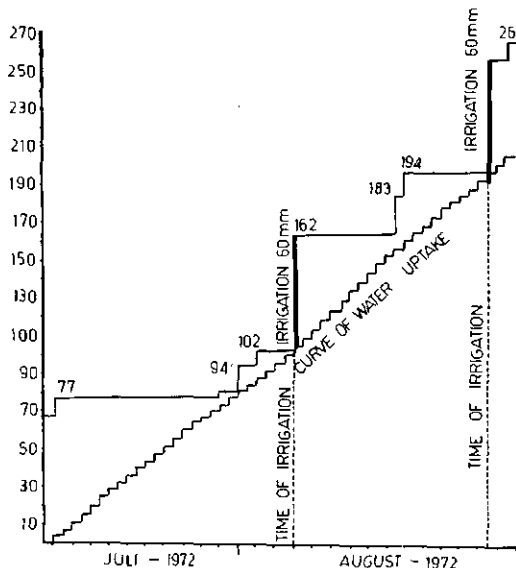
FIG.5.   Graphic presentation of water influx and consumption, and irrigation dates in 1972.

a formula for calculating ETP (evapotranspiration) potential based on air temperature and latitude. Sharov [13] calculated water expenditure in cultured plants on the basis of air temperature. Relying on their results as well as our own long-term data, we made a formula for calculating water requirements of sugar-beet grown in the agroclimatic region of Vojvodina Province:

$$E_t \sim k \cdot \Sigma_t (m^3/ha)$$

E_t = total water expenditure in a certain period
t = sum of mean daily air temperatures, °C
k = phytobioclimatic coefficient.

   The average coefficient for sugar-beet vegetation, determined experimentally by following regularly the soil water balance, was found to be $K-1.8$.
   The phytobioclimatic coefficient varied monthly, in accordance with the changes in water expenditure in the course of sugar-beet growth and development. The calculated values for April, May, June, July, August, and September were 1.5, 1.5, 2.0, 2.1, 2.0, and 1.2, respectively.
   The sugar-beet irrigation schedule was determined by daily calculations of potential evapotranspiration and water uptake and release balancing. These data are given in Fig. 5.

TABLE II. NUMBER OF IRRIGATIONS, TOTAL IRRIGATION WATER, AND
SUGAR-BEET REQUIREMENTS FOR WATER DURING EXPERIMENT

Year	No. of irrigations	Total irrigation water (mm)	Total water requirements (mm)
1970	2	120	552
1971	5	280	592
1972	3	160	577
1973	3	180	575
1974	2	120	541
1975	1	60	569
1976	2	120	542
1977	2	120	569
1978	3	180	566
Average	2.5	150	565

TABLE III. SUGAR-BEET YIELD (t/ha) DEPENDING ON METHOD OF
IRRIGATION SCHEDULING

Year	Method 1	Method 2	Method 3	Method 4
1970	60.4	63.9	61.6	59.8
1971	70.4	65.2	67.1	67.2
1972	75.7	71.5	75.8	73.8
1973	73.9	68.6	69.7	73.3
1974	65.6	62.1	64.7	64.9
1975	53.7	48.1	49.4	50.0
1976	71.8	61.8	64.1	62.7
1977	73.4	76.3	72.2	79.4
1978	60.9	59.6	56.3	62.2
Average	67.3	64.1	65.4	65.9

The method showed that sugar-beet varied in the annual water expenditure from 541 to 592 mm. The average for the experimental period was 565 mm (Table II).

In our trial, the method produced satisfactory results. Generally, it is widely accepted and used because it is simple, quick, and fairly reliable.

EFFECT OF THE TESTED METHODS ON SUGAR-BEET YIELD

Sugar-beet yields varied from year to year, according to prevailing weather and agro-ecological conditions. It means that the yield level is influenced by a complex of factors, not only by the quantity and distribution of rainfall. The differences in sugar-beet yields between the methods were not great — the highest were obtained by Method 1 (Table III), the lowest by Method 2. The difference of 3.2 t/ha or 5% was not significant at LSD 5%[1], but may be considerable in terms of large-scale commercial production.

Our results show that all four methods may be used since they all increased sugar-beet yields in relation to the unirrigated variant by 9.0 t/ha or 16% on an average for the experiment. Method 1 is recommended only if a neutron probe or another piece of equipment for rapid determination of soil moisture is available. If not, we recommended the bioclimatic method.

REFERENCES

[1] RODE, A.A., Pochvennaya Vlaga, Izd-vo Akad. Nauk SSSR, Moscow (1952).

[2] MAKSIMOV, N.A., Izbrannye raboty po zasukhoustojchivosti i zimostojkosti rastenii.
     I. Vodnyj rezhim i zasukhoustojchivost' rasteniya, 1, Izd-vo Akad. Nauk SSSR, Moscow
     (1952).

[3] IZRAELSEN, O.W., Irrigation Principles and Practices, John Wiley and Sons (1955).

[4] DRAGOVIĆ, S., Irrigation of sugarbeet on chernozem at different nutrient levels, Matica
     Srpska, Proc. Nat. Sci. 51 (1976).

[5] KOSTYAKOV, A.N., Osnovy melioratsij, Izd-vo Sel'khozgiz, Moscow (1951).

[6] FILIPOVICH, R., The application of neutron method for moisture measuring in
     different soils, Soil Plant 3 (1973).

[7] McHENRY, J.R., Theory and application of neutron scattering in the measurement
     of soil moisture, Soil Sci. 95 (1963).

[8] ORLOVSKIJ, N.I., Osnovy biologii sakharnoj svekly, Gosel'khozizdam, Kiev (1961).

[9] SNITKO, A.I., Osobennosti formirovaniya urozhaya i rezhim orosheniya sakharnoj
     svekly v usloviyakh Kulundijskoj stepi. Polivnoe svekloseyanie, Sbornik Trudov, Kiev (1970).

[10] SHTOJKO, D.A., ANDRUSENKO, I.I., Sposoby opredeleniya srokov polivov sakharnoj
     svekly, Vestn. S-kh. Nauki (Moscow) 16 No. 11 (1971).

---

[1] LSD = least significant difference.

[11] LOBOV, M.F., Diagnostirovanie srokov polivov ovoshchnykh kul'turov po kontseht-ratsii kletochnogo soka, Biologicheckie osnovy ovoshchaemogo zemledeliya, Izd-vo Akad. Nauk SSSR, Moscow (1957).

[12] THORNTHWAITE, C.W., An approach toward a rational classification of climate, Geograph. Rev. 38 (1948).

[13] SHAROV, I.A., Ehkcpluatatsiya gidromeliorativnykh sistem, Izd-vo Sel'khozgiz, Moscow (1959).

SIMULATED OPTIMIZATION OF CROP YIELD THROUGH IRRIGATION SYSTEM DESIGN AND OPERATION BASED ON THE SPATIAL VARIABILITY OF SOIL HYDRODYNAMIC PROPERTIES

L. GUROVICH, J. STERN, R. RAMOS
Pontificia Universidad Católica
   de Chile,
Santiago, Chile

Abstract

SIMULATED OPTIMIZATION OF CROP YIELD THROUGH IRRIGATION SYSTEM DESIGN AND OPERATION BASED ON THE SPATIAL VARIABILITY OF SOIL HYDRODYNAMIC PROPERTIES.

Spatial autocorrelation and kriging techniques were applied to soil infiltrability data from a 20 hectare field, to separate homogeneous irrigation units. Border irrigation systems were designed for each unit and combinations of units by using DESIGN, a computer model based on soil infiltrability and hydraulics of surface water flow, which enables optimal irrigation systems to be designed. Water depths effectively infiltrated at different points along the irrigation run were determined, and the agronomic irrigation efficiency of the unit evaluated. A modification of Hanks' evapotranspiration model, PLANTGRO, was used to evaluate plant growth, relative crop yield and soil-water economy throughout the growing season, at several points along each irrigation unit. The effect of different irrigation designs on total field yield and total water used for irrigation was evaluated by integrating yield values corresponding to each point, volume and inflow time during each irrigation. For relevant data from winter wheat grown in the central area of Chile during 1981, simulation by an interactive and sequentially recurrent use of DESIGN and PLANTGRO models, was carried out. The results obtained indicate that, when a field is separated into homogeneous irrigation units on the basis of the spatial variability of soil infiltrability and the border irrigation systems are designed according to soil characteristics, both a significant yield increase and less water use can be obtained by comparison with other criteria of field zonification for irrigation management. The use of neutrometric determinations to assess soil-water content during the growing season, as a validation of the results obtained in this work, is discussed.

INTRODUCTION

Knowledge of the influence of non-uniform water infiltration on crop yield is important both to irrigation system design and management and to agronomic and economic evaluation of irrigation methods. When a field is

irrigated by any surface method, i.e. borders, furrows or unchecked flooding, water application expressed as water depths effectively infiltrated at different points over the irrigation run is non-uniform to some degree. Hence, the crop yield is expected to vary from point to point.

Field variability of crop yield is a result of variability in plant genetic properties as well as environmental factors such as climate, management and soil variability. Extensive quantitative information about the effect of soil heterogeneity on soil infiltrability and other hydrodynamic properties has been published [1-5]. The effect of soil heterogeneity on crop yield, as a result of differential water depths infiltrated into the field, has been discussed by several authors [6-9] suggesting that, when considering a whole field, crop potential yield can be obtained in only a few locations; total yield may increase if an optimal irrigation system is designed for each management unit that is considered homogeneous in relation to some relevant soil characteristics affecting irrigation design.

Finally, it is extremely important to evaluate the economic soundness of investments in irrigation technology applied to increase yield and water application efficiency, since productive resources such as capital, labour and inputs − in particular water because of its scarcity − must be allocated according to marginal benefit criteria [10]. An analysis of these aspects is beyond the scope of this study.

An approximate measure of soil uniformity, with respect to any soil parameter, may be given by the autocorrelation function and the values of the integral scale of the pertinent field parameters. The integral scale can be interpreted as the largest average distance for which the parameter is correlated with itself [11].

The autocorrelation function has been used to evaluate the spatial variability of a parameter in the field [12-14], and the framework for expressing such relationships has been developed in time series and spatial analysis, in a discipline generically known as geostatistics.

The values of the integral scale and the autocorrelation function have been used to interpolate between observed values [15], thus enabling a field to be separated into homogeneous zones with respect to a specific parameter; this procedure is known as "kriging".

Surface irrigation design involves balancing the water advance and recession water flows, to achieve a similar opportunity time for infiltration at any point along an irrigation run. Hydraulics of surface water flow and soil infiltrability determine the behaviour of advance and recession functions [16], which define actual opportunity time for infiltration.

When a field presents zones with different infiltrabilities it is obvious that a greater uniformity in water depths stored in the soil profile along the irrigation run can be achieved if the system is designed specifically for each zone, according to its characteristics.

Irrigation system design through the use of computer models has been reported [17, 18]. This approach is useful for irrigation design when the complexities of surface water and soil-water flow processes, interacting during irrigation, are considered.

Several investigators have proposed models for predicting plant yield as influenced by water use. The evapotranspiration model, PLANTGRO, developed by Hanks [1], has proved widely applicable for estimating seasonal crop yield, incorporating differential water applications, potential and actual evapotranspiration, soil-water storage, and drainage.

For a given crop and year relative transpiration is equal to relative yield [1], as given by

$$Y/Y_p = T/T_p \tag{1}$$

where Y_p is potential yield when transpiration is equal to potential transpiration, T_p.

Hanks [1] proposed general transpiration relations to soil-water status and to potential transpiration. The simplest one is typified by the equation:

$$T = T_p \, (SWS/AW) \tag{2}$$

where SWS is the actual soil-water storage, and AW the amount of available water. SWS is the product of the depth of the root zone and the difference between actual volumetric water content and wilting point; AW is the product of the depth of the root zone and the difference in volumetric water content between field capacity and wilting point. Obviously, the amount of actual soil-water storage in a dry season depends on the irrigation regime. Non-uniform water infiltration will cause some areas in the field to be low in soil-water storage and, therefore, in crop yield.

Field studies on the effect of design and management of irrigation systems upon crop yields, as a first approach, are difficult and expensive. Thus, a simulation of field spatial variability of soil infiltrability on wheat yield and water use is presented; this work is based on the interactive use of DESIGN and PLANTGRO models, the first developed by the authors, and the second by Hanks [1].

Field validation of the simulation results is now in its initial stages; neutrometric determinations of soil-water depths at different locations along each irrigation unit are carried out intensively before and after each irrigation, to evaluate actual evapotranspiration and infiltrated water depths.

The study presented here aims to design alternative border irrigation systems for a field divided into several management units, related to soil infiltrability, through the use of spatial autocorrelation and kriging techniques. At the same

time the objective is to integrate crop yield and water use on the whole field, simulating the behaviour of wheat in the irrigation units, or combinations of units, thus evaluating alternative management approaches.

MATERIAL AND METHODS

Using methods based on Gaussian functions, described by the authors [19], a set of soil infiltrability data was generated. These data were associated with 64 specific locations, evenly distributed on a grid (Fig.1), in such a way that the field was divided into two apparently homogeneous zones of different dimensions. To test the homogeneity of soil infiltrability of each zone, the autocorrelation function was applied to data on basic soil intake rates and the integral scale was calculated in a procedure described by the authors [2].

For this field, the following irrigation design and management alternatives are compared:

(1) Independent design for each apparently homogeneous unit, as indicated before;
(2) Irrigation design, considering the whole field to be homogeneous, using the average soil infiltrability of the largest unit;
(3) Same as (2), using the mean value of soil infiltrability of the whole field;
(4) Same as (2), using the weighted mean value of soil infiltrability of the whole field; and
(5) Irrigation design for two zones of equal length of run, using mean soil infiltrability values corresponding to the predominant soil on each unit.

The border irrigation systems design for each management alternative was obtained using the DESIGN computer model [20]. Water depths infiltrated along the irrigation runs, surface runoff and deep percolation, were determined. By taking into consideration the discharge and inflow time into the border, the total volume of water applied on each irrigation was evaluated. Thus, the application, storage, uniformity and agronomic efficiencies for irrigation [21] were obtained.

The PLANTGRO model [1] was used to define production functions of wheat grain yield in relation to irrigation water depths infiltrated into the soil. These functions were obtained for irrigation frequencies of 12, 20 and 30 days, starting irrigation at the beginning of the dry season.

Wheat grain yield at each location along the irrigation run was obtained by evaluating the production function with the water depth effectively infiltrated at this location, thus assessing the effect of irrigation design on crop yield.
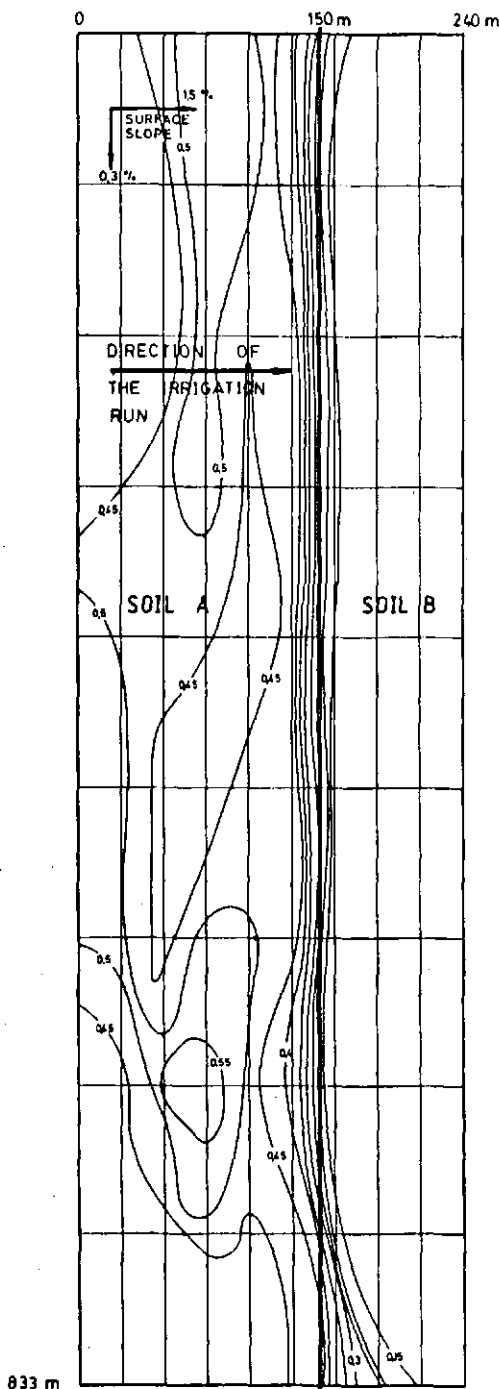
FIG.1. Simulated field.

RESULTS AND DISCUSSION

As a result of soil formation processes, it is usual to find on irrigated fields areas with different textures and structural characteristics, which determine zones of different soil infiltrability. However, the variation in soil hydraulic characteristics is not randomly distributed on the field, but usually follows a certain spatial pattern which may be gradual or steep.

The integral scale of soil infiltrability, calculated for all 64 generated values of the whole field, is 67 m, indicating a spatial variability of soil infiltrability in this field; thus, it is necessary to select zonification criteria to divide the field into homogeneous units for irrigation management. Several data-clustering alternatives were tested, selecting an arbitrary division into two units, 1/3 and 2/3 of the field as the alternative giving the highest soil homogeneity (Fig.1); on each unit integral scales of soil infiltrability values were 96 m and 147 m, respectively, indicating that each zone is relatively uniform in relation to this parameter.

To define a more precise separation of the field into two uniform units, a weighted interpolation between the integral scales and the mean soil infiltrability values for each zone was carried out according to kriging techniques published in the literature [15]. This procedure indicates that the field should be separated into two zones of 150 and 90 m long, as shown in Fig.1, where iso-soil steady-state intake rate lines are presented.

Irrigation management considerations may indicate the advantages and possibilities of dividing the field in relation to the spatial variability of soil infiltrability, on the basis of its integral scale. Any other criteria of irrigation system design and operation will create a situation where water depths infiltrated towards the end of the infiltration run, will be less than that needed to replenish water evapotranspirated by the crop if no water is allowed to percolate and run-off at the beginning and the end of the infiltration run, i.e. if an adequate irrigation application efficiency is to be obtained.

When field zonification is done according to the values of the integral scale of soil infiltrability (alternative 1), water-depth distribution along the run is uniform, as shown in Fig.2. If the field is irrigated as one unit (240 m length of irrigation run) (alternative 2), the change in the infiltrated water depth along the irrigation run is very steep (Fig.2), since soil A presents higher infiltrability than soil B, thus remaining only a small water volume for effective infiltration into soil B. Only if the inflow time is significantly increased over its optimum value in relation to application efficiency is it possible to obtain the necessary infiltrated water depth at the end of the run that will restore the field capacity on the soil profile at this location.

If the field is arbitrarily divided into units of equal length (i.e. 120 m for each irrigation run) (alternative 5), the irrigation design will enable an adequate
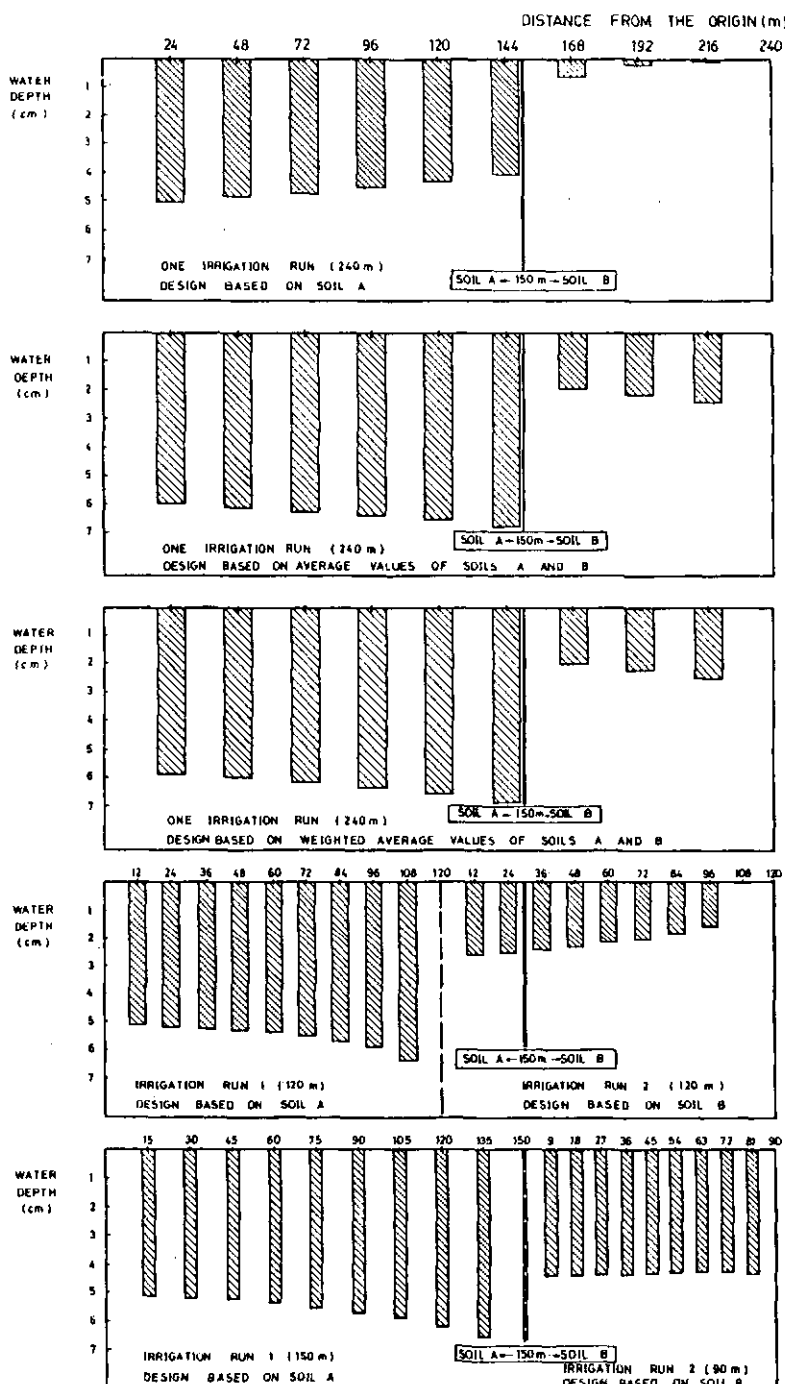
FIG.2.   Water depths infiltrated into the soil for each irrigation.

$$Y/_{Y_0} = 100 \left(1 - 0.6794\, e^{\beta x} \right)$$

WATER   DEPTH   INFILTRATED   ON   EACH   IRRIGATION   (cm)

□	FREQ = 12 DAYS	β = -0.54	r² = 0.782	SSR = 159.12
◇	FREQ = 20 DAYS	β = -0.32	r² = 0.744	SSR = 188.02
×	FREQ = 30 DAYS	β = -0.24	r² = 0.764	SSR = 192.42
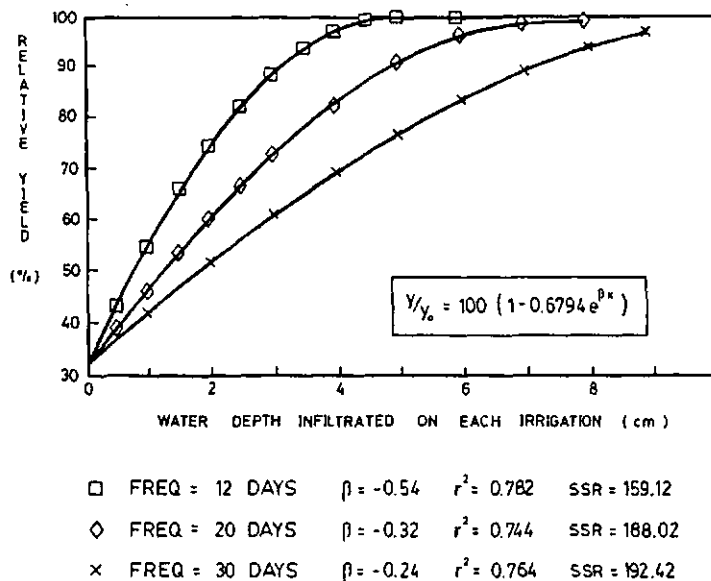
FIG.3.   Water-production functions.

distribution to be obtained of infiltrated water depths in the unit in which only one kind of soil, in relation to its infiltrability, is present. If at one unit two soils with different infiltrabilities coexist, water-depth distribution along the run is expected to be highly non-uniform (Fig.2).

Production functions of infiltrated water depths for three different irrigation frequencies are presented in Fig.3. The effect of irrigation frequencies on crop yield is clearly shown; for example, for a 5 cm water depth infiltrated on each irrigation the losses in relative yield, when the specific location is irrigated every 30 and 20 days, is 22 and 9% respectively, as compared with the same location irrigated every 12 days.

A definite trade-off between irrigation frequencies and infiltrated water depths is presented in Fig.3. Thus, 80% of relative yield can be obtained with 2.2 cm water depth if the irrigation is repeated every 12 days, but if the irrigation frequency is every 20 and 30 days 3.8 and 5.2 cm, respectively, must be infiltrated, to obtain the same yield. The decision regarding which irrigation regime is to be followed on a specific field will depend on the amount of water available and its relative price, since high-frequency irrigation requires more water when the total season is considered, owing to considerations of application efficiency.

Water-production functions presented in this study, obtained through the use of Hanks' PLANTGRO model [1], are similar to those published by

TABLE I. TOTAL WATER APPLIED, AGRONOMIC EFFICIENCY OF
IRRIGATION AND WHEAT YIELD[a]

Irrigation run alternative		Agronomic efficiency	Total water applied/irrigation	Wheat yield for irrigation frequency		
Length (m)	Design based on:	(%)	(m³/ha)	12 days	20 days	30 days
150+90	Soils A and B independently	35.5	176.8	96.6 (6.28)	83.4 (5.42)	79.7 (5.18)
240	Only Soil A	21.1	362.8	76.5 (4.97)	68.8 (4.47)	63.7 (4.14)
240	Average, Soils A and B	31.19	589.3	92.2 (5.99)	83.2 (5.41)	77.1 (5.01)
240	Weighted Average, Soils A and B	35.1	535.2	92.5 (6.01)	83.4 (5.42)	77.1 (5.01)
120+ 120	Soils A and B independently	25.3	115.2	85.2 (5.54)	75.7 (4.92)	69.7 (4.53)

[a] Relative grain yield (%), (and grain yield (kg/ha) when potential yield is 6.5 t/ha).

others [22, 23]. One of the outstanding features of the PLANTGRO model
is the set of parameters that relate available water in the soil profile to its
effects on crop yield. Data sets for wheat, corn and other crops have been
reported, defining these parameters for the conditions of the corresponding
experiments. However, it is not clear if these parameters can be applied
universally or if there is a need to evaluate them specifically for a given set
of crop variety, soil and climatic conditions [24, 25]. This aspect needs
further field evaluation to assess relevant values for specific situations.

Values of relative grain yield for the different irrigation management
alternatives studied are presented in Table I. These values are obtained by
integrating relative yields corresponding to each of the nine locations along
each irrigation run, which are evaluated using the water-production functions
for the water depth infiltrated at the specific location on each irrigation.

A significant yield increment is obtained when irrigation design takes
into consideration the uniformity of infiltrated water depths' distribution
along the irrigation run; for example, when the field is divided according to
the integral scale of soil infiltrability values (alternative 1), a 26% yield
increment is obtained in relation to an irrigation design based only on the
predominant soil (alternative 2), and the yield increment is 46% when

alternative 1 is compared with an irrigation design based on equal irrigation run lengths with mean values of the pertinent soil characteristic parameters (alternative 5).

For a field, arbitrarily divided into two irrigation units, each 120 m long (alternative 5), a definite relation between the uniformity of infiltrated water depths and the relative wheat grain yield is obtained; at the first irrigation unit, where only one kind of soil is present (soil A), a relative yield of 89.43% is obtained but, on the second unit, where both soils coexist, only 61.9% of the potential yield can be reached for a 20-day irrigation frequency. Results for 12 and 30 days' frequency present similar differences.

The potential wheat yield for the edapho-climatic conditions of this study, which correspond to those of an alluvial irrigated soil in central Chile, is 6.5 t/ha, obtained under optimal field conditions. In Table I, the grain yield is also presented for comparison purposes. Relative prices of inputs, as well as for wheat grain, must be considered in relation to the results presented here, in order to decide alternative strategies for dealing with the spatial variability of soil infiltrability values in connection with irrigation management possibilities.

The agronomic efficiency of irrigation, which is the product of application efficiency, relative replenishment of soil water up to field capacity, and Christiansen's coefficient of uniformity [21], vary in a similar way to the yield (Table I), owing to a greater uniformity of infiltrated water depths, and a higher application efficiency, which is obtained for irrigation designs that follow more closely the differences in soil infiltrability along the field. For example, for a field divided according to the integral scale of soil infiltrability values (alternative 1), an increment of 14.5% on agronomic efficiency of irrigation can be obtained, as compared with a complete field, where irrigation design is based on values corresponding to the predominant soil only (alternative 2).

Agronomic efficiency of irrigation is an adequate index for evaluating this practice from the standpoint of yield; values obtained on this work for border irrigation (21.0 to 35.5%) are in the range reported in other studies [21], indicating that, although efficiency can be significantly enhanced by management, this kind of optimal design is inherently inefficient as compared with sprinkler or drip irrigation systems. Thus, a significant amount of water applied to the field will not be available to the crop and will be lost by run-off and deep percolation, so that a certain uniformity on infiltrated water depths can be attained.

Total water volume applied to each irrigation (Table I) is one of the aspects most affected by irrigation management as a result of irrigation design based on field zonification. One third of the total volume of water is needed if the field is divided according to the integral scale (alternative 1), and if optimum irrigation management is done on each zone, as compared with a

240-m irrigation run, on which irrigation design is based on the predominant
soil (alternative 2). Even with that significantly lower applied water volume,
the total field yield is 26% higher, owing to the uniformity of infiltrated
water depths.

For surface irrigation systems, farmers tend to underestimate the value
of total water applied to crops, and the cost of labour needed for that application.
However, as water and labour are becoming more and more expensive in
relation to crop returns, savings obtained through improved irrigation manage-
ment are a priority; criteria of irrigation management such as those presented
in this paper can result in these savings without too much investment; these
economic considerations are now being tested.

Irrigation frequency is a determinant parameter of irrigation management.
In this study, the irrigation frequencies considered were constant throughout
the season; thus, at the beginning and end of the season, irrigation design is
over-dimensioned in relation to the actual water depth to be replenished in
the soil profile, since the design considers a constant replenishment water depth
according to peak crop evapotranspiration, and a constant opportunity
time for infiltration that takes place at each location of the irrigation run.
To improve the agronomic efficiency of irrigation, a variable water application
frequency is now being considered — the frequency criterion — to start
irrigation when a constant water depth has been consumed by the crop.

Surface irrigation system design is significantly affected by the degree and
distribution of field slope; when the slope is non-uniform along the irrigation
run, infiltrated water depths will also be non-uniform since surface water flow
velocity will change at different locations and an effective opportunity time
for water to infiltrate will differ along the run. Variable field slopes were not
considered at this stage of the research, but they are now being studied to
evaluate alternative management practices such as land grading versus field
zonification for irrigation, to account for slope variation.

In many irrigated soils, infiltrability values usually tend to diminish
throughout the crop growing season, mainly due to the mechanical and chemical
effects of agricultural practices. Thus, a certain degree of compactation due
to machinery traffic, or fertilizer and soluble salts migrating towards the surface
can be expected, as well as crust formation due to seasonal dispersion and
structure alterations caused by water flowing over the soil surface.

Irrigation system design and operation are planned according to the average
values of soil infiltrability, true only for one or two irrigations in the middle of
the season, and in some cases this time variation of soil infiltrability values
can significantly affect water-depth distribution along the irrigation run. The
evaluation of this time effect on irrigation system design and subsequent
application efficiency of irrigation water has seldom been reported.

Surface water flow velocity over the irrigation run is a result of soil roughness and plant density, which interact to determine a parameter known as the Manning coefficient of roughness. Both components of this coefficient vary during the growing season of a crop, thus affecting the irrigation system management in a way similar to that discussed previously for field slope effects [26].

In this study the eventual negative effect of limited soil profile drainage on crop yield is not considered, since the PLANTGRO model does not take this aspect into consideration. This effect may occur at some locations along the irrigation run owing to non-uniformities on infiltrated water-depth distribution.

The effect of irrigation design upon crop yield, based on soil zonification, is now being confirmed by field work. The results obtained through the approach presented in this paper should enable specialists to select, among the many irrigation design and operation alternatives, those field treatments that represent actual possibilities so as to enhance total field crop yield and water use efficiency, by adapting irrigation management to spatial variability of soil infiltrability values.

The intensive use of neutrometric determinations of soil water, before and after each irrigation, for different soil profiles along each irrigation run, is now being considered. These measurements will determine the soil-water depth infiltrated at each location, and the difference between consecutive measurements represents the actual crop evapotranspiration if no drainage is measured. Thus, soil-water economy will be monitored during the growing season, and its effects upon plant growth and yield will be assessed, so as to establish the relative effect of soil water availability upon crop development.

The results presented here are based on the use of two simulation models that require, as inputs, the environmental and management data; if field validation of these results indicate that good predictions on field yield and water use can be obtained through the use of the simulation models, this approach will be extended to other crops and irrigation methods, such as corn and furrow or pastures, and unchecked flooding systems.

The contribution of the work presented here is the practical combination of three disciplines: geostatistics, engineering design of irrigation systems and evapotranspiration-crop yield modelling — in order to predict economic solutions for agronomic problems related to the actual irrigation of a specific field.

CONCLUSIONS

The results presented in this paper enable the following conclusions to be reached:

1. For a field, where soil infiltrability is spatially variable, an irrigation design based on the values of the integral scale can bring about an increment of relative yields and a reduction of total water applied.

2. If, from agronomic considerations, the field cannot be divided into different irrigation managements units, it is useful to design and operate irrigation according to the average (or weighted average) values of soil infiltrability, corresponding to the soils present on the field, rather than taking into consideration only the dominant soil type.

3. If on an irrigation management unit two areas with different soil infiltrability coexist, a significant reduction of relative crop yield can be expected because non-uniformity of the distribution of water depths infiltrated into the soil along the irrigation run.

4. Agronomic efficiency of the irrigation system, designed on the basis of spatial variability of soil infiltrability values, can be improved as a result of a better distribution uniformity of infiltrated water depths obtained along the irrigation run.

5. The total water volume needed to be applied on a field that is divided according to the integral scale of its soil infiltrability need be only one third of that required for an undivided field.

6. Intensive neutrometric determinations of the soil water present in the profile along the irrigation run, before and after each irrigation, seem to be the best approach to confirm the field results of this work.

REFERENCES

[1] HANKS, R.J. Model for predicting plant growth as influenced by evapotranspiration and soil water, Agron. J. 66: (1974) 660.

[2] GUROVICH, L., STERN, J. Variabilidad espacial de la velocidad de infiltración en el suelo. II. Análisis geoestadístico y estructura espacial, Ciencia e Investigación Agraria 10 (1983) in press.

[3] NIELSEN, D.R., BIGGAR, J.W., EHR, K.T. Spatial variability of field measured soil water properties, Hilgardia 42 (1973) 215.

[4] WARRICK, A.W., MULLER, G.J., NIELSEN, D.R. Predictions of the soil water flux based upon field measured soil water properties, Soil Sci. Soc. Amer. J. 41: (1977) 388.

[5]   STOCKTON, J.G., WARRICK, A.W.   Spatial variability of unsaturated hydraulic conductivity, Soil Sci. Soc. Amer. Proc. 35 (1971) 847.

[6]   STERN, J.   Non-uniform sprinkler irrigation and corn yield. M.Sc. Thesis, Hebrew University of Jerusalen (1981).

[7]   BRESLER, E., DAGAN, G., HANKS, J.   Statistical analysis of crop yield under controlled line source irrigation, Soil Sci. Soc. Amer. J. 46: (1982) 841.

[8]   BRESLER, E., COHEN, O.P.   The effect of non-uniform water application on soil moisture content, moisture depletion, and irrigation efficiency, Soil Sci. Soc. Amer. Proc. 31 (1967) 117.

[9]   ZASLAVSKY, D., BURAS, N.   Crop yield response to non-uniform applications of irrigation water.   Trans. ASAE 10 (1967) 196.

[10] VENEZIAN, E., GUROVICH, L.   Uso eficiente del agua de riego en Chile a través de una moderna política de aguas, Ciencia e Investigación Agraria 7 (1980) 115.

[11] RUSSO, D., BRESLER, E.   Soil hydraulic properties as stochastic processes. I. An analysis of field spatial variability, Soil Sci. Soc. Amer. J. 45 (1981) 682.

[12] GUROVICH, L., STERN, J.   Estructura de la variabilidad espacial de las propiedades hidrodinámicas de los suelos, Ciencia e Investigación Agraria 9 (1982) 243.

[13] WARRICK, A.W., NIELSEN, D.R.   Spatial variability of soil physical properties in the field, In: "Applications of Soil Physics" by Hillel, D. Academic Press, N. York (1980) 319.

[14] VACHAUD, G.   Soil Physics Research and Water Management, 12th International Conference of Soil Science, N. Delhi (1982) 32.

[15] MATHERON, G.   The theory of regionalized variables and its applications.   Ecole des Mines, Fontainebleu, France (1971).

[16] HART, W.E., COLLINS, H.G., WOODWARD, G., HUMPHERYS, A.S. Design and operation of gravity or surface systems, In: "Design and Operation of Farm Irrigation Systems", Jensen, M.E. (ed.). ASAE Monograph 3 (1980) 501.

[17] FANGMEIER, D.D., STRELKOFF, T.   Mathematical models and border irrigation design, Trans. of the ASAE 22 (1979) 92.

[18]   FONKEN, D.W., CARMODY, T., LAURSEN, E.M., FANGMEIER, D.D.
        Mathematical model of border irrigation, J. of the Irriga
        tion and Drainage Division, ASCE 106 (1980) 203.

[19]   GUROVICH, L., STERN, J.   Variabilidad espacial de la velo
        cidad de infiltración del agua en el suelo. I. Generación
        de datos, Ciencia e Investigación Agraria 10 (1983) 35.

[20]   RAMOS, R.   Diseño computarizado del riego por bordes.
        M.Sc. Thesis, Pontificia Universidad Católica de Chile
        (1983).

[21]   GUROVICH, L.   Conceptualización de la eficiencia de riego
        a nivel predial.   Análisis de algunas situaciones en Chile,
        Ciencia e Investigación Agraria 5 (1978) 171.

[22]   HEADY, E.O., HEXEM, R.W.   Water production functions of
        irrigated agriculture, The Iowa State University Press
        (1978).

[23]   SHALHEVET, J., MANTELL, A., BIELORAI, H., SHIMSHI, D.
        Irrigation of field and orchard crops under semi-arid con
        ditions, International Irrigation Information Center. Pu
        blic. N° 1, (1976).

[24]   STEWART, J.I., HAGAN, R.M.   Function to predict effects of
        crop water deficits, J. of the Irrigation and Drainage Di
        vision ASCE 99 (LR4) (1973) 421.

[25]   STEWART, J.I., HAGAN, R.M., PRUITT, W.O.   Functions to
        predict optimal irrigation programs, J. of the Irrigation
        and Drainage Division ASCE 100 (IR2) (1974) 179.

[26]   SHIH, S.F., RAHI, G.S.   Seasonal variations of Manning
        roughness coefficient in a subtropical marsh.   Trans. of
        the ASAE 25 (1982) 116.

MISE AU POINT,
A L'AIDE D'UN HUMIDIMETRE A NEUTRONS,
D'UN MODE RATIONNEL
D'IRRIGATION A LA RAIE
BASE SUR L'EMPLOI DE TENSIOMETRES

P. PEYREMORTE
Société du Canal de Provence et
    d'aménagement de la région provençale,
Aix-en-Provence

M. AKHTAR BHATTI
Institut national polytechnique,
Toulouse,

France

Abstract—Résumé

USE OF A NEUTRON MOISTURE GAUGE TO DEVELOP A RATIONAL METHOD OF
FURROW IRRIGATION BASED ON TENSIOMETERS.
    Surface irrigation continues to be the commonest worldwide method distributing water
and the interest in it has been revived since the rise in the cost of energy. Mastery of this
method requires in agricultural practice a simple technique for determinating the variation in time
in the state of the soil water so as, first, to improve the uniformity of application and, second,
to estimate the time for re-application without the need for systematic encroachment upon the
irrigation frequency. The use of tensiometers, which are simple and easy to operate, was tried
out by a method appropriate for the purpose of improving furrow irrigation management in
the case of maize crops. The results show the extent of possible improvements.

MISE AU POINT, A L'AIDE D'UN HUMIDIMETRE A NEUTRONS, D'UN MODE RATIONNEL
D'IRRIGATION A LA RAIE BASE SUR L'EMPLOI DE TENSIOMETRES.
    L'irrigation de surface reste le mode de distribution de l'eau le plus employé à l'échelle
mondiale et connaît un regain d'intérêt depuis l'augmentation du coût de l'énergie. La maîtrise
de ce mode d'irrigation nécessite de disposer, à l'échelle de la pratique agricole, d'un moyen
simple pour apprécier l'évolution de l'état hydrique du sol; d'une part, pour améliorer l'uni-
formité des arrosages, d'autre part, pour apprécier l'opportunité de renouveler les apports afin
de ne pas intervenir systématiquement au régime du «tour d'eau». L'emploi de tensiomètres,
appareils simples dont l'utilisation est peu contraignante, a été testé selon une méthode de mise
en œuvre adaptée aux objectifs d'amélioration de la conduite des irrigations à la raie sur des
cultures de maïs. Les résultats obtenus montrent l'importance des progrès possibles.

1.   INTRODUCTION

L'irrigation de surface reste prédominante et connaît même un regain d'intérêt dans les pays industrialisés depuis l'augmentation du coût de l'énergie. L'importance de la consommation énergétique des techniques modernes d'arrosage a été souvent évoquée: Kemper et al. [1] ont indiqué, à ce sujet, que la mise sous pression nécessaire pour l'aspersion pouvait exiger jusqu'à 4 à 5 fois plus d'énergie que les besoins de traction concernant l'ensemble des autres interventions utiles pour certaines grandes productions.

Il s'ensuit que de très nombreux programmes de recherche tendent actuellement à réhabiliter l'irrigation de surface notamment par des moyens permettant de mécaniser la distribution à la parcelle.

La maîtrise de ce mode d'arrosage est difficile à obtenir. A ce propos, Keller et al. [2] ont signalé que les irrigants n'ont, jusqu'à présent, que très peu bénéficié des travaux réalisés par les chercheurs.

Les principes fondamentaux de la conduite des irrigations à la raie ont pourtant été développés par de nombreux auteurs aux cours des dernières décennies [3–6] et permettent aux techniciens d'avoir une bonne approche de l'ensemble des situations concernées.

En Provence, où les trois quarts des superficies sont arrosés de cette façon, on constate que les modes de conduite sont devenus exclusivement dépendants des disponibilités en main-d'œuvre au mépris des paramètres techniques à respecter pour garantir l'efficacité des irrigations. Ainsi réalisé, l'arrosage constitue le principal facteur limitant comparativement au progrès des autres techniques (variétés, fertilisation, etc.) et les agriculteurs ont conscience de la nécessité de reconsidérer les pratiques actuelles.

Dans ce contexte, nous avons pensé que le meilleur moyen de faire progresser la conduite des irrigations était de mettre à la disposition des agriculteurs une méthode d'appréciation objective de l'état hydrique du sol.

Dans les conditions de la pratique agricole, cela impose de prendre en compte les impératifs de simplicité des appareils à mettre en œuvre, raison pour laquelle nous avons envisagé l'usage de tensiomètres [7, 8].

La mise au point d'une méthode pratique d'emploi de ces appareils en vue d'assurer un mode rationnel d'irrigation à la raie n'a été possible qu'à partir de l'usage d'un moyen approprié pour analyser la teneur en eau des sols; nous avons utilisé pour cela un humidimètre à neutrons.

2.   CONDITIONS GENERALES DES ESSAIS – MATERIELS ET METHODES

2.1. Conditions générales

La recherche a été réalisée dans la vallée de la Durance, près d'Oraison, dans une région sous l'influence du climat méditerranéen qui se caractérise par une longue période de sécheresse estivale. Le sol est une alluvion récente à prédominance de limons (teneurs moyennes: argile 26%, limon 52%, sable 22%). Un horizon plus dense s'opposant à la pénétration des racines a été décelé entre les niveaux 45 et 55 cm.

La parcelle sur laquelle ont été réalisées les observations a une surface de 4 ha cultivée en maïs. Dans le sens de l'arrosage, elle a en moyenne 160 m de longueur avec une pente de 0,38%. Les lignes de culture sont espacées de 0,75 m. Les raies d'arrosage, distantes de 1,5 m, n'occupent qu'un interligne sur deux. L'irrigation est soumise à la contrainte du tour d'eau hebdomadaire.

2.2. Mesures climatiques

Les pluies ont été mesurées à proximité du lieu d'essai. L'estimation de l'évapotranspiration maximale de la culture a été établie à partir de l'évapo-transpiration potentielle (ETP) corrigée par un coefficient cultural établi dans la région.

2.3. Mesures des quantités d'eau engagées

Le débit d'irrigation a été contrôlé à l'aide des canalisations de Parshall. Les collatures ont fait l'objet de mesures en continu.

2.4. Mesures de l'état hydrique du sol

2.4.1. Humidimétrie

La teneur en eau du sol a été appréciée avant chaque arrosage à l'aide d'un humidimètre à neutrons. Le matériel (une sonde NEA neutronique et gammamétrique) a été mis à notre disposition par le Centre d'étude du machinisme agricole, du génie rural et des eaux et forêts d'Aix-en-Provence. Les mesures effectuées aux niveaux 25, 50, 75, 100 cm de profondeur, respectivement désignés H1, H2, H3 et H4, ont permis d'analyser l'évolution de la teneur en eau du sol sur une épaisseur supérieure à celle contribuant directement à l'alimentation de la culture. A cette fin, en 1981, des tubages ont été implantés à proximité d'une raie d'arrosage et, au milieu de l'espace séparant deux de ces raies, en quatre sites équidistants dans le sens longitudinal. Ne seront présentés que les résultats des deux sites

extrêmes, le premier, S1, placé à 20 m du point d'alimentation des raies, et le second, S2, placé à 140 m de ce point d'alimentation. En 1982, S1 et S2 ont été maintenus, sur chaque comparaison d'irrigation, à 40 et 120 m de distance du point d'alimentation des raies.

2.4.2. Tensiométrie

L'état de tension de l'eau du sol a été apprécié par des mesures effectuées tous les deux jours. Les tensiomètres, de marque Irrometer, ont été éprouvés au laboratoire chaque année avant leur positionnement pour connaître la réponse des manomètres Bourdon qui les équipent. Les appareils étaient placés entre les deux tubages destinés aux mesures d'humidité, en chacun des deux sites, aux profondeurs 45, 60, 90, 120, 150 cm en 1981 et 30, 40, 60, 75, 90 cm en 1982.

2.5. Mesures agronomiques

Outre l'observation du comportement de la culture, le rendement en grain a été établi par la récolte de 6 rangs effectuée à la moissonneuse-batteuse.

2.6. Variables imposées et dispositif expérimental

En 1981, l'étude a eu essentiellement pour but d'analyser la conduite assurée selon la pratique courante de l'agriculture: apports hebdomadaires avec un débit de $0,35 \ L \cdot s^{-1}$/raie.

En 1982, un essai systématique à trois répétitions a permis de comparer trois traitements correspondant à des modes de conduite améliorés:
– TA: traitement irrigué hebdomadairement au débit de $0,55 \ L \cdot s^{-1}$/raie;
– TB: limitation du nombre d'arrosages en tenant compte des observations tensiométriques, irrigation à un débit de $1,4 \ L \cdot s^{-1}$/raie pour l'humectation et à $0,7 \ L \cdot s^{-1}$/raie pour l'entretien;
– TC: autre régime d'arrosage (non présenté ici).

De plus, au cours de ces essais, une méthode de mise en œuvre des tensiomètres a été testée; cette méthode a pour base:
– d'une part d'apprécier la qualité de la distribution au long des raies, facteur principal de l'efficience de l'arrosage; dans ce but, des tensiomètres sont placés à plusieurs niveaux en deux sites: l'un entre 1/4 et 1/3 de la longueur des raies, l'autre entre les 2/3 et les 3/4 de cette longueur;
– d'autre part de juger l'opportunité de réaliser ou renouveler l'arrosage.

Le premier arrosage n'est effectué que lorsque la tension atteinte au premier niveau de mesures est jugée suffisante pour révéler un besoin d'irrigation. La profondeur choisie pour ce premier niveau est telle que la première irrigation n'est réalisée que lorsque la tension atteint la limite supérieure de fonctionnement

des tensiomètres (80 centibars). Cette profondeur peut se situer nettement en dessous de l'épaisseur du sol concernée par l'enracinement de la culture.

Les apports ne sont renouvelés que lorsqu'il y a eu exploitation suffisante des réserves reconstituées au cours de l'irrigation précédente, ce que révèle une tendance à l'accroissement des tensions aux divers niveaux. La présence d'appareils à plusieurs niveaux permet de garder les informations même lorsqu'il y a eu désamorçage des appareils situés à moindre profondeur.

Trois niveaux sont proposés en chaque site. Pour prendre en compte le gradient de distribution inhérent à ce mode d'arrosage, le niveau 1 du site 2 est placé à même profondeur que le niveau 2 du site 1. Ces niveaux doivent être adaptés à chaque culture et à chaque condition de sol [8].

3.   RESULTATS

3.1. Résultats obtenus en 1981 [9]

Le rendement de la culture a été de 114 quintaux à l'hectare de grains à 15% d'humidité.

L'exploitation des mesures a montré que l'irrigation traditionnellement employée était beaucoup trop abondante. De plus, le fait de connaître ces informations a induit l'exploitant à supprimer deux arrosages par rapport à sa conduite habituelle. Malgré cela, huit apports ont été réalisés totalisant 443 mm d'apport soit, compte tenu des pluies, 130 mm de plus que les besoins estimés à partir du bilan d'évapotranspiration maximale.

L'appréciation des quantités globales d'eau distribuées ne permet pas de juger la qualité de l'arrosage car l'excès apparent peut s'accompagner d'une forte différence de distribution entre le début et la fin des raies.

3.1.1. L'observation de l'évolution de la teneur en eau du sol, appréciée par les mesures neutroniques effectuée avant chaque arrosage, permet les commentaires suivants:

a)   les horizons H3 et H4 n'ont pas eu à participer directement à l'alimentation de la culture;

b)   au site 1, H1 et H2 ne se différencient pas et restent tous deux à une teneur élevée qui a dû provoquer de fortes pertes par percolation, tandis qu'au site 2, la teneur en eau du sol reste nettement plus basse pour H1; de plus, H2 présente une tendance à l'assèchement dans le temps;

c)   la prise en compte de l'état hydrique du sol à proximité de la raie d'arrosage et de celle de l'interligne ne montre pas de différence marquée au S1, alors qu'elle est très important au S2.
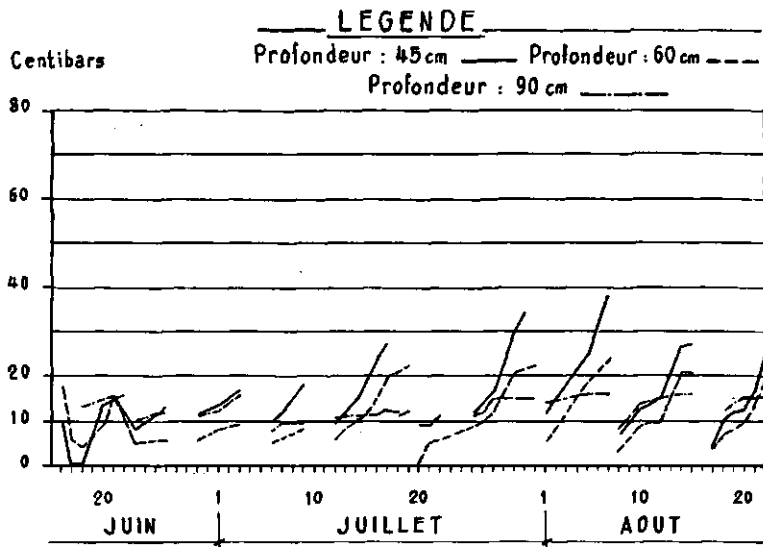
FIG.1.   Année 1981. Site n° 1.
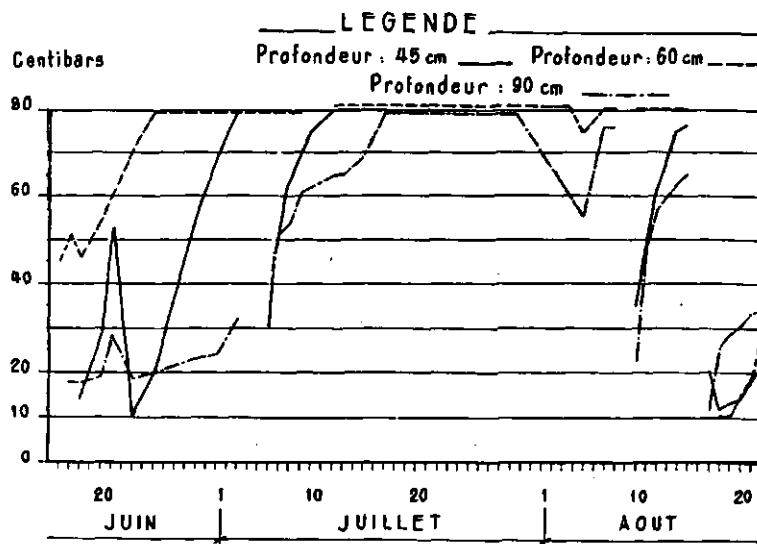
FIG.2.   Année 1981.   Site n° 2.

Cet état de fait dénote la très mauvaise répartition de l'eau qui est surabon-
dante tant dans l'inter-raie que sur la raie d'arrosage en tête de parcelle, alors
que les inter-raies sont insuffisamment irriguées à l'autre extrémité du champ.

3.1.2. Les mesures tensiométriques ont, tout aussi bien démontré que les
mesures neutroniques l'état de fait signalé précédemment. On constate la grande
différence de comportement de l'état hydrique du sol entre les sites 1 et 2
(fig. 1 et 2).

De plus un certain rapprochement a pu être fait entre les valeurs de tension
et celles de teneur en eau; comme on pouvait s'y attendre, le désamorçage des
tensiomètres se produit alors que les réserves sont encore abondantes. Cela ne
condamne pas l'emploi des tensiomètres mais constitue une limite à considérer
pour définir les conditions de leur mise en œuvre.

3.2. Résultats obtenus en 1982 [11]

3.2.1. Résultats des mesures tensiométriques

Les mesures effectuées sur les parcelles TA (voir paragraphe 2.5.) permettent:
— d'une part, d'apprécier, par comparaison des deux sites, l'amélioration de
l'uniformité de la distribution par rapport à 1981, du fait de l'adoption d'un
débit accru d'arrosage:
— d'autre part, de constater que les arrosages renouvelés toutes les semaines ne
se justifiaient pas, ce que traduisent des tensions modérées à presque tous les
niveaux.

Les parcelles TB n'ont reçu que 4 arrosages, représentant un apport total
de 417 mm, contre 8 arrosages, totalisant 553 mm pour TA.

L'évolution de l'état hydrique du sol de TB a été fort différente (fig. 3 et 4).
La comparaison des deux sites permet d'apprécier la bonne concordance des
courbes révélatrices de l'homogénéité de la distribution obtenue grâce à l'emploi
de deux débits successifs. On constate de plus une nette élévation des tensions
aux divers niveaux.

Le résultat agronomique n'est pas significativement différent entre les
traitements. La production a été élevée: 142 quintaux par hectare de grains
aux normes commerciales, ce qui n'avait jamais été atteint sur ces sols.

Le rendement hydraulique est amélioré d'environ 25% en faveur de TB alors
que TA est déjà en progrès par rapport au mode de conduite empirique (meilleure
uniformité, suppression des derniers arrosages). Notons de plus que la demande
climatique en 1982 atteint 108% de celle de 1981.

PEYREMORTE et AKHTAR BHATTI
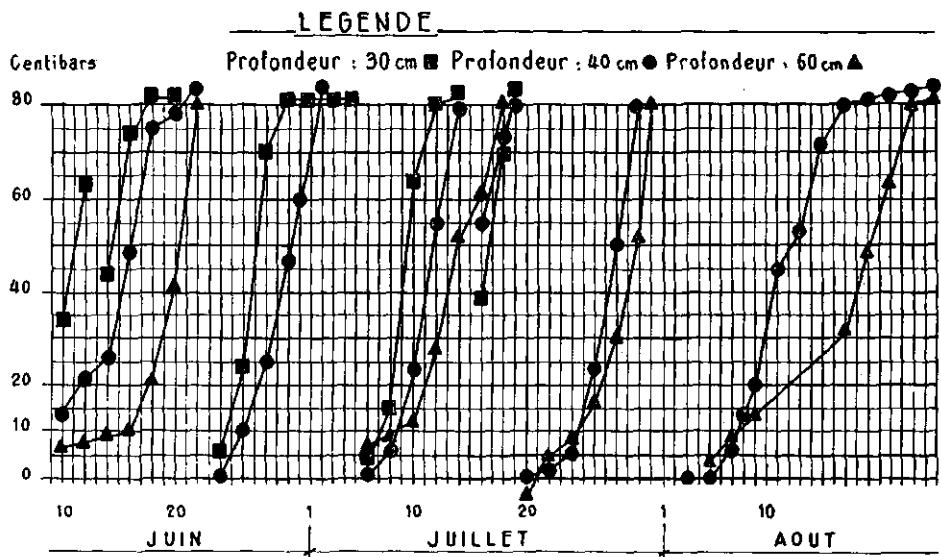
FIG.3. Année 1982. Traitement TB. Site n° 1.
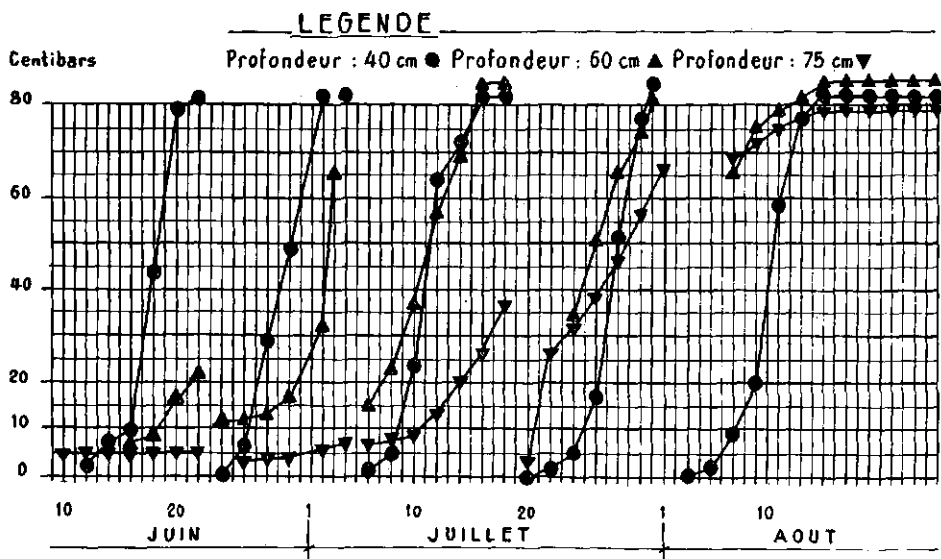
FIG.4. Année 1982. Traitement TB. Site n° 2.

3.2.2. Contrôles effectués à l'humidimètre à neutrons

Pour s'assurer que les observations tensiométriques étaient dignes de confiance, des mesures neutroniques ont été simultanément effectuées. L'analyse de ces mesures démontre que le régime d'arrosage de TA conduit à une élévation de la teneur en eau du sol après le troisième arrosage, ce que laisse prévoir l'évolution des mesures tensiométriques. L'utilisation de l'eau du sol est nettement meilleure pour TB qui présente une contribution significative à l'horizon H2. Ces informations sont donc tout à fait conformes à celles des mesures tensiométriques, tout au moins en ce qui concerne les aspects pratiques de la conduite de ces arrosages.

4. CONCLUSIONS

Ces premiers résultats ont montré que les tensiomètres, malgré leurs limites inhérentes à la faible gamme d'humidité dans laquelle ils peuvent fonctionner, sont aptes à rendre de précieux services pour améliorer la maîtrise de l'irrigation à la raie.

La méthode de mise en oeuvre proposée et testée a donné satisfaction dans les circonstances de l'essai. Il s'entend que son extrapolation à d'autres cultures ne pourra être faite qu'après avoir obtenu une bonne connaissance du milieu, et plus particulièrement de la relation tension-teneur en eau du sol. Ce préalable étant acquis, par exemple par l'emploi simultané d'un humidimètre à neutrons et de tensiomètres, il reste primordial de pouvoir mettre à la disposition des irrigants une technique simple afin que les progrès permis par les résultats des recherches passent effectivement au niveau de la pratique agricole. Actuellement, en attendant mieux, les tensiomètres doivent pouvoir rendre ce service.

REFERENCES

[1] KEMPER, W.D., HEINEMANN, W.H., KINCAID, D.C., WORSTELL, R.V., «Cable controlled plugs in perforated supply pipes for automatic furrow irrigation», Transactions of the ASAE 24 6 (1981) 1526.

[2] KELLER, J., COREY, F., WALKER, W.R., VAVRA, M.E., «Evaluation of irrigation systems», Proc. 2nd National Irrigation Symposium, University of Nebraska, Lincoln (1980) 95.

[3] BOOHER, L.J., L'irrigation de surface, FAO, Rome (1974).

[4] MARR, J.C., Furrow irrigation, Agricultural Extension Service Manual n° 37, University of California (1967).

[5] Furrow irrigation, National Engineering Handbook, Section 15, US Department of Agriculture, Washington DC (1979).

[6] REDDY, J.M., CLYMA, W., «Optimal design of furrow irrigation systems», Transactions of the ASAE 24 3 (1981) 617.

[7] MOUTONNET, P., COUCHAT, Ph., MARCESSE, J., Etude expérimentale et simulation numérique de l'économie de l'eau sous culture, Agricultural Meteorology 16 (1976) 193.

[8] PEYREMORTE, P., Des tensiomètres pour améliorer la conduite de l'aspersion ou des irrigations traditionnelles de surface, Eau et Aménagement 31 (1982).

[9] AKHTAR BHATTI, M., Etat actuel de la conduite des irrigations dans la région d'Oraison, éléments d'étude destinés à une thèse de docteur-ingénieur (1981).

[10] AKHTAR BHATTI, M., Compte rendu des recherches effectuées à Oraison en 1982, éléments d'étude destinés à une thèse de docteur-ingénieur.

USE OF NEUTRON SOIL-MOISTURE PROBE TO DETERMINE WATER-DISTRIBUTION UNIFORMITY IN FURROW IRRIGATION

M. AKHTAR BHATTI
Institut National Polytechnique de Toulouse,
Toulouse, France

Abstract

USE OF NEUTRON SOIL-MOISTURE PROBE TO DETERMINE WATER-DISTRIBUTION
UNIFORMITY IN FURROW IRRIGATION.
     In the case of furrow irrigation the efficiency of an irrigation depends upon the lateral
spread of water. Hence, this is directly related to the distribution uniformity of water applied.
Two methods of water application, with advance ratios of 1/2 and 1/3, were analysed in the
field under normal conditions using a neutron soil-moisture probe. The resulting distribution
uniformities showed that the advance ratio of 1/3 in combination with cut-back can be the best
solution for distribution uniformity problems. The advance ratio of 1/2 is also far better than
traditional practices in the region of Provence in southeastern France.

1. INTRODUCTION

Furrow irrigation is carried out by running parallel water streams in small
channels (furrows) that carry the water as it moves down or across the slope of
the field. The water seeps into the bottom and the sides of the furrows to provide
the desired wetting of soil laterally and vertically. In contrast to other methods
of surface irrigation, furrow irrigation does not wet the entire soil surface. There-
fore, irrigation efficiency largely depends upon the lateral movement of water from
the furrow. This movement is important not only for wetting the soil but also for
the movement of soluble salts, fertilizers and herbicides carried with the irrigation
water.

Small inflow rates are employed for the furrow system, practised widely in
Provence in southeastern France. They take 80% of the total irrigation time to
reach the lower end [1]. This produces very poor distribution uniformity. Although
the quantities of water applied are nearly twice the evapotranspiration, the lower
third of the field is under-irrigated.

To improve the distribution uniformity two methods of water application
were proposed. This paper presents the distribution uniformity for both methods
determined by using a neutron soil-moisture probe.

2.   LITERATURE REVIEW

The principal factors affecting the application of water to a furrow-irrigated field are: field length, field slope, furrow inflow rate, intake rate, roughness and shape.

Among these factors the furrow inflow rate is the only one which can be varied after the furrow irrigation system has been installed.

2.1. Inflow rate

The furrow inflow rate or unit flow (the size of stream delivered into each furrow, measured in litres/second or gallons/minute) is of the utmost importance for the efficient use of irrigation water.

Small inflow rates are used for the furrow system, widely practised in the region of Provence. The water advance ratio (AR = t_a/T where t_a = the fraction of the total time of irrigation during which water advances in overland flow from the upper field boundary towards the lower field boundary and T is the total time of irrigation) observed is 8/10 while irrigating every other furrow. This produces very poor distribution uniformity [1]. The lateral spread of water at any point in a furrow is dependent upon soil infiltration characteristics as well as the time the water is applied at that point (opportunity time). When the soil infiltration characteristics are more or less the same in the field, or more precisely along the furrow, the lateral movement is directly related to the opportunity time. *This opportunity time is a function of the water advance ratio (AR) in the case of furrow irrigation.*

An AR ratio approaching 1/1 results in the excessively deep infiltration of significant quantities of water at the upper end, but produces little run-off. But an AR ratio of 1/2 usually results in a distribution uniformity of about 85% and moderate run-off [2]. If the initial stream is large enough to cause the flow to arrive at the lower end in one fourth of the total time of irrigation (AR = 1/4), very high uniformity is ensured. The most uniform distribution is usually obtained by starting the irrigation with the largest unit flow that can be safely carried in the furrow. This implies AR ratios of from 1/4 to 1/3, and is achieved by employing large inflow rates at the beginning of irrigation and cutting back when the water reaches the lower end [3]. The maximum flow rate allowable at the beginning of the irrigation is determined by the need to prevent excessive run-off, over-topping of the beds, and soil erosion. Several authors have specified different procedures to estimate the maximum non-erosive flow rate given particular site and field conditions [3−5]. Ley et al. indicate that proper flow in the furrows is perhaps the most easily controlled variable and the single most important factor in efficient water application given particular field and site conditions [6].

2.2. Water application uniformity

The distribution uniformity (DU) is considered as the index of uniform water application.

2.2.1. Distribution uniformity

2.2.1.1. *Description:* This term indicates the uniformity of infiltration through-out the field and the magnitude of the distribution problem. This does not consider the adequacy of irrigation, but evaluates how efficiently water has been distributed in a field.

$$DU(\%) = \frac{\text{Average depth infiltrated in the lowest quarter or half of the area}}{\text{Average depth infiltrated in the area}} \times 100$$

The low-quarter (LQ) concept was developed by the USDA soil conservation service and is recommended as the standard for comparing alternative conditions. The average low-quarter depth of water infiltrated is the lowest quarter of the measured or estimated values where each value represents an equal area. In the case of furrow irrigation this is considered as the quarter situated at the lower end of the furrows.

2.2.1.2. *Estimation:* Generally, distribution uniformity is estimated by infiltration data and opportunity time which is calculated from water advance and recession ratios. Several procedures are outlined based on opportunity time ratios and infiltration characteristics [7–9]. It has already been mentioned that in the furrow system DU depends upon the lateral movement. The latter is not easy to estimate from the infiltration data which is collected by "Double-ring infiltro-meters".

The "Blocked furrow infiltrometer" method used for determining infiltration characteristics, although a good estimate, does not consider the surface sealing and smoothing effects.

In this paper the estimation of DU is based on the soil-moisture content measured directly in the field under normal practices with a neutron soil-moisture probe.

3.   MATERIALS AND METHODS

3.1. Field characteristics

The field had furrows 160 m long with a regular slope of 0.38%. The average textural composition determined by the soil analysis was clay 26%, silt 52% and sand 22%. The structure was more or less uniform except for a zone situated at a depth of between 45 and 55 cm. The latter was found to be slightly more dense. The furrows were made every 75 cm and only one to two weeks before the first irrigation. The irrigation was carried out for every other furrow. The distance between the maize crop rows was 75 cm. The field was reasonably homogeneous.

3.2. Experiment design

Two advance ratios of 1/3 and 1/2 were used for the analysis of their respective DU in the field. An AR of 1/3 requires a high unit flow and it is estimated that unless it is cut back heavy run-off will occur. The two following treatments were employed.

First treatment (hereafter called TA): A unit flow of 1.4 L/s (litres/second) was used at the beginning, and once the water approached the lower end the flow was reduced by 50% and total time of irrigation was $3 \times t_a$.

Second treatment (hereafter called TB): A unit flow of 0.8 L/s was used and the total time of water application was determined by the time it took to reach the lower end. The total time of irrigation was $2 \times t_a$.

Both treatments were repeated three times for crop yield. Each repetition involved eight furrows of irrigation. Water distribution at the upper end was controlled by siphons and measured by small Parshall flumes. At the lower end run-off volume was also measured using Parshall flumes. Irrigation was carried out every second week.

3.3. Soil-moisture content

3.3.1. Method

The standard gravimetric method is used widely in the field to determine the soil-moisture content. This involves weighing a sample of wet soil, drying it to a constant weight at a temperature of 105 to 110°C and weighing it again to determine the amount of water lost on drying. This method is time-consuming and laborious. Moreover, repeated measurements cannot be made in the same place.

Other methods like porous blocks, gamma-ray attenuation, extraction of water with methyl alcohol, generation of acetylene gas by adding carbide to wet soil etc.,

have not been widely used. However, the accuracy of most of these methods is said to be about the same as routine oven-drying. Moreover, they are not always suitable for field measurements.

The neutron scattering method for estimating soil-moisture content used to estimate DU has gained wide acceptance in recent years. It has an advantage over the standard gravimetric method because repeated measurements may be made at the same location and depth, thus minimizing the effect of soil variability on successive measurements. It also determines water content on a volume basis. The soil-moisture probe used in this study was the "SOLO 20". The gravimetric method was used for its calibration in the field.

3.3.2. Measurements

Soil-moisture distribution measurements were carried out for both treatments on the measurement tubes installed at a distance of 25% of the total length of the furrows from both the upper and the lower end. Three measuring tubes were installed on each site in such a way that the first one was half way between two irrigated furrows, the second was in the irrigated furrow and the third half way between the first and the second, that is to say exactly on the maize crop row. The first and second were installed at parallel points but the third was installed slightly further down to avoid the compaction of measuring areas. The layout of the experiment is shown in Fig.1.

The measuring depths were D1 (25 cm), D2 (50 cm), D3 (75 cm) and D4 (100 cm). Soil-moisture measurements were performed every week but the results presented are those obtained before each irrigation.

Soil-moisture profiles were observed after completion of an irrigation for 24-, 48- and 72-hour intervals to see the evolution of DU as a function of time.
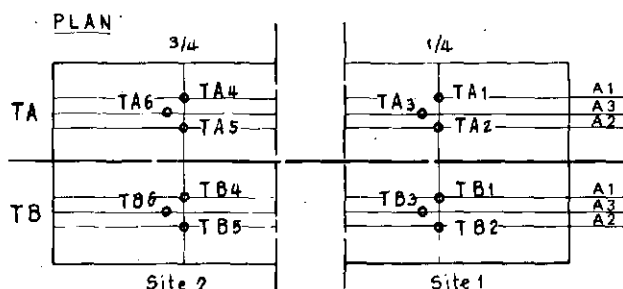
FIG.1. Experimental plan. TA1, TA4 − TB1, TB4 (A1) = tubes in non-irrigated furrow. TA2, TA5 − TB2, TB5 (A2) = tubes in irrigated furrow. TA3 − TA6 − TB3, TB6 (A3) = tubes on the crop row.

3.4. Calculation of distribution uniformity (DU)

Three areas were analysed for DUs along the furrows using three tubes installed on each site:

Area 1 (A1) = situated at the maximum distance from the irrigated furrow
Area 2 (A2) = situated around the irrigated furrow
Area 3 (A3) = situated half way between A1 and A2, under the maize crop row

$$DU\%\,(D) = \frac{(P_a - P_b) \text{ at site } 2}{((P_a - P_b) \text{ site } 1 + (P_a - P_b) \text{ site } 2)/2} \times 100$$

Where
P_a = % soil moisture after irrigation
P_b = % soil moisture before irrigation
D = corresponding depth

4.   RESULTS AND DISCUSSION

The irrigations were applied fortnightly (compared with weekly as is usually practised in the region) totalling four irrigations during the whole irrigation season 1982. The quantities applied were 417 and 465 mm for TA and TB, respectively. The rainfall during the irrigation period was only 30 mm. The run-off volumes were 11 and 13% for TA and TB, respectively.

Soil-moisture content before each irrigation is shown for D1 and D2 in Figs 2 to 7. The measurements representing the same areas are compared. The soil-moisture content at site No. 1 for both treatments is more or less the same. This indicates that in the upper half of all the three areas (A1, A2, A3) have more or less the same moisture content for both treatments, whereas at site No. 2 the results are not the same. TB4 compared with TA4 indicates a net decrease in soil-moisture content with the passage of time. This shows a small lateral spread of water at the lower end of the furrows. Also TB6 compared with TA6 indicates that only small quantities of water infiltrated. Therefore, areas A1 and A3 were not sufficiently irrigated for TB during the irrigations.

Soil-moisture content for D3 and D4 are not presented here because they did not vary much. However, they showed the same tendencies which are observed very clearly for D1 and D2.
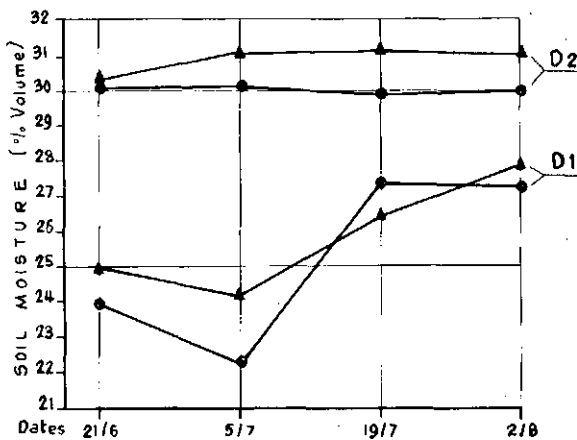
FIG.2.   Tubes in non-irrigated furrow (A1) at site 1.
   ● = TA1; ▲ = TB1
   (NB for all Figs: TA = 1st treatment; TB = 2nd treatment; D1 and D2 = 25 and 50 cm depth, respectively).
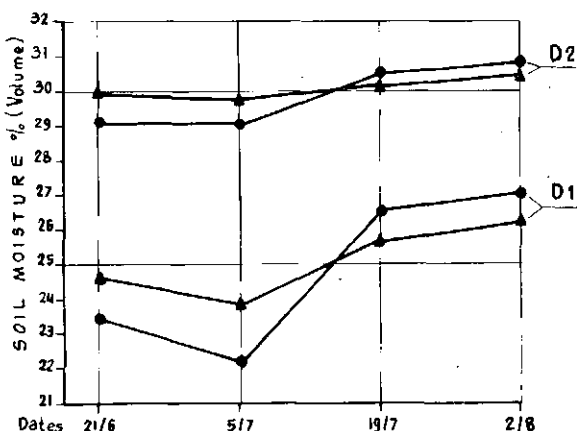
FIG.3.   Tubes in irrigated furrow at site 1.
   ● = TA2; ▲ = TB2
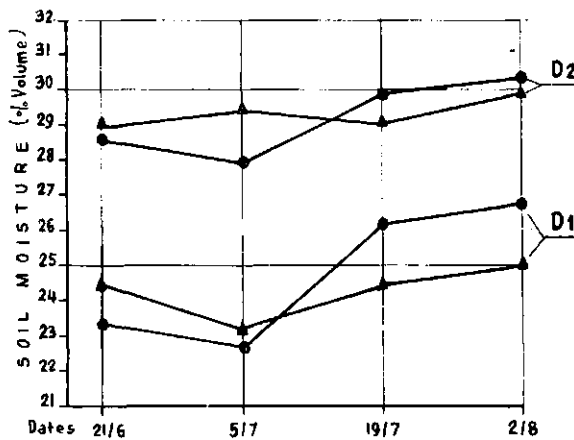
FIG.4.   Tubes on the crop row at site 1.
● = TA3; ▲ = TB3
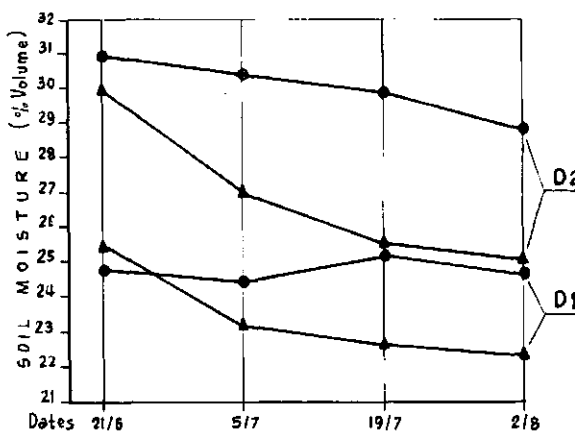
FIG.5.   Tubes in the non-irrigated furrow at site 2.
● = TA4; ▲ = TB4
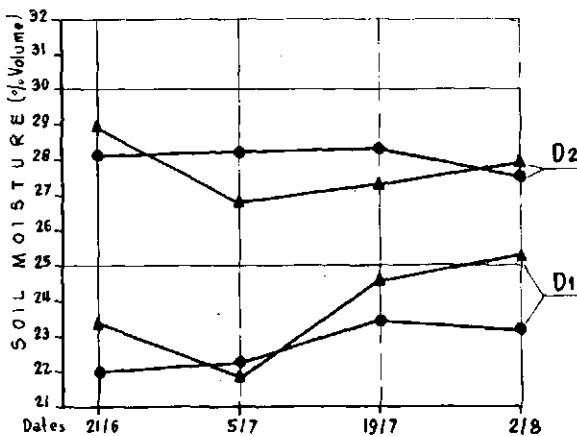
FIG.6.   Tubes in the irrigated furrow at site 2.
● ≈ TA5; ▲ ≈ TB5
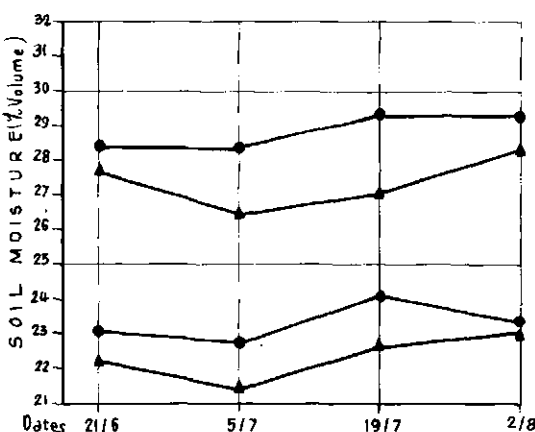
FIG.7.   Tubes on the crop row at site 2.
● = TA6; ▲ = TB6

TABLE I. DISTRIBUTION UNIFORMITIES IN PERCENTAGE

Treatment	Depth	Area A1	Area A2	Area A3	Average
TA	D1	73	91	89	84
	D2	70	90	86	82
TB	D1	52	92	73	72
	D2	48	94	70	71

The DU calculated for D1 and D2 based on the lower half are presented in Table I. They are calculated from the moisture content observed 24 hours after the completion of an irrigation. They are presented for their corresponding areas.

The DUs presented in Table I confirm the results seen in Figs 2—7.

Although the results obtained in both treatments are quite satisfactory, improvements are possible in the case of TB. Two options can be considered — either a decrease in the AR ratio or irrigation of every furrow. The first option must be combined with cut-back, otherwise heavy run-off losses will occur. For the second, the unit flow and the time of application should be calculated according to the amount of water distributed in each furrow.

Average crop yields for three repetitions were 14.2 and 13.8 t for TA and TB, respectively — high yields previously unattained in this region, proving the importance and necessity of DU.

5.   CONCLUSIONS

Utilization of the soil-moisture probe allowed repeated measurements in the same places to analyse more precisely the distribution uniformity along the furrow while minimizing the soil variability effects. It would have been difficult to obtain the same precision and rapidity using other techniques.

This study shows better uniformity of water distribution for method A as compared with method B. This is mainly due to an increase in the wetted perimeter, higher opportunity time and large unit flow at the lower end of the furrow. Method B is found to be less efficient, even though it is far better than conventional methods.

The crop yields obtained in the experimental area have never been achieved before at this farm or even in this region by using furrow irrigation. Therefore, it can be concluded that, along with other improved crop practices, distribution uniformity of water applied has its role to play.

REFERENCES

[1] AKHTAR BHATTI, M., "Etat actuel de la conduite des irrigations dans la région d'Oraison", Part of the applied research performed at the Society of Canal de Provence, France, Ph.D. 1981.

[2] MERRIAM, J.L., SHEARER, M.N., "Evaluating irrigation systems and practices", Design and Operation of Farm Irrigation System (M.E. JENSEN, Ed.) Am. Soc. Agric. Eng. (1980) Ch. 17.

[3] BOOHER, L.J., L'irrigation de surface, FAO, Rome (1974).

[4] MARR, J.C., Furrow Irrigation, University of California Agricultural Extension Service Manual No.37 (1967).

[5] CRIDDLE, W.D., DAVIS, S., PAIR, C.H., and SHOCKLEY, D.G., Methods of Evaluating Irrigation Systems, United States Dept. of Agric./Soil Conservation Sci., USDA Handbook No.82 (1956).

[6] LEY, W.T., CLYMA, W., Furrow irrigation practices in northern Colorado, Trans. Am. Soc. Agric. Eng. (1981) 610–16.

[7] AKHTAR BHATTI, M., "Compte rendu des recherches effectuées à Oraison en 1982", Part of the applied research performed at the Society of Canal de Provence, France, Ph.D. (draft), 1981.

[8] SMERDON, E.T., GLASS, L.T., Surface irrigation water distribution efficiency related to soil infiltration, Am. Soc. Agric. Eng. (1965) 76–82.

[9] CLEMMENS, A.J., DEDRICK, A.R., Estimating distribution uniformity in level basins, Trans. Am. Soc. Agric. Eng. (1981) 1177–87.

EVALUATION OF DIFFERENT METHODS
OF MEASURING EVAPOTRANSPIRATION
AS A SCHEDULING GUIDE FOR
DRIP-IRRIGATED COTTON

E. RAWITZ, A. MARANI, Y. MAHRER, D. BERKOVICH
The Faculty of Agriculture,
The Hebrew University of Jerusalem,
Rehovot, Israel

Abstract

EVALUATION OF DIFFERENT METHODS OF MEASURING EVAPOTRANSPIRATION
AS A SCHEDULING GUIDE FOR DRIP-IRRIGATED COTTON.
Evapotranspiration in a drip-irrigated cotton field was estimated by the energy balance
method, net radiation, standard evaporation pan, evaporation pan in the field at canopy height,
and by the Penman equation, and the results were compared with the soil-water balance based
on neutron meter and tensiometer data from seven obseravation sites. Evapotranspiration
according to the soil-water balance was only about 85% of that determined by the energy
balance method, and this is attributed to the fact that irrigation laterals were placed every second
row, and the soil-water balance was determined in the irrigated rows. The crop also utilized
moisture stored from winter rains in the unirrigated inter-row spaces, which was detected by
the energy balance method. Actual evapotranspiration (ET) was 96% of potential ET (Penman),
and the latter equalled 98% of net radiation energy. The actual ET equalled 90% of free water
evaporation from the pan in the field at canopy height, and 88% of net radiation. The high-
frequency drip regime maintained ET very close to potential ET, and under these conditions
the field-installed evaporation pan, or the net radiometer, are good indicators of crop water use,
with the latter being adaptable to computer-controlled irrigation.

1. Introduction

Drip irrigation is now used on 25% of the irrigated cotton
area of Israel and is steadily expanding. The practice that has
developed differs considerably from conventional practice under
sprinkler or furrow irrigation insofar as no deep wetting of the
soil is carried out by a pre-irrigation, the date of the first
irrigation is advanced by several weeks, small irrigations are
applied twice a week, nitrogen fertilizer is applied at frequent
intervals with the irrigation water, and thus water and root
penetration are limited to a shallower layer than under a con-
ventional regime. As a consequence of these features, the role
of the soil as a reservoir of water and nutrients has been

largely eliminated. This makes the crop vulnerable to undesirable moisture stress as a result of malfunctions of the irrigation system or of gradual drying out of the root zone due to inadvertent under-irrigation.

In spite of highly successful results, with seed-cotton yields of up to 7,000 kg/ha being achieved, the choice of irrigation amounts is largely based on empirical experience of individual farmers. This results in considerable variations in both water application amounts and yields, with the general tendency being to over-irrigate. The most common guide for irrigation is a Class-A evaporation pan sited on a dry, fallow plot of land, but both site conditions and choice of pan coefficient vary appreciably between farms in the same general area. The farming system is highly intensive, including pesticide spraying by airplane and monitoring and control of the irrigation system by computer. This, together with the limited water availability, impart a very high alternative value to every unit of water saved. The growers therefore are in need of a reliable irrigation indicator that would ideally also be inexpensive, simple to operate, and suitable for integration into the computerized irrigation system. The major aim of this research was to compare a number of methods that could fill the above need. The secondary objective was to develop preliminary information in preparation for a similar study of conventional irrigation regimes where some water stress presumably occurs.

2. Materials and Methods

2.1. Site description

The experiment was carried out within a large area of irrigated cotton at kibbutz Nahal Oz ($34^{\circ}29'$ E, $31^{\circ}28'$ N) in the southern coastal plain of Israel. The soil is a calcareous loess with uniform properties to a depth of at least 120 cm. The mechanical composition is 33% sand, 42% silt and 24% clay, containing 18% $CaCO_3$, pH is 8.2, dry bulk density 1.47 t m^{-3} and water content at field capacity is 18 wt% [1]. The dimensions of the study area were 162 x 81 m, surrounded by irrigated cotton at least 400 m in all directions.

2.2. Agronomic conditions

Both in 1981 and 1982 cotton of the variety Acala SJ-2 was sown in the first days of April in rows spaced 96 cm apart. The soil profile was wet to more than 100 cm, and the first irrigation of 30-35 mm was given in mid-June. After this, irrigation was given twice weekly at a rate ranging between 2.5 and 6.5 mm/day, determined by the grower based on pan evaporation, leaf water potential, and crop development stage.

Drip lines were placed every second row, so that as soil water
was exhausted by the crop in the unirrigated inter-row spaces,
the plants received water in only one half of their rooting
volume. Nitrogen fertilizer solution was injected into the irri-
gation water once a week until the end of July.

2.3. Measurements

2.3.1. Meteorological measurements

     All observations except for standard pan evaporation were
taken at a station located in the center of the plot. Net radia-
tion and incoming and outgoing global radiation were measured
2 m above canopy height; soil heat flux was measured at nine
points at a depth of 3 cm in both irrigated and unirrigated rows;
the Bowen ratio [2,3] was determined with the aid of two psychro-
meters using FD-300 diodes on a reversing mechanism similar to
the design of McNeil and Shuttleworth [4] and Perrier et al. [5],
with the lower psychrometer 0.5 m above canopy height and a ver-
tical distance of 0.5 m between the sensors. Wind run was
measured at 2 m above canopy level. Sensor outputs were recorded
on a Campbell Scientific CR-5 battery powered data logger, which
also gave the signal for activating the Bowen ratio device
reversing mechanism. A Class-A evaporation pan was installed at
this site, and was raised periodically together with its standard
wood base so as to be approximately at canopy height. Another
Class-A pan was also maintained in a standard enclosure, which
consists of dry, bare ground in Israel, within about 1 km of the
experimental field, and both pans were read daily.

2.3.2. Field water balance

     Water input was measured by integrating water meters with
electrical output, wired directly to the computer in the control
room of the farm. Soil water storage was measured at seven sites
in the field with neutron meters, with three access tubes at each
site at a distance of 15, 35, and 50 cm from a drip emitter. The
0 - 15 cm layer was measured with a Troxler moisture-density sur-
face probe, and the 15 - 105 cm layer by a Troxler neutron depth
probe at 30 cm intervals. Soil water potential was measured at
the same sites by tensiometers spaced every 15 cm to a depth of
120 cm. The seven observation sites were located following a
preliminary study of soil moisture distribution using geostatis-
tical methods adapted from the work of Matheron [6] by Burgess
and Webster [7], Gajem et al. [8], Vachaud [9] and Vieira et al.
[10]. The minimal distance between independent observations
ranged between 42 m and 58 m depending on the depth layer, which
compares well with the distance of 46 m reported by Gajem et al.[8],

Table I.   Comparison of energy and water fluxes in a cotton field.

Period	ET(WB)[a]	ET(EB)[b]	J_n[c]	E_{ps}^d	E_{pc}^d
	mm day^{-1}				
17-06-81 - 23-07-81	4.8	6.4	7.3		
24-07-81 - 28-08-81	5.0	5.9	6.7	6.8	5.4
17-06-81 - 28-08-81	4.9	6.2	7.1		
20-06-82 - 25-07-82	5.4	5.9[e]	6.7	6.9	6.4
26-07-82 - 30-08-82	4.8	5.1	5.8	6.8	5.4
20-06-82 - 30-08-82	5.1	5.5	6.2	6.8	5.9

a - ET based on soil water balance by neutron meter
b - ET by energy balance-Bowen ratio method
c - converted from measured net radiation using
    58 Ly = 1 mm evaporation
d - evaporation from standard pan and pan at canopy height,
    respectively
e - calculated values, $0.88(J_n)$

3.   Results and Discussion

3.1.   Soil water balance.

     The principal results of the two seasons are summarized in
Table I.   Energy balance data were obtained only during the
latter part of the 1981 season, because at the beginning of that
season the farm had technical problems with the irrigation instal-
lation, which also interfered with some of the research activities,
while no energy balance data were obtained in 1982 due to the
unanticipated absence of key technical personnel.   While the net
radiation input during the first six weeks of the 1981 summer was
higher than in 1982, evapotranspiration (ET) as measured by the
soil water balance was lower, reflecting the inability to irri-
gate as per plan.   This is confirmed by the temporary depletion
of soil water storage as shown in Fig. 1.   Detailed analysis by
depth layers showed that about 25% of this depletion came from
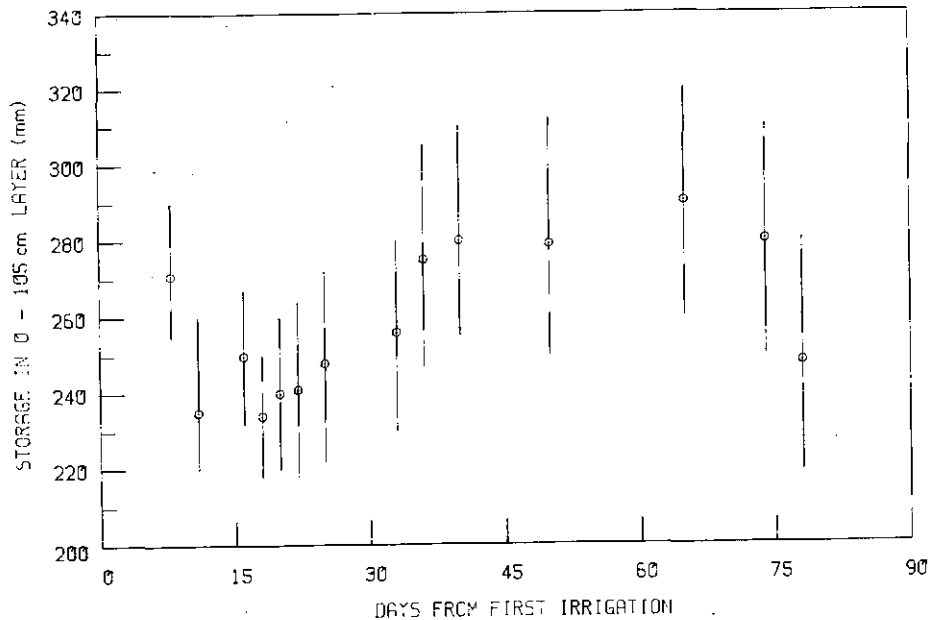
FIG.1.   Seasonal soil-water storage (average and SD).
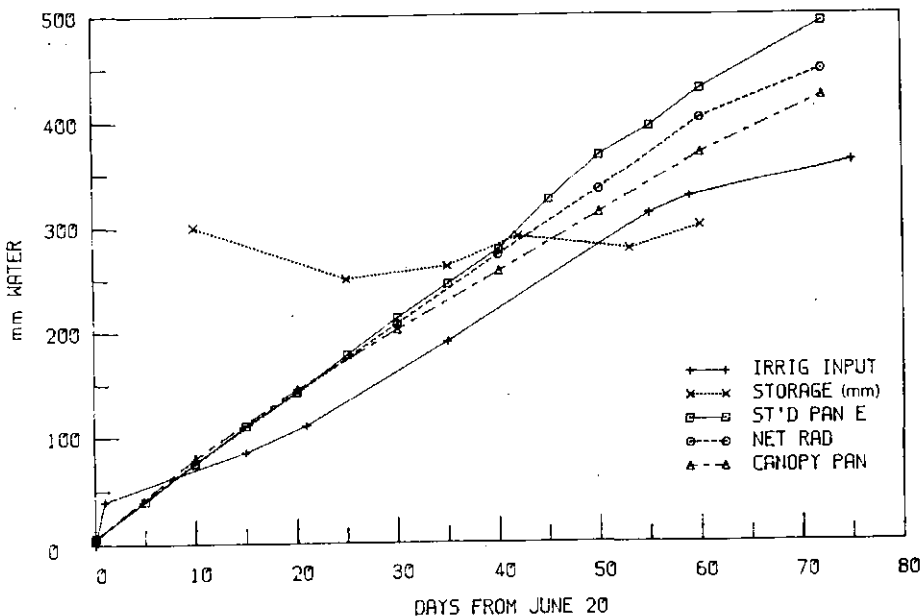
FIG.2.   Comparison of irrigation indices.

the 75-105 cm layer, and that after the planned regime was reestablished, the active root zone was limited to the 0 - 60 cm layer. During the entire season, the hydraulic gradient was either zero or upward between the 120 cm depth and the 90 cm depth, and upward between 90 and 75 cm, and consistently downward between 60 cm and 75 cm. The water content and hydraulic gradient data indicate that there was no downward flux of water past the lower root-zone boundary. The standard deviation of water storage in Fig. 1, based on seven observation sites, demonstrates the limitations of the neutron meter for the purposes of detecting small changes of water content. Additional sampling sites would be of little benefit since the distance between them would then be less than the minimal distance between independent observations, and the error must be accepted as an inherent soil property.

In 1982 the irrigation proceeded according to plan, and the soil profile storage remained essentially constant throughout the season. Since moisture changes were again limited to the upper 60-75 cm, the application rate may be viewed as the actual ET rate. During the peak demand period from mid-July to mid-August this rate is equal to the evaporation that can be accounted for by the energy supplied by net radiation (Fig. 2), indicating that ET was proceeding at the potential rate. Up to mid-July the application rate was lower, and on the evidence of the soil moisture depletion, it was less than adequate to maintain potential ET.

3.2. Climatological indices

As calculated from the data in Table I, during both seasons ET based on the water balance was 74% of standard pan evaporation, and 92% and 89% respectively of evaporation from a pan in the canopy for the parallel periods in 1981 and 1982. The coefficient of variation of the relation is 6.5%.

ET as measured by the energy balance method amounted to 88% of the energy gained by net radiation in 1981, with a correlation coefficient of 0.94 (Fig.3). The value of ET by the energy balance was consistently higher than that obtained by the water balance method in 1981, and likewise in 1982 when the ET was calculated as 88% of net radiation. The discrepancy is explained by the fact that the water balance was determined only on the basis of the changes in the irrigated furrows, whereas the crop actually also depleted the stored water from the unirrigated furrow. In 1981, the difference between the two terms for ET over the season is 94 mm of water. Total water storage capacity in the 0 - 120 cm layer is 360 mm, and "available water" is about half of this amount, or 180 mm. Thus if one takes one-half the total soil volume, it would contain 90 mm of available water, or the amount equal to the discrepancy between the two ET estimates. Fig. 3 was chosen as an
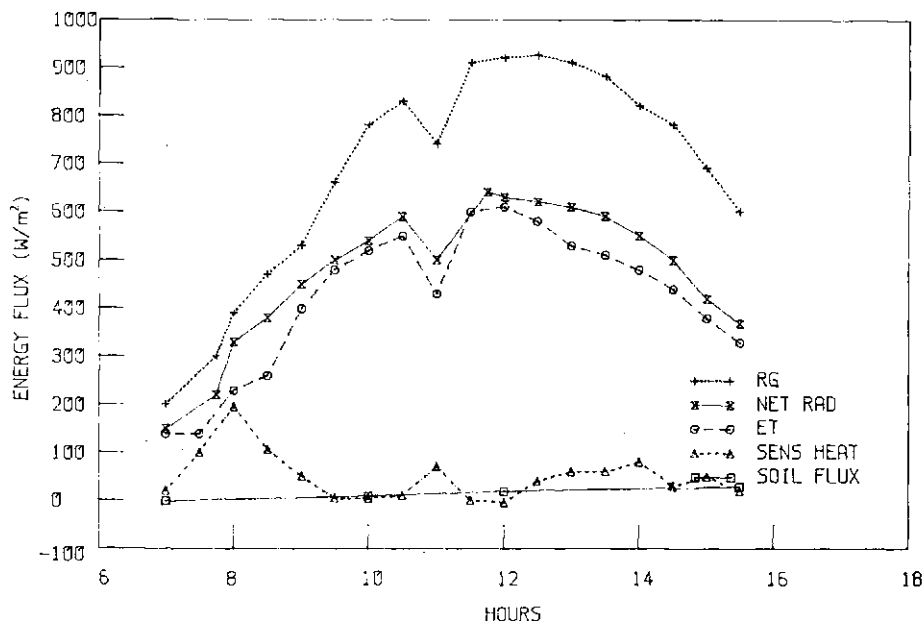
FIG.3.   Energy balance in field, 5 August 1981.

illustration because of the sudden temporary decrease in radiation just before noon, and thus the record demonstrates the sensitivity of global and net radiation and of the calculated ET to small environmental changes, in this case apparently caused by the passing of a cloud. The albedo ranged between about 15% in the early part of the season before full ground cover, to about 22% in mid-August. The relation between ET based on the energy balance and potential ET according to Penman [11] was determined at 30-minute intervals on four days, and ET was found to equal 96% of ETP, with a correlation coefficient of 0.94. Statistical analysis of all possible regressions showed that 88% of ET was explained by net radiation, and 89% by net radiation and dry-bulb temperature taken together. Similarly, 98.5% of potential ET was explained by net radiation, and 99.5% by the addition of wind run, with no appreciable further improvement by the consideration of additional factors.

In conclusion, it can be stated that ET based on the energy balance, free water evaporation from a pan mounted at canopy height, and net radiation were all excellent measures of actual ET, with the latter two indices being much the simpler to determine. Since the high-frequency irrigation regime typical of drip irrigation maintains a high soil water potential, it is reasonable that actual

ET should very nearly equal potential ET, and that most of the
available radiation energy should be dissipated as latent heat.
This regime does not favor the use of the neutron meter for moni-
toring short-term soil moisture changes. Net radiometry shows
promise for this purpose and appears suitable for automated irri-
gation control, at least in drip systems. Additional information
is required on its sensitivity to fluctuating conditions as
under sprinkling, where some plant water stress may occur towards
the end of each irrigation cycle.

REFERENCES

[1]   BERKOVICH, D., "A comparison of different methods of
       measuring evapotranspiration in a drip-irrigated cotton
       field." M.Sc. Thesis, The Hebrew University of Jerusalem,
       The Faculty of Agriculture, Rehovot (1982). (Offset,
       Hebrew, Engl. summary) 93 pp.
[2]   GAY, L.W., Evapotranspiration from irrigated alfalfa and
       riparian saltcedar in an arid environment, 15th Conf. Agric.
       Forest Meteorol. (1981) 94.
[3]   TANNER, C.B., Energy balance approach to evapotranspiration
       from crops, Soil Sci. Soc. Am. Proc. 24(1969)1.
[4]   McNEIL, D.D., SHUTTLEWORTH, W.J., Comparative measurements
       of the energy fluxes over a pine forest, Boundary-Layer
       Meteorol. 9(1975)297.
[5]   PERRIER, A.B., ITIER, J.M., KATERJI, M., A new device for
       continuous recording of the energy balance of natural sur-
       faces, Agric. Meteorol. 16(1976)71.
[6]   MATHERON, G., The theory of regionalized variables and
       its applications, Cah. Cent. Morphol. Math. 5(1971)211.
[7]   BURGESS, T.M., WEBSTER, R., Optimal interpolation and
       isarithmic mapping of soil properties, I: The semi-
       variogram and punctual kriging, J. of Soil Sci. 31(1980)
       315.
[8]   GAJEM, Y.M., WARRICK, A.W., MYERS, D.E., Spatial
       dependence of physical properties of a typic torrifluvent
       soil, Soil Sci. Soc. Am. J. 45(1981)709.
[9]   VACHAUD, G., Large scale determination of flux of water
       and solute through the soil in situ in the semi-arid
       zone taking into account the spatial variability, 12eme
       Cong. International de Sciences de Sol, New Delhi (1982).
[10]   VIEIRA, S.R., NIELSEN, D.R., BIGGAR, J.W., Spatial
       variability of field-measured infiltration rate, Soil
       Sci. Soc. Am. J. 45(1981)1040.
[11]   PENMAN, H.L. Natural evaporation from open water bare
       soils and grass, Roy. Soc. London Proc. Ser. A. 193
       (1948)120.

NUCLEAR METHODOLOGY

(Sessions 7 and 8)

Chairman (Session 7)

T.J. D'SOUZA

Chairman (Session 8)

N.N. BARTHAKUR
Canada

Invited Paper

GAMMA-RAY ATTENUATION TO MEASURE
WATER CONTENTS AND/OR BULK
DENSITIES OF POROUS MATERIALS

E.S.B. FERRAZ
Department of Physics and Meteorology,
Escola Superior de Agricultura "Luiz
    de Queiroz" (ESALQ), and
Center for Nuclear Energy in Agriculture,
University of São Paulo, Brazil

Abstract

GAMMA-RAY ATTENUATION TO MEASURE WATER CONTENTS AND/OR BULK
DENSITIES OF POROUS MATERIALS.
    Attenuation of gamma radiation during transmission through soil and porous materials
has been used for approximately three decades as a method for determining volumetric water
content, θ, and bulk density, ρ. This method is particularly suited for laboratory determinations
of θ and ρ in soil columns but it also has been used with success under field conditions. Measure-
ments of attenuation of a collimated beam of monoenergetic gamma-rays has been used
successfully by many investigators to provide rapid, non-destructive determinations for small
volumes of soil. For stable soils, i.e. soils which do not swell upon wetting or shrink upon
drying, ρ may be assumed to remain constant during water flow through the soil, and thus
changes in intensity or transmitted radiation may be attributed to changes in water content, θ.
However, for unstable soils, the dry bulk density is subject to change with time during water
flow through the soil and cannot be assumed to be a constant. Several investigators have
utilized either a single beam of dual-energy gamma photons or two separate monoenergetic
photon beams with greatly different energies to simultaneously determine θ and ρ in these
soils. A general review of gamma-ray attenuation methods for determining θ and ρ in laboratory
soil cores and in field soil profiles is reported in this paper. Theoretical equations for trans-
mission and attenuation of gamma radiation in soils are presented for both single and double
beams of gamma photons. Sensitivity, precision, accuracy, and experimental errors for
the method are evaluated and discussed with respect to the theory.

1. INTRODUCTION

Attenuation of gamma radiation during transmission
through soil has been used for approximately three decades as
a method to determine volumetric water content and dry bulk
density. This method is particularly recommended for flow
studies in laboratory soil columns and other porous materials
as it is indestructible, fast and with good sensitivity.

The idea to use radiation interactions with water as a method to study the physical characteristics of a sample came from Rutherford who, in 1911, gave an important contribution to science on atomic structure by using the scattering of alpha particles.

Probably the first successful experiment based on radiation with matter phenomena was performed by Belcher et al. [1] in 1950. They developed a method to measure water content in soil by neutron moderation and bulk density by gamma ray scattering. Later, gamma-ray attenuation methods were used for a wide range of purposes: to determine fluid level in tanks [2], uniformity of several different materials [3], density of concrete [4], concentration of solids in fluids [5], concentration of heavy metals in aqueous solution [6] [7].

Today, the gamma-ray attenuation method is used for several purposes in science and technology. The availability of new gamma radiation sources, the advances in electronic equipment and automation facilities, made this method popular all over the world, as of the most important tools of science.

2. THEORY

2.1. *Attenuation Equation for Single-Energy Gamma Radiation*

If a collimated beam of monoenergetic gamma rays with intensity I_0 (number of photons per cm^2 per sec) passes through a substance having density ρ (g/cm^3) and thickness x (cm), the radiation becomes attenuated in accordance with the Lambert-Beer equation:

$$I = I_0 \exp\left[-\mu\rho x\right] \tag{1}$$

where I is the resulting intensity (number of photons per cm^2 per sec) and μ is a proportionality constant referred to as the mass attenuation coefficient (cm^2/g). The decrease in intensity during radiation transmission occurs primarily as a result of absorption and scattering interaction between photons and the substance. Compton effect, which includes absorption and scattering, is the major attenuation process; however, photo-electric, pair-production and Raleigh effects may also be important for some ranges of radiation energy.

The gamma-ray attenuation method is based upon the measurement of the intensity of a single-energy collimated beam of gamma photons after the beam has passed through a selected absorber material. This method has been used under laboratory conditions to soil bulk density or volumetric water content in soil columns and for general studies of flux in porous materials.

In a system consisting of porous material and a fluid
passing through the material, attenuation of gamma-ray occurs
not only by all the absorbers along the path of the photons,
but also by the porous material, fluid and air components.
However, attenuation by air layer can be neglected in most
situations, as it represents values 10^3 to 10^4 smaller than
the other components. Thus, equation (1) can be written:

$$I = I_0 \exp \left[-x(\mu_s \rho + \mu_\omega \rho_\omega \theta)\right] \tag{2}$$

where I_0 is the intensity (number of photons per cm^2 per sec),
I is the resulting intensity; x is the thickness of the
sample; ρ the bulk density of the porous material; μ_s the mass
attenuation coefficient of the porous material; μ_ω the mass
attenuation coefficient of the fluid; ρ_ω the density of the
fluid and θ, the volumetric content.

If the fluid is water under standard conditions of
temperature and pressure, the water density can be considered
as one: $\rho_\omega = 1$. In this case, equation (2) is written in the
current form used in soil-water studies:

$$I = I_0 \exp \left[-x(\mu_s \rho + \mu_\omega \theta)\right] \tag{3}$$

Attenuation of monoenergetic gamma-rays can be used to
determine θ if ρ is known or ρ if θ is known.

If gamma radiation is transmitted through a soil column
either as a single collimated beam of dual-energy photons or
as two separate beams of monoenergetic photons with different
energies, two attenuation equations similar to equation (3)
result. These two equations may be solved simultaneously to
obtain the two unknown variables θ and ρ [8]:

$$\theta = \frac{\mu_{sa} \ln \left(\frac{Ic}{I_{oc}}\right) - \mu_{sc} \ln \left(\frac{Ia}{I_{oa}}\right)}{x \left(\mu_{sa} \mu_{\omega c} - \mu_{sc} \mu_{\omega a}\right)} \tag{4}$$

$$\rho = \frac{\mu_{\omega a} \ln \left(\frac{Ic}{I_{oc}}\right) - \mu_{\omega c} \ln \left(\frac{Ia}{I_{oa}}\right)}{x \left(\mu_{sa} \mu_{\omega c} - \mu_{sc} \mu_{\omega a}\right)} \tag{5}$$

where a indicates one photon energy and c the other photon
energy.

Americium-241, which emits 60 keV photons and Cesium-137,
which emits 662 keV photons, are commonly used as radiation
sources for simultaneous determination of θ and ρ.

Experimental measurements of I and I_0 are subject to errors due to statistical fluctuations in radioactive disintegration events. When measuring a number I of events, the uncertainty, at 68% probability level, is equal to the square root of I. For small increases of I, it is possible to make the following approximation:

$$\frac{dI}{I} \simeq \frac{1}{\sqrt{I}} \tag{6}$$

A fractional change in the measurement of intensity dI/I, causes variations in the determination of ρ or θ. The sensitivity of the method is mainly limited by the errors in I_0 and I determination, because errors due to determination of the other parameters are negligible. It is important to note that errors in bulk density and in water content measurements with the double-beam method are greater than errors when the single beam method is used. In the single-beam method, errors in determination of ρ do not influence the determination of θ, but with the double-beam method, errors in determination of ρ tend to increase the error in θ determination. Therefore, the double-beam method must be used only when necessary.

2.2. *Single-Energy Gamma Radiation Method*

The single-energy gamma radiation method is commonly used to determine bulk density, water content and flux variations in laboratory studies. When correctly used it provides rapid, easy, practical, accurate and nondestructive measurements. Several factors control the precision and accuracy: statistics of countings precision in the mass attenuation coefficient measuremnts; homogeneity of sample; sensitive of electronic equipment; and optimum collimation geometry.

The best possible determination can be obtained when errors are minimal. This occurs when the function of errors passes by the point of minimum. Certain parameters of these measurements cannot be easily changed, but the thickness of the sample can be changed as needed. Theoretically the optimum thickness (x*) for soil-water determination is given as follows |9|:

$$x^* = \frac{2}{\mu_s \rho + \mu_\omega \theta} \tag{7}$$

For a beam of low-energy gamma photons, the chemical composition of the sample strongly affects the mass attenuation coefficient values. Therefore, the optimum

thickness (x*) determination is very important for best results.

2.3. *Determination   of* θ *and* ρ *using dual-energy gamma radiation*

The simultaneous measurement of water content and bulk density using a dual-energy gamma beam has been very useful in studies of shrinking and swelling soils. Basically, the method is based on equations (4) and (5) and requires good resolution and prior knowledge of water and soil mass attenuation coefficients for both energies, the thickness of the sample, and the unattenuated beam intensities for both energies, I_{oa} and I_{oc}.

The variables I_a and I_c can be obtained by two ways: simultaneously or alternately. For simultaneous measurement of I_a and I_c the complex energy spectrum with two peaks, one of low energy and other of high energy, can be electronically separated with a two-channel analyser and the counting ratios recorded with two scalers. In this procedure special attention should be observed to minimize and correct the high energy peak interferences in the low-energy peak countings. Several authors, such as Gardner, Campbell and Calissendorf, 1972, [10], Corey, Peterson, and Wakat, 1971, [11], Mansell, Hammond and McCurdy, 1973, [12], and Nofziger and Swartzendruber, 1974, [13] have examined these interferences.

Another procedure is to obtain the attenuated beam intensity in the high peak channel (I_c) alternately with that in the low peak channel (I_a), in order to prevent such interferences. Ferraz, 1974 [14], used a geometry with two parallel beams, where the high energy radiation is shielded when the low energy peak is being counted. Bridge and Collis-George, 1973 [15], used a mechanical device in order to change the position of the sources in the collimator. Strossnidjer and De Swart, 1974 [16], used a cross-beam device with two independent counting systems to accomplish the same objectives.

Theoretical considerations of errors in simultaneous determinations of θ and ρ due to random fluctuations in radiation have been reported by Gardner et al., 1972 [10], Ferraz, 1974 [14] and Ferraz and Mansell, 1979 [9].

The main use of the dual-energy gamma method is to study water movement in shrinking-swelling soils. One example is the determination of soil water diffusivity as a function of water content and time.

Studies of θ and ρ measurements in natural soil compaction due to use of heavy equipment, such as harvesting machines, etc. were possible only with the dual-energy method. Samples

of undisturbed soil in a sugar-cane culture were removed,using
special techniques, with a "u"-shaped alluminum sheet (Ferraz,
1974) [14].

3. SYSTEM PARAMETERS

3.1. *Gamma Radiation Sources*

Most determinations of ρ and θ by soil scientists have
been made with ^{137}Cs (662 keV) source, but the use of ^{241}Am
(60 keV) as a gamma-ray source has also become increasingly
popular. Several other gamma ray sources have been used
according to the material studies and the thickness of the
sample. In the selection of a radiation source, the following
elements shoud be considered:
a) Monoenergetic spectrum. The radiation spectrum must
show a well-distinguished primary energy peak in a region free
of interfering radiation, because the detector used in most
cases is the solid NaI(Tℓ) scintillator which has limited
resolution but high efficiency.
b) Half-life. The radioisotope half-life must be of the
same or greater order as the duration of the programmed
experiments to minimize or eliminate corrections for decay.
Also the cost of the system assembly should be considered.
c) Activity. In this case the total activity and
specific activity of the source are important. Because of
errors due to the random nature of radioactive disintegration,
a large number of photons must reach the detector. The actual
number of photons counted is a function of source activity and
specific activity, geometry and collimation.
Usually a source with 100 to 200 mCi is used for a
collimated beam in laboratory, but certain investigators have
used stronger sources (greater than 250 mCi). High activity
provides high values of beam intensity, and this although good
for statistics of counting, increases the errors due to the
dead time of the electronic equipment.
d) Energy. The sample thickness, its density and the
gamma radiation energy, determine the optimum experimental
conditions. The product of density and thickness determines
the best energy to be used. For most soil columns 4 to 8 cm
thickness, the 60 keV ^{241}Am is recommended. For soil columns
with thickness between 15 and 25 cm or for dense material,such
as concrete and rocks, the 662 keV ^{137}Cs is normally used, and
sometimes in special cases, 1170 and 1310 keV of ^{60}Co or 1250
keV of ^{22}Na. For very thick samples, and light materials,
X-ray and very low energy, such as ^{55}Fe can also be used [17].
Two very well-distinguished energies are required for the
dual-energy gamma method. These energies must provide

adequate mass attenuation coefficients for the porous material
and the fluid, in order to give good resolution with
simultaneous equations. Careful examination of a radioisotope
table shows that only a few radioisotopes can be used, due to
the reported considerations. Today, most of the investigations
with the double-beam method for simultaneous measurements of
bulk density and water content in soils are made with paired
^{241}Am and ^{137}Cs gamma-ray sources. This method is also used
for wood [28].

3.2. Geometry and Detection

    Collimation is especially important in the gamma-ray
attenuation method and particularly in simultaneous
measurements with two energy gamma beams. The collimator is
necessary to supply a beam as thin as possible, but with
maximum intensity. Such an ideal collimator is impossible to
obtain due to the practical geometry limitation and specific
activity of the source, but many authors have obtained good
results.
    Collimators are generally made of lead and sometimes of
tungsten or other heavy metals. The cross-section and its
length are determined by resolution and beam intensity. Some
scientists have used a circular cross-section with different
sizes, like 2 or 3 mm^2 and 80 or 100 mm^2; others used
rectangular slits of cross-section smaller than 1 mm^2 or
larger than 100 mm^2. For best results, collimation of the
radiation is required on both source and detector sides. A
good procedure for testing collimation involves a comparison
between theoretical and experimental mass attenuation
coefficients for a known material, such as water.
    The NaI(Tℓ) scintillator detector optically coupled to a
photomultiplier tube connected to a single-channel pulse
analyser is the equipment currently used. The thickness of
the scintillator crystal depends on the photon energy.
Resolution better than 16% for 60 keV and 10% for 662 keV was
easily obtained.
    Although used extensively in gamma spectroscopy analysis,
the high resolution Ge-Li detector (and other solid state) has
not been used, primarily because of its low efficiency, which
is about 100 times less than the NaI(Tℓ).
    A finite resolving time in measurements of radiation
intensity for the gamma-ray spectrometer contributes to a
coincidence loss or counting error. For good statistics, a
large counting rate is necessary, however, in this case there
may be a significant decrease in counting due to losses by
resolving time of the electronic equipment.

4. PRACTICAL USES OF THE GAMMA-RAY METHOD

4.1. *Soil Physics*

Ferraz and Mansell [9] published an extended paper showing theoretical and experimental considerations about the uses of the gamma-ray attenuation method in soil physics, with a large number of references.

A narrow collimated beam of gamma radiation was first used in laboratory investigations by Gurr [8] and Ferguson and Gardner [19] and Davidson, Biggar and Nilsen [20]. These early studies provided important contribution to the development and dissemination of methodology. They used a ^{137}Cs source, NaI(Tl) scintillator detector and a single-channel analyser: the same arrangement now used by most scientists.

The radioisotope [241]Am was proposed by King [21] in 1962 and used in soil physics after 1966 by many investigators.

The possibility of using radiation from two gamma-ray sources was first considered theoretically by Durante et al. [22] in 1957. Soane [8] in 1967 and Gardner, Campbell and Calissendorf, 1969 [23] successfully tested this method to simultaneously determine water content and bulk density of soil columns.

In situ, the use of an uncollimated beam of gamma radiation is a means to determine relative changes in water content with good approximation. However, this method is not recommended for absolute water content and bulk density determinations. Essentially, this method consists of placing two access tubes into the soil, 20 - 30 cm apart, one for the gamma radiation source and the other for the detector.

4.2. *Wood*

The method for determination of wood density and water content by gamma ray was suggested by some investigators in the 1950's and subsequently presented by Loos [24] in 1961. Most of these earlier authors used ^{137}Cs as a gamma-ray source, which has a very high energy for light material, such as wood. Due to the low density of the material and the low values of its mass attenuation coefficient, the interaction of photons of this energy band is not sufficient to provide good sensitivity, even for large samples.

Ferraz [25] in 1976 introduced the use of [241]Am because of its low energy, 60 keV. The method then became important for density determinations and mainly for water-flow studies, due to its sensitivity and simplicity.

Studies of water vapour diffusion are very important to wood science and technology, mainly in drying and impregnation processes. The main parameter sought is the water diffusion coefficient, when the water content of the medium is below the fiber saturation point (ca. 30% moisture). The best way to determine this coefficient is through a steady-state study, where the gradient of moisture of a sample is measured by gamma ray [26].

Another application of the gamma radiation methodology in wood science is the density variability measurement and growth ring identification. Ferraz and Mortatti [27] used samples of dry wood 20 mm thick, a 60 keV ^{241}Am source and a collimator with 0.2 x 5 mm rectangular cross-section by 30 mm length, on both sides. Cown [17] used 2 mm thick samples, a collimator 2.0 x 0.1 mm cross-section and a ^{55}Fe gamma-ray source 5.9 keV energy.

4.3. Other uses

The gamma-ray attenuation methodology is now used for many purposes, but its most important application is in porous media flow studies.

Several papers have been written reporting experiments with gamma-ray applications, and many others have not been reported as they were being too simple. The gamma-ray attenuation method, with a large number of adaptations, was been used in the evaluation of biomass;of wood internal defects by sweeping the cross-section of the standing tree; water stored in internal cavities; the variability of density in sugar-cane for entomology studies; the density of bovine bones; salt concentration in solutions; movement of solid particles in aqueous media; studies of problems of mixture of liquids; flow of bifasic fluids in porous media with temperature gradients; and in many other applications.

5. CONCLUSIONS

The gamma-ray attenuation method is one of the most important tools available to investigators, and its utilization depends on individual ingenuity.

Basically, three parameters are important and interdependent: density, thickness and mass attenuation coefficient of the material to be studied. The thickness of the samples can sometimes be modified to obtain best results. The mass attenuation coefficient depends on the chemical composition of the sample and the energy of the photon of

gamma ray. Then, the selection of gamma-ray energy is very important to work close to optimum experimental conditions.

In the single-beam method, an error in the determination of density does not influence the determination of fluid content, since density is considered constant. But for the double-beam method, errors in determination of density tend to increase the errors in fluid content determination. For example, in soil physics, errors in bulk density and water content measurements with the double-beam method are greater than errors when the single-beam method is used. Therefore, the double-beam method must be used only when necessary, that is, when the bulk density changes with the water content.

REFERENCES

[1] BELCHER, D.J., CUYKENDALL, T.R., SACK, H.S., The measurement of soil moisture and density by neutron and gamma-ray scattering. Technical Development Report no. 127, Civil Aeronautics Administration, Washington. D.C. (1950).

[2] SMITH, E.E., WHIFFIN, A.C., Density measurement of concrete slabs using gamma radiation,Engineers 194 (1952) 278.

[3] BERMAN, A.I., HARRIS, J.N., Precision measurement of uniformity of materials by gamma-ray transmission. Rev. Sci. Inst., 25 (1954) 21.

[4] GLASHEEN, R.W., Automatic control over materials movement. Chem. Engr. Progr. 50 (1954) 487.

[5] BARTOLOMEW, R.N., CASAGRANDE, R.M., Measuring solids concentration in fluid systems by gamma-ray absorption. Ind. Eng. Chem. 49 30 (1957) 428.

[6] SEYMOUR, F.D., Density determination of uranium pulp and uranyl solution by gamma-ray absorption. AERE E/R (1957) 2269.

[7] WATT, J.S., LAWTHER, K.R., Measurement of concentration of tungsten suspensions and density of liquid sodium by gamma-ray absorption. *In* Symposium on the peaceful uses of atomic energy in Australia, Canberra, (1958) 610.

[8] SOANE, B.D., Double energy gamma transmission for moisture and density measurements in soil tillage studies. *In* Soil water symposium, Prague, (1967).

[9] FERRAZ, E.S.B., MANSELL, R.S., Determining water content and bulk density of soil by gamma-ray attenuation methods. Univ. of Florida, IFAS. Technical Bulletin 807 (1979) 51.

[10] GARDNER, W.H., CAMPBELL, G.S., CALISSENDORF, C., Systematic and random errors in dual gamma energy soil bulk density and water content measurement. Soil Sci. Soc. Amer. Proc., 36 (1972) 393.

[11] COREY, J.C., PETERSON, S.F., WAKAT, M.A., Measurement of attenuation of ^{241}Am gamma-rays for soil density and water content determinations. Soil Sci. Soc. Amer. Proc., 35 (1971) 215.

[12] MANSELL, R.S., HAMMOND, L.C., McCURDY, R.M., Coincidence and interference corrections for dual-energy gamma-ray measurements of soil density and water content. Soil Sci. Soc. Amer. Proc., 37 (1973) 500.

[13] NOFZIGER, D.L., SWARTZENDRUBER, D., Material content of binary physical mixtures as measured with a dual-energy beam of γ-rays. J. App. Phys., 45 (1974) 5443.

[14] FERRAZ, E.S.B., Determinação simultânea de densidade e umidade de solos por atenuação de raios gama do ^{137}Cs e ^{241}Am. Thesis, University of São Paulo, Brazil, (1974) 120.

[15] BRIDGE, B.J., COLLIS-GEORGE, N., A dual source gamma-ray traversing mechanism suitable for the nondestructive simultaneous measurement of bulk density and water content in columns of swelling soil. Aust. J. Soil Res., 11 (1973) 83.

[16] STROOSNIJDER, L., DeSWART, J.G., Collimation of a 60-KeV column scanner with simultaneous use of ^{241}Am and ^{137}Cs gamma radiation. Soil Sci., 118 2 (1974) 61.

[17] COWN, D.J., X-ray densitometry using an ^{55}Fe source. Wood Microdensitometry Bulletin 2 2 (1982) 25.

[18] GURR, C.G., Use gamma-rays in measurement of water content and permeability in unsaturated columns of soil. Soil Sci. 94 (1962) 224.

[19] FERGUSON, H., GARDNER, W.H., Water content measurement in soil columns by gamma ray absorption. Soil Sci. Soc. Amer. Proc., 26 (1962) 11.

[20] DAVIDSON, J.M., BIGGAR, J.W., NIELSEN, D.R., Gamma
     radiation attenuation for measuring bulk density and
     transient water flow in porous materials. J. Geophys.
     Res. 68 (16) (1963) 4777.

[21] KING, L.G., Gamma-ray attenuation for soil-water-content
     measurement using [241]Am. *In* Symposium on the use of
     measurement using [241]Am, Isotope and Radiation Techniques in Soil
     Physics and Irrigation Studies, (Proc. Symp. Istanbul, 1967), IAEA, Vienna
     (1967) 17.

[22] DURANTE, V.A., KOGAN, J.L., FERRONSKY, V.I., NOSAL, S.I.,
     Field investigations of soil densities and moisture
     contents. Proc. Fourth Int. Conf. Soil. Mech. Found.
     Eng. 1 (1957) 216.

[23] GARDNER, W.H., CAMPBELL, G.S., CALISSENDORF, C., Water
     content and soil bulk density measured concurrently using
     two gamma photo energies. Oak Ridge, United States Atomic
     Energy Commision, Report RLO, 1543 6 (1969) 42.

[24] LOOS, W.E., Gamma-ray absorption and wood moisture content
     and density. Forest Prod. J. 11 (3) (1961) 145.

[25] FERRAZ, E.S.B., Determinação da densidade da madeira por
     atenuação de raios gama de baixa energia. Bol. IPEF,
     Brazil, 12 (1976) 61.

[26] FERRAZ, E.S.B., AGUIAR, O., Wood density and moisture
     content determination by gamma-ray attenuation technique.
     IUFRO FAST GROWING TREES SYMPOSIUM, ÁGUAS DE SÃO PEDRO,
     Brasil (1980).

[27] FERRAZ, E.S.B., MORTATTI, J., Determining density of wood
     by gamma-ray attenuation method - Growth ring
     identification. Wood Microdensitometry Bulletin 2 2 (1982)
     26.

[28] MORTATTI, J., NASCIMENTO FO, V.F., FERRAZ, E.S.B.,
     Aplicação do método de atenuação de dois raios gamas em
     linha em amostras de madeira. Energia Nuclear e
     Agricultura (1983) (submitted).

SOME POTENTIAL USES OF THE BETA GAUGE IN AGRICULTURAL RESEARCH

N.N. BARTHAKUR
Department of Agricultural Chemistry
    and Physics,
Macdonald Campus of McGill University,
Ste. Anne de Bellevue,
Quebec, Canada

Abstract

SOME POTENTIAL USES OF THE BETA GAUGE IN AGRICULTURAL RESEARCH.
    Moisture stress and drought endurance characteristics of three plant species were explored in the laboratory with a β-gauge. Non-stress time periods were found to be between 2 and 15 days after the plants were exposed to artificially produced drought conditions. The concept of a critical transmission rate is proposed to determine the onset of moisture stress and optimum timing of irrigation of crops. Stomatal dynamics to relative leaf turgidity relationship was studied. Stomatal movement caused about 3 to 10% change in the β-transmission through leaves. The β-gauge was tested as a leaf surface wetness indicator in the laboratory. Field measurements of the amount and the duration of dew formation demonstrated another potential use of the β-gauge in agriculture.

1. INTRODUCTION

The β-gauge was used to measure water content of leaves [1—11]. The relative advantages and disadvantages of the technique, as used in plant science, were critically reviewed [8]. The instrument could not be operated non-destructively because of calibration requirements inherent in water-content determinations of live leaves. The usefulness of the β-gauging technique in plant breeding experiments was demonstrated [9]. The amount of dew formation on soil surfaces was measured more accurately by the β-absorption method than those obtained by conventional dewmeters [12]. Other potential uses of the β-gauge in agricultural research remained unexplored.

This paper investigates potential uses of the β-gauge in plant/water relations that could be relevant to the agriculture of semi-arid regions.

461

2.   MATERIALS AND METHODS

A ^{204}Tl source (0.222 MBq), a pure β-emitter, was mounted on an adjustable
laboratory stand. A G-M detector of 3.5 cm diameter and 1.4 mg/cm^2 window
thickness was positioned 4 cm directly below the source on the same stand.
Mature but attached leaves of potted, greenhouse-grown plants were placed
horizontally 0.2 cm above the window of the detector. Free air movement
between the leaf and the detector prevented condensation from forming on the
window. Source-leaf-detector geometry was kept constant and any variation of
air density within this short distance did not affect the count rates. For plant
moisture stress determinations, the pots were initially filled with water to field
capacity. Water in the pots was then allowed to deplete with time via evapo-
transpiration. Tobacco (*Nicotania tobacum*), marble queen (*Scindapsus aureus*),
and wax bean (*Phaseolus vulgaris*) were selected for drought endurance studies.

Count rates were continuously recorded by a ratemeter-recorder system
whose RC time constant was held fixed at 10 s. The fractional standard deviation
in the average count rate (N) was determined from the equation $\sigma/N = 1/\sqrt{Nt}$,
where t was the recording time (t $\geqslant$ RC). Twenty minutes of running average
for the highest (10 000 counts/min) and the lowest (1000 counts/min) count
rates in these experiments gave about 0.2 and 0.7% standard deviation respectively.
The coincidence correction of the G-M detector was neglected. The average
background count rate was 25 counts/min. G-M detector characteristics were
known not to change for a wide range of environmental temperature variations [13].

Stomatal movement studies were conducted under natural light conditions.
Stomates were counted under an optical microscope by taking epidermal
specimens from an isopositional leaf which was similarly exposed to sunlight as
the experimental leaf. Epidermal specimens were immediately immersed in
absolute alcohol before they were mounted on microscope slides so as to count
the number of stomates.

A circular lanolin ring 5 cm^2 in area and 0.2 cm rim thickness was constructed
on the experimental materials and centred above the detector for surface wetness
measurements. Leaves were wetted with measured amounts of water inside the
lanolin rings which prevented runoff. Leaf temperature was measured by a
copper-constantan thermocouple. Wind velocity over surfaces was measured by a
hot-wire anemometer. Relative humidity was determined from the wet and dry
bulb temperatures.

3.   RESULTS AND DISCUSSION

The plot of percentage transmission versus time for plant species produced
characteristic curves (Fig. 1). Any significant increase in the percentage trans-
mission could be assumed to indicate moisture stress in the plant. Tobacco, a
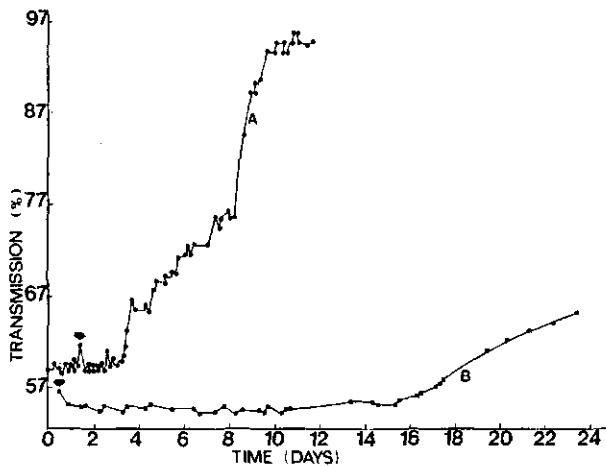
FIG.1. *Transmission versus time for tobacco (A) and marble queen (B) plants at RH = 50%; air temperature = 24.5°C; leaf temperature = 23.4°C; and incident radiation = 19 W/m². Arrows indicate watering.*
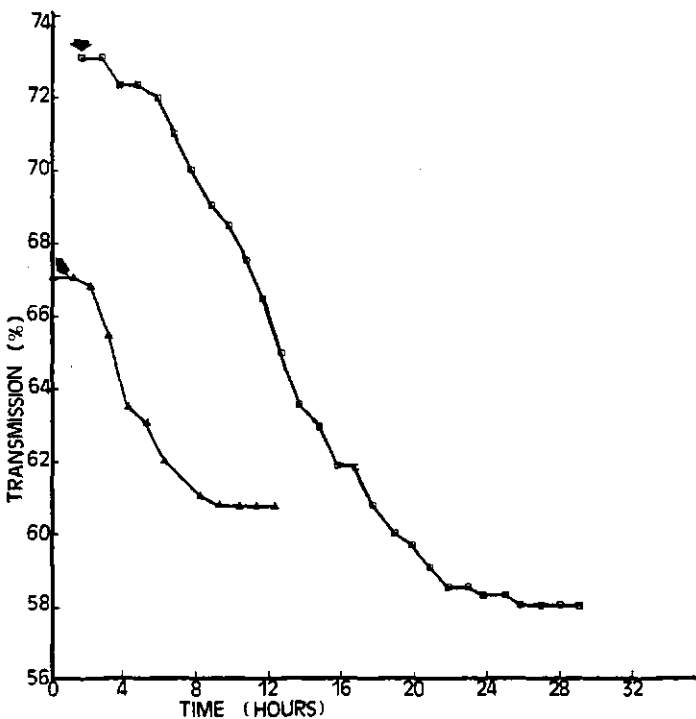
FIG.2. *Water uptake by tobacco plants. Arrows indicate watering. RH = 50%; air temperature = 24.5°C; leaf temperature = 23.4°C; and incident radiation = 19 W/m².*
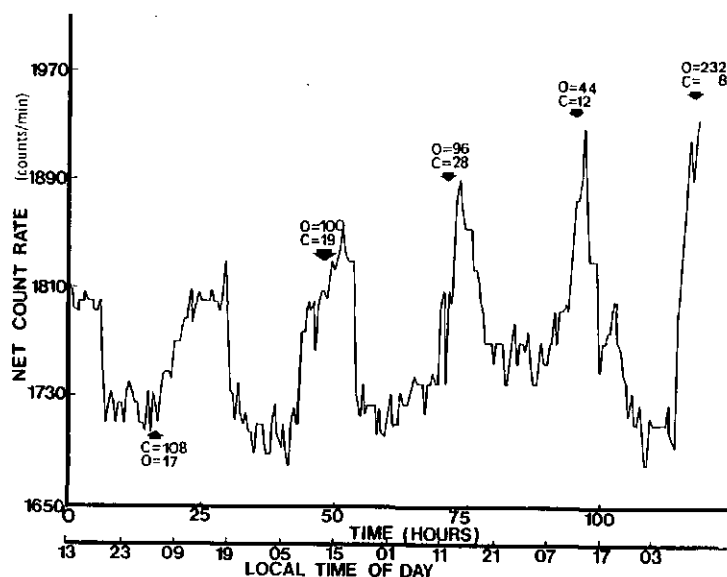
FIG.3.   Count rate versus time for tobacco exposed to sunlight. RH = 60%; air temperature = 26.5°C. Stomates opened (0); closed (C).
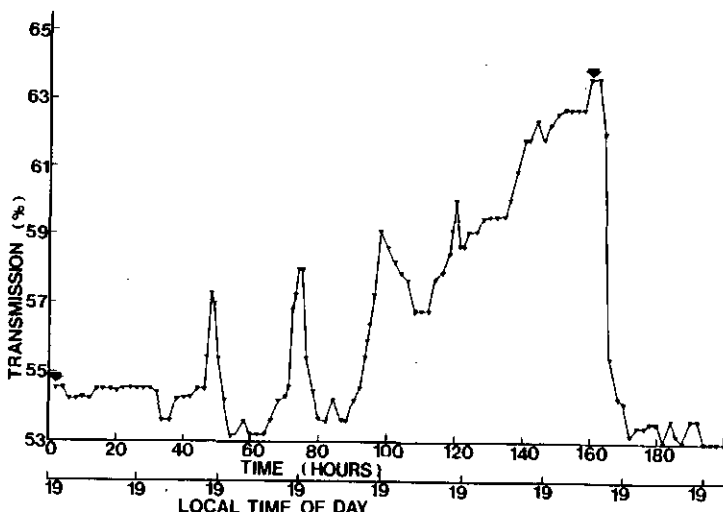
FIG.4.   Transmission versus time for tobacco exposed to sunlight. Arrows indicate watering. RH = 63%; air temperature = 26°C.
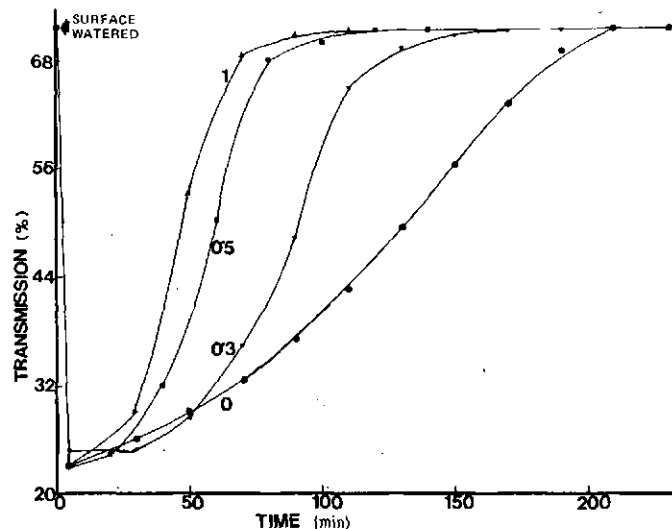
FIG. 5. Transmission versus time of a wet plastic disc. The numerals alongside the curve represent wind velocity in m/s. RH = 42%; air temperature = 24.4°C; incident radiation = 19 W/m².
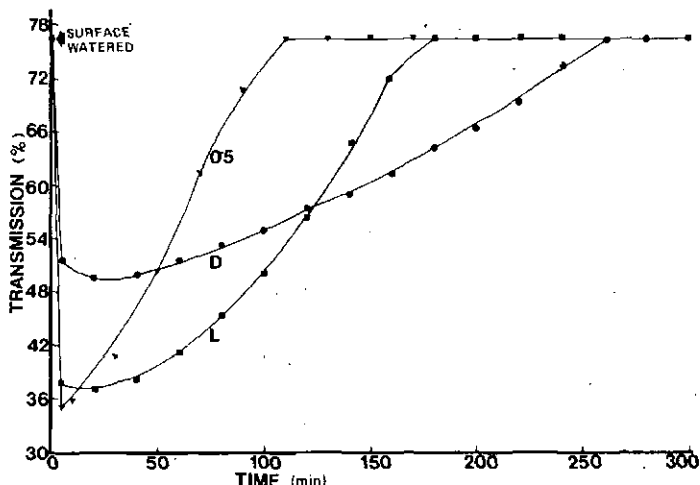
FIG. 6. Transmission versus time for wet poinsettia leaves. RH = 28%; air temperature = 22.7°C; incident radiation = 19 W/m². Surface wetted with drops (D) or with a wetting agent (L) by the same amount of water. The curve with 0.5 m/s wind speed is shown.
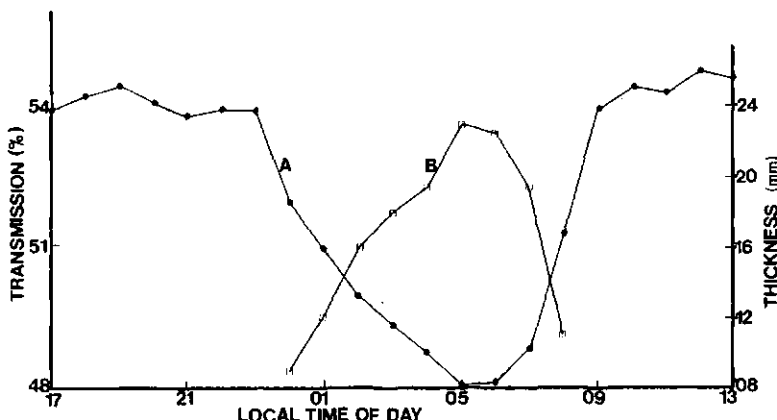
FIG.7.   Dew curves obtained with the β-gauge at the canopy height of a wax bean crop.
Curve A: transmission versus time; Curve B: dew thickness versus time.

TABLE I. DEW MEASUREMENTS BY THE BETA GAUGE

Date (1983)	Conditions	Time: wet	Time: dry	Wet duration	Maximum dew thickness (mm)
Aug. 3−4	Dew, then sunny	24:35	08:15	7·67	0·12
Aug. 4−5	Rain, dew, then sunny	18:35	09:55	15·33	0·20
Aug. 5−6	Dew, then sunny	22:30	09:00	10·50	0·30
Aug. 6−7	Dew, then sunny	23:00	09:00	10·00	0·23
Aug. 8	Heavy rain	19:00	−	−	−

mesophyte, showed about two non-stress days after the plants were watered.
Marble queen, a xerophyte, did not manifest water stress for about 15 days. Wax
bean was found to have about four non-stress days under similar conditions. The
ability to maintain the same transmission for a length of time by a representative
leaf of a species, without replenishing water, could serve as an index of drought
endurance. The slope of the curve for tobacco during the stress period was higher
than that for marble queen (Fig. 1). This must be due to the presence of some
water conservation mechanism in the latter species.

The concept of a critical transmission rate (CTR) could be proposed − CTR
may be defined as that transmission value below which no plant injury may occur.

The CTR could be arrived at by simultaneously measuring a plant growth parameter or nutrient uptake as transmission was allowed to increase. Once the CTR is evaluated for a species in the laboratory, the concept could serve as an objective criterion for determining the optimum timing of irrigation of field crops. At present, no suitable method exists for determining irrigation schedules. The proposed method will have some advantages over soil moisture or plant water potential measurements. The β-gauge is non-destructive and measures the actual water status in the plant. Water uptake by stressed plants showed the sensitivity of the method (Fig. 2). A 15% transmission difference between a moderately stressed and a turgid leaf was usually observed.

Continuous recording of the count rate versus time revealed the effect of stomatal movement when a well-watered plant was exposed to sunlight (Fig. 3). The number of stomates opened was found to be much higher than those closed when the transmission was higher. The reverse was true when the transmission was low during the night. The rythmic variations follow the light and dark cycles of the day. The amplitudes of these rythmic variations damped out as the plant was subjected to moisture stress (Fig. 4). The stomatal closure phenomenon stimulated by water stress was demonstrated before [14]. The damping out of the amplitudes of the rythmic variations could constitute a 'distress signal' from the plant for water.

The β-gauge as an indicator of leaf surface wetness was tested in the laboratory. Evaporation as a function of wind velocity for a hydrophobic surface showed the asymptotic behaviour (Fig. 5). Surface dryness time may be defined as the time required for the surface to attain the pre-wet percentage transmission value. Surface dryness as determined visually agreed well with those indicated by the β-gauge for materials like plastics. For a real leaf surface, visual dryness apearances did not coincide with those given by the β-gauge. Evaporation from a real leaf surface showed non-asymptotic behaviour (Fig. 6). Foliar absorption of water could contribute to this phenomenon. The β-gauge was field tested as a dewmeter (Fig. 7) The times of initiation and termination of dew as recorded by the β-gauge were much clearer than those measured by dew balances [12]. The amount of dew could be determined accurately by calibrating the β-gauge with added water on leaf surfaces. The results of dew measurements on four successive nights are shown in Table I.

REFERENCES

[1] MEDERSKI, H.J., Determination of internal water status of plants by beta ray gauging, Soil Sci. 92 (1961) 143.

[2] WHITMAN, P.C., WILSON, G.L., Estimations of diffusion pressure deficit by correlation with relative turgidity and beta radiation absorption, Aust. J. Biol. Sci. 16 (1963) 140.

[3] NAKAYAMA, F.S., EHRLER, W.L., Beta ray gauging techniques for measuring leaf water content changes and moisture status of plants, Plant Physiol. **39** (1964) 95.

[4] EHRLER, W.L., VAN BAVEL, C.H.M., NAKAYAMA, F.S., Transpiration, water absorption and internal water balance of cotton plants as affected by light and changes in saturation deficit, Plant Physiol. **41** (1966) 71.

[5] JARVIS, P.G., SLATYER, R.O., Calibration of β-gauges for determining leaf water status, Science 153 (1966) 78.

[6] ROLSTON, D.E., HORTON, M.L., Two beta sources compared for evaluating water status of plants, Agron. J. **60** (1968) 333.

[7] BIELORAI, H., Beta-ray gauging technique for measuring leaf water content changes of citrus seedlings as affected by the moisture status in the soil, J. Exp. Bot. **19** (1968) 489.

[8] JONES, H.G., Estimation of plant water status with the beta-gauge, Agric. Meteorol. **11** (1973) 345.

[9] ANTOSZEWSKI, R., "Some nuclear techniques applicable for physiological characterization of plant material", Tracer Techniques for Plant Breeding (Proc. Panel Vienna, 1974), IAEA, Vienna (1975) 25.

[10] KIELAK, Z., ANTOSZEWSKI, R., SLOWIK, K., Radiometric studies on water stress in the strawberry plant, Fruit Sci. Reps **2** (1975) 75.

[11] OBRIGEWITSCH, R.P., ROLSTON, D.E., NIELSON, D.R., NAKAYAMA, F.S. Estimating relative leaf water content with a simple beta gauge calibration, Agron. J. **67** (1975) 729.

[12] BUNNENBERG, C., KUHN, W., Application of the β-absorption method to measure dew on soil and plant surfaces, Int. J. Appl. Radiat. Isot. **28** (1977) 751.

[13] KORFF, S.A., SPATZ, W.D.B., HILLBERY, N., Temperature coefficients in self-quenching counters, Rev. Sci. Instrum. 13 (1942) 127.

[14] DAVIES, W.J., Stomatal responses to water stress and light in plants grown in controlled environments and in the field, Crop. Sci. **17** (1977) 735.

USE OF A SURFACE GAMMA-NEUTRON GAUGE TO MEASURE BULK DENSITY, FIELD CAPACITY, AND MACROPOROSITY IN THE TOPSOIL

L.R. AHUJA, R.D. WILLIAMS
Water Quality and Watershed
    Research Laboratory,
Agricultural Research Service,
US Department of Agriculture,
Durant, Oklahoma,
United States of America

Abstract

USE OF A SURFACE GAMMA-NEUTRON GAUGE TO MEASURE BULK DENSITY, FIELD CAPACITY, AND MACROPOROSITY IN THE TOPSOIL.
    A surface gamma-neutron gauge (Troxler, Model 3411-B) was used to determine bulk densities and average moisture contents of 0−100, 0−200, and 0−300 mm soil layers at 26 sites in two soils, and the results were compared with measurements made on soil cores. Bulk densities (D) from the gauge using factory calibration were generally smaller than the core values, while the neutron moisture contents (θ) were higher. Recalibration of the neutron response improved both moisture content and density determinations. To improve density results further, the gamma probe was recalibrated by two methods. In Method 1, both soil and water attenuation constants were obtained by a least-squares procedure from some core D and θ data. In Method 2 only the water constants were revised, based on core data. Both methods improved agreement between gamma-probe and soil-core bulk densities to nearly the same extent. Standard deviation of differences between gamma and core values was about ± 0.03 Mg/m^3 for a bare silt loam soil, and ± 0.04 for a grassed and stony fine sandy loam. The mean differences were very small. Deviations were random and probably caused by variability in soil composition, surface roughness, and errors in measuring actual densities by cores.

1. INTRODUCTION

Spatial measurements of soil bulk density, moisture holding capacity, and macroporosity can aid hydrologic characterization of a variable field soil, and can be used to evaluate the effects of tillage systems, cropping, and erosion-depositions on water infiltration, water storage, and air movement in the soil. Macroporosity can be estimated from bulk density (which gives total porosity) and moisture content at field capacity. A surface gamma-neutron gauge, such as the

469
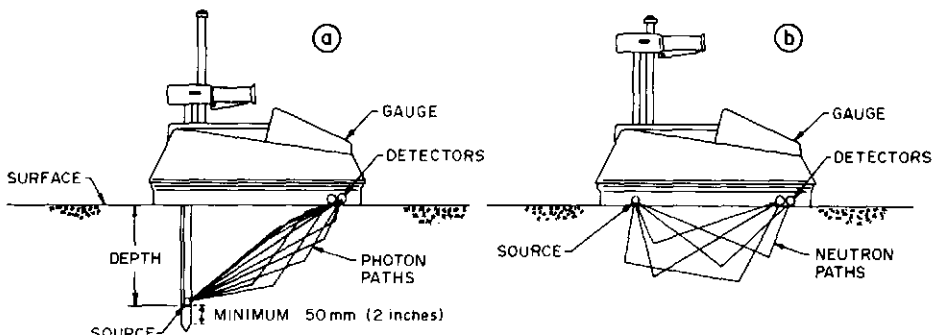
FIG.1.   *Direct transmission (a) and back-scatter (b) geometry of the Troxler surface gamma-neutron gauge.*

Troxler Electronics Laboratories' Model 3401-B or 3411-B[1], may be a useful tool for rapidly measuring soil bulk density and moisture content in the topsoil at a large number of locations within a field. The bulk density is determined using the gamma probe after determining moisture content using the neutron probe. The instrument is placed on the soil surface. The gamma source (8 mCi ^{137}Cs) is permanently mounted on an indexed steel rod which is lowered into an access hole in increments of 50 mm below the surface, down to a depth of 300 mm. The radiation is transmitted through the soil diagonally to the detector located at the soil surface (Fig. 1a). Since source rod is permanently attached to the instrument base, the geometric relationships between source and detector are fixed for any depth increment. The neutron source (40 mCi ^{241}Am-Be) and detector, both of which are permanently located at the base of the instrument, are used to measure soil moisture content in the surface layer by back-scatter geometry (Fig. 1b). A separate unit containing a reference standard is supplied with the instrument for both gamma and neutron counting. The reference counts are taken in the back-scatter geometry, with the instrument placed over the reference unit.

Vigier and Campbell [1] used the gamma probe in a surface gauge to measure wet bulk densities of two organic soils. Smajstrla and Clark [2] explored its use to measure moisture contents in soil surface layers, with known bulk densities.

---

[1] Trade names are given for convenience of the readers. No endorsement, by the US Department of Agriculture, is implied.

The objective of this study was to investigate the use of
Troxler Model 3411-B surface gamma-neutron gauge for deter-
mining dry bulk densities and moisture contents in thin layers
of the topsoil under field conditions. Factory calibration and
two methods of in situ field calibration based on undisturbed
soil cores were examined.

2.   THEORY

For the direct transmission geometry of Fig. 1a, the
Troxler Electronics Laboratories [3] have found the following
equation adequately describes the transmission of gamma rays
through a given material:

$$I/I_s = A \exp(-BD)-C \qquad (1)$$

where I is the intensity of gamma rays exiting the material, I_s
is the intensity after passing through a reference standard, D
is density of the material, and A, B, and C are constants. The
A and C are related to source size, detector efficiency, and
primarily the geometric factors that cause response deviations
from an exponential function. The constant B contains the mass
attenuation coefficient and path length. Values of all the
constants thus depend upon the location depth of the source.
The constants A and C are determined by Troxler by counting
through three metallic standards, and are assumed to remain
unchanged for use of the instrument in soils. The value of the
constant B for use with soils is obtained as an average of
values for standard blocks of granite and limestone. In a
moist soil, soil bulk density is obtained using Eq. (1) as:

$$D = \ln[A/(C+I/I_s)]/[B]-1.05[\theta] \qquad (2)$$

where θ is the volumetric soil moisture content. It is im-
plicitly assumed that the gamma attenuation coefficient of soil
water is 1.05 times that of the dry soil. The moisture content
θ obtained with the surface neutron probe is assumed constant
with depth [3].
It is recognized that the gamma attenuation coefficient of
soil depends upon the soil composition, especially the fraction
of hydrogen contained in materials other than water, as well as
upon the nature of medium surrounding the beam path [4].
Similarly, attenuation coefficient of soil water and the ratio
of soil and water coefficients may also vary appreciably [4].
It may be better to use separate attenuation coefficients for
soil and water, and determine them by calibration with in situ
field data, under actual conditions of operation. For this
purpose. Eq. (2) for a given location of the gamma source may
be written as:

$$D = \ln[A/(C+I/I_s)]/[B_s] - (B_w/B_s)\bar{\theta} \qquad (3)$$

where B_s is the pooled attenuation-path length constant for soil and B_w for soil-water, and $\bar{\theta}$ is the average soil water content from soil surface to depth of the source. We determined the constants B_s and B_w by two methods. In Method 1, both B_s and B_w were obtained by a least-square fit of Eq. (3) to a set of D and $\bar{\theta}$ values measured on undisturbed soil cores for location of gamma source at either 100, 200, or 300 mm depth below the soil surface. Number of core values in the set were either 4, 8, or 12 for each depth. In Method 2, the soil coefficient B_s was set equal to the factory value B, while a B_w was obtained directly from Eq. (3) for each known D and $\bar{\theta}$. Average B_w for either 4, 8, or 12 core values was employed in evaluations. After B_s and B_w were determined, the bulk density for each site was calculated using the measured average gravimetric soil water content, $\overline{W}$ (kg/kg), in the specified depth interval:

$$D = \ln[A/(C+I/I_s)]/[B_s+B_w\overline{W}] \qquad (4)$$

This equation can be used for determining bulk density when only gravimetric soil water content is measured in conjunction with gamma probe reading.

3. EXPERIMENTAL

Soil bulk densities and moisture contents were measured at 12 sites on a bare Kirkland silt loam soil (Udertic Paleustolls) and 14 sites on a grassed Ruston fine sandy loam (Typic Paleudults). After allowing the instrument to warm up for 20 min, the Reference Standard unit was placed on a 600 mm high dry concrete block in an open area, and standard counts for gamma photons and neutrons were taken for 4 min. While the standard counts were being taken, a 300 x 300 mm level area was selected. In the grassed field, the grass was clipped as close as possible to the ground level. The soil surface was smoothed with a steel scrap plate, with the minimum of digging, to allow the smallest possible air gap between the soil surface and the bottom of the instrument. A 22 mm diameter access hole was then made with a soil tube to a depth of 350 mm. The gauge was placed in position and four 1-min gamma and neutron counts were taken with the source located at 100, 200, and 300 mm depths. Immediately after completing the measurements, undisturbed soil cores (100 mm diameter x 75 mm long) were taken from directly under the instrument with one core for each depth interval of 0-100, 100-200, and 200-300 mm. Moisture content and bulk density were determined on each core. Average moisture contents and bulk densities of the 0-200 and 0-300 mm soil layers
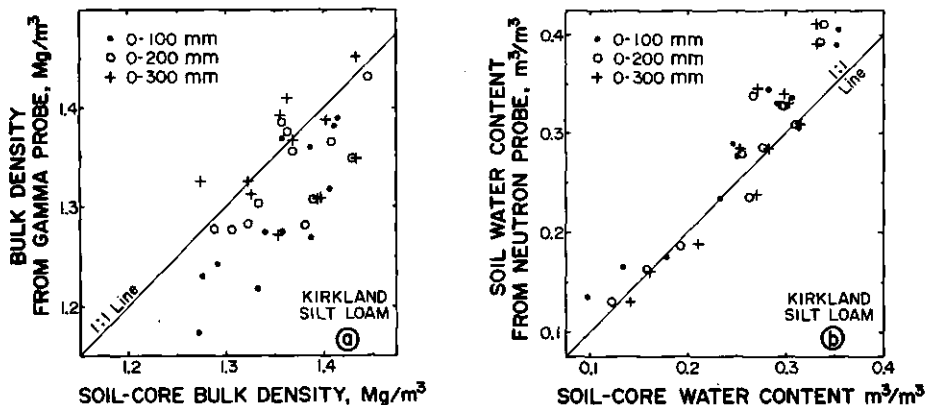
FIG.2.   Soil bulk densities in Kirkland silt loam topsoil determined by gamma and neutron probes using Troxler calibration (Eq. (2)), compared with soil-core values (a); and soil water contents determined by surface neutron probe, using Troxler calibration, compared with soil-core values (b).

were obtained as mean values for the first two and all three cores, respectively.

4.   RESULTS AND DISCUSSION

Soil bulk densities for different depth intervals of the bare Kirkland silt loam topsoil determined with the gamma-neutron probe, using factory calibration (Eq. (2)), are compared with measurements on soil cores in Fig. 2a. Probe bulk density values are generally smaller than the soil-core values, and there is large variability in the data points. The moisture contents determined with the neutron probe fairly well agree with the core values in the lower half of the water content range, but are higher than the core values in the upper half (Fig. 2b). Thus, at least part of the discrepancy in gamma probe bulk density values may be due to error in θ values used in Eq. (2). For the grassed Ruston soil the discrepancies between probe and core values were greater than for Kirkland soil, especially in moisture contents (data not presented).

The surface neutron probe was recalibrated against soil-core water contents in the top 0-100 mm layer, since the probe senses moisture primarily in this layer [3]. When soil water contents obtained from the improved calibration were used in Eq. (2), the bulk density values determined by the gamma probe were in better agreement with the soil-core values in both

Table I. B_s and B_w of Eq. (3) for different locations of gamma source in soil as determined By Methods 1 and 2, from core data of D and $\bar{\theta}$ for 4, 8, or 12 sites, and Troxler calibration A, C, and B values.

Method and soil	Location of gamma source (mm)	No. of core $D,\bar{\theta}$ data pairs used					
		4		8		12	
		B_s	B_w	B_s	B_w	B_s	B_w
Method 1, Kirkland	100	1.0964	0.9197	1.1262	0.7838	1.0983	0.9079
	200	1.5330	1.7673	1.6899	1.0845	1.6256	1.4767
	300	2.3409	1.3293	2.4982	0.6242	2.3494	1.4403
Method 1, Ruston	100	1.0117	1.5856	0.9694	1.7955	0.9944	1.6711
	200	1.5503	2.2142	1.5660	2.0659	1.5401	2.2193
	300	2.1542	2.8516	2.1600	2.7337	2.1919	2.5503
Method 2, Kirkland	100	--	0.9917	--	1.0660	--	1.0188
	200	--	1.4530	--	1.5832	--	1.6353
	300	--	2.0528	--	2.2898	--	2.3686
Method 2, Ruston	100	--	1.1544	--	1.1024	--	1.1044
	200	--	1.8661	--	1.8267	--	1.7899
	300	--	2.6803	--	2.5984	--	2.6317

		A	C	B
Troxler calibration, all soils	100	10.9859	0.1069	1.0779
	200	14.0756	-0.0012	1.5991
	300	13.6570	-0.0122	2.1796
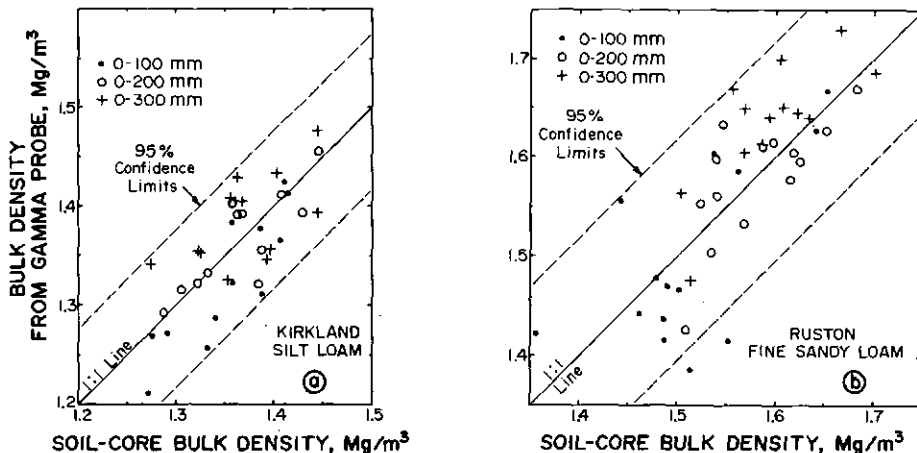
FIG.3. Comparison of soil bulk densities determined by gamma probe, using water contents from improved calibration of neutron probe, and soil-core bulk densities: (a) Kirkland silt loam; (b) Ruston fine sandy loam. The 95% confidence limits are based on analysis of residuals of the two sets of data.

soils (Fig. 3a,b) for all depth intervals. The differences between probe and core values were not statistically signi- ficant, while the correlation coefficients between them (0.744 for Kirkland and 0.794 for Ruston soil) were highly signi- ficant. Mean difference for Kirkland soil was -0.00364 Mg/m³ with a standard deviation of +0.0397, and for Ruston soil 0.00571 with a standard deviation +0.0558. However, there was appreciable scatter in the data points, more so in Ruston soil due to presence of grass roots and stones. Also the moisture content was less uniform with depth for Ruston, causing greater error in densities calculated for 0-200 and 0-300 mm soil thicknesses.

The constants B_s and/or B_w of Eq. (3) determined by Methods 1 and 2, and the constants A, C, and B for our gamma- neutron gauge provided by the Troxler calibration are presented in Table I. In Method 1, the least-squares values of constant B_s for a given soil and location of gamma source varied less with number of data pairs used in determining them than the value of water constant B_w. Furthermore, B_s values in both soils were within 10% of the corresponding Troxler B values, except one value for Kirkland soil which was 15% higher. Thus, the use of Troxler B in place of B_s may be acceptable. The Method 2 B_w values in Kirkland soil are within 10% of Troxler B values, but those in Ruston soil are higher for gamma source locations greater than 100 mm.

Table II. Mean (M_r) and standard deviation (SD_r) of differences between probe and soil-core bulk densities, and correlation coefficient (R) between probe and core values pooled for all depth intervals in different cases of Table I.

Soil	No. of $D,\bar{\theta}$ pairs used to determine B_s and/or B_w	Method 1			Method 2		
		M_r	$SD_r(\pm)$	R	M_r	$SD_r(\pm)$	R
Kirkland	4	0.0139	0.0320	0.7991	0.0183	0.0310	0.8035
	8	0.0019	0.0328	0.8169	-0.0006	0.0309	0.7945
	12	-0.0003	0.0286	0.8294	-0.0025	0.0305	0.7928
Ruston	4	-0.0123	0.0391	0.8822	-0.0125	0.0427	0.8531
	8	-0.0044	0.0387	0.8835	-0.0053	0.0434	0.8466
	12	-0.0067	0.0388	0.8843	-0.0050	0.0434	0.8461
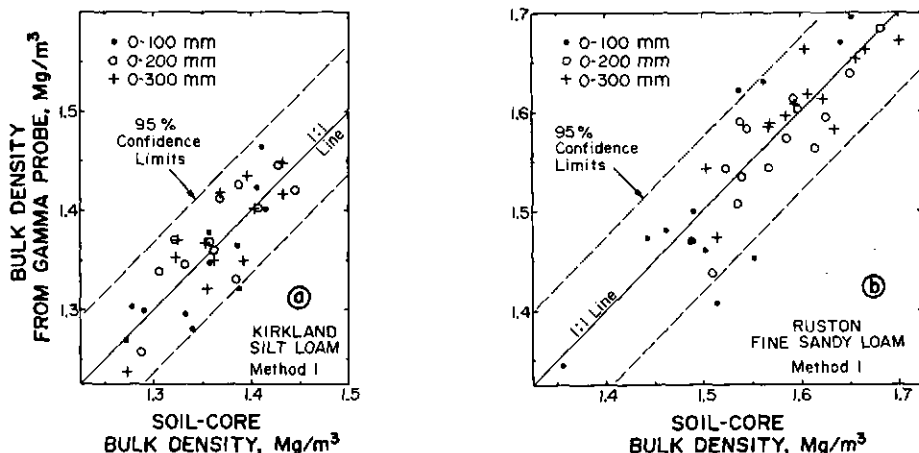
FIG.4. Comparison of soil bulk densities determined by gamma probe, using Eq. (4) with B_s and B_w constants obtained by Method 1 (8 data pairs) and gravimetric soil-core water contents, with soil-core bulk densities: (a) Kirkland soil; (b) Ruston soil.

For each set of constants in Table I, bulk densities (D) were calculated by Eq. (4). There were no significant differences in calculated D values due to number of data pairs used to determine the constants within a given method or between the two methods, as well as no significant difference between soil-core values and any set of calculated values. However, there was a significant difference between densities for different soil depth intervals. Mean difference between probe and soil-core bulk densities, over 36 or 42 points, was very small in all cases (Table II). The standard deviation of the differences was higher in Ruston than in Kirkland soil, and Method 1 was better than Method 2 in Ruston. The correlation coefficients also indicated slight superiority of Method 1 (Table II). Overall, it appears that no more than eight $D,\bar{\theta}$ data pairs are necessary to obtain the constants, and four pairs may be adequate.

In Fig. 4a,b, we present comparisons of bulk densities obtained from gamma probe using Method 1, 8 data-pairs, coefficients with soil-core bulk densities. The plots in Fig. 4 and the data in Table II indicate appreciable variability or scatter in the data points, despite the fact that the coefficients were determined from in situ core measurements. The differences between the probe and core value seemed to be random, since no correlation was found between the residuals and the magnitude of soil-core bulk densities. The deviations may be due to variability in soil composition and hence its

gamma attenuation characteristics, errors in measuring actual
bulk densities (that the gamma rays encounter) by soil cores,
and variability in air gaps between soil surface and the
instrument. A mean of 10 to 20 probe values would agree
closely with similar number of soil-core values.

5.   CONCLUSIONS

With proper calibration, this instrument is useful for
measuring topsoil bulk densities and moisture contents in a
field. Calibration on four to eight soil-core measurements
should be sufficient. Measurements made in a field 2 to 3 days
after a heavy rainfall will give information on a soil's field
capacity and macroporosity, which are indicative of its hy-
draulic conductivity. Moisture contents at this time will be
more uniform with depth for surface-neutron gauging. However,
a measurement of gravimetric soil water content on the soil
sample, removed from the hole required for gamma source, will
further improve the results.

REFERENCES

[1]   VIGIER, B., CAMPBELL, J. A., Canadian J. Soil Sci. 60
      (1980) 133.
[2]   SMAJSTRALA, A. G., CLARK, G. A., Am. Soc. Agr. Engn.
      Paper No. 81-2030, Am. Soc. Agr. Engn., St. Joseph, MI,
      U.S.A. (1981).
[3]   TROXLER ELECTRONICS LABORATORIES, 3400-B Series Instru-
      ment Manual - Surface Moisture-Density Gauges. Research
      Triangle Park, N.C., U.S.A. (1980).
[4]   RAWITZ, E., ETKIN, H., HAZAN, A., Soil Sci. Soc. Am. J.
      46 (1982) 461.

SOME CONSIDERATIONS FOR SOIL MOISTURE GAUGING WITH NEUTRONS

S. KASI, J. IMMONEN, K. SAIKKU
Physics Laboratory,
Helsinki University of Technology,
Espoo, Finland

Abstract

SOME CONSIDERATIONS FOR SOIL MOISTURE GAUGING WITH NEUTRONS.

The sensitivity of the moisture gauge, especially the neutron gauge, is discussed. The neutron gauge is very sensitive to hydrogen content. The interference of other elements including the most significant absorbers of thermal neutrons is computed. The so-called composition effect is made quantitative. Normally it is not very significant. A calculation of the weight function of the neutron gauge is reported, and a simple formula given for the 95% "sphere" of influence. To simulate the subsurface gauge a procedure is presented and applied by using available experimental data. The procedure is not a very good approximation of the transport theory:diffusion theory with a neutron absorbing sphere. The position and size of this sphere were two fitting parameters; altogether five gauge parameters were used for a fitting.

1. SENSITIVITY OF THE MOISTURE GAUGE

In agricultural use of soil its moisture content should not remain long below wilting-moisture content and above field capacity. Irrigation or drainage is needed to keep water within this range. On the other hand, the soil may have pores for relatively large amounts of gravitational water. All these moisture quantities — wilting moisture, available water, moisture deficit, field capacity, saturating water content etc. [1], can be presented as density quantities which have the unit kg/m^3. Let us denote this quantity by w.

The user of a moisture gauge can have a requirement Δw for its accuracy. Roughly a constant absolute accuracy of moisture determination is often appropriate. Then the sensitivity quantity

$$S = \frac{1}{R} \frac{dR}{dw} \tag{1}$$

where R is the response of the moisture gauge, offers a good basis for comparing instruments which have a response function of the type $R = R(w)$. In some such comparisons it is better to use[2] the relative sensitivity $S_r = (dR/R)/(dw/w)$.

479

For neutron gauges many types of sensitivity evaluation have been proposed.
S of Eq. (1) has been used, e.g. in Ref. [3]; the relative sensitivity, see Ref. [4],
is best when a constant $\Delta w/w$ is demanded (as in many mass gaugings); the
sensitivity quantity dR/dw [5] has the advantage of being proportional to source
strength, but these sensitivity evaluators have no basis in the statistical error of
radioactivity such as the quantity

$$E = \frac{1}{R^{1/2}} \frac{dR}{dw} \tag{2}$$

presented in Ref. [6] has (see Ref. [7:a]). The higher E is, the smaller is the
statistical error in the moisture w measured. The modifications of E in the cases
of measured background or standard count-rate comparison have been given in
Ref. [6].

A requisite for a nuclear gauge is that radiation risk must be at a minimum.
This certainly has been achieved when natural radiation is used. Relatively slow
moisture processes near the soil surface can be followed by cosmic radiation [8].

The neutron measurement used for moisture determination is in first place
the protium (^1H) density determination. Therefore, the hydrogen content of the
matrix must be very accurately known. Consider gaugings with a "point probe",
i.e. with the probe where the source and detector are close. When you measure
very organic soil matter, e.g. peat, and when its dry density $\rho = \rho_t - w$ does
not vary (ρ_t is the total density), then $R \propto \rho_t$, and thus $S \simeq 1/\rho_t$. In this matter
the point neutron and gamma probes gauge similarly [9]. For neutron gauging
in mineral soil, where the matrix includes little hydrogen, the effect of density
is relatively weak and the counting rates, at least without background, are small
for a point in dry substance. Thus, $S \simeq 1/w$.

2.   BASIC CALIBRATIONS

For a neutron moisture gauge the dependence of calibration on matrix density
is minimal when the substance is free from hydrogen. When the hydrogen content
of the matrix is known, the equivalent moisture content can be used [10], and the
calibration which was done for a substance which has no hydrogen in its composition.

The hydrogen content of the soil matrix should be determined accurately.
For this, thermogravimetric methods can be useful. Many other soil elements that
considerably interfere with the neutron measurement cannot be analysed easily.
Fortunately, the effect of composition is not usually very significant, (see Section 4).
For calibration, a basic composition can be selected which is most representative
for the tasks of the gauge. For soil studies the best basic matrix composition is

TABLE I. INTERFERING POWER S_i $(kg/m^3)/(kg/m^3)$ OF THE ELEMENT i
CALCULATED FOR A NEUTRON MOISTURE GAUGE WHEN THE DETECTOR,
BLACK FOR THERMAL OR EPITHERMAL NEUTRONS, IS A CONCENTRIC
SPHERE WITH A POINT AmBe SOURCE.

The free density of the matrice substance is 1500 kg/m^3 and it has the averaged
composition of the earth's crust, except the hydrogen content p_H = 0. The
moisture content w = 100 kg H_2O/m^3

| Element | Content p_i | Interfering power S_i in | |
i	value ± SD	thermal	epithermal
O	464 ± 30 g/kg	0.11	0.36
H	0 ± 0	8.0	6.0
Si	282 ± 100 g/kg	0.04	0.22
Al	82 ± 30 g/kg	0.025	0.19
Fe	56 ± 30 g/kg	−0.08	0.20
Ca	41 ± 20 g/kg	0.005	0.14
Na	24 ± 10 g/kg	0.06	0.4
Mg	23 ± 10 g/kg	0.07	0.27
K	21 ± 10 g/kg	−0.13	0.13
Ti	5.7 ± 3 g/kg	−0.3	0.24
P	1050 ± 500 mg/kg	0.04	0.20
Mn	950 ± 450 mg/kg	−0.6	0.27
S	260 ± 120 mg/kg	−0.004	0.17
C	200 ± 90 mg/kg	0.17	0.5
Cl	130 ± 60 mg/kg	−2.6	0.15
N	20 ± 9 mg/kg	−0.23	0.5
Li	20 ± 9 mg/kg	−32	−0.3
B	10 ± 5 mg/kg	−219	−6.6
Gd	7.3 ± 3.6 mg/kg	−708	−1.0
Sm	7.3 ± 3.6 mg/kg	−187	−2.3
Eu	1.2 ± 0.6 mg/kg	−115	−4.0
Cd	200 ± 100 μg/kg	−84	0.07
In	100 ± 50 μg/kg	−5	−0.08
		measurement	

that of the earth's crust, but even for some mineral soils it must be modified, e.g. for $CaCO_3$ [11].

For light organic soils, which usually include a high water content, a good basic calibration is that which has been determined for H_2O.

3.   INTERFERENCE OF ELEMENT

An increase of density ρ_i of an element i in a substance causes a change of gauge counting rate. A certain change of water density will cause the same counting rate change. We can define the ratio of this water density change (increasing or decreasing) to the increase of the element density, i.e.

$$S_i = -(\partial w/\partial \rho_i)_R. \tag{3}$$

as the interfering power of this element, or as the sensitivity of the gauge to the density of this element.

To make calculational investigations concerning the basic calibration for mineral soils, the composition of the earth's crust was taken from Krauskopf [12]. For hydrogen the content zero was selected. The composition and the result of a calculation are presented in Table I. The first elements up to manganese are the most common in the earth's crust. The last seven elements have a very high absorption cross-section for thermal neutrons. They absorb 30% of thermal neutrons in the soil when it is dry. One can calculate, when w = 10% by volume, that an increase of 3.6 ppm in gadolinium content causes $\Delta w = -3.8$, and that a 5 ppm increase in boron content gives $\Delta w = -1.6$ kg H_2O/m^3 as the error of moisture reading.

The hydrogen sensitivity is generally higher in gauges that detect thermal than in those that detect epithermal neutrons — see Table I [7:b, 13]. In calculations with models of different "point" gauges we found that in the thermal measurements S_i for hydrogen varies between 6—9 for rather mineralized soil, and decreases with moisture. In the case of epithermal detection S_i may in such cases be below the value of 4. The reason for the low epithermal sensitivity is that the increase of slowing-down power decreases flux with respect to the slowing-down density at the same energy; the growth in the response is due to the decrease of diffusion. Otherwise, when the detector is a very strong absorber of even epithermal neutrons, the spectrum of detectable neutrons is to be hardened considerably. For this case, our 3-group diffusion calculations (though comprising flux depression treatment) may be misleading.

Now we also define, by the same means as S_i,

$$S_\rho = -(\partial w/\partial \rho)_R \tag{4}$$

TABLE II. THE INTERFERING POWER OF DENSITY S_ρ, ITS VARIANCE D_c AND THEIR RATIO E_c

The type of gauge, matter and moisture as in Table I. The used estimates of $\sigma(p_i)$ are also presented there

Neutron detector	$S_\rho \pm D_c$	E_c
Thermal	0.0500 ± 0.0069	13.8%
Epithermal	0.283 ± 0.026	9.4%

to be the interfering power of dry density ρ. The values of this are given in Table II for the same cases as in Table I. The increase $\Delta\rho = 100$ kg/m^3 is eliminated with $\Delta w \simeq -5$, or $\simeq -28$ kg H$_2$O/m^3 in thermal or epithermal detection, respectively.

Change of density does not generally cause a unique S_ρ. We define it to be the change of dry density without any change of composition, i.e. $d\rho_i = p_i d\rho$. Thus,

$$S_\rho = \sum_i p_i S_i. \tag{5}$$

4. EFFECT OF COMPOSITION

It is supposed that the variance of the content of each element i is known. $\sigma(p_i)$ is the standard deviation. If we suppose that the p_i are independent — though their sum must be 1 and they co-exist in many minerals — then Eq. (5) gives the variance

$$\sigma^2(S_\rho) = \sum_i S_i^2 \sigma^2(p_i) \tag{6}$$

Thus, the composition causes in S_ρ the standard deviation

$$D_c = \sigma(S_\rho) \tag{7}$$

The interfering effect of composition is properly defined, we consider, with the measure

$$E_c = D_c/S_\rho \tag{8}$$

D_c and E_c, in addition to S_ρ, have been calculated in Table II for the case we have been using as an example.
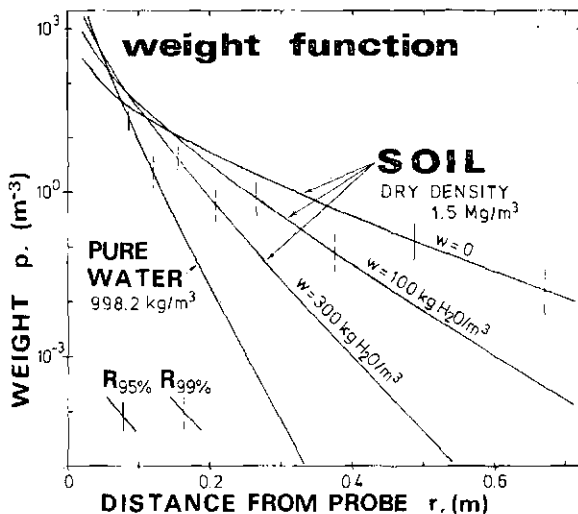
FIG.1. The weight function p(r) calculated with the model of a "point" probe in homogeneous media: water and a soil with three values of moisture. The soil has the composition of the earth's crust - see Table I – with an H content of 1400 mg/kg. The radii of the 95% and 99% influence spheres around the probe are shown.

5. ILLUSTRATION OF SAMPLE VIRTUALLY GAUGED

The region measured by a neutron gauge is often represented as a sphere [14]. A soil hole, surface, etc., however, considerably deforms this picture [13], even for a "point" probe. There have been few attempts to determine a weight function [15] appropriate for the real geometry of measurement, while the subsurface gauge calculations with a finite sphere, in which the probe is in the centre, have been common.

For our basic soil composition with w = 100 kg H_2O/m^3 the slowing-down effect of water below 100 keV represents about 90% of the total slowing-down power. We can rather definitely define the weight function p by considering the number of hydrogen scatterings during the slowing-down of the detected neutrons: we establish that the ratio of the number of these scatterings in a small soil element dV to their total number is given by pdV [14]. In the model of a point source in homogeneous medium we have

$$\int_0^{R_t} p 4\pi r^2 \, dr = t \tag{9}$$

where t = 1 when $R_t = \infty$. The solution R_t of Eq. (9) is the radius of the 100 t% influence sphere in moisture gauging.

The weight function p decreases very rapidly with the distance from the point probe — see Fig. 1. In the calculations, a 3-group diffusion model has been used [14].

In Fig. 1 the radii of the spheres that have an influence of 95% and 99% in the counting rate are presented. For the radius of the 95% region of influence, in the case of a point probe in a Danish soil (composition near that of the earth's crust) which has a hydrogen content 0.326%, we have the formula

$$R_{95\%} = \frac{4.3}{L_1^{-1} + L_2^{-1}} \tag{10}$$

Eq. (10) is based on the observation presented in Ref. [14] concerning the relation between 3-group and 2-group diffusion results. L_1 and L_2 are the slowing-down length and thermal diffusion length, respectively. Their formulae can be found in the references.

6. SIMULATIONS OF GAUGE

The exact theory of a neutron gauge is the transport theory [16]. Its normal form and the combined one [16] can be used. The latter gives the probability of detecting a neutron. Both are needed for exact determination of the weight function — Section 5 and Ref. [14].

We have found such a model to calculate the fitting to any measured data which seem to be useful. The rather poor data that must be used in calibration today are presented in Fig. 2. The data were neasured with the Danish subsurface probe BASC and a Miniscaler in an access iron tube.

In our model we use a point source in an infinite medium and calculate with a 3-group diffusion model. The detector is a sphere at a certain distance from the source and it absorbs all incoming thermal neutrons and part of the epithermal ones. The effect of the detector is taken into account by depressing the fluxes calculated in a homogeneous medium.

As soil parameters in our data we have had to use: (1) moisture, (2) heating loss, and (3) bulk density, but not the absorption of thermal neutrons, although we have made a certain effort with our facilities to measure the absorption cross-section, as has been determined elsewhere, e.g. Ref. [11]. As instrumental fitting parameters we had: (1) distance between source and detector; (2) radius of detector sphere; (3) multiplier for the calculated counting rate; (4) fraction of the detected epithermal neutrons; and (5) an additional constant term (it made fitting better).
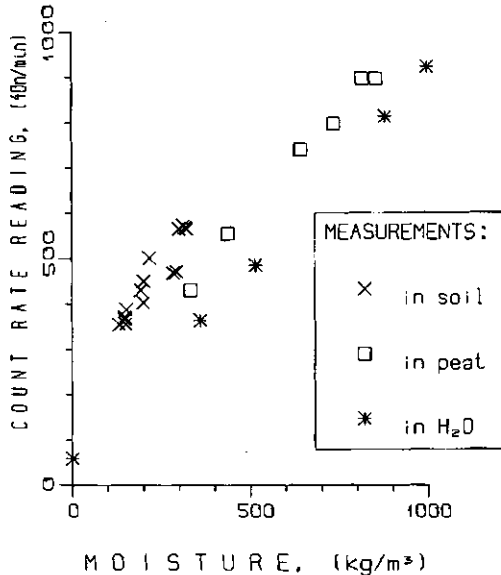
FIG.2.   The present experimental data of subsurface gaugings using an iron access tube. The soil data were measured in the lysimeter of Helsinki university [17], at least 0.5 m below the surface of each soil column.   The dry densities of these sandy soils are about 1500 kg/m³ and they have hydrogen contents from 0.3 to 0.5%.   The samples for weighing were taken 0.5 m from the access tube.   Peat measurements in field (dry density ≃ 73 kg/m³ and ash content ≃ 3%) may have suffered from moisture inhomogeneity. The samples were taken just around the access tube.   In H₂O measurements in ice and snow it required a considerable effort to make the gauge function in the cold.   The zero moisture value was obtained with the probe in air.
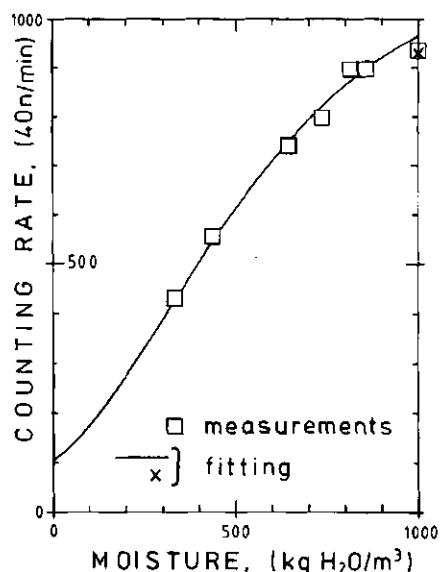
FIG.3.   The optimized calibration to the peat and water data of FIG.2.   The computer model and parameters are described in the text.

A fitting with our model is shown in Fig. 3. For the geometric fitting parameters this gave the value 6.2 cm for the distance between source and detector sphere, and 1.38 cm for the radius of the sphere; these values are in accordance with the probe measurements.

The trivial geometry and incompatible theory need improvements in our simulation. The best experimental data for the calibration can be achieved by making measurements in a laboratory with homogeneous materials which have certain elemental compositions. We prefer to get different "moisture" contents by mixing materials which possibly contain water of crystallization.

The simulation depends considerably on gauge type, and on special features in the soil geometry (surface against air, etc.).

ACKNOWLEDGEMENT

REFERENCES

[1] LINSLAY, R.K., Jr., KOHLER, M.A., PAULUS, J.L.H., Hydrology for Engineers, McGraw-Hill Kogakusha, Ltd., Tokyo (1975) 192.

[2] SEGAL, Y., NOTEA, A., SEGAL, E., "A systematic evaluation of nondestructive testing methods", Research Techniques in Nondestructive Testing (SHARPE, R.S., Ed.) Vol. 3, Academic Press (1977) 293.

[3] ARTSYBASHEV, V.A., Yaderno-Geofizicheskaya Razvedka, Atomizdat, Moscow (1980) 146.

[4] INTERNATIONAL ATOMIC ENERGY AGENCY, Neutron Moisture Gauges, Technical Reports Series No. 112, IAEA, Vienna (1970).

[5] GARDNER, R.P., ELY, R.L., Jr., Radioisotope Measurement Applications in Engineering, Reinhold Publishing Corp., New York (1967) 254.

[6] KASI, S.S.H., Consideration for evaluation and design of radiation gauges, Isotopenpraxis, to be published.

[7] FILIPPOV, E.M., Yadernaja Geofizika, Vols 1 and 2, Izdatelstvo "Nauka", Sibirskoe otdelenie, Novosibirsk (1973). [a] Vol. I, p.173; [b] Vol. II, p. 21.

[8] KASTNER, J., "Effects of soil and water on cosmic ray", Extra-Terrestrial Matter, Northern Illinois Univ. Press (1969) 265.

[9] ØLGAARD, P.L., "Neutron and gamma gauges, their design and application", Radiation Engineering in Academic Curriculum (Proc. Study Group, Haifa, 1973), IAEA, Vienna (1975) 147.

[10] CAMERON, J.F., "Nucleonic soil density and moisture gauges", Nucleonic Techniques and Mineral Resources (Proc. Symp. Buenos Aires, 1968), IAEA, Vienna (1969) 81.

[11] COUCHAT, Ph., et al., "The measurement of thermal neutron constants of the soil;
      Application to the calibration of neutron moisture gauges and to the pedological study
      of soil", Proc. 4th Conf. Nuclear Cross Sections and Technology, CEA-CONF-3167,
      USA, 3–7 March 1975.

[12] KRAUSKOPF, K., Introduction to Geochemistry, McGraw Hill Book Co. (1967) 639.

[13] COUCHAT, Ph., Mesure Neutronique de l'Humidité des Sols, Rep. FRNC-TH-566,
      Toulouse (1974).

[14] KASI, S.S.H., An attempt to calculate correctly the region of influence in gauging moisture
      with neutrons, Int. J. Appl. Radiat. Isot. 33 8 (1982) 667.

[15] FEARON, R.E., Neutron well logging, Nucleonics 4 6 (1949) 32.

[16] BELL, G.I., GLASSTONE, S., Nuclear Reactor Theory, New York (1970).

[17] VAKKILAINEN, P., Maa-alueelta Tapahtuvan Haihdunnan Arvioinnista, Acta Univ.
      Oul. C 20.1981, Oulu (1982) 24.

[18] VIRKKUNEN, J., A Cyclic Coordinate Ascent Algorithm in Linearly Constrained
      Nonlinear Optimization, Rep.-HTKK-MAT-A57, Espoo (1974).

TWO NEW DESIGNS OF TWO-SOURCE SOIL-MOISTURE GAUGES*

G. CHRISTALLER, R. THIES
Laboratory for Nuclear Radiation
    Measurement,
Technische Fachhochschule Berlin,
Berlin (West)

Abstract

TWO NEW DESIGNS OF TWO-SOURCE SOIL SOIL-MOISTURE GAUGES.

This paper discusses how to avoid the well-known disadvantages when measuring soil moisture by the established radiometric method. These disadvantages are: (1) To get absolute values of moisture it is mandatory to know the bulk density; (2) The detectors used have a strong temperature sensitivity; (3) Use of multi-point cables, especially for bore-hole probes, may produce problems with respect to water-tightness; (4) Interpretation of data by using calibration curves based on laboratory measurements does not allow adjustments during field measurements. To eliminate, or to compensate for, these disadvantages the following special features are introduced. (1) The use of two radiation sources — gamma + neutron or gamma + gamma; (2) Using on-line gain control in a closed-loop configuration; (3) Using only one coaxial cable for both signal and power supply; and (4) Using a CMOS-based intelligence data logger. This preliminary data show how this works (CMOS = complementary metal-oxide silicon).

INTRODUCTION

Numerous publications deal with applications of radiometric methods for soil-moisture measurements, so only a selection can be referred to [1--3]. These publications contain descriptions of methods, including theoretical background, experimental results, discussion of calibration and the influence of different parameters on accuracy. One of the main problems is the variability of bulk density by swelling or shrinking with the absorbed water. This can be dealt with by using two sources, either a neutron and a gamma source or two gamma sources with different main photon energies [4, 5]. A most efficient detector for both neutron and gamma detection is reported to be the scintillation counter [6]. But, besides its excellent detection efficiency, much less is reported on its main disadvantage, i.e. the strong temperature dependence of its output pulse-height per unit energy.

Our main design goals were fourfold:

(1) The use of a two-source technique: To measure the volume moisture in a
     bore-hole we planned to use an Am-Be neutron source combined with a
     ^{137}Cs gamma source. To measure the subsurface fast-changing moisture
     after irrigation we planned to use an ^{241}Am or a ^{57}Co gamma source and
     a ^{137}Cs gamma source.
(2) To introduce some modularity in the mechanical and electronic design
     for higher flexibility.
(3) The use of an on-line gain stabilization method which we designed for
     radiometric measurements in industrial environments (steel or aluminium
     mills) and which we have proved to work satisfactorily [7].
(4) To introduce an intelligent battery-operated data logger. It should have the
     possibility of changing the fitting parameters in the field [8, 9].

The theoretical background and the mathematical treatment of the neutron
slowing-down process, and the gamma absorption and scattering process, are
described in detail in many publications [2–5, 10–13], so I shall not repeat
this. Only for the new two-source subsurface probe is some mention made in
Appendix 1.

The designs are not complete, so in some respects descriptions and data
given are preliminary and subject to change.

1.   THE NEUTRON GAMMA PROBE

At first sight (Fig. 1) this probe seems to be conventional in design: an
Am-Be neutron source, ^{137}Cs gamma source, scintillation detector with ^{6}Li
enriched lithium glass scintillator. But on examining the details several un-
common features appear (Fig. 2).

1.1. Mechanical part

There is only one coaxial cable connector, and a Lemo-type-1 water-tight
plug and socket, which is used to transfer the signal from the probe to the data
logger and to carry the supply current at a voltage of 12 V DC from the data logger
to the probe. In the probe, whose diameter is given by the scintillation counter
(35 mm outer dia.), are a DC/DC converter generating the high voltage and a
DC/DC converter generating a negative voltage of 10 V which is used in the pre-
amplifiers and stabilization circuit.

The probe itself is divided into three compartments, the first of which houses
the summing and cable-driving amplifiers and the negative voltage generator. The
second compartment contains the high-voltage generator, the stabilizing circuitry,
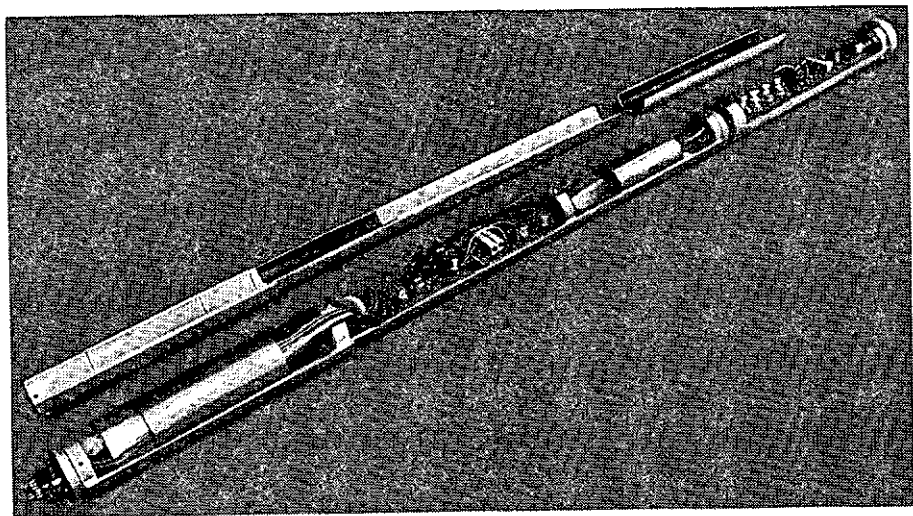
FIG.1. n-γ probe: general view.
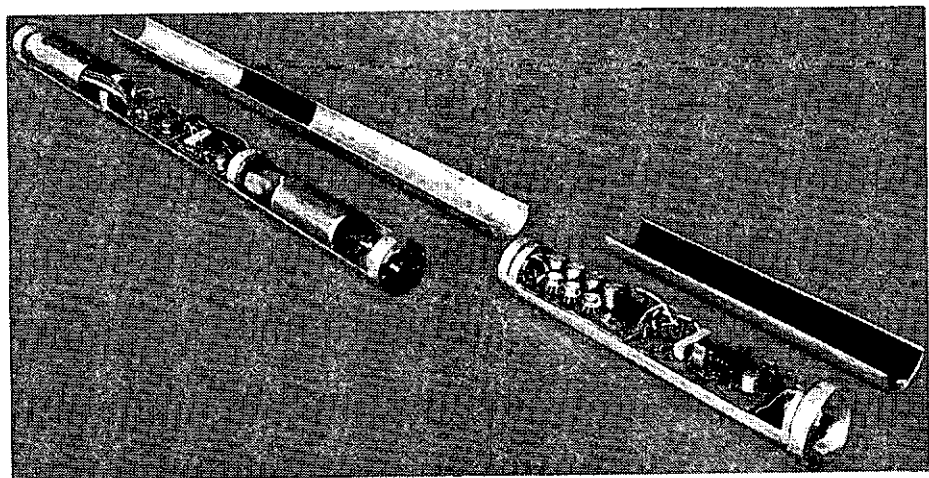
FIG.2. n-γ probe: two modules.

the charge-sensitive preamplifier and the scintillation detector. The third — not shown — contains the source, which will be either a neutron or a gamma source. Should both be used two source compartments will be plugged together. Even if another detector is required, e.g. a special gamma detector with a NaI, a $Bi_4Ge_3O_{12}$, or a NE 142 Pb-doped plastic scintillator [7], this can be used instead of the lithium glass detector, or in addition. The connector between the compartments is a rugged high-quality one. The ready assembled probe is then pushed into a water-tight tube which is fitted by an O-ring in the top flange carrying the Lemo plug.

1.2. Electronic part

As already mentioned the detector is a scintillation counter which can be equipped with different scintillators. The high-voltage supply is a DC/DC converter whose output voltage is proportional to its input voltage[1]. This makes it possible to control the gain of the photomultiplier tube by a referenced control circuit. In this manner the pulse-height shifts due to temperature-dependent gain shifts in the PM tube and temperature-dependent changes in light collection efficiencies will be reduced by a factor of 1/20 to 1/50. The reference in this case is an aged light-emitting diode (LED) in a circuit similar to that mentioned in Ref. [14]. The continuous light output of the LED leads to a continuous current of the PM output which is detected and amplified by an operational amplifier whose output controls the input of the high-voltage generator.

The charge-sensitive preamplifier is a very conventional and simple one using a fast integrated-circuit operational amplifier.

2.   THE GAMMA-GAMMA PROBE

This probe was designed with no prior example. It should be used to study subsurface water transport after irrigation. This work will be done at the Institut für physische Geographie und Landschaftsökologie, Technische Universität Braunschweig. To resolve the water transport in different subsurface layers the probe is equipped with four measuring channels (Fig.3). Each is fitted with a collimated ^{241}Am or a ^{57}Co gamma source and a small gamma detector housed in another box. The collimation is such that the irradiated area at the detector side at a distance of ~20 cm will be 1 cm^2 or less. In these channels the measuring is done via the absorption of the primary gamma beam. Because of the change of the bulk density it is necessary to use a second gamma source (^{137}Cs), the

---

[1]   Erie-Murata type 15 PPA 15

1   ^{241}A-source
2   ^{137}C-source
3   Scintillation counter
4   High voltage supply
5   Preamplifier
6   Stabilizer circuits

FIG.3.   Two-source/four-level soil-moisture probe.
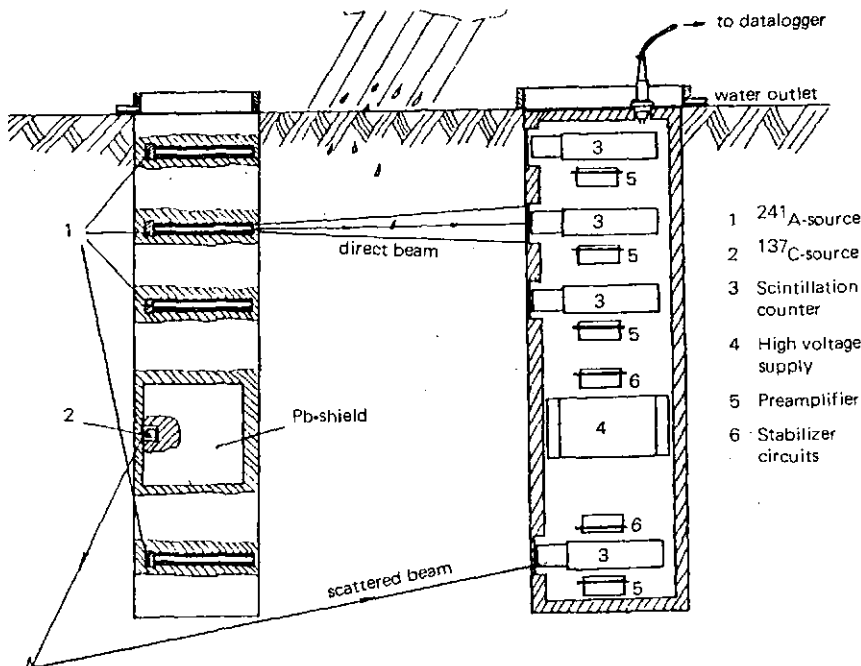
radiation of which is detected after having undergone Compton scattering. The direct path between this single source and the four detectors is blocked by lead screening.

2.1. Mechanical part

The probe consists of two rectangular boxes which will be installed opposite each other in the subsurface area. For proper alignment the two boxes can be screwed to a common handle. The tops of the boxes are built as little circular pans with a water outlet nozzle at the bottom for connecting a PVC hose.

One box contains four ^{241}Am sources or, for expanding the source-detector distance, four ^{57}Co sources with a source strength of $10-100$ mCi ($0.37 -3.7$ GBq). In addition, this box contains the ^{137}Cs source in a Pb slab.

The other box, which is somewhat larger, contains the four gamma detectors with the associated preamplifiers, and a high-voltage power supply, again with a stabilizing circuitry. Both boxes can be seen in Figs 4 and 5.
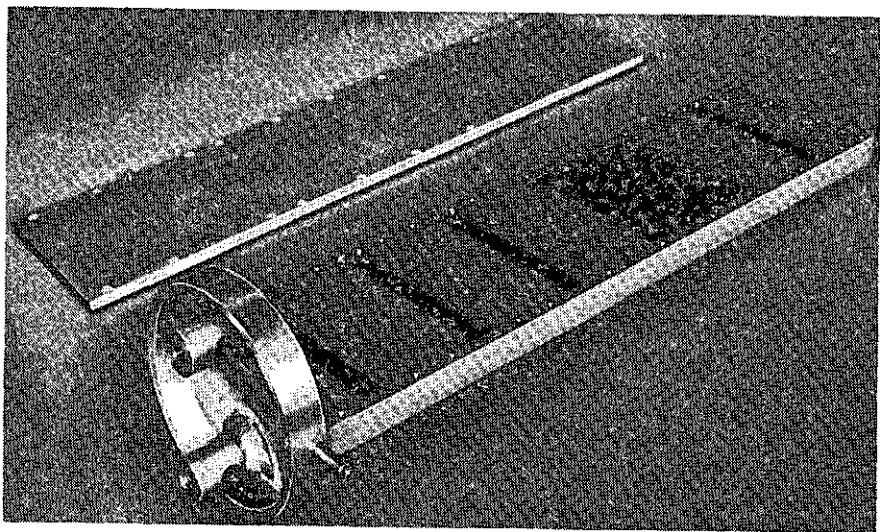
FIG.4. γ-γ probe: source container.
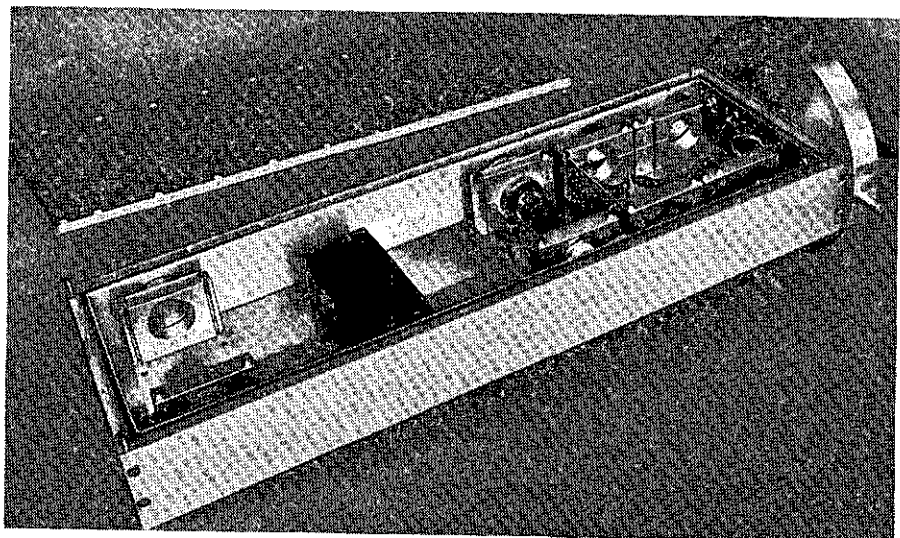
FIG.5. γ-γ probe: detector container.

2.2. Electronic part

NaI as a scintillator will only be used for the prototype. For measuring in the field we plan to use either $Bi_4Ge_3O_{12}$ or the Pb-doped plastic scintillator NE-142[2], because NaI will not withstand temperature shocks which can easily happen in the subsurface range. The photomultiplier tube is a small 6-dynode type. The preamplifier is the same as for the bore-hole probe. We use a single high-voltage generator for all four detectors, with a voltage-sensitive control input for setting and controlling the high voltage. But the control mechanism will be different from that used in the aforementioned probe, because the LED will produce too high a noise level in the 60-keV region (^{241}Am). There we shall use the ^{241}Am photopeak itself as a reference. This method is described in more detail in Ref. [7].

3.   THE DATA LOGGER

The data logger is based on a commercially available system[3] for which we have designed many attachments. The data logger uses CMOS[4] independent circuits wherever possible. It can be equipped with two different central processor unit (CPU) cards, one based on the NSC-800 microprocessor, the other on the MC-146805 microprocessor [9]. The cards are standard Eurocards with a standard DIN plug in a standard crate, 19 in. wide or smaller. The system is bus-oriented so additional cards can be supplied very easily. The data logger can be either powered from a main supply or from a 12-V battery.

The data logger may be equipped with different cards according to application requirements. For radiometric measurements these cards are linear amplifier with gain and time constant settings, differential discriminators for distinguishing different pulse heights resulting from energies released in the detector, scaler-timers to determine the count rate, and a liquid crystal display in connection with a user-operated keyboard.

For an intelligent data logger the software package is most important. The basis is an operating system [8] which is modular and extremely user-oriented. It guides the user through the initial phase, asking for operating modes, detectors, scaling factors, measuring time, and certain constants and parameters used for the moisture and density calculation (see Appendix 1). Because of the modular design it is very easy to expand or to change the operating system, or to incorporate special user programs.

---

[2] Nuclear Enterprises, Sighthill, Edinburgh, UK.

[3] ELSA GmbH, Heketweg 20, D-5190 Stolberg.

[4] CMOS = complementary metal-oxide silicon.

There is also a laboratory version of this data logger available, which is equipped with a double floppy disc and runs with the widely used CP/M^5 operating system.

4.   CONCLUSIONS

The main parts of the two probes described, the data logger with its hard- and software, are now designed and assembled, and the first laboratory-based measurements are in progress for testing and calibrating. The first field experience and measuring results will be reported elsewhere.

APPENDIX 1

To limit the number of calculations to be done by a special program, the complex dependencies in interpreting and combining the readings of a two-source probe have to be treated mathematically with the aim of incorporating that program in the data logger. Many publications deal with the calibration of a n-γ probe [2—5] but only a few deal with a two-γ probe [3]. We want to use the two-γ sources simultaneously, the one with the lower energy (^{241}Am) in the absorption mode, the other with the higher energy (^{137}Cs) in the scattering mode. Below is a brief representation of the mathematical treatment.

1.   Absorption method (Index 1)

The general absorption law reads

$$I_1 = I_{10} \cdot B \cdot \exp(-\mu_1' \cdot \rho \cdot 1) \tag{1}$$

I_1, I_{10} = the radiation intensities in the detector with and without absorber

B = Build-up factor — can be neglected for proper collimation and pulse-height discrimination

μ_1', ρ = the mass absorption coefficient and the overall density

1 = distance source-detector

If, with index s we denote the dry soil, with index m the moist soil, and with index w the water, Eq. (1) can be rewritten as follows:

$$I_{1m} = I_{10} \cdot \exp(-\mu_{1s}' \cdot \rho_s \cdot 1) \cdot \exp(-u \cdot \mu_{1w}' \cdot \rho_w \cdot 1) \tag{2}$$

u = m_w/m_s = water content

---

[5] CP/M is a registered trade mark of **Digital Research**.

For the reference medium, e.g. the dry soil, Eq. (2) reads

$$l_{1s} \qquad = I_{10} \cdot \exp(-\mu'_{1s} \cdot \rho_s \cdot 1) \qquad\qquad (3)$$

Dividing Eq. (2) by (1) gives

$$I_{1m}/I_{1s} \qquad = \exp(-u \cdot \mu'_{1w} \cdot \rho_w \cdot 1)$$

Rewriting for u reads

$$u \qquad = (1/k_1) \cdot \ln(I_{1s}/I_{1m}) \qquad\qquad (4)$$
$$k_1 \qquad = \mu'_{1w} \cdot \rho_w \cdot 1$$

Equation (4) is only valid if ρ_s is constant over the whole moisture range. If this is not true, Eq. (4) has to be written as

$$u \qquad = (1/k_1) \cdot [\ln(I_{1s}/I_{1m}) - k'_1 \cdot \Delta\rho_s] \qquad\qquad (5)$$
$$k'_1 \qquad = \mu'_{1s} \cdot 1$$
$$\Delta\rho_s \qquad = \rho'_s - \rho_s = \text{difference of bulk density}$$

Because $\Delta\rho_s$ cannot be determined with just one measurement, a second independent measurement is needed — in this application a measurement of the scattered γ-ray of a ^{137}Cs source.

2. Scattering method (Index 2)

The equivalent general equation for scattered γ-rays reads

$$I_2 \qquad = I_{20} \cdot P \qquad\qquad (6)$$

with P   = integral probability of detection of a scattered γ-quantum [10]
$$= \int P_1 \cdot P_2 \cdot P_3 \cdot P_4$$

P_1 $= (1/4\pi r^2) \exp(-\mu'_p \cdot \rho_m \cdot r) \cdot r^2 \cos\theta \, d\theta \, d\phi$
        = probability of a γ-quantum reaching the volume element
          $dV = r^2 \cos\theta \, d\theta \, d\phi$

with θ = angle between symmetry axis and direction of γ-quantum
ϕ = azimuthal angle
μ'_p = mass-absorption coefficient for primary γ-energy
r   = distance from source to dV
ρ_m = density of moist soil = $\rho_s + \Delta\rho_s + u \cdot \rho_w$

P_2 $= [(Z \cdot N_A \cdot \rho_m)/A] \cdot (d\sigma/d\Omega) \cdot dr$
        = probability of γ-quantum scattering in dV

with Z   = nuclear charge number
    A   = nuclear mass number
    N_A = Avogadro's number
    $d\sigma/d\Omega$ = differential cross-section with Klein-Nishina formula

    P_3 = $\exp(-\mu'_{sc} \cdot \rho_m \cdot t)$
              = probability of a scattered γ-quantum reaching the detector
with μ'_{sc} = mass-absorption coefficient for scattered γ-energy
    t   = distance from dV to detector

    P_4 = $\exp(-\mu_d \cdot d)$
              = probability that a γ-quantum reaching the detector produces
                 a countable event (detection efficiency)
with μ_d = linear attenuation coefficient for the detector material used
    d   = linear geometrical value of the detector (a combination of
                 diameter and thickness)

To solve Eq. (6) one has to integrate over the entire volume and energy. This can only be done by using complicated mathematical methods like Monte Carlo calculations (see, e.g. Ref. [4]). But, by making some simplifying assumptions, e.g. reading P_4 as a device constant and putting all the integrating in a parameterized constant K_2, we can write Eq. (6) as

$$I_{2m} \qquad = I_{20}(Z/A)_m \cdot \rho_m \cdot K_2 \tag{7}$$

and for a reference measurement in dry soil

$$I_{2s} \qquad = I_{20}(Z/A)_s \cdot \rho_s \cdot K_2 \tag{8}$$

Dividing Eqs (7) by (8) and re-ordering reads

$$\rho_m \qquad = \rho_s + \Delta\rho_s + u \cdot \rho_w$$
$$= [(Z/A)_s \cdot \rho_s/(Z/A_m)] \cdot (I_{2m}/I_{2s}) \tag{9}$$
$$= K'_2$$
$$\Delta\rho_s \qquad = K'_2 - (\rho_s + u \cdot \rho_w) \tag{10}$$

So the recommended procedure is as follows:

(1) From Eq. (4) a preliminary u' is calculated;
(2) With this u' a $(Z/A)_m$ is read from a table;
(3) With this $(Z/A)_m$ with $(Z/A)_s = 0.499$ and with user-submitted ρ_s, K'_2 is calculated and $\Delta\rho_s$ determined from Eq. (10);
(4) The final u is calculated from Eq. (5).

ACKNOWLEDGEMENTS

REFERENCES

[1] BERLINER, M.A., Feuchtemessung (German edition), VEB-Verlag, Technik, Berlin
(West) (1980).

[2] CAMERON, J.F. (Ed.), Neutron Moisture Gauges, Tech. Reps Series No. 112, IAEA,
Vienna (1970).

[3] INTERNATIONAL ATOMIC ENERGY AGENCY, Isotope and Radiation Techniques
in Soil Physics and Irrigation Studies – I. (Proc. Symp. Istanbul, 1967), IAEA, Vienna
(1967); and II. (Proc. Symp. Vienna, 1973), IAEA, Vienna (1974).

[4] CHRISTENSEN, E.R., "Use of the gamma density gauge in combination with the neutron
moisture probe" ibid. II., pp. 27–44.

[5] GARDNER, W.H., CALISSENDORFF, C., "Gamma-ray and neutron attenuation in
measurement of soil bulk density and water content", ibid I., pp. 101–13.

[6] JENSEN, P.A., SOMER, E., "Scintillation techniques in soil-moisture and density measure-
ments", ibid. I., pp. 31–48.

[7] CHRISTALLER, G., "Application of fast detectors and fast electronics in connection with
microcomputers on radiometric measurements", in Proc. 10th World Conf. Non-Destructive
Testing, Vol. 6, Moscow (1982) 62.

[8] WAECKEN, H., WOITZIK, P., "Entwicklung eines Echtzeit-Betriebssystems für einen
NSC-800 Rechner", Dipl.-Arbeit, TFH Berlin (West) (1983).

[9] BRACHAT, P., SOERRIES, M., "CMOS-Mikrocomputer", Dipl.-Arbeit, TFH Berlin
(West) (1983).

[10] SEDA, J., STRACHOTA, J., CECHAK, Th., KLUSOW, J., Nucl. Instrum. Methods 144
(1977) 557.

[11] KING, L.G., "Gamma-ray attenuation for soil-water-content measurements using ^{241}Am ",
Isotope and Radiation Techniques in Soil Physics and Irrigation Studies (Proc. Symp. Vienna,
1967), IAEA, Vienna (1967) 17–29.

[12] GRODSTEIN, G.W., X-ray attenuation coefficients from 10 keV to 100 MeV, NBS
Circular 583 (1957).

[13] BECKURTS, K.H., WIRTZ, K., Neutron Physics, Springer, Berlin (West) (1964).

[14] FRASER, H.J., Nucl. Instrum. Methods 136 (1976) 513.

SOIL-DENSITY AND MOISTURE-CONTENT DISTRIBUTION FUNCTIONS STUDIED BY MEANS OF 60 keV AND 660 keV GAMMA RADIATION AND NEUTRONS

H. BAUMBACH
Technical University, Leipzig

M. FRENZEL, J.W. LEONHARDT, M. BAER
Central Institute of Isotope and
    Radiation Research, Leipzig

German Democratic Republic

Abstract

SOIL-DENSITY AND MOISTURE-CONTENT DISTRIBUTION FUNCTIONS STUDIED
BY MEANS OF 60 keV AND 660 keV GAMMA RADIATION AND NEUTRONS.
    The density and moisture distributions of turf-earth, calcareous earth and clay soil
were studied by means of gamma transmission experiments and neutron moderation. The
mass attenuation coefficients of the soils studied are 0.32, 0.38 and 0.29 cm^2/g respectively,
and the densities 0.76, 0.73 and 100 g/cm^3. H_2O migration could also be studied as H_2O
depth profiles. The studies aimed at clarifying the potential of nuclear techniques in
producing data for relevant parameters in soil sciences.

1. DETERMINATION OF THE MEAN MASS ATTENUATION COEFFICIENTS AND THE MEAN DENSITIES OF VARIOUS TYPES OF SOIL BY 60 keV and 660 keV γ-RADIATION

Experimental

The experimental arrangement used is schematically given in Fig.1. The
γ-ray sources used were 11 GBq ^{241}Am and 0.15 GBq ^{137}Cs, sensitive for mass
attenuation coefficient (μ^{60}) and density (ρ), respectively. The transmission
measurements were carried out by a 3-mm narrow γ-beam. Earth samples were
filled into a flat box with parallel walls. The attemuation of the γ-radiation
within a 3.3-cm thick earth layer was determined at 60 different points. This
procedure was repeated five times with each sample. From the measured count
rates the count-rate frequency distribution was obtained. This distribution is
an infinitely compound Poisson distribution [1]. From the parameters of this
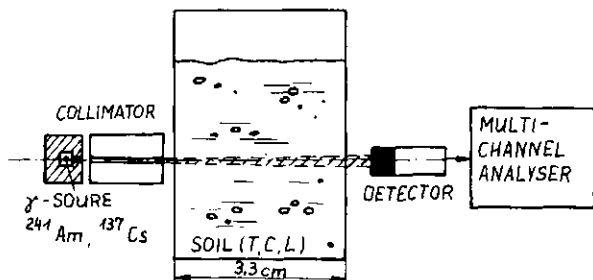
FIG.1.   Scheme of the experimental arrangement for the μ and ρ·x determination.
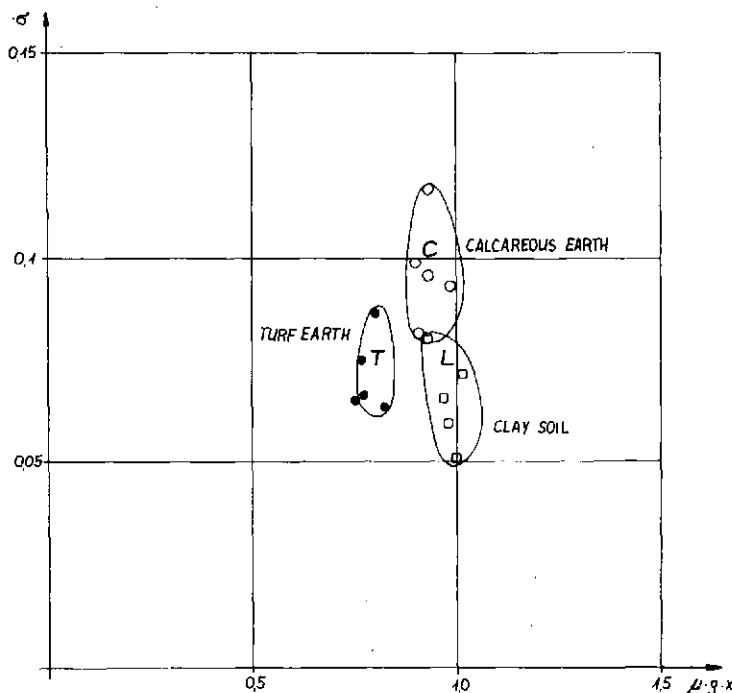
FIG.2.   Standard deviations σ of turf earth ●, calcareous earth ○, and clay soil □ on μ·ρ·x determined by 60 keV γ-radiation.   T,C,L: Mean values of all points measured.   T = turf; C = calcareous earth;   L = clay soil.
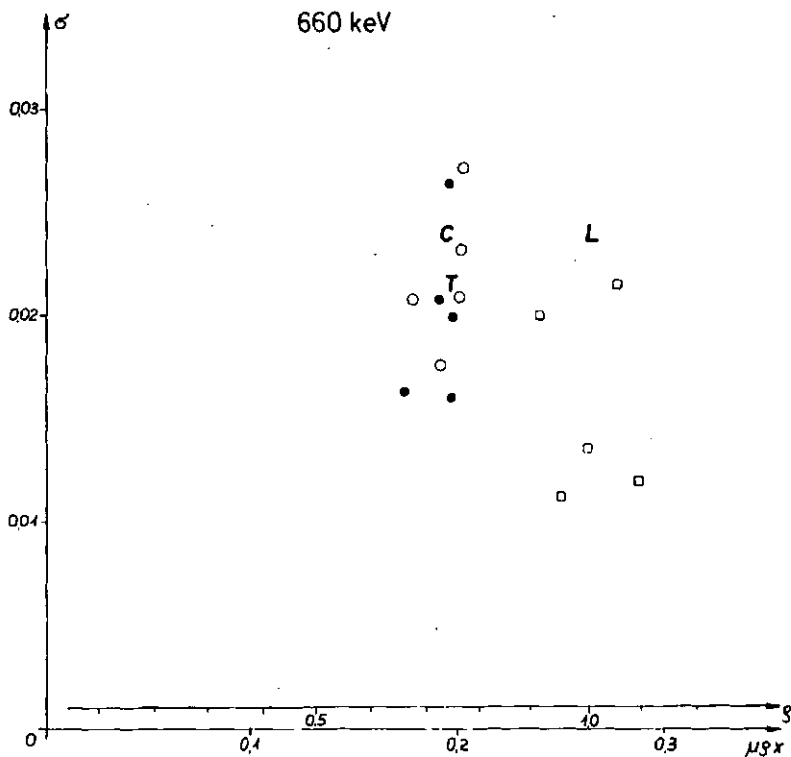
FIG.3.   Standard deviations σ of T, C, and L soils on ρ·x determined by 660 keV
γ-radiation. ●, ○, ◻: Mean values of σ for 60-point measurements for T, C, L.
T, C, L: Mean values of σ for all measuring points for T, C, L.

distribution the mean value of the product $\mu\rho x$ and the standard deviation σ
were determined for each of the five 60-point measurements and also for the
five measurements together. These σ values reflect the inhomogenities of
each kind of soil sample.

Results and discussion

In Fig.2 the mean standard deviation σ is plotted versus $\mu^{60} \cdot \rho \cdot x$ for
60 keV γ-radiation. Using the determined values of $\mu^{660} \cdot \rho \cdot x$ by means of
660 keV γ-rays ($\mu^{660} = 0.08$ cm^2/g) the following mass attenuation coefficients
were determined:

Turf earth (T) 0.32 ± 0.05 cm^2/g
Calcareous earth (C) 0.38 ± 0.05 cm^2/g
Clay soil (L) 0.29 ± 0.05 cm^2/g

Despite any fluctuations in their densities the soil samples used can be distinguished by means of their μ^{60} values. Figure 3 (660 keV) shows the σ values versus the product $\mu^{660} \cdot \rho \cdot x$. In this case the values of turf earth and calcareous earth overlap. These samples cannot be distinguished by means of radiometric density-determination.

Turf earth (T) 0.76 ± 0.10 g/cm^3
Calcareous earth (C) 0.73 ± 0.10 g/cm^3
Clay soil (L) 1.00 ± 0.10 g/cm^3

2. WATER MIGRATION STUDY IN SOIL BY MEANS OF NEUTRON TRANSMISSION MEASUREMENTS

Experimental

The experimental arrangement used is given in Fig.4. Four ^{252}Cf sources with neutron fluxes of 10^6, 0.9×10^6, 0.9×10^6, 0.9×10^6 neutrons/s were used. BF detectors count the thermal neutrons slowed down by incoming water. A simple Fe reflector was used to improve the counting statistic. Neutron counters were installed at soil depths of 2, 12, 22 and 32 cm below the soil surface.

Results and discussion

The changes in H_2O content of soil according to time after irrigation are given in Fig.5 for four positions due to the soil depth profile. The curves for position 1 (2 cm) and position 2 (12 cm) show clear maximums before some stationary values are reached. The reason for this effect is the relatively high amount of water passing the upper horizons at first. The stationary values at 22 cm and 32 cm depths are reached after 10 and 14 minutes, respectively.

By analysing the stationary moisture contents in arbitrary units of all points measured, some moisture depth profiles in turf earth can be evaluated. The rising fronts of the curves may be used for some information about migration speeds.
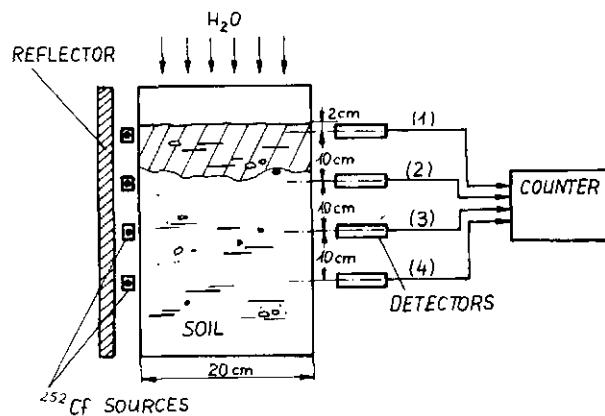
FIG.4. Scheme of the experimental arrangement used for H_2O determination by neutrons.
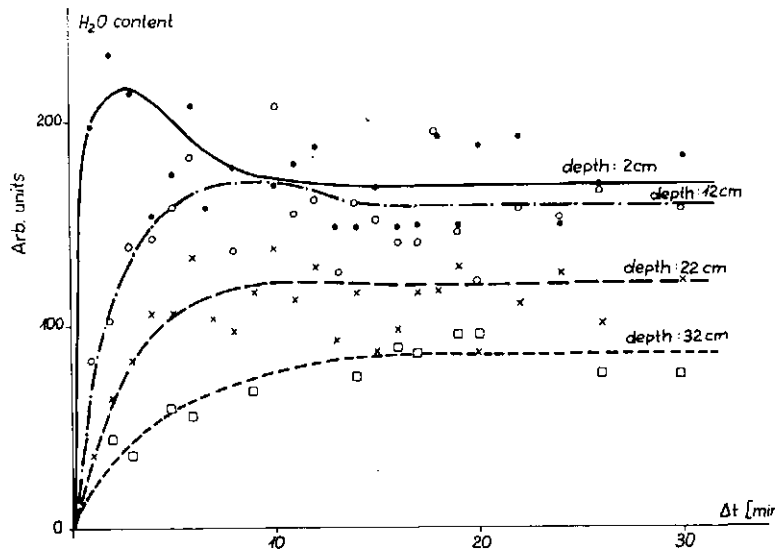
FIG.5. Water content in dependence on the time difference to the start of irrigation at different soil depths.
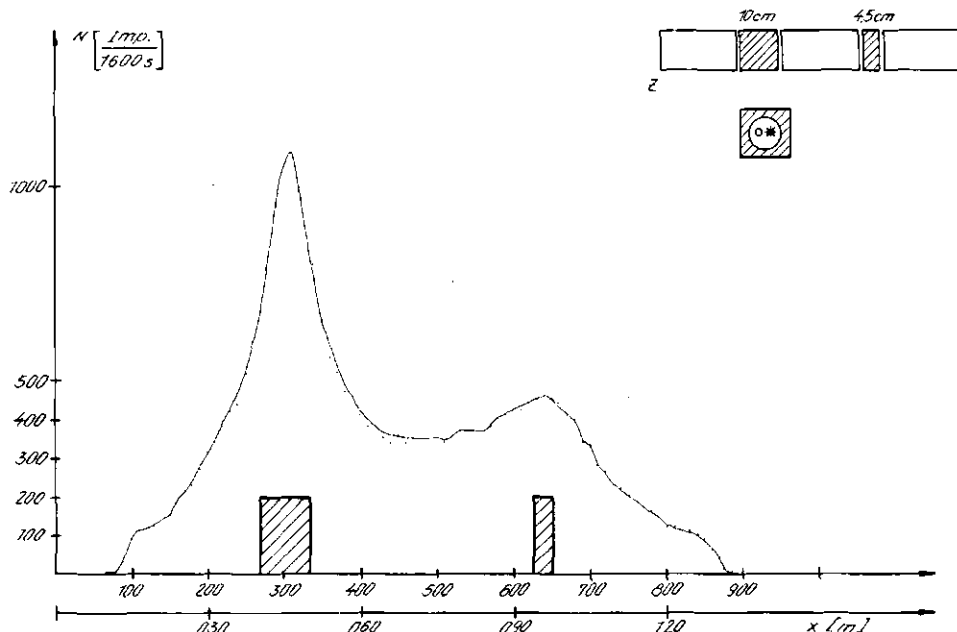
FIG.6. Water content distribution in soil measured by a position-sensitive neutron counter arrangement.

3. MOISTURE DISTRIBUTION DETERMINATION IN SOIL BY MEANS OF A POSITION-SENSITIVE NEUTRON COUNTER

The principle of the position-sensitive counter has been known since at least 1966 [2]. There are arrangements for determining the two-dimensional radiation flux distribution [3, 4]. In a position-sensitive counter the electron pulse will be conducted to both ends of the counter. The relation between the amplitudes on both ends include information about the co-ordinates of the incoming neutron:

$$U(x) = \frac{U_1}{U_1 + U_2} = \frac{1 + (1 - x) \cdot \rho/R_A}{2 + 1\,\rho/R_A}$$

U   is the pulse height (V); index 1 on the left side and index 2 on the right side of the wire ends;

x   the co-ordinate from the left end (cm);

l   the length of the wire inside the counter;

ρ the specific resistance (Ω/cm) of the counter wire (10–50 Ω/cm);

R_A the working resistor (Ω).

Experimental

A ^{3}He-filled neutron counter (NEM 525 M, ZDAU IBJ, Warsaw) was used to determine neutron fluxes along x. A linear Pu-Be neutron source (5×10^7 ns) moving pneumatically in the tube was installed. CAMAC modules and a multi-channel analyser NTA 1024 were used.

Results and discussion

Figure 6 shows the moisture distribution in soil of more than one metre distance measured by the means described above with a position-sensitive neutron counter and a linear neutron source. The moisture content at the maximum was 0.30 g/cm^3, and the thickness of the water-enriched layer was both 10 and 4.5 cm.

This arrangement has the following advantages:

(1) The local resolution power is better if position-sensitive counters are used (mm range);
(2) The interpretation of the results is improved by using a linear neutron source if the modulation transfer function of the arrangement is known;
(3) It will be possible to measure short time changes in the moisture content for dynamic studies.

REFERENCES

[1] GREENWOOD, M., YULE, G.U., J. R. Statist. Soc. **83** (1920) 255.
[2] KUHLMANN, W.R., LAUTERJUNG, K.W., SCHIMMER, B., LISTEMICH, K., Nucl. Instrum. Methods **40** (1966) 118–20.
[3] TURES, A., ZIEMIURSKI, A., Nucl. Instrum. Methods **44** (1966) 119–22.
[4] ABEND, K., SCHMATZ, W., SCHELTEN, J., MÜLLER, K.D., Nuclear Instrum. Methods **83** (1970) 111–14.

Mémoire présenté sur invitation

LES APPLICATIONS
DE LA METHODE NEUTRONIQUE
DANS LA RECHERCHE AGRONOMIQUE

Ph. COUCHAT
Département de biologie,
CEA, Centre d'études nucléaires de Cadarache,
Saint-Paul-lez-Durance, France

Abstract–Résumé

APPLICATIONS OF NEUTRON METHODS IN AGRONOMIC RESEARCH.
      Calculation of soil-water content from neutron moisture gauge measurements requires
that the instrument's calibration curve should be known. This curve represents graphically, for
a given site, the relation between the moisture gauge count and the water content averaged over
the soil volume considered for the measurement. The calibration curve depends on the
measuring instrument – the characteristics of its source, its detector and measuring geometry,
especially the diameter of the access tube – and on the type of soil, i.e. its dry bulk density
and chemical composition. The parameters associated with the instrument are taken into
account by comparison with a reference moisture gauge. The influence of the soil's chemical
composition is expressed by its neutron constants, which are determined directly in the
laboratory. The thermal neutron diffusion and absorption constants for the soil can be used to
plot the moisture gauge calibration curve by determining dry bulk density in addition. This
quick method has a wide range of applications, including for mineral and organic soils. Apart
from the moisture gauge, the neutron method has other uses in agronomy – simultaneous
detection of thermal and epithermal neutrons, by which water content can be determined
independently of dry bulk density; measurement of photoneutrons from the γ-n reaction in
deuterated water, so that the later can be used as a tracer in field experiments; and lastly, in-situ
neutron radiography of roots.

LES APPLICATIONS DE LA METHODE NEUTRONIQUE DANS LA RECHERCHE
AGRONOMIQUE.
      Le calcul de la teneur en eau des sols à partir des mesures faites à l'aide d'un humidimètre
à neutrons requiert la connaissance de la courbe d'étalonnage de l'appareil. Cette courbe
représente graphiquement, pour un site donné, la relation entre le comptage fourni par l'humi-
dimètre et la teneur en eau moyennée sur le volume de sol pris en compte par la mesure. La
courbe d'étalonnage de l'humidimètre dépend de l'appareil de mesure à travers les caractéristiques
de sa source, de son détecteur et de sa géométrie de mesure, en particulier le diamètre du tube
d'accès; elle dépend ensuite du type de sol par l'intermédiare de sa densité sèche et de sa
composition chimique. La prise en compte des paramètres liés à l'appareil est réalisée par
comparaison avec un humidimètre de référence. L'influence de la composition chimique du sol
est exprimée par ses constantes neutroniques dont la mesure directe s'effectue en laboratoire.
Les constantes de diffusion et d'absorption par le sol des neutrons thermiques permettent le

calcul de la courbe d'étalonnage de l'humidimètre, moyennant une détermination complémentaire de densité sèche. Cette méthode rapide est applicable à une large gamme incluant les sols minéraux et organiques. Par delà l'humidimètre, la méthode neutronique a d'autres applications en agronomie: détection conjointe des neutrons thermiques et épithermiques qui permet une détermination de la teneur en eau indépendante de la densité sèche; mesure des photoneutrons issus de la réaction γ-n sur l'eau deutérée qui fournit le moyen d'utiliser cette dernière comme traceur dans des expériences sur le terrain; enfin neutronographie des racines en place.

Dans un monde où les pratiques défectueuses, aussi bien pour la culture que pour l'irrigation, peuvent gaspiller une quantité d'eau presque égale à celle qui est utilisée, ... l'humidimètre à neutrons ... semble destiné à prendre un intérêt économique immense.

Etude de base FAO, n° 22, 1970.

INTRODUCTION

La méthode neutronique appliquée à la mesure de l'humidité des sols a connu ses premiers développements il y a près de 40 ans [3]; depuis, elle est l'objet d'une diffusion continue dans le monde auprès du physicien des sols et de l'agronome.

Si le geste qui consiste à introduire une sonde à neutrons dans un tubage préalablement installé dans le sol est relativement simple, l'information fournie par l'humidimètre est, quant à elle, sujette à beaucoup d'interprétations. L'apparente simplicité de la démarche de celui que l'on peut appeler le «neutrono-agronome» masque en réalité la complexité de cette mesure de teneur en eau du sol.

Dans cet article de synthèse qui ne se veut pas exhaustif, nous voudrions aborder quelques uns des aspects de cette complexité, ne serait-ce que pour dissiper les vieux démons qui nous portent vers l'une ou l'autre des deux facilités extrêmes que représentent le rejet pur et simple de la méthode ou son accueil inconditionnel.

Après un bref rappel théorique, nous envisagerons les questions liées à l'humidimètre lui-même, à la géométrie de sa mesure, puis au sol en distinguant densité apparente sèche et nature chimique.

LA THEORIE

La méthode neutronique de mesure de l'humidité des sols est basée sur l'interaction des neutrons émis par une source artificielle de neutrons rapides et des noyaux des éléments présents dans un sol humide, spécialement l'hydrogène de l'eau. Son objet est la mesure de l'humidité volumique H_v (g/cm³), qui est définie comme le produit de l'humidité pondérale H_p (g d'eau/g de sol) par la densité apparente sèche ρ_s (en g/cm³), et qui est exprimée en pourcentage.

L'introduction dans un sol humide d'une source de neutrons rapides crée un flux de neutrons thermiques dont les propriétés dépendent de la source, du sol et de la géométrie du système de mesure. Les sources couramment utilisées sont constituées d'un mélange ^{241}Am-Be; elles émettent des neutrons dont l'énergie s'étend sur plusieurs MeV autour d'une valeur moyenne de 5,5 MeV, et qui proviennent de la réaction suivante:

$$^{4}_{2}\text{He} + ^{9}_{4}\text{Be} \rightarrow ^{12}_{6}\text{c} + ^{1}_{0}\text{n} + 5,71 \text{ MeV}$$
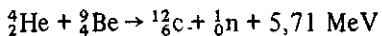
$^{4}_{2}$He représentant le rayonnement alpha issu de l'américium 241.

Par suite de leur interaction avec les noyaux présents dans le sol, ces neutrons occupent tous les niveaux d'énergie: rapides (au-dessus de 1 keV), intermédiaires (de 1 eV à 1 keV), épithermiques (de l'ordre de l'électron-volt) et thermiques (environ 0,0025 eV à 20°C, niveau correspondant à l'énergie d'agitation thermique des molécules du milieu). Quatre principaux types d'interaction prennent alors naissance: la diffusion élastique, qui préside au ralentissement et à la diffusion des neutrons, la capture radiative, responsable de l'absorption des neutrons thermiques et accompagnée d'une émission de photon γ, la diffusion inélastique et, enfin, la capture avec émission de particules chargées qui permet la détection des neutrons de basse énergie par les compteurs proportionnels.

A chacun de ces phénomènes correspond une probabilité d'interaction σ qui a la dimension d'une surface: c'est la section efficace microscopique. Pour un milieu homogène, on définit une section efficace macroscopique par:

$$\sum = \frac{N_o}{M} \rho_\sigma$$

avec Σ cm^{-1}, N_o nombre d'Avogadro, M masse du noyau, ρ densité. Dans un sol humide, Σ devient:

$$\sum = \frac{N_o}{M_{H_2O}} (2\,\sigma_H + \sigma_o)\,H_v + \left(\sum_{i=1,\,n} \frac{N_o}{M_i}\,p_i\,\sigma_i \right) \rho_s \tag{1}$$

où σ_H, σ_o et σ_i sont les sections efficaces microscopiques de l'hydrogène, de l'oxygène et de l'élément i du sol «sec» dont le pourcentage pondéral est p_i, H_v est l'humidité volumique et ρ_s est la densité apparente sèche. La formule de Σ montre que l'interaction neutron-sol dépend de H_v et du sol par ρ_s et sa composition chimique.

La description des flux de neutrons est faite à partir d'une simplification des modèles mathématiques utilisés dans l'analyse des réacteurs nucléaires; pour l'humidimètre, le modèle doit fournir des valeurs relatives de flux et permettre le traitement simple de différentes géométries de mesure et de différents sols. De nombreux auteurs ont présenté des solutions soit analytiques [7, 18, 31, 37], soit numériques [8, 10, 15], soit basées sur l'analyse des processus stochastiques d'interaction [10, 20, 24]. Dans la théorie multigroupe et en coordonnées cylindriques, le flux thermique a pour expression:

$$\phi_2(r, z) = \frac{Q}{4 \pi^2 D_2} \frac{L_2^2}{L_1^2 - L_2^2} \int_{-\infty}^{+\infty} e^{-\eta R} (1 + \eta R)$$

$$\left[\frac{K_0 (\xi_1 r)}{\xi_1 R K_1(\xi_1 r)} - \frac{K_0 (\xi_2 r)}{\xi_2 R K_1 (\xi_2 r)} \right] e^{-i \eta z} d\eta \tag{2}$$

avec Q:force de la source; D_2, L_2 :coefficient et longueur de diffusion thermique; L_1 : longueur de diffusion rapide; $\xi_1 = \sqrt{\eta^2 + \frac{1}{L_1^2}}$; $\xi_2 = \sqrt{\eta^2 + \frac{1}{L_2^2}}$; R:rayon du tubage; K_0 et K_1 :fonctions de Bessel modifiées d'ordre 0 et 1.

Types d'humidimètres à neutrons

Les humidimètres actuellement utilisés se différencient par la nature de la source et du détecteur ainsi que par la géométrie de mesure.

Source

La figure 1 donne les spectres de quelques sources utilisables. Pour une énergie supérieure à 2 MeV, un phénomène de *diffusion inélastique* peut intervenir, entre autres avec le fer. L'incidence de cet effet, que l'on peut prendre en compte par la théorie multigroupe, s'est avérée négligeable sur ces valeurs relatives de comptage, comme l'a mis en évidence la comparaison entre une source Am-Be et une source Sb-Be.

En fait, le passage d'un type de source à l'autre s'effectue par une simple relation linéaire entre les comptages des humidimètres équipés de ces sources. Une
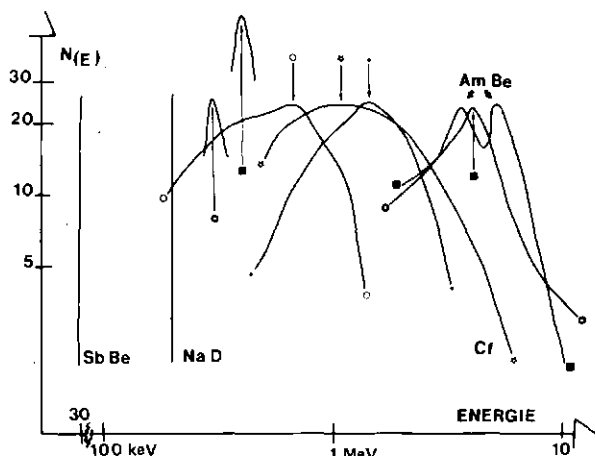
FIG.1. *Spectres des sources artificielles utilisables dans la mesure neutronique de l'humidité des sols. On note trois zones d'énergie possibles: 5 MeV (Am-Be ✪; Ra-Be □), 1 MeV (²⁵²Cf ✫, Am-F ✖), 500-200 keV (Am-Li ◯, Po-Li ◯, Na-D).*

étude comparative des sources ^{241}Am-Be, ^{244}Cm-Be et ^{252}Cf montre par le tableau I [40] l'avantage de ces deux dernières du point de vue de la protection biologique.

Détecteur

Les principaux détecteurs utilisés sont à remplissage de BF_3 ou d'^{3}He. Les détecteurs à ^{3}He, plus sensibles, permettent l'utilisation de sources de faible activité (10 mCi) et sont aptes à la mesure des flux épithermiques; pour chacun, la réponse suit une loi en $1/v$ (v vitesse des neutrons). Les neutrons épithermiques, d'énergie supérieure à 0,8 eV, sont détectés dans une proportion allant de 4 à 8% du flux thermique pour les compteurs en bore et jusqu'à 15% pour les détecteurs à ^{3}He. Les mesures faites sur le terrain [10] montrent que ce rapport dépend très peu du type de sol et que le passage d'un détecteur à l'autre s'effectue par une simple relation linéaire de comptages.

Géométrie de mesure

Les principaux paramètres sont la position de la source vis-à-vis du détecteur et le diamètre du tube utilisé.

Dans les humidimètres, les sources sont disposées soit au milieu du détecteur soit en son embout. Le comptage fourni par l'humidimètre résulte de l'intégration du flux thermique tel qu'il est donné par la formule (2) sur tout le volume utile

TABLEAU I. COMPARAISON DES SOURCES ^{241}Am-Be, ^{244}Cm-Be ET ^{252}Cf

Source, désignation	Américum-béryllium (^{241}Am-Be)	Curium-béryllium (^{244}Cm-Be)	Californium (^{252}Cf)
Type d'enveloppe	SNA 2 (poudre d'Am-Be) Forme annulaire	SNA 2 (poudre de Cm-Be) Forme annulaire	SNA 2 (émail de Cf) Forme annulaire
N° de la source et date de la fabrication	057 5 novembre 1975	400 19 août 1980	422 19 août 1980
Radioactivité [a]	10 mCi ± 10% (3,7 X 10^8 Bq)	10 mCi ± 10% (3,7 X 10^8 Bq)	0,005 mCi ± 10% (18,5 X 10^6 Bq)
Emission neutronique [a]	2,3 X 10^4 N · s^{-1} · μm^{-2} ± 10%	2,2 X 10^4 N · s^{-1} · μm^{-2} ± 10%	3 X 10^4 N · s^{-1} · μm^{-2} ± 10%
Période	433 ans	17,6 ans	2, 64 ans
Débit d'équivalent de dose — au contact, en neutrons [b] — à un mètre, en neutrons — au contact, en gamma [c] — à un mètre, en gamma	2,25 mrem · h^{-1} Inférieur à 0,15 mrem · h^{-1} 8 mrem · h^{-1} 0,2 mrem · h^{-1}	2,25 mrem · h^{-1} Inférieur à 0,15 mrem · h^{-1} 1 mrem · h^{-1} Inférieur à 0,1 mrem · h^{-1}	1,50 mrem · h^{-1} Inférieur à 0,15 mrem · h^{-1} 0,7 mrem · h^{-1} Inférieur à 0,1 mrem · h^{-1}
Energies — émission alpha	(Pour ^{241}Am) Raies à: 5,48 MeV (85%) 5,44 MeV (13%) 5,31 MeV 5,54 MeV	(Pour ^{244}Cm) Raies à: 5,80 MeV (77%) 5,76 MeV (23%)	6,11 MeV (82%) 6,07 MeV (15%)
— émission gamma	Raies à: 0,060 MeV 0,304 MeV 0,033 MeV 0,370 MeV 0,027 MeV	Raies à: 0,043 MeV 0,100 MeV 0,150 MeV	0,043 MeV (15%) 0,100 MeV
Mode d'obtention des neutrons	Réaction (alpha, neutron)	Réaction (alpha, neutron)	Fission spontanée
Zone d'énergies	5 MeV	5 MeV	1 MeV

[a] Données fournies par le fabricant.
[b] Mesuré par le "Neutron Meter" équipé d'une sphère en polyéthylène donnant une réponse en mrem · h^{-1}.
[c] Mesuré par un débitmètre d'exposition à chambre ionisante babyline, donnant un débit d'équivalent de dose dû aux rayons gamma.

du détecteur: soit de 0 à 6 cm de la source (source au centre), soit de 0 à 15 cm (source en embout). On vérifie qu'il existe une relation unique non rigoureusement linéaire entre les comptages des deux types de sonde quel que soit le sol.

La figure 2 montre l'influence du diamètre du tubage sur la droite d'étalonnage de l'humidimètre: le passage de 40 à 50 mm de diamètre se traduit par une diminution de pente de 13% d'humidité, et, à 30% d'humidité, par une diminution de comptage équivalent de 3,5% d'humidité. Il existe cependant une relation linéaire entre les comptages fournis par les humidimètres avec les deux types de tubage et quel que soit le sol.

La règle essentielle de construction d'un humidimètre est celle du maximum de sensibilité vis-à-vis des variations de teneur en eau; il s'y ajoute, bien sûr, le souci d'un minimum de contraintes pour ce qui concerne la protection biologique. Une source annulaire de 10 mCi positionnée en partie médiane du détecteur permet l'usage d'un tubage de faible diamètre et répond à ces deux critères. Le passage
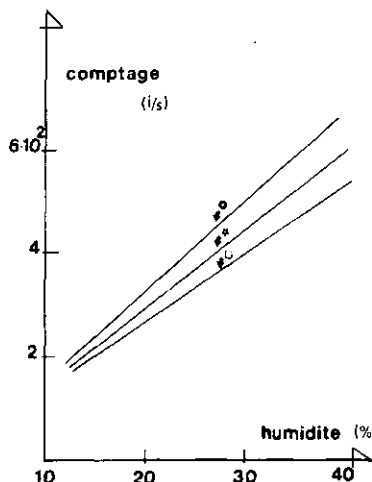
FIG.2. Variation de la courbe d'étalonnage en fonction du diamètre du tube. Comptage en impulsions/seconde (i/s). ●40 mm ✳50 mm ☐60 mm.

d'un appareil à l'autre, d'après ce que nous avons vu, ne nécessite que la construction sur le terrain de la relation de passage unique pour tous les sols, entre les comptages fournis par les deux appareils.

La méthode qui consiste à utiliser une sonde de référence et des standards en absorbants plastiques paraît intéressante [29].

Intervention du type de sol

L'influence du type de sol sur la courbe d'étalonnage est l'objet, depuis plusieurs décennies, de nombreuses recherches. En effet, les premières expériences effectuées en laboratoire ou sur le terrain ont vite montré que la courbe d'étalonnage de l'humidimètre à neutrons dépendait du sol [2, 4, 18]. Ainsi, la plupart des utilisateurs, abandonnant la courbe fournie par le constructeur qui se révèle souvent erronée [34, 35], ont cherché à déterminer eux-mêmes la courbe adéquate. Plusieurs procédures ont vu le jour, les unes étant pratiquées sur le terrain [1, 17, 42, 43, 44], d'autres étant réalisées en laboratoire dans des fûts [21, 22, 38] et certaines s'appuyant sur ces deux voies [10,,12].

Toutes ces approches confirment l'intervention du sol de façon significative sur la réponse de l'humidimètre; cette intervention passe par la densité apparente sèche (quantité volumique de noyaux présents dans le sol) et la composition chimique (nature des noyaux). Cependant, aucune méthode d'étalonnage ne paraît actuellement avoir permis une harmonisation des résultats et des procédures.
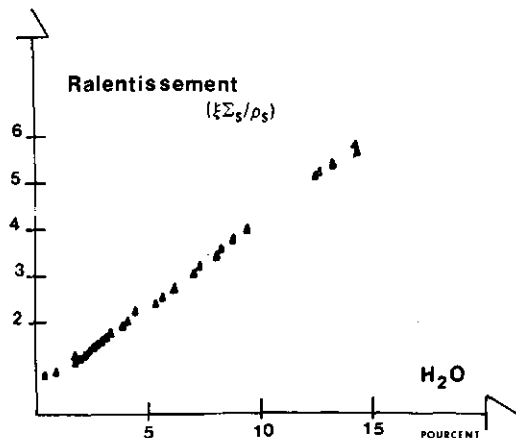
FIG.3.   *Evolution du ralentissement ($\xi\Sigma_s/\rho_s$), en fonction de la teneur en eau de constitution.*
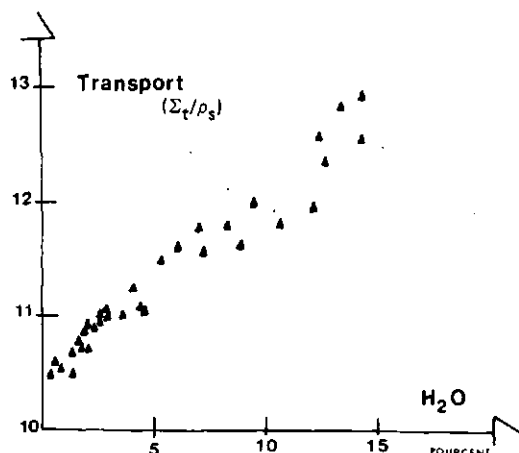
FIG.4.   *Evolution du transport (Σ_t/ρ_s) en fonction de la teneur en eau de constitution.*

La formule (1) distingue l'intervention du sol par sa densité sèche et sa composition chimique. Le sol est envisagé en tant qu'il est séché à l'étuve à 105°C pendant 24 h. On considère séparément une partie appelée eau de constitution et obtenue par calcination à 1000°C pendant 1 h au plus en présence d'argon.

Les termes de la formule qui exprime l'incidence du sol sur la section efficace macroscopique d'interaction des neutrons s'écrivent alors:
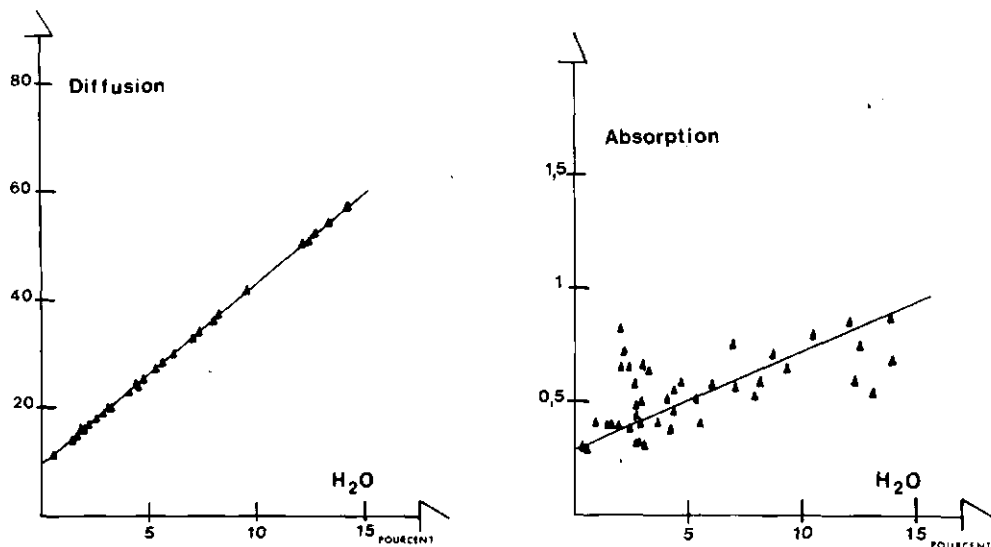
FIGS. 5 et 6. Evolution de la diffusion totale (Σ_s/ρ_s) et de l'absorption totale (Σ_a/ρ_s) d'un sol, exprimées en $mm^2 \cdot g^{-1}$, en fonction de la teneur en eau de constitution.

$$\Sigma_s = \left[\frac{N_o}{M_{H_2O}} (2\,\sigma_H + \sigma_o)\,\rho_{H_2O} + \sum_{i=1,\,n} \left(\frac{N_o}{M_i} \rho_i\,\sigma_i\right) \right] \rho_s \qquad (3)$$

ρ_{H_2O} étant le pourcentage pondéral d'eau de constitution, et ρ_1 le pourcentage pondéral de chaque élément du sol.

A partir de la formule (3), nous avons calculé, pour une quarantaine de sols différents, les valeurs des sections efficaces (en $mm^2 \cdot g^{-1}$, soit Σ/ρ_s) des sols secs relatives aux processus de ralentissement, de transport rapide, de diffusion thermique et d'absorption. Les figure 3, 4, 5 et 6 présentent les résultats obtenus.

La teneur en eau de constitution définit entièrement, quel que soit le sol, le pouvoir de ralentissement et la diffusion thermique. Le transport rapide est obtenu avec un coefficient de corrélation de 0,9743 mais aucune corrélation n'existe entre l'absorption thermique et la teneur en eau de constitution des sols.

La section efficace de diffusion Σ_d, par l'intermédiaire de l'eau de constitution, et la section efficace d'absorption Σ_a définissent l'intervention de la nature du sol sur la réponse de l'humidimètre à neutrons; la limite de cette proposition est donnée par la corrélation qui existe au niveau du transport rapide.

La mesure de Σ_d et de Σ_a se présente donc comme un moyen de définir le sol vis-à-vis de l'humidimètre à neutrons.
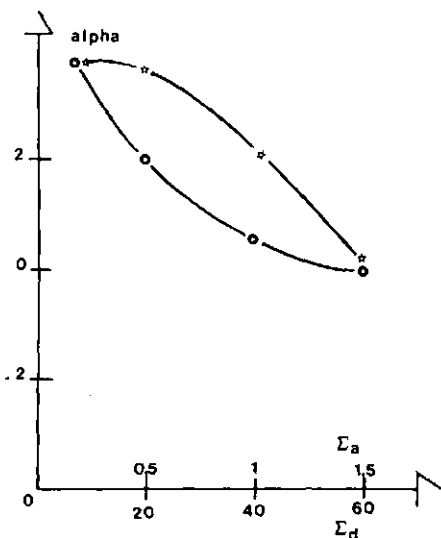
FIG.7. *Evolution de* α *en fonction des variations d'absorption et de diffusion exprimée en* $mm^2 \cdot g^{-1}$. ⊛*courbe pour l'absorption,* ✸*courbe pour la diffusion.*
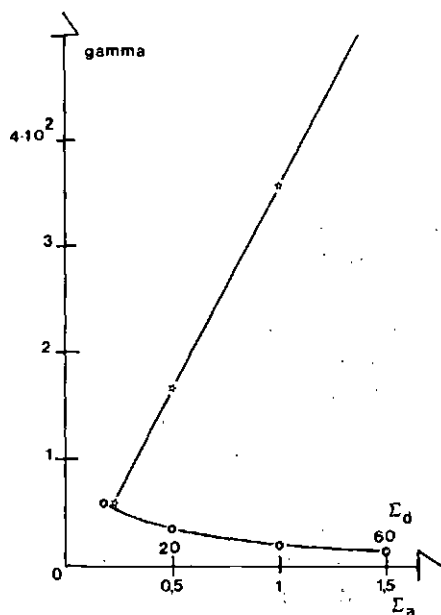

FIG.8. *Evolution de* γ *en fonction des variations d'absorption et de diffusion exprimées en* $mm^2 \cdot g^{-1}$. ⊛*courbe pour l'absorption,* ✸*courbe pour la diffusion.*
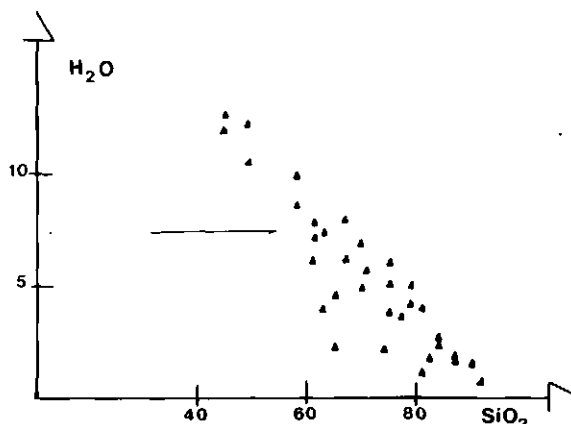
FIG.9.   *Valeurs des pourcentages d'eau obtenue par séchage à 1000°C sur des sols préalablement étuvés à 105°C.*

Le modèle numérique, qui applique la théorie multigroupe en géométrie cylindrique [8, 10], fournit une représentation simple de la courbe d'étalonnage de l'humidimètre à neutrons, pour un sol donné:

$$N = (\alpha \rho_s + \beta) \, H_v + \gamma \rho_s + \delta$$

avec N:taux de comptage, H_v: humidité volumique, ρ_s:densité sèche et α, β, γ, δ: constantes représentant l'intervention du sol. Cette équation est relative à un humidimètre à source centrée.

Les quatre constantes α, β, γ, δ sont interdépendantes et définies, à la corrélation près du transport rapide, par le couple Σ_d, Σ_a; leur calcul s'effectue par le modèle.

A titre d'exemple, nous présentons les courbes fournissant α et γ lorsque Σ_a et Σ_d varient (figures 7 et 8). On voit que plus le sol est diffusant (teneur en eau de constitution croissante), plus α diminue et plus γ augmente: cela signifie que, lorsque la teneur en eau de constitution augmente, l'incidence de la densité sèche sur la pente est plus faible mais, par contre, cette incidence augmente sur l'ordonnée à l'origine de la droite d'étalonnage.

D'un autre côté, lorsque l'absorption du sol augmente, α et γ diminuent, ce qui traduit une incidence plus faible de la densité sèche dans le cas d'un sol absorbant.

La relation entre la teneur en eau de constitution et le pourcentage de SiO_2 du sol (fig. 9) nous permet de dire que l'incidence de la densité sèche sur la courbe d'étalonnage est d'autant plus forte que le sol est sableux.
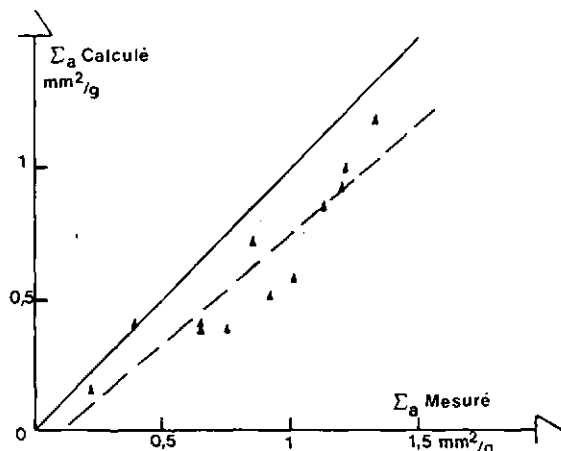
FIG. 10. *Comparaison entre les valeurs mesurées et calculées à partir de l'analyse chimique des sections efficaces d'absorption de divers sols.*

En conclusion, deux sols possédant le même couple de valeurs Σ_a et Σ_d présenteront des courbes d'étalonnage identiques. La mesure de Σ_a et Σ_d est donc un moyen de prévoir l'intervention de la nature du sol sur l'étalonnage de l'humidimètre; nous allons voir quelle procédure permet cette mesure.

Mesure directe de la diffusion Σ_d et de l'absorption Σ_a

Des deux constantes, la plus simple à déterminer est probablement Σ_d que l'on déduit de la section efficace totale Σ_T calculée à partir du coefficient d'atténuation d'un faisceau de neutrons thermiques $\Sigma_T = \Sigma_a + \Sigma_d$; l'écart entre Σ_a et Σ_d est tel (fig. 5 et 6) que l'erreur commise en négligeant Σ_d dans Σ_T est faible; par suite, Σ_T donne Σ_d.

La mesure de Σ_a est, quant à elle, plus complexe: elle s'appuie sur la perturbation qu'entraîne un échantillon de sol placé à l'intérieur d'un flux de neutrons thermiques.

Ce flux peut être fourni par un réacteur: on introduit l'échantillon de sol et on lui imprime un mouvement périodique; la modulation du flux neutronique, propagée dans tout le réacteur, est recueillie en un point par une chambre d'ionisation. Le fondamental du signal est proportionnel à la section efficace d'absorption de l'échantillon [5]. On a mesuré par cette méthode sur la pile Zoé (Fontenay-aux-Roses) les sections efficaces Σ_a de douze sols.

Les résultats présentés sur la figure 10 montrent que le calcul de Σ_a à partir de l'analyse chimique conduit à des résultats systématiquement par défaut.
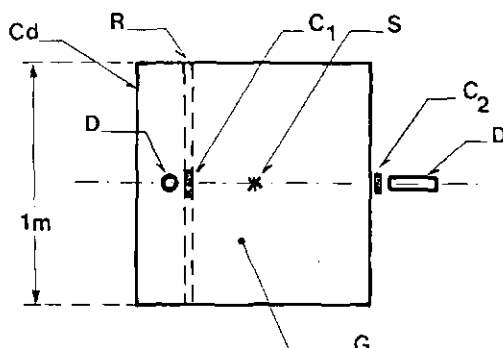
FIG.11. *Empilement graphite pour la mesure des constantes neutroniques des sols.*
Cd: cadmium; R: réglette; D: détecteur; C_1: échantillon 1; C_2: échantillon 2; S: source; G: graphite.

Cet écart est à associer à la difficulté de dosage des éléments tracés, spéciale-
ment les terres rares à fort pouvoir d'absorption; il confirme les limites de l'étalon-
nage théorique par la voie de l'analyse chimique des sols.

Cette procédure de mesure a été utilisée par ailleurs [25], mais son coût
élevé ne permet pas de la généraliser; c'est pourquoi nous avons développé, pour
des échantillons de sols, la méthode mise au point pour les évaluations de teneur
en bore d'échantillons d'aluminium [6]. Dans un cube de graphite de 1 m³,
(figure 11), une source Am-Be de 3 Ci génère un flux de neutrons thermiques
représentatif d'un milieu peu absorbant (pas d'hydrogène).

Un détecteur au trifluorure de bore détermine la perturbation induite par
l'introduction d'un échantillon de 300 g de sol entre la source et le détecteur. La
variation du comptage dépend de Σ_a et a un degré moindre de Σ_d. Sur le même
massif, une mesure de l'atténuation par échantillon de sol du flux sortant par
l'une des faces est effectuée; cette seconde mesure dépend de Σ_d et en second lieu
de Σ_a. Ainsi les comptages fournis par les deux détecteurs permettent le calcul de
Σ_d et Σ_a.

Courbe d'étalonnage des humidimètres à neutrons

L'application de la mesure directe des constantes neutroniques à l'étalonnage
des sols pour la mesure de teneur en eau repose sur la précision de la détermination
de Σ_a et Σ_d et sur la validité du modèle numérique permettant de passer de
Σ_a et Σ_d à α, β, γ et δ.

Dans un article conjoint du présent colloque [28], on a montré que Σ_a
est obtenu à ± 0,07 mm² · g⁻¹ et que Σ_d est obtenu à ± 1,58 mm² · g⁻¹. Ceci
correspond à une incertitude de 2,3% sur le bilan en eau et 0,5 point d'humidité
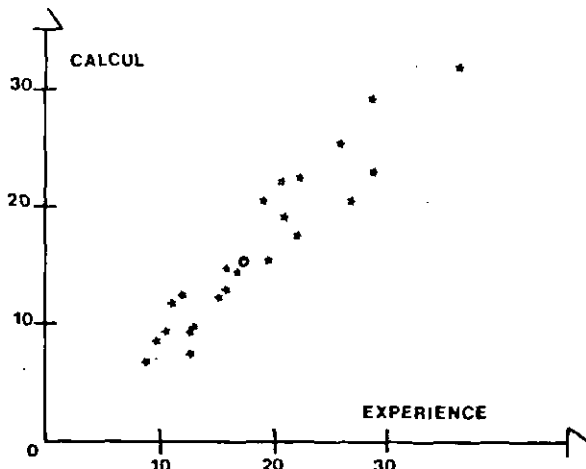
FIG.12.　Comparaison de la représentation théorique avec l'expérience.　Points moyens pour chaque sol.　Valeurs calculées et expérimentales d'humidité pondérale données en pourcent.

mesurée.　La figure 12 montre la comparaison entre l'expérience et le calcul issu du modèle utilisé pour déterminer α, β, γ, δ à partir de Σ_a et Σ_d.

Le principe selon lequel deux sols possédant les mêmes valeurs de Σ_a et Σ_d auront nécessairement la même courbe d'étalonnage permet de comprendre l'intérêt de la mesure directe et rapide de Σ_a et Σ_d.

La prospection préliminaire d'un site permet de prévoir s'il y aura lieu d'utiliser une ou plusieurs courbes d'étalonnage avant même d'entreprendre d'éventuelles procédures expérimentales longues et onéreuses.　On peut réaliser une cartographie à trois dimensions du site à étudier.　Dans le cas difficile d'une rizière [33], cette méthode rapide d'analyse a permis d'interpréter et de corriger les profils d'humidité obtenus, là où l'étalonnage expérimental s'avérait presque impossible, à cause de l'inondation.

Variabilité spatiale de la courbe d'étalonnage

La mesure de Σ_a et Σ_d nous permet d'appréhender les composantes de la variance dans l'estimation des caractéristiques hydrodynamiques des sols; le traitement de ces dernières est effectué en tant qu'il s'agit de processus stochastiques décrits par une analyse statistique [30, 36].　Parmi les composants de la variance, on retient [32] l'erreur d'étalonnage, laquelle intervient directement sur les variables de teneur en eau H_v et de bilan hydrique sH_v [37].　Puisque l'erreur sur le comptage peut être minimisée, les paramètres d'erreur restent la densité sèche et la nature du sol.　La mesure rapide des constantes neutroniques
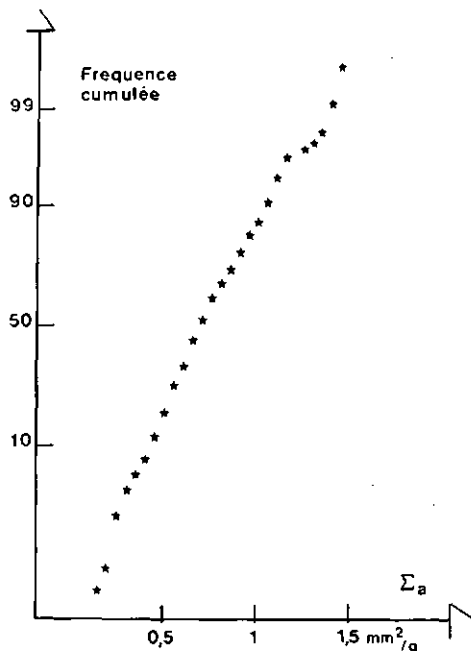
FIG.13. Loi de distribution des valeurs de Σ_a pour un ensemble de 407 échantillons de sol.

du sol fournit un moyen de prendre en compte le paramètre de variabilité spatiale de l'étalonnage du sol.

Celle-ci est supérieure à l'erreur de la mesure de Σ_a et Σ_d dans le cas d'un sol réputé homogène [28]; on peut alors fixer une procédure pour l'échantillonnage du du sol en vue d'apprécier la composante de variabilité due à l'intervention de la nature du sol dans la détermination de H_v et sH_v par l'intermédiaire de la courbe d'étalonnage de l'humidimètre à neutrons.

Applications de la mesure de Σ_a et Σ_d à l'étude des sols

A partir de plus de 400 mesures effectuées sur divers sols, nous avons déterminé les lois de distributions de Σ_a et de Σ_d. Les graphiques des figures 13 et 14 montrent que la loi de distribution de Σ_a est normale, alors que celle de Σ_d est log-normale. Au niveau actuel de nos recherches, il n'est pas encore possible de préciser quelle est la signification de cette différence entre les lois obtenues pour les deux constantes. On peut seulement noter que la distribution de Σ_d semble plus liée à celle des argiles, alors que celle de Σ_a recouvre l'ensemble du domaine textural des sols.
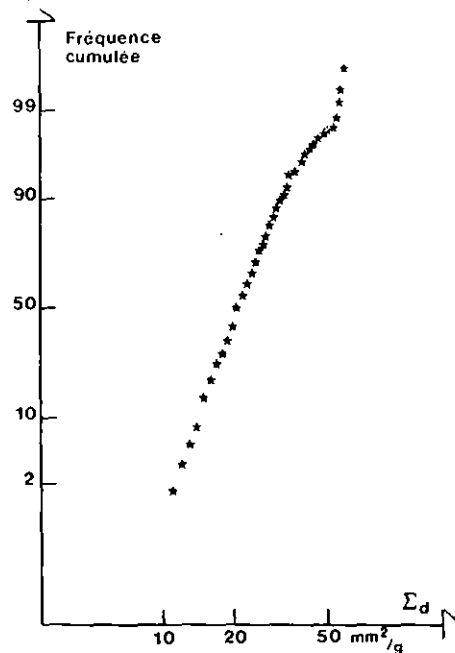
FIG.14.   Loi de distribution de Σ_d pour un ensemble de 407 échantillons de sol.
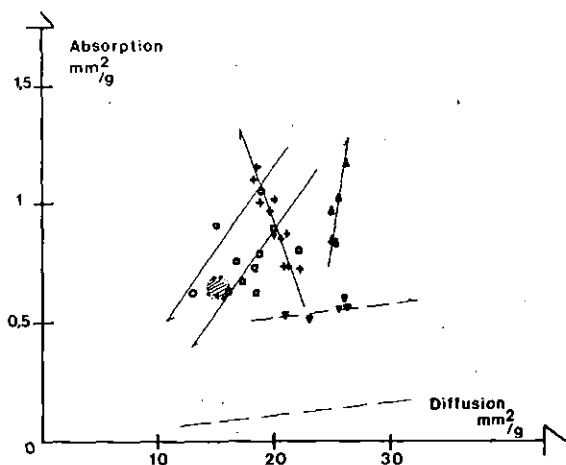

FIG.15.   Graphe des points images de valeurs $\Sigma_a = f(\Sigma_d)$ pour divers sols.   Le sens de la flèche indique le sens de prélèvement des échantillons de la surface vers la profondeur.
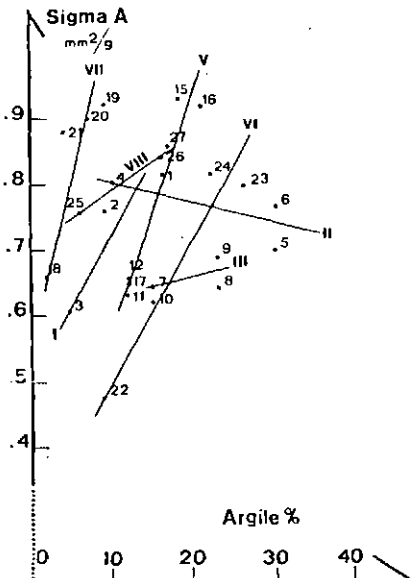
FIG.16.   Valeurs de Σ_a en fonction de la teneur en argile ($\leqslant 2$ μm). Les chiffres font référence aux sols numérotés de 1 à 27 rassemblés sur les droites I à VIII.

Les points images des valeurs de Σ_a et Σ_d caractérisent chaque site de mesure (fig. 15) de telle sorte que la mesure rapide des constantes neutroniques peut se présenter comme une méthode complémentaire dans la classification pédologique des sols.

Lorsque, pour un site donné, seule varie la teneur en eau de constitution lorsqu'on passe d'un échantillon à l'autre, les points images de [Σ_d, Σ_a] se répartissent sur une droite parallèle à une droite «fictive» correspondant à l'incidence de la variation de la teneur en eau sur le couple [Σ_a, Σ_d]. Ce cas peut se produire lorsque dans un site donné les échantillons de sol ne reflètent qu'une évolution de la granulométrie avec le même type d'argile et sans lessivage d'éléments absorbants. Dans les autres circonstances et notamment si l'on passe d'un type d'argile à un autre, s'il y a lessivage ou stratification, les points images pourront présenter une répartition différente, en général ils se situeront sur une droite de pente plus forte que la droite «Eau». Les figures 16 et 17 illustrent cette intervention différentielle de l'eau de constitution et des éléments absorbants. Les résultats portent sur l'analyse de 27 sols canadiens faite en relation avec le département des ressources terrestres de l'Université de Guelph. L'analyse des variations de Σ_a et Σ_d en fonction du pourcentage d'éléments inférieurs à 2 μm appelé argile montre qu'il y a une bonne corrélation pour Σ_d, qui traduit l'incidence prépondérante de l'eau de constitution, mais que Σ_a n'est pas corrélé à la teneur en argile.
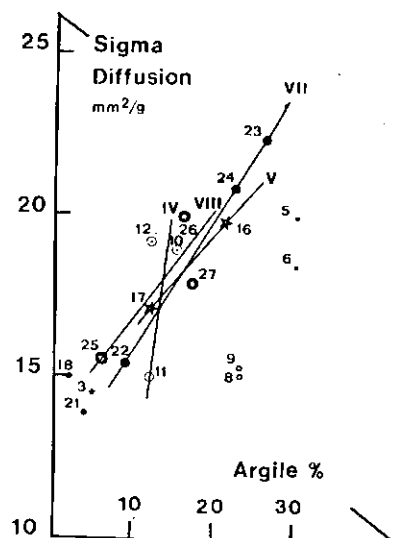
FIG.17. Valeurs de Σ_d en fonction de la teneur en argile ($\leqslant 2 \mu m$). Les chiffres font référence aux sols numérotés de 1 à 27 rassemblés sur les droites I à VIII.
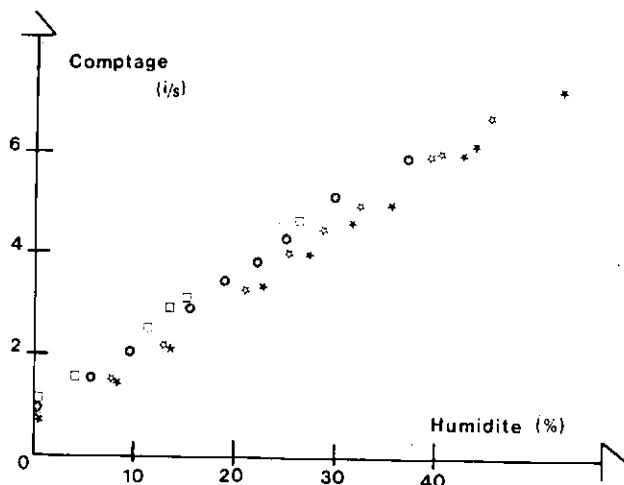

FIG.18. Points d'étalonnage des comptages thermiques en fonction de l'humidité volumique; les densités sèches correspondantes varient de 1 à 2 g·cm⁻³ (✹, ✩, ⬤, ☐).
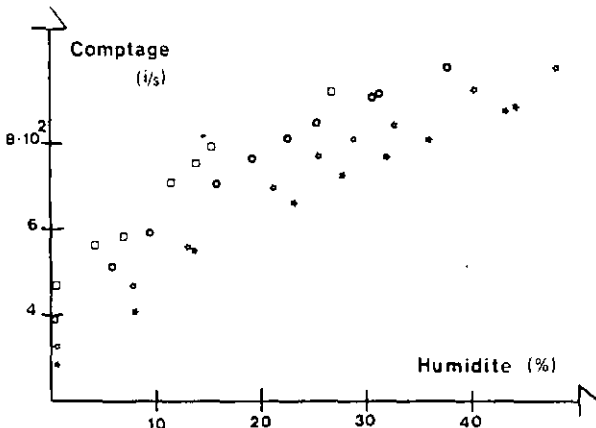
FIG.19. Points d'étalonnage des comptages épicadmiques (énergie ≥ 0,8 eV) en fonction de l'humidité volumique; les densités sèches correspondantes varient de 1 à 2 g·cm⁻³ (✳, ✢, ●, □).

Intervention de la densité apparente sèche

Cet aspect de l'intervention du sol a été assez développé par de nombreux auteurs [10, 16, 22, 23]. Nous n'y reviendrons pas. Il s'agit de connaître par une mesure conjointe avec un densimètre γ les variations spatio-temporelles de ρ_s à affecter à la formule de la courbe d'étalonnage.

Une correction empirique a été proposée [16] pour tenir compte de l'incidence de la densité sèche; elle suppose que le comptage relié à la teneur en eau totale est proportionnel à la racine carrée de la densité apparente sèche.

Nous savons que l'influence de ρ_s est d'autant plus faible que Σ_a augmente (figures 7 et 8); cette constatation nous conduit à penser que le flux de neutrons épithermiques devrait être plus sensible à la variation de ρ_s que le flux de neutrons thermiques, c'est ce que montrent les figures 18 et 19. Par suite, on montre qu'à partir des relations qui lient le comptage thermique et le comptage épithermique à la teneur en eau et à la densité apparente sèche, on peut calculer la teneur en eau H_v en fonction du comptage thermique et du comptage épithermique:

$$
\begin{cases}
N = (\alpha\rho + \beta)\, H_v + \gamma\rho_s + \delta \\[2mm]
N' = (\alpha'\rho_s + \beta')\, H_v + \gamma'\rho_s + \delta
\end{cases}
$$

$$
\text{d'où } H_v = \frac{N - cN' - d}{a\, N' + b}
$$
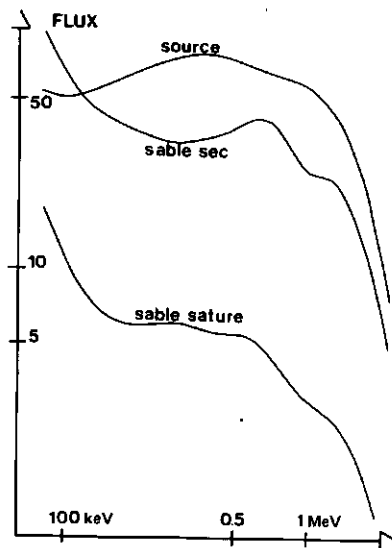
FIG.20.   Evolution du flux rapide par transmission à travers une épaisseur de 25 cm de sable sec et humide.   Le spectre source est déformé par des diffusions dues au montage expérimental.
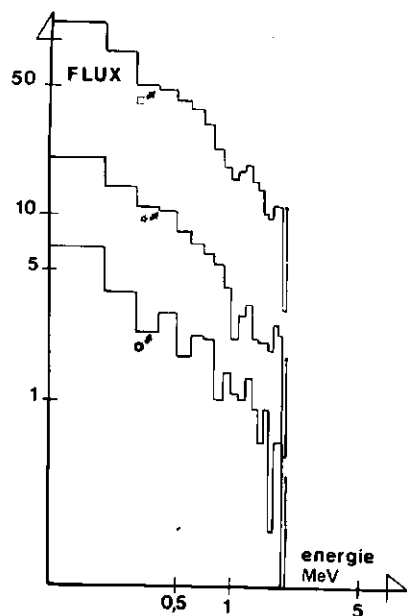

FIG.21.   Spectre calculé de neutrons rapides à travers un massif de sable de 20 cm pour une source de 2 MeV.   □0%, ✿20%, ●40%.

Les valeurs normalisées de a, b, c et d en fonction de Σ_a ont été calculées [10]; la seule connaissance de Σ_a (à partir d'une mesure directe; voir les paragraphes précédents) permet d'obtenir a, b, c et d. Aussi est-il possible de réaliser une double sonde thermique-épithermique dans laquelle le comptage épithermique intervient comme une correction du comptage thermique prenant en compte la densité apparente sèche.

Dans le cas de sols homogènes, l'utilisation d'un tel appareil relativement complexe ne se justifie pas; cependant, nous avons montré que l'influence des cailloux, déjà mise en évidence [1, 23], passait par celle de la densité apparente sèche. En effet, la présence de cailloux peut être prise en compte, indépendamment de la granulométrie, si l'on effectue la correction correspondante de densité sèche. Dans ce domaine des sols caillouteux, l'utilisation d'une double sonde thermique-épithermique peut se justifier.

BILAN ET PERSPECTIVES

La méthode neutronique de mesure de l'humidité des sols a maintenant atteint un stade de développement élevé. Parmi les paramètres qui interviennent dans la construction de la courbe d'étalonnage, le sol est le plus délicat à prendre en compte. La mesure des constantes neutroniques fournit le moyen de prendre en compte de façon sûre et rapide l'incidence de la nature du sol. Ce faisant, on a montré que cette mesure se présente comme une méthode complémentaire d'analyse des sols eux-mêmes. La définition de l'influence de la densité apparente sèche se fait par l'intermédiaire de la mesure densimétrique gamma. Enfin, le passage d'un type de sonde à l'autre s'effectue en construisant simplement, à l'occasion de mesures sur le terrain, la relation de passage unique pour tous les sols entre les comptages d'une sonde et celle de la sonde à laquelle on veut la comparer.

La méthode neutronique ne se limite pas à la seule mesure de teneur en eau des sols par l'humidimètre. La détection des flux de neutrons rapides peut être un moyen de mesure dans le cas des colonnes de sol ou des sols caillouteux [9]. Les figures 20 et 21 montrent l'évolution, mesurée et calculée par un programme Monte-Carlo, des flux de neutrons rapides obtenus par transmission à travers un sable humide.

La réaction photoneutronique sur l'eau deutérée permet la détermination in situ des propriétés dispersives des sols et fournit donc un moyen d'apprécier la part du mouvement des nitrates sous culture due aux transferts d'eau. Enfin la neutrographie en réacteur pulsé conduit à l'obtention de photographies des racines in situ; cette dernière méthode a été appliquée avec succès à l'étude de l'incidence du déficit hydrique et de la réhumectation sur le développement des racines du riz pluvial.

BIBLIOGRAPHIE

[1] BABALOLA OLAOLU, Field calibration and use of the neutron moisture meter on some Nigerian soils, Soil Sci. **126** 2 (1977) 118.

[2] BLOEMEN, G.W., L'étalonnage du champ de l'humidimètre à neutrons, Instituut voor Cultuurtechniek en Waterhuishouding, Mededeling 10 (1962).

[3] BRUMMER, E., MARDOCK, E.S., «A neutron method for measuring saturations in laboratory flow experiments» (Proc. Meeting, Los Angeles, 1945) American Inst. of Mining, Metallurgical and Petroleum Eng. Inc., New York (1945).

[4] BURN, K.N., Effect of iron on the determination of moisture content by the neutron method, Can.J. Earth. Sci. **34** (1966) 129.

[5] CARRE, J.C., VIDAL, R., Mesure des sections efficaces thermiques d'absorption de l'Al, du Mg, du P et du Cu par la méthode d'oscillation, Rapport CEA-R-2485 (1964).

[6] CARRE, J.C., LETOUR, C., Empilement boréal pour le contrôle de la teneur en bore d'échantillons d'alliage bore-aluminium, Revue Phys. Appl. (1971) 267.

[7] COUCHAT, Ph., «Détermination de la courbe d'étalonnage de l'humidimètre à neutrons à partir de l'analyse chimique des sols», Isotope and Radiation Techniques in Soil Physics and Irrigation Studies (C.R. Coll. Istamboul 1967) AIEA, Vienne (1967) 67.

[8] COUCHAT, Ph., «Etude en géométrie cylindrique de quelques problèmes posés par la méthode neutronique de mesure de l'humidité des sols» Réunion RILEM-AIEA, Brno (1969).

[9] COUCHAT, Ph., RAMODIHARILAFY, J., La mesure neutronique de l'humidité des sols caillouteux, Int. J. Appl. Radiat. Isot. 23 5 (1972) 229.

[10] COUCHAT, Ph., Mesure neutronique de l'humidité des sols, Thèse d'état, Faculté des Sciences de Toulouse (1974).

[11] COUCHAT, Ph., CARRE, C., MARCESSE, J., LEHO, J., «The measurement of thermal neutron constants of the soil: application to the calibration of neutron moisture and to the pedological study of soil» Nuclear Cross-sections Technology (SCHRACH and BOWMAN Eds.) (1975) 516.

[12] COUCHAT, Ph., Aspects méthodologiques et technologiques de la mesure neutronique de l'humidité des sols. Ann. Agron. **28** 5 (1977) 477.

[13] COUCHAT, Ph., MOUTONNET, P., PUARD, M., The application of the gamma-neutron method for transport studies in field soils, Water Resour. Res. **6** (1979) 1583.

[14] COUCHAT, Ph., MOUTONNET, P., Study of corn seedling root and shoot growth by neutron radiography, Agron. J. **72** (1980) 321.

[15] GEMMEL, W., GREGOR, B., MOSS, G.F., Estimation of moisture content by neutron scattering: theory, calculation and experiment, Int. J. Appl. Radiat. Isot. **17** (1966) 615.

[16] GREACEN, E.L., SCHRALE, G., The effect of bulk density on neutron meter calibration, Aust. J. Soil Res. **14** (1976) 159.

[17] GREACEN, E.L., MIGNETT, C.T., Sources of bias in the field calibration of a neutron meter, Aust. J. Soil Res. **17** (1979) 405.

[18] HOLMES, J.W., Calibration and field use of the neutron scattering method for measuring soil water content, Aust. J. Appl. Sci. **7** (1956) 45.

[19] INTERNATIONAL ATOMIC ENERGY AGENCY, Neutron Moisture Gauges, Technical Reports Series n° 112, IAEA, Vienna (1979).

[20] KASHI, S., KOSKINEN, J., Analysis, calculation and measurement concerning the moisture measuring by the neutron method, Nucl. Eng. Des. **4** (1966) 74.

[21] LAKSHMIPATHY, A.V., GANGADHBRAN, A., Minimum size of soil sample for laboratory calibration of subsoil neutron moisture probe, Nucl. Instrum. Methods **142** (1977) 577.

[22] LAL, R., Concentration and size of gravel in relation to neutron moisture and density probe calibration for some tropical soils, Soil Sci. 177 4 (1974) 183.

[23] LAL, R., Concentration and size of gravel in relation to neutron moisture and density probe calibration, Soil Sci. 127 1 (1979) 41.

[24] LIPPOLD, W.J., Monte-Carlo simulation of neutron thermalization in soils, Thèse, North Carolina State University (1969).

[25] McCULLOCH, D.B., WALL, T., A method of measuring the neutron absorption cross-sections of soil samples for calibration of the neutron moisture meter, Nucl. Instrum. Methods 137 (1976) 577.

[26] MOUTONNET, P., La mesure neutronique de l'humidité des sols: intérêts et limitations, Bull. Groupe Fr. Humidimétrie Neutronique 3 (1978) 37.

[27] MOUTONNET, P., COUCHAT, Ph., Heavy water tracing of soil water transfers under irrigation, Soil Sci. Soc. Am. J. 46 2 (1982) 435.

[28] MOUTONNET, P., PERROCHET, P., COUCHAT, Ph., «Variabilité spatiale des caractéristiques neutroniques d'un sol: incidence sur la détermination des courbes d'étalonnage des humidimètres à neutrons», Isotope and Radiation Techniques in Soil Physics and Irrigation Studies (C.R. Coll. Aix-en-Provence, 1983) AIEA, Vienne (1983) présent volume.

[29] NAKAYAMA, F.S., REGINATO, R.J., Simplifying neutron moisture meter calibration, Soil Sci. 133 I (1982) 48.

[30] NIELSEN, D.R., BIGGAR, J.W., ERH, K.T., Spatial variability of field measured soil water properties, Hilgardia 42 7 (1973) 215.

[31] OLGAARD, P.L., On the theory of neutronic method for measuring the water content, Risø Report n° 97 (1965).

[32] PARKES, M.E., SIAM, N., Error associated with measurements of soil moisture change by neutron probe, Agric. Eng. 24 (1979) 87.

[33] PUARD, M., COUCHAT, Ph., MOUTONNET, P., Application de la méthode gamma neutronique à une étude d'infiltration d'eau sous rizière, Agron. Trop. 35 1 (1980) 25.

[34] RAHI, G.S., SHIM, S.F., MYHRE, D.L., Calibration and sensitivity of neutron moisture probe for histosols, Soil Sci. Soc. Am., Proc. 38 (1979) 87.

[35] RAWLS, W.J., ASMUSSEN, Neutron probe field calibration for soils in the Georgia coastal plain, Soil Sci. 116 4 (1972) 262.

[36] RUSSO, D., BRESLER, E., 1982 − Soil hydraulic properties as stochastic processus: II, Errors of estimates in a heterogeneous field, Soil Sci. Soc. Am. J. 46 (1982) 20.

[37] SEMMLER, R.A., Neutron moderation moisture meters, Final report, USAEC Chicago Operations Office (1963) 712.

[38] SHIRAZI, G.A., ISOBE, M., Calibration of neutron probe in some selected Hawaïan soils, Soil Sci. 122 3 (1976) 165.

[39] SINCLAIR, D.F., WILLIANS, J., Components of variance involved in estimating soil water content and water content change using a neutron moisture meter, Aust. J. Soil Res. 17 (1979) 237.

[40] SICAMOIS, D., Etude comparative des sources 241Am-Be, 244Cm-Be et 252Cf pour équiper les humidimètres à neutrons, Bull. Groupe Fr. Humidimétrie Neutronique 8 (1980) 35.

[41] STIRK, G.B., «Moisture measurements in swelling clay soils», Physical Aspects of Swelling Clay Soils (Proc. Symp. 1972) Univ. of New England (1972) 53.

[42] VACHAUD, G., ROYER, J.M., COOPER, J.D., Comparison of methods of calibration of a neutron-capture model, J. Hydrol. 34 (1977) 343.

[43] VACANCOGNE, Ch., FOUERE, A., AHO, N., Contrôle de l'étalonnage basé sur l'étude neutronique d'échantillons de sols, Bull. Groupe Fr. Humidimétrie Neutronique 1 (1977) 61.

[44] WILLIAMSON, R.J., TURNER, A.K., Calibration of a neutron moisture meter for catchment hydrology, Aust. J. Soil Res. 18 (1980) 1.

ANALYSE DES ERREURS
LIEES A L'UTILISATION
DE L'HUMIDIMETRE NEUTRONIQUE

M. VAUCLIN, R. HAVERKAMP, G. VACHAUD
Institut de mécanique de Grenoble,
Saint-Martin-d'Hères, France

Abstract–Résumé

ANALYSIS OF ERRORS ASSOCIATED WITH USE OF THE NEUTRON MOISTURE GAUGE.
The variance associated with estimating water contents by means of a neutron moisture
gauge is analysed theoretically. The analysis shows the respective contributions of the
instrument (Poisson-type random neutron emission) and calibration (statistical treatment of the
correlation between count rate and moisture content) to the total error associated with any
determination of moisture content. On this basis one can formulate some simple rules for
the optimum use of the moisture gauge (counting time, number of repetitions at each measure-
ment point, and selection of the reference medium). It is also shown that when plotting
the calibration line account should be taken not only of the moisture measurement errors
(sampling and use of a gamma densimeter) but also of errors associated with the neutron
emission itself so as to obtain an unbiased estimate of the linear regression coefficients. The
theoretical analysis is then applied to an experiment conducted over a 2000 m^2 plot. The
hydric relations were monitored at the sites of 17 access tubes, and the moisture gauge was
calibrated with the use of gravimetric samples and a depth gamma densimeter. The results
show that the absolute accuracy for moisture content ($\pm$ 0.015 cm^3/cm^3) and water storage
($\pm$ 7 mm for a 390 mm storage) is basically a function of the calibration quality. In the case
of spatial studies, it is also shown that uncertainties in calibration may completely mask the
variance associated with the natural variability in moisture content and its variations in time;
contrary to what one might think, the uncertainty of the mean values cannot be reduced
systematically by increasing the number of access tube sites.

ANALYSE DES ERREURS LIEES A L'UTILISATION DE L'HUMIDIMETRE NEUTRONIQUE.
Une analyse théorique de la variance associée à l'estimation des teneurs en eau par
humidimétrie neutronique est présentée. Elle met en évidence les contributions respectives de
l'appareil (émission neutronique aléatoire de type Poisson) et de l'étalonnage (traitement
statistique de la corrélation entre taux de comptage et humidité) à l'erreur totale associée à
toute détermination de l'humidité. Cela permet d'établir quelques règles simple d'utilisation
optimum de l'humidimètre (temps de comptage, nombre de répétitions en chaque point de
mesure, choix du milieu de référence). On montre également que, pour l'établissement de la
droite d'étalonnage, il convient de prendre en compte, d'une part, les erreurs sur les mesures
d'humidité (prélévement d'échantillons, utilisation d'un gamma-densimètre), et d'autre
part, les erreurs liées à l'émission neutronique elle-même, afin d'obtenir une estimation non
biaisée des coefficients de la régression linéaire. L'analyse théorique est ensuite appliquée
à une expérimentation menée sur une parcelle de 2000 m^2. Un suivi hydrique a été
effectué en 17 verticales. L'étalonnage de l'humidimètre a été réalisé par prélévements

d'échantillons remaniés associés à l'utilisation d'un gamma-densimètre de profondeur. Les résultats montrent que la précision absolue sur les humidités ($\pm$ 0,015 cm^3/cm^3) et sur les stock hydriques ($\pm$ 7 mm pour un stock de 390 mm) est essentiellement fonction de la qualité de l'étalonnage. Dans le cas des études spatiales, on montre également que les incertitudes de l'étalonnage peuvent masquer complètement la variance liée à la variabilité naturelle de l'humidité et de ses variations temporelles: augmenter le nombre de verticales de mesure ne permet pas de réduire systématiquement l'incertitude sur les valeurs moyennes, comme on pourrait le penser.

INTRODUCTION

Alors que l'humidimètre neutronique est très classiquement et intensivement utilisé pour déterminer au champ, les teneurs en eau, les stocks hydriques et leurs variations dans le temps, peu d'études ont été effectuées sur l'estimation des erreurs associées à ces déterminations. HEWLETT et al [1] mettent en évidence l'influence de l'appareil de mesure et du temps de comptage sur l'estimation des erreurs associées à une mesure d'humidité. Plus récemment, SINCLAIR et WILLIAMS [2] présentent une analyse de variance sur la valeur moyenne de k mesures. Aucune de ces études ne fait mention des difficultés d'ordre statistique soulevées lors de l'établissement de la relation d'étalonnage de l'humidimètre : recherche d'une corrélation non biaisée entre deux séries d'observations (humidités et taux de comptage) entachées d'erreurs expérimentales.

Dans cette communication, on se propose d'examiner les points suivants :

. Analyse et estimation des erreurs (exprimées en terme de variance) associées à une détermination d'une valeur de l'humidité à une cote et à un temps donné.

. Analyse et estimation des erreurs liées au calcul du stock hydrique, à partir de la mesure d'un profil hydrique.

. Analyse et estimation des erreurs associées au calcul de valeurs moyennes de k mesures de l'humidité à la même cote et de ses variations temporelles.

. Etude de l'influence du mode de traitement statistique utilisé pour établir la droite d'étalonnage de l'humidimètre.

POSITION DU PROBLEME

Il est bien connu que la relation d'étalonnage d'un humidimètre neutronique est représentée par le modèle linéaire suivant :

$$\theta = a_o + a_1 n + e \qquad (1)$$

où θ est l'humidité volumique (cm^3/cm^3), a_0 et a_1 sont les coefficients de la régression ; e représente la déviation au modèle linéaire telle que son espérance mathématique $E\{e\}$ soit nulle et sa variance $E\{e^2\}$ = var(e) soit constante (hypothèse d'homoscédasticité).

Le taux de comptage réduit n est défini par :

$$n = \frac{\bar{N}}{\bar{N}_S} \qquad (2)$$

où $\bar{N}$ est le taux de comptage moyen (coups/sec) résultant de p répétitions N_i à la même cote z_i durant la période T_c (secondes) et $\bar{N}_S$ est le taux de comptage moyen correspondant à q répétitions N_{Si} dans un milieu de référence (eau, bloc de paraffine, etc...) durant la période T_S.

En fait, les "vraies valeurs" θ et n sont entachées d'incertitudes expérimentales et seules sont accessibles les estimations $\hat{\theta}$ et $\hat{n}$ définies par :

$$\hat{n}_i = n_i + u_i$$
$$\hat{\theta}_i = \theta_i + v_i \qquad (3)$$

où u_i et v_i sont les erreurs de mesure telles que leurs espérances mathématiques soient nulles et leurs variances var(u) et var(v) soient définies. Ainsi, en pratique, la relation d'étalonnage est de la forme :

$$\hat{\theta} = \hat{a}_0 + \hat{a}_1 \hat{n} \qquad (4)$$

où $\hat{a}_0$ et $\hat{a}_1$ sont des estimations de a_0 et a_1 respectivement telles que $E\{\hat{a}_0\}$ = a_0 et $E\{\hat{a}_1\}$ = a_1 pour un traitement statistique non biaisé.

1 - *Analyse de variance associée à la détermination individuelle d'une valeur de l'humidité.*

On se pose ici le problème de l'estimation d'une valeur particulière de l'humidité $\hat{\theta}_0$, correspondant à une mesure neutronique $\hat{n}_0$ et de la variance associée qui constitue une mesure de l'erreur affectée à cette détermination.

L'analyse statistique détaillée [3] montre que cette variance est donnée par :

$$s^2(\hat{\theta}_0) = \{\hat{a}_1^2 - s^2(\hat{a}_1)\} \cdot \{\frac{\hat{n}_0}{pT_c} + \frac{\hat{n}_0^2}{qT_S}\} \frac{1}{\bar{N}_S} + s^2(\hat{a}_0) + \hat{n}_0^2 s^2(\hat{a}_1)$$

$$+ 2\hat{n}_0 s(\hat{a}_0, \hat{a}_1) + s^2(e_0) \qquad (5)$$

où $s^2(\hat{a}_o)$ et $s^2(\hat{a}_1)$ sont les variances associées à $\hat{a}_o$ et $\hat{a}_1$ respectivement et $s(a_o, a_1)$ est la covariance entre ordonnée à l'origine et pente de la droite de régression (Eq. 4).

L'équation (5) montre que la variance totale associée à une estimation $\hat{\theta}_o$ est constituée de deux composantes :

a) - composante instrumentale

$$s_I^2(\hat{\theta}_o) = \{\hat{a}_1^2 - s^2(a_1)\} \cdot \{\frac{\hat{n}_o}{pT_c} + \frac{\hat{n}_o^2}{qT_S}\} \frac{1}{\bar{\bar{N}}_S} \tag{6}$$

Elle correspond à l'erreur aléatoire associée à l'émission neutronique elle-même selon un processus de Poisson [4]. On notera que le second terme de la deuxième parenthèse $(\hat{n}_o^2/qT_S)$ provient de l'utilisation du taux de comptage réduit dans l'équation (4). Cela a l'avantage d'éliminer l'influence de dérives électroniques mais l'inconvénient d'amplifier l'importance de $s_I^2(\hat{\theta}_o)$, par rapport à celle qui résulterait de l'utilisation du taux de comptage $\bar{\bar{N}}_o$.

b) - composante liée à l'étalonnage

$$s_c^2(\hat{\theta}_o) = s^2(\hat{a}_o) + \hat{n}_o^2 s^2(\hat{a}_1) + 2 \hat{n}_o s(\hat{a}_o, \hat{a}_1) + s^2(e_o) \tag{7}$$

Elle quantifie la plus ou moins grande qualité de la régression linéaire elle-même.

2 - *Analyse de variance associée à la détermination du stock hydrique.*

Dans de nombreuses études, il est fait appel au stock d'eau contenu dans une tranche de sol (O-z). Sa vraie valeur est définie par :

$$S = \int_o^z \theta(z) \, dz \tag{8}$$

Puisque l'utilisation d'un humidimètre neutronique permet seulement une estimation $\hat{\theta}(z)$ du profil hydrique qui, dans le cas général ne conduit pas à une expression analytique directement intégrable, seule une estimation $\hat{S}$ du stock hydrique est obtenue. Sa variance associée peut alors être estimée par :

$$s^2(\hat{S}) = s_1^2(\hat{S}) + s_2^2(\hat{S}) \tag{9}$$

où $s_1^2(\hat{S})$ représente la contribution des erreurs associées à la détermination du profil hydrique $\hat{\theta}(z)$ et $s_2^2(S)$ est la variance résultant de la méthode numérique utilisée pour intégrer la fonction $\hat{\theta}(z)$.

3 - *Analyse de variance associée à la détermination des valeurs moyennes spatiales de l'humidité.*

Il s'agit ici de déterminer la variance $s^2(<\hat{\theta}_o>)$ associée à la valeur moyenne $<\hat{\theta}_o>$ de k estimations $\hat{\theta}_{o,j}$ de l'humidité volumique à une profondeur donnée.

L'analyse précédente effectuée sur la valeur moyenne, en supposant que les k observations $\hat{n}_{o,j}$ sont indépendantes entre elles, afin d'appliquer le théorème central limite [5] conduit à l'expression suivante [6] :

$$s^2(<\hat{\theta}_o>) = \{\hat{a}_1^2 - s^2(\hat{a}_1)\} \frac{s^2(L_o)}{k \overline{\hat{N}_S^2}} + \{\hat{a}_1^2 - s^2(\hat{a}_1)\}\{\frac{<\hat{n}_o>}{pT_c} + \frac{<\hat{n}_o>^2}{qT_S}\} \frac{1}{k\overline{\hat{N}_S}}$$
$$+ s^2(\hat{a}_o) + <\hat{n}_o>^2 s^2(\hat{a}_1) + 2<\hat{n}_o> s(\hat{a}_o, \hat{a}_1) \qquad (10)$$

où $s^2(L_o)$ exprime la variabilité spatiale proprement dite de l'humidité.

Cette équation montre que la variance totale est constituée de trois composantes :

a) - *composante instrumentale*

$$s_I^2(<\hat{\theta}_o>) = \{\hat{a}_1^2 - s^2(\hat{a}_1)\}\{\frac{<\hat{n}_o>}{pT_c} + \frac{<\hat{n}_o>^2}{qT_S}\} \frac{1}{k\overline{\hat{N}_S}} \qquad (11)$$

b) - *composante liée à l'étalonnage*

$$s_c^2(<\hat{\theta}_o>) = s^2(\hat{a}_o) + <\hat{n}_o>^2 s^2(\hat{a}_1) + 2<\hat{n}_o> s(\hat{a}_o, \hat{a}_1) \qquad (12)$$

c) - *composante liée à la variabilité spatiale*

$$s_L^2(<\hat{\theta}_o>) = \{\hat{a}_1^2 - s^2(\hat{a}_1)\} \cdot \frac{s^2(L_o)}{k\overline{\hat{N}_S^2}} \qquad (13)$$

On notera que seul $s_c^2(<\hat{\theta}_o>)$ est indépendant du nombre de mesures. Augmenter k revient à réduire $s_I^2(<\hat{\theta}_o>)$ et $s_L^2(<\hat{\theta}_o>)$.

4 - *Analyse de variance associée aux moyennes spatiales des variations de l'humidité dans le temps.*

Il s'agit ici d'estimer la variance $s^2(<\Delta\hat{\theta}>)$ associée aux valeurs moyennes $<\Delta\theta>$ de k observations $\Delta\theta_j = \theta_{j1} - \hat{\theta}_{j2}$ où

$\hat{\theta}_{j1}$ et $\hat{\theta}_{j2}$ sont des estimations de l'humidité au site j et à deux instants t_1 et t_2.

Par la même analyse, on peut aisément montrer que $s^2(<\Delta\hat{\theta}>)$ est également constituée de trois composantes :

a) - composante instrumentale

$$s_{\overline{I}}^2(<\Delta\hat{\theta}>) = \{\hat{a}_1^2 - s^2(\hat{a}_1)\}\{\frac{<\hat{n}_1>}{p_1 T_{c_1}\overline{\hat{N}}_{S_1}} + \frac{<\hat{n}_1>^2}{q_1 T_{S_1}\overline{\hat{N}}_{S_1}} + \frac{<\hat{n}_2>}{p_2 T_{c_2}\overline{\hat{N}}_{S_2}}$$
$$+ \frac{<\hat{n}_2>^2}{q_2 T_{S_2}\overline{\hat{N}}_{S_2}}\} \frac{1}{k} \tag{14}$$

b) - composante liée à l'étalonnage

$$s_c^2(<\Delta\hat{\theta}>) = <\Delta\hat{n}>^2 . s^2(\hat{a}_1) \tag{15}$$

c) - composante liée à la variabilité spatiale

$$s_L^2(<\Delta\hat{\theta}>) = \{\hat{a}_1^2 - s^2(\hat{a}_1)\}.\{\frac{s^2(L_1)}{\overline{\hat{N}}_{S_1}^2} + \frac{s^2(L_2)}{\overline{\hat{N}}_{S_2}^2} - \frac{2s(L_1,L_2)}{\overline{\hat{N}}_{S_1}\overline{\hat{N}}_{S_2}}\} \frac{1}{k} \tag{16}$$

où $s^2(L_1)$ et $s^2(L_2)$ expriment la variabilité spatiale de l'humidité aux temps t_1 et t_2 et $s(L_1,L_2)$ rend compte d'éventuelles incertitudes sur la position relative des sites de mesure. $<\Delta\hat{n}>$ est la moyenne des variations du taux de comptage réduit.

On notera que ces expressions sont générales puisqu'elles permettent de tenir compte des variations du taux de comptage $\overline{\hat{N}}_S$ entre deux séries de mesure ($\overline{\hat{N}}_{S_1}$ et $\overline{\hat{N}}_{S_2}$) ainsi que l'éventuels changements de la durée de comptage et du nombre de répétitions (p_1, p_2) ; (q_1, q_2).

EXPERIMENTATION

Une parcelle gazonnée de 2000 m^2, située sur le Campus Universitaire de Grenoble a été équipée de 17 tubes d'accès pour humidimètre neutronique implantés jusqu'à 1 m de profondeur et disposés aux sommets de triangles équilatéraux de 10 m de côté.

Les mesures ont été effectuées tous les 10 cm ; la première mesure étant faite à 10 cm de la surface. L'humidimètre

utilisé avait la particularité d'être une sonde combinée gamma-neutron. Il est constitué d'une source Am/Be de 50 mC et d'un détecteur au He^3. Sa sphère d'influence a été estimée à 18 cm dans l'eau. L'étalonnage en humidité a été réalisé de la façon suivante :

a) - à l'implantation des tubes, des échantillons de sol remaniés de 20 cm de longueur ont été prélevés afin de déterminer les teneurs massiques en eau $\hat{W}_i$.

b) - la masse volumique humide $\hat{\rho}_i$ a été mesurée, tous les 20 cm, la sonde fonctionnant en gamma-densimètre ; l'étalonnage ayant été préalablement effectué sur des blocs de matériaux de densités connues (tableau I).

c) - les comptages neutroniques $\hat{N}_i$ ont été effectués tous les 10 cm et rapportés aux comptages dans l'eau avec $T_S = T_c = 30$ secondes, q = 5 et p = 2.

d) - les teneurs massiques en eau ont été converties en teneurs volumiques par l'expression :

$$\hat{\Theta}_i = \hat{\rho}_i \cdot \frac{\hat{W}_i}{1 + \hat{W}_i} \qquad (17)$$

Les couples ($\hat{n}_i$, $\hat{\Theta}_i$) sont reportés fig. 1 pour la cote z = 10 cm et les cotes plus profondes. Les erreurs u_i et v_i associées à chaque observation sont également reportées. Elles ont été respectivement estimées par :

$$u_i^2 = s^2(\hat{n}_i) = \left| \{\frac{\hat{n}_{oi}}{pT_c} + \frac{\hat{n}_{oi}^2}{qT_S}\}/\bar{\hat{N}}_S \right| \qquad (18)$$

$$v_i^2 = s^2(\hat{\Theta}_i) = \frac{1}{(1+\hat{W}_i)^2} \{\hat{\rho}_i^2 s^2(\hat{W}_i) [1 + \frac{\hat{W}_i^2}{(1+\hat{W}_i)^2}] + \hat{W}_i s^2(\hat{\rho}_i)\} \qquad (19)$$

L'équation (19) s'obtient aisément en appliquant à l'équation (17) les règles de calcul des variances de fonctions aléatoires [7].

RESULTATS

1 - Etablissement de l'équation d'étalonnage de l'humidimètre.

Puisqu'il s'agit de corréler des valeurs ($\hat{n}_i$, $\hat{\Theta}_i$) entachées d'erreurs, le traitement statistique classique fondé sur la technique des moindres carrés conduit à une estimation biaisée des paramètres de la régression [8].

TABLEAU I. PARAMETRES D'ETALONNAGE DE LA SONDE GAMMA-NEUTRON POUR LES TRAITEMENTS NON BIAISE (1) ET BIAISE (2) [a]

		$\hat{a}_o$	$\hat{a}_1$	$10^2 \cdot s^2(\hat{a}_o)$	$10^2 \cdot s^2(\hat{a}_1)$	$10^2 \cdot s(\hat{a}_o, \hat{a}_1)$	$10^4 \cdot s^2(e)$	r	observations
GAMMA DENSIMETRE	10 cm	2,895	-0,560	6,029	1,207	-2,689	47,72	-0,938	(1)
HUMIDIMETRE	10 cm	-0,444	1,340	0,408	0,981	-0,632	0,654	0,968	(1)
	10 cm	-0,362	1,212	1,871	4,495	-2,898	3,311	0,855	(2)
	≥ 20 cm	-0,0259	0,604	0,153	0,373	-0,238	3,278	0,833	(1)
	≥ 20 cm	-0,0165	0,589	0,242	0,588	-0,376	5,320	0,760	(2)

[a] Les calculs ont été faits avec $s^2(u) = 4,8 \cdot 10^{-5}$ et $s^2(v) = 2,6 \cdot 10^{-4} (cm^3/cm^3)^2$.
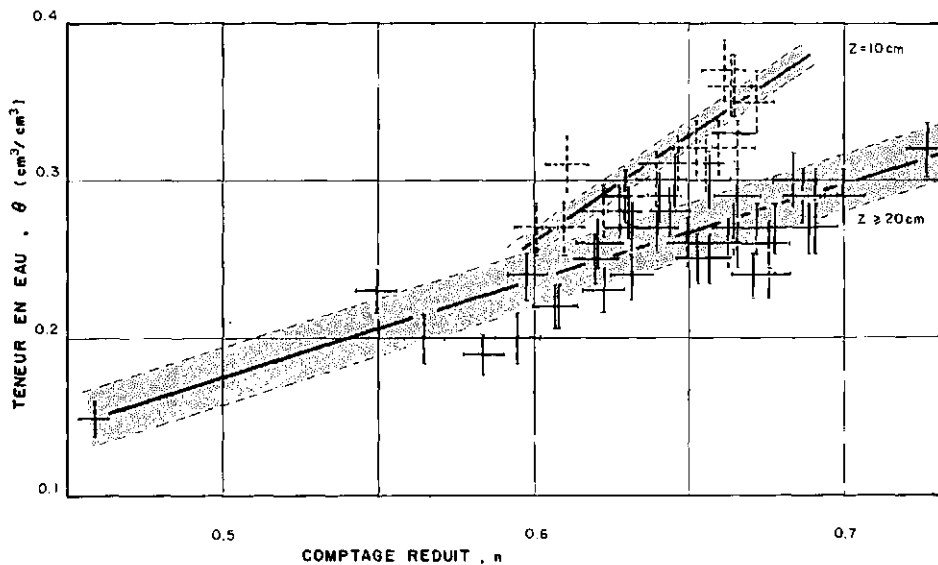
FIG.1. Etalonnage de l'humidimètre neutronique: les barres horizontales et verticales corres-
pondent aux erreurs de mesures. Droites de régression et bande de confiance à 68% sont
reportées pour le traitement non biaisé.
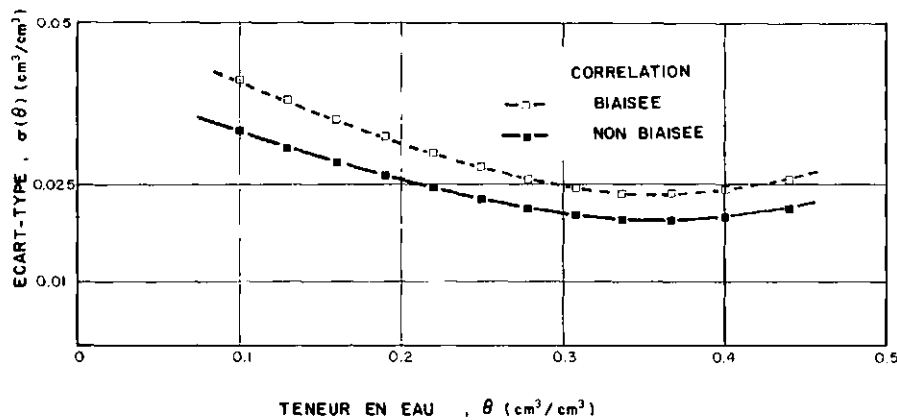
FIG.2. Évolution de l'écart-type σ(θ) en fonction de l'humidité.

Le traitement non biaisé doit prendre en compte les erreurs u_i^2 et v_i^2. Il conduit alors aux expressions de $\hat{a}_o$, $\hat{a}_1$ de leurs variances associées et de la covariance $s(\hat{a}_o, \hat{a}_1)$ rappelées en annexe. Les résultats correspondant sont donnés tableau I. A titre indicatif, on donne également les valeurs obtenues, dans le cas du traitement avec biais statistique. On notera que ce traitement revient à sous-estimer la pente $\hat{a}_1$ de la droite de régression, donc les variations temporelles de l'humidité qui lui sont proportionnelles.

2 - *Variance associée à la détermination des teneurs en eau.*

La figure 2 donne la valeur absolue de l'écart-type $|s(\hat{\theta}_o)|$ estimée par l'équation (5) en fonction de valeur hypothétiques de $\hat{\theta}_o$ calculées en utilisant successivement les relations d'étalonnage biaisée et non biaisée. Tous les calculs ont été effectués avec p = 2 ; q = 5 ; $T_C = T_S$ = 30 sec et $\hat{N}_S$ = 250 coups/sec. Elle amène les commentaires suivants :

- Sur le domaine d'humidité rencontré lors de l'étalonnage de l'humidimètre ($0,15 < \hat{\theta}_o < 0,40$ cm3/cm3), $|s(\hat{\theta}_o)|$ est relativement constant.

- Les valeurs de $|s(\hat{\theta}_o)|$ sont très notablement réduites en considérant le traitement non biaisé, ce qui justifie son emploi systématique.

Toutes les mesures obtenues sur le site expérimental ont été analysées selon cette procédure. A titre d'exemple, le tableau II fournit les résultats relatifs à une verticale de mesure. Les valeurs $\hat{\theta}_o$ à chaque profondeur ont été calculées avec les coefficients relatifs au traitement non biaisé (tableau I). Les composantes $s_I^2(\hat{\theta}_o)$ et $s_C^2(\hat{\theta}_o)$ ont été calculées selon les équations (6) et (7) avec p = 1 ; q = 5 et $\hat{N}_S$ = 249 coup/sec. Les remarques suivantes peuvent être faites :

- $|s(\hat{\theta}_o)|$ est pratiquement constant sur tout le profil à l'exception de la cote z = 10 cm pour laquelle la relation d'étalonnage est différente (tableau I).

- L'incertitude relative $s(\hat{\theta}_o)/\hat{\theta}_o$ est de l'ordre de ± 5 % environ.

- La composante instrumentale contribue faiblement (5 % environ) à la variance totale. Cependant, si besoin en était, la théorie exposée (Eq. 6) donne la manière de réduire $s_I^2(\hat{\theta}_o)$: augmenter les temps de comptage T_C et T_S, augmenter le nombre de répétitions, choisir un humidimètre ayant un taux de comptage $\hat{N}_S$ le plus élevé possible.

TABLEAU II. EXEMPLE DE CALCUL D'UN PROFIL HYDRIQUE ET DE
VARIANCES ASSOCIEES.

z(cm)	$\hat{n}$	$\hat{\theta}$	$10^5 . s_I^2(\hat{\theta})$	$10^4 . s_c^2(\hat{\theta})$	$10^4 . s^2(\hat{\theta})$	$10^2 . s(\hat{\theta})$
10	0,677	0,463	9,188	0,779	1,691	1,300
20	0,686	0,388	1,886	3,437	3,636	1,904
30	0,644	0,363	1,757	3,358	3,534	1,879
40	0,616	0,346	1,672	3,379	3,546	1,883
50	0,599	0,336	1,621	3,42	3,582	1,893
60	0,645	0,364	1,76	3,359	3,535	1,880
70	0,704	0,399	1,941	3,511	3,706	1,925
80	0,687	0,389	1,889	3,441	3,629	1,905
90	0,586	0,328	1,582	3,466	3,624	1,904
100	0,557	0,311	1,49	3,614	3,764	1,940

3 - *Variance associée à la détermination du stock hydrique*.

L'analyse de variance appliquée au stock hydrique corres-
pondant au profil du tableau **II** et calculé par la méthode des tra-
pèzes conduit à :

$$\hat{S}_o^{105 \ cm} = 391,8 \ mm \overset{+}{-} 7,1 \ mm$$

La variance associée à l'incertitude du profil hydrique étant
$s_1^2(\hat{S}) = 36,4 \ mm^2$ et celle résultant de la méthode numérique d'in-
tégration $s_2^2(\hat{S}) = 14,1 \ mm^2$. On notera que l'utilisation de la re-
lation d'étalonnage biaisée conduit aux valeurs suivantes :

$$\hat{S}_o^{105 \ cm} = 391,1 \ mm \overset{+}{-} 8,7 \ mm$$

avec $s_1^2(\hat{S}) = 62,4 \ mm^2$ et $s_2^2(\hat{S}) = 14,1 \ mm^2$.

Là encore on voit l'intérêt d'un traitement statistique
rigoureux de la corrélation afin de réduire les variances.

TABLEAU III. EXEMPLE DE CALCUL DES HUMIDITES MOYENNES A
3 PROFONDEURS ET DES VARIANCES ASSOCIEES: TRAITEMENTS NON
BIAISE (1) ET BIAISE (2) DE LA RELATION D'ETALONNAGE.

	$\langle \hat{n} \rangle$	$s^2(\langle \hat{n} \rangle)$	$\langle \hat{\theta} \rangle$	$s^2(\langle \hat{\theta} \rangle)$	$s_I^2(\langle \hat{\theta} \rangle)$	$s_C^2(\langle \hat{\theta} \rangle)$	$s_L^2(\langle \hat{\theta} \rangle)$	
z=30 cm	0.637	$1.203\ 10^{-5}$	0.3588	$1.236\ 10^{-5}$	$2.042\ 10^{-6}$	$8.018\ 10^{-6}$	$2.300\ 10^{-6}$	(1)
	"	"	0.3587	$1.670\ 10^{-5}$	$1.928\ 10^{-6}$	$1.260\ 10^{-5}$	$2.167\ 10^{-6}$	(2)
z=50 cm	0.624	$4.947\ 10^{-5}$	0.3510	$2.679\ 10^{-5}$	$1.995\ 10^{-6}$	$8.927\ 10^{-6}$	$1.586\ 10^{-5}$	(1)
	"	"	0.3510	$3.091\ 10^{-5}$	$1.884\ 10^{-6}$	$1.404\ 10^{-5}$	$1.498\ 10^{-5}$	(2)
z=70 cm	0.621	$3.308\ 10^{-4}$	0.3491	$1.287\ 10^{-4}$	$1.985\ 10^{-6}$	$9.316\ 10^{-6}$	$1.174\ 10^{-4}$	(1)
	"	"	0.3492	$1.275\ 10^{-4}$	$1.874\ 10^{-6}$	$1.465\ 10^{-5}$	$1.109\ 10^{-4}$	(2)

4 - *Variance associée à la valeur moyenne de l'humidité.*

L'analyse de variance liée à l'estimation des valeurs
moyennes de l'humidité à toute cote de mesure a été effectuée
selon la méthode précédemment exposée. On ne présente ici que
les résultats relatifs aux profondeurs z = 30, 50 et 70 cm qui
correspondent respectivement à une faible moyenne et forte va-
riabilité spatiale pour le site considéré.

L'analyse statistique classique [6] a montré que les
mesures neutroniques $n_{o,i}$ sont normalement distribuées à toute
profondeur. Cela permet d'estimer correctement valeurs moyen-
nes $\langle n_o \rangle$ et variances $s^2(\hat{n}_o)$ par les deux premiers moments de
la loi de distribution ainsi identifiée.

L'analyse géostatistique [6] effectuée à l'aide du semi-
variogramme a mis en évidence l'absence de structure spatiale du
champ de mesures neutroniques à toutes les profondeurs. Cela as-
sure la pertinence de l'hypothèse d'indépendance pour estimer la
variance de la moyenne à partir de la variance de l'échantillon
constitué des 17 observations.

L'ensemble des résultats pour les 3 cotes est donné
tableau III. Les composantes $s_I^2(\langle \hat{\theta}_o \rangle)$ et $s_C^2(\langle \hat{\theta}_o \rangle)$ ont été cal-
culées respectivement par les équations (11) et (12). La compo-
sante $s_L^2(\langle \hat{\theta}_o \rangle)$ due à la variabilité spatiale proprement dite a

été obtenue par simple différence : $s^2(<\hat{\theta}_0>) - (s^2_c(<\hat{\theta}_0>) + ...$
$+ s^2_f(<\hat{\theta}_0>))$. A titre de comparaison, tous les calculs ont été ef-
fectués en utilisant les coefficients d'étalonnage correspon-
dants aux traitements biaisé et non biaisé. Les commentaires
suivants peuvent être faits :

    - La nature du traitement statistique de la relation
d'étalonnage affecte principalement $s^2_c(<\hat{\theta}_0>)$.

    - La composante instrumentale est faible, comparée aux
autres composantes.

    - Dans les situations où $s^2_L(<\hat{\theta}_0>)$ est faible, en rai-
son d'une grande homogénéité (cas de la cote z = 30 cm), la com-
posante due à l'étalonnage constitue la contribution majeure à
la variance totale.

    Alors que cette étude a été réalisée à partir d'une sé-
rie spatiale de 17 observations, l'analyse théorique (Eq. 10)
permet d'étudier l'influence du nombre de mesures sur l'estima-
tion de la variance totale et de ses différentes composantes.

    A titre d'exemple, la figure 3 donne $s^2(<\hat{\theta}_0>)$ et ses
3 composantes en fonction de k aux cotes z = 30 et 70 cm. Elle
amène les remarques suivantes :

    - $s^2(<\hat{\theta}_0>)$ diminue à mesure que k augmente pour tendre
asymptotiquement vers $s^2_c(<\hat{\theta}_0>)$ qui est invariant avec k (Eq. 12).

    - à la cote z = 30 cm, $s^2_L(<\hat{\theta}_0>)$ devient inférieure à
$s^2_c(<\hat{\theta}_0>)$ pour k supérieur à 5 mesures. Cela signifie qu'en si-
tuation de faible variabilité spatiale, il est illusoire d'aug-
menter le nombre de mesures pour espérer réduire la variance.
Il sera plus profitable d'améliorer, si faire se peut, la qua-
lité de l'étalonnage.

    - en cas de plus forte variabilité (z = 70 cm) la va-
riance totale ainsi que $s^2_f(<\hat{\theta}_0>)$ peuvent être notablement ré-
duits en augmentant le nombre de points de mesure.

5 - *Variance associée à la valeur moyenne des variations d'humidité.*

    Les mesures neutroniques effectuées aux 17 points de
la parcelle et à différents temps permettent également d'obte-
nir les variations temporelles de l'humidité et leur moyenne
spatiale. A titre d'exemple, le tableau IV donne les résultats
relatifs aux mesures effectuées à la cote z = 70 cm à deux da-
tes : 3/06/81 et 25/08/81. Les variances $s^2_c(<\Delta\hat{\theta}>)$ et $s^2_L(<\Delta\hat{\theta}>)$ ont
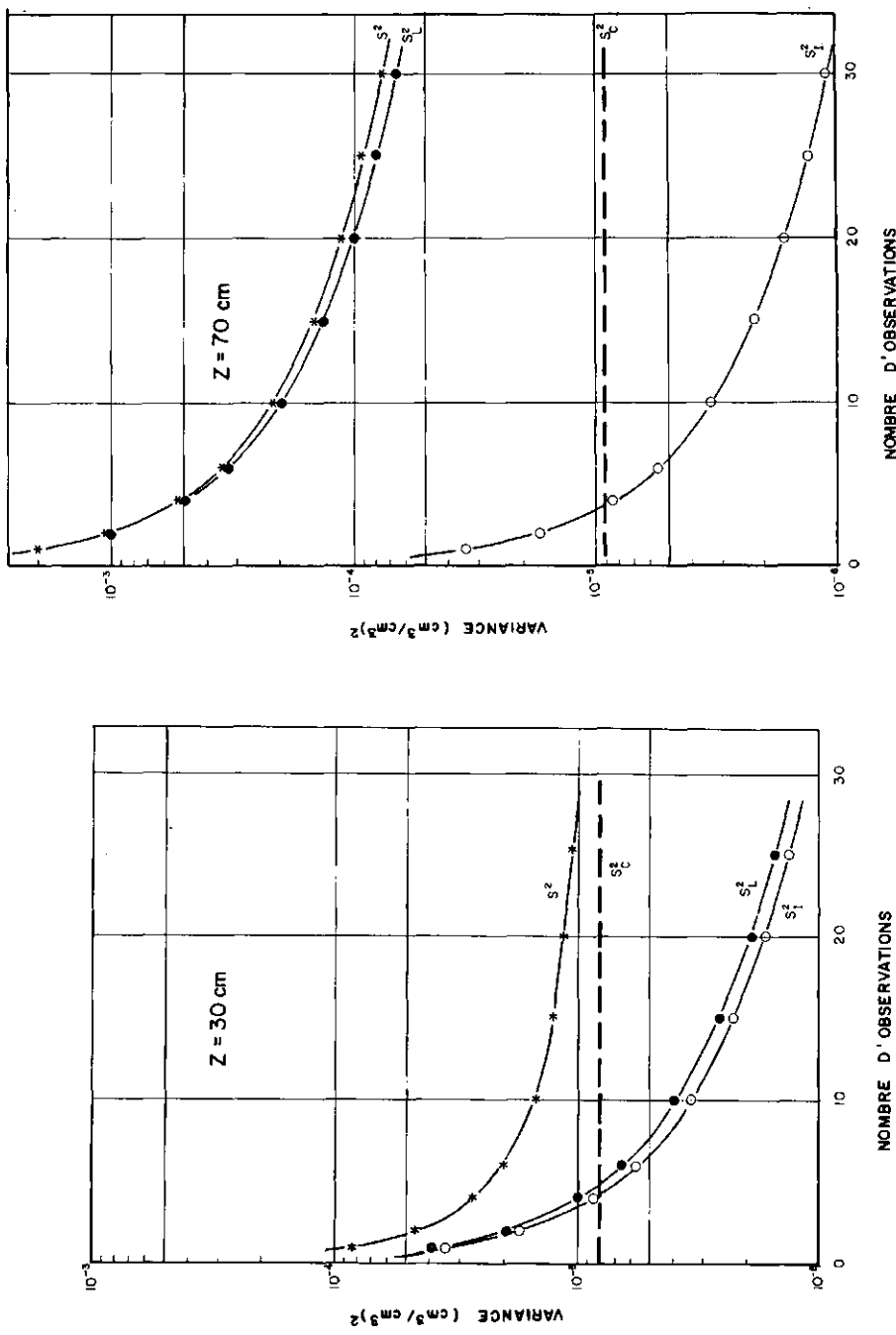
FIG.3. *Evolution des différentes composantes de la variance associée aux valeurs moyennes de l'humidité en fonction du nombre de sites de mesures.*

TABLEAU IV. EXEMPLE DE CALCUL DES VARIATIONS MOYENNES
D'HUMIDITE POUR z = 70 cm ET DE LA VARIANCE ASSOCIEE.

Dates	$\hat{<n>}$	$<\hat{\Delta n}>$	$<\hat{\Delta\theta}>$ cm^3/cm^3	$s^2(<\hat{\Delta\theta}>)$ $(cm^3/cm^3)^2$	s_I^2	s_c^2	s_L^2
3/06/81	0,621						
		0,091	0,0549	6.10^{-5}	2.10^{-6}	$3,08.10^{-5}$	$2,72.10^{-5}$
25/08/81	0,530						

été calculées selon les équations (14) et (15) avec les coeffi-
cients relatifs à l'étalonnage non biaisé.

La variance $s_L^2(<\hat{\Delta\theta}>)$ a été obtenue par différence avec
la variance totale $s^2(<\hat{\Delta\theta}>)$ estimée à partir de la série des 17
observations. Toutes les mesures, donc les calculs, ont été ef-
fectués avec $p_1 = p_2 = 1$; $q_1 = q_2 = 5$; $\hat{N}_{S_1} = 249$ coups/sec et
$\hat{N}_{S_2} = 252$ coups/sec. On notera que pour k = 17 observations, la
contribution majeure à la variance totale sur $<\Delta\theta>$ provient de
l'étalonnage de l'humidimètre dont la variance est indépendante
de k.

CONCLUSIONS

A la faveur de cette étude, les conclusions suivantes
peuvent être dégagées.

1 - *Au plan local*

L'analyse de variance associée à toute détermination
individuelle de la teneur en eau par humidimétrie neutronique
a mis en évidence les contributions respectives de l'instrument
et de l'étalonnage.

Réduire la variance nécessite le respect des straté-
gies suivantes :

i) - *Stratégie de la mesure* : le nombre de répétitions
et la durée des comptages dans le milieu de référence doivent
être suffisamment grands pour que la contribution supplémentai-
re liée à l'utilisation du comptage réduit (au lieu des compta-
ges bruts) soit minimum.

ii) - *stratégie statistique* : le traitement non biaisé de la relation d'étalonnage "in-situ" de l'humidimètre s'impose puisqu'il réduit très notablement la variance de calibration.

iii) - *stratégie commerciale* : il peut être d'intérêt de choisir un appareil donnant des valeurs élevées de comptages dans un milieu de référence. Cela est en relation notamment avec la nature du détecteur et l'électronique utilisée.

2 - *Au plan spatial*

La même analyse effectuée sur les valeurs moyennes permet d'avoir accès à la variance de l'humidité et de ses variations temporelles liée uniquement à l'hétérogénéité du sol. Ce point est capital dans les études de variabilité spatiale. On retiendra plus particulièrement que dans le cas où la composante due à l'étalonnage est importante ; il ne sert à rien d'augmenter le nombre de sites de mesures pour espérer diminuer la variance des observations.

ANNEXE

On rappelle ici les expressions des différents paramètres intervenant dans le traitement non biaisé de la relation d'étalonnage :

$$\hat{a}_1 = \frac{s(\hat{n},\hat{\theta})}{s^2(\hat{n}) - \frac{m-2}{m-1} s^2(u)} \tag{A1}$$

$$\hat{a}_o = \overline{\hat{\theta}} - \hat{a}_1 \overline{\hat{n}} \tag{A2}$$

$$s^2(\hat{a}_1) = \frac{s^2(e)}{(m-1) s^2(\hat{n}) - (m-2) s^2(u)} \tag{A3}$$

$$s^2(\hat{a}_o) = s^2(\hat{a}_1) \frac{1}{m} \sum_{i=1}^{m} \hat{n}_i^2 \tag{A4}$$

$$s(\hat{a}_o,\hat{a}_1) = - s^2(\hat{a}_1) \frac{1}{m} \sum_{i=1}^{m} \hat{n}_i \tag{A5}$$

$$s^2(e_o) = \frac{m-1}{m-2} \{s^2(\hat{\theta}) - \hat{a}_1 s(\hat{n},\hat{\theta})\} - s^2(v) \tag{A6}$$

Dans ces équations, $s^2(\hat{n})$ et $s^2(\hat{\theta})$ sont respectivement les estimations non biaisées des variances de $\hat{n}$ et $\hat{\theta}$ calculées à partir de m paires d'observations $(n_i, \hat{\theta}_i)$; $s(\hat{n},\hat{\theta})$ est l'estimation non biaisée de la covariance entre n_i et $\hat{\theta}_i$; $s^2(u)$ et $s^2(v)$

sont les variances des erreurs affectées aux mesures de $\hat{n}$ et $\hat{\theta}$. Elles sont estimées par :

$$s^2(u) = \frac{1}{m-1} \sum_{i=1}^{m} s^2(\hat{n}_i) \tag{A7}$$

$$s^2(v) = \frac{1}{m-1} \sum_{i=1}^{m} s^2(\hat{\theta}_i) \tag{A8}$$

où $s^2(\hat{n}_i)$ et $s^2(\hat{\theta}_i)$ sont données par les équations (18) et (19).

REFERENCES

[1] HEWLETT, J.D., DOUGLAS, J.E., CLUTTER, J.L., Instrumental and soil moisture variance using the neutron scattering method, Soil Sci. 97 (1964) 19.

[2] SINCLAIR, D.F., WILLIAMS, J., Components of variance involved in estimating soil water content and water content change using a neutron moisture meter, Aust. J. Soil Res. 17 (1979) 237.

[3] HAVERKAMP, R., VAUCLIN, M., VACHAUD, G., Error analysis in estimating soil water content from neutron probe measurements. I-Local Standpoint, à paraître dans Soil Sci. (1983).

[4] Van BAVEL, C.H.M., Accuracy and Source Strength in soil moisture neutron probes, Soil Sci. 26 (1962) 405.

[5] HAAN, C.T., in Statistical methods in hydrology, Iowa State University Press, Ames (1977).

[6] VAUCLIN, M., HAVERKAMP, R., VACHAUD, G., Error analysis in estimating soil water content from neutron probe measurements. II-Spatial Standpoint, à paraître dans Soil Sci. (1983).

[7] KENDALL, M.G., STUART, A., in The advanced theory of statistics, Charles Griffin and Co, London (1963) 1.

[8] JOHNSTON, J., in Econometric methods, Mac Graw Hill Book Co, New York (1963).

EFFETS D'UN STRESS HYDRIQUE SUR LE COMPORTEMENT RACINAIRE ET AERIEN DU RIZ PLUVIAL

J.F. BOIS
Antenne ORSTOM,
Centre d'études nucléaires de Cadarache,
Saint-Paul-lez-Durance

Ph. COUCHAT
Service de radio-agronomie,
CEA, Centre d'études nucléaires de Cadarache,
Saint-Paul-lez-Durance,
France

Abstract–Résumé

EFFECTS OF WATER STRESS ON THE ROOT AND SHOOT BEHAVIOUR OF RAIN-FED RICE.
Application of the neutron technique to the roots of rain-fed rice seedlings during water stress has shown that there is a noticeable decrease in root diameter because of water loss and a slowing down of growth. At the leaf level the water deficiency results in modified gas exchanges due to closure of the stomata. Transpiration and photosynthesis appear to be independent of the soil-water potential above a threshold value in the neighbourhood of -600 mbar. Below this critical potential the closure of the stomata is progressive and proportional to the drop in water potential.

EFFETS D'UN STRESS HYDRIQUE SUR LE COMPORTEMENT RACINAIRE ET AERIEN DU RIZ PLUVIAL.
L'application de la technique de neutronographie des racines à des plants de riz pluvial au cours du stress hydrique a permis de montrer une diminution notable du diamètre des racines due à la perte d'eau et un ralentissement de croissance. Au niveau foliaire, le déficit hydrique se manifeste par une modification des échanges gazeux à la suite de la fermeture des stomates. Il apparaît que la transpiration et la photosynthèse sont indépendants du potentiel hydrique du sol au dessus d'une valeur seuil proche de -600 mbar. Au dessous de ce potentiel critique, la fermeture des stomates est progressive et proportionnelle à la baisse de potentiel hydrique.

INTRODUCTION

La culture du riz pluvial *Oriza sativa* L. est importante en Afrique de l'Ouest où elle représente 75% des surfaces cultivées en riz [1]. Mais, du fait de l'irrégularité des pluies et de la faible réserve en eau des sols, les rendements sont médiocres et très variables car le riz n'est guère tolérant à la sécheresse.

L'amélioration des rendements passe par la sélection de variétés résistantes, ce qui suppose l'établissement de critères de sélection fiables. Pour cela, une bonne connaissance des mécanismes mis en œuvre par la plante pour éviter la sécheresse est nécessaire.

En période défavorable, la plante peut éviter le déficit hydrique par le maintien de l'absorption et par la réduction des pertes par la transpiration. La première stratégie fait intervenir l'activité du système racinaire par sa capacité à maintenir sa croissance pour prospecter des horizons plus profonds. La seconde implique le fonctionnement du système foliaire et, surtout, l'efficacité de l'appareil stomatique.

Nous nous sommes attachés à étudier sur plante entière les modifications qu'entraîne un stress hydrique suivi d'une réhumidification. Au niveau racinaire, nous avons utilisé la neutronographie pour visualiser les effets du stress et mesurer la croissance des racines. Au niveau foliaire, nous avons enregistré en cellule de culture les transferts d'eau entre la plante et l'atmosphère ainsi que les liaisons avec les échanges de CO_2 lors de stress hydriques obtenus sur sol par arrêt d'irrigation et, en culture hydroponique, par chocs osmotiques.

1.   MATERIEL ET METHODE

1.1. Généralités

Les variétés utilisées sont IRAT 13 et Iguape Cateto.

Les plants sont cultivés en phytotron avec une photopériode de 12 heures, un éclairement de 300 microeinstein $\cdot$ m$^{-2} \cdot$ s^{-1}, 28°C de température et 70% d'humidité relative le jour, 22°C et 90% la nuit.

Les expérimentations sont faites sur des plants au stade végétatif (début de tallage).

1.2. Neutronographie des racines

La neutronographie est une technique non destructive, analogue à la radiographie aux rayons X. Elle permet de visualiser les racines d'une plante cultivée sur milieu sableux. Son principe repose sur l'utilisation du contraste d'humidité qui existe entre les racines vivantes et le sol. L'objet à analyser est placé dans un flux de neutrons thermiques issu d'un réacteur. Ce flux est modifié par les éléments légers tels que l'hydrogène de l'eau. Il impressionne un film sensible par l'intermédiaire d'un convertisseur de gadolinium qui transforme les neutrons en rayonnements béta et gamma.

Les neutronographies sont faites au Centre d'études nucléaires de Valduc (France) avec le réacteur Mirène selon le protocole décrit ailleurs [2]. Les
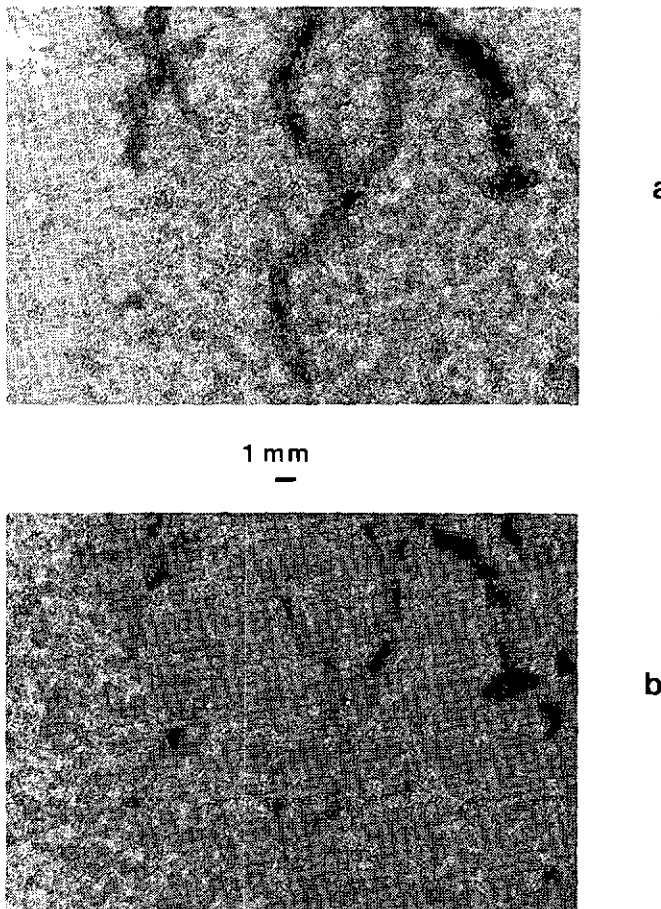
FIG.1. Neutronographie des racines: a) avant stress (50e jour); b) après stress (54e jour).

plants sont cultivés en bacs individuels d'aluminium (de 40 cm de haut, 24 cm de large, 2 cm d'épaisseur) sur sable avec une solution nutritive. La période de stress hydrique débute au 50e jour après semis et dure 4 jours. Elle est obtenue par arrêt de l'approvisionnement en eau. Elle est incluse entre deux périodes témoins de trois jours à irrigation régulière. Les neutronographies sont effectuées au début et à la fin de chaque période: aux 47e, 50e, 54e et 57e jours après semis.

1.3. Dispositif de mesure de la transpiration et des échanges de CO_2

1.3.1. Cellule de culture sur sol

Le dispositif utilisé a déjà été décrit [3]. Il permet de mesurer en continu les échanges en H_2O et CO_2 entre le feuillage et l'atmosphère d'un plant cultivé

TABLEAU I. CROISSANCE DU SYSTEME RACINAIRE DE DEUX PLANTS DE RIZ ENTRE CHAQUE NEUTRONOGRAPHIE

Périodes	Nombre de racines en élongation		Taux d'élongation $(mm \cdot d^{-1}/racine)$	
	Plant 1	Plant 2	Plant 1	Plant 2
Du 47e au 50e jour (Irrigation)	26	23	5	5,3
Du 50e au 54e jour (Stress hydrique)	17	8	2	1,6
Du 54e au 57e jour (Irrigation)	18	7	4,1	4,6

en conditions contrôlées. Il comprend principalement une cloche en verre à double paroi sur laquelle se raccorde de façon étanche un pot de culture contenant environ 2 kg de sol. La cloche est traversée par un courant d'air conditionné en humidité et en température (60% et 25°C). Après modification par la plante des teneurs en H_2O et CO_2, l'air de sortie passe dans des analyseurs différentiels à infrarouge où il est comparé à l'air d'entrée.

La lumière est fournie par une lampe aux halogènes de 1000 W donnant un éclairement de 500 microeinstein $\cdot m^{-2} \cdot s^{-1}$ pendant une photopériode de 12 h.

Le potentiel hydrique du sol est suivi par une batterie de tensiomètres couplés à un capteur de pression.

Les plants élevés en phytotron sont mis en cellule au stade début du tallage. Le stress hydrique est obtenu par arrêt d'irrigation et par épuisement des réserves du sol par la plante en quelques jours.

1.3.2. Cellule de culture sur solution nutritive

Le principe de la cellule est le même [4]. Le compartiment racinaire est un récipient en verre à double paroi pour la régulation thermique. Il est isolé parfaitement du compartiment aérien et peut être vidangé rapidement de sa solution nutritive. La mesure de l'humidité de l'air est faite par un hygromètre à point de rosée.

Le stress hydrique est obtenu par l'application de chocs osmotiques au niveau racinaire en remplaçant la solution nutritive par des solutions de polyéthylène glycol (PEG 6000) dont le potentiel osmotique est contrôlé par cryoscopie.
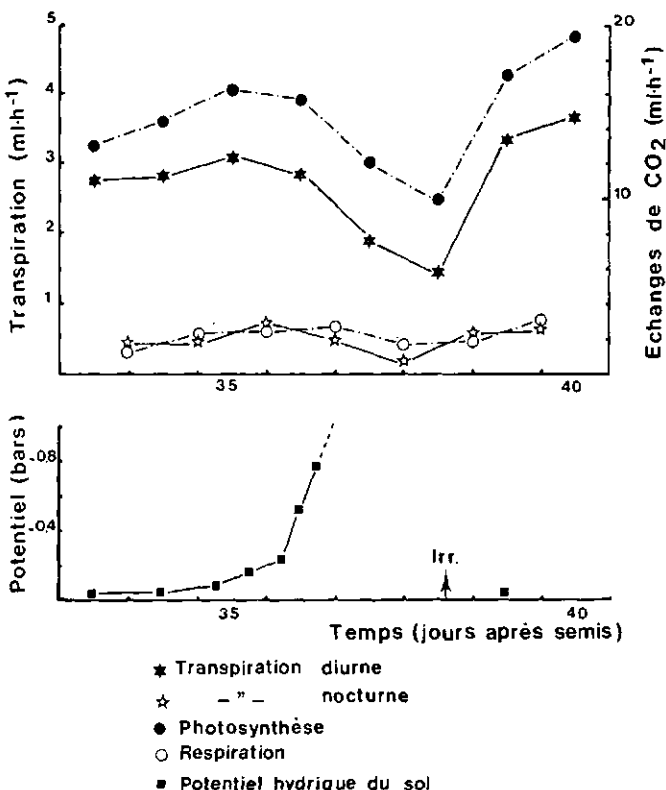
FIG.2. Evolution des échanges gazeux et du potentiel hydrique du sol au cours du cycle dessèchement-irrigation.

2. RESULTATS

2.1. Effets du stress hydrique au niveau racinaire

La figure 1 montre un agrandissement photographique des neutronographies du système racinaire d'un plant de riz prises avant et après une période sans irrigation de 4 jours. La comparaison des deux clichés met en évidence une importante diminution du diamètre apparent des racines. On peut évaluer cette diminution à environ 40%. Des réductions de diamètre de cet ordre ont déjà été notées au cours d'un dessèchement sur des racines d'*Helianthus annuus* [5]. Ce changement de forme des racines est la matérialisation du déficit hydrique qui provoque une perte de turgescence. Celle-ci entraîne un ralentissement de la croissance qui apparaît dans le tableau I: le taux délongation de la période sèche
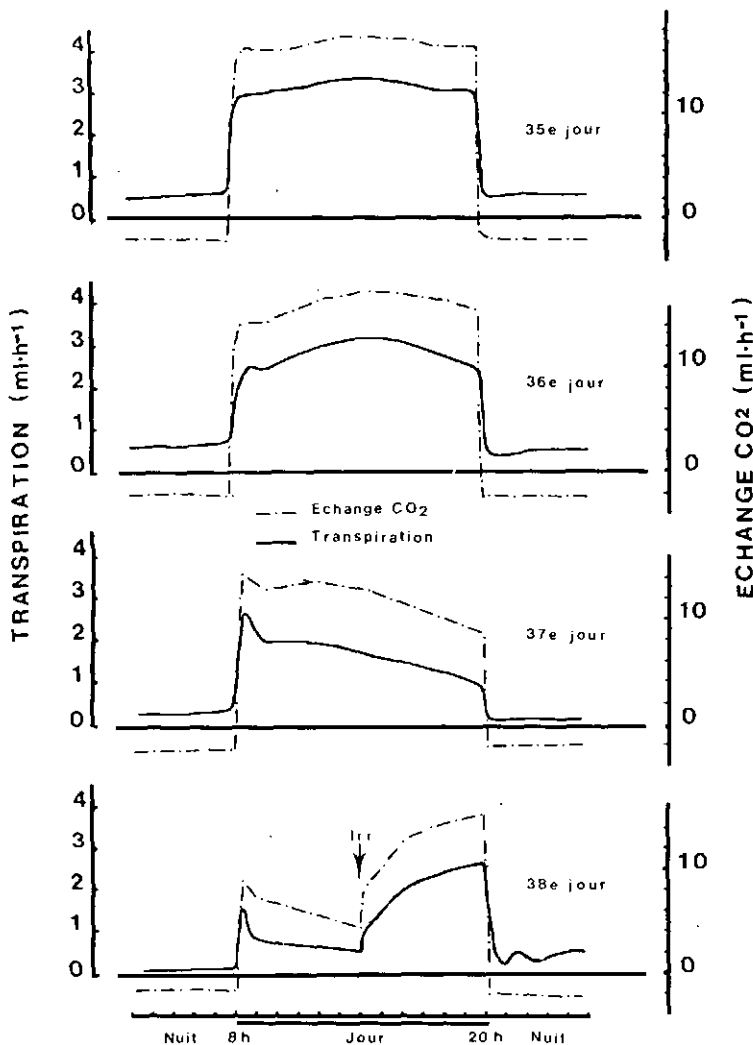
FIG.3. Cycles journaliers de photosynthèse et de transpiration au cours du dessèchement.

chute de 60 à 70% par rapport à celui de la période initiale. La période consécutive au stress se caractérise par une reprise de croissance à un taux voisin de celui de la première période mais avec un nombre plus faible de racines en élongation. Dans un autre travail [6], nous avons montré que la reprise de la croissance s'accompagnait d'une émission de racines secondaires (ramifications de 1er ordre des racines primaires).
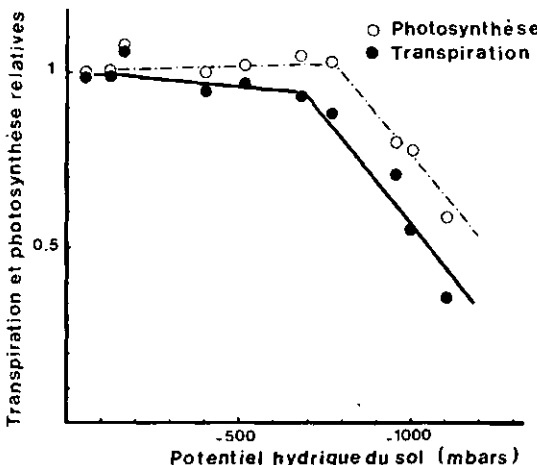
FIG.4.   Relation entre les échanges gazeux au niveau foliaire et le potentiel hydrique du sol au cours du dessèchement.

2.2. Effets du stress hydrique au niveau foliaire

2.2.1. Modification de la transpiration et de la photosynthèse

La figure 2 montre l'évolution au cours du temps des taux moyens de transpiration nocturne et diurne ainsi que de respiration nocturne et de photosynthèse lors d'une séquence de dessèchement suivie d'une irrigation. Jusqu'au 35ᵉ jour après semis, les paramètres mesurés croissent régulièrement en raison de l'augmentation de surface foliaire. Le potentiel hydrique moyen du sol reste supérieur à – 200 mbar et la plante a une alimentation hydrique suffisante. Par contre, au 36ᵉ jour, le potentiel hydrique chute rapidement, le déficit hydrique s'installe, la transpiration et la photosynthèse diminuent notablement. La respiration nocturne est moins affectée. Cette diminution des échanges gazeux est due à l'arrêt de croissance et à la fermeture des stomates. Au 38ᵉ jour intervient une irrigation. L'augmentation des échanges gazeux est immédiate. On retrouve les valeurs antérieures au bout d'un jour.

Sur la figure 3, on peut voir l'évolution des cycles journaliers de transpiration et de photosynthèse du 35ᵉ jour au 38ᵉ jour, donc au cours de l'installation du stress hydrique jusqu'au début de la reprise. Le premier cycle montre l'évolution des échanges gazeux avec une alimentation hydrique suffisante. La photosynthèse et la transpiration suivent un cours parallèle. Au 36ᵉ jour, une différence apparaît sur l'enregistrement de la transpiration qui diminue de 25% en fin de période diurne par rapport au maximum diurne. La plante ferme partiellement
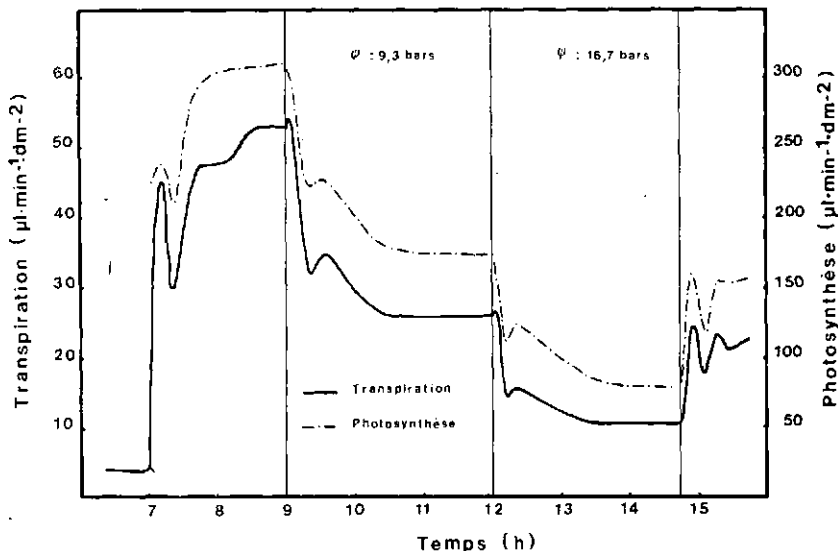
FIG.5. Influence de chocs osmotiques sur la transpiration et la photosynthèse.

ses stomates pour limiter le déficit hydrique interne. La photosynthèse n'est que faiblement affectée par ce phénomène. Au 37e et au 38e jour, après un pic à l'illumination, transpiration et photosynthèse décroissent régulièrement pour atteindre des valeurs ne représentant que 16% et 25% respectivement des valeurs atteintes le 35e jour à la même heure. Lorsqu'intervient l'irrigation, le 38e jour, la reprise est très rapide, transpiration et photosynthèse augmentent immédiatement et atteignent en fin de journée des valeurs proches de celles de la 35e journée. Ceci laisse penser que le déficit hydrique a peu affecté les mécanismes internes dans ce cas.

2.2.2. Contrôle stomatique et potentiel hydrique du sol

L'établissement du stress hydrique se manifeste donc par une modification importante des échanges gazeux à la suite du contrôle stomatique, surtout dans la période diurne. La figure 4 met en relation l'évolution des échanges gazeux avec celle du potentiel hydrique du sol dans la phase de dessèchement. La photosynthèse et la transpiration sont présentées en valeurs relatives en prenant comme référence les valeurs obtenues lorsque l'alimentation hydrique est suffisante (34e et 35e jours). Il apparaît que photosynthèse et transpiration sont pratiquement indépendantes du potentiel hydrique du sol au dessus d'une valeur seuil proche ici de −700 mbar. Au dessous de ce potentiel critique, la baisse de transpiration et de photosynthèse est proportionnelle à la baisse de potentiel

hydrique. La fermeture des stomates dépend donc d'un potentiel critique et cette fermeture est progressive. Nous avons montré par ailleurs [7] que les variétés de riz pluvial présentent une différence de comportement vis-à-vis de variétés irriguées: leur potentiel critique se situe autour de $-600, -700$ mbar contre -450 mbar pour les riz aquatiques. La figure 4 montre que la photosynthèse est moins affectuée que la transpiration par la fermeture stomatique. Ceci s'explique par l'existence d'une résistance du mésophylle au transfert du CO_2 qui minimise l'effet de l'augmentation de la résistance stomatique [8]. La transpiration diminue plus que la photosynthèse ce qui conduit à une augmentation du rapport photosynthèse sur transpiration donc de l'efficience de l'eau, tant que les mécanismes biochimiques de la photosynthèse ne sont pas lésés.

2.2.3. Chocs osmotiques

La simulation de stress hydriques en milieu hydroponique à l'aide de solutions de polyéthylène glycol (PEG) de potentiel osmotique croissant a permis de confirmer l'existence d'un seuil en deçà duquel la régulation stomatique ne se fait pas.

La figure 5 montre l'effet de deux chocs osmotiques successifs sur la transpiration et la photosynthèse. Dès le changement de solution dans le compartiment racinaire, on observe une chute importante et rapide des taux d'échanges gazeux qui se stabilisent au bout de deux heures environ. Le niveau du palier atteint est proportionnel au potentiel osmotique de la solution utilisée.

CONCLUSION

S'il est facile de constater les manifestations du déficit hydrique au niveau foliaire (enroulement des feuilles, fanaison), il n'en est pas de même au niveau racinaire. C'est là l'intérêt de la méthode neutronographique qui permet de visualiser les pertes d'eau des racines et de quantifier le ralentissement de croissance pendant le dessèchement.

La mesure en continu des échanges gazeux au niveau foliaire montre les réactions du système stomatique à l'abaissement du potentiel hydrique du sol. Au dessous d'un potentiel critique, la fermeture stomatique est progressive et proportionnelle au potentiel hydrique.

REFERENCES

[1]   DE DATTA, S.K., «Upland rice around the world», Major Research in Upland Rice, International Rice Research Institute, Los Banos, Philippines (1975) 2.

[2]   COUCHAT, Ph., MOUTONNET, P., HOUELLE, M., PICARD, D., In situ study of corn seedling root growth by neutron radiography, Agron. J. 72 (1980) 321.

[3]   PICARD, D., COUCHAT, Ph., MOUTONNET, P., Particularité du cycle nycthéméral de transpiration de la variété de riz pluvial IRAT 13 comparé à celui de Morobérékan, Plant Soil **59** (1981) 481.

[4]   LASCEVE, G., COUCHAT, Ph., Le transfert de l'eau dans la plante en régime transitoire, Ann. Agron. **31** 3 (1980) 273.

[5]   CRUZIAT, P., Détermination des pertes en eau subies par les différents organes d'une plante soumise au dessèchement, Ann. Agron. **25** 4 (1974) 539.

[6]   BOIS, J.F., COUCHAT, Ph., Comparison of the effects of water stress on the root systems of two upland rice cultivars, à paraître dans Ann. Bot.

[7]   BOIS, J.F., COUCHAT, Ph., MOUTONNET, P., Etude de la réponse à un stress hydrique de quelques variétés de riz pluvial et de riz irrigué, à paraître dans Plant Soil.

[8]   SLATYER, R.O., dans Plant Water Relationships, Academic Press, London, New York (1967).

SOL-PLANTE-ATMOSPHERE:
CONTRIBUTION A L'ETUDE
DE LA COMPOSITION ISOTOPIQUE DE L'EAU
DES DIFFERENTES COMPOSANTES DE CE SYSTEME

T. BARIAC, A. FERHI,
C. JUSSERAND, R. LETOLLE
Laboratoire de géologie dynamique,
Université Pierre et Marie Curie,
Paris, France

Abstract–Résumé

SOIL-PLANT-ATMOSPHERE: A CONTRIBUTION TO THE STUDY OF THE ISOTOPIC
COMPOSITION OF WATER IN THE DIFFERENT COMPONENTS OF THIS SYSTEM.
It is essential to know the isotopic composition of water vapour for a geochemical study of
systems controlled by evaporation. Owing to difficulties of analysis, however, this composition is
most often only estimated (from water balances and precipitation). The authors' intention is to
study the content of ^{18}O in the vapour of continental water at the soil-atmosphere interface on
the assumption that, locally, the isotopic composition of vapour, which is a mixture of continental
and oceanic vapours, should reflect these different origins if they are sufficiently pronounced. A
number of samples were taken at the station of the Villeau National Institute of Astronomy and Geo-
physics (France) with a view to verifying this hypothesis. The study was made possible through
use of a new analytical technique by which routine analysis can be made of the ^{18}O content
of vapour in a limited volume of air and in moduled time steps. It was found that: (1) regional
water vapour was likely to have very wide isotopic variations in time, associated with the origin
and history of the air mass; (2) this regional isotopic signal was strongly perturbed in the first
few metres above the soil and plant cover, where there was evidence of a local vapour source.
At the level of this source the water vapour was re-equilibrated with the isotopic composition
of the soil water, the extent of this phenomenon depending on the conditions of meteoro-
logical circulation.

SOL-PLANTE-ATMOSPHERE: CONTRIBUTION A L'ETUDE DE LA COMPOSITION
ISOTOPIQUE DE L'EAU DES DIFFERENTES COMPOSANTES DE CE SYSTEME.
La connaissance de la composition isotopique de la vapeur d'eau est essentielle pour l'étude
géochimique des systèmes contrôlés par l'évaporation. Or cette composition est le plus souvent
estimée (bilans hydriques, précipitations) du fait de la difficulté d'analyse. On se propose
d'étudier ici la teneur en oxygène 18 de la vapeur d'eau continentale à l'interface sol-atmosphère.
En effet, localement, la composition isotopique de la vapeur, mélange entre des vapeurs
océanique et continentale, devrait refléter ces diverses origines, si celles-ci sont suffisamment
marquées. Afin de vérifier cette hypothèse, on a effectué un certain nombre de prélèvements,
à la station de l'Institut national d'astronomie et de géophysique de Villeau (France). Cette
étude est rendue possible grâce à l'emploi d'une nouvelle technique analytique permettant
d'analyser la teneur en oxygène 18 de la vapeur en routine sur un volume d'air restreint et un pas
de temps modulable. On a pu constater que: 1) la vapeur d'eau régionale est susceptible de

présenter de très fortes variations isotopiques temporelles, liées à l'origine et à l'histoire de la masse d'air; 2) ce signal isotopique régional se trouve fortement perturbé dans les premiers mètres au-dessus du sol et du couvert végétal, où est mise en évidence une source de vapeur locale. Au niveau de cette source, se produit un phénomène de rééquilibration de la vapeur d'eau avec la composition isotopique de l'eau du sol, phénomène plus ou moins important suivant les conditions de circulation météorologique.

INTRODUCTION

La détermination de la composition isotopique (δ_v) de la vapeur d'eau atmosphérique[1] constitue l'une des donnés fondamentales de l'étude isotopique des échanges liquide-vapeur dans le cycle hydrologique: δ_v est l'un des principaux facteurs de contrôle de la teneur isotopique des masses d'eau en voie d'évaporation [1] et reste le plus mal connu.

Cette composition isotopique a été jusqu'à présent déterminée:

— soit indirectement, notamment à partir des bilans hydriques [2], d'où une grande approximation des résultats obtenus, ou à partir des précipitations en supposant l'existence d'un équilibre isotopique liquide-vapeur [3];

— soit directement, après piégeage cryoscopique de cette vapeur, ce qui intègre nécessairement un volume d'air important sur un intervalle de temps relativement long [4].

Une technique de prélèvement instantanée couplée à une détermination de la teneur en ^{18}O de la vapeur portant sur quelques microlitres d'eau nous permet de suivre sur un pas de temps très court l'évolution de la composition isotopique d'un volume d'air restreint [5, 6].

Nous avons appliqué cette nouvelle technique à la mesure de la teneur en ^{18}O de la vapeur d'eau à l'interface sol-atmosphère. Nous pensons en effet que, localement, la composition isotopique de la vapeur, résultant d'un mélange entre de la vapeur d'eau océanique et la vapeur d'eau continentale, doit refléter ces différentes origines si celles-ci sont suffisamment marquées.

1.   MATERIEL ET METHODE

1.1. Prélèvements

Les prélèvements suivants ont été effectués à Villeau[2]. Cette station dispose en effet d'un pylône de 100 m de hauteur installé en plein champ, équipé pour

---

[1] Le δ est exprimé en parts pour mille par rapport au «Standard Mean Ocean Water» (SMOW):

δ échantillon $= (\dfrac{R \text{ échantillon}}{R \text{ standard}} - 1) \times 10^3$ avec $R = \dfrac{^{18}O}{^{16}O}$

[2] Station de l'Institut national d'astronomie et de géophysique, Villeau, Eure-et-Loir, France.
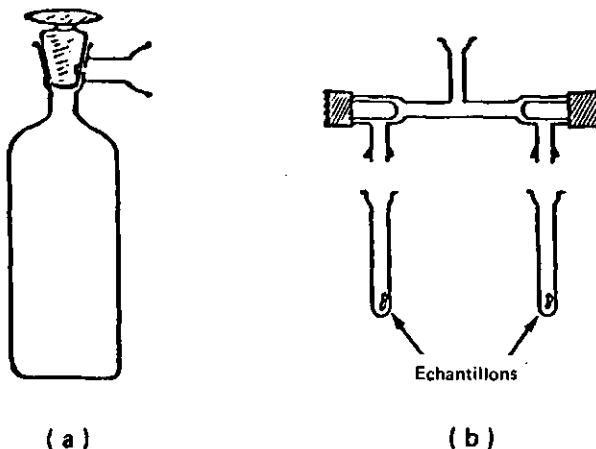
FIG.1.   Ampoule pour l'analyse des teneurs en ^{18}O dans la vapeur d'eau atmosphérique (a) et porte-échantillons pour l'analyse des teneurs en ^{18}O de l'eau des sols et des plantes (b).

la mesure de paramètres climatiques et donc parfaitement adapté à notre type d'étude. On a effectué:

— des prélèvements d'échantillons de vapeur d'eau le long du mât de 100 m, de façon à pouvoir examiner la répartition dans l'espace et dans le temps de la composition isotopique de la masse d'eau (ampoules de 250, 500 et 1000 ml suivant l'humidité relative des échantillons) (fig. 1);

— des prélèvements d'échantillons de vapeur d'eau dans les parcelles environnantes de façon à contrôler l'influence éventuelle du couvert végétal et du sol sur la composition isotopique générale de la vapeur d'eau atmosphérique;

— des prélèvements d'échantillons de sol et de végétaux de façon à déterminer les relations existantes entre la teneur en ^{18}O de l'eau de ces échantillons et celle des vapeurs (fig. 1).

1.2. Analyses

Au laboratoire, après piégeage cryoscopique (− 77°C) de l'eau des échantillons, les gaz atmosphériques incondensables à cette température sont éliminés par pompage. Puis les échantillons sont traités sur la ligne de préparation représentée à la figure 2.

La vapeur est réduite sur la poudre de diamant portée à la température de 1050°C, suivant la réaction:

$$H_2O + C \longrightarrow H_2 + CO$$
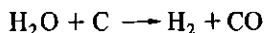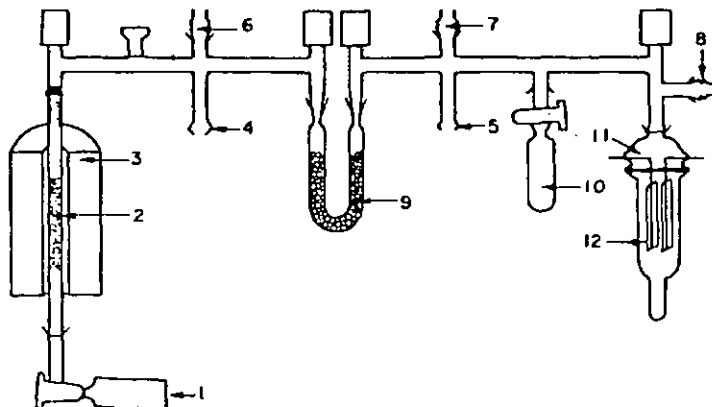
FIG.2. Ligne de réduction-conversion. 1: ampoule; 2: poudre de diamant; 3: four; 4, 5: vannes de pompage; 6, 7, 8: têtes de jauge; 9: silicagel; 10: porte-échantillon; 11: tête de convertisseur CO-CO_2; 12: éprouvette du convertisseur.

L'hydrogène évacué, le monoxyde de carbone est adsorbé sur le silicagel refroidi à $-170°C$. Le monoxyde de carbone ainsi formé est alors transformé en dioxyde de carbone dans un convertisseur à décharge électrique:

$$2\,CO \rightleftharpoons CO_2 + C$$
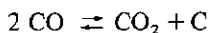
La teneur en ^{18}O du CO_2 est déterminée au spectromètre de masse à double collecteur VG 602D.

Il nous a été possible, pour tester cette méthode, de déterminer à $25°C$ le fractionnement isotopique eau-vapeur d'eau (tableau I) et d'examiner l'influence du volume des ampoules de prélèvements sur les résultats ainsi obtenus (tableau II).

Les résultats obtenus au cours de ces différents contrôles montrent que la méthode est très fiable pour l'analyse de micro-quantités d'eau (3 à 20 micro-litres d'eau).

2.   RESULTATS

L'un des résultats auxquels nous sommes parvenus est la mise en évidence d'une forte hétérogénéité isotopique de la vapeur d'eau à la fois dans l'espace (teneurs en ^{18}O variant entre $-9,5‰$ et $-30,3‰$) et dans le temps ($-10,5‰$ à $-32,25‰$) (figures 3, 4 et 5).

TABLEAU I. DETERMINATION DU COEFFICIENT D'ENRICHISSEMENT
LIQUIDE/VAPEUR A 25°C

$\delta^{18}O$		$\epsilon\%_o = \left[\dfrac{10^{-3}\,\delta_v + 1}{10^{-3}\,\delta_L + 1} - 1 \right] 10^3$
H$_2$O (liquide)	H$_2$O (vapeur)	
− 6,43	− 15,03	− 8,66
− 6,43	− 15,65	− 9,28
− 6,43	− 15,15	− 8,78
− 7,43	− 16,32	− 8,96
− 14,13	− 23,48	− 9,38
− 14,13	− 22,94	− 8,84
		valeur moyenne mesurée − 8,98
		valeur théorique − 9

TABLEAU II. INFLUENCE DU VOLUME DE L'AMPOULE SUR LA
TENEUR EN ^{18}O DE LA VAPEUR D'EAU (h = 0, 84, θ = 15,6°C) D'UN
MEME ECHANTILLON

Volume de l'ampoule (mL)	Quantité d'eau présente dans l'ampoule (μL)	$\delta^{18}O$ par rapport au SMOW (± 0,4$\%_o$)
250	2,79	− 13,85, − 13,74
500	5,79	− 14,50
1000	11,18	− 13,69
1500	16,77	− 14,32
		Moyenne = − 14,02
		σ = 0,37

Soit par exemple le profil général (fig. 3) réalisé le 4 septembre 1979 montrant
les variations de la teneur en ^{18}O de la vapeur d'eau en fonction de l'altitude du
prélèvement. Ce profil se traduit par un enrichissement isotopique de la vapeur
tout au long du mât avec une nette perturbation dans les premiers mètres au-dessus
du sol.
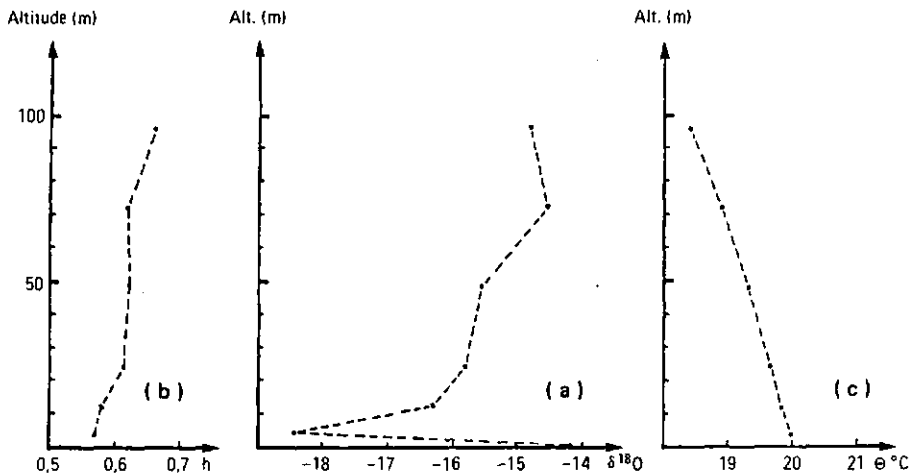
FIG.3.   a) Profil de la composition isotopique de la vapeur d'eau en fonction de l'altitude
(4/7/79) (sol nu); b) Profil d'humidité relative de l'air en fonction de l'altitude; c) Profil de
température de l'air en fonction de l'altitude; δ eau sol = − 5,80.
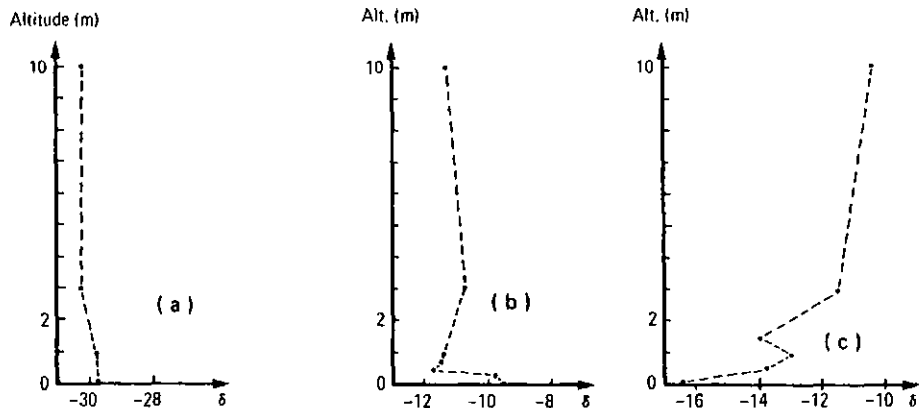
FIG.4.   Profil de la composition isotopique de la vapeur d'eau en fonction de la hauteur du
prélèvement. a) (13/2/83) couvert végétal:blé, 10 cm; δ eau sol = − 10,06; δ eau blé = − 10,40
(h = 0,70, θ = − 2°C); b) (10/6/82) couvert végétal:blé, 96 cm; δ eau sol = − 3,80;
δ eau blé = + 6,88 (h = 0,72, θ = 23,7°C); c) (29/9/80) couvert végétal: maïs, 1,90 m;
δ eau sol = − 4,42; δ eau maïs = + 2,16 (h = 0,81, θ = 17,4).
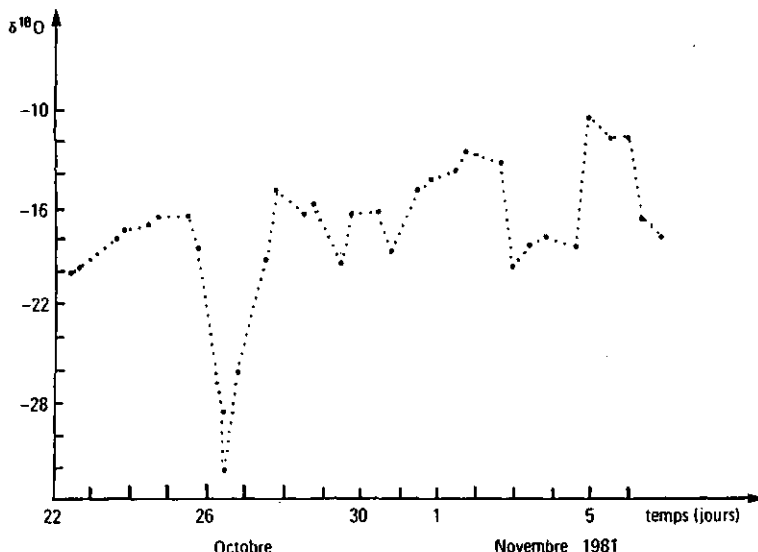
FIG.5. Evolution de la composition isotopique de la vapeur d'eau régionale au cours du temps.

Il semble donc que l'on puisse ainsi mettre en évidence deux types de vapeur en fonction de leur origine:

— l'une régionale, susceptible de présenter des variations de composition isotopique à grande échelle;

— l'autre locale, en relation directe avec le sol et les végétaux. C'est à ce type de vapeur que nous avons consacré l'essentiel de notre étude, limitant les prélèvements dans les dix premiers mètres au-dessus du sol dans la mesure où la perturbation du signal isotopique enregistrée à la figure 3 a affecté principalement cette zone.

Les profils ainsi réalisés peuvent être regroupés suivant trois familles:

— profils homogènes (fig. 4a);

— profils hétérogènes avec enrichissement de la teneur en ^{18}O de la vapeur d'eau à la base du profil (fig. 4b);

— profils hétérogènes avec appauvrissement de la teneur en ^{18}O de la vapeur d'eau à la base du profil (fig. 4c).

3.   DISCUSSION

La composition isotopique de la vapeur d'eau (δ_v) en un point de ces divers profils est donnée par les relations (1) et (2) en supposant un simple processus de mélange entre la vapeur régionale et la vapeur locale:

$$\delta_v = x \, \delta_E + (1 - x) \, \delta_A \qquad (1)$$

δ_v : $\delta^{18}O$ vapeur d'eau de l'échantillon prélevé
δ_A : $\delta^{18}O$ vapeur d'eau régionale
δ_E : $\delta^{18}O$ vapeur d'eau due à l'évapotranspiration
x : % vapeur d'eau due à l'évapotranspiration

avec

$$\delta_E = y \, \delta_{vp} + (1 - y) \, \delta_{vs} \qquad (2)$$

δ_{vp} : $\delta^{18}O$ vapeur d'eau issue des plantes
δ_{vs} : $\delta^{18}O$ vapeur d'eau issue du sol
y : % vapeur d'eau issue de végétaux.

Il s'agit maintenant d'examiner les différentes contributions isotopiques de ces vapeurs ainsi que les masses d'eau dont elles sont issues.

3.1. Teneur en ^{18}O de la vapeur d'eau régionale (δ_A)

Les prélèvements (fig. 5) ont été effectués au cours du temps de façon à déterminer l'amplitude des variations isotopiques de cette vapeur.

L'échantillonnage a été effectué deux fois par jour durant 15 jours, à 20 m de hauteur de façon à limiter tout risque de pollution de ce signal isotopique par de la vapeur d'eau d'origine différente.

Ces résultats montrent d'importantes variations qui sont probablement en relation avec l'histoire de ces masses d'air [7]. Celles-ci subissent tout d'abord, lors de leur formation, le fractionnement isotopique provoqué par l'évaporation de l'eau des océans. Puis la vapeur océanique ainsi formée voit sa composition isotopique se modifier du fait des précipitations qui appauvrissent en isotopes lourds la vapeur d'eau résiduelle, du fait des mélanges avec des vapeurs océaniques et continentales par suite des échanges avec des eaux locales. La composition isotopique ainsi mesurée reflète l'intégration de toute l'histoire antérieure de la masse d'air.

Il n'est pas encore possible à l'heure actuelle d'établir une relation nette entre les variations isotopiques mesurées et les paramètres météorologiques observés, mais l'existence de ces variations montre que la mesure systématique de δ_A doit être envisagée pour ce type d'étude.

+4,6

+5,4

+22,7

détail d'une feuille

+3,3

+2,2

−0,2 (eau du sol)
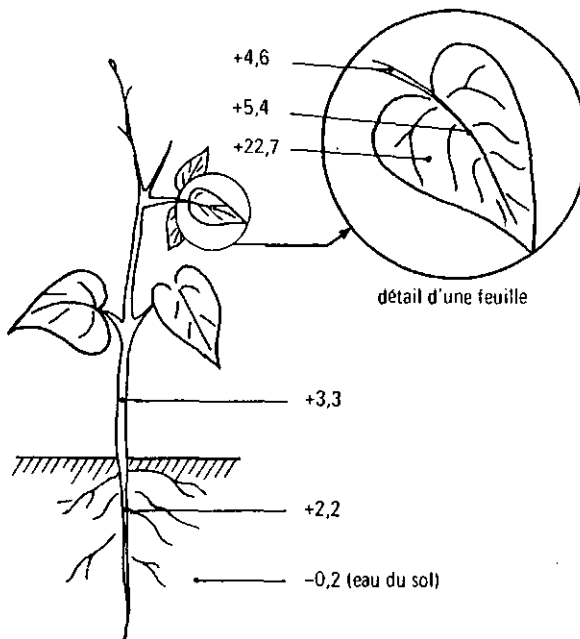
FIG.6.   Composition isotopique de l'oxygène de l'eau dans différentes parties d'un plant de haricot croissant dans les conditions de milieu suivantes: $\delta^{18}O$ de l'eau d'arrosage: − 0,2‰; humidité relative: 41%; température: 26°C; luminosité: lumière du jour; source de carbone: CO_2 atmosphérique.

3.2.   Teneur en ^{18}O de la vapeur d'eau locale

3.2.1.   Composition isotopique de l'eau circulant dans les végétaux

Dès 1965, Gonfiantini [8] a montré l'existence d'une discrimination des teneurs en ^{18}O dans l'eau foliaire par rapport à l'eau d'alimentation. Ce phénomène a été attribué à la transpiration; de plus, Zimmermann [9] a montré que l'absorption radiculaire ne provoquait pas de fractionnement isotopique.

L'utilisation de la méthode micro-analytique nous a permis de déterminer la composition isotopique des différents organes végétaux chez *Phaseolus vulgaris* L. (fig. 6).

Ces mesures montrent une grande hétérogénéité de la composition de l'eau de ces différents organes avec un enrichissement progressif depuis les racines jusqu'aux feuilles où les teneurs atteignent leurs valeurs maximales.

Cet enrichissement peut se justifier par l'existence de deux flux d'eau:

— l'un ascendant («sève brute») qui amène l'eau du sol aux feuilles;

— l'autre descendant, qui répartit la «sève élaborée» entre les différents organes; or, cette sève s'est enrichie en ^{18}O dans les feuilles.
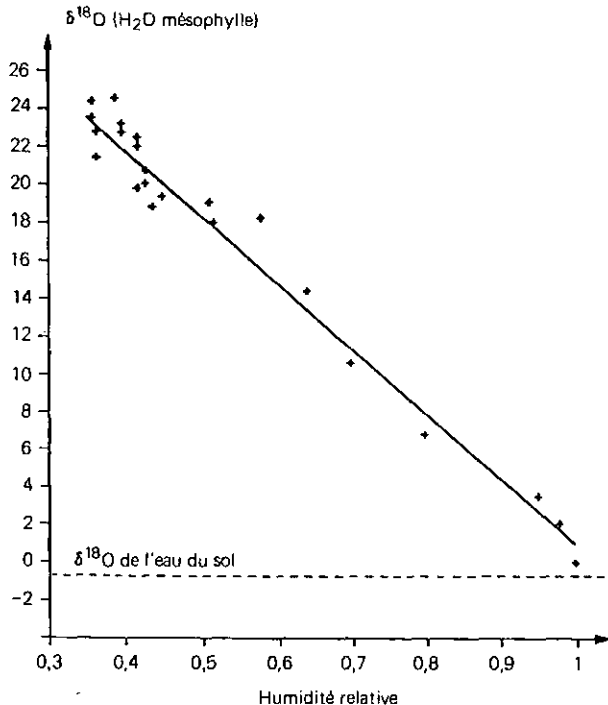
FIG. 7. Variation des $\delta^{18}O$ de l'eau au niveau du mésophylle de plants de haricot en fonction de l'humidité relative de l'air. L'eau du sol a un $\delta^{18}O$ de $- 0,7\%_0$.

Les prélèvements effectués intègrent ces deux types de sève, ce qui permet d'expliquer les valeurs moyennes observées entre la racine et la feuille.

Dongmann et al. [10], Förstel et al. [11], Förstel [12], Farris et Strain [13] ont montré l'existence d'une corrélation inverse entre l'humidité relative atmosphérique et l'enrichissement isotopique de l'eau foliaire et une corrélation directe entre la température et cet enrichissement, ce qui peut caractériser indirectement la transpiration. Bariac [14] a mis en évidence, en milieu contrôlé, l'existence d'une relation linéaire entre l'humidité relative et le $\delta^{18}O$ de l'eau foliaire (δ_L) chez Phaseolus vulgaris L., lorsque les autres paramètres sont maintenus constants (fig. 7):

$$\delta_L = - 35\,h + 36 \qquad\qquad (3)$$

Il faut noter sur cette figure, d'une part l'absence totale de fractionnement isotopique par rapport à l'eau du sol lorsque l'humidité relative atteint 100% et,

d'autre part, les très fortes valeurs atteintes par la composition isotopique de l'eau foliaire lorsque l'humidité relative diminue (h = 40%, δ_L = + 23‰).

L'essentiel de ces travaux conduit aujourd'hui à admettre qu'il est possible d'appliquer aux végétaux l'équation générale du modèle isotopique d'évaporation de l'eau libre (Ferhi et al. [15]):

$$\delta_L = \delta_L^{\circ} \left[\frac{V^{\circ} + D \cdot t}{V^{\circ}} \right]^X$$

$$+ \left[\frac{q\delta_a (1-h) + h(\delta_A - \epsilon_k) + \epsilon_e + \epsilon_k}{q(1-h) + h} \right] \left\{ 1 - \left[\frac{V^{\circ} + D \cdot t}{V^{\circ}} \right]^X \right\} \tag{4}$$

avec:

$$X = \frac{-\phi_a - h \cdot \phi_E/(1-h)}{\phi_a - \phi_E}$$

$$D = \phi_a - \phi_E, \ q = \phi_a/\phi_E$$

et où:

δ_L: $\delta^{18}O$ de l'eau foliaire
δ_L°: $\delta^{18}O$ de l'eau foliaire à l'instant t_o
V°:   volume d'eau contenu dans la feuille à l'instant t_o
ϕ_E: flux d'évaporation net
h: humidité relative
δ_a: $\delta^{18}O$ de l'eau des apports
ϵ_e: coefficient d'enrichissement isotopique à l'équilibre
ϵ_k: coefficient d'enrichissement isotopique cinétique
δ_A: $\delta^{18}O$ de la vapeur d'eau atmosphérique
ϕ_a: flux des apports

Dans le contexte particulier où la feuille se comporte, en ce qui concerne le fractionnement isotopique, comme un bassin évaporatoire à niveau constant et homogénéisation rapide (Ferhi, Létolle [16]):

$$\delta_L = \delta_L^o \cdot e^{-\dfrac{\phi_E}{V(1-h)}t} + \left[(1-h)\,\delta_a + \epsilon_e + \epsilon_k + h\,(\delta_A - \epsilon_k) \right]$$

$$\times \left[1 - e^{-\dfrac{\phi_E}{V(1-h)}t} \right] \tag{5}$$

Pour une humidité relative et une composition isotopique de l'eau d'alimentation données, la teneur en ^{18}O de l'eau foliaire tend vers une valeur limite δ_L^S (6):

$$\delta_L^S = (1-h)\,\delta_S + \epsilon_e + \epsilon_k + h\,(\delta_A - \epsilon_k) \tag{6}$$

avec δ_S: composition isotopique de l'eau du sol.

L'équation (4) peut également être appliquée à l'eau libre et à l'eau présente dans le sol: tel le cas d'un bassin à réduction de volume (fig. 8) (Ferhi [17]):

$$\delta_L = \delta_L^o \left[\dfrac{V}{V^o} \right]^{\dfrac{a+h}{1-h-a}}$$

$$+ \dfrac{\left[a \cdot \delta_a + h\,(\delta_A - \epsilon_k) + \epsilon_e + \epsilon_k \right]\left[1 - \left[\dfrac{V}{V^o} \right]^{\dfrac{a+h}{1-h-a}} \right]}{h} \tag{7}$$

avec $a = \dfrac{\phi_a\,(1-h)}{\phi_E}$

Dans le cas particulier où ϕ_a est nul, l'équation (7) devient:

$$\delta_L = \left[\delta_L^o - \dfrac{h\,(\delta_A - \epsilon_k) + \epsilon_e + \epsilon_k}{h} \right]\left[\dfrac{V}{V^o} \right]^{\dfrac{h}{1-h}}$$

$$+ \dfrac{h\,(\delta_A - \epsilon_k) + \epsilon_e + \epsilon_k}{h} \tag{8}$$
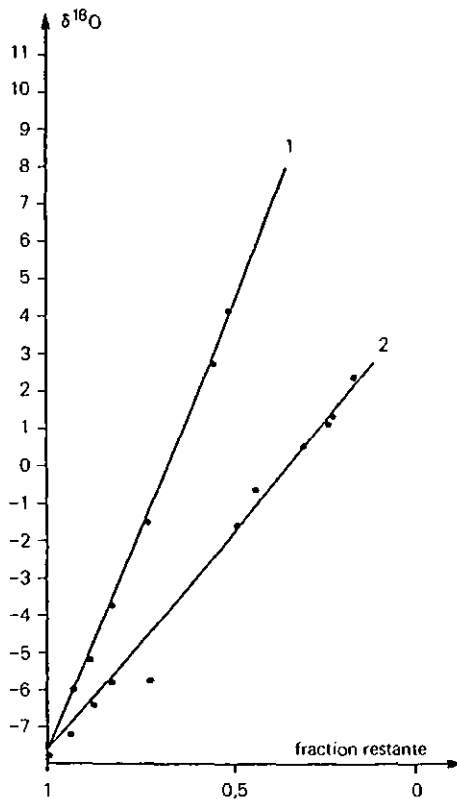
FIG.8.   Variation des $\delta^{18}O$ de l'eau en état d'évaporation: 1) à l'état libre, 2) dans le sol. Les points (·) correspondent aux résultats expérimentaux, les droites (——) sont déterminées à partir de l'équation (8) avec: $\delta° = -7,56$; $h = 0,5$; $\delta_A = -16$; $\epsilon_e = 9$ et $\epsilon_k = 14$ pour l'eau libre et 2 pour l'eau du sol.

3.2.2. Composition isotopique de la vapeur d'eau due à la transpiration

La teneur en ^{18}O du flux de vapeur d'eau δ_{ϕ_E}, issu de l'eau libre est donnée par la relation (Merlivat [18], Fehri [15]):

$$\delta_{\phi_E} = \frac{\delta_L - \epsilon_e - h(\epsilon_A - \epsilon_k)}{1-h} \qquad (9)$$

Dans le cas où la composition isotopique de l'eau foliaire δ_L atteint l'état stationnaire δ_L^S (état où l'absorption radiculaire compense exactement les pertes dues à la transpiration):

$$\delta_{\phi_E} = \delta_s \qquad (10)$$

   Les premières mesures effectuées en milieu contrôlé confirment cette hypothèse et feront l'objet d'un prochain article.

   Cette identité isotopique entre les compositions isotopiques de l'eau du sol et de la vapeur d'eau transpirée laisse supposer, dans la nature, l'existence de vapeur dont la teneur en ^{18}O plus élevée que celle observée sur le plan régional. En effet, l'eau des précipitations, et donc du sol, a, par le fractionnement isotopique à l'équilibre, une teneur en ^{18}O plus enrichie que la vapeur dont elle est issue.

   En supposant, dans les régions tempérées, que la composition isotopique de l'eau du sol δ_s reste en moyenne égale à celle des précipitations (la moyenne de celle-ci conservant une composition isotopique constante au-dessus d'une même région), il est alors possible de considérer δ_s comme peu variable.

   Par ailleurs, on peut penser que la composition isotopique de la vapeur d'eau (δ_v) au contact du sol est influencée par la composition isotopique de l'eau du sol du fait des processus d'échanges isotopiques.

   La composition isotopique δ_v mesurée à l'interface sol-atmosphère sera donc fonction:

   — de la teneur en ^{18}O de la vapeur d'eau régionale,

   — de la teneur en ^{18}O de la vapeur d'eau issue des stomates,

   — du temps de résidence de la masse d'air en contact avec le sol (processus de rééquilibration).

   Les familles de profils mesurés peuvent, suivant ces hypothèses, être interprétées de la façon suivante:

   a) Lorsque l'évapotranspiration est réduite (basses températures dans l'atmosphère et dans le sol), et la vitesse du vent atteignant des valeurs très élevées, on n'enregistre plus de contribution isotopique de la part de la vapeur d'eau locale. La vapeur d'eau régionale impose sa teneur en ^{18}O à l'ensemble du profil comme le montre la figure 4a. Les teneurs en ^{18}O mesurées le 13 février 1983 sont alors à mettre en relation avec l'origine de la masse d'air.

   b) Lors d'une transpiration intense de la part des végétaux, et par vent faible, les teneurs en ^{18}O de la vapeur enregistrées sont, dans les premiers 50 cm, plus enrichies que celles de la vapeur régionale (fig. 4b). Ce qui peut s'expliquer en appliquant les relations (8) et (9). Cependant, les teneurs en ^{18}O enregistrées dans la vapeur ne sont pas aussi élevées qu'elles devraient l'être d'après la relation (10):

$$\delta_v = -9,5\text{‰}$$
$$\delta_s = -3,8\text{‰}$$

   La vitesse du vent étant réduite dans le couvert végétal, on assiste probablement à un début de rééquilibration de la teneur en ^{18}O de la vapeur d'eau transpirée avec celle de l'eau du sol.

c) Lors d'une évaporation intense du sol et d'une absence de transpiration (végétaux en voie de fanaison), la vitesse du vent étant également réduite, la composition isotopique de la vapeur d'eau au-dessus du sol se rééquilibre avec l'eau présente dans le sol; d'où les valeurs appauvries en ^{18}O mesurées sur le terrain dans les premiers mètres au-dessus du sol (fig. 4c).

Cette étude nous amène donc aux conclusions suivantes:

Il existe une forte hétérogénéité isotopique de la vapeur d'eau atmosphérique à la fois dans le temps et l'espace. La mesure de la teneur en ^{18}O de la vapeur en fonction de la hauteur du prélèvement nous a amené à distinguer deux sources:

— une source régionale, dont la composition isotopique dépend de l'origine et de l'histoire de la masse d'air;

— une source locale, proche de l'interface sol-atmosphère, où se produit un phénomène de rééquilibration avec la composition isotopique de l'eau du sol plus ou moins important suivant les conditions de circulation atmosphérique.

REFERENCES

[1] CRAIG, H., GORDON, L.J., «Deuterium and oxygen-18 variations in the ocean and marine atmosphere», Proc. Conf. Stable Isotopes in Oceanographic Studies and Paleo-temperatures, Spoleto (1965) 9.

[2] GAT, J.R., «Environmental isotope balance of lake Tiberias», Isotope Hydrology 1970 (C.R. Coll. Vienne, 1970), AIEA, Vienne (1970) 109.

[3] CRAIG, H., HORIBE, Y., Isotopic characteristics of marine and continental water vapor, Trans. Am. Geophys. Union 48 (1967) 135.

[4] FONTES, J.Ch., GONFIANTINI, R., Composition isotopique et origine de la vapeur d'eau atmosphérique dans la région du lac Léman, Earth Planet. Sci. Letters 7 (1970) 325.

[5] BARIAC, T., JUSSERAND, C., LETOLLE, R., A routine method for ^{18}O analysis of water vapor, Int. J. Appl. Radiat. Isot. 33 (1982) 1365.

[6] FERHI, A., BARIAC, T., JUSSERAND, C., LETOLLE, R., An integrated method for isotopic analysis of oxygen from organic compounds, in water vapor and leaf water, à paraître dans Int. J. Appl. Radiat. Isot. (1983).

[7] O'NEIL, J.R., EPSTEIN, S., A method for oxygen isotope analysis of milligram quantities of water and some of its applications, J. Geophys. Res. 71 20 (1966) 4955.

[8] GONFIANTINI, R., GRATZIU, S., TONGIORGI, E., «Oxygen isotopic composition of water in leaves», Isotopes and Radiation in Soil-Plant Nutrition Studies (C.R. Coll. Ankara, 1965), AIEA, Vienne (1965) 405.

[9] ZIMMERMANN, U., EHHALT, D., MÜNNICH, K.O., «Soil-water movement and evapo-transpiration: Changes in the isotopic composition of the water», Isotopes in Hydrology (C.R. Coll. Vienne, 1966) AIEA, Vienne (1967) 567.

[10] DONGMANN, G., NURNBERG, H.W., FORSTEL, H., WAGENER, K., On the enrichment of $H_2^{18}O$ in the leaves of transpiring plants, Radiat. Environ. Biophys. 11 (1974) 41.

[11] FÖRSTEL, H., PUTRAL, A., SCHLESER, G., LIETH, H., «The world pattern of oxygen-18 in rainwater and its importance in understanding the biogeochemical oxygen cycle», Isotope Ratios as Pollutant Source and Behaviour Indicators (C.R. Coll, Vienne, 1974), AIEA, Vienne (1975) 3.

[12] FÖRSTEL, H., The enrichment of ^{18}O in leaf water under natural conditions, Radiat.
       Environ. Biophys. 15 (1978) 167.

[13] FARRIS, F., STRAIN, B.R., The effects of water stress on leaf $H_2^{18}O$ enrichment,
       Rad. and Environ. Biophys. 15 (1978) 167.

[14] BARIAC, T., La plante comme système fractionnant (^{18}O) dans le transfert de l'eau à
       l'interface sol-atmosphère, Thèse de doctorat 3e cycle, Université Pierre et Marie Curie,
       Paris, (1980).

[15] FERHI, A., BARIAC, T., LETOLLE, R., «$^{18}O/^{16}O$ ratios in leaf water and in cellulose
       of aquatic and terrestrial plants», Palaeoclimates and Palaeowaters: A Collection of
       Environmental Isotopes Studies (C.R. Groupe d'experts, Vienne, 1980), AIEA, Vienne
       (à paraître).

[16] FERHI, A., LETOLLE, R., Relation entre le milieu climatique et les teneurs en
       oxygène 18 de la cellulose des plantes terrestres, Physiol. Vég. 17 1 (1979) 107.

[17] FERHI, A., Variation des $\delta^{18}O$ de la matière organique d'origine végétale. Application
       à l'étude des paléoenvironnements, Thèse de Doctorat d'Etat, Université Pierre et
       Marie Curie, Paris, 1980.

[18] MERLIVAT, L., JOUZEL, J., Global climatic interpretation of the deuterium-oxygen-18
       relationship for precipitation, J. Geophys. Res. 84 C8 (1970) 5029.

SUMMARY REPORT OF AN
FAO/IAEA ADVISORY GROUP MEETING ON
THE EFFECT OF IRRIGATION WATER
QUALITY ON YIELD AND CROP WATER
REQUIREMENTS WITH SPECIAL EMPHASIS
ON SALT-AFFECTED SOILS*

Participants

M. Kutílek (Czechoslovakia)
A.T.A. Moustafa (Egypt)
F.I. Massoud (FAO)
K. Reichardt (FAO/IAEA)
S.K.A. Danso *(Scientific Secretary)* (FAO/IAEA)
G. Vachaud (France)
I.P. Abrol (India)
E. Rawitz (Israel)
C. Dirksen (Netherlands)
S.H. Mujtaba Naqvi (Pakistan)
J.A. Estrada (Peru)
D.R. Nielsen (United States of America)
I. Pla-Sentis (Venezuela)

BACKGROUND

A group of consultants met in Aix-en-Provence during the symposium to assist the Joint FAO/IAEA Division of Isotope and Radiation Applications of Atomic Energy for Food and Agricultural Development to determine whether or not programmes involving irrigation water quality, and the use of salt-affected soils for crop production, should be developed by the Joint Division and if so, what specific types of programme might be considered.

The first part of the meeting consisted of the presentation of papers by the participants at the symposium. Sessions III and IV included papers on this subject, and discussions related to up-to-date advances in knowledge concerning the origin of salinity; surveys of the extent of salt-affected areas; the physical properties of saline and alkaline soils under irrigation; water-crop-soil management approaches for evaluating irrigation water quality; the management of saline and

---

* This Advisory Group Meeting was held concurrently with the symposium.

sodic soils; principles of water uptake by roots; soil salinity and crop yield for optimizing irrigation management; the reclamation of saline soils; and the effects of drainage on salt movement and distribution in salt-affected soils.

The second part of the meeting consisted of several discussion sessions, held in parallel with the symposium, in which each participant contributed to the contents of this document.

INTRODUCTION

Agricultural production in many parts of the world is severely limited by high salt contents of soils. These soils, classified as either saline or sodic/saline, depending on the alkalinity of the soil, normally support very little vegetative growth.

While some soils are intrinsically high in salt content, others have induced salinity attributable to faulty soil management, such as inadequate drainage associated with the irrigation system, or the use of poor-quality irrigation water (especially in areas where water is scarce).

According to statistics released by FAO, at the current rate of growth the world population is expected to double by 2000 A.D. This rise in population calls for at least a doubling in food production by the end of the century, in a world which is already undernourished. Part of this increase is expected to be met by the adoption of more advanced technology, such as the use of high-yielding, fertilizer-responsive varieties, especially in the developing countries. However, a significant proportion of the increase in food production is expected to come from increased acreage brought under cultivation. This would certainly put great pressure on the existing agricultural land, and the need to reclaim land which would otherwise be classified as unsuitable for cultivation, such as saline/sodic soils, would assume great importance. In addition, water is often a scarce natural commodity which severely limits crop yields. Therefore, in many cases increased food production will be strongly linked to the provision of irrigation water, whose quality may not be good, and could lead to the development of saline/sodic soils, unless properly managed.

The Advisory Group Meeting was therefore convened to examine the problems associated with the use of saline/sodic soils for agricultural production and to examine existing or potential methods available for reclaiming such soils. In addition, the group reviewed the effect of poor-quality irrigation water on the physico-chemical as well as the biological properties of soils, and the effect on the productivity of land irrigated with such water, and made proposals regarding what management practices would be compatible with the use of poor-quality water for irrigation.

The Food and Agricultural Organization (FAO) has already devoted much attention to the problem (see FAO Irrigation and Drainage Papers Nos 7, 13, 16 and 29)[1] and continues to carry out many projects in developing Member States. Since nuclear-aided techniques have played a key role in many studies related to soil water and soil nutrient uptake, the major task assigned to the Advisory Group was to recommend to the Joint FAO/IAEA Division what role nuclear-aided techniques could play in studies designed to make adequate use of salt-affected soils or poor-quality water.

Co-ordinated Research Programmes carried out by the Joint FAO/IAEA Division have shown that neutron moisture meters can be successfully used, not only to measure soil-water content, but also to measure the soil's water retention and transmission properties under field conditions. The method has proved to be extremely suitable for characterizing spatially variable soils, thus contributing to the understanding of water behaviour over large areas used for crop production. The inclusion of this methodology, together with the use of tracers, in the subject matter of this Advisory Group Meeting, is a natural consequence.

GENERAL PROPOSALS

A better understanding of the dynamics of "salts" in soils is necessary, especially where soils are intrinsically high in salt content, where faulty management has induced salinity, and where "problem" waters have to be used for irrigation. The problem of salinity is regional and the proportions have become gigantic in many areas. It should be tackled from a multidisciplinary approach, so as to derive maximum benefits from recommended research. This may necessitate the expertise of soil physicists, agronomists, geneticists and plant breeders, soil microbiologists, irrigation and drainage engineers and soil fertility experts. Links already established between the Joint FAO/IAEA Division's soil section and recognized multidisciplinary Institutes in Member States, well advanced in these problems, are valuable for the success of any recommended programmes so as to ensure that research plans take into consideration available information at the local, regional and international levels, thereby avoiding duplication.

The intrinsic aspects of the problem call for programmes which should not depend on observation made on a few small experimental plots. Experimental field plots should be selected, taking into account whole regions, so that findings could be applicable to locations and regions outside the experimental sites. The time required to achieve answers in such studies is often longer that that for many other agricultural programmes.

---

[1] No.7: Salinity Seminar, Baghdad (1971); No.13: Water-Use Seminar, Damascus (1972); No.16: Drainage of salty soils (1973); No.29: Water quality for agriculture (1976).

The advantages of nuclear methods over classical approaches, such as tracing salts and easy rapid monitoring of water dynamics under field conditions, indicate that they are essential for obtaining additional information to help solve the problem of crop production under these adverse conditions. The Joint FAO/IAEA Division, because of its multidisciplinary interests, especially the work of its soil section, could usefully contribute to programmes where isotope applications are studied. Co-ordinated research programmes, the training of scientists from developing Member States through IAEA fellowship and training programmes, and the holding of regular scientific meetings are suggested.

SPECIFIC PROPOSALS

The Advisory Group recognizes that the salinity of soil and water is a great impediment to the development of agriculture in various countries, particularly those in the semi-arid tropics. The salinity problem has to be seen as a complex hydro-pedo-biological problem, the understanding of which requires an awareness of the importance of several interrelated disciplines. Specific proposals are listed below with no attempt to set priorities:

(i)   Few data are available on the possible causes of soil salinity, but a thorough understanding of these is essential for correct soil management. The reasons why soil salinity develops may vary under different climatic and geological conditions. Some information is available on saline soils, but additional data are needed on sodic soils. Monitoring drainage rates and water-table levels, and the establishment of the dynamics of water and salt balances, which can be carried out conveniently through the judicious use of neutron probes and isotopic tracers, could help indicate measures to be adopted so as to avoid salinization processes in "potentially" salt-affected soils.

(ii)   Soil-water conservation in saline/sodic soils is possible by improving physical and chemical characteristics of soils. Soil-water permeability is often a serious problem in these soils. Research objectives should include the identification of ways to improve the physico-chemical characteristics of soils so as to increase the infiltration rate of water in soil, as well as the soil's ability to retain water. Research could help identify crop species that are tolerant to and/or adapted to saline conditions, and which can therefore grow in these soils. For example, the breaking up of a soil pan through root penetration of a salt-tolerant species would, in turn, create routes for water to infiltrate. Extensive or diffuse root growth and subsequent decomposition in the top soil layer could provide organic matter, which would further enhance soil-water holding capacity and other soil properties.

The use of soil amendments, organic matter, and soil conditioners such as acrylic gel, to improve the ability of saline/sodic soils to conserve moisture and/or limit evaporation losses, should also be investigated. The establishment of water balances through the use of neutron moisture meters and the evaluation of fertilizer use efficiency through the use of isotope-labelled fertilizers would be most helpful.

(iii) Various biological processes such as symbiotic or asymbiotic N_2 fixation in plants, or soil and mycorrhizal infection, are capable of supplying resources that limit plant growth. Enhanced plant growth then subsequently affect the soil's physico-chemical-biological status. Studies to find various legumes, non-legumes and grasses capable of growth and N_2-fixation in saline/sodic soils are of extreme importance.

Investigations into isolating, identifying, multiplying and inoculating soil or N_2-fixing plants with halophylic (salt-tolerant) N_2-fixing microorganisms, assessments of N_2 amounts fixed in various crops inoculated with suitable microbial strains in saline/sodic soils, studies on the susceptibility/tolerance of various crops to saline/sodic conditions when infected with mycorrhiza, or when not, should indicate means of improving food production under these adverse conditions.

These studies should include observations on water balance, water use efficiency by the crop, salt balance, nutrient/fertilizer uptake as related to soil and/or water salinity and crop yield.

CHAIRMEN OF SESSIONS

Session 1	D.R. NIELSEN	United States of America
Session 2	E.G. YOUNGS	United Kingdom
Session 3	I. P. ABROL	India
Session 4	G. VACHAUD	France
Session 5	Ph. COUCHAT	France
Session 6	J. A. ESTRADA	Peru
Session 7	T.J. D'SOUZA	India
Session 8	N.N. BARTHAKUR	Canada

SECRETARIAT OF THE SYMPOSIUM

Scientific Secretary:	K. REICHARDT	Joint FAO/IAEA Division of Isotope and Radiation Applications of Atomic Energy for Food and Agricultural Development, IAEA, Vienna
Administrative Secretary:	Caroline de MOL VAN OTTERLOO	Division of External Relations, IAEA, Vienna
Editor:	Monica KRIPPNER	Division of Publications, IAEA, Vienna

LIST OF PARTICIPANTS AND DESIGNATING
MEMBER STATES AND ORGANIZATIONS

BELGIUM

Agneessens, J.P.

Chaire hydraulique agricole,
Faculté des sciences agronomiques de l'Etat,
B-5800 Gembloux

De Boodt, M.

Faculté des sciences agronomiques,
Université de Gent,
Coupure 653, B-9000 Gent

De Smedt, F.

Laboratory of Hydrology,
Free University of Brussels,
Pleinlaan 2, B-1050 Bruxelles

Dreze, Ph.
Paguot-Gasia, M.-C.

Chaire de chimie physique,
Faculté des sciences agronomiques de l'Etat,
8, avenue de la Faculté, B-5800 Gembloux

BRAZIL

Ferraz, E.S.B.

Centro de Energia Nuclear na Agricultura (CENA),
Caixa Postal 96, 13.400 Piracicaba, S.P.

CANADA

Barthakur, N.N.

Department of Agricultural Chemistry and Physics,
Macdonald Campus of McGill University,
21111 Lakeshore Road,
Ste Anne de Bellevue, Quebec, H9X 1C0

CHILE

Gurovich, L.

Pontificia Universidad Católica de Chile,
P.O. Box 114-D, Santiago

CONGO

Ondongo, G.   Direction de l'agriculture,
                               Ministère de l'Agriculture et de l'élevage,
                               B.P. 387, Brazzaville

CUBA

Labrada Remón, Aleida   Instituto de Investigaciones Fundamentales en
                                   Agricultura Tropical (INIFAT).
                               Calle 1 esq. 2, Santiago de las Vegas,
                               Ciudad de La Habana

CYPRUS

Orphanos, P.I.   Agricultural Research Institute,
                               Nicosia

CZECHOSLOVAKIA

Kutílek, M.   Soil Science Laboratory, Technical University,
                               Thákurova 7, CS-166 29 Praha 6

EGYPT

Azzam, R.   Nuclear Chemistry Department,
                               Atomic Energy Authority,
                               101 Kasr El Eini Street, Cairo

El-Hady, O.   Soils and Water Laboratory,
                               National Research Center,
                               Dokki, Giza

Moustafa, A.T.A.   Soils and Water Research Institute,
                               Agricultural Research Centre,
                               Ministry of Agriculture,
                               Giza

FINLAND

Kasi, S.   Laboratory of Physics,
                               Helsinki University of Technology,
                               Otakaari 1, SF-02150 Espoo 15

FRANCE

Akhtar Bhatti, M.	Société du Canal de Provence et d'aménagement de la région provençale, B.P. 100, F-13603 Aix-en-Provence Cedex
Bariac, T.	Laboratoire de géologie dynamique, Université Pierre et Marie Curie, 4, place Jussieu, Tour 26, F-75230 Paris Cedex 05
Berthome, P.	Centre national d'étude du machinisme agricole, du génie rural et des eaux et forêts (CEMAGREF), B.P. 99, F-13603 Aix-en-Provence Cedex
Bois, J.F.	Office de la recherche scientifique et technique Outre-Mer (ORSTOM), 24, rue Bayard, F-75008 Paris
Brissaud, F.	Laboratoire d'hydrologie mathématique, Université des sciences et techniques du Languedoc, F-34060 Montpellier Cedex
Brouwers, M.	Institut de recherches agronomiques tropicales (IRAT), 110, rue de l'Université, F-75340 Paris Cedex 07
Bruckler, L.	Station de sciences du sol, Institut national de la recherche agronomique (INRA), Domaine Saint-Paul, B.P. 91, F-84140 Montfavet
Chossat, J.C.	CEMAGREF, 50, avenue de Verdun, F-33610 Cestas
de Cockborne, A.M.	INRA, Station de sciences du sol, Domaine Saint-Paul, B.P. 91, F-84140 Montfavet
Collas, P.	CEMAGREF, 50, avenue de Verdun, F-33610 Cestas
Couchat, Ph.	Service de radio agronomie, CEA, Centre d'études nucléaires (CEN) de Cadarache, B.P. 1, F-13115 Saint-Paul-lez-Durance
Doulbeau, S.	ORSTOM, 24, rue Bayard, F-75008 Paris
Dumas, M.	CEA, CEN de Fontenay-aux-Roses (FAR), B.P. 6, F-92260 Fontenay-aux-Roses

FRANCE (cont.)

Gascuel-Odoux, C.	INRA, Station de sciences du sol, 65, rue de St-Brieuc, F-35042 Rennes Cedex
Gaujé, P.M.	Institut de recherche de la sidérurgie (IRSID), 185, avenue du Président Roosevelt, F-78105 St-Germain-en-Laye Cedex
Guennelon, R.M.	INRA, Station de sciences du sol, Domaine Saint-Paul, B.P. 91, F-84140 Montfavet
Guetat, P.	CEA, CEN FAR, B.P. 6, F-92260 Fontenay-aux-Roses
Isberie, C.	CEMAGREF, B.P. 99, F-13603 Aix-en-Provence Cedex
Jusserand, C. Létolle, R.	Laboratoire de géologie dynamique, Université Pierre et Marie Curie, 4, place Jussieu, Tour 26, F-75230 Paris Cedex 05
Marcesse, J. Marini, P.	CEA, CEN de Cadarache, B.P. 1, F-13115 Saint-Paul-lez-Durance
Marucic, J.-A.	Laboratoire central des Ponts et Chaussées, 58, boulevard Lefebvre, F-75732 Paris Cedex 15
Merot, P.	INRA, Laboratoire de sciences du sol, 65, rue de St-Brieuc, F-35042 Rennes Cedex
Mignée, A.	CEA, B.P. 561, F-92542 Montrouge Cedex
Moutonnet, P.	Service de radio agronomie, CEA, CEN de Cadarache, B.P. 1, F-13115 Saint-Paul-lez-Durance
Nicou, R.	IRAT, 110, rue de l'Université, F-75340 Paris Cedex 07
Normand, M.	CEMAGREF, Division Hydrologie-hydraulique, B.P. 121, F-92164 Antony Cedex
Oliver, J.	CEA, 31–33, rue de la Fédération, B.P. 510, F-75752 Paris Cedex 15

Paulet, B.	Service de l'hydraulique, Direction de l'aménagement, Ministère de l'Agriculture, 19, avenue du Maine, F-75732 Paris Cedex 15
Penadille, Y.	CEMAGREF, B.P. 99, F-13603 Aix-en-Provence Cedex
Peyremorte, P.	Société du Canal de Provence et d'aménagement de la région provençale, B.P. 392, F-13603 Aix-en-Provence Cedex
Rambal, S.	Centre d'études phytosociologiques et écologiques (CEPE), Centre national de la recherche scientifique (CNRS), Route de Mende, B.P. 5051, F-34033 Montpellier Cedex
Roose, E.	ORSTOM, 24, rue Bayard, F-75008 Paris
Saint-Lebe, L.	Service de radio agronomie, Département de biologie, CEA, CEN de Cadarache, B.P. 1, F-13115 Saint-Paul-lez-Durance
Schmidt, F.	CEA, CEN de Cadarache, B.P. 1, F-13115 Saint-Paul-lez-Durance
Sicamois, D.	Société Nardeux, Avenue d'Islande, 2A Courtabœuf, F-94910 Les Ulis
Sicot, A.M.	INRA, Centre de Toulouse, B.P. 12, F-31320 Castanet-Tolosan,
Thevenet, G.	Institut technique des céréales et des fourrages, B.P. 52, F-17700 Surgères
Vachaud, G.	Institut de mécanique de Grenoble, B.P. 68, F-38402 Saint-Martin-d'Hères Cedex
Vallerie, M.	ORSTOM, 24, rue Bayard, F-75008 Paris
Vauclin, M.	Institut de mécanique de Grenoble, B.P. 68, F-38402 Saint-Martin-d'Hères Cedex
Vieillefon, J.	Mission Orstom, 18, avenue Charles Nicolle, Tunis, Tunisie

GERMAN DEMOCRATIC REPUBLIC

Baer, M.   Zentralinstitut für Isotopen- und Strahlenforschung,
                                           Akademie der Wissenschaften der DDR,
                                           Permoserstrasse 15, DDR-7050 Leipzig

Markgraf, G.   Sektion Pflanzenproduction, Humboldt-Universität,
                                           Invalidenstrasse 43, DDR-1040 Berlin

GERMANY, FEDERAL REPUBLIC OF

Christaller, G.   Technische Fachhochschule Berlin,
Krämer, R.   Luxemburger Strasse 10, D-1000 Berlin 65
Thies, R.

GUATEMALA

Rueda Calvet, J.L.   Dirección General de Energía Nuclear,
                                           Diagonal 17, 29–78, Zona 11, Apartado Postal 1421,
                                           Ciudad de Guatemala

INDIA

Abrol, I.P.   Central Soil Salinity Research Institute,
                                           Karnal-132001

D'Souza, T.J.   Biology and Agriculture Division,
                                           Bhabha Atomic Research Centre,
                                           Trombay, Bombay 400 085

INDONESIA

Mitrosuhardjo, M.M.   Center for the Application of Isotopes and Radiation,
                                           PAIR - BATAN,
                                           P.O. Box 2, Kebajoran Lama, Jakarta-Selatan

IRAN, ISLAMIC REPUBLIC OF

Alemzadeh, M.   Nuclear Research Centre,
                                           North Kargar Avenue, P.O. Box 41-1198, Tehran

IRAQ

Abdullah, I.   Ministry of Irrigation,
Khalil, F.R.   Baghdad

ISRAEL

Rawitz, E.   The Seagram Centre for Soil & Water Sciences,
                                            The Faculty of Agriculture, The Hebrew University
                                                of Jerusalem,
                                            P.O. Box 12, Rehovot 76—100

ITALY

Chamard, P.   Lab. Ecologia Continentale e Diffusione Atmosferica,
                                            ENEA, CSN Casaccia,
                                            CP 2400, I-00100 Roma

LIBYA

Abdulgader, A.   Tajoura Nuclear Research Center,
Khalifa, O.   P.O. Box 30878, Tajoura

MALAYSIA

Razley Bin Mohd,Nordin   Tun Ismail Atomic Research Centre,
                                            No. 4, Jalan 1/4, Bandar Baru Bangi, Selangor

NETHERLANDS

Bouma, J.   Netherlands Soil Survey Institute (Stiboka),
                                            P.O. Box 98, NL-6700 AB Wageningen

Dirksen, C.   Department of Soils and Fertilizers,
                                            Agricultural University,
                                            De Dreijen 3, NL-6703 BC, Wageningen

NORWAY

Steenberg, K.   Isotope Laboratory,
                                            Agricultural University of Norway,
                                            P.O. Box 26, N-1432 Aas — NLH

PAKISTAN

Haq M.I.   Nuclear Institute for Agriculture & Biology,
Naqvi, S.H. Mujtaba   Jhang Road, P.O. Box 128, Faisalabad

PERU

Estrada, J.A.

Universidad Nacional Agraria "La Molina",
Instituto Regional de Desarrollo Costa,
Apartado Postal 456, Lima

PORTUGAL

Oliveira, C.

Laboratório Nacional de Engenharia e
     Tecnologia Industrial (LNETI),
Estrada Nacional No.10, P-2685 Sacavém

SWITZERLAND

Calame, F.

Station fédérale de recherches agronomiques de
     Changins,
CH-1260 Nyon

Mermoud, A.

Institut de Génie rural, EPFL,
En Bassenges, CH-1024 Ecublens

Regamey, P.

Institut de Génie rural, Ecole Polytechnique,
Lausanne

TUNISIA

Chaabouni, Z.

Centre de recherche du Génie rural,
B.P. 10, Ariana

Mhiri, A.

Institut national agronomique de Tunisie,
43, avenue Charles Nicolle, Tunis

UNITED KINGDOM

Henshall, J.K.

Scottish Institute of Agricultural Engineering,
Bush Estate, Penicuik,
Midlothian, Scotland EH26 0PH

Youngs, E.G.

Rothamsted Experimental Station,
Harpenden, Herts AL5 2JQ

UNITED STATES OF AMERICA

Ahuja, L.R.

Water Quality and Watershed Research Laboratory,
United States Department of Agriculture,
P.O. Box 1430, Durant, OK 74702

Nielsen, D.R.   Department of Land, Air and Water Resources,
                                      University of California,
                                      Veihmeyer Hall, Davis, CA 95616

UPPER VOLTA

Some, B.L.   Institut voltaïque de recherche agronomique et
                                          zootechnique,
                                      B.P. 7192, Ouagadougou

VENEZUELA

Pla-Sentis, I.   Instituto de Edafología, Faculdad de Agronomía,
                                      Universidad Central de Venezuela,
                                      Apartado 189, Maracay

YUGOSLAVIA

Dragović, S.   Institute of Field and Vegetable Crops,
                                      Faculty of Agriculture Novi Sad,
                                      St. M. Gorkog 30, YU-21000 Novi Sad

ORGANIZATIONS

FOOD AND AGRICULTURE ORGANIZATION OF THE UNITED NATIONS (FAO)

Alaerts, M.   Kuleuven, Lab. Landtechniek,
Massoud, F.   Kard. Mercierlaan 92, B-3030 Heuerlee

INTERNATIONAL ATOMIC ENERGY AGENCY (IAEA)

Danso, S.K.A.   Joint FAO/IAEA Division of Isotopes and
                                          Radiation Applications of Atomic Energy
                                          for Food and Agricultural Development,
                                      P.O. Box 100, A-1400 Wien, Austria

Zifferero, M.   Department of Research and Isotopes,
                                      P.O. Box 100, A-1400 Wien, Austria

AUTHOR INDEX

INDEX OF PAPERS BY NUMBER

HOW TO ORDER IAEA PUBLICATIONS

■ An exclusive sales agent for IAEA publications, to whom all orders
and inquiries should be addressed, has been appointed
in the following country:

UNITED STATES OF AMERICA   UNIPUB, P.O. Box 433, Murray Hill Station, New York, NY 10157

■ In the following countries IAEA publications may be purchased from the
sales agents or booksellers listed or through your
major local booksellers. Payment can be made in local
currency or with UNESCO coupons.

ARGENTINA	Comisión Nacional de Energía Atomica, Avenida'del Libertador 8250, RA-1429 Buenos Aires
AUSTRALIA	Hunter Publications, 58 A Gipps Street, Collingwood, Victoria 3066
BELGIUM	Service Courrier UNESCO, 202, Avenue du Roi, B-1060 Brussels
CZECHOSLOVAKIA	S.N.T.L., Spálená 51, CS-113 02 Prague 1
	Alfa, Publishers, Hurbanovo námestie 6, CS-893 31 Bratislava
FRANCE	Office International de Documentation et Librairie, 48, rue Gay-Lussac, F-75240 Paris Cedex 05
HUNGARY	Kultura, Hungarian Foreign Trading Company P.O. Box 149, H-1389 Budapest 62
INDIA	Oxford Book and Stationery Co., 17, Park Street, Calcutta-700 016
	Oxford Book and Stationery Co., Scindia House, New Delhi-110 001
ISRAEL	Heiliger and Co., Ltd., Scientific and Medical Books, 3, Nathan Strauss Street, Jerusalem 94227
ITALY	Libreria Scientifica, Dott. Lucio de Biasio "aeiou", Via Meravigli 16, I-20123 Milan
JAPAN	Maruzen Company, Ltd., P.O. Box 5050, 100-31 Tokyo International
NETHERLANDS	Martinus Nijhoff B.V., Booksellers, Lange Voorhout 9-11, P.O. Box 269, NL-2501 The Hague
PAKISTAN	Mirza Book Agency, 65, Shahrah Quaid-e-Azam, P.O. Box 729, Lahore 3
POLAND	Ars Polona-Ruch, Centrala Handlu Zagranicznego, Krakowskie Przedmiescie 7, PL-00-068 Warsaw
ROMANIA	Ilexim, P.O. Box 136-137, Bucarest
SOUTH AFRICA	Van Schaik's Bookstore (Pty) Ltd., Libri Building, Church Street, P.O. Box 724, Pretoria 0001
SPAIN	Diaz de Santos, Lagasca 95, Madrid-6
	Diaz de Santos, Balmes 417, Barcelona-6
SWEDEN	AB C.E. Fritzes Kungl. Hovbokhandel, Fredsgatan 2, P.O. Box 16356, S-103 27 Stockholm
UNITED KINGDOM	Her Majesty's Stationery Office, Agency Section, Room 008, Publications Centre, 51 Nine Elms Lane, London SW8 5DR
U.S.S.R.	Mezhdunarodnaya Kniga, Smolenskaya-Sennaya 32-34, Moscow G-200
YUGOSLAVIA	Jugoslovenska Knjiga, Terazije 27, P.O. Box 36, YU-11001 Belgrade

---

■ Orders from countries where sales agents have not yet been appointed and
requests for information should be addressed directly to:

**Division of Publications
International Atomic Energy Agency
Wagramerstrasse 5, P.O. Box 100, A-1400 Vienna, Austria**